



Deng, Lin (2016) *The role of non-coding RNA in the development of pulmonary arterial hypertension*. PhD thesis.

<http://theses.gla.ac.uk/7828/>

Copyright and moral rights for this work are retained by the author

A copy can be downloaded for personal non-commercial research or study, without prior permission or charge

This work cannot be reproduced or quoted extensively from without first obtaining permission in writing from the author

The content must not be changed in any way or sold commercially in any format or medium without the formal permission of the author

When referring to this work, full bibliographic details including the author, title, awarding institution and date of the thesis must be given

Glasgow Theses Service  
<http://theses.gla.ac.uk/>  
theses@gla.ac.uk

# **The Role of Non-coding RNA in the Development of Pulmonary Arterial Hypertension**

**Lin Deng MRes**

Submitted in fulfillment of the requirements for the  
Degree of Doctor of Philosophy, Institute of  
Cardiovascular and Medical Sciences, University of Glasgow

Institute of Cardiovascular and Medical Sciences  
College of Medical, Veterinary and Life Sciences  
University of Glasgow



**University  
of Glasgow**

**2016**

**Lin Deng**

# Author Declaration

I declare that this thesis has been written entirely by myself and is a record of research performed by myself with the exception of *in situ* hybridization of miR-143-3p in lung sections from human patients with PAH (Dr Ruifang Lu) and hypoxia neonatal calves and Brisket disease (Professor Kurt Stenmark lab), the Taqman qRT-PCR analysis the miR-143/145 cluster expression in PASMCs (healthy donors and PAH patient samples) with multiple scratches (Dr Francisco J. Blanco), analysis of miR-143 expression in mouse cardiomyocytes and fibroblasts (Dr Hannah Stevens), *in situ* hybridization of right ventricle of miR-143-3p (Dr Hannah Stevens), analysis of miR-143-3p expression in the SU5416/hypoxia rat model of PH (Dr Jenny Grant). This work has not been submitted previously for a higher degree. The research was carried out at the Institute of Cardiovascular and Medical Sciences, University of Glasgow and Centre for Cardiovascular Science, University of Edinburgh under the supervision of Professor Andrew H. Baker and Dr Angela C. Bradshaw.

Lin Deng

August 2016

# Acknowledgments

First and foremost, I would like to thank my supervisors Professor Andrew H. Baker and Dr Angela C. Bradshaw for their excellent advice, support, help and guidance throughout my studies. In particular, I would like to thank Professor Baker for giving the opportunities to study in his lab during the last four years. Additionally, I would like to thank the University of Glasgow and China Scholarship Council for the support and funding of this work.

I would like to say a special thank you to Dr Kevin White, for kindly teaching me the surgery for hemodynamic measurements and the chronic hypoxia induced PH mouse model and for his advice on my project. Thank you to Professor Margaret R. MacLean who allowed me to use her *in vivo* equipment for animal studies. I'd also like to thank the Professor Nicholas Morrell, Professor Kurt Stenmark, Professor Joseph M. Miano and Dr Xiaochun Long research groups for the wonderful collaboration.

Thanks to everyone who I have been fortunate enough to work with in the BHF Glasgow Cardiovascular Research Centre and Centre for Cardiovascular Science, University of Edinburgh. Special thanks to Dr Francisco J. Blanco, Dr Hannah Stevens, Dr Ruifang Lu, Dr Jiangtao Ma, Dr Robert McDonald, Dr Raghu Bhushan, Dr Axelle Caudrillier, Dr Rachel Dakin, Dr Laura Denby, Dr Jenny Grant, Margaret D. Ballantyne, Nicola Britton, Gregor Aitchison, and Yvonne Harcus for their first-class knowledge and support in the lab.

A special thank you to the girls and boys who share the office with me during this fantastic experience, Chris, Valters, Margaret, Emma, Estrella, Lisa, Liz and Hannah. Also thank to my Chinese friends meet in Glasgow, Jiangtao Ma, Yan Yang, Xuan Meng, Liyu Cao, Cui Zhang, Runlin Chen, Jie Luo, Yongxin Min, and Yaqing Cui. Especially to Yan and Xuan, thank you guys coming to my wedding in Chengdu.

I would like to say a heartfelt thank you to my family, especially my Mum, and Dad and for always believing in me and encouraging me even when the going gets tough. I couldn't have done it without you. I spent very little time with them during these years in Scotland. I owe too much to my parents as the only child of them. I wish all my best to them. Massive thanks to the family members and friends for helping preparing the wedding in Jiangjin and Chengdu.

And last but not least, thanks to my amazing wife Jing Ju, who I absolutely could not have done this without. Your support and love have been unwavering and I will always be in your debt for all the help you've given me. Thanks you so much. I dedicate this to you, and our baby, who will arrive soon and give me a new life.

# Table of Contents

<b>AUTHOR DECLARATION</b> .....	<b>I</b>
<b>ACKNOWLEDGMENTS</b> .....	<b>II</b>
<b>LIST OF FIGURES</b> .....	<b>IX</b>
<b>LIST OF TABLES</b> .....	<b>XIII</b>
<b>LIST OF PUBLICATIONS, PRESENTATIONS AND AWARD</b> .....	<b>XIV</b>
<b>DEFINITIONS/ABBREVIATIONS</b> .....	<b>XV</b>
<b>ABSTRACT</b> .....	<b>XX</b>
<b>1 INTRODUCTION</b> .....	<b>1</b>
1.1 PULMONARY CIRCULATION .....	2
1.1.1 <i>Structure of the Pulmonary Circulation</i> .....	2
1.1.2 <i>Structure of the Pulmonary Vessels</i> .....	4
1.1.3 <i>Function of the Pulmonary Circulation</i> .....	5
1.1.4 <i>Control of the Pulmonary Circulation</i> .....	6
1.1.5 <i>Pulmonary Vascular Resistance</i> .....	6
1.2 PULMONARY ARTERIAL HYPERTENSION .....	8
1.2.1 <i>Classification</i> .....	8
1.2.2 <i>Clinical Definition and Diagnosis</i> .....	13
1.2.3 <i>Epidemiology of Pulmonary Arterial Hypertension</i> .....	14
1.2.4 <i>BMPR2 Mutations in PAH</i> .....	15
1.2.5 <i>Pathobiology of Pulmonary Arterial Hypertension</i> .....	16
1.2.5.1 Vasoconstriction .....	17
1.2.5.1 Pulmonary Vascular Remodelling .....	18
1.2.6 <i>Cellular Components of PAH</i> .....	21
1.2.6.1 Endothelial Cells .....	22
1.2.6.2 Smooth Muscle Cells.....	23
1.2.6.3 Fibroblasts.....	24
1.2.6.4 Inflammatory Cells.....	26
1.2.7 <i>Current Approved Therapeutic Strategies in PAH</i> .....	27
1.2.7.1 Prostacyclin Analogues.....	30
1.2.7.2 Endothelin Receptor Antagonists.....	31
1.2.7.3 Phosphodiesterase Type 5 Inhibitors.....	32
1.2.8 <i>Combination Therapy</i> .....	33
1.2.9 <i>Traditional Animal Models of Pulmonary Hypertension</i> .....	34
1.2.9.1 Chronic Hypoxia.....	34
1.2.9.2 Monocrotaline (MCT) Injury Model .....	36
1.2.10 <i>Alternative Animal Models of PAH</i> .....	38
1.2.10.1 Sugren 5416 (SU5416) and Hypoxia.....	39
1.2.10.2 Overexpression of S100A4/Mts in Mice .....	41
1.2.10.3 IL-6 Overexpression in Mice .....	42
1.2.10.4 BMPR2 Mutant Mice.....	43

1.3 NON-CODING RNA(NCRNA).....	45
1.3.1 <i>MicroRNAs</i> .....	46
1.3.1.1 MicroRNA Genomics and Biogenesis .....	46
1.3.1.2 The Function of MiRNAs.....	50
1.3.1.3 MicroRNAs Involved in PAH.....	52
1.3.1.3.1 MiR-204 .....	52
1.3.1.3.2 MiR-21.....	54
1.3.1.3.3 MiR-17/92 .....	57
1.3.2 <i>Long non-coding RNAs (lncRNAs)</i> .....	59
1.3.2.1 Biogenesis and Function of LncRNAs .....	59
1.3.2.2 Long non-coding RNA in PAH.....	62
1.4 EXOSOMES .....	64
1.4.1 <i>Exosome Biogenesis</i> .....	64
1.4.2 <i>Exosome Composition</i> .....	67
1.4.3 <i>The Function of Exosomes</i> .....	68
1.4.4 <i>The Role of Exosomes in PAH</i> .....	69
1.5 AIMS .....	70
<b>2 MATERIALS &amp; METHODS.....</b>	<b>71</b>
2.1 CHEMICALS.....	72
2.2 ETHICAL INFORMATION .....	72
2.3 ANIMALS .....	72
2.3.1 <i>Wild-type Mice</i> .....	72
2.3.2 <i>MiR-143 Knockout Mice</i> .....	73
2.3.3 <i>Chronic Hypoxia Model of PH</i> .....	73
2.4 ANTIMiR-143/145 ADMINISTRATION.....	73
2.4.1 <i>PAH Prevention Study</i> .....	74
2.4.2 <i>PAH Reversal of Study</i> .....	74
2.4.3 <i>Intranasal Delivery of antimir-145-5p</i> .....	74
2.4.4 <i>Hypoxia/SU5416 rat model of PH</i> .....	75
2.4.5 <i>Neonatal calf model</i> .....	76
2.5 ASSESSMENT OF PH .....	77
2.5.1 <i>Anaesthetic Induction</i> .....	77
2.5.2 <i>Right Ventricular Systolic Pressure measurements</i> .....	77
2.5.3 <i>Systemic Arterial Pressure</i> .....	78
2.5.4 <i>Right Ventricular Hypertrophy</i> .....	80
2.5.5 <i>Pulmonary Vascular Remodelling</i> .....	80
2.6 HISTOLOGY .....	80
2.6.1 <i>Fixation, Paraffin Embedding and Sectioning of Lung Tissue</i> .....	80
2.6.2 <i>Immunohistochemistry</i> .....	81
2.6.3 <i>Immunofluorescence</i> .....	82
2.6.4 <i>Immunocytochemistry (ICC)</i> .....	83
2.6.5 <i>Haematoxylin and Eosin Staining</i> .....	83
2.6.6 <i>In Situ Hybridisation</i> .....	84
2.7 CELL CULTURE.....	85

2.7.1 Human Pulmonary Artery Smooth Muscle Cells (PASCs)	85
2.7.2 Human Pulmonary Endothelial Cells (PAECs)	86
2.7.3 Human Embryonic Kidney (HEK) 293T cell	87
2.8 CELL TRANSFECTION AND TRANSDUCTION	87
2.8.1 MiRNA Transfection	87
2.8.2 SiRNA Transfection	88
2.8.3 Cell Transduction	89
2.9 CELLULAR FUNCTION ASSAYS	89
2.9.1 Proliferation Assay	89
2.9.1.1 BrdU Cell Proliferation Assay	89
2.9.1.2 EdU Proliferation Assay	90
2.9.2 Apoptosis Assay	91
2.9.3 Wound Healing Migration Assay	92
2.9.4 Multiple Scratches Assay	92
2.9.5 In Vitro Tube Formation Assay	93
2.10 DNA DAMAGE ASSAY	93
2.11 WESTERN BLOTTING	94
2.11.1 Protein Extraction and Preparation	94
2.11.2 Protein Quantification	95
2.11.3 SDS-PAGE	95
2.11.4 Immunoblotting	96
2.12 RNA EXTRACTION, PURIFICATION AND QUANTIFICATION	97
2.12.1 Cells	97
2.12.2 Tissues	98
2.12.3 Nano-Drop	98
2.12.4 Agilent Testing of RNA Quality	99
2.13 REVERSE TRANSCRIPTION POLYMERASE CHAIN REACTION (RT-PCR)	99
2.13.1 MiRNA Reverse Transcription	99
2.13.2 mRNA Reverse Transcription	100
2.14 TAQMAN QUANTITATIVE REAL-TIME PCR	101
2.15 EXOSOME EXTRACTION, PURIFICATION AND QUANTIFICATION	102
2.16 NANOPARTICLE TRACKING ANALYSIS (NTA)	103
2.17 MICROARRAY ANALYSIS	103
2.18 LENTIVIRUS PRODUCTION AND TITERING	104
2.19 CO-CULTURE MODEL	106
2.20 LABELLING PRE-MiR-143-3P PRECURSOR WITH CY3 <i>IN VITRO</i>	107
2.21 STATISTICAL ANALYSIS	108

<b>3 EVALUATION OF MIR-143/145 IN PULMONARY ARTERIAL HYPERTENSION PATIENT SAMPLES AND IN EXPERIMENTAL ANIMAL MODELS OF PAH</b>	<b>109</b>
3.1 INTRODUCTION	110
3.2 AIMS	115
3.3 RESULTS	116
3.3.1 MiR-143 is Highly Expressed in PASCs Compared to PAECs	116
3.3.2 MiR-143-3p is Upregulated in PAH Patients	117

3.3.3 <i>MiR-143-3p is Upregulated in Animal Models of Pulmonary Hypertension</i> .....	119
3.3.4 <i>Genetic Deletion of miR-143 in Mice Prevents Chronic Hypoxia Induced PH</i> .....	126
3.3.5 <i>Pharmacological Inhibition of miR-143-3p in Mice Alleviates the Development of PH</i> .....	130
3.3.6 <i>AntimiR-143-3p Treatment Shows Therapeutic Effect in Chronic Hypoxia Induced PH Mice</i> .....	137
3.3.7 <i>Intranasal Delivery of antimiR-145-5p Significantly Reduced the miR-145-5p Level in Pulmonary System</i> .....	142
3.3.8 <i>Intranasal Delivery of antimiR-145-5p does not Attenuate Chronic Hypoxia Induced Pulmonary Arterial Hypertension</i> .....	146
3.4 DISCUSSION .....	150
<b>4 THE ROLE OF MIR-143 REGULATION OF SMOOTH MUSCLE AND ENDOTHELIAL CELL CROSSTALK IN PULMONARY ARTERIAL HYPERTENSION</b> .....	<b>156</b>
4.1 INTRODUCTION.....	157
4.2 AIMS .....	162
4.3 RESULTS .....	163
4.3.1 <i>MiR-143 Expression is Significantly Upregulated During Scratch Closure in PSMCs</i> .....	163
4.3.2 <i>MiR-143-3p Expression is Dysregulated During Scratch Closure in Distal PSMCs from HPAH/IPAH Patients and Controls</i> .....	166
4.3.3 <i>Overexpression and Knockdown of miR-143-3p in PSMCs Affects Cell Migration</i> ....	170
4.3.4 <i>Manipulation of miR-143-3p Affects PSMC Apoptosis but not Proliferation</i> .....	173
4.3.5 <i>DNA Damage in PSMCs Induces miR-143-3p Expression</i> .....	176
4.3.6 <i>Extracellular Vesicles from PSMC-derived Culture Medium can Transfer miR-143-3p to PAECs</i> .....	178
4.3.7 <i>MiR-143-3p Secreted by PSMC Induces PAEC Cell Migration</i> .....	181
4.3.8 <i>Isolation and Characterisation of Exosomes Derived from PSMCs</i> .....	184
4.3.9 <i>MiR-143-3p Enriched Exosomes Treatment and Direct Transfection of pre-miR-143-3p Induced Cell migration and Angiogenesis in PAECs</i> .....	187
4.3.10 <i>Overexpression of miR-143-3p in PAECs Has No Effect on Cell Proliferation and Apoptosis</i> .....	191
4.3.11 <i>Cy3-labelled pre-miR-143-3p is Transferred from PSMC to PAEC in Exosomes</i> .....	194
4.3.12 <i>AntimiR-143-3p Treatment Reversed the Pro-migratory Effect of miR-143-3p Enriched Exosomes Derived from PSMCs</i> .....	196
4.3.13 <i>Pathway Analysis of PSMCs and PAECs</i> .....	199
4.4 DISCUSSION .....	208
<b>5 THE ROLE OF LONG NON-CODING RNA IN PAH</b> .....	<b>217</b>
5.1 INTRODUCTION.....	218
5.2 AIMS .....	224
5.3 RESULTS .....	225
5.3.1 <i>LncRNA MYOSLID</i> .....	225
5.3.1.1 <i>Identification and Genomic Location of MYOSLID</i> .....	225
5.3.1.2 <i>MYOSLID is Upregulated by Multiple Triggers of PH in PSMC and PAH Patients</i> .....	226
5.3.1.3 <i>Downregulation MYOSLID Induces Apoptosis and Inhibits Cellular Migration in PSMCs</i> .....	231

5.3.1.4 <i>MYOSLID</i> Knockdown Decreased the Proliferation of PAEC .....	235
5.3.1.5 <i>MYOSLID</i> Knockdown Modulates the Expression of BMP Pathway Components in PASCs.....	238
<b>5.3.2 <i>LncRNA Myolnc16</i> .....</b>	<b>243</b>
5.3.2.1 Genomic Location of <i>Myolnc16</i> .....	243
5.3.2.2 Inflammatory Cytokines Induced <i>Myolnc16</i> Expression in PASCs .....	244
5.3.2.3 <i>Myolnc16</i> Knockdown Induced IL-1 and TNF- $\alpha$ Expression and Inhibited IL-6 Expression.....	246
5.3.2.4 <i>Myolnc16</i> Knockdown Decreased the Chemokine 1,6 8 Expression .....	249
5.3.2.5 <i>Myolnc16</i> Knockdown Decreased the MAPK/ERK Pathway .....	251
5.3.2.6 <i>Myolnc16</i> Knockdown Decreased the Migration and Proliferation in PASCs .....	253
5.4 DISCUSSION .....	255
<b>6 GENERAL DISCUSSION .....</b>	<b>264</b>
<b>7 BIBLIOGRAPHY .....</b>	<b>278</b>

# List of Figures

Figure 1.1 Schematic of the pulmonary circulation .....	3
Figure 1.2 Schematic representation of <i>bmpr2</i> functional domains.....	16
Figure 1.3 Histopathologically changes observed in pulmonary vascular remodelling in human patients with PAH.....	20
Figure 1.4 Schematic showing the different cells types involved in pulmonary vascular remodelling.....	21
Figure 1.5 Major pathways approved for current therapies for PAH patients .....	29
Figure 1.6 MiRNA biogenesis.....	49
Figure 1.7 Overview of the genome location and functions of lncRNAs.....	63
Figure 1.8 Biogenesis of exosomes.....	66
Figure 2.1 Rat 14 week hypoxia/SU5416 <i>in vivo</i> study design .....	76
Figure 2.2 Representative recording of right ventricular systolic pressure .....	78
Figure 2.3 Representative recording of systemic arterial pressure.....	79
Figure 2.4 PASMCs migration with multiple scratches .....	93
Figure 2.5 Co-culture model of cell-to-cell communication.....	107
Figure 3.1 Analysis of miR-143 expression levels in pulmonary vascular cells .....	116
Figure 3.2 Analysis of miR-143 expression in PAH patients and healthy controls.....	118
Figure 3.3 Analysis of miR-143 in chronic hypoxia induced PH mouse model .....	121
Figure 3.4 <i>In situ</i> hybridization analysis of miR-143-3p in right ventricle.....	122
Figure 3.5 Analysis of miR-143 expression in mouse cardiomyocytes and fibroblasts .....	123
Figure 3.6 Analysis of miR-143-3p expression in SU5416/hypoxia rat PH model.....	124
Figure 3.7 <i>In situ</i> hybridization analysis of miR-143-3p expression in hypoxia neonatal calf PH model and brisket disease .....	125
Figure 3.8 Effect of miR-143 knockout on systemic arterial pressure and heart rate .....	127
Figure 3.9 Effect of miR-143 knockout on right ventricular systolic pressure .....	128
Figure 3.10 Effect of miR-143 knockout on right ventricular hypertrophy and pulmonary vascular remodelling.....	129
Figure 3.11 Prevention study of antimiR-143-3p <i>in vivo</i> study design.....	132
Figure 3.12 Analysis of MiR-143-3p expression in lung, PA and RV of antimiR-143-3p prevention study.....	133
Figure 3.13 Quantification of PH indices antimiR-143-3p prevention study .....	135
Figure 3.14 Effect of antimiR-143-3p treatment on the pulmonary vascular remodelling.....	136
Figure 3.15 Reverse study of antimiR-143-3p <i>in vivo</i> study design.....	138
Figure 3.16 Analysis of miR-143-3p expression in lung, PA and RV from antimiR-143-3p prevention study.....	139
Figure 3.17 Quantification of PH indices antimiR-143-3p reversal study .....	140

<b>Figure 3.18 Effect of anti-miR-143-3p reversal study on the pulmonary vascular remodelling.....</b>	<b>141</b>
<b>Figure 3.19 Schematic of experimental normoxic mice model with anti-miR-145-5p administration.....</b>	<b>143</b>
<b>Figure 3.20 Analysis of miR-145-5p lung, PA and RV from anti-miR-145 treated mice .....</b>	<b>144</b>
<b>Figure 3.21 Analysis of target genes expression of the anti-miR-145-5p treated mice .....</b>	<b>145</b>
<b>Figure 3.22 Schematic of experimental mice PH model with anti-miR-145-5p administration.....</b>	<b>147</b>
<b>Figure 3.23 Analysis of target genes expression of miR-145 in lung from the anti-miR-145 intranasal study.....</b>	<b>148</b>
<b>Figure 3.24 Effect of miR-145-5p inhibition on the development of PAH .....</b>	<b>149</b>
<b>Figure 4.1 Analysis of the expression of pri-miR-143 and pri-miR-145 during PASMCMigration <i>in vitro</i> .....</b>	<b>164</b>
<b>Figure 4.2 Analysis of the expression of miR-143/145 lead and passenger strands during PASMCMigration <i>in vitro</i>.....</b>	<b>165</b>
<b>Figure 4.3 Comparative analysis of migration in distal PASMCMigration from healthy donors .....</b>	<b>167</b>
<b>Figure 4.4 Comparative analysis of migration in distal PASMCMigration from HPAH patients .....</b>	<b>168</b>
<b>Figure 4.5 Comparative analysis of migration in distal PASMCMigration from IPAHPatients .....</b>	<b>169</b>
<b>Figure 4.6 Assessment of miR-143-3p overexpression on cell migration in wound healing assay .....</b>	<b>171</b>
<b>Figure 4.7 Assessment of miR-143-3p knockdown on cell migration in wound healing assay.....</b>	<b>172</b>
<b>Figure 4.8 Evaluation of the proliferation of PASMCMigration after transfection with pre-miR-143-3p.....</b>	<b>174</b>
<b>Figure 4.9 Analysis of apoptosis in PASMCMigration with miR-143-3p overexpression and knockdown.....</b>	<b>175</b>
<b>Figure 4.10 Analysis of miR-143-3p expression following induction of DNA damage in PASMCMigration.....</b>	<b>177</b>
<b>Figure 4.11 Analysis of cell-to-cell communication between PASMCMigration and PAECs...179</b>	
<b>Figure 4.12 Analysis the cell-to-cell communications between PASMCMigration and PAECs via miR-143-3p.....</b>	<b>180</b>
<b>Figure 4.13 Analysis cell migration of PAECs in co-culture with PASMCMigration with pre-miR-143-3p transfection .....</b>	<b>182</b>
<b>Figure 4.14 Analysis cell migration of PAECs treated with conditioned medium from PASMCMigration with pre-miR-143-3p transfection.....</b>	<b>183</b>
<b>Figure 4.15 Identification of PASMCMigration-derived exosomes and analysis of miR-143 expression in exosomes.....</b>	<b>185</b>
<b>Figure 4.16 Analysis of miR-143-3p exosomes derived from PASMCMigration with</b>	

pre-miR-143-3p transfection at different concentration .....	186
Figure 4.17 Analysis cell migration of PAECs treated miR-143-3p enriched exosomes derived from PSMCs with pre-miR-143-3p transfection.....	188
Figure 4.18 Analysis cell migration of PAECs with pre-miR-143-3p transfection .....	189
Figure 4.19 Angiogenesis analysis of PAECs with miR-143-3p overexpression via treated with miR-143-3p enriched exosomes and transfected with pre-miR-143-3p.....	190
Figure 4.20 Proliferation analysis of PAECs with miR-143-3p transfection.....	192
Figure 4.21 Apoptosis analysis of PAECs with miR-143-3p overexpression via pre-miR-143-3p transfection and treated with miR-143-3p enriched exosomes .....	193
Figure 4.22 Tracking analysis of cell-to-cell communication between PSMCs and PAECs via Cy3-labeled pre-miR-143-3p.....	195
Figure 4.23 Schematic diagrams to shown the experiments work model.....	197
Figure 4.24 Migration analysis of PAECs with modulation of miR-143-3p expression with transfection and/or miR-143-3p enriched exosome treatment.....	198
Figure 4.25 Validation of miR-143-3p expression in PSMCs and PAECs array samples .....	200
Figure 4.26 Pathway analysis in PSMC by microarray .....	201
Figure 4.27 Pathway analysis in PAEC by microarray .....	202
Figure 4.28 Proposed mechanism of miR-143/145 cluster in PAH.....	216
Figure 5.1 Genomic location of <i>MYOSLID</i> .....	225
Figure 5.2 Analysis of <i>MYOSLID</i> in the cells with hypoxia exposure .....	227
Figure 5.3 Analysis of <i>MYOSLID</i> expression in PSMCs with TGF- $\beta$ and BMP4 stimulation .....	228
Figure 5.4 Analysis of <i>MYOSLID</i> in PSMCs and PAECs with various stimulations .....	229
Figure 5.5 Analysis of <i>MYOSLID</i> in PAH patients .....	230
Figure 5.6 Analysis of <i>MYOSLID</i> in PSMCs during the cell migrations.....	232
Figure 5.7 Analysis of the migration of PSMCs with <i>MYOSLID</i> knock down.....	233
Figure 5.8 Analysis of proliferation and apoptosis of PSMCs with <i>MYOSLID</i> knock down .....	234
Figure 5.9 Analysis of cell migration of PAECs upon <i>MYOSLID</i> knockdown.....	236
Figure 5.10 Analysis of proliferation in PAECs with <i>MYOSLID</i> knocking down.....	237
Figure 5.11 Analysis of BMP pathway components with <i>MYOSLID</i> knockdown .....	239
Figure 5.12 Analysis of BMP pathway components with <i>MYOSLID</i> overexpression.....	240
Figure 5.13 Analysis of <i>BMPR2</i> protein level with <i>MYOSLID</i> knockdown and overexpression.....	241
Figure 5.14 Effect of <i>MYOSLID</i> knockdown on the canonical and non-canonical BMP pathway.....	242
Figure 5.15 Genomic location of <i>Myolnc16</i> .....	243
Figure 5.16 Analysis of <i>Myolnc16</i> expression with inflammatory cytokines stimulation .....	245

<b>Figure 5.17 Analysis of IL-6 expression with <i>Myolnc16</i> knockdown with or without TNF-<math>\alpha</math> stimulation.....</b>	<b>247</b>
<b>Figure 5.18 Analysis of IL-1 and TNF-<math>\alpha</math> expression in PASMCs with <i>Myolnc16</i> knockdown.....</b>	<b>248</b>
<b>Figure 5.19 Analysis of chemokine gene expression in PASMCs with <i>Myolnc16</i> knockdown.....</b>	<b>250</b>
<b>Figure 5.20 Effect of <i>Myolnc16</i> knockdown on ERK1/2 and p38 activation in PASMCs.....</b>	<b>252</b>
<b>Figure 5.21 Effect of <i>Myolnc16</i> knockdown on PASMC cell functions .....</b>	<b>254</b>

# List of Tables

<b>Table 1-1 WHO Classification of Pulmonary Hypertension .....</b>	<b>11</b>
<b>Table 1-2 New York Heart Association/World Health Organization (NYHA/WHO) functional classification of pulmonary hypertension.....</b>	<b>12</b>
<b>Table 1-3 Classification for Drug-and Toxin-Induced PAH .....</b>	<b>12</b>
<b>Table 2-1 Tissue processing for paraffin embedding .....</b>	<b>81</b>
<b>Table 2-2 Patient information for human pulmonary arterial smooth muscle cells....</b>	<b>86</b>
<b>Table 2-3 The siRNA sequences of lncRNA .....</b>	<b>88</b>
<b>Table 2-4 The Click-it reagent components .....</b>	<b>91</b>
<b>Table 2-5 Antibodies used for western blotting .....</b>	<b>97</b>
<b>Table 2-6 MiRNA reverse transcription primers .....</b>	<b>100</b>
<b>Table 4-1 Disease and function annotation relating to migration in the smooth muscle cell gene expression dataset.....</b>	<b>203</b>
<b>Table 4-2 Gene expression data from the ‘migration of cancer cell’ functional annotation relating to migration in the smooth muscle cell gene expression dataset.....</b>	<b>205</b>
<b>Table 4-3 Gene expression data from the ‘cell death and survival’ functional annotation relating to survival in the endothelial cell gene expression dataset.....</b>	<b>206</b>
<b>Table 4-4 Gene expression data from the ‘cell death and survival’ functional annotation relating to survival in the endothelial cell gene expression dataset.....</b>	<b>207</b>

# List of Publications, Presentations and Award

**Deng L**, Bradshaw AC, Baker AH. Role of noncoding RNA in vascular remodelling. *Current Opin Lipidol*. 2016 July 28.

**Deng L\***, Blanco FJ\*, Stevens H, Lu R, Caudrillier A, McBride M, McClure JD, Grant J, Thomas M, Frid M, Stenmark K, White K, Seto AG, Morrell NW, Bradshaw AC, MacLean MR, Baker AH. MicroRNA-143 Activation Regulates Smooth Muscle and Endothelial Cell Crosstalk in Pulmonary Arterial Hypertension. *Circ Res*. 2015 Oct 23; 117 (10): 870-83. (\*joint first author)

Stevens HC, **Deng L**, Grant JS, Pinel K, Thomas M, Morrell NW, MacLean MR, Baker AH, Denby L. Regulation and function of miR-214 in pulmonary arterial hypertension. *Pulm Circ*. 2016 Mar; 6 (1): 109-17.

Ma J, Duffy MR, **Deng L**, Dakin RS, Uil T, Custers J, Kelly SM, McVey JH, Nicklin SA, Baker AH. Manipulating adenovirus hexon hypervariable loops dictates immune neutralisation and coagulation factor X-dependent cell interaction *in vitro* and *in vivo*. *PloS Pathog*. 2015 Feb 6; 11 (2): e 1004673.

## Presentations:

**Deng L**, White K, Stevens HC, Bradshaw AC, Maclean MR, Baker AH. The role of miR-143 in pulmonary arterial hypertension. ECCPS/PVRI Meeting in Bad Nauheim, January 2014. (Poster communication).

**Deng L**, Bradshaw AC, Morrell NW, Miano JM, Long XL, Baker AH. Role of lncRNA MyolncRNA6v1 in human pulmonary artery smooth muscle cell function. Keystone: long noncoding RNA: From evolution to Function. Keystone Resort. Keystone, Colorado USA. March 2015. (Poster communication).

## Award:

Graham Wilson Travelling Scholarship Award, 2015

## Definitions/Abbreviations

3'-UTR	3'-untranslated region
5'-UTR	5'-untranslated region
6-MWD	6-min walking distance
5-HT	Serotonin or 5-hydroxytryptamine
$\alpha$ SMA	$\alpha$ -Smooth muscle actin
ACE	Angiotension Converting Enzyme
Ang II	Angiotensin II
ANOVA	Analysis of variance
AA	Arachidonic acid
Ago2	Argonaute 2
Apo E	Apolipoprotein E
ALK1	Activin receptor-like kinase type 1
$\alpha$ -SMA	Alpha smooth muscle actin
BMP	Bone morphogenetic protein
BMPR1 $\alpha$	Bone morphogenetic protein receptor 1 $\alpha$
BMPR1 $\beta$	Bone morphogenetic protein receptor 1 $\beta$
BMPR2	Bone morphogenetic protein type 2 receptor
BMSC	Bone marrow stromal cell
BSA	Bovine serum albumin
Bcl2	B-cell lymphoma 2
Bcl-xL	B-cell lymphoma extra long
Bp	Base pair
BrdU	Bromodeoxyuridine
CAD	Coronary artery disease
CHX	Cycloheximide
cDNA	Complementary deoxyribonucleic acid
Ct	Cycle threshold
CDKN2A/B	Cyclin dependent kinase inhibitor 2A/B
CLs	Concentric lesions
COX	Cyclo-oxygenase
cGMP	Cyclin guanosine monophosphate
CTEPH	Chronic thromboembolic pulmonary hypertension
CM	Conditioned medium
CXCL	C-X-C motif chemokine
DDR	DNA damage response
DMEM	Dulbecco's Modified Eagle Medium
DEPC	Diethylpyrocarbonate
DIG	Digoxigenin
DNA	Deoxyribonucleic acid
dNTPs	Deoxynucleoside triphosphates
DTT	Dithiothitol

DOCK	Dedicator of cytokinesis
DGCR8	DiGeorge syndrome critical region 8
EC	Endothelial cell
EdU	5-ethynyl-2-deoxyuridine
ET <sub>A</sub> R	Endothelin A receptor
ET <sub>B</sub> R	Endothelin B receptor
ET-1	Endothelin-1
ENG	endoglin
EGFR	Epidermal growth factor receptor
EpCAM	Epithelial cell adhesion molecule
ECG	Electrocardiography
ECM	Extracellular matrix
EGFR	Endothelial growth factor receptor
EGTA	Ethylene glycol tetraacetic acid
eRNAs	Enhancer RNAs
EVs	Extracellular vesicles
ERK1/2	Extracellular signal-regulated kinase 1/2
EDTA	Ethylenediaminetetraacetic acid
FGF2	Fibroblast growth factor 2
FC	Functional classification
EXP5	Exportin-5
FCS	Fetal calf Serum
FDA	Food and Drug Administration
FMOD	Fibromodulin
GAPDH	Glyceraldehyde 3-phosphate dehydrogenase
GC	Golgi complex
HAS2	Hyaluronan synthase 2
HK II	Hexokinase II
HIV	Human immunodeficiency virus
hPAEC	Human pulmonary artery endothelial cell
HPAH	Heritable pulmonary arterial hypertension
HR	Heart rate
HFD	High fat diet
HPV	Hypoxic pulmonary vasoconstriction
HEK293T	Human embryonic kidney 293 T cell
HIF-1 $\alpha$	Hypoxia-inducible factor 1 $\alpha$
HSP90	Heat shock protein 90
HER	Human epidermal growth factor receptor
H <sub>2</sub> O <sub>2</sub>	Hydrogen Peroxide
hPASMC	Human pulmonary artery smooth muscle cell
IPAH	Idiopathic pulmonary arterial hypertension
ILV	Intraluminal vesicles
ID1	Inhibitor of DNA binding-1
ID3	Inhibitor of DNA binding-3

IL-1	Interleukin-1
IL-6	Interleukin-6
IL-10	Interleukin-10
IPF	Idiopathic pulmonary fibrosis
iPSCs	Induced-pluripotent stem cells
ITGB1	Integrin subunit beta 1
ITGB8	Integrin subunit beta 8
IV	Intravenous
IR	Ionizing Radiation
KO	Knockout
KCNK3	Potassium channel subfamily K member 3
KLF-2	Kruppel-like factor 2
KLF4	Kruppel-like factor 4
KLF5	Kruppel-like factor 5
LncRNAs	Long non-coding RNAs
LNA	Locked Nucleic acid
LV+S	Left ventricle plus septum
MCT	Monocrotaline
MAPK	Mitogen activated protein kinase
MEJ	Myoendothelial junction
MHC	Myosin heavy chain
MRI	Magnetic resonance imaging
MSC	Mesenchymal stem cell
mRVP	Mean right ventricular pressure
mTOR	Mammalian target of rapamycin
MMP	Matrix metalloproteinase
MRTF	Myocardin related transcription factor
Myocd	Myocardin
miRNA	Micro ribonucleic acid (MicroRNA)
mM	Milli molar
MVBs	Multivesicular bodies
MPI	Multiple-pathological-insult
mPAP	Mean pulmonary arterial pressure
mRNA	Messenger ribonucleic acid
nM	Nanomolar (nanomoles per litre)
NcRNAs	Non-coding RNAs
NANOG	homeobox protein NANOG
NFAT	Nuclear factor of activated T-cells
NIH	National Institutes of Health
NYHA	New York Heart Association
NTA	Nanoparticle Tracking Analysis
NO	Nitric oxide
nt	Nucleotide
O <sub>2</sub>	Oxygen

OCT4	Octamer-binding transcription factor 4
ORF	Open reading frame
PAWP	Pulmonary artery wedge pressure
PiRNAs	Piwi-interacting RNAs
PARs	Promoter-associated RNAs
PA	Pulmonary artery
PAH	Pulmonary arterial hypertension
PPH	Primary pulmonary hypertension
PPH1	Primary pulmonary hypertension 1
PH	Pulmonary hypertension
PGH2	Prostaglandin H2
PEG2	Prostaglandin E2
PCR	Polymerase chain reaction
PDCD4	Programmed cell death protein 4
PDE-5	Phosphodiesterase type 5
PDGF	Platelet derived growth factor
PFA	Paraformaldehyde
PGI2	Prostacyclin
PPRA- $\alpha$	Peroxisome proliferator-activated receptor receptor alpha
PCNA	Proliferating cell nuclear antigen
PDLIM5	PDZ and LIM domain 5
PMSF	Phenylmethanesulfonylfluoride
PPAR- $\gamma$	Peroxisome proliferator-activated receptor gamma
PTEN	Phosphatase and tensin homologue
PI3K	Phosphoinositide-3-kinase
PBS	Phosphate buffered saline
PVR	pulmonary vascular resistance
Pre-miRNA	Precursor microRNA
Pri-miRNA	Primary microRNA
PDH	Pyruvate dehydrogenase
qRT-PCR	Quantitative real-time polymerase chain reaction
RISC	RNA-induced silencing complex
RHC	Right heart catheterisation
RV	Right ventricle
RV/LV+S	Ratio of right ventricle to left ventricle plus septum
RNA	Ribonucleic acid
RBPs	RNA-binding proteins
RCTs	Randomized controlled trials
RVH	Right ventricular hypertrophy
RVSP	Right ventricular systolic pressure
ROS	Reactive oxygen species
RhoB	Ras homolog family member B
$\gamma$ -H2AX	Gamma H2AX (H2AX phosphorylated at serine 139)
RER	Rough endoplasmic reticulum

RPM	Revolutions Per Minute
RT	Reverse Transcriptase (RT)
SAP	Systemic arterial pressure
SHP2/PTPN11	Tyrosine-protein phosphatase non-receptor type 11
SATB1	SATB homeobox 1
SPRY2	Sprout homolog 2
SDS-PAGE	Sodium dodecyl sulphate polyacrylamide gel electrophoresis
SEM	Standard error of the mean
SOX2	SYR box-containing factor 2
STAT3	Signal transducer and activator of transcription 3
SU5416	Sugen-5416; a VEGF receptor inhibitor
SMC	Smooth muscle cell
SiRNA	Short interfering ribonucleic acid
SRF	Serum response factor
SPI	Single-pathological-insult
SSC	Saline Sodium Citrate
sGC	Soluble guanylate cyclase
TAC	Transverse Aortic Constriction
TBST	Tris Buffered Saline with Tween <sup>®</sup> 20
TNF- $\alpha$	Tumour necrosis factor alpha
TXA2	Thromboxane A2
TRBP	Trans-activating response RNA binding protein
TRPM3	Transient receptor potential melastatin 3
TTCW	Time to clinical worsening
TSS	Transcriptional start site
TLDAs	Taqman low density arrays
TrxG/MLL	Trithorax group/Mixed lineage leukemia
Treg	Regulatory T cell
UV	Ultraviolet
V	Volt
v/v	Volume/volume
VEGF	Vascular endothelial growth factor
VEGFR	Vascular endothelial growth factor receptor
WT	Wild type
WIF1	Wnt inhibitory factor 1
WHO	World Health Organisation
YOD1	YOD1 deubiquitinase

# Abstract

Pulmonary arterial hypertension (PAH) is a progressive disease of the small pulmonary arteries, characterised by pulmonary vascular remodelling due to excessive proliferation and resistance to apoptosis of pulmonary artery endothelial cells (PAECs) and pulmonary artery smooth muscle cells (PASMCs). The increased pulmonary vascular resistance and elevated pulmonary artery pressures result in right heart failure and premature death. Germline mutations of the bone morphogenetic protein receptor-2 (*bmpr2*) gene, a receptor of the transforming growth factor beta (TGF- $\beta$ ) superfamily, account for approximately 75%-80% of the cases of heritable form of PAH (HPAH) and 20% of sporadic cases or idiopathic PAH (IPAH). IPAH patients without known *bmpr2* mutations show reduced expression of *BMPR2*. However only  $\sim 20\%$  of *bmpr2*-mutation carriers will develop the disease, due to an incomplete penetrance, thus the need for a 'second hit' including other genetic and/or environmental factors is accepted. Diagnosis of PAH occurs most frequently when patients have reached an advanced stage of disease. Although modern PAH therapies can markedly improve a patient's symptoms and slow the rate of clinical deterioration, the mortality rate from PAH remains unacceptably high. Therefore, the development of novel therapeutic approaches is required for the treatment of this multifaceted disease.

Noncoding RNAs (ncRNAs) include microRNAs (miRNAs) and long noncoding RNAs (lncRNAs). MiRNAs are  $\sim 22$  nucleotide long and act as negative regulators of gene expression via degradation or translational inhibition of their target mRNAs. Previous studies showed extensive evidence for the role of miRNAs in the development of PAH. LncRNAs are transcribed RNA molecules greater than 200 nucleotides in length. Similar to classical mRNA, lncRNAs are translated by RNA polymerase II and are generally alternatively spliced and polyadenylated. LncRNAs are highly versatile and function to regulate gene expression by diverse mechanisms. Unlike miRNAs, which exhibit well-defined actions in negatively regulating gene expression via the 3'-UTR of mRNAs, lncRNAs play more diverse and unpredictable regulatory roles. Although a number of lncRNAs have been inten-

sively investigated in the cancer field, studies of the role of lncRNAs in vascular diseases such as PAH are still at a very early stage. The aim of this study was to investigate the involvement of specific ncRNAs in the development of PAH using experimental animal models and cell culture.

The first ncRNA we focused on was miR-143, which is up-regulated in the lung and right ventricle tissues of various animal models of PH, as well as in the lungs and PASMCs of PAH patients. We show that genetic ablation of miR-143 is protective against the development of chronic hypoxia induced PH in mice, assessed via measurement of right ventricular systolic pressure (RVSP), right ventricular hypertrophy (RVH) and pulmonary vascular remodelling. We further report that knockdown of miR-143-3p in WT mice via anti-miR-143-3p administration prior to exposure of mice to chronic hypoxia significantly decreases certain indices of PH (RVSP) although no significant changes in RVH and pulmonary vascular remodelling were observed. However, a reversal study using anti-miR-143-3p treatment to modulate miR-143-3p demonstrated a protective effect on RVSP, RVH, and muscularisation of pulmonary arteries in the mouse chronic hypoxia induced PH model.

*In vitro* experiments showed that miR-143-3p overexpression promotes PASMC migration and inhibits PASMC apoptosis, while knockdown miR-143-3p elicits the opposite effect, with no effects observed on cellular proliferation. Interestingly, miR-143-3p-enriched exosomes derived from PASMCs mediated cell-to-cell communication between PASMCs and PAECs, contributing to the pro-migratory and pro-angiogenic phenotype of PAECs that underlies the pathogenesis of PAH.

Previous work has shown that miR-145-5p expression is upregulated in the chronic hypoxia induced mouse model of PH, as well as in PAH patients. Genetic ablation and pharmacological inhibition (subcutaneous injection) of miR-145-5p exert a protective against the development of PAH. In order to explore the potential for alternative, more lung-targeted delivery strategies, miR-145-5p expression was inhibited in WT mice using

intranasal-delivered anti-miR-145-5p both prior to and post exposure to chronic hypoxia. The decreased expression of miR-145-5p in lung showed no beneficial effect on the development of PH compared with control anti-miRNA treated mice exposed to chronic hypoxia. Thus, miR-143-3p modulated both cellular and exosome-mediated responses in pulmonary vascular cells, while the inhibition of miR-143-3p prevented the development of experimental pulmonary hypertension.

We focused on two lncRNAs in this project: Myocardin-induced Smooth Muscle Long noncoding RNA, Inducer of Differentiation (*MYOSLID*) and non-annotated *Myolnc16*, which were identified from RNA sequencing studies in human coronary artery smooth muscle cells (HCASMCs) that overexpress myocardin. *MYOSLID* was significantly increased in PASMCs from patients with IPAH compared to healthy controls and increased in circulating endothelial progenitor cells (EPCs) from *bmpr2* mutant PAH patients. Exposure of PASMCs to hypoxia *in vitro* led to a significant upregulation in *MYOSLID* expression. *MYOSLID* expression was also induced by treatment of PASMC with BMP4, TGF- $\beta$  and PDGF, which are known to be triggers of PAH *in vitro*. Small interfering RNA (siRNA)-mediated knockdown *MYOSLID* inhibited migration and induced cell apoptosis without affecting cell proliferation and upregulated several genes in the BMP pathway including *bmpr1a*, *bmpr2*, *id1*, and *id3*. Modulation of *MYOSLID* also affected expression of *BMPR2* at the protein level. In addition, *MYOSLID* knockdown affected the BMP-Smad and BMP-non-Smad signalling pathways in PASMCs assessed by phosphorylation of Smad1/5/9 and ERK1/2, respectively. In PAECs, *MYOSLID* expression was also induced by hypoxia exposure, VEGF and FGF2 treatment. In addition, *MYOSLID* knockdown significantly decreased the proliferation of PAECs. Thus, *MYOSLID* may be a novel modulator in pulmonary vascular cell functions, likely through the BMP-Smad and –non-Smad pathways.

Treatment of PASMCs with inflammatory cytokines (IL-1 and TNF- $\alpha$ ) significantly induced the expression of *Myolnc16* at a very early time point. Knockdown of *Myolnc16* *in vitro* decreased the expression of *il-6*, and upregulated the expression of *il-1* and *il-8* in

PASMCs. Moreover, the expression levels of chemokines (*cxcl1*, *cxcl6* and *cxcl8*) were significantly decreased with *Myolnc16* knockdown. In addition, *Myolnc16* knockdown decreased the MAP kinase signalling pathway assessed by phosphorylation of ERK1/2 and p38 MAPK and inhibited cell migration and proliferation in PASMCs. Thus, *Myolnc16* may be a novel modulator of PASMCs functions through anti-inflammatory signalling pathways.

In summary, in this thesis we have demonstrated how miR-143-3p plays a protective role in the development of PH both *in vivo* animal models and patients, as well as *in vitro* cell culture. Moreover, we have showed the role of two novel lncRNAs in pulmonary vascular cells. These ncRNAs represent potential novel therapeutic targets for the treatment of PAH with further work addressing to investigate the target genes, and the pathways modulated by these ncRNAs during the development of PAH.

# **1 Introduction**

## **1.1 Pulmonary Circulation**

### **1.1.1 Structure of the Pulmonary Circulation**

The pulmonary circulation carries oxygen-depleted blood away from the heart, to the lungs, and returns oxygenated blood back to the heart. The pulmonary vasculature consists of thin-walled, low-pressure arteries, unlike the thick-walled high-pressure arteries of the systemic vasculature. Under physiological conditions, the pulmonary circulation facilitates the oxygenation of blood in the lungs, where gaseous exchange occurs between the pulmonary capillaries and the air-filled alveolar sacs. The right ventricle of the pulmonary circulation receives mixed venous blood (deoxygenated blood) draining into the right atrium from the systemic circulation via the superior and inferior vena cava. After the deoxygenated blood enters the right ventricle through the tricuspid valve, contraction of the right ventricle forces blood against the tricuspid valve through the pulmonary semilunar valve to enter the pulmonary trunk and its branches, the pulmonary arteries. Upon relaxation of the right ventricle, the pulmonary semilunar valve closes, preventing blood from re-entering the right ventricle. The pulmonary artery originates at the anterior base of the right ventricle, from which it bifurcates to become the *left* and *right* pulmonary artery, which both enter into the lung hilum. The human lungs are divided into five independent lobes, with a lobar fissure separating the lung lobes. The anatomy of the left lung is divided into the left upper (superior) and the left lower (inferior) lobes, separated by the oblique fissure and each received an arterial branch from the left pulmonary artery. In contrast, the right lung is partitioned into the right upper lobe (superior), middle lobe (middle), and the lower lobe (inferior), separated by the oblique and horizontal fissures and each supplied with a branch from the bifurcation of the right pulmonary artery (Ding et al., 2009). Each of these five lobes can be further subdivided into distinct anatomical compartments, which are bronchopulmonary segments. Each of these segments contains segmental bronchi and corresponding pulmonary arterial branch. In addition, each segment is anatomically and functionally distinct. The pulmonary arteries continue branching irregularly but in parallel series with the bronchial tree until the terminal alveoli reach at the periphery of the lung

pleural. Then the oxygenated blood is carried from the lungs to the left atrium via the pulmonary veins. Contraction of the left atrium forces the blood pass through the bicuspid valve into the left ventricle. Further contraction of the left ventricle forces the blood through the aortic semilunar valve into the aorta, and the oxygenated blood is distributed throughout the body via the systemic circulation (Figure 1.1).

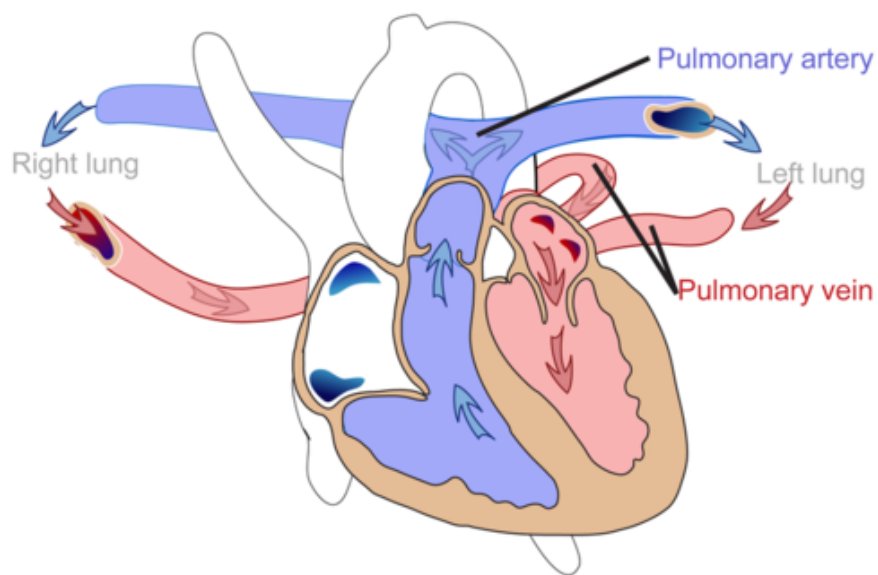


**Figure 1.1 Schematic of the pulmonary circulation**

Deoxygenate blood in the right heart pump into the pulmonary artery and bifurcates into the right and left lung where gaseous exchange takes place. Oxygenated blood is then returned to the left heart via pulmonary vein. With the left ventricle contraction, oxygenated blood is pumped into the aorta and distributed throughout the body. Adapted from (<http://www.freelearningchannel.com/>).

## 1.1.2 Structure of the Pulmonary Vessels

The pulmonary vasculature comprises three anatomic compartments connected in series: the arterial tree, and extensive capillary bed, and the venular tree (Townsend, 2012). A total of 15 orders of arteries were found between the main pulmonary artery and the capillaries in the left lung and a total of 15 orders of veins between the capillaries and the left atrium in the right lung. In convergence, the most peripheral pulmonary arteries (the smallest noncapillary vessels) are termed order 1 vessel. This numbering continues with each proximal branch-point until the large proximal pulmonary vessel, which is defined as order 15. These orders are categorised using the Strahler ordering system, which shows the order 1 arteries have an average diameter of 20  $\mu\text{m}$ , whereas the diameter of order 15 pulmonary arteries is 14.8 mm (Huang et al., 1996). The large proximal elastic arteries of order 15-13 have an internal diameter general  $> 1000 \mu\text{m}$  and are highly compliant with increased elastic laminae in the tunica media to facilitate compliance. The more distal muscular arteries (order 12-4) have a reduction of diameter between 100 to 1000  $\mu\text{m}$  and progressively lose their compliance with continual branching due to the increased smooth muscle and decreased elastic laminae in the tunica media. These pulmonary arteries are important in the blood pressure regulation as these vessels characterised with increased presence of medial smooth muscle. The most distal pulmonary arteries (order 3-1) are less than 100  $\mu\text{m}$  in diameter and characterised with non-muscular pre-capillary arteries that medial smooth muscle is completely diminished. These pulmonary vessels are extremely thin-walled composed of endothelial cells and pericytes (undifferentiated smooth muscle cells) to facilitate the blood-gas exchange.

The adult human lung contains approximately 300 million alveoli, each of which made up of approximately 1000 capillary segments with the entire network connecting to 300 million arterioles and venules. That it approximately 85-95% of alveolar surface is intertwined with pulmonary capillaries, with 280 billion capillaries supplying 300 million alveoli. Each capillary has an internal diameter less than 10  $\mu\text{m}$  and supplies blood to several alveoli. Thus, the pulmonary capillary bed is a huge reservoir with a large surface area about 125

m<sup>2</sup> and the gas exchange surface is very thin (0.2 - 0.5 µm), which efficiently facilitates the blood oxygenation. The exchange of oxygen from the alveolus into the pulmonary capillary blood occurs rapidly with the pressures equalizing in the two areas in 0.25 second. And the blood requires 0.75 second to move through the pulmonary capillary bed under resting conditions.

### **1.1.3 Function of the Pulmonary Circulation**

In the pulmonary circulation, the left and right sides of the heart operate in series, that is, blood flows sequentially from the left heart to the right heart and back to the left heart. Thus, in the steady state, the cardiac output of the right ventricle (pulmonary blood flow) equals the cardiac output of the left ventricle. The cardiac output increases from the resting value of approximately 5 litres per minute and can reach 25 litres per minute (or even 35 litres per minute in elite athletes). The primary function of the pulmonary circulation is to facilitate the oxygenation of the deoxygenated blood arriving from the systemic circulation by close contact with the alveoli to all gas exchange (Comroe, 1966). After the deoxygenated blood arriving from the systemic circulation, which is oxygenated by the rapid unloading of excess CO<sub>2</sub> and subsequent binding of O<sub>2</sub> molecules to haemoglobin that resides within the red blood cells. The protein haemoglobin is molecule that is responsible for carrying almost all the oxygen in the blood. It is composed of four subunits, each with a heme group plus a globin chain (Pittman, 2011). This CO<sub>2</sub>/O<sub>2</sub> exchange within the lung produces the re-oxygenation blood, which is vital to maintain the metabolic throughout the body.

Apart from the gas exchange function, the pulmonary circulation also participates other important non-respiratory functions. The pulmonary circulation is proposed to function as a blood reservoir. The pulmonary vessels normally contain about 600ml of blood and most of this is in readily distensible vessels. This blood and the blood in the left atrium together serve as a reservoir that supplies blood to fill the left ventricle and maintain the cardiac output (Comroe, 1966). Another function is served as blood filter and physical barrier,

which can filter and prevent the passage of inhaled foreign bodies from the respiratory system to the cardiovascular system and dissipation of small emboli by pulmonary endothelium, fibrinolysis, and absorption of air emboli. In addition, the pulmonary circulation also can mediate the metabolic activity, which can activation/inactivation of vasoactive substances such as prostacyclin and nitric oxide synthesised and released from pulmonary arterial endothelial cells.

#### **1.1.4 Control of the Pulmonary Circulation**

As mentioned above, the pulmonary circulation is a low pressure, low resistance, highly compliant circulation and pulmonary vessels are thinner walled and have less smooth muscle and elastic components compared with the systemic counterparts. Especially for the pulmonary capillaries, which are exceptionally thin walled (Kilner, 2004). As a consequence, the pulmonary arterial pressure (PAP) is typically 24/9 mmHg (systolic/diastolic), which is significantly lower than the systemic arterial pressure (SAP) that is typically 120/80 mmHg) Thus, the mean pulmonary arterial pressure (mPAP) for a healthy adult is 10-20 mmHg, whereas mean systemic arterial pressure is 70-105 mmHg. Similarly, the cardiac output is pumped through the pulmonary circulation at a much lower pressure than through the systemic circulation. The 10 mmHg pressure gradient across the pulmonary circulation drives the same blood flow as the pressure gradient almost 100mmHg in the systemic circulation.

#### **1.1.5 Pulmonary Vascular Resistance**

Pulmonary vascular resistance (PVR) is defined as the total peripheral resistance which must be overcome to maintain continuous blood flow through the pulmonary arteries. The PVR is mainly related to the geometry of small distal resistive pulmonary arterioles. According to the Poiseuille's law, PVR is inversely related to the fourth power of arterial radius, which indicates that even small changes in lumen diameter are likely to significantly result in large changes in PVR. Thus, PVR is considered to mainly reflect the functional status of pulmonary vascular /smooth muscle cell coupled system. PVR is also posi-

tively related to blood viscosity and may be influenced by changes in perivascular alveolar and pleural pressure (Chemla et al., 2002). Intimal thickening due to the vascular remodeling of the pulmonary vascular wall results in an irreversible reduction of lumen diameter and consequently results in sustained increases in PAP.

## 1.2 Pulmonary arterial hypertension

### 1.2.1 Classification

Primary pulmonary hypertension (PPH) was first described by Dresdale et al. in 1951, when a clinical description together with cardiac catheterization data was published (Dresdale et al., 1951). The first classification of pulmonary hypertension (PH) was proposed in 1973 at an international conference on PPH endorsed by the World Health Organisation. At that time, PH was classified into two categories: primary pulmonary hypertension (PPH) or secondary pulmonary hypertension, depending on the presence or absence of identifiable causes or risk factors (1973). The 2<sup>nd</sup> World Symposium on Pulmonary Arterial Hypertension (PAH) was held in Evian, France in 1998. The aim of the “Evian classification” was to individualise different categories of PH sharing similarities in pathophysiological mechanisms, clinical features, and therapeutic options and management (Galie et al., 2015, Galie et al., 2009b). Five groups of disorders that cause PH were identified: pulmonary arterial hypertension (Group 1); pulmonary hypertension due to left heart disease (Group 2); pulmonary hypertension due to chronic lung disease and/or hypoxia (Group 3); chronic thromboembolic pulmonary hypertension (Group 4); and pulmonary hypertension due to unclear multifactorial mechanisms (Group 5). Such a clinical classification allowed investigators to conduct clinical trials in a well-defined group of patients with a shared underlying pathogenesis.

The 3<sup>rd</sup> World Symposium on PAH was held in Venice, Italy in 2003. At this conference, the most notable change was to abandon the term PPH in favour of idiopathic pulmonary arterial hypertension (IPAH), familial PAH if there is a family history of PAH; or associated PAH if another cause (Simonneau et al., 2004). The 4<sup>th</sup> World Symposium on PAH was held in Dana Point, California in 2008. The modifications adopted in this meeting mainly concerned Group 1 PAH, which included patients with PAH and a family history of disease, or patients with idiopathic PAH possessing germline mutations (e.g., mutations in the genes encoding bone morphogenetic protein receptor-2 (*bmpr2*), activin receptor-like ki-

nase type 1 (*alk1*) and/or endoglin (*eng*) (Simonneau et al., 2009). The 5<sup>th</sup> World Symposium was held in 2013 in Nice, France. The consensus of this meeting was to maintain the general disposition of previous clinical classification, albeit with some modifications and updates especially for Group 1 PAH. It was also decided in agreement with the Task Force on Paediatric PH to add some specific items relating to paediatric PH, in order to have a comprehensive classification common for adults and children. The most up-to-date classification of pulmonary hypertension is listed in (Table 1-1) (Galie and Simonneau, 2013).

Despite well-defined groups of PAH; functional classification (FC) is widely used as marker of disease severity in pulmonary hypertension and is strongly predictive of mortality (Bennett et al., 2002). The published treatment guidelines include functional classification in their recommendations for the evaluation and treatment of patients with PAH (Galie et al., 2009b, Rubin and American College of Chest, 2004), based on the severity of the symptoms and the patient's ability performing physical tasks. PAH patients can be further categorised into groups according to severity using the New York Heart Association/World Health Organisation (NYHA/WHO) functional classification system (Table 1-3). This classification is based on the physical limitations imposed on the patients, with four different stages from early stage Class 1 and the late stage Class 4 (patients with right heart failure). The NYHA/WHO classification is a very powerful predictor of survival in PH patients (Benza et al., 2010). For example, in untreated patients with IPAH or HPAH, median survival was six months for patients with NYHA/WHO FC IV, two and a half years for NYHA/WHO FC 3 and six years for NYHA/WHO FC1 and FC 2. In addition, FC is also an important endpoint in clinical trials of PAH therapy as the therapeutic changes can be easily measured and assessed within three months of therapy and are predictive of mortality (D'Alonzo et al., 1991).

The focus of this project is Group 1 PAH, which is divided into disease subgroups that include idiopathic PAH (IPAH), heritable PAH (HPAH, formerly familial PAH) and PAH associated with a variety of other systemic diseases or drug/toxin exposures (Austin and Loyd, 2014). IPAH describes a sporadic disease with neither a family history of PAH nor

an identified risk factor. HPAH is diagnosed in those patients with two or more family members presenting with disease, as well as in those patients without family history found to have genetic mutations in genes known to be associated with PAH (McLaughlin and McGoon, 2006). Germline mutations in the bone morphogenetic protein receptor type 2 (*bmpr2*) gene, as well as genes encoding a number of transforming growth factor- $\beta$  (TGF- $\beta$ ) signalling pathway members can be identified in ~80% of families with multiple cases of PAH. In addition, about 5% patients with PAH have rare mutations in other genes belonging to the TGF- $\beta$  super family including activin-like receptor 1 (*alk1*), endoglin (*eng*), and mothers against decapentaplegic homolog 9 (*Smad9*) (Simonneau et al., 2013). Recently, two new PAH-associated genes have been identified; caveolin-1 (*cav-1*), a membrane protein present in caveolae that is abundant in the endothelial cells of the lung, and *kcnk3*, a gene encoding potassium channel super family K member-3. However, there are still approximately 20% of patients with no detectable mutations genes are currently known to be associated with PAH (Austin and Loyd, 2014). In addition, a number of drugs and toxins have been demonstrated as risk factors for the development of PAH, which were categorised in (Table 1-3).

**Table 1-1 WHO Classification of Pulmonary Hypertension**

Reproduced from (Simonneau et al., 2013).

---

<b>1 Pulmonary arterial hypertension</b>
1.1 Idiopathic PAH
1.2 Heritable PAH
1.2.1 BMPR2
1.2.2 ALK1, ENG, SMAD9, CAV1, KCNK3
1.2.3 Unknown
1.3 Drug and toxin induced
1.4 Associated with:
1.4.1 Connective tissue disease
1.4.2 Portal hypertension
1.4.3 HIV infection
1.4.4 Congenital heart diseases
1.4.5 Schistosomiasis
1' Pulmonary veno-occlusive disease and/or pulmonary capillary hemangiomatosis
1'' Persistent pulmonary hypertension of the newborn (PPHN)

---

<b>2 Pulmonary hypertension due to left heart disease</b>
2.1 Left ventricular systolic dysfunction
2.2 Left ventricular diastolic dysfunction
2.3 Valvular disease
2.4 Congenital/acquired left heart inflow/outflow tract obstruction and congenital Cardiomyopathies

---

<b>3 Pulmonary hypertension due to lung diseases and /or hypoxia</b>
3.1 Chronic obstructive pulmonary disease
3.2 Interstitial lung disease
3.3 Other pulmonary diseases with mixed restrictive and obstructive pattern
3.4 Sleep-disordered breathing
3.5 Alveolar hypoventilation disorders
3.6 Chronic exposure to high altitude
3.7 Developmental lung diseases

---

<b>4 Chronic thromboembolic pulmonary hypertension</b>
--

---

<b>5 Pulmonary hypertension with unclear multifactorial mechanisms</b>
5.1 Hematologic disorders: chronic hemolytic anemia, myeloproliferative disorders, splenectomy
5.2 Systemic disorders: sarcoidosis, pulmonary histiocytosis, lymphangioliomyomatosis
5.3 Metabolic disorders: glycogen storage disease, Gaucher disease, thyroid disorders
5.4 Others: tumoral obstruction, fibrosing mediastinitis, chronic renal failure, segmental PH

---

**Table 1-2 New York Heart Association/World Health Organization (NYHA/WHO) functional classification of pulmonary hypertension**

<b>Class</b>	<b>Description</b>
1	Patients with pulmonary hypertension but without resulting limitation of physical activity. Ordinary physical activity does not cause undue dyspnea or fatigue, chest pain or near syncope.
2	Patients with pulmonary hypertension with slight limitation of physical activity. They are comfortable at rest. Ordinary physical activity causes undue dyspnea or fatigue, chest pain or near syncope.
3	Patients with pulmonary hypertension with marked limitation of physical activity. They are comfortable at rest. Less than ordinary physical activity causes undue dyspnea or fatigue, chest pain or near syncope.
4	Patients with pulmonary hypertension with inability to carry out any physical activity without symptoms. These patients manifest signs of right heart failure. Dyspnea and/or fatigue may even be present at rest. Discomfort is increased by any physical activity.

**Table 1-3 Classification for Drug-and Toxin-Induced PAH**

Reproduced from (Simonneau et al., 2013)

<b>Definite</b>	<b>Possible</b>
Aminorex	Cocaine
Fenfluramine	Phenylpropanolamine
Dexfenfluramine	St. John's wort
Toxic rapeseed oil	Chemotherapeutic agents
Benfluorex	Interferon $\alpha$ and $\beta$
SSRIs	Amphetamine-like drugs
<b>Likely</b>	<b>Unlikely</b>
Amphetamines	Oral contraceptives
L-Tryptophan	Estrogen
Methamphetamines	Cigarette smoking
Dasatinib	

### **1.2.2 Clinical Definition and Diagnosis**

PH is a rare, progressive disease characterised by vasoconstriction and remodelling of the pulmonary vasculature and a rise in right ventricular pressure, resulting in right heart failure and eventual death. PH is currently defined by a mean pulmonary artery pressure (mPAP) of  $> 25$  mmHg at rest measured by right heart catheterisation (RHC). Due to the insufficient evidence of exercise conditions, an exercise criterion to the PH definition is excluded. PH is also characterised hemodynamically by the presence of pre-capillary PH, including an end-expiratory pulmonary artery wedge pressure (PAWP)  $< 15$  mmHg and a pulmonary vascular resistance  $> 3$  Wood units (Hoeper et al., 2013).

In the early phases of the disease, PH may be asymptomatic. Patients usually present with dyspnea exacerbated by exertion, fatigue, chest pain, and palpitations. These symptoms are ambiguous and not specific, which often lead to delays in the diagnosis of PH. The differential diagnosis includes congestive heart failure, coronary artery disease, pulmonary embolism, and chronic obstructive pulmonary disease. PH patients in advanced stages of the disease may exhibit clinically evident right-sided heart failure, dizziness, syncope, edema, or cyanosis (Stringham and Shah, 2010). Due to the classifications of PH, the diagnosis of disease needs a series of investigations to confirm the diagnosis and establish the cause of PH and determine the severity. A detailed patient history, thorough physical examination, and a high index of suspicion are essential to diagnosing PH. Other investigations include laboratory tests (blood tests), chest radiography, electrocardiography (ECG), echocardiography, pulmonary function tests, lung scintigraphy, computed tomography scans, cardiac magnetic resonance imaging (MRI), positron emission tomography scanning, vasodilator testing, assessment of ventriculoarterial coupling, and right heart catheterisation (RHC) (Rich and Rich, 2014).

### **1.2.3 Epidemiology of Pulmonary Arterial Hypertension**

PAH is a rare disease, with an estimated worldwide prevalence ranging from 10 to 52 cases per million of population (Peacock et al., 2007). In the United Kingdom (UK.) and Ireland registry, the incidence is between 2001 and 2009 was shown to be 1.1 per million per annum (Ling et al., 2012). A US National Institutes of Health (NIH) registry study conducted in the 1980s showed that IPAH patients were typically diagnosed in young adults with a mean age of  $36\pm 15$  years (Rich et al., 1987). Data from the PH registry of the UK and Ireland in 2001-2009 found that 26% of patients were aged 51-65 years and 23% were aged > 65 years (Ling et al., 2012). A recent audit of PAH patient in the UK from 2013, similar to previous audits in 2010-2012 reported that 21% of PAH patients were in the 60-69 years' age bracket. In general, registry data show a greater incidence of PAH in female patients, with approximately 70-80% female PAH patients in most registries. This strong gender bias has increased since the 1980s, when the NIH registry in the US showed that 63% of PAH patients were female (Rich et al., 1987). The recent five-year outcomes of patients enrolled in the Registry to Evaluate Early and Long-term PAH Disease Management (REVEAL Registry) showed that female patients account for 79.4% of the registry membership (the female: male ratio is 3.9:1.0). The female: male ratio is variable when evaluated by functional classes (FCs) including FC 1 (2.9:1.0), FC 2 (3.4:1.0), FC 3 (4.6:1.0), and FC 4 (4.2:1.0) (Farber et al., 2015). The underlying reasons for this variance in female/male ratio across functional class include several factors such as geography, age and aetiology.

Analysis study characterises the 5-year survival in the United States of a cohort included 2039 previously diagnosed and 710 newly diagnosed patients stratified by baseline functional class (FC). Observes survival rates in the PAH patients at 1, 3, and 5 years were 90.4%, 76.2%, and 65.4% respectively; in newly diagnosed patients, survival rate were 86.3%, 69.3, and 61.2% respectively. In according to the function classification (FC), previous diagnosed patients in FC 1, 2, 3, and 4 had an estimated 5-year survival rate of 88.0%, 75.7%, 57.0%, and 27.2%, respectively, compared with 72.2%, 71.7%, 60%, and

43.8% for newly diagnosed patients in FC 1, 2, 3, and 4, respectively (14). In addition, the UK and Ireland registry described a 1-, 3-, and 5-year survival of 92.7%, 73.3%, and 61.1% respectively (Ling et al., 2012).

#### **1.2.4 BMPR2 Mutations in PAH**

PAH is a disease with an underlying genetic susceptibility. Cases of HPAH occur due to mutations in PAH predisposing genes, most frequently with autosomal dominant modes of inheritance. This accounts for the familial distribution of HPAH, as each child of an affected individual is at a 50% risk of inheriting the mutant allele (Thompson and McRae, 1970). The first report of linkage in HPAH showed the disease locus was mapped to a 27-cM region on chromosome 2q31-q32, and was termed primary pulmonary hypertension 1 (*pph1*) (Morse et al., 1997). Subsequent studies identified that HPAH can be caused by mutations in the bone morphogenetic protein type II receptor gene (*bmpr2*), a serine/threonine kinase which binds a specific subset of the TGF- $\beta$  superfamily of ligands (International et al., 2000). We now know that *bmpr2* mutations are responsible for the majority of HPAH cases (80%) and for a significantly subset of sporadic PAH patients (Austin et al., 2013, Fessel et al., 2011, Morrell, 2010). There are over 300 different *bmpr2* mutations have been identified (Evans et al., 2016). The *bmpr2* gene is located on chromosome 2q33 and contains 13 exons. Exons 1-3 encode an extracellular domain, exon 4 encodes the transmembrane domain, exons 5-11 encode a serine/threonine kinase domain, and exons 12 and 13 encode a very large intracellular C-terminus (Newman et al., 2004) (Figure 1.2). In normal lung vasculature, *bmpr2* is predominantly localised to the vascular endothelium, with much lower levels of expression in vascular smooth muscle and fibroblasts (Atkinson et al., 2002). The expression of *bmpr2* is decreased in the pulmonary vasculature of *bmpr2* mutant HPAH patients as well as in IPAH patients without *bmpr2* mutation, suggesting the important role of *bmpr2* in the pathogenesis of PAH (Morrell, 2010, Evans et al., 2016). The average penetrance of *bmpr2* pathogenic variants is very low, with approximately 20% overall penetrance, and is sex dependent. For example, the lifetime risk of developing HPAH with a *bmpr2* pathogenic variation in males is 14%, whereas in a

female is 42% (Austin and Loyd, 2013). Therefore, it is suggested that additional genetic or environmental factors are involved in the pathogenesis of HPAH.

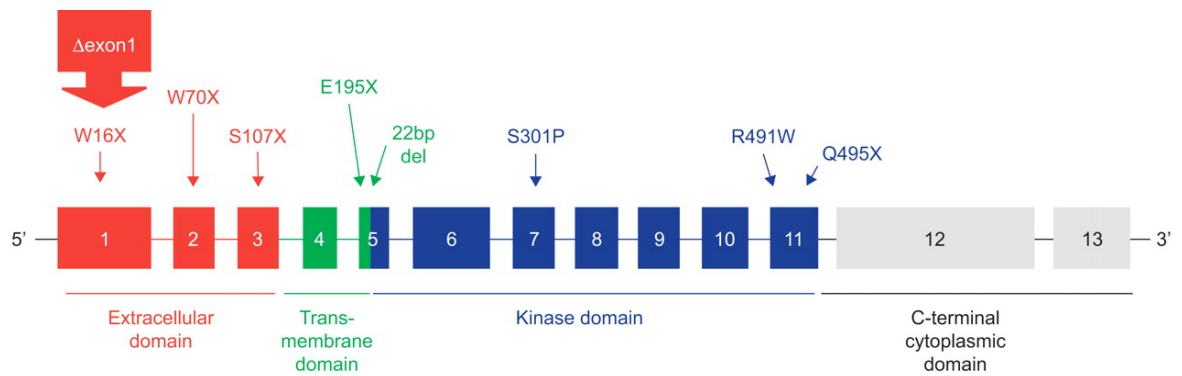


**Figure 1.2 Schematic representation of *bmpr2* functional domains**

Genetic characteristics of patients with PAH demonstrated the range of *bmpr-2* mutations and indicated the nature of amino acid substitution or nonsense mutations (X). Adapted from (Dewachter et al., 2009)

### 1.2.5 Pathobiology of Pulmonary Arterial Hypertension

PAH has a multifactorial pathobiology. Vasoconstriction, remodelling of the pulmonary vessel wall, and thrombosis contribute to increased pulmonary vascular resistance in PAH (Rubin, 1995). The pulmonary vascular remodelling process involves all layers (adventitia, media, and intima) of the pulmonary vessel wall and is complicated by cellular heterogeneity within each cellular compartment of the vessel wall (Jeffery and Morrell, 2002).

All pulmonary vascular cell types (endothelial cell (ECs), smooth muscle cells (SMCs), fibroblasts), as well as inflammatory cells and platelets contribute to the pathogenesis of PAH (Hassoun et al., 2009, Morrell et al., 2009, Humbert et al., 2004b). Pulmonary vasoconstrictions, initiated by hypoxia, elevations in cytoplasmic  $Ca^{2+}$  or decreased voltage-gated  $K^+$  channel depolarisation, are believed to be an early initiation factor of the pulmonary hypertensive process (Mandegar et al., 2004). Excessive and sustained eleva-

tion of vasoconstriction is related to endothelial dysfunction, which further leads to medial hypertrophy, a central aspect of pulmonary vascular remodelling. Indeed, it is widely recognised that the hallmarks of PAH are sustained vasoconstriction and vascular remodelling, leading to a progressive increase in pulmonary artery pressure (Shimoda and Laurie, 2013). PAH often leads to right heart failure, the primary cause of mortality in patients with PAH, although in the early stages of the disease there is a compensatory increase in right ventricular hypertrophy (Zangiabadi et al., 2014). There are several specific signalling pathways known to regulate pulmonary vasoconstriction and remodelling in PAH including bone morphogenetic proteins (BMPs)/transforming growth factor- $\beta$  (TGF- $\beta$ ) pathways (Long et al., 2009, Zaiman et al., 2008), endothelin-1 (ET-1), nitric oxide (NO), and prostacyclin (PGI<sub>2</sub>) pathways (Humbert et al., 2004c). The identification and pharmacological targeting of these signalling pathways are considered as the therapeutic strategies for diseased treatment of PAH.

#### **1.2.5.1 Vasoconstriction**

Vasoconstriction of the small pulmonary arteries is an essential initiating factor in the pathogenesis of PAH. Vasoconstriction represents an early and potentially reversible stage in the development of PAH when it occurs without complications such as microthrombosis and pulmonary vascular remodelling (Mandegar et al., 2004). Hypoxic pulmonary vasoconstriction, or HPV, is a physiological response to alveolar hypoxia that distributes pulmonary capillary blood flow to alveolar areas of high oxygen partial pressure. HPV is caused by hypoxia-driven decreases in the expression of potassium channel proteins, which result in PASMC membrane depolarisation and subsequent induction of calcium influx and calcium release from intracellular stores, leading to smooth muscle cell contraction (Sommer et al., 2008, Arrigo and Huber, 2013). The sustained vasoconstriction induced in the early stages of PAH leads to endothelial cell dysfunction alongside impaired production of vasodilators including prostacyclin, and nitric oxide (NO), and increased synthesis of vasoconstrictors such as endothelin-1 (ET-1) (Lai et al., 2014), all of these three pathways are involved in the development and progression of PAH (Humbert et al.,

2004c). These three mediators act to regulate the diameter of the pulmonary vessel by further reducing vasodilatation (NO and prostacyclin) or by exacerbating hypoxia-induced vasoconstriction (ET-1) (Chester and Yacoub, 2014). Under physiological conditions, all these mediators maintain pulmonary vascular tone at an optimal level. In PAH disease, the profile of endothelium-released vasoactive factors is dysregulated, with reduced production of vasodilator agents NO and prostacyclin (Ghofrani et al., 2002, McLaughlin and McGoon, 2006, Mitchell et al., 2008). In addition, NO and prostacyclin also exert an inhibitory effect on the regulation of smooth muscle cell proliferation and platelet activation (Mitchell et al., 2008).

### **1.2.5.1 Pulmonary Vascular Remodelling**

PAH is associated with structural and mechanical changes in the pulmonary vascular bed that increase the right ventricular afterload, leading to narrowing and stiffening of both proximal and distal pulmonary arteries. PAEC apoptosis occurs in the early stages of the vascular remodelling process results in the selection of an apoptosis-resistant, proliferation and phenotypically altered EC phenotype and the damage of EC may stimulate PSMCs phenotype change due to the exposure to the circulating mitogenic factors (Sakao et al., 2009, Sakao et al., 2005). It is widely recognised that the hallmarks of PAH are sustained vasoconstriction and pulmonary vascular remodelling (Stacher et al., 2012). PAH is characterised primarily by increase in proliferation, migration, resistance to apoptosis, and glycolytic metabolism in pulmonary artery smooth muscle, fibroblasts, and endothelial cells (Archer et al., 2010). Remodelling might involve both arterial and venous components of the pulmonary vascular bed: especially in small distal pulmonary arteries (Dorfmuller et al., 2010). Typically, a transverse section of a remodelled pulmonary artery reveals neointimal thickening and fibrosis, smooth muscle hypertrophy arising from PSMC hyperplasia and adventitial thickening and/or fibrosis (Figure 1.3).

There are several histopathological subtypes observed in the pulmonary vascular remodelling in human patients with PAH (Cool et al., 2005). Hyperplasia and thickening of smooth

muscle, adventitial fibrosis, and increased medial thickness occur in most form of mild/moderate-stage PAH, which leads to occlusion and eventual loss of small pulmonary arteries and results in reduced perfusion of the lung (Moledina et al., 2011, Humbert et al., 2004b). In addition to affect the distal pulmonary arteries, pulmonary vascular remodelling also affects the large proximal pulmonary artery. Medial and adventitial hypertrophy occurs in the large proximal leads to the loss of pulmonary vascular compliance and proximal pulmonary artery stiffening, which can predict mortality in patients with PAH (Tian and Chesler, 2012). In severe/end-stage PAH, plexiform lesions are usually observed in the most severe subtype of pulmonary vascular remodelling. The plexiform lesion is a focal proliferation of endothelial channels lined by myofibroblasts, SMCs, and connective tissue matrix, which represent an extreme example of pulmonary vascular remodelling usually observed in severe patients with PAH (Pietra et al., 2004). These lesions are most commonly formed just distal to the bifurcation site of small pulmonary arteries (approximately 50 to 300  $\mu\text{m}$ ) (Tuder et al., 1994). Fibrin thrombi and platelets are frequently present in the plexiform lesions (Pietra et al., 2004). The endothelial cells within the plexiform lesions express high levels of vascular endothelium growth factor (VEGF) and VEGF receptor (Cool et al., 1999), key regulators of endothelial angiogenesis, as well as the cell adhesion molecule CD44. The cell adhesion molecule CD44 have been demonstrated involved in angiogenesis, endothelial cell proliferation and migration (Ohta-Ogo et al., 2012). Thus, the disordered angiogenesis, proliferation and migration of endothelial cells are believed to contribute to the plexiform lesions formation.

The presence of inflammatory cells in the surrounding area of plexiform lesions composed of T cells, B cells and macrophages also are thought to be involved in the development of the plexiform lesion (Tuder et al., 1994). The consequence of plexiform lesion formation is the complete obliteration of the distal small pulmonary arteries, resulting in the severe impairment and cessation of the blood flow and leading to increased pulmonary vascular resistance. Targeting the disordered angiogenesis, proliferation, apoptosis, and inflammatory is believed to resulting in inhibition of the pulmonary vascular remodelling process and considered the effective therapeutic strategies in treatment of PAH. For example,

peroxisome proliferator-activated receptor-gamma (*ppar-γ*) has anti-proliferative, pro-apoptotic and anti-inflammatory functions as well as inhibiting angiogenesis (Humbert et al., 2004b, Hassoun et al., 2009, Pullamsetti et al., 2011). The decreased expression of *ppar-γ* is observed in plexiform lesions of patients with PAH (Ameshima et al., 2003) and *PPAR-γ* agonist has shown to mediate a protective role in the experimental PH model (Hansmann et al., 2008).

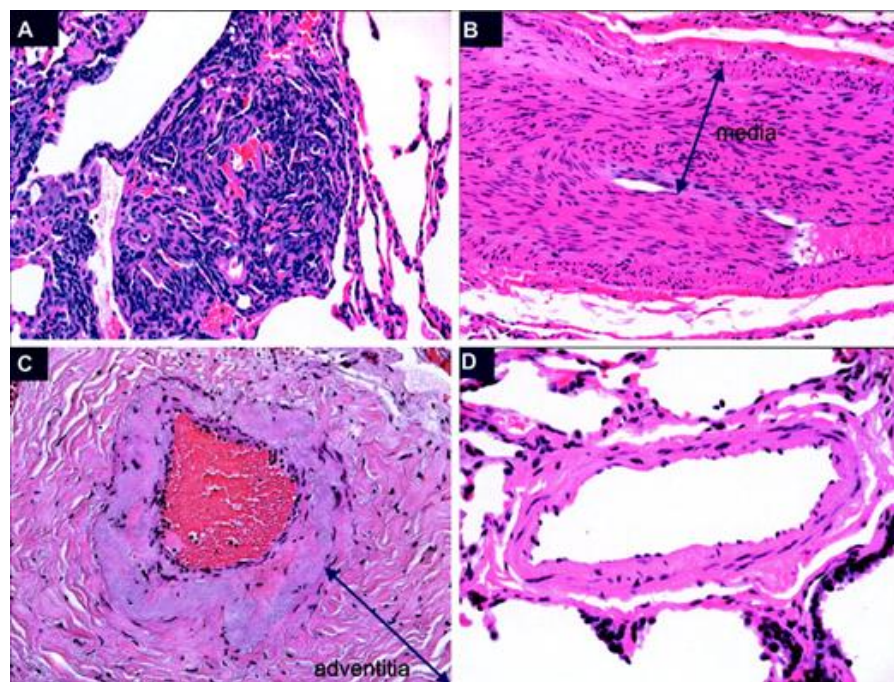


**Figure 1.3 Histopathologically changes observed in pulmonary vascular remodelling in human patients with PAH**

The comparison of the Histopathologically subtypes of PAH. *Top left, A:* plexiform lesion characterised by exuberant proliferation of cells and lumen obliteration. *Top right, B:* Smooth muscle hypertrophy/hyperplasia typically observed in mild/moderate human PAH. *Bottom left, C:* Adventitial fibrosis observed in moderate PAH patients. *Bottom right, D:* a normal pulmonary artery. Adapted from (Cool et al., 2005).

## 1.2.6 Cellular Components of PAH

As illustrated in the previous section, pulmonary endothelial cell (ECs), smooth muscle cells (SMCs), and fibroblasts of the pulmonary vessel wall, as well as platelets and inflammatory cells play an important role in PAH pathogenesis. The interactions including ECs, SMCs, fibroblasts, circulating platelets and inflammatory cells are regulated by several autocrine and paracrine mediators, contributing to the pathophysiologic features of PAH (Hung et al., 2011). Vascular stressors, such as endothelial injury, inflammation, flow/shear stress, and hypoxia can result in constrictive remodelling of the pulmonary vessels, which in PAH primarily affects the small distal pulmonary arteries (Cabali et al., 2011, Pugliese et al., 2015) (Figure 1.4).

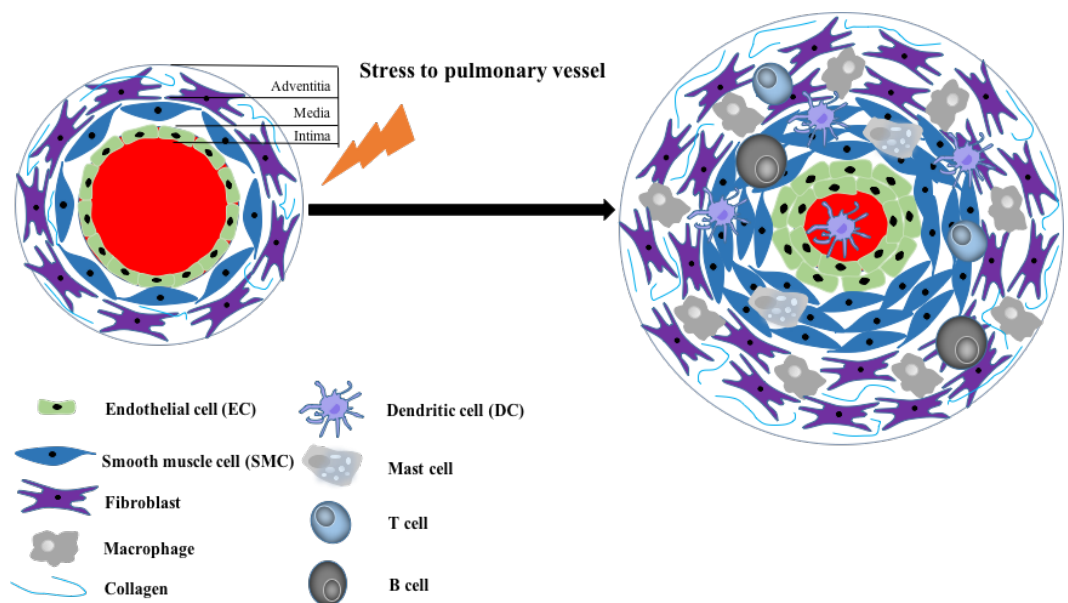


**Figure 1.4 Schematic showing the different cells types involved in pulmonary vascular remodelling**

In PAH, the pulmonary artery undergoes changes to all three layers of the vessel, including adventitial thickening with fibroblast proliferation and inflammatory cells recruitment (macrophages, dendritic cells, mast cells, B cells, and T cells), proliferation, resistance to apoptosis and hypertrophy of pulmonary artery smooth muscle and endothelial cells result in medial and intimal thickening of the pulmonary vessel wall.

### 1.2.6.1 Endothelial Cells

Endothelial cells (ECs) are located in the inner layer of the pulmonary artery wall. Endothelial damage and dysfunction play a key role in the initial event in PAH. The mechanisms underlying these observations are largely unknown, however the insults may include hypoxia, inflammation, viral infection, mechanical stretch or shear stress, and/or aberrant responses to drugs or toxins on a background of genetic susceptibility (Pullamsetti et al., 2011). In severe and end-stage PAH, the formation of ‘plexiform’ vascular lesions is caused by dramatically increased EC proliferation and resistance to apoptosis in response to the initial EC attrition that occurs in the early stages of the disease (Sakao et al., 2009). The bone morphogenetic proteins have showed anti-apoptosis effect in PAECs (Hirose et al., 2000). The impaired BMP signalling due to the loss of function mutations in *bmpr2* leads to increased PAEC apoptosis could explain the loss of PAECs in the early stages of PAH (Teichert-Kuliszewska et al., 2006). In IPAH patients, the apoptosis-resistant ECs exert robust proliferation and migration than the ECs from healthy donors (Masri et al., 2007). Endothelial cells also regulate the vasoconstriction and thrombosis processes through the production and release of several vasodilatory and vasoconstrictory mediators. The imbalance between these vasoactive mediators can lead to dysregulation of vascular tone (Wilkins, 2012). In addition, growth factors released by endothelial cells can modulate SMC proliferation and migration, contributing to the abnormal vascular remodelling process that is the hallmark of PAH. For example, over-production of fibroblast growth factor 2 (FGF2), serotonin, and endothelin-1 (ET-1) by PAECs leads to increased PASMC proliferation, which is a critical component of the abnormal crosstalk between these two cell types contributing to pulmonary vascular remodelling during the progression of PAH (Izikki et al., 2009). The excessive autocrine release of endothelial-derived FGF2 in PAH also contributes to the acquisition and maintenance of an abnormal endothelial phenotype, enhancing proliferation through constitutive activation of ERK1/2 and decreasing apoptosis by increasing B-cell lymphoma 2 (*bcl2*) and B-cell lymphoma extra-long (*bcl-xl*) (Tu et al., 2011). Fluid shear stress decreases the expression of the tumour suppressor gene peroxisome proliferator-activated receptor- $\gamma$  (*ppar-\gamma*) in endothelial cells and that loss of *ppar-\gamma*

expression characterises an abnormal, proliferating, apoptosis-resistant endothelial cell phenotype (Ameshima et al., 2003). This is of particular relevance to PAH, as complex vascular lesions within the lungs of patients with severe PAH show decreased or absent *ppar-γ* expression (Ameshima et al., 2003).

### **1.2.6.2 Smooth Muscle Cells**

Smooth muscle cells (SMCs) located in the medial layer of the vessel wall can present various phenotypes including cell morphology, proliferation and migration rates and the expression of protein markers, which are depending on their functions (Nogueira-Ferreira et al., 2014). For example, elongated cells with slow proliferative and migratory rates typify the contractile SMC phenotype. On the contrary, a rhomboid morphology and higher proliferative and migratory features typify the synthetic phenotype (Hao et al., 2003). The mechanisms involved in the SMC phenotype modulation include pathways/mediators such as the transforming growth factor beta (TGF- $\beta$ ) superfamily, tumour necrosis factor- $\alpha$  (TNF- $\alpha$ ), PDGF platelet-derived growth factor (PDGF), and angiotensin II (Rensen et al., 2007). PASMC derived from PAH patients exhibit a significant resistance to apoptosis inducers such as bone morphogenetic protein 2 (*BMP2*) and bone morphogenetic protein 7 (*BMP7*) (Voelkel and Tuder, 1997) and show more proliferative and increased migration phenotypes, which suggest that increased PASMC proliferation, migration and decreased PASMC apoptosis can concurrently mediate thickening of the pulmonary vasculature, subsequently narrowing the inner-lumen diameter of pulmonary arteries leading to pulmonary vascular resistance increasing (Savai et al., 2014, Voelkel and Tuder, 1997). The distal extension of smooth muscle into non-muscular small peripheral pulmonary arteries resulting in muscularisation of the terminal portion of the pulmonary artery due to the differentiation and hypertrophy of SMC precursor cells and pericytes already present in the vessel wall (Stenmark et al., 2002, Aggarwal et al., 2013). In addition, the medial SMC layer exhibits a variety of changes during PAH pathogenesis, including SMC hypertrophy, SMC hyperplasia and extensive extracellular matrix protein deposition (collagen and elastin). SMC hypertrophy is a predominant feature of larger proximal pulmonary vessels, whereas

the small distal pulmonary vessels undergo hyperplasia (Aggarwal et al., 2013, Stenmark et al., 2006b). Recently study found that bone morphogenic protein-4 (BMP4), TGF- $\beta$ , Serotonin or 5-hydroxytryptamine (5-HT), and ET-1 can induce the PASMC hypertrophy, which showed increased cell size, protein synthesis, and contractile protein expression (Deng et al., 2010). Moreover, PAEC can also directly influence the behaviour of PASMC during PAH pathogenesis, for example by secreting growth factors that stimulate the proliferation of PASMC such as platelet-derived growth factor (PDGF) and FGF2 or by reducing and/or failing to produce factors that suppress PASMC proliferation, such as apelin (Crosswhite and Sun, 2014).

### **1.2.6.3 Fibroblasts**

The adventitia of the vessel wall is predominantly composed of fibroblasts, and undergoes a variety of changes during the development of PAH. The fibroblast populations are heterogeneous within specific tissues including the lung and with significantly diversity populations comprising the pulmonary artery adventitia. This can explain only certain subsets of fibroblasts are in responding to injury and stress (Das et al., 2002). Fibroblasts response to injury and other pathophysiological stimuli through activation of vascular NADPH oxidases, inducing the production of reactive oxygen species (ROS) (Meier et al., 1989). The hypoxia induced ROS generated by pulmonary artery adventitial fibroblasts drives hypoxia induced fibroblast proliferation and can act as paracrine effect on neighbouring SMCs to increase their contraction (Li et al., 2008, Touyz and Schiffrin, 2004). In addition, adventitial fibroblasts in response to ROS or other stimuli are capable of releasing a number of mediators such as ET-1, PDGF, FGF2, and Heat shock protein 90 (HSP-90), which could affect vascular tone. Activated resident fibroblasts are also affecting SMC proliferation and extracellular matrix (ECM) production by releasing cytokines and growth factors (Herrmann et al., 2002, Stenmark et al., 2011). The mechanisms of hypoxia induced adventitial fibroblast proliferation include the activation of G $\alpha$ i and G $\alpha$ q family members and subsequent stimulation of protein kinase C and mitogen-activated protein kinase (MAPK) family members (Das et al., 2001, Das et al., 2000). The activation of phosphatidylinosi-

tol-3-kinase (PI3K), synergistic interactions with Akt mammalian target of rapamycin (mTOR), and p70 ribosomal protein S6 kinase has also been implicated (Gerasimovskaya et al., 2005, Krick et al., 2005).

From the activated adventitial fibroblasts, a subset population of activated fibroblasts can differentiate into a myofibroblast phenotype (Stenmark et al., 2002). Myofibroblasts express  $\alpha$ -Smooth muscle actin ( $\alpha$ -SMA), which is the most common marker for myofibroblast identification (Desmouliere et al., 2005, Phan, 2002). The differentiation of fibroblasts into myofibroblasts is regulated by a variety of factors including growth factors, cytokines, adhesion molecules, and ECM. All these factors including TGF- $\beta$ , thrombin, ET-1, Angiotensin II (Ang-II), and Interleukin-6 (IL-6) can induce the differentiation of fibroblasts into a myofibroblast phenotype and are upregulated by hypoxia stimulation and observed in the pulmonary artery adventitia of chronic hypoxic animals (Stenmark et al., 2002, Gao et al., 2003, Gallucci et al., 2006, Shi-Wen et al., 2004). In addition, hypoxia can stimulate the transition of fibroblast to myofibroblast along with the induction of proliferation of pulmonary artery adventitial fibroblasts (Short et al., 2004). There is early and dramatic increase in the appearance of  $\alpha$ -SMA expressed myofibroblasts in the adventitia in the chronic hypoxia induced PH (Sobin et al., 1983). Myofibroblasts are also the main producers of collagen and other ECM proteins such as fibronectin, tenascin and elastin (Stenmark et al., 2006a). An excessive deposition of ECM proteins was observed in the adventitia in PAH (Durmowicz et al., 1994).

The composition of the adventitial ECM is largely regulated by fibroblasts. The production of ECM is dependent on the stresses or injuries on the fibroblast, which accumulation can have a profound effect on vascular structure and function (Stenmark et al., 2011). In addition to secreting ECM proteins, fibroblasts produce matrix metalloproteinases (MMPs), which allow fibroblasts to move through the adventitial matrix into the media or intima by promoting ECM remodelling (Shi et al., 1999). Taken together, the changes of adventitial fibroblasts in response to vascular stimuli and injuries facilitate fibroblast proliferation, migration, and differentiation, which can affect the vascular function, structure and the

vascular remodelling.

#### **1.2.6.4 Inflammatory Cells**

Inflammatory cells have been demonstrated as major pathogenic components of the pulmonary vascular remodelling (Hassoun et al., 2009). Pulmonary vascular lesions occurring in PAH patients and animal models of PH are characterised by varying degrees of perivascular inflammatory infiltrates, comprising T- and B-lymphocytes, macrophages, dendritic cells and mast cells (Rabinovitch et al., 2014). T cells are increased in pulmonary vasculature in lungs of PAH patients. Cytotoxic CD8<sup>+</sup> T cells constitute the major part of the inflammatory component in plexiform lesions (Savai et al., 2012) and deficiency of cytotoxic CD8<sup>+</sup> T cell in patients is associated with an increased risk of death in PAH patients (Edwards et al., 2013). In addition, decreased regulatory T cell (Treg) function, which can control T-cells and regulate monocytes, macrophages, dendritic cells, natural killer cells, and B cells, may predispose individuals to PAH as well as in animals (Rabinovitch et al., 2014). For example, the failure of Treg control endothelial injury may lead to PAH, which suggest that Treg normally function to limit vascular injury and may protect against the development of PAH (Tamosiuniene et al., 2011).

Increased numbers of macrophages are observed in the plexiform lesions of patient with severe PAH (Gerasimovskaya et al., 2012). Activation of macrophages induced the release of inflammatory cytokines such as Interleukin-1(IL-1), Interleukin-6 (IL-6), TNF- $\alpha$ , and Interleukin-10 (IL-10) which are involved in the pathogenesis of PAH (Stow et al., 2009). Macrophages activation is also linked to epigenetic changes that stimulate and induce proliferation of vascular fibroblasts in patients and in experimental models of PH (Li et al., 2011). Macrophages can secret MMPs, which inappropriate expression is contribute to the pathogenesis of PAH (Brauer, 2006). In addition, mast cell population was shown to be abundantly present in patients with PAH (Dahal et al., 2011). And the activation of mast cell contribute to the vascular remodelling and dysfunction in PAH (Farha et al., 2012). Peripheral blood lymphocyte analysis showed B cells are activated in IPAHA patients, which

have a distinct RNA expression profile of the peripheral blood B-lymphocytes compared to healthy controls (Ulrich et al., 2008).

### **1.2.7 Current Approved Therapeutic Strategies in PAH**

PAH is a complex disease that requires an integrated therapeutic approach involving multiple clinical disciplines. As discussed above there are many cell types and signalling pathways involved in the pathobiology of PAH, and the incomplete understanding of the molecular pathways resulting to the lack of sufficient treatment strategies. Over the past decade, recent advances in the understanding of the mechanisms underlying the development of PAH have led to major progress in treatment options for PAH patients. Unfortunately, while modern PAH therapies can markedly improve patient symptoms and slow the rate of clinical deterioration, there is currently no cure for PAH (Galie et al., 2009b, Humbert et al., 2010a). Although the life expectancy for PAH patients is now significantly improved compared to the 1980's, with 5-year mortality rates increasing from 60% in the 1987 NIH registry to 40% in the recent U.K. and Ireland registry (Rich et al., 1987, Ling et al., 2012), the mortality rates remain unacceptably high. Thus there is great rationale to development new therapeutic routes or drugs to reduce pulmonary arterial pressure and decrease the pressure in the right ventricular in order to prevent right ventricular failure, which are the fundamental aims of PA treatment. The current three therapeutically exploited signalling pathways involved in the pathology of PAH are the prostacyclin (also called prostaglandin I<sub>2</sub> (PGI<sub>2</sub>)), endothelin and nitric oxide pathways (Humbert et al., 2004c, Mubarak, 2010, Norel, 2007, Hata and Breyer, 2004, Whittle et al., 2012, Abramovitz et al., 2000, Kuwano et al., 2008, Aronoff et al., 2007, Chen et al., 2013, Ghofrani and Humbert, 2014, Shao et al., 2011, Stitham et al., 2011, Wilson and Giles, 2005, Woodward et al., 2011) (Figure 1.5). Treatments that target these three signalling pathways in PAH have now been approved for clinical use (Galie et al., 2016, Galie et al., 2013), and other novel targets for drug treatment are currently under investigation including guanylate cyclase activators and tyrosine kinase inhibitors (Hu et al., 2015). Currently approved treatments for PAH include prostacyclin analogues and the IP receptor agonist selexipag, which target the

prostacyclin pathway; endothelin receptor antagonists (ERAs), which target the endothelin pathway; and the phosphodiesterase type 5 inhibitors (PDE-5I) and soluble guanylate cyclase stimulators, which target the nitric oxide pathway. The current PAH treatment algorithm, updated following the 5<sup>th</sup> World Symposium on Pulmonary Hypertension, recommends targeting at least one of the three main disease pathways (Galie et al., 2009b, Farber et al., 2013). The evidence provided by longer term randomised controlled trials (RCTs) indicates that specific combination therapies for PAH may provide an effective therapeutic approach for patients (Ghofrani and Humbert, 2014) Thus, combination therapy is now considered an important part of the treatment algorithm for PAH (Ghofrani and Humbert, 2014).

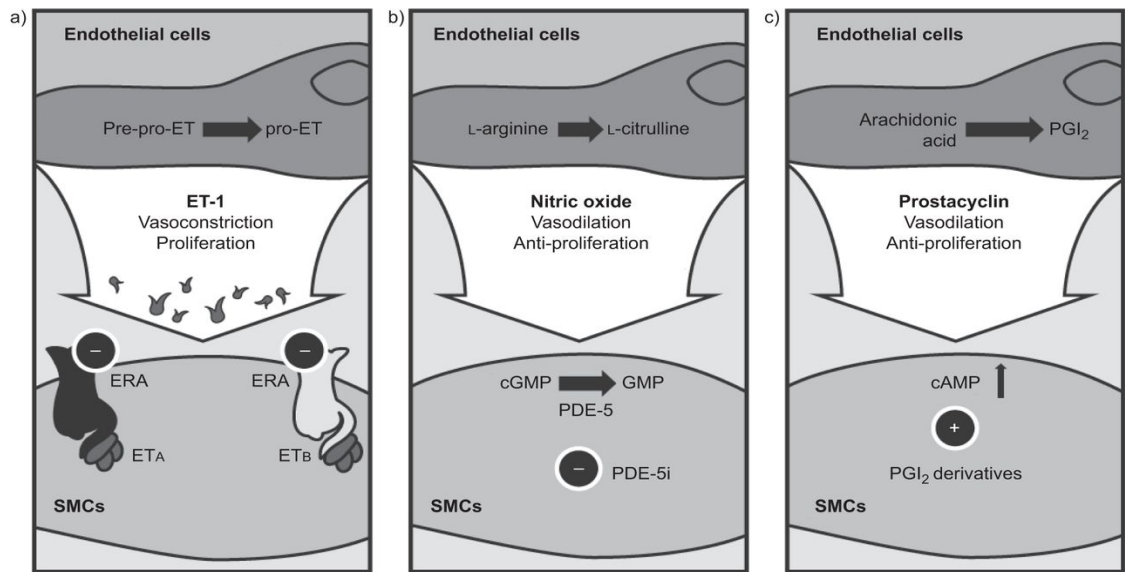


**Figure 1.5 Major pathways approved for current therapies for PAH patients**

Three pathways were targeted for PAH treatment including a) endothelin (ET) (ET receptor antagonists), b) nitric oxide (NO) (phosphodiesterase type-5 inhibitors (PDE-5 inhibitors)), and c) prostacyclin (PGI<sub>2</sub>) (prostacyclin analogues) pathways. Adapted from (Sitbon and Morrell, 2012).

### 1.2.7.1 Prostacyclin Analogues

Prostacyclin is produced primarily by pulmonary artery endothelial cells and is a natural ligand for the prostacyclin IP receptor, which is widely expressed in the vasculature, including in the aorta, coronary arteries, pulmonary arteries, the cerebral arteries, where its expression was confined to smooth muscle cells (Oida et al., 1995, Norel, 2007, Narumiya, 2007). Prostacyclin is synthesised from arachidonic acid (AA) by the concerted actions of the enzymes cyclo-oxygenase (COX) and prostacyclin synthase. AA is liberated by from plasma phospholipids by phospholipase enzymes, and after which it is metabolised to prostaglandin (PGH<sub>2</sub>) by COX. PGH<sub>2</sub> is then further metabolised by prostacyclin synthase to PGI<sub>2</sub>, and by PGE<sub>2</sub> synthases/isomerases to PGE<sub>2</sub> or thromboxane synthase to thromboxane (TXA<sub>2</sub>) (Mitchell et al., 2014). Studies have demonstrated that the PGI<sub>2</sub> pathway has an important role in increasing vasodilation and inhibiting vascular smooth muscle cell proliferation and migration (Sitbon and Morrell, 2012). The activation of the IP receptor by prostacyclin or its analogues also inhibits platelet aggregation (Mubarak, 2010). Conversely, TXA<sub>2</sub> elicits the opposite effect, acting as a potent pulmonary vasoconstrictor and activator of platelet aggregation. An imbalance between these vasoactive prostanoids (prostacyclin and TXA<sub>2</sub>) has been demonstrated in PAH patients (Christman et al., 1992). PAH is associated with reduced urinary markers of prostacyclin and increased marker of thromboxane. Similarly, there is reduced prostacyclin synthase in the pulmonary arteries of patients with idiopathic PAH (Christman et al., 1992, Tuder et al., 1999). The observation of reduced levels of prostacyclin in PAH provides a rationale for therapies targeting the prostacyclin pathway. In pre-clinical animal models, PGI<sub>2</sub> receptor (PGI-R) knockout mice developed more severe pulmonary hypertension and vascular remodelling following chronic hypoxic exposure compared with the WT mice (Hoshikawa et al., 2001). The transgenic mice overexpressing prostacyclin synthase selectively in the pulmonary vasculature are protected against chronic hypoxia induced PH and rats with gene transfer of human prostacyclin synthase ameliorated the MCT-induced PH (Gubrij et al., 2014, Nagaya et al., 2000, Geraci et al., 1999). Further, engineered endothelial-like progenitor cells producing prostacyclin and mesenchymal stem cell-based prostacyclin synthase gene therapies pro-

tected against the development of experimental pulmonary hypertension (Zhou et al., 2013, Takemiya et al., 2010). The currently available drugs that target the prostacyclin pathway are epoprostenol, iloprost, treprostinil and beraprost. These drugs are recommended for the treatment of patients at FC III–IV, according to the WHO/NYHA functional classification (Galie et al., 2016, Galie et al., 2013).

Epoprostenol was the first prostacyclin analogue to be approved by the FDA, and is the first exogenous prostanoid to be used in the treatment of PAH (Mubarak, 2010). Epoprostenol is a chemically unstable compound with a short half-life (of about 6 min) which must be administered continuously via intravenous infusion (Badesch et al., 2007). As Epoprostenol showed rapidly effective therapy in PAH, it has been recommended as an initial treatment for patients in FC III and IV stages. Epoprostenol treatment has improved the prognosis of patients with PAH, and has also been shown to improve hemodynamic measures (Rubin et al., 1990) (McLaughlin et al., 2002) and exercise capacity (Barst et al., 1996, Badesch et al., 2000, McLaughlin et al., 2002). Apart from monotherapy, short-term studies have shown the efficacy of combining epoprostenol with PDE-5i and/or ERAs (Humbert et al., 2004a). Despite substantial evidence to support the use of epoprostenol in PAH, its short half-life, inconvenient route of administration and side effects (attributed to the vasodilatory effects of epoprostenol including flushing, jaw pain, arthralgias, myalgias, and headache (Myers et al., 2004, Delcroix and Howard, 2015)) mean that it is underused as a treatment for PAH. Fortunately, thermostable formulation of epoprostenol is now in development, while a variety of prostacyclin analogues are now available for clinical use.

#### **1.2.7.2 Endothelin Receptor Antagonists**

Endothelin-1 (ET-1), originally isolated from endothelial cells, is a potent vasoconstrictor and has a proliferative effect on pulmonary artery smooth muscle cells (Davie et al., 2002). Plasma levels of ET-1 are increased in PAH patients and correlate with PAH severity and prognosis (Rubens et al., 2001). There are two types of ET receptors: endothelin receptor A (ET<sub>A</sub>R) and B (ET<sub>B</sub>R), which are both upregulated in PAH patients (Davie et al., 2002).

ET<sub>A</sub>R is mainly expressed in PASMCs, and is thought to mediate ET-1-induced contraction and proliferation of PASMCs during PAH pathogenesis (Rubin, 2012, Frumkin, 2012); ET<sub>B</sub>R promotes vasodilation and clearance of ET-1 in endothelial cells (where it is highly expressed) and has vasoconstrictive and proliferative actions in PASMCs (Seo et al., 1994, Raja and Dreyfus, 2008, Raja, 2010, Eguchi et al., 1993). Currently, both selective and nonselective ET receptor antagonists (ERA) are approved and used for treatment of PAH patients. The dual ERAs bosentan and macitentan, and the selective ET<sub>A</sub>R antagonist ambrisentan target the actions of ET-1 in the pulmonary vasculature by binding and blocking activation of the ET receptors, preventing ET-1-mediated responses (Humbert and Ghofrani, 2016).

Bosentan is a nonselective orally active dual endothelin receptor antagonist used for the treatment of FC III and IV stages patients (Humbert et al., 2007), as well as for FC II patients (Task Force for et al., 2009). The first randomised placebo-controlled 12-week clinical study showed that bosentan could increase exercise capacity and improved hemodynamics in patients with PAH (Channick et al., 2001). Another larger multicenter study assessing 213 PAH patients for 16 weeks showed orally administered bosentan significantly improved exercise capacity and increased the time to clinical worsening in patients with severe PAH either primary or associated with connective-tissue disease (Rubin et al., 2002). The side effects of bosentan are associated with hepatic toxicity, headaches, flushing and syncope, which are probably due to the effects of bosentan on the systemic vasculature and associated systemic vasodilatation (Gabbay et al., 2007).

### **1.2.7.3 Phosphodiesterase Type 5 Inhibitors**

Nitric oxide (NO) released from endothelial cells induces relaxation and inhibition of PASMC proliferation by binding to soluble guanylyl cyclase (sGC) to increase intracellular cyclic guanosine monophosphate (cGMP) levels (Vakrilova, 2014). The key enzyme phosphodiesterase type-5 (PDE-5) is abundantly and predominantly expressed in PASMCs and shows increased activity in animal models of PH which can degrade cGMP levels in

smooth muscle cells to terminate the action of cGMP (Corbin et al., 2005, Li and Chen, 2013). Inhibition of PDE-5 activity by sildenafil and tadalafil has shown both acute and long-term beneficial effects in patients with PAH (Galie et al., 2005, Galie et al., 2009a).

Sildenafil is a highly potent and selective PDE-5 inhibitor, which can inhibit the hydrolysis of cGMP to GMP to allowing accumulation of NO-mediated cGMP and subsequently induce vasodilation and inhibit proliferation (Ghofrani et al., 2006, Michelakis et al., 2002). *In vivo* studies have shown that oral sildenafil treatment can attenuate chronic hypoxia- and MCT-induced pulmonary hypertension (Zhao et al., 2001, Schermuly et al., 2004). The SUPER-1 trial with sildenafil treatment showed improvements in 6MWD, NYHA FC and pulmonary haemodynamics, but with adverse events including headache, flushing and dyspepsia (Galie et al., 2005). The follow-up SUPER-2 trial showed sustained improvements in 6 MWD and NYHA FC with an estimated 3-year survival rate of 79% (Rubin et al., 2011). Currently, sildenafil is approved for the treatment of patients with FC II–III in Europe and FC II–IV in the USA.

### **1.2.8 Combination Therapy**

In most cases, monotherapy does not adequately control disease progression in PAH patients due to the involvement and interaction of several signalling pathways contributing to PAH pathogenesis. Using more than one class of drug to target multiple disease pathways may potentially increase the overall impact on each or all of the mechanisms involved in PAH to improve the treatment efficiency (Humbert et al., 2004c, McGoon, 2014). In sequential combination therapy studies, there was no significant improvement in 6MWD observed in the 16-week FREEDOM-C1 and FREEDOM-C2 trials, both investigating oral trepostinil on a background of bosentan and/or sildenafil (Tapson et al., 2012, Tapson et al., 2013). In the upfront combination therapy study, the efficacy and safety of first-line combined bosentan plus epoprostenol versus epoprostenol alone was investigated in patients with severe PAH. This double blind, placebo-controlled prospective study showed a greater improvement in hemodynamic measurements, exercise capacity and function capacity in

the combined treatment group compared with monotherapy (Humbert et al., 2004a). In addition, triple upfront combination therapy has been trialled in patients with severe PAH. The observational analysis in PAH patients showed significant improvements in haemodynamics, WHO functional class status and 6MWD using combination therapy with *i.v.* epoprostenol, bosentan, and sildenafil compared with baseline (Sitbon et al., 2014). Taken together, these clinical studies indicate that specific combination therapies for PAH might provide an effective therapeutic approach for patients. Further studies are required to investigate the optimal combination treatment algorithm for PAH in order to provide the patients with the treatment plan that will result in the best possible outcome.

### **1.2.9 Traditional Animal Models of Pulmonary Hypertension**

In order to investigate the molecular mechanisms involved in the pathophysiology of PAH and to perform preclinical studies for drug development, appropriate animal models of PAH are required. Indeed, animal models are an essential platform for investigating and understanding the pathophysiological processes that underlie PAH progression. The most commonly used animal models of PH are the chronic hypoxic model and the monocrotaline (MCT) injury model, which are single-pathological-insult models.

#### **1.2.9.1 Chronic Hypoxia**

The right heart catheterisation studies carried out several decades ago in people born and living at high altitudes compared with people born and living at sea level showed mild pulmonary hypertension and moderate increases in pulmonary vascular resistance and right ventricular load in persons living at high altitude compared to those living at sea level (Arias-Stella and Saldana, 1963). Moreover, a much greater increase in pulmonary artery pressure in response to exercise is observed in people living at high altitude compared with sea-level dwellers (Arias-Stella and Saldana, 1963, Sime et al., 1963). Based on these findings, researchers maintained various animals (mouse, rat, calf, and pig) at high altitude, or simulated high altitudes using tools such as hypobaric chambers. These treatments resulted in the development of a pulmonary hypertension disease phenotype (Hislop and

Reid, 1976, Stenmark et al., 1987, James and Thomas, 1968, Hassoun et al., 1989), showing that chronic hypoxia makes a significant contribution to PH. The most popular hypoxic animal models are using mice and rats, with PH induction achieved in the lab using hypobaric hypoxic chambers with exposure to 10% O<sub>2</sub> for 2-4 weeks. This model is widely used, as it is very predictable and reproducible within a selected animal strain (Stenmark et al., 2009). Exposure of mice and rats to chronic hypoxia exposure results in a reliable increase in right ventricular systolic pressure (RVSP) of about 10 mmHg in mice and higher in rats, together with right ventricular hypertrophy and remodelling of the pulmonary vasculature (Das et al., 2012).

There are a number of features observed in the pulmonary arteries (PAs) (all the three layers of the vessel) in mammals following chronic exposure to chronic hypoxia. These structural changes include muscularisation of small, normally nonmuscular arteries in the alveolar and increases in the appearance of cells expressing  $\alpha$ -smooth muscle actin in the previously nonmuscularised vessels, as well as medial and adventitial thickening of the muscular and elastic vessels (Stenmark et al., 2006b). The contributors to these changes are including smooth muscle cell hypertrophy, proliferation, and migration, differentiation of pericytes, recruitment and differentiation of local fibroblasts, mononuclear cell/progenitor cell recruitment, transdifferentiation of endothelial cells into mesenchymal-like cells, and the increased deposition of extracellular matrix proteins (Meyrick and Perrett, 1989, Stenmark et al., 2006b, Stenmark et al., 2006a). Furthermore, chronic hypoxia also induces an early and persistent pulmonary artery specific vascular inflammatory response, which suggests inflammation playing a significant role in the hypoxia induced remodelling process (Burke et al., 2009). Although significant stiffening of the conduit vessels, severe inflammatory and fibrotic lesions have been noted, unlike human PAH disease, chronic hypoxia induced PH in animals can be reversed following a return to normoxic conditions (Lammers et al., 2008, Stenmark et al., 2009).

The phenotype of chronic hypoxia induced PH models differs between strains of animal and indeed species. For example, exposure of mice to chronic hypoxia induces minimal

vascular remodelling compared to rats (Dempsey et al., 2009, Frank et al., 2008, Nozik-Grayck et al., 2008). In hamsters, chronic hypoxia induced PH also causes less muscularisation of the precapillary arteries than in rats (Walker et al., 1984). In contrast, neonatal calves exposed to chronic hypoxia develop very severe PH with exceeded systemic pressures and vascular remodelling in both distal and proximal pulmonary arteries, which is far more striking compared with mouse and rat model (Orton et al., 1988, Stenmark et al., 1987, Stenmark et al., 2006b). In addition, intimal morphology changes are usually minimal in the hypoxic rat and mouse models but with very pronounced intimal thickening in the hypoxic neonatal calves (Meyrick and Reid, 1980, Stenmark et al., 2006b). Microarray analysis demonstrates that chronic hypoxia induced lung gene expression profiles show distinct differences between species. For example, rats exposed to hypoxic conditions show increased expression of genes involved in endothelial cell proliferation and decreased expression of those associated with apoptosis; while the gene expression pattern in hypoxic mouse lung shows decreased expression of genes that regulate vascular smooth muscle proliferation (Bull et al., 2007, Hoshikawa et al., 2003).

The main advantage to chronic hypoxia is its simplicity and reliability, and widely used as PH model in the literature. The shortcomings of the chronic hypoxia induced PH model include the absence of significant pulmonary vascular remodelling, especially within the mouse model, and the absence of plexiform lesions even following longer exposure times, which cannot fully recapitulate the pulmonary vascular damage observed in human patients (Voelkel and Tuder, 2000, Herget et al., 1978, Campian et al., 2006). Moreover, while chronic hypoxia can induce right ventricular hypertrophy (RVH) in animals there is little evidence of right ventricular failure, which is the main cause of death in patients with PAH (Drexler et al., 2008, Stenmark et al., 2009).

#### **1.2.9.2 Monocrotaline (MCT) Injury Model**

Monocrotaline (MCT) is a toxic pyrrolizidine alkaloid present in the plant *Crotalaria spectabilis* and it is known for its ability to cause hepatotoxicity and PH (Heath et al., 1975,

Kay, 1994). Feeding rats with the seeds of *Crotalaria spectabilis* or by injecting nonhuman primates with a suspension of MCT results in a pulmonary hypertensive phenotype characterised by RVH and pulmonary vascular remodelling due to the medial hypertrophy in the distal pulmonary vessels (Kay et al., 1967, Chesney and Allen, 1973b, Chesney and Allen, 1973a, Kolettis et al., 2007). Following administration of MCT, it is metabolised into pyrrolic derivatives in the liver by the enzyme cytochrome-P450, which initiates endothelial injury in the pulmonary vessel wall (Shah et al., 2005). Due to differences in hepatic metabolism by cytochrome P-450, the response to MCT is variable among species, strains, and even animals. The ideal species for the MCT-induced PH model is the rat. Although injection or oral administration of MCT in mice causes liver damage (Miranda et al., 1983), modest pulmonary fibrosis (Yasuhara et al., 1997, Molteni et al., 1989, Hayashi et al., 1995), and immunotoxicity (Deyo and Kerkvliet, 1990, Deyo and Kerkvliet, 1991), they do not develop a PH.

The histological features of the pulmonary vasculature of MCT-induced PH include intimal hyperplasia, medial hypertrophy, and adventitial thickening. This model is also characterised by increased apoptosis of endothelial cells, proliferation and resistance to apoptosis of PASMCs (Kolettis et al., 2007, Gomez-Arroyo et al., 2012, Stenmark et al., 2009, Ryan et al., 2011). Although the exact mechanism of MCT-induced PH has not yet been fully characterised, it is widely accepted that MCT metabolism causes endothelial cell damage and then triggers pulmonary vasculitis and obstructive pulmonary vascular remodelling (Jasmin et al., 2001). This is consistent with the observations showing that rats exposed to MCT only develop increased pulmonary arterial pressures and vascular remodelling 1-2 weeks after the initial MCT dose (Meyrick et al., 1980). In the MCT model, inflammatory cells (macrophages, dendritic cells, and mast cells) and cytokines (IL-1, and IL-6) play a pivotal role in the early stages of pulmonary vascular remodelling (Savai et al., 2012, Dahal et al., 2011, Henriques-Coelho et al., 2008b). Macrophage and dendritic cell accumulation are believed to facilitate the inflammatory response in PH, thereby contributing to pulmonary vascular remodelling. In addition, mast cells are thought to have direct vasoactive effects and to stimulate remodelling by increasing the production of matrix metallo-

proteinases (Dorfmueller et al., 2003, Price et al., 2012, Thienemann et al., 2004). It has also been demonstrated that right heart failure in the MCT-induced rat PH model is associated with up-regulated expression and infiltration of both neutrophils and monocytes/macrophages (Campian et al., 2010).

The MCT-induced PH model is widely used by researchers. The procedure is relatively simple and does not require meticulous technical skills, and is also reproducible and inexpensive (Gomez-Arroyo et al., 2012). One of the advantages of this model is that it is a good model to investigate the pulmonary vascular remodelling process and its role in PAH pathophysiology. However, there are several shortcomings of the MCT model. The side effects of MCT treatment include significant liver and kidney damage, and also consisting of pulmonary interstitial edema, myocarditis, and hepatic veno-occlusive disease that is uncharacteristic of severe human PAH disease (Gomez-Arroyo et al., 2012). The myocarditis caused by MCT affects both the right and left ventricle, which complicates the study of the right ventricular hypertrophy/failure associated with the severe PH (Miyachi et al., 1993). The disease progression toward death in MCT model might be too short for compensatory mechanisms to develop (Buermans et al., 2005), and most experimental treatment studies seem to improve, reverse, and prevent pulmonary vascular damage and PH, which has resulted in criticisms that this model does not accurately recapitulate the progression of PH observed in humans (Stenmark et al., 2009, Ryan et al., 2011). In addition, the use of MCT is restricted to rats due to the differences in cytochrome P-450-mediated hepatic metabolism between species (Dumitrascu et al., 2008).

### **1.2.10 Alternative Animal Models of PAH**

As mentioned above, traditional models of PH provided a vast amount of knowledge in the understanding of the disease pathophysiology of PH. However, the chronic hypoxia and MCT models do not recapitulate certain aspects of PAH, such as neointimal and plexogenic arteriopathy. As a result, new experimental strategies based on the two principal models of PAH have been developed, aimed at including progressive pulmonary vascular

disease with neointimal changes observed in human PAH disease. These models include the multiple-pathological-insult (MPI) models, which appear to correlate better with PAH disease in humans. In addition, several genetic modified mice models have been used for PH studies, which provide a tool to study specific genes and pathways in the pathobiology of PAH.

#### **1.2.10.1 Sugen 5416 (SU5416) and Hypoxia**

In the lungs of PAH patients, affected pulmonary arteries exhibit deregulated angiogenesis, caused by abnormal proliferation of endothelial cells into the lumen. VEGF and its receptor (VEGFR-2) are required for normal endothelial cell maintenance, function and signaling, and blockade of VEGF induces endothelial cell dysfunction and death, while promoting apoptosis-resistant endothelial cell proliferation (Stenmark et al., 2009). In order to develop a better PH model to recreate the plexiform neointimal lesions observed in patients with PAH, a combination of VEGFR-2 blockade (using the tyrosine kinase inhibitor SU5416) and chronic hypoxia showed a severe, irreversible PH associated with precapillary arterial occlusion by proliferating endothelial cells in rats (Taraseviciene-Stewart et al., 2001). These severe and irreversible phenotypes were confirmed by a single subcutaneous with SU5416 with chronic hypoxia and then return to normoxic condition develop a severe, sustained PH in the last stage accompanied by severe right ventricular pressure overload and the formation of lesions that are indistinguishable from the pulmonary arteriopathy of human PAH. This PH model provides a new and rigorous approach for investigation the genesis, hemodynamic effects and reversibility of plexiform and other occlusive lesions in PAH (Abe et al., 2010). Under normoxic conditions, treatment with SU5416 also resulted in mild PH and pulmonary vascular remodelling in normoxic exposure rats (Taraseviciene-Stewart et al., 2001, Fong et al., 1999). In addition, the SU5416-injected rats exhibited increase vascular smooth muscle cell proliferation due to the Vascular endothelial growth factor (VEGF) receptor blockade caused endothelial cell apoptosis, indicating that the endothelial cell VEGF receptor can regulate pulmonary vascular SMC growth (Stenmark et al., 2009, Taraseviciene-Stewart et al., 2001). Furthermore, the VEGF receptor

blockade by SU5416 only affects the lung rather than other organs and does not find perivascular infiltration of monocytes/macrophages in this model (Burke et al., 2009).

Contrary to rats, which require a single injection of SU5416, mice require weekly injections of SU5416 during a 3-week hypoxic exposure for induction of severe PH. Compared with chronic hypoxia alone, mice which receive multiple SU5416 injections show exacerbations in all measures of PAH pathology such as RVSP and RVH and pulmonary vascular remodelling. In addition, hypoxia/SU5416 treatment steadily decreases cardiac output, indicating incipient heart failure. Molecular analysis showed a dysregulated TGF- $\beta$ /BMP/Smad axis as well as augmented induction of IL-6 and Hypoxia-inducible factor 1  $\alpha$  (HIF-1 $\alpha$ ) in SU5416-and/or hypoxia-treated mice (Ciuclan et al., 2011). In contrast to the rat model, mice injected with SU5416 weekly during three-week chronic hypoxia and then with 10-week recovery in normoxia. Following ten weeks after hypoxic exposure, several indices of PH are reduced including RVSP, angioobliterative lesions and the PH and RV dysfunction does not show even worse (Vitali et al., 2014), which suggest this PH model is reversible. Although this mouse model of PH is less severe than the rat model, it is still a useful adjunct to other PH models, particularly when genetic modification or long-term intervention is desired.

The SU5416/hypoxia model has proved to be a particularly robust model of PH, which resemble human PAH disease more closely than the single insult models. This is in accordance with 'multiple hit' hypothesis for the development of PH including the genetic and environment insults (Geraci et al., 2010). This indicates that MPI models developed from SPI models of PH are more correlated with human PAH disease. In addition, the SU5416/hypoxia model is unresponsive to treatments such as calcium-entry blocker, ACE inhibitors, and bosentan, and displays increased RVSP and RVH. This model appeared progressive and refractory to treatment and the unresponsiveness to treatment and irreversibility of PH features are more relevant to human PAH (Nicolls et al., 2012). Thus, the data generated from this new model may add greater clinical relevance.

### **1.2.10.2 Overexpression of S100A4/Mts in Mice**

The S100A4/Mts-1 gene was identified as a differentially expressed gene in highly metastatic mouse mammary adenocarcinoma cells (Ebralidze et al., 1989). S100A4/Mts-1 is a metastasis-promoting protein belonging to the S100 family of calcium-binding proteins. The S100 family members are involved in numerous physiological functions include cell proliferation, differentiation, cytoskeleton dynamics, and apoptosis (Schafer and Heizmann, 1996). The first S100A4/Mts-1 transgenic mouse was created in 1998 (Ambartsumian et al., 1998), and about 5% of transgenic mice overexpression S100A4/Mts-1 developed pulmonary arterial changes resembling human plexogenic arteriopathy with intimal hyperplasia leading to occlusion of the arterial lumen (Greenway et al., 2004). SMC-like and endothelial-like cells are found in the plexogenic lesions of S100A4/Mts-1 overexpressing mice; while a marked periarterial inflammatory response in plexogenic arteriopathy, suggesting that inflammatory insult may trigger the development of plexogenic arteriopathy in these mice (Greenway et al., 2004). The expression of S100A4/Mts-1 was absent in human lungs with no PH or early-stage disease, but the expression was markedly increased in the late-stage plexogenic arteriopathy. This suggests that S100A4/Mts-1 is not involved in the initial responses but may be functionally significant in the development of the more severe arterial lesions seen in the end-stage disease. In addition, lung biopsies from children with PH associated with congenital heart defects showed increased expression of S100A4/Mts-1 in PSMCs of lesions associated with neointimal formation and plexiform lesions (Greenway et al., 2004).

One of the principal reasons for using this model to study PAH is that most animal PH models lack neointimal thickening and plexiform lesions. In addition, these mice show gender differences. Female mice overexpression S100A4/Mts-1 developed plexiform lesions and increased RVSP but not observed in male mice (Greenway et al., 2004). Furthermore, S100A4/Mts-1 overexpressing mice showed greater pulmonary arterial pressure increases and more RVH in the chronic hypoxia condition, and will sustain the disease phenotype even after 3 months normoxia exposure. The S100A4/Mts-1 mice develop sim-

ilar peripheral vascular disease as control mice in response to hypoxia. Interestingly, those changes did not regress after normoxic exposure in S100A4/Mts-1 mice. The protein fibulin-5 might contribute to these findings, which is a matrix component necessary for elastin fibrin assembly (Merklinger et al., 2005).

### **1.2.10.3 IL-6 Overexpression in Mice**

Interleukin 6 (IL-6) is a cytokine produced mainly by T cells and macrophages. IL-6 is not only involved in inflammation and infection responses but also plays a role in the regulation of metabolic, regenerative, and neural processes (Scheller et al., 2011). Both human PAH patients and animal PH models showed elevated levels of IL-6 and IL-6 seems to correlate well with disease severity and mortality (Dorfmueller et al., 2003, Price et al., 2012, Humbert et al., 1995). In order to investigate the role of IL-6 in the development of PH, transgenic mice overexpression lung-specific IL-6 were created. The transgenic mice exhibited elevated RVSP and RVH with corresponding pulmonary vasculopathic changes, all of which were exacerbated by chronic hypoxia exposure. In addition, the mice had muscularisation of the proximal arterial tree, and chronic hypoxia enhanced this effect. Similar to what is observed in PAH patients, muscularisation and proliferative arteriopathy was seen in the distal arteriolar vessels. In the later stages of disease, animals developed occlusive neointimal angioproliferative lesions composed of endothelial cells and T-lymphocytes. This is thought to be due to the IL-6-induced activation of a proangiogenic factor, vascular endothelial growth factor (VEGF), the proliferative kinase extracellular signal-regulated kinase, proliferative transcription factors c-MYC and MAX, and the anti-apoptotic proteins survivin and Bcl-2 and downregulation of the growth inhibitor TGF- $\beta$  and proapoptotic kinases JNK and p38 (Steiner et al., 2009). Thus, this IL-6 transgenic mouse model recapitulated similar features seen in patients with severe PAH including concentric intimal wall thickening, arteriolar wall muscularization, plexogenic lesions and recruitment of inflammatory cells (Steiner et al., 2009). In order to further confirm the important role for IL-6 in the development of PH, IL-6 knockout mice exposed to chronic hypoxia displayed reduced RVSP, RVH, and both the number and medial thickness of

muscular pulmonary vessels. These knockout mice also showed less inflammatory cell recruitment in the lungs compared with wild-type mice as analysed by protein levels and immunostaining for the specific macrophage marker F4/80 (Savale et al., 2009).

#### 1.2.10.4 BMPR2 Mutant Mice

As mentioned in Section 1.2.4, the genetic basis of HPAH and IPAH is related to mutations in *bmpr2*. A total of 298 different *bmpr2* mutations have been identified in PAH patients (Machado et al., 2006). Due to the high proportion of PAH patients possessing mutations in *bmpr2*, genetic models of *bmpr2* have been used to investigate the role of *bmpr2* in the pathogenesis of PAH.

Initial studies attempted to generate homozygous *bmpr2* genetic ablation mice, however these failed to develop due to an absence of organised mesoderm (Beppu et al., 2000). Therefore, mice heterozygous for a *bmpr2* mutant allele (*bmpr2*<sup>+/-</sup>) were developed for PAH studies. These mice showed normal survival rates and reproduced normally, despite a 50% reduction in *bmpr2* mRNA expression in isolated PSMCs. This is consistent with the human observations that heterozygous *bmpr2* mutations themselves are insufficient to account for the clinical manifestation of PAH and multiple environmental or genetic hits are required to trigger the disease (Morrell, 2006). In basal conditions, one study reported that *bmpr2*<sup>+/-</sup> mice (a mutant *bmpr2* allele lacking exons 4 and 5) exhibit mild PH with muscularisation and thickening of the pulmonary arteries, and a mild increase in pulmonary arterial pressure (Beppu et al., 2004). However, the mice carrying a heterozygous partially inactivation (hypomorphic) mutation at the *bmpr2* locus (*bmpr2*<sup>Δex2/+</sup>) does not develop mild spontaneous PH (Frank et al., 2008) and silence *bmpr2* expression by RNA interference in mice does not increase pulmonary arterial resistance (Liu et al., 2007). This phenotype variation may due to the different *bmpr2* gene mutations have different effects on *BMPR2* protein production, which are likely to cause differences in phenotype (Austin et al., 2009). Importantly, these *bmpr2*<sup>+/-</sup> mice exposed with a secondary insult (e.g. hypoxia, serotonin, or inflammation) result in development of PH such as increased pulmo-

nary artery pressure and pulmonary vascular remodelling (Long et al., 2006, Song et al., 2005, Frank et al., 2008, Beppu et al., 2004). These observations are similar to human patients, which the penetrance of the *bmpr2* mutations is remarkably low, with only 20-30% of carriers actually developing HPAH (Newman et al., 2001, Newman et al., 2004).

The smooth muscle cell-specific transgenic mice expressing a dominant-negative *bmpr2* under control of a tetracycline gene switch (SM22-tet-BMPR2 (delx4<sup>+</sup>) mice) developed increased RVSP, RVH, and pulmonary arterial muscularisation (West et al., 2004). Another smooth muscle-specific doxycycline-inducible *bmpr2* mutation with an arginine to termination mutation at amino acid 899 (SM22-rtTAx TetO (7)-BMPR2 (R899X)) mice developed elevated RVSP, associated with extensive vascular pruning, muscularisation of small pulmonary vessels, and development of large structural pulmonary vascular changes 9 weeks after transgene induction. Pulmonary vascular lesions were filled with smooth muscle cells and endothelial cells, and were surrounded by a large numbers of macrophages and T cells (West et al., 2008b). These features were confirmed with the later study using SM22-tet-BMPR2 (R899X) mice showed elevated RVSP, RVH, muscularisation of small pulmonary arteries, and associated disturbed blood flow in their lungs (Yasuda et al., 2011).

In normal lungs, *bmpr2* expression is prominent on the vascular endothelium. In pulmonary hypertension cases, however, the expression of *bmpr2* is markedly reduced in the peripheral lung of HPAH patients, especially with heterozygous *bmpr2* mutations (Atkinson et al., 2002). The mice with *bmpr2* conditional knockout in endothelial cells revealed, but not all mice, elevated RVSP, developed RVH, and increased the number and wall thickness of muscularised ( $\alpha$ SMA-positive) distal pulmonary arteries. In addition, there are elevated proteins involved in the pathogenesis of PAH include serotonin transporter and tenascin-C in the distal arteries and with a high incidence of perivascular leukocyte infiltration and in situ thrombosis (Hong et al., 2008).

The conditional knockout *bmpr2* in SMCs and ECs is sufficient to induce PH within a

subsection of mice, which demonstrated that conditional heterozygous or homozygous *bmpr2* deletion predisposes mice to develop PH (Hong et al., 2008). This is in accordance with human that *bmpr2* mutations predispose patients to develop PAH. Thus, the genetic models of *bmpr2* mutations provide useful genetic resources to further investigate the pathogenesis regarding gene mutations in PAH. Furthermore, these models also present opportunities to further identify environmental and genetic factors that involved in the development.

Taken together, various animal models of PH provide valuable knowledge to understanding the pathophysiology of PH. Although there is no perfect animal model can mimic human PAH disease, a number of MPI animal models developed from SPI animal models are more closely correlate with human disease. The MPI models tend to correlate better with severe PAH in human than do SPI models. However, the SPI models provide the early stages of PAH disease in humans, which can be reversed with proper treatment. Unfortunately, PAH patients in their early stages are often missed diagnosis. Therefore, different animal models can be used to assess various stages of the disease progression. There is still a long way to cure PAH disease, and more animal models of PH need to be developed to provide better preclinical studies.

### **1.3 Non-coding RNA(ncRNA)**

High-throughput transcriptomic analyses have revealed that eukaryotic genomes transcribe up to 90% of the genomic DNA. Only 1-2% of these transcripts encode for proteins, whereas the vast majority are transcribed as non-coding RNAs (ncRNAs) (Consortium, 2004). These non-protein-coding sequences increasingly dominate the genomes of multicellular organisms as their complexity in contrast to protein-coding genes. NcRNAs are expressed in a cell/tissue-specific manner or in a developmental stage-specific manner (van Rooij, 2011, Ward et al., 2015). There are mounting evidences that ncRNAs are involved in the pathogenesis of human diseases such as cancer, cardiovascular, neurological, developmental, and other diseases (Esteller, 2011).

NcRNAs can be divided into infrastructural ncRNAs and regulatory ncRNAs. Constitutively-expressed infrastructural ncRNAs include ribosomal, transfer, small nuclear, and small nucleolar RNAs. Regulatory ncRNAs can be classified into microRNAs (miRNAs), Piwi-interacting RNAs (piRNAs), small interfering RNAs (siRNAs), long non-coding RNAs (lncRNAs), promoter-associated RNAs (PARs), enhancer RNAs (eRNAs), and circular RNAs (Cech and Steitz, 2014). This project is focused on miRNAs and lncRNAs.

### 1.3.1 MicroRNAs

#### 1.3.1.1 MicroRNA Genomics and Biogenesis

MiRNAs are a novel class of endogenous, small/short noncoding transcripts of 16 to 29 nucleotide RNAs that negatively regulate gene expression via degradation or translational inhibition of their target mRNAs (Bartel, 2004, van Rooij and Olson, 2007). The first miRNA identified in 1993, when researchers discovered that the *lin-4* gene in *C.elegans* encoded a pair of short RNA transcripts rather a protein (Lee et al., 1993). These RNA transcripts were able to regulate larval development through translational repression of *LIN-14* protein (Le Contel et al., 1995). They found that *lin-4* transcripts in *C.elegans* contain sequences complementary to a repeated sequence element in 3'UTR of *lin-14* mRNA. *lin-4* regulates *lin-14* through RNA-RNA interactions with the 3' untranslated region (Le Contel et al., 1995, Parant et al., 1995). In 2000, a second miRNA, let-7, was discovered, and since then thousands more miRNAs have been identified (Reinhart et al., 2000). In its most recent version, miRBase reports ~ 2000 human miRNAs (version 20: [www.mirbase.org](http://www.mirbase.org) 2014) and current estimates suggest that over 30% of human genes are regulated by miRNAs (Filipowicz et al., 2008), leading to diverse effects on multiple cellular processes. MiRNA genes can be classified into four groups according to their genomic location: intronic miRNA encoded in noncoding transcriptional units; exonic miRNA encoded in noncoding transcriptional units; intronic miRNA encoded in protein-coding transcript units, and exonic miRNAs encoded in protein-coding transcripts (Rodriguez et

al., 2004). Nearly half of the known human miRNAs are found in clusters, which are transcribed as polycistronic primary transcripts (Lagos-Quintana et al., 2001, Lau et al., 2001). Each cluster usually contains two or three miRNA genes and the largest cluster, at 13q31, is composed of seven genes (Calin et al., 2004, He et al., 2005). About 37% of mammalian miRNAs appear to be located within the introns of protein-coding genes, linking their expression to the promoter-driven regulation of the host gene (Lutter et al., 2010, Baskerville and Bartel, 2005). Human miRNAs are located on all chromosomes except the Y chromosome, and are nonrandomly distributed in the human genome.

MiRNA transcripts are synthesised and processed through a series of cleavage steps (Figure 1.6). The biogenesis of miRNA begins with transcription of a primary miRNAs (pri-miRNA) from a miRNA gene by RNA polymerase II in the nucleus (Pedron et al., 1993). Pri-miRNAs are structurally analogous to mRNA as they are 5'-capped and spliced and bear a 3' poly-A tail, and often can produce more than one functional miRNA (Cai et al., 2004, Lee et al., 2004). Following association with the Drosha-DGCR8 complex, pri-miRNAs are processed into approximately 70 nucleotides (nt) long precursor hairpin structures (Pre-miRNA) in the nucleus (Gregory et al., 2004, Han et al., 2004). The pre-miRNA is characterised by a two nucleotide single stranded overhang on the 3' end, which is recognised by Exportin-5 (XPO5) and Dicer for further processing (Du and Zamore, 2005). Exportin-5 is a member of the karyopherin family of nucleocytoplasmic transport factors that can bind pre-miRNAs in the presence of a Ran-GTP cofactor, exporting precursor miRNAs into the cytoplasm. Once in the cytoplasm, hydrolysis occurs converting RanGTP into RanGDP and releasing the pre-miRNA from the Exportin-5/RanGTP complex (Yi et al., 2003). Following export of the pre-miRNAs from the nucleus, pre-miRNAs are further processed by a cytoplasmic RNase III endonuclease (Dicer) in complex with the double-stranded RNA-binding protein TRBP, which digests the pre-miRNAs resulting in an imperfect miRNA-miRNA duplex. This mature miRNA duplex is about 22 nucleotides in length, and containing the mature miRNA guide or lead strand and the passenger strand (Lee et al., 2002). After separation of the two miRNA strands by the helicase enzyme, the passenger strand is degraded, and the guide strand of

the mature miRNA is loaded with Argonaute (Ago2) proteins and incorporated into the RNA-induced silencing complex (RISC). Depending on the complementarity of the “seed region” of mRNA targets, the guide stand recognises and binds the 3’ untranslated regions (UTRs) of target mRNAs via Watson-Crick base pairing. This interaction leads to either translational repression/activation or degradation of its target mRNAs, and repression of protein translation (Winter et al., 2009).

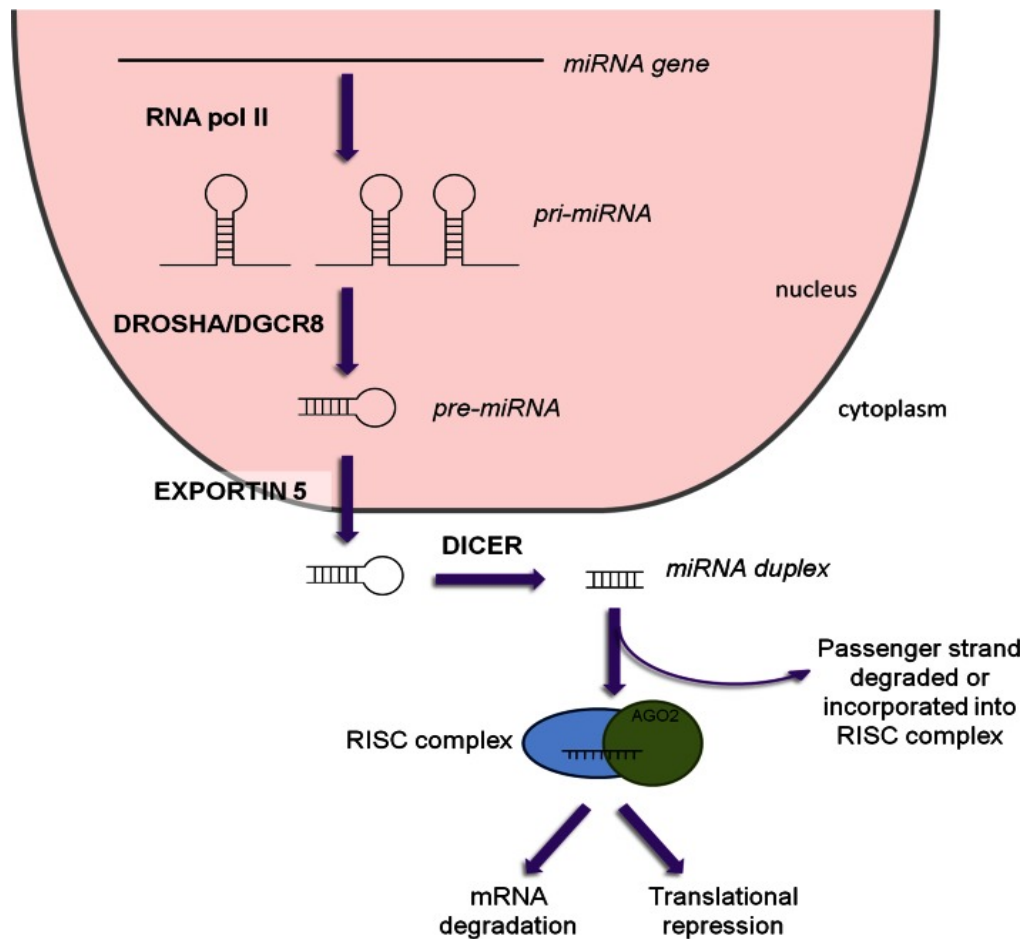


**Figure 1.6 MiRNA biogenesis**

Transcription by RNA polymerase II gives rise to the pri-miRNA, which can produce multiple mature miRNAs. Processing by the RNase III enzyme Drosha along with cofactor DGCR8 produces the stem-loop pre-miRNA that is exported out of the nucleus by Exportin-5. In the cytoplasm, cleavage by Dicer results in a miRNA duplex, ~22 nucleotides long. The mature miRNA is incorporated into the RNA-induced silencing complex (RISC) and targets the 3'-UTR of mRNA. Gene silencing is achieved by either mRNA degradation or translational repression (adapted from (Grant et al., 2013))

### 1.3.1.2 The Function of MiRNAs

The regulatory functions of miRNAs are accomplished through the RNA-induced silencing complex (RISC). MiRNAs assembled into RISC function as guides, directing the silencing of target mRNA. Ago2 is the only argonaute protein that possesses endonuclease activity and is required for mediating mRNA cleavage. However, all four Ago proteins are associated with miRNAs as well as RISC activity in human cell lines (Meister et al., 2004). Structural analyses have shown that the Ago2 PIWI domain is similar to ribonuclease H, which cleaves mRNA to form 5' phosphate and 3' hydroxyl groups products, and mutations within a cryptic ribonuclease H domain with Ago2 inactivate RISC (Song et al., 2004, Liu et al., 2004). The activated RISC binds target mRNA by complementary base pairing the guide strand and the 3'UTR of the target mRNA. The target recognition relies heavily on base pairing between the highly evolutionary conserved 'seed sequence' nucleotides 2-8 at the 5' end and the corresponding 3' region of its target mRNA (Lewis et al., 2003, Grimson et al., 2007). The degree and nature of complementarity between the guide miRNA and the target mRNA appear to determine the gene silencing mechanism (either mRNA degradation or repression; (Zeng et al., 2003). Full complementarity of miRNA with the 'seed region' in the target mRNA 3' UTR can lead to target mRNA cleavage, a process that is much more common in plants compared to animal cells (Rhoades et al., 2002, Davis et al., 2005). Conversely, incomplete complementation between MiRNA and mRNA target 3'UTR triggers the repression of mRNA translation rather than mRNA cleavage and degradation (Zeng et al., 2003). This incomplete binding can prevent the initiation of mRNA translation, and can also inhibit mRNA translation that has already been initiated (Petersen et al., 2006, Nottrott et al., 2006). Incomplete complementation of miRNAs: mRNAs have showed to regulate target expression via initiating degradation pathways. This has been found act through accelerating deadenylation and decapping of the their target mRNAs (Rehwinkel et al., 2005, Wu et al., 2006). In addition, in addition to binding to the 3'UTR of target mRNA, some miRNAs have demonstrated to binding to the 5'-UTR and coding sequences of the mRNA (Tay et al., 2008). For example, in human Hela cells, which express endogenous let-7a miRNA. Let-7a can bind both 3'-UTR and 5'-UTR to mediate

translation repression of target mRNAs (Lytle et al., 2007). Thus, a variety of regulation mechanisms are involved in the regulation of mRNA by miRNA-RISC complex, which mainly depend on the miRNA: mRNA complementarity.

It is generally accepted that the passenger strand of the miRNAs duplex is degraded during miRNA biogenesis and only the guide strand is incorporated into RISC as a functional mature miRNA. However, some miRNA passenger strands are not degraded and can also target mRNAs (Yang et al., 2013, Eulalio et al., 2012, Kos et al., 2012). For example, overexpression of miR-590-3p or miR-199a-3p *in vitro* promoted cell cycle re-entry of adult cardiomyocytes and induced cardiomyocytes proliferation in both neonatal and adult animals. In a mouse model of myocardial infarction, overexpression of these miRNAs stimulated marked cardiac regeneration and almost completely recovery of cardiac functional parameters (Eulalio et al., 2012). Another passenger miRNA, miR-21-3p, is enriched in fibroblast - derived exosomes, which cause hypertrophy when taken up by cardiomyocytes (Bang et al., 2014). Transfection of pre-miR-21-3p or inhibitor of miR-21-3p in cardiomyocytes was showed an increase or opposite effect on the cardiomyocytes cell size. In addition, miR-21-3p was shown to inhibit the expression of target genes sorbin and SH3 domain-containing protein 2 (*sorbs2*) and PDZ and LIM domain 5 (*pdlim5*), which have been reported involved in the cardiac pathologies and cardiomyopathy (Cheng et al., 2010, Kakimoto et al., 2013). Furthermore, miR-21-3p expression was elevated in pericardial fluid of mice with transverse aortic constriction-induced cardiac hypertrophy and administration of miR-21-3p antagomiR to mice with angiotensin II-induced cardiac hypertrophy resulted in reduced heart/body weight ratio and decreased cardiomyocytes diameter (Bang et al., 2014). In addition, some miRNAs showed both strands were functionally inhibited target expression. Both miR-126-5p and miR-126-3p were shown to directly inhibit stromal cell-derived factor-1 alpha (*sdf-1 $\alpha$* ) to inhibit lung metastasis by breast tumour cells in a mouse xenograft model (Zhang et al., 2013c).

### 1.3.1.3 MicroRNAs Involved in PAH

#### 1.3.1.3.1 MiR-204

MiR-204 were among the first studies to show a mechanistic link between miRNA dysregulation and signalling pathways involved in the pathogenesis of PAH (Courboulin et al., 2011). The *miR-204* gene is located in the intronic region of the transient receptor potential melastatin 3 (*trpm3*) (Wang et al., 2010a). The decreased expression levels of miR-204 were found in total lung and plexiform lesions from patients with PAH, as well as animal PH models (chronic hypoxia mouse model and MCT rat model) (Courboulin et al., 2011) (Brock et al., 2014). The expression level of miR-204 also found correlated with PAH severity (Courboulin et al., 2011). In addition, *in vivo* study showed that intratracheal nebulization of miR-204 by administration with miR-204 mimics decreased the pulmonary artery pressure, right ventricular wall thickness and reduced medial hypertrophy of pulmonary arteries in the MCT-induced rat PH model (Courboulin et al., 2011). These findings suggest miR-204 is important in the pathogenesis of PAH and can be served as a potential clinical biomarker of PAH disease.

Mechanically, previous studies showed that in retinal epithelial cells and several cancer cells, miR-204 down-regulation has been demonstrated associated with enhanced proliferation and membrane potential depolarization (Lee et al., 2010, Wang et al., 2010a). The pro-proliferative phenotype was associated in part with the activation of the Src-STAT3 (accounting for *bmpr2* down-regulation) (Wong et al., 2005) and NFAT pathways in several cancer cells (Bonnet et al., 2007). In PAH setting, miR-204 is primarily expressed in PSMCs, and the expression of miR-204 is decreased in PSMCs isolated from distal pulmonary arteries from IPAH patients compared with controls (Courboulin et al., 2011). *In vitro* study showed miR-204 inhibition increased proliferation and resistance to apoptosis in control PSMCs, which were similar to those seen in the PSMCs isolated from patients with PAH. And increasing miR-204 expression level in PAH-PSMCs reversed the pro-proliferation and anti-apoptotic phenotype (Courboulin et al., 2011). These beneficial

effects of miR-204 exert on PASMCM proliferation and apoptosis activation of Src-STAT3-NFAT pathway in PASMCMs. The PAH-induced growth factors PDGF, endothelin-1 and angiotensin II can stimulate the activation of STAT3 to mediate the down-regulation of miR-204. Knockdown of STAT3 abolished the down-regulation of miR-204 in PAH-PASMCMs, which suggest STAT3 is responsible for the decreased of miR-204 in PAH-PASMCMs (Courboulin et al., 2011). The STAT3 activation suppresses the miR-204 and leads to the up-regulation of *shp2*, which is the direct target of miR-204. The increased *shp2* expression further activates the Src kinase and NFAT. STAT3 also directly induces NFATc2 expression. The activations of STAT3 and NFATc2 were observed in PAH lungs (Bonnet et al., 2007). Both *nfat* and *shp2* were needed to sustain PAH-PASMCMs proliferation and resistance to apoptosis (Courboulin et al., 2011).

The activation of miR-204-Scr-STAT3-NFAT pathway in the development of PAH also confirmed in the experimental rat model. In the MCT-induced rat model of PH, the activation of STAT3 in the pulmonary arteries is earlier than the decrease of miR-204. This further confirms the activation of STAT3 drives the down-regulation of miR-204. The down-regulation of miR-204 leads to the increase of SHP2, which further pushed up the activation of STAT3. This positive feedback between STAT-3 and miR-204 may contribute to the development and progression of PAH. Once the STAT3 activation becomes maximal, and then NFAT gets activated and results in NFAT-dependent PASMCM proliferation and resistance to apoptosis and increasing pulmonary artery remodelling and pressures (Courboulin et al., 2011). The activation of STAT3 signalling in PAH is also found in the chronic hypoxia induced mouse PH model. Administration of mesenchymal stromal cell-derived exosomes inhibited the vascular remodelling and chronic hypoxia induced PH. The mechanism of the protective effect is mesenchymal stromal cell-derived exosomes suppresses the activation of STAT3 and increases the lung levels of miR-204 (Lee et al., 2012a).

In systemic vascular diseases, reduced expression of miR-204 promotes vascular biomineralization by augmenting the expression of the transcription factor *RUNX2* (Huang et al., 2010). In the PAH disease, *runx2* expression was up-regulated in lungs, distal PAs and

primary cultured human PSMCs isolated from patients with PAH. MiR-204 inhibition induced *runx2* up-regulation and the sustained *runx2* expression activated *hif-1 $\alpha$*  activation, leading to aberrant proliferation, resistance to apoptosis and subsequent trans-differentiation of PAH-PSMCs into osteoblast-like cells. *In vivo* model showed that inhibition of *runx2* reversed the SU5416/hypoxia induced PH rat model (Ruffenach et al., 2016).

MiR-204 also involved in the DNA damage in PAH. Distal PSMCs from patients with PAH exhibit increased DNA damage and overexpression of *parp-1*. *parp-1* activation accounts for miR-204 downregulation and subsequent activation of the transcription factors nuclear factor of activated T cells (*NFAT*) and hypoxia-inducible factor 1- $\alpha$  (*HIF-1 $\alpha$* ) in PAH-PSMCs. *In vitro* *PARP-1* inhibitor using the chemical inhibitor ABT-888 in PAH-PSMCs increases miR-204 expression and thereby decreases *NFAT* and *HIF-1 $\alpha$*  activation. Inhibition of *PARP-1* *in vivo* improves PAH prognosis in MCT-and SU5416/hypoxia-induced PAH rat models (Meloche et al., 2014b), which is consistent with overexpression of miR-204 exerts protective role in the development of MCT-induced PH rat model (Courboulin et al., 2011).

### **1.3.1.3.2 MiR-21**

MiR-21 is a very extensively studied miRNA in human diseases and miR-21 has been found to be upregulated in many pathological conditions including cancer and cardiovascular diseases (Jazbutyte and Thum, 2010). There are considerable studies that have been carried out to investigate the role of miR-21 in the development of PAH using both *in vitro* cell culture and *in vivo* animal PH models. MiR-21 is significantly upregulated in human PSMCs after 6 h of hypoxia and remained high till 24 h of hypoxia (Sarkar et al., 2010). Both mature miR-21 and pri-miR-21 are increased in human PAECs after hypoxia (Parikh et al., 2012). *In situ* hybridization showed miR-21 expression increased in the distal diseased pulmonary vessels (< 200  $\mu$ m) and the plexiform lesions in patients with PAH (Bockmeyer et al., 2012, Parikh et al., 2012). In the PH animal models include chronic hypoxia induced PH model

(Yang et al., 2012), SU5415/hypoxia mice PH model, and MCT-induced rat PH model (Parikh et al., 2012) revealed increased expression of miR-21. However, another study showed that miR-21 expression significantly reduced in MCT-induced rat PH model (Caruso et al., 2010).

Due to the dysregulation of miR-21 expressions in PAH patients and various animal PH models, the effect of manipulation of miR-21 on PH progression and development was investigated. Yang and colleagues performed sequestration of miR-21 by LNA-modified anti-miR-21 treatment, either before or after chronic hypoxia exposure, diminished chronic hypoxia induced pulmonary hypertension and attenuated the pulmonary vascular remodeling in the chronic hypoxia included mouse model. The potential mechanism of this protective role is the upregulation of the putative targets of miR-21 including *bmpr2*, SATB homeobox 1 (*satb1*), and YOD1 deubiquitinase (*yod1*) (Yang et al., 2012). As the increased expression of *BMPR2* is beneficial to the development PAH (Morrell et al., 2001, Nakaoka et al., 1997). Consistent results obtained with another study use anti-miR-21 treatment in chronic hypoxia induced mice PH model, which showed reduced RVSP, and decreased pulmonary arterial muscularization but no effect on RVH (Pullamsetti et al., 2012). Contrary to these findings, Parikh and colleagues use miR-21 knockout mice exposed to the SU5416/hypoxia conditions showed exaggerated manifestations in PH phenotype such as increased RVSP, RVH and pulmonary vascular remodelling. The potential mechanism is the increased expression of ras homolog family member B (RhoB) in the vascular intima and media of small pulmonary vessels. These vessels display increased Rho kinase-dependent levels of phosphorylated myosin phosphatase in miR-21 knockout mice. In addition, these treated mice exhibits a substantial increase in the transcriptional expression of at least one Rho-dependent vasoconstrictive effector of PH, such as endothelin-1 (Parikh et al., 2012). In the pulmonary vasculature RhoB enhances vasoconstriction and remodelling pulmonary arteries and genetic deletion of RhoB prevents the development of hypoxia induced PH (Wojciak-Stothard et al., 2012). This exaggerated phenotype further confirmed by using both miR-21 knockout mice and miR-21 overexpression transgenic mice in the SU5416/hypoxia induced PH model. The potential mechanism for is the loss of

miR-21 leads to the direct activation of PDCD4/caspase-3 axis and as a consequence results in the onset of progressive PH and *vice versa* (White et al., 2014).

*In vitro*, miR-21 has been showed to modulate the cellular behaviours of PASMSs such as proliferation, migration, and contractility, which are key components contribute to the development of PAH. MiR-21 knockdown significantly reduced chronic hypoxia induced proliferation, and migration in PSMCs and overexpression of miR-21 reverses these behaviours by targeting phosphatase and tensin homologue (*pten*), programmed cell death protein 4 (*pdc4*), sprout homolog 2 (*spry2*) and peroxisome proliferator-activated receptor receptor alpha (*ppra- $\alpha$* ) (Sarkar et al., 2010) (Green et al., 2015). MiR-21 also demonstrated involved in cell cycle, cell proliferation and apoptosis by affecting the expression of proliferating cell nuclear antigen (*pcna*), *cyclin d1*, and *bcl-xl* in PSMCs (Yang et al., 2012). In addition, miR-21 expression is modulated by BMP signalling pathway. BMP4 stimulated miR-21 expression and further directly target members of the dedicator of cytokinesis (DOCK) 180-related protein superfamily including *DOCK4*, -5, and -7 to modulate cell migration and contractility (Kang et al., 2012). In PAECs, miR-21 has plentiful target genes including the proteins integral to BMP, BMPR2, and RhoB/Rho-kinase signalling, which connect miR-21 to hypoxia, inflammation and angiogenesis signalling pathways associated with the pathogenesis of PAH (Parikh et al., 2012).

From the studies discussed above, while conflicting, highlights the complex role of miR-21 in the PAH disease. The variation among different studies may due to the different experimental conditions such as animal strain and species difference, gender difference, age, and different PH models. The different pharmacological manipulation strategies of miR-21 *in vivo* also should be considered. However, based on the findings of miR-21 in PAH, it is clearly deserving further research attention designed to investigate the true potential in the development of PAH.

### 1.3.1.3.3 MiR-17/92

The miR-17-92 cluster is one of the best-characterised miRNA families located on human chromosome 13 consists of six distinct mature miRNAs: miR-17, miR-18a, miR-19a, miR-20a, miR-19b-1, and miR-92-1, each of which have a specific set of target genes that exert their functions (Tanzer and Stadler, 2004). With regard to the hypoxia and PAH, it has been reported that miR-17-92 cluster expression is regulated positively by the *c-myc* transcription factor (O'Donnell et al., 2005) and the IL-6/STAT3 pathway (Steiner et al., 2009, Brock et al., 2009). *C-myc* gene expression levels are increased in the lungs and PASMCs of the chronic hypoxia induced rat PH model (Cai et al., 1996, Luo et al., 1996), which can active the expression of miR-17-92 cluster (specifically miR-17-5p and miR-20a) directly target transcription factor *E2F1*, which can promote cell cycle progression (O'Donnell et al., 2005, Woods et al., 2007). The IL-6 expression levels were elevated in the PAH patients and animal models of PH. And miR-17-92 cluster is modulated by IL-6. IL-6 induced arteriopathic changes were accompanied with pro-proliferative transcription factor C-myc, which is a potential mechanism to induce the expression of miR-17-92 cluster in the PAH setting (Steiner et al., 2009). In addition, IL-6 also activates STAT3 in human PAECs, which bind directly to a highly conserved STAT3 binding site in the promoter region of miR-17-92 gene to regulate miR-17-92 expression (Brock et al., 2009).

A reduction or mutation of *bmpr2* is found in majority of HPAH and isolated cases of IPAH. *In silico* analysis revealed the *bmpr2* was a putative target of the miR-17-92 cluster. Experimental overexpression of miR-17-92 results in a strong reduction of the *BMPR2* protein, and reporter gene assay showed that *bmpr2* is directed targeted by miR-17-5p and miR-20a in PAECs. Interestingly, the persistent activation of STAT3 also leads to repressed protein expression of *BMPR2* (Brock et al., 2009). These studies describe novel IL-6-STAT3-miR-17-92-BMPR2 pathways involved in the development of PAH and provide a possible mechanism to explain the loss of *bmpr2* during PAH development.

Individual miRNAs from this cluster have been investigated in PAH. AntagomiR of

miR-17 treatment reversed the PH phenotype in both the chronic hypoxia induced mouse model and MCT rat model. The potential mechanism is that miR-17 targets cyclin-dependent kinase inhibitor 1A (p21) to regulate PASMCs proliferation, which overexpression of miR-17 reduces the expression of p21 and increases the proliferation of PASMCs (Pullamsetti et al., 2012). In addition, MiR-17 expression levels are significantly elevated with the chronic hypoxia exposure and associated with an increase in arginase II in PASMCs, and their expression levels are positively related (Jin et al., 2014). Furthermore, Chen and colleagues found decreased expression levels of miR-17-92 cluster in PASMCs from patients with PAH as well as the decrease of TGF- $\beta$  and SMC markers. Overexpression of miR-17-92 restored the expression of TGF- $\beta$ , Smad3, and SMC markers in patients with IPAH. SMC-specific knockout of miR-17-92 attenuated chronic hypoxia induced PH in mice, and reconstitution of miR-17-92 restored chronic hypoxia induced PH in these mice. The mechanism is that miR-17-92 direct target PDZ and LIM domain 5 (*pdlim5*), which expression levels are elevated in hypertensive human and mouse PASMCs. Suppression *pdlim5* increased expression of SMC marker and enhanced TGF- $\beta$ /Smad2/3 activity *in vitro* and enhanced chronic hypoxia induced PH *in vivo*, whereas overexpression of *pdlim5* attenuated chronic hypoxia induced PH (Chen et al., 2015). This study demonstrates that miR-17-92 induced TGF- $\beta$ /Smad3 pathway via inhibiting *pdlim5* expression contributing to the pathogenesis of PAH.

### **1.3.2 Long non-coding RNAs (lncRNAs)**

Long noncoding RNAs (lncRNAs) are currently defined as RNA transcripts longer than 200 nucleotides with no potential to encode for functional proteins of more than 30 amino acids, which separate them from miRNAs and from protein-coding genes (Rinn and Chang, 2012). Due to the development of next generation sequencing techniques, many new lncRNAs are discovered and annotated each year. Thus far, more than 100,000 lncRNA genes have been defined in human genome. In comparison, there are currently 20,345 annotated protein-coding genes in the human genome. This suggests a dominant role of lncRNA genes in mammalian genome (O'Donnell et al., 2005). The biological functions of most lncRNAs are currently still unknown, as only a handful of lncRNAs have been studied in detail. LncRNAs can be classified into different subtypes based on their genomic location: sense lncRNAs (when they overlap one or more exons of another transcript on the same strand); antisense lncRNAs (when they overlap one or more exons of another transcript on the opposite strand); bidirectional lncRNAs (when their expression and that of a neighbouring coding transcript on the opposite strand are initiated in close genomic proximity); intronic lncRNAs (when they are derived from an intron of a second transcript); and intergenic lncRNAs (when found as an independent unit within the genomic interval between two genes) (Figure 1.7) (Thum and Condorelli, 2015).

#### **1.3.2.1 Biogenesis and Function of LncRNAs**

LncRNAs can be transcribed from intergenic regions, promoter regions or be interleaved, overlapping or antisense to annotated protein-coding genes and display remarkable similarity to classical mRNA in that they are generally transcribed by RNA polymerase II. Following RNA polymerase production, the individual lncRNA is subjected to 5'-capped (m<sup>7</sup>G), alternative splicing, RNA editing, and 3'-polyadenylated (Sun and Kraus, 2015). Final lncRNA developments essentially involve the formation of a stable secondary (and tertiary) structure, which confer the individual lncRNA with its unique function roles (Li and Chen, 2013). In most cases, they lack any biochemical distinction from mRNAs be-

sides the absence of translated open reading frame (ORF). There are other more general features of lncRNAs that distinguish them from mRNAs, including their shorter length, having fewer but longer exons, and being expressed at relatively low levels with poor primary sequence conservation (Derrien et al., 2012, Cabili et al., 2011). Based on their molecular mechanisms of action, lncRNAs can be classified into four archetypes (Fig 1-6) (Wang and Chang, 2011). An individual lncRNA may fulfil several archetypes and these archetypes are not meant to be mutually exclusive.

#### Archetype I: Signals.

lncRNAs are expressed in cell type-, tissue-, developmental stage or disease state-specific manner (Flynn and Chang, 2014, Batista and Chang, 2013) and respond to diverse stimuli, suggesting that lncRNA expression is under considerable transcriptional control. Thus, lncRNA can serve as molecular signals due to the temporal and spatial restriction of their transcription to integrate developmental cues and interpret cellular context or as a response to specific stimuli. For example, lincRNA-RoR is required in the process of somatic cell reprogramming of induced-pluripotent stem cells (iPSCs). LincRNA-RoR was showed to be directly targeted by the key pluripotency factors octamer-binding transcription factor 4 (*OCT4*), SYR box-containing factor 2 (*SOX2*), and homeobox protein NANOG (*NANOG*) through colocalisation of the three factors in close proximity to lincRNA-ROR promoters (Loewer et al., 2010).

#### Archetype II : Decoys.

The central role of lncRNAs is regulating transcription both positively and negatively (Guenther et al., 2007). This indicates that lncRNAs regulate transcription via diverse mechanisms, a major one of which is to act molecular decoys. This archetype of lncRNA is transcribed and then binds and titrates away a target protein but does not exert any additional functions functions (Wang and Chang, 2011). Thus lncRNAs within this archetype can function as a “molecular sink” for RNA-binding proteins (RBPs), transcription factors, chromatin modifiers, or other regulatory factors. For example, the lncRNA p21-associated ncRNA DNA damage-activated (PANDA) is induced in a p53-dependent manner in human

fetal lung fibroblasts FL3. The PANDA is located approximately 5 kilobases upstream of the *cdkn1a* transcriptional start site (TSS) together with 5'-capped and polyadenylated non-spliced lncRNA that is transcribed antisense to *cdkn1a*. The induction of PANDA during DNA damage is p53-dependent. Depletion of PANDA or *cdkn1a* has no effect on each other's response to DNA damage. Importantly, PANDA acts as a decoy binding to transcription factor *NF-YA* to prevent *NF-YA* binding to occupy target gene promoter to repress expression of pro-apoptotic genes (Hung et al., 2011).

#### Archetype III: Guides.

The guide lncRNAs act as molecular chaperones and localise the ribonucleoprotein complex to specific genomic targets. These lncRNAs can also guide changes in gene expression either in *cis* (on neighbouring genes) or in *trans* (distantly located genes) in a manner that is difficult to predicted based on the lncRNA sequence. For example, the lateral mesoderm-specific lncRNA fetal-lethal non-coding development regulatory RNA (Fendrr) can bind to both the polycomb repressive complex 2 (PRC2) and Trithorax group/Mixed lineage leukemia (TrxG/MLL) complexes, which play pivotal roles in determining the activation state of gene controlling pluripotency, lineage commitment, and cell differentiation (Grote et al., 2013). Fendrr can guide PRC2 to target genes to increase PRC2 occupancy and H3K27 trimethylation or decrease H3K4 trimethylation (Grote et al., 2013). Similarly, LincRNA-p21, which is regulated by p53, can guide hnRNP-K to the promoter of the p21 gene and act as a co-activator for p53-dependent p21 transcription to mediate gene repression and apoptosis in the p53 pathway (Huarte et al., 2010). This study proposes a model whereby transcription factors activate lncRNAs that serve as key repressors by physically associating with repressive complexes and modulates their localization to set of previously active genes (Huarte et al., 2010).

#### Archetype IV: Scaffolds.

Scaffold lncRNAs have multiple domains, enabling them to form complexes with proteins such as transcription factors or components of chromatin modifying complexes that allows them to function as transcriptional activators or repressors. For example, the lncRNA

HOTAIR serves as a scaffold for at least two distinct histone modification complexes. The 5' domain of HOTAIR binds Polycomb repressive complex-2 (PRC2), whereas its 3' domain binds to the LSD1/CoREST/REST complex (Tsai et al., 2010). This ability to tether two distinct complexes enables RNA-mediated assembly of PRC2 and LSD1 and coordinates targeting of PRC2 and LSD1 to chromatin for coupled histone H3 lysine 27 methylation and lysine 4 demethylation (Tsai et al., 2010). Taken together, these studies demonstrate that lncRNAs can serve as scaffolds by providing surfaces to assemble select histone modification enzymes to specify the pattern of histone modifications on target genes (Figure 1.7).

### **1.3.2.2 Long non-coding RNA in PAH**

Accumulating evidence suggests that lncRNAs play a significant role in a wide variety of important biological processes including regulating gene transcription, splicing, translation, cell cycle and apoptosis, cell differentiation, stem cell pluripotency and reprogramming, and heat shock response (Loewer et al., 2010). In addition, lncRNAs have been demonstrated play important roles in many diseases including cancer (Sahu et al., 2015, Huarte, 2015) and cardiovascular disease (Uchida and Dimmeler, 2015, Lorenzen and Thum, 2016, Schonrock et al., 2012). However, to date there have been very few studies investigating the role of lncRNA in PAH. The only study on lncRNA in PAH to date assessed the expression of lncRNAs in lung tissue from rats following hypoxia-mediated induction of PH (Wang et al., 2016). Microarray analysis and qRT-PCR target validation revealed 362 lncRNAs that were differentially expressed in hypoxic animals compared to normoxic controls (Wang et al., 2016). A related study performed microarray analysis on endothelial tissues from the pulmonary arteries of chronic thromboembolic pulmonary hypertension (CTEPH) patients and healthy controls, identifying 185 differentially-expressed lncRNAs observed in the CTEPH tissues compared with healthy controls. Gene ontology and pathway analysis suggested that these lncRNAs might play a role in the regulation of the inflammatory response, responses to endogenous stimuli and antigen processing and presentation (Gu et al., 2015). In addition, RNA-seq analysed the expression of lncRNAs in hu-

man heart failure, which is the primary cause of death in patients with PAH. There are 105 differentially expressed lncRNAs in heart failure heart compared with donor hearts (Di Salvo et al., 2015). The expression profiles of lncRNAs in animal models and human tissues show that lncRNAs may participate into the pathogenesis of PAH.

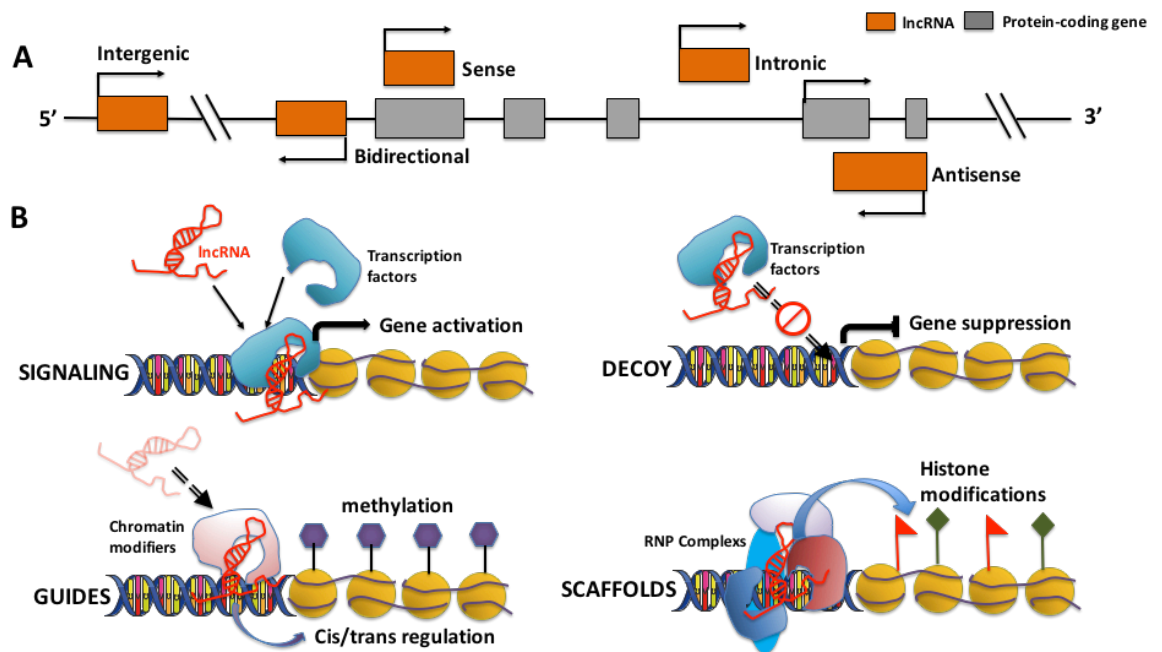


**Figure 1.7 Overview of the genome location and functions of lncRNAs**

(A) Based on their genomic locations, lncRNA transcripts can be classified as sense (transcribed from the sense strand of a protein-coding gene) antisense (transcribed from the antisense strand of a protein-coding gene) intronic (transcribed entirely from an intron of a protein-coding gene); intergenic (transcribed sequences is not located near any other protein-coding loci) or bidirectional (transcribed sequences are located on the opposite strand from a protein-coding gene whose transcription is initiated less than 1000 base pairs away). (B) The main functions of lncRNA include SIGNALING: lncRNA can function as molecular signal or indicator of transcriptional activity; DECOY: lncRNAs can preclude the access of regulatory proteins to DNA; GUIDES: lncRNA can be required for the localisation of specific protein complexes either in *cis* (on neighbouring genes) or in *trans* (on distantly located genes); SCAFFOLDS: lncRNAs can serve as adaptors to bring two or more proteins into discrete complexes (adapted from (Deng et al., 2016)).

## 1.4 Exosomes

Extracellular vehicles (EVs) consist of a lipid bilayer membrane, containing diverse cargoes including proteins, RNA species (mRNA, miRNA, lncRNA, and other RNA species), DNAs (mtDNA, ssDNA, and dsDNA), and lipids that can be transported and exchanged between cells as a means of intercellular communication at both paracrine and systemic levels. EVs are released from virtually all cell types (Simpson et al., 2009, Colombo et al., 2014, Rajendran et al., 2014). A number of different EV subpopulations have been described, classified based on their size and mode of biogenesis. The most extensively studied of these are exosomes, which range from 30 to 130 nm in diameter and are generated by reverse budding of multivesicular bodies within cells before their secretion (Raposo and Stoorvogel, 2013). Other notable EVs include microvesicles (100 nm to 1  $\mu$ m in diameter), which are directly shed from the plasma membrane of cells, and apoptotic bodies (ranging from 1  $\mu$ m to  $> 2 \mu$ m in diameter), which arise from cells undergoing apoptosis.

### 1.4.1 Exosome Biogenesis

The generation of exosomes through budding from the limiting membrane of intracellular vesicles was first reported in sheep during reticulocyte maturation (Pan et al., 1985). Exosome biogenesis is initiated when small amounts of intracellular fluid are engulfed, forming a small intracellular body called an endosome (They et al., 2002, Keller et al., 2006). These early endosomes are subjected to a maturation process that includes an interaction with the Golgi complex to develop into the late endosome, which is characterised by the formation of intraluminal vesicles (ILV) inside the lumen of the endosome. Endosome maturation can also be detected by observing a change in their shape and location: while early endosomes are tube-like in shape and are usually located in the outer portion of the cytoplasm, the late endosome is spherical and found closer to the nucleus (Keller et al., 2006). ILVs are formed by inward budding of the endosomal membrane, randomly engulfing portions of the cytosol and incorporating transmembrane and peripheral proteins into the invaginating membrane. Late endosomes that contain ILVs are called multivesicular bodies (MVBs) (van Niel et al., 2006, They et al., 1999). MVBs undergo fusion with

lysosomes, following which the MVB contents are degraded through hydrolysis. Subsequent lysosome fusion with the plasma membrane leads to the release and exocytosis of ILVs, also known as exosomes (Figure 1.8) (Waldenstrom and Ronquist, 2014, Beach et al., 2014).

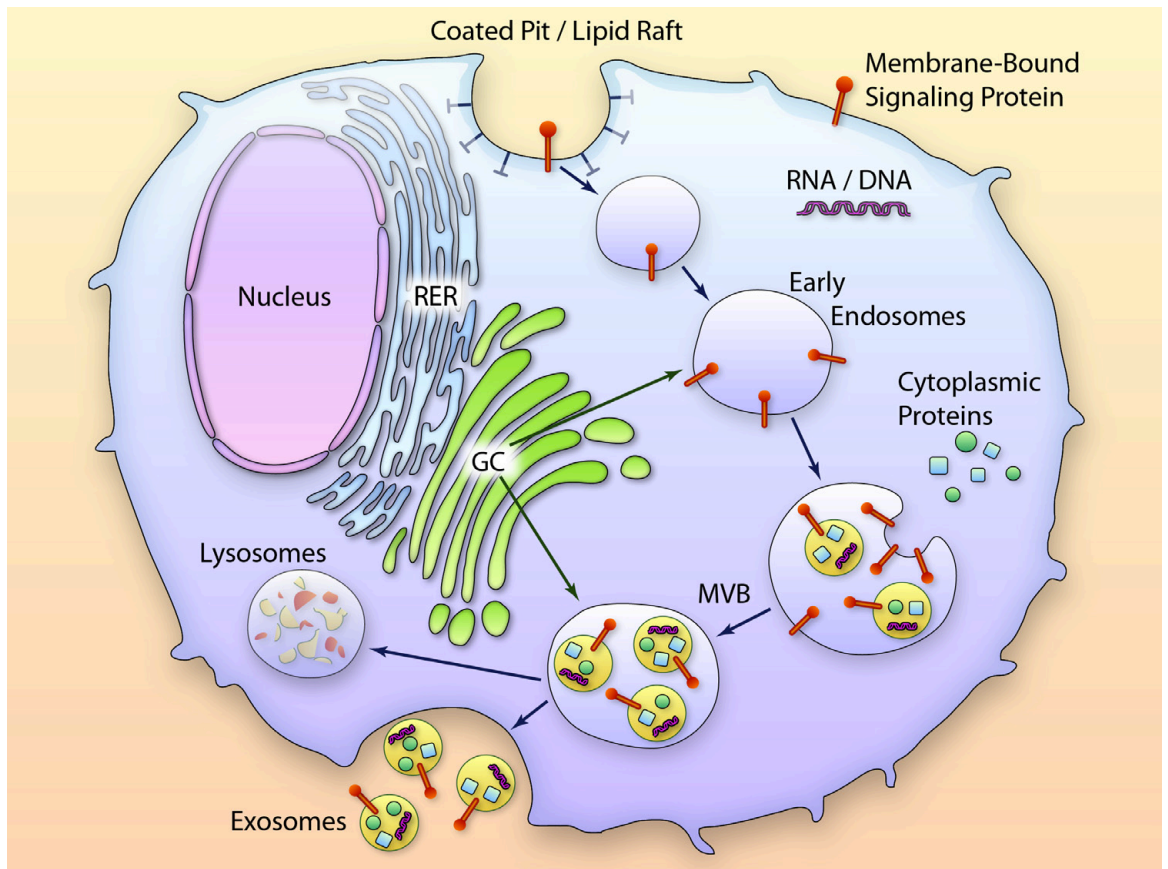


**Figure 1.8 Biogenesis of exosomes**

Exosomes are generated in the late endosomal compartment and carry recycled proteins from coated pits/lipid rafts in the cellular membrane, proteins directly sorted to the MVBs from rough endoplasmic reticulum (RER) and Golgi complex (GC), mRNA, microRNA, and DNA. Note that the generation of exosomes by inward budding of the limiting membrane of MVB ensures that the membrane-bound proteins preserve the same orientation and folding on the exosomal membrane as those on the plasma membrane. The exosome-filled MVBs are either fused with the plasma membrane to release exosomes or sent to lysosomes for degradation. Adapted from (Waldenstrom and Ronquist, 2014)

## 1.4.2 Exosome Composition

Exosomes contain various types of biomolecules including protein, carbohydrates, lipids and nucleic acids. In addition to most cell lines, exosomes have been isolated from most body fluids including saliva, urine, and plasma (Mathivanan et al., 2010, Dragovic et al., 2011, Caby et al., 2005, Lasser et al., 2011). Exosome composition is dynamic and varies depending on the cellular origin and release site, as well as the body's physiological or pathological state (Sreekumar et al., 2010). The lipid composition of exosomes includes cholesterol, sphingomyelin, hexosylceramides, phosphatidylserine, and saturated fatty acids, all of which are components of the synthesising cell plasma membrane (Colombo et al., 2014). The proteome of exosomes includes endosomal, plasma, cytosolic, and nuclear proteins. Exosomes also contain tetraspanins (*CD9*, *CD63*, *CD81*, and *CD82*), as well as co-stimulatory molecules (*CD86*) and adhesion molecules (*CD11b* and *CD54*). Other common exosomal proteins include heat shock proteins (*HSP70* and *HSP90*), integrins, MHC class II proteins, epithelial cell adhesion molecules (EpCAM), and members of the human epidermal growth factor receptor (HER) family (Beach et al., 2014, Kalluri, 2016). Many exosomal proteins are required for exosome biogenesis, while other proteins that are enriched in exosomes reflect the composition of the cell or tissue of origin. Exosome protein composition proteins present on the surface of the exosomes can engage cell surface receptors on recipient cells to induce intracellular signalling (Raposo and Stoorvogel, 2013, Colombo et al., 2014, Zhang et al., 2015). For example, exosomes produced by human cancer cells (A431 human squamous cell carcinoma cell line) containing activated endothelial growth factor receptors (EGFR) can be taken up by cultured endothelial cells, in which they elicit EGFR-dependent responses, including activation of mitogen-activated protein kinases (MAPK) and Akt pathways (Al-Nedawi et al., 2009). Moreover, a number of proteomic and transcriptomic profiling analyses have been performed on exosomes showed that exosomes contain cell-type specific proteins that define their functional activity (Simpson et al., 2008, Thery et al., 2001). Thus, the composition of the exosome membrane, and by extension the state of the cell from which the exosomes are released, is a critical determining factor in their biological function.

In addition to their protein and lipid cargoes, exosomes also contain diverse nucleic acid species, including mRNA and miRNA. Pioneering work carried out by two independent groups demonstrated that exosomes could –mediate the transfer of mRNA and miRNAs from host to recipient cells (Ratajczak et al., 2006, Valadi et al., 2007). Subsequently, other RNA species were also founded in exosomes including transfer RNAs (tRNAs), lncRNAs, and viral RNA (Gusachenko et al., 2013, Yang et al., 2016). Importantly, different types of RNAs such as miRNAs and lncRNAs present within exosomes are biologically active, indicating that they can function to modulate the protein profile, transcriptome, and cellular state of the recipient cells (Lee et al., 2012c, Melo et al., 2014, Chen et al., 2014b). In addition, exosomal RNA content can also vary depending on the cellular origin, the physiological or pathological state of the originating cell, indicating that the incorporation of RNA into exosomes is a regulated and selective event (Schorey and Harding, 2016).

### **1.4.3 The Function of Exosomes**

As shown in the previous sections, there are a large variety of constitutive elements in exosomes including > 4563 proteins, 193 lipids, 1639 mRNA, 764 miRNA and other components, underlining the complexity and potential functional diversity of exosomes (Mathivanan et al., 2012, Mathivanan and Simpson, 2009). Exosomes are emerging as important mediators of cell-to-cell communication in both the physiological and pathological context such as cancer (Zhang et al., 2015), and cardiovascular diseases (Zhao et al., 2015c). Exosomes can be transported between different cells and can activate or inactivate different pathways on surrounding or remotely-located cells depending on their molecular composition, which is influenced by the activation state of the secreting cell and cell type of origin. Exosomes can also interact with recipient target cells by fusion with the plasma membrane or adhesion to corresponding receptors on the plasma membrane (Lakkaraju and Rodriguez-Boulan, 2008). When the recipient cells uptake the exosomes, which will mediate functional and phenotypic changes in recipient cells such as proliferation and migration (Pfeifer et al., 2015). Furthermore, exosomes also observed in the blood, body flu-

ids and tissues, which suggest that exosomes can be served as novel biomarkers for clinical diagnosis (Lin et al., 2015).

#### **1.4.4 The Role of Exosomes in PAH**

There are several studies showing the emerging role of exosomes in PAH. Aslam and colleagues administered bone marrow stromal cell-conditioned media (BMSC-CM) via the superficial temporal vein to neonatal mice on postnatal day 4 of a 14-day period of hypoxia. BMSC-CM injection reduced alveolar loss and lung inflammation, attenuating both pulmonary vessel remodelling and alveolar injury, and preventing the development of pulmonary hypertension (Aslam et al., 2009). A related study used mesenchymal stem cell conditioned media (MSC-CM) from hypoxic cells to treat pulmonary artery rings, which significantly reduced acute hypoxia induced pulmonary vasoconstriction (Patel et al., 2007). These studies suggested that BMSCs and MSCs could have a protective role in PAH by acting through a paracrine mechanism. Subsequent studies showed that both BMSCs and MSCs could release exosomes into conditioned media (Wang et al., 2014, Yu et al., 2014), indicating that this protective role may be due to the biological functions of the secreted exosomes. The first demonstration of the therapeutic potential of MSC-derived exosomes for pulmonary hypertension was achieved by Lee and colleagues by using fractionated mouse and human umbilical cord MSC-CM and showed that the biologically active component included exosomes (Lee et al., 2012a). In the chronic hypoxia induced mouse model of PH, intravenous delivery of MSC-derived exosomes suppressed the influx of macrophages to the lungs of hypoxic animals, as well as the induction of proinflammatory and proliferative mediators, inhibiting vascular remodelling. In addition, MSC-derived exosomes suppressed the hypoxic activation of STAT3 and upregulation of the miR-17 superfamily, increasing the expression of miR-204 (Lee et al., 2012a). Intravenous injection of MSC-derived microvesicles in the MCT-induced rat PH model also ameliorated the mean pulmonary artery pressure (mPAP), mean right ventricular pressure (mRVP), RVH, and pulmonary arteriole area index and thickness index (Chen et al., 2014a). These studies show administration of MSC-derived microvesicles/exosomes produce similar beneficial

effects in different animal models of PH, which provide a potential therapeutic application of cell-free approach in stem cell therapy in PAH. The potential mechanisms underlie the protective effect of MSC-derived exosomes are dependent on their cargoes, such as miRNAs. For example, the injection of exosomes derived from the plasma and lung from MCT-induced mice PH model increased the RVH and the pulmonary vascular remodelling in healthy mice. MSC-derived exosomes prevented any increase in RVH and pulmonary vascular remodelling when given at the time of MCT injection and reversed the increase in these indices when given after MCT administration. The microarray analyses of the exosomes from MCT-induced mice PH and human IPAH patients showed increased expression of miRNA-19b, 20a, 20b, and -145, whereas miRNAs isolated from MSC-derived exosomes had increased levels of anti-inflammatory, anti-proliferative miRNAs including miRNA-34a, -122, -124, and -127 (Aliotta et al., 2016, Aliotta et al., 2013).

## 1.5 Aims

Building evidence indicates that ncRNAs (particularly miRNAs and lncRNAs) may be central mediators of PAH pathogenesis. However, despite intensive studies of miRNAs in PAH, the mechanisms of miRNA regulating the disease onset and pathogenesis are still largely unknown. In particular, there is a paucity of data on how exosome RNA cargoes influence the dysfunctional vascular cell behaviour that characterises PAH. Moreover, there have been very few studies investigating the role of lncRNAs in PAH. Therefore, the principal research aim of this thesis was to investigate the role of miR-143 in the pulmonary vasculature using clinical samples from PAH patients, *in vivo* models and *in vitro* experiments. The specific aims of this project were:

- To identify the role of miR-143 in the development of PAH using both *in vivo* and *in vitro* techniques
- To investigate the role of exosomal miR-143 in cell-to-cell communication between pulmonary vascular cells during PAH pathogenesis
- To determine the role of the lncRNAs *MYOSLID* and *Myolnc16* in human pulmonary

## **2 Materials & Methods**

## **2.1 Chemicals**

All chemicals and reagents unless otherwise indicated were supplied from Sigma-Aldrich (Dorset, UK). All tissue culture reagents unless otherwise stated were obtained from Gibco (Paisley, UK). All transfection reagents were purchased from Life Technologies (Paisley, UK) unless otherwise stated.

## **2.2 Ethical Information**

All experimental procedures conform to the United Kingdom Animal Procedures Act (1986) and to the 'Guide for the Care and Use of Laboratory Animals' published by the US National Institutes of Health (NIH publication No. 85-23, revised 1996). All transgenic mice were bred under the Home Office project licence 60/4429 held by Professor A. H. Baker (University of Glasgow, UK). *In vivo* procedures using the hypoxic mice model of PH were conducted under Home Office project licence 60/3773 held by Professor M. R. MacLean (University of Glasgow, UK) and Lin Deng personal licence 60/13805 (University of Glasgow, UK). Experimental procedures using human pulmonary artery smooth muscle cells conform to the principles outlined in the declaration of Helsinki.

## **2.3 Animals**

All animals were housed either at the Central Research Facility (CRF) or the licensed facility located in the West Medical Building, University of Glasgow. All animals were maintained in a continuous 12 h light/dark cycle with access to water and food *ad libitum*. Cages were cleaned and replaced twice a week. The genetically modified animals were ear clipped by CRF staff and genetic background confirmed by genotyping.

### **2.3.1 Wild-type Mice**

Inbred wild-type (WT) mice (C57 BL6/J) at 7 weeks old were obtained from Charles River (United Kingdom). The mice were housed at the CRF for a one-week acclimatization and

monitoring period before any experimental procedures were performed.

### **2.3.2 MiR-143 Knockout Mice**

MiR-143 knockout (KO) mice were kindly supplied by Eric Olson (University of Texas SouthWestern, USA). The KO mice were generated at the University of Texas SouthWestern and have previously been described (Xin et al., 2009). Briefly, the targeting strategy deleted the 70-bp pre-miRNA stem-loop sequence of miR-143 and replaced it with a neomycin resistance cassette flanked by loxP sites. Chimeric mice obtained by blastocyst injection of targeted embryonic stem (EC) cells transmitted the mutant allele through the germline, yielding mice heterozygous for miR-143 allele. The neomycin resistance cassette was removed by breeding these mice with mice expressing a ubiquitously expressed CAG-Cre transgene. Breeding of these heterozygous mice produced global knockout of the miR-143.

### **2.3.3 Chronic Hypoxia Model of PH**

Pulmonary hypertension (PH) was induced in mice by exposure to chronic hypoxia using a hypobaric hypoxia chamber. The hypoxic chamber was depressurised over the course of two days to 550 mbar (equivalent to 10% O<sub>2</sub>) to allow for acclimatization of animals. The development of chronic hypoxic PH in mice was achieved through a continuous 14-day exposure to chronic hypoxia resulting in pulmonary vasoconstriction (Hoepfer and Welte, 2006). Normoxic mice were exposed to atmospheric pressure. The temperature and relative humidity were constantly monitored and cages were changed and cleaned every three days, with food and water accessible *ad libitum*.

## **2.4 AntimiR-143/145 Administration**

An antimiRNA targeting mature miR-143/145 (antimiR-143/145) was used to silence miR-143-3p and miR-145-5p *in vivo*. AntimiR-143/145 (in collaboration with miRagen Therapeutics Ltd, Boulder, Colorado) are 16 nt in length with phosphorothioate backbones and consisted of a mixture of LNA and DNA bases complementary to the 5' end of mature

miR-143-3p (antimiR-143-3p) or miR-145-5p (antimiR-145-5p). The antimiRNA was suspended in PBS at 5 mg/kg or 25 mg/kg and stored at -80 °C. Scramble/control antimiRNA (similar molecular composition to the antimiR-143/145 but directed against a miRNA in *C.elegans*) was used as control.

#### **2.4.1 PAH Prevention Study**

Adult female C57BL/6J mice (aged 8 weeks) were administered antimiR-143-3p, control antimiRNA or PBS subcutaneously at a dose of 25 mg/kg at day 0 and day 7 in a blinded study. Mice were maintained in hypoxic or normoxic conditions for 14 days. On day 14, hemodynamic pressures were taken and right ventricle hypertrophy (RVH) measured prior to tissue harvest. The design of the antimiR-143-3p prevention study is shown in Figure 3-11 (Chapter 3).

#### **2.4.2 PAH Reversal of Study**

Adult female C57BL/6J mice (8 weeks old) were maintained in a hypoxic chamber (10% O<sub>2</sub>) for 14 days to develop the PH phenotype. Then, subcutaneous administration of antimiR-143-3p, control antimiRNA or PBS was performed at a dose of 25 mg/kg on day 14 and day 17 in a blinded study with another 7 days chronic hypoxia exposure. On day 21, hemodynamic pressures were taken and right ventricle hypertrophy (RVH) measured prior to tissue harvest. The antimiR-143-3p reversal *in vivo* study design is shown in Figure 3-15 (Chapter 3).

#### **2.4.3 Intranasal Delivery of antimiR-145-5p**

Adult female C57BL/6J mice (aged 8 weeks) were treated with antimiR-145-5p by intranasal delivery. All intranasal instillations were performed using 200 µl sterile pipette tips, with fresh tips used for each mouse. Prior to intranasal instillation, the mice were anaesthetised via exposure to 3% (v/v) isoflurane in O<sub>2</sub>. Once the animals were under shallow anaesthesia, mice were held with the body tilted at a 45° angle. Using a 200 µl pipette, 25 µl were administered dropwise to each nare, waiting between drips to ensure the

mouse has inhaled the liquid. The total administration volume did not exceed 50  $\mu$ l (25/nare). Animals were then returned to their cages.

Normoxic animals received intranasal instillation of antimiR-145-5p at day 1, 7, 14, and 21, with mice culled at day 28 for tissue harvest. Animals maintained in hypoxic conditions received antimiR-145-5p by intranasal instillation at days 1 and 7 (under normoxic conditions), and were then maintained in a hypoxic chamber for two weeks from day 14 of the procedure, with a further two doses of antimiRNA at days 14 and 21. Hemodynamic measurements, RVH assessment and tissues harvests were performed on day 28. The anti-miR-145-5p intranasal delivery study design is shown in Figure 3.19 and Figure 3.22 (Chapter 3).

#### **2.4.4 Hypoxia/SU5416 rat model of PH**

Adult male Wistar Kyoto rats (150-200 g body weight) were maintained in normoxic (~21% O<sub>2</sub>) or in a normobaric hypoxic chamber (10% O<sub>2</sub>) for 14 days with subcutaneous administration of SU5416 or vehicle at a dose of 20 mg/kg on day 0. This was then immediately followed by varying lengths of time in normoxia (Figure 2.1). At each time point a group of animals (n = 5) were tested for hemodynamic pressures and tissues were harvested.

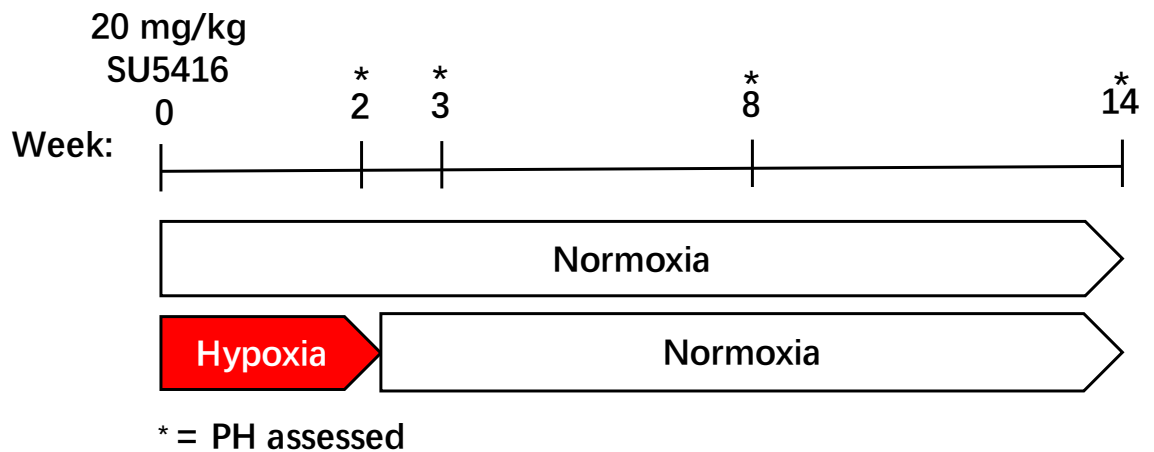


**Figure 2.1 Rat 14 week hypoxia/SU5416 in vivo study design**

Male Wistar Kyoto rats were maintained in normoxic or hypoxic conditions for 14 days with SU5416 or vehicle administered subcutaneously at 20 mg/kg on day 0. This was then followed by varying lengths of time in normoxic conditions. At each time point, hemodynamic measurements were taken along with right ventricular hypertrophy assessment and tissues harvested.

### 2.4.5 Neonatal calf model

The neonatal calf model of severe hypoxia-induced pulmonary hypertension includes the development of pulmonary artery (PA) pressure equal to, or exceeding, systemic pressure, accompanied by remarkable PA remodelling with medial and adventitial thickening, as well as perivascular inflammation. Briefly, one-day-old male Holstein calves were exposed to hypobaric hypoxia (PB = 445 mmHg) for 2 weeks, while age-matched controls were kept at ambient Denver altitude (PB = 640 mmHg). Standard veterinary care was used following Institutional guidelines, and procedures were approved by Colorado State University IACUC and performed at Department of Physiology, School of Veterinary Medicine, Colorado State University (Fort Collins, CO). Animals were euthanized by overdose of sodium pentobarbital (160 mg/kg body weight).

## **2.5 Assessment of PH**

### **2.5.1 Anaesthetic Induction**

Anaesthesia was induced in an induction chamber containing 3% (v/v) isoflurane (Abbot Laboratories, Berkshire, United Kingdom) supplemented with O<sub>2</sub> (flow rate, 0.5 L/min). Post-induction, mice were immediately weighed before being enclosed in a facemask supplied with 1.5% (v/v) isoflurane supplemented with O<sub>2</sub> (flow rate, 0.5 L/min). The appropriate level of anaesthesia was confirmed by the absence of hind limb reflex before and throughout the surgery.

### **2.5.2 Right Ventricular Systolic Pressure measurements**

Right ventricular systolic pressure (RVSP) was measured by a transdiaphragmatic approach by catheterization of the right ventricle of the heart to allow measurement of right ventricular pressure (RVP). The continuous measurement of RVSP was achieved by using a calibrated 25 mm gauge heparinized saline filled needle attached to an Elcomatic E751A pressure transducer connected a MP100 data acquisition system (BIOPAC Systems Inc, Santa Barbara, USA). Specifically, mean RVSP, systolic and diastolic RVSP were measured at three independent areas of the steady trace.

Briefly, the anterior sternum was exposed by removing a small portion of skin from the ventral chest. A 25 mm gauge heparinised needle was centrally aligned and then advanced into the mid-portion of the abdomen using a micromanipulator (Warner Instruments, Connecticut, U.S.A). Needle entry into the diaphragm has a negative effect on pressure and RVSP was monitored to ensure correct positioning and puncture of the right ventricle free wall by looking for a characteristic waveform (such as in Figure 2.1). Following a five-to-eight min trace, the measurement of RVSP was used as a surrogate of PH. For analysis, the RVSP and heart rate was obtained from the pressure readings. A noticeable puncture wound could be found in the right ventricle free wall to confirm the needle puncturing into the right ventricle wall.

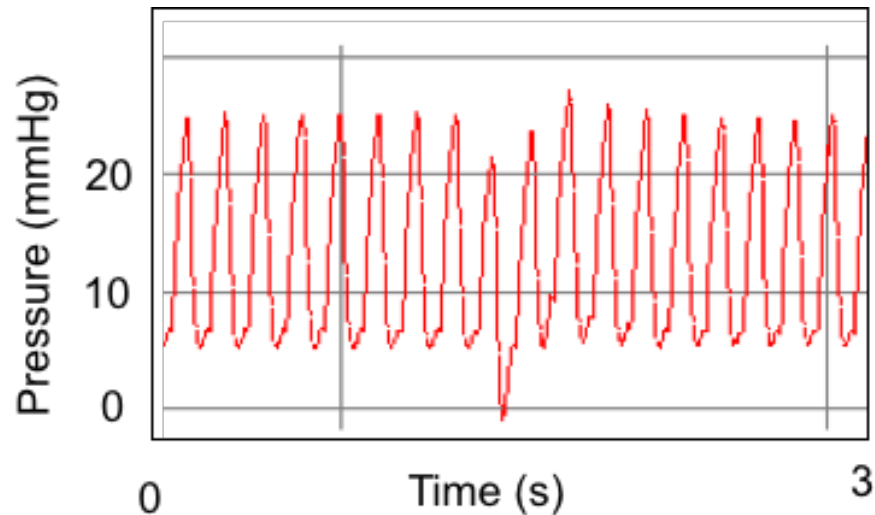


**Figure 2.2 Representative recording of right ventricular systolic pressure**

Three-second representative measurement of right ventricular systolic pressure in normoxia mice. Y-axis expressed in mmHg.

### **2.5.3 Systemic Arterial Pressure**

The systemic arterial pressure (SAP) was measured by cannulation of the left common carotid artery. An incision was made in the ventral neck and we carefully blunt dissected the smooth muscle layers until the trachea was reached. The left common carotid artery is typically positioned ~ 2 mm lateral (left) and less than ~ 1mm posterior to the trachea and can be identified by its pulsation and the presence of the vagus nerve (white in appearance) running alongside. Then the carotid artery was isolated by precision dissection from the vagus nerve without severing the nerve and cleaned of any connecting tissues. The carotid artery was ligated at the proximal (head) end with a surgical silk monofilament suture (size 5.0, Harvard Apparatus, Massachusetts, U.S.A). A microsurgical artery clip (Fine Science Tools, Heidelberg, Germany, FST18055-04) was placed on the distal end of the carotid artery to temporarily occlude blood flow through the lumen proximal to the heart. A small

incision was made in the carotid artery above the suture tie and inserted a heparinised saline-filled micro-cannula (Harvard Apparatus, Massachusetts, U.S.A) with curved forceps to open the incision. A micro-cannula was then advanced gently into the lumen of the carotid artery and ligated in place with a 5.0 silk suture before removal of the artery clip. Continuous measurement of SAP was obtained using the same technique as for RVSP using an Elcomatic E751A pressure transducer and an MP100 data acquisition system.

After the measurement of RVSP and SAP, mice were killed by cervical dislocation. The heart and lungs were gently flushed with ice-cold PBS by injection through the right ventricle and dissected out immediately and placed in ice cold PBS. Liver, spleen, kidneys were also dissected out and then snap frozen in liquid nitrogen and further put into -80 °C freezer until further use. A typical SAP waveform is shown in Figure 2.2.

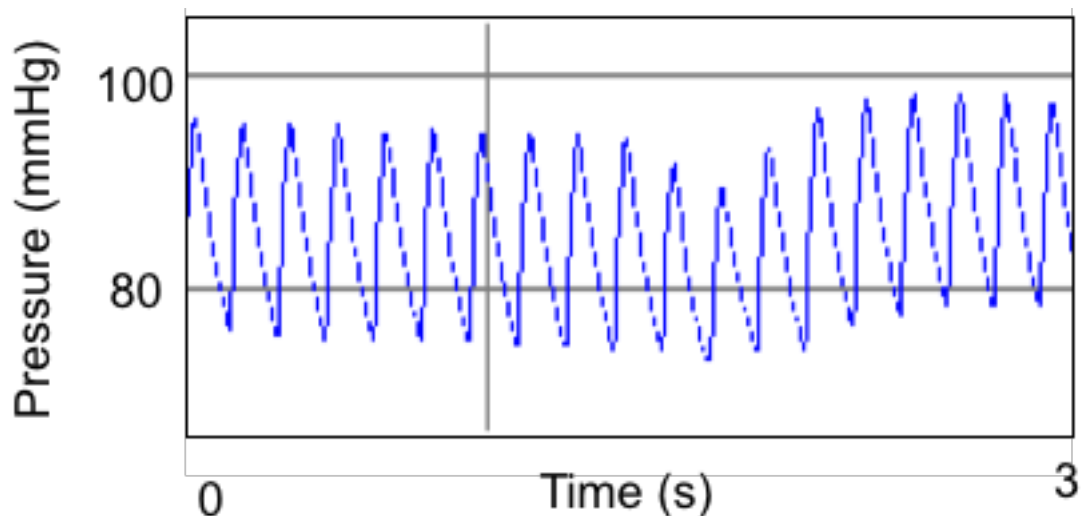


**Figure 2.3 Representative recording of systemic arterial pressure**

Three-second representative measurement of systemic arterial pressure in normoxia mice. Y-axis expressed in mmHg.

## **2.5.4 Right Ventricular Hypertrophy**

The excised whole hearts were cleared of adjoining fatty tissue and blood vessels. After removing the right and left atria, the right ventricle (RV) was dissected from the left ventricle plus septum (LV + S) and both were dry blotted and weighed. Measurement of right ventricular hypertrophy (RVH) was determined by the ratio of RV over LV + S, and the ratio (RV/LV + S) was used in the PAH assessment methodology.

## **2.5.5 Pulmonary Vascular Remodelling**

In order to assess the extent of pulmonary vascular remodelling in PH, 3 µm frontal plane lung sections were prepared and stained immunohistochemically for  $\alpha$ -smooth muscle actin ( $\alpha$ -SMA) and microscopically examined for non-remodelled and remodelled pulmonary arteries < 80 µm external diameter in a blinded fashion. The arteries were considered muscularised by the presence of a visible distinct thick vascular wall. In  $\alpha$ -SMA stained pulmonary arteries, a ratio of vascular wall thickness: vascular diameter was determined and used as a surrogate value to define the extent of pulmonary vascular thickness and remodelling. Lung sections from 6-8 mice for each experimental group were assessed. Five small pulmonary arteries were quantitatively analysed in each animal to generate a mean vasculopathy score per animal.

## **2.6 Histology**

### **2.6.1 Fixation, Paraffin Embedding and Sectioning of Lung Tissue**

Following Schedule I cull of animals, the inferior and middle lobes of the right lung and right ventricle (RV) were dissected free and fixed in 10% (v/v) neutral buffered formalin (NBF) overnight at room temperature with gentle agitation. Tissues were processed through a series of dehydration steps and to xylene and finally to 62 °C paraffin wax using the Shandon Excelsior tissue processor (Thermo Scientific, United Kingdom). An overview of the process is shown in Table 2-1.

**Table 2-1 Tissue processing for paraffin embedding**

<b>Solution</b>	<b>Incubation Period</b>
70% Ethanol	30 min
95% Ethanol	30 min
100% Ethanol	30 min
100% Ethanol	30 min
100% Ethanol	45 min
100% Ethanol	45 min
100% Ethanol	60 min
Xylene	30 min
Xylene	30 min
Xylene	30 min
Paraffin wax	30 min
Paraffin wax	45 min
Paraffin wax	45 min

Following the tissue processing sequence, lungs and right ventricle (RV) were placed in the right position in biopsy cassettes and embedded in paraffin wax using the Shandon Histocenter 3 (Thermo Scientific, United Kingdom). Paraffin embedded lung blocks were stored at room temperature. Lung blocks were placed in 4 °C overnight or -20 °C for 1 h prior to sectioning to aid with the cutting process. 3-5 µm frontal plane lung sections were cut using a Leica microtome and transferred to a 45 °C water bath from where they were mounted onto silanised glass microscopic slides and then baked overnight at 60 °C in a histology oven.

### **2.6.2 Immunohistochemistry**

Tissue sections were de-paraffinised then rehydrated by placing in two changes of Histo-Clear (Fisher Scientific Ltd, Leicestershire, UK) and followed by 100%, 95%, 70%, 50% ethanol and distilled water each for 5 min. Rehydrated sections were then immersed in 10

mM citric acid buffer at pH 6 and boiled in a microwave for 4 x 5min to perform antigen retrieval. Lung sections then were then cooled to room temperature for 20 min in the citric acid buffer, followed by washing in running tap water for 10 min. Sections were then incubated with 20% normal goat serum/PBS for 60 min to reduce non-specific background staining in a humidified chamber at room temperature. The sections were then incubated with primary antibodies at appropriate dilutions in 2% goat serum in PBS and incubated at 4 °C overnight in a humidified chamber. An immunoglobulin G (IgG) negative control was used on duplicate tissue sections at the same concentration to observe any non-specific binding. After primary antibody incubation, lung sections were washed three times in tris-buffered saline (TBS) for 10 min and then incubate with HRP-conjugated secondary antibodies (Vector Labs BA-1000) diluted 1/200 in PBS with 1% BSA for 60 min in a humidified chamber at room temperature. After incubation, sections were then washed three times in TBS for 10 min. Sections were then incubated with Extravidin-Peroxidase LSAB reagent (Sigma E2886) diluted 1/200 in PBS with 1% BSA for 30 min at room temperature. Following three TBS 10 min washes. Protein immunolocalisation was visualised by incubation with DAB solution (Vector Labs SK-4100) for 3 or 5 min. Dark brown staining was indicative of positive immunolocalisation. To quench the reaction, sections were immersed in running tap water for 10 min. Lung sections were then counterstained with haematoxylin (Cell Pathology Ltd, Newtown Powys, UK) for 1 min and washed in running tap water for 10 min. Lung sections were dehydrated by a water/alcohol gradient consisting of 70% ethanol for 1 min, 90% ethanol for 1 min, 100% ethanol for 1 min and finally twice in Histo-clear for 5 min. The lung sections were mounted with glass coverslips using DPX non-aqueous mounting medium (Merck Millipore, Darmstadt, Germany).

### **2.6.3 Immunofluorescence**

For mouse lung immunofluorescence, all the steps before the lung sections blocking were the same as immunohistochemistry in section 2.6.2. Lung sections were then incubated in 20% goat serum for 60 min in a humidified chamber at room temperature, and then incubated with primary antibodies in PBS-1% BSA overnight at 4 °C. Lung sections were

washed three times for 10 min in TBS prior to incubation with secondary antibodies (Alexa Fluor®488/590, dilution 1:500) (ThermoScientific, United Kingdom) for 1 h at room temperature protected from light. After three times wash with TBS for 10 min in the dark and then sections were mounted with glass coverslides using ProLong® Gold antifade reagent with Dapi (Molecular Probes).

#### **2.6.4 Immunocytochemistry (ICC)**

PASMCs were plated on sterile coverslips in 24-well plates and further treated with inflammatory cytokines to induce DNA damage. When the cells reached the desired density, culture media were removed from each well and cells washed twice with PBS. The cells then were fixed with 4% PFA at room temperature for 10 min, the PFA discarded and washed twice with PBS. After washing, cells were permeabilised with PBS-Triton (0.05%) at room temperature for 10 min and followed by three washes with PBS. Cells were blocked using 10% goat serum diluted in PBST for 30 min at room temperature to avoid non-specific staining. Cells were washed with PBST once and incubated with primary antibodies diluted in 1% goat serum PBST (1:200) overnight at 4 °C. The next day, cells were washed three times with PBS and incubated with secondary antibodies diluted 1:500 in PBS at room temperature for 1 h in the dark. Then cells were washed with PBS three times in the dark and coverslips were carefully removed from the wells and blotted to remove any excess PBS. Cells were mounted on microscope slides using ProLong® Gold antifade reagent with DAPI (Molecular Probes). The mounted slides were stored on the bench at room temperature in the dark overnight to allow the mounting medium to harden.

#### **2.6.5 Haematoxylin and Eosin Staining**

Haematoxylin and eosin (H&E) staining was performed on the right ventricle (RV) of mouse. 5 µm RV sections were deparaffinised and rehydrated by placing in two changes of Histo-Clear (Fisher Scientific Ltd, Leicestershire, UK) and followed by 100%, 95%, 70%, 50% ethanol and distilled water each for 5 min. Nuclei were stained with Harris' modified haematoxylin (Cell Pathology Ltd, Newtown Powys, UK) for 5 min and then rinsed in

running tap water for 5 min and transferred to 70% ethanol for 1 min. RV sections were further counterstained in eosin Y solution (Sigma-Aldrich) for 2 min to stain cytoplasmic structures before being dehydrated in two changes of each of the following: 95% ethanol, 100% ethanol and Histo-Clear each for 5 min. The RV sections were mounted with glass coverslips using DPX non-aqueous mounting medium (Merck Millipore, Darmstadt, Germany).

### **2.6.6 *In Situ* Hybridisation**

*In situ* hybridisation was performed to detect miR-143-3p in tissues from experimental mice, hypoxia-exposed neonatal calves, Brisket disease cattle and human PAH patients. 5 µm sections were deparaffinised and rehydrated with Histo-Clear and graded concentrations of ethanol same as described in previous sections. Antigen retrieval was performed by boiling slides for 10 min in DEPC treated 10 mM sodium citrate buffer (pH 6.0). After being cooled to room temperature on the bench, slides were immersed in 0.2 M HCL for 20 min. After three washes in DEPC-PBS, 0.3% Triton-X-100/PBS was added on the slides for 10 min, then incubated with 10 µg proteinase K at 37 °C for 15 min and finally fixed with 4% PFA for 10 min. Following incubation with hybridization buffer (50% (v/v) formamide, 4 X SSC, 2.5 X Denhardt's solution, 2.5 mg/ml salmon DNA, 0.6 mg/ml yeast tRNA, 0.025% (v/v) SDS and 0.1% (w/v) blocking reagent) at 60 °C for 1 h followed by overnight incubation with 40 nM miR-143-3p or scramble miRCURY LNA™ Detection probe, 5'-DIG labelled (Exiqon, Denmark) in the same buffer at 60 °C. After stringency washing with different concentrations of SSC buffer and DEPC-PBS, sections were blocked in 1% (w/v) blocking reagent in PBS and 10% FCS for 1 h at room temperature. Immunodetection was performed by 4 °C incubation with an anti-DIG antibody (Roche Applied Science, Indianapolis, IN, USA) diluted 1:500 overnight. After washing in DEPC-PBS with agitation, slides were then incubated with 0.1M Tris pH 9.0 twice for 5 min. In order to visualise hybridised miR-143-3p probes, BM purple solution or NBT/BCIP solution (Roche Applied Science, Mannheim, Germany) was added to each section, respectively and left at room temperature overnight. Slides were checked the next

day and excessive development of the purple colouration was stopped by washing with PBS. Finally, slides were mounted using glass coverslips and Vectamount AQ (Vector Labs).

## **2.7 Cell Culture**

All cell culture procedures were carried out under sterile conditions using class II Biological Safety vertical laminar flow cabinet. Cells were maintained in a humidified incubator with a constant supply of 5% CO<sub>2</sub> and 95% air. All the PSMCs and PAECs used in this study are derived from females.

### **2.7.1 Human Pulmonary Artery Smooth Muscle Cells (PSMCs)**

Distal human female pulmonary artery smooth muscle cells (PSMCs) were generated and provided by Prof N.W Morrell, University of Cambridge, UK. Distal PSMCs were isolated from distal pulmonary arteries (~1-3 mm external diameter) from female patients with PAH and non-PAH patients (Table 2-2). Proximal female human PSMCs were purchased from Lonza (Slough, UK). PSMCS were maintained in T150 culture flasks cultured in smooth muscle cell medium 2 (Promocell, Heidelberg, Germany) containing 15% FCS, 0.5 ng/ml epidermal growth factor, 2 ng/ml basic fibroblast growth factor, 5 µg/ml insulin, 2 mM L-glutamine, and 100 U/mL penicillin/streptomycin.

PSMCs were routinely passaged when monolayer cell growth reached 85%-95% confluence, avoiding cell growth arrest via contact inhibition. For passaging, cells were washed twice with sterile Dulbecco's calcium and magnesium free phosphate buffered saline (PBS) and incubated with trypsin EDTA (0.05% trypsin, 0.02% EDTA) at 37 °C and 5% CO<sub>2</sub> incubator until cells had detached from the flasks. Following detachment of cells, 5ml of full growth medium was added to the flasks to neutralise the trypsin. Cells were pelleted by centrifugation at 1,500 g for 5 min and resuspended in fresh full growth medium. Where

necessary for sub-culturing purposes, cells density was assessed via cell counts using a haemocytometer.

**Table 2-2 Patient information for human pulmonary arterial smooth muscle cells**

<b>Name</b>	<b>Gender</b>	<b>Age</b>	<b>Type</b>	<b>Disease Status</b>
MP27	F		CTL	N/A
MP32	F	58	CTL	Mild Emphysema
MP77	F	64	CTL	Mild Emphysema
MP79	F	N/A	CTL	
82MP	F	N/A	CTL	
83MP	F	N/A	CTL	
MP84	F	59	CTL	Squamous cell carcinoma
MP85	F		CTL	N/A
9MP	M	72	CTL	N/A
34MP	M	62	CTL	Emphysema
78MP	M	68	CTL	Lung Carcinoma
73MP	F	30	hPAH(R899X)	
MP35	F		hPAH(N903S)	
67MP	M	17	hPAH(W9X)	
56MP	F	N/A	hPAH(C347R)	
MP37	F	24	IPAH	
MP23	M	43	APAH	Eisenmengers
36MP	F	33	IPAH	
38MP	F	N/A	PAH	
98MP	F	N/A	IPAH	
113MP	F	N/A	IPAH	

### **2.7.2 Human Pulmonary Endothelial Cells (PAECs)**

Female pulmonary arterial endothelial cells (PAECs) were purchased from Lonza (Lonza, Slough, UK) and cultured in EBM-2 Endothelial Growth Basal Medium supplemented with BulletKit™ (Lonza, Slough, UK, CC-3162), 15% FBS, 2 mM L-glutamine, and 100 U/mL penicillin/streptomycin. PAECs cell culture was carried out as described in section 2.7.1 except the culture media was EBM-2 Endothelial Growth Basal Medium.

### **2.7.3 Human Embryonic Kidney (HEK) 293T cell**

HEK293T cells were cultured in Dulbecco's Modified Eagle Medium (DMEM) supplemented with 10% FBS, 2 mM L-glutamine, 1 mM sodium pyruvate and 100 U/mL penicillin/streptomycin. HEK293T cells were grown in T150 flasks and routinely passaged when monolayer cell growth reached 85%-95% confluence. For passaging, cells were washed twice with sterile Dulbecco's calcium and magnesium free phosphate buffered saline (PBS) and incubated with 5 ml 1 X citric saline at 37 °C and 5% CO<sub>2</sub> incubator until cells had detached from the flasks. The full growth medium was added to the flasks to pipet the cells up and down to disperse them. Cells were pelleted by centrifugation at 1,500 g for 5 min and resuspended in fresh full growth medium in fresh flasks.

## **2.8 Cell Transfection and Transduction**

### **2.8.1 MiRNA Transfection**

Reverse transfection of human PSMCs and PAECs with pre-miR-143-3p or anti-miR-143-3p was performed using siPORT NeoFX Transfection Agent according to manufacturer's instructions. Briefly, Siport NeoFX Transfection Agent was diluted 1:20 into 100ul of Opti-MEM<sup>®</sup> reduced serum medium and incubated in the hood for 10 min at room temperature. Pre-miR-143-3p and anti-miR-143-3p were diluted in a total volume of 100 µl Opti-MEM<sup>®</sup> reduced serum medium to various final concentrations including 10 nM, 50nM, and 100nM. siPORT NeoFX/Opti-MEM<sup>®</sup> and diluted pre-/anti-miRNA-143-3p/ Opti-MEM<sup>®</sup> were combined and mixed gently and incubated for a further 10 min at room temperature to allow transfection complexes to form. During the time for transfection complex preparation, cells were trypsinised with 1 X TE as described in section 2.7.1. Transfection complexes were then added to 6 well plates (200 µl per well) and then the cell suspension overlaid on to the transfection mix complex (1800 µl cell suspension with  $2 \times 10^5$  cells). The final volumes were 2000 µl for 6 well plates. Cells were incubated with transfection complexes/culture media overnight at 37 °C and 5% CO<sub>2</sub> incubator. The following day media was removed and cells were used for further experi-

ments.

PASMC cells ( $2.5 \times 10^5$ ) were transfected with 100 nm of Cy3 labelled pre-miR miRNA precursor using siPORT NeoFX Transfection Agent and cultured in full SMC media for 24 h described above. The day after transfection, cells were washed with PBS, and the medium was switched to fresh exosome-free SMC media. After incubation for 36 h, the culture media was collected and used for exosome preparation according to section 2.15.

## 2.8.2 SiRNA Transfection

PASMCs and PAECs were transfected with siRNAs using Lipofectamine® 2000. Briefly, PASMCs and PAECs were seeded in 6-well plates overnight. The following day 5 µl (10 nM) siRNA oligomer was diluted into 250 µl Opti-MEM® per well and mixed gently. At the same time, 5 µl Lipofectamine® 2000 were diluted into 250 µl Opti-MEM® and mixed gently and incubated for 5 min at room temperature. After the incubation, Lipofectamine® 2000/ Opti-MEM® and siRNA/ Opti-MEM® were combined and mixed gently and incubated for a further 20 min at room temperature to allow transfection complexes to form. During the incubation time, cells were washed with PBS twice and 500 µl of 5% FCS added to the culture medium without penicillin/streptomycin. Then, 500 µl transfection complexes were added to each well containing 500 µl media and incubated at 37 °C and 5% CO<sub>2</sub> for 6-8 h and changed with fresh full culture media after. The cells were ready for the further experiments. The siRNA sequences were described in table 2-3

**Table 2-3 The siRNA sequences of lncRNA**

Name of siRNA	Sequence
siMYOSLID-1-Sense	5' rGrGrArGrArArUrGrArArCrUrUrCrUrUrArArArGrCrUrGAA 3'
siMYOSLID-1-Antisense	5' rUrUrCrArGrCrUrUrUrArArGrAr ArGrUrUrCrArUrUrCrUrCrArC 3'
siMYOSLID-2-Sense	5' rGrArGrCrCrArCrCrUrUrGrCrUrCrUrArGrGrArUrGrUrGCC 3'
siMYOSLID-2-Antisense	5' rGrGrCrArCrArUrCrCrUrArGrArGrCrArArGrGrUrGrGrCrUrCrUrU 3'
siMyolnc16-1-Sense	5' rGrCrArArCrArUrGrCrArGrCrCrArGrCrCrArUrUrUrCrCAG 3'

siMyolnc16-1-Antisense	5' rCrUrGrGrArArArUrGrGrCrUrGrGrCrUrGrCrArUrGrUrUrGrCrUrU 3'
siMyolnc16-2-Sense	5' rUrGrCrCrArCrCrCrUrGrUrArArGrArUrArUrGrArCrUrUGC 3'
siMyolnc16-2-Antisense	5' rGrCrArArGrUrCrArUrArUrCrUrUrArCrArGrGrGrUrGrGrCrArGrG 3'

### 2.8.3 Cell Transduction

Lentiviral transduction of PSMCs was performed in 6 well plates. PSMCs were seeded into 6 well plates at a density of  $1.5 \times 10^5$  per well. The following day, media was replaced with fresh full media containing appropriate amount of virus. Cells were incubated at 37 °C and 5% CO<sub>2</sub> for 48 h. After the experimental period, cells were lysed for RNA extraction and following gene expression analysis.

## 2.9 Cellular Function Assays

### 2.9.1 Proliferation Assay

#### 2.9.1.1 BrdU Cell Proliferation Assay

Cell proliferation was measured by BrdU incorporation using Proliferation Assay Kits (Millipore BrdU Cell Proliferation Assay Kit) according to the manufacturer's instructions. PSMCs and PAECs were seeded into a 96-well culture plates at densities of  $1 \times 10^4$  and  $5 \times 10^3$ , respectively. Where required, cells were transfected the next day. The day following transfection, cells were serum-starved for 24 h (PAECs) and 48 h (PSMCs) in serum starvation media (0.2% FCS media). Cells were then treated with PDGF (20 ng/μl) (PSMCs) and VEGF (50 ng/μl) (PAECs) for 72 h (PSMCs) and 48 h (PAECs). A working stock of BrdU was prepared by diluting the BrdU stock 1:2000 into fresh cell culture media and pipetting 20 μl of this working stock to each well after 5 h stimulation with PDGF and VEGF. Two types of controls were set up to ensure validity of the experiments, including a blank control: a no cells control, and a background control: cells without BrdU added. The BrdU incorporation was stopped by removing the contents of wells by invert-

ing over sink and blotting gently on paper towels and then adding 200  $\mu$ l of the Fixative/Denaturing Solution to each well and allowing to incubate at room temperature for 30 min. Antibody solution was prepared by diluting the 100 X Anti-BrdU antibody 1:100 into the Antibody Dilution Buffer and then added to the wells and incubated at room temperature for 1 h after removed the Fixative/Denaturing Solution. The wells were washed three times with 1 X Wash Buffer making sure each well was filled completely and blotted the plate gently on paper towels. Conjugate solution were prepared by diluting the reconstituted (in 1 X PBS) Peroxidase Goat Anti-Mouse IgG HRP Conjugate into the Conjugate Diluent and then added 100  $\mu$ l into each well and incubated for 30 min at room temperature. The entire plate was flooded with dH<sub>2</sub>O and then washed by 1 X Wash Buffer three times. We then added 100  $\mu$ l of Substrate Solution to each well and incubated in the dark at room temperature for 15 min and followed by adding 100  $\mu$ l Stop Solution to each well to stop the reaction. The absorbance was measured in each well using a spectrophotometric plate reader, Victor (Perkin Elmer, Waltham, USA) at dual wavelengths of 450-540 nm in 30 min after adding the Stop Solution.

### **2.9.1.2 EdU Proliferation Assay**

Cell proliferation also quantified using EdU proliferation assay (Click-iT® Plus EdU Alexa Fluor® 488 Flow Cytometry Assay Kit, C10633) according to the manufacturer's instructions. Briefly, PSMCs seeded in 6-well plates were stimulated with full culture medium and EdU (20  $\mu$ g/ml in 2 ml culture media) was added at the point of stimulation for the remaining time to allow cell proliferation to occur for 48 h. The cells were trypsinised and harvested after 48 h stimulation and placed in 15 ml falcon tubes and centrifuged at 600 g for 6 min. Following centrifugation, the supernatants were discarded and cells resuspended in 0.5 ml PBS and fixed by adding 4.5 ml 70% ethanol overnight. Fixed cells were then centrifuged at 600 g for 6 min and 5 ml 0.2% Triton X-100 added following removal of supernatants. Samples were mixed and incubated for 30 min at room temperature. 0.5 ml PBS + 1% BSA was then added to cells, which were mixed for 60 sec and then centrifuged at 600 g for 6 min allowing removal of the supernatant. The Click-it Alexa

reagent stock was prepared as described in Table 2-4. 0.5 ml Click-it reagent was added per tube, mixed well and incubated at room temperature for 60-90 min in the dark. Following incubation, 5 ml PBS + 1% BSA was added to cells which were then centrifuged at 600 g for 5 min and removed the supernatant. Finally, 500  $\mu$ l PBS to each sample of pelleted cells and resuspended cells were transferred to Fluorescence Activated Cell Sorting (FACS) tubes for FACS analysis.

**Table 2-4 The Click-it reagent components**

Reaction Component	Number of reactions (500 $\mu$ L volumes)						
	1	2	3	4	6	9	10
PBS	438 $\mu$ l	875 $\mu$ l	1.3 ml	1.75 ml	2.6 ml	3.95 ml	4.38 ml
CuSO <sub>4</sub> (2 mM final concentration) Component F (Room temp)	10 $\mu$ l	20 $\mu$ l	30 $\mu$ l	40 $\mu$ l	60 $\mu$ l	90 $\mu$ l	100 $\mu$ l
Alexa Fluor azide - 7.14 $\mu$ g/ $\mu$ l Component B – 18 $\mu$ g/reaction (18ng/ $\mu$ l; 23 $\mu$ M final concentration) (-20°C)	2.5 $\mu$ l	5 $\mu$ l	7.5 $\mu$ l	10 $\mu$ l	15 $\mu$ l	22.5 $\mu$ l	25 $\mu$ l
1X Reaction buffer additive (-20°C)	50 $\mu$ l	100 $\mu$ l	150 $\mu$ l	200 $\mu$ l	300 $\mu$ l	450 $\mu$ l	500 $\mu$ l

## 2.9.2 Apoptosis Assay

PASMC and PAEC apoptosis was analysed by measuring Caspase3/7 activity using Caspase-Glo® 3/7 Assay (Promega, G8091) according to the manufacturer's protocol. PASMCS and PAECs were seeded in 96-well plates and followed by different treatments. To induce apoptosis, PASMCS were treated with H<sub>2</sub>O<sub>2</sub> (50  $\mu$ M) for 12 h and PAECs were treated with Cycloheximide (CHX, 25 ng/ml) and TNF- $\alpha$  (4 ng/ml) for 7 h. Briefly, the Caspase-Glo® 3/7 Buffer and lyophilised Caspase-Glo® 3/7 Substrate were equilibrated to room temperature and mixed the Substrate and buffer. The 96-well plates were removed from the incubator and allowed to equilibrate to room temperature, after which 100  $\mu$ l of Caspase-Glo® 3/7 Reagent was added to each well of the 96-well plate containing 100  $\mu$ l of blank, negative control cells or treated cells in culture medium. The well contents were gently mixed using a plate shaker and incubated at room temperature for 2 h. The solution

was transferred to a white-walled 96-well plate and luminescence measured in a plate luminometer (VICTOR X3 Multimode Plate Reader, PerkiElmer) in the wavelength range of 510-570 nm.

### **2.9.3 Wound Healing Migration Assay**

Migration of PSMCs and PAECs was analysed using the scratch wound-healing assay in 6-well plates. All cells were serum-starved for 24 h after various treatments (transfections, conditioned medium, and exosomes treatment), and vertical scratches were drawn through the confluent monolayer of cells using a P200 pipette tip. Cells were washed with PBS to remove any cell debris caused by induction of the wound and fresh full cell culture media (10% FBS) was added to the cells. For migration assay, it is recommended to use a lower percentage of serum in the growth medium to minimize the cell proliferation, however sufficient serum is required to prevent apoptosis and/or cell detachment, which is a particular concern for transfection experiments. Scratches were imaged at 0, 10, or 12 h post scratch using the Nikon Eclipse TS100 microscope and imaged on QICAM Fast 1394 camera (QImaging, Burnaby, Canada), with three images captured for each well. Migration distance analysis was performed using Image J software where a grid composed of 10 horizontal lines was placed over the photo. The distance between the edges of the scratch wound was measured along the grid lines and a relative migrated distance was expressed as a proportion of the migrated distance based on 0 h time point. Independent experiments were performed three times, with three independent wells per condition.

### **2.9.4 Multiple Scratches Assay**

The multiple scratches are to apply a high density field of scratches to maximize the area of wound edges, while leaving sufficient undamaged cells to migrate into the gap. This form of high density wounding creates a high proportion of migrating cells to quiescent monolayer cells, which permits sensitive detection of the biochemical events occurring, specifically in the migrating cell population. Briefly, each well of the 6-well plate was scratched 10-12 scratches horizontally and vertically using P200 pipette tip. Then the wells

were washed with PBS and supplemented with full medium. After the desired time, media is removed and gently washed with PBS. Cells were harvested for RNA extraction and further analysed by Taqman PCR. The PSMCs closure after multiple scratches at different time points were shown in Figure.

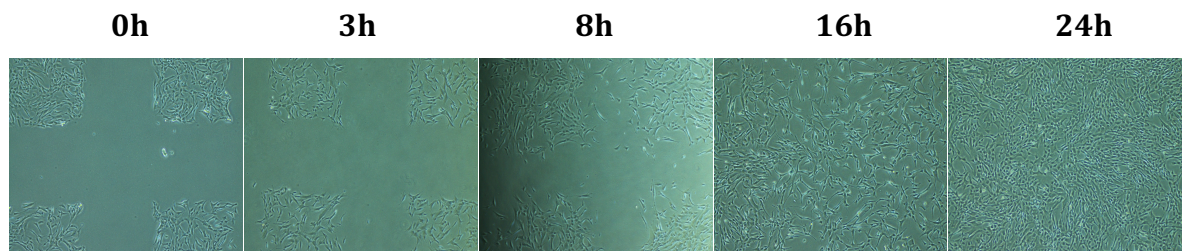


**Figure 2.4 PSMCs migration with multiple scratches**

PASMCs were scratched with P200 pipette tip in 6 well plate. Pictures were shown the cell migration at different time points.

### **2.9.5 *In Vitro* Tube Formation Assay**

PAEC tube formation assays were performed in 96-well plates containing 50  $\mu$ l Matrigel (*in vitro* angiogenesis assay ECM625, Millipore, USA) according to the manufacturer's protocol. Briefly, Matrigel solution was added to the wells of a 96-well plate and allowed to solidify and polymerize in a 5% CO<sub>2</sub> incubator at 37 °C for 1 h. PAECs were then dissociated, centrifuged at 1200 rpm for 5 min and resuspended in full endothelial cell media at a density of  $1 \times 10^4/100 \mu$ l. 100  $\mu$ l of cell suspension was layered on top of the Matrigel. After 6-12 h incubation at 37 °C and 5% CO<sub>2</sub>, tube formation was inspected using a light microscope. Tube-like formations were evaluated in 15 pictures per condition (magnification 10x) and the number of cells, number of branches, average length of the capillary branches, number of branches to the length of capillaries ratio and the pattern of branching were assessed using the angiogenesis analyser module for Image J.

### **2.10 DNA Damage Assay**

PASMCs were seeded in 6-well plates and treated with TNF- $\alpha$  (100 ng/ml), IL-6 (100 nm) and PDGF (30 ng/ml) for 48 h in cell incubator at 37 °C and 5% CO<sub>2</sub>. Immunocytochemis-

try for  $\gamma$ -H2AX was performed as section 2.6.4 using a monoclonal antibody directed against  $\gamma$ -H2AX (ab11174, Abcam) at 1: 200 dilutions. The DNA damage *in vitro* was imaged with a Zeiss LSM510 confocal microscope. Cells were classified based on the number of foci in the nucleus: cells with greater than 10 foci were counted as positive DNA damage.

## **2.11 Western Blotting**

### **2.11.1 Protein Extraction and Preparation**

Protein lysis buffer was prepared on ice including the following reagents: 20mM Tris pH 7.5, 1 mM EDTA, 150 mM NaCl, 1 mM Ethylene glycol tetra-acetic acid (EGTA), 1 mM  $\beta$ -glycerophosphate, 2.5 mM Na pyrophosphate, 1 mM  $\text{Na}_3\text{VO}_4$ , 0.5% (w/v) sodium deoxycholate, 1 mM phenylmethylsulfonylfluoride (PMSF), 2 mM NaF, 1 $\mu$ g/ml leupeptin. Protease inhibitor cocktail (1 tablet diluted in 10 ml lysis buffer) (Roche Applied Sciences), and phosphatase inhibitor cocktail 2 (1:100 in dilution in lysis buffer) were added freshly before protein extraction.

PASMCs and PAECs were seeded in 6-well plates and grown to 80% confluence. Following various stimulations for the required time, experiments were stopped by 6-well plate incubation on ice. Immediately, the cell culture media was aspirated and washed with ice-cold PBS twice. Ice-cold protein lysis buffer (120  $\mu$ l) was then added to each well for 15 min. Keeping the 6-well plate on ice, the cells were scraped using a sterile plastic scraper and cell lysates collected in a pre-chilled 1.5 ml Eppendorf tube. These samples were further incubated on ice for 30 min and then centrifuged at 14,000 g for 10 min at 4 °C. The protein supernatant was collected and store at -80 °C for western blot analysis.

To prepare protein lysates of tissues, 200  $\mu$ l ice-cold protein lysis buffer was added to 2 ml Eppendorf tubes containing about 25 mg frozen tissues and one 5mm stainless steel bead (Qiagen, United Kingdom), which was placed in a Tissue Lyser II (Qiagen, United Kingdom) for homogenisation. High-speed shaking was performed for 4 X 30 sec intervals. Af-

ter homogenisation, samples were incubated at 4 °C for 1h with shaking, then centrifuged at 14,000 g for 30 min at 4 °C. Supernatants were collected and stored at -80°C for western blot analysis.

### **2.11.2 Protein Quantification**

Quantification of total protein was performed using the Pierce Bicinchonic Acid (BCA) protein Assay Kit (ThermoScientific, United Kingdom, catalog number: 23225) according to the manufacturer's instructions. Bovine serum albumin was diluted at different concentrations ranging from 25 µg/ml to 2000 µg/ml to prepare diluted BSA standards. These standard samples were used to generate a standard curve. Working reagent was prepared by mixing 50 parts of BCA reagent A with 1 part of BCA reagent B. Protein samples and standards (10 µl each well) were added to the 96-well plate with 200 µl of working reagent, mixed thoroughly, protected from light and incubated at 37 °C for 30 min. Absorbance was measured at 560 nm using the Wallac 1420 Victor<sup>2</sup>™ plate reader (Wallac). Sample protein concentrations were calculated using the standard curve generated by the protein standards.

### **2.11.3 SDS-PAGE**

Protein was separated by molecular weight using SDS-PAGE on a XCell4 SureLock™ Midi-Cell Electrophoresis System (ThermoFisher Scientific, UK) according to the manufacturer's instructions. Briefly, 20 µg protein samples were mixed with NUPAGE® 4 X LDS Sample Buffer and denatured by heating at 95 °C for 10 min. Samples were loaded into the precast NuPAGE Novex 4-12% Bis-Tris Midi Gels along with a rainbow marker (Amersham). Electrophoresis was performed at 80-160 V in NuPAGE MOPS SDS running buffer until adequate migration and separation of protein samples was achieved.

Proteins were transferred onto Amersham Hybond P nitrocellulose membranes (0.2 µm pore) (GE Life Sciences) at 100 V for 1.5 h in transfer buffer (25 mM Tris, 0.2 M glycine, 20% (v/v) methanol) at 4 °C. The membranes were soaked into distilled H<sub>2</sub>O for 5 min and

balanced in the transfer buffer for 10 min before transfer.

#### **2.11.4 Immunoblotting**

Immunoblotting was performed to quantitatively evaluate protein expression. Following transfer, nitrocellulose membranes were washed with PBS for 5 min. For specific protein analysis, the membranes were blocked at room temperature for 1h on a shaker in blocking buffer containing 50% Odyssey® Blocking Buffer in Tris buffered saline plus tween (TBST) (150 mM NaCl, 2mM KCl, 25 mM Tris and 1% (v/v) Tween-20). Membranes were incubated with specific primary antibodies (see Table 2-5 for a complete list) at 4 °C overnight. The following day membranes were washed in TBST for 3 X 10 min and then incubated with fluorescently-labelled secondary antibodies (1:10000) in Odyssey® blocking buffer diluted 1:1 in TBST for 1 h at room temperature with gentle shaking. The membrane was then washed in TBST for 3 X 10 min and another wash with PBS for 10 min with gently shaking and protected from light. Membranes were then imaged on a Li-COR Odyssey imager.

**Table 2-5 Antibodies used for western blotting**

<b>Antibody</b>	<b>Dilution</b>	<b>Supplier</b>
PCNA (rabbit) (100 µg/ml)	1:1000	Abcam-18197
CD63 (rabbit) (200 µg/ml)	1:1000	Santa Cruz Biotech (sc-15363)
CD9 (rabbit) (200 µg/ml)	1:1000	Santa Cruz Biotech (sc-9148)
GAPDH (rabbit) (100 µg/ml)	1:1000	Cell Signalling (2118)
β-Tubulin (rabbit) (100 µg/ml)	1:1000	Cell Signalling (2146)
MAPK Family Antibody Kit (rabbit)	1:1000	Cell Signalling (9926)
Smad 1/5/9 Antibody Kit (rabbit)	1:1000	Cell Signalling (12656)
BMPR2 (mouse) (250 µg/ml)	1:500	BD Biosciences (612292)
IRDye® 800CW Goat anti-Mouse IgG (goat) (100 µg/ml)	1:10000	LI-COR (P/N 925-32210)
IRDye® 800CW Goat anti-Rabbit IgG (goat) (100 µg/ml)	1:10000	LI-COR (P/N 925-33211)

## **2.12 RNA Extraction, Purification and Quantification**

### **2.12.1 Cells**

Total RNA from PSMCs and PAECs was extracted using the QIAGEN miRNeasy mini kit (including on-column DNase treatment) following manufacturer's instructions. Briefly, cells were lysed directly with 700 µl QIAzol lysis reagent and homogenised by repeated pipetting. The cell homogenate was added to 140 µl chloroform and mixed by shaking the tube vigorously for 10-15 sec. After incubation for 3 min at room temperature, samples were centrifuged at 12,000 g for 15 min at 4 °C to separate the sample into aqueous and organic phases. The upper aqueous phase was transferred to a new collection tube 1.5 volumes of 100% ethanol was added and mixed thoroughly by pipetting. Samples were transferred into an RNeasy Mini spin column and centrifuged at 8,000 g for 1 min at room temperature. Total RNA was bound to the silica membrane while contaminants, such as

phenol, were washed away in the subsequent wash steps. Columns were washed with 350  $\mu$ l buffer RWT at 8,000 g for 1 min at room temperature. At this stage, on-column DNase digestion was performed to remove contaminating genomic DNA from the samples, which could interfere with downstream applications. DNase stock solution was diluted 1:8 (v/v) in buffer RDD (10  $\mu$ l to 70  $\mu$ l). The DNase/RDD mixture (80  $\mu$ l) was added directly onto the column membrane and incubated at room temperature for 15 min.

The columns were washed once with 350  $\mu$ l buffer RWT and twice with 500  $\mu$ l buffer RPE with centrifugation at 8,000 g for 1 min at room temperature between each wash. The columns were placed into a fresh collection tubes and centrifuged at 14,000 g for 2 min at room temperature to remove any buffer contaminants. Spin columns were then transferred to new RNase-free tubes and RNA was eluted by adding 30  $\mu$ l RNase-free H<sub>2</sub>O to the columns and centrifuging at 8,000 g for 1 min at room temperature. In order to increase RNA yield, the RNA eluates were collected and re-eluted through the column.

### **2.12.2 Tissues**

Total tissue RNA was extracted using the QIAGEN miRNeasy mini kit including on-column DNase treatment following manufacturer's instructions. Snap frozen tissues were stored at -80 °C until processing. Tissues were lysed using 700  $\mu$ l QIAzol lysis reagent and disrupted and homogenised using 5 mm stainless steel beads in the TissuLyser (QIAGEN) at 25 Hz FOR 1-2 min until full tissue disruption. Following homogenisation, 140  $\mu$ l chloroform was added to each sample and followed the next steps described in section 2.12.1.

### **2.12.3 Nano-Drop**

Total RNA was quantified using the NanoDrop 1000 Spectrophotometer (Thermo Scientific). The spectrophotometer measured the absorbance of each sample at 260 nm (absorbance of RNA) and 280 nm (absorbance of protein) and 230 nm (absorbance of contaminations). The ratio of absorbance at 260 nm and 280 nm is used to assess the purity of DNA

and RNA. A 260 nm/280 nm ratio of ~2.0 is generally accepted as “pure” for RNA. If the ratio is appreciably lower in either case, it may indicate the presence of protein, phenol or other contaminants, which absorb strongly at or near 280 nm. The 260 nm/ 230 nm ratio is used as a secondary measure of nucleic acid purity. The 260/230 values for “pure” nucleic acid often higher than the respective 260/230 values. Expected 260/230 value are commonly in range of 2.0-2.2. If the ratio is appreciably lower than expected, it may indicate the presence of contaminants which absorb at 230 nm.

#### **2.12.4 Agilent Testing of RNA Quality**

The RNA extracted from PSMCs and PAECs for microarray assays were further analysed by a Small RNA Assay performed on the Agilent Bioanalyzer 2100 system (Agilent Technologies, Berkshire, UK) at the Sir Henry Wellcome Functional Genomics Facility, Microarray Unit at the University of Glasgow. The negatively charged RNA molecules were electrophoretically separated by size to produce gel images and electropherograms, allowing assessment of RNA quality. The percentage of miRNA (relative to small RNA) in the sample was also calculated using the Agilent 2100 software.

### **2.13 Reverse Transcription Polymerase Chain Reaction (RT-PCR)**

#### **2.13.1 MiRNA Reverse Transcription**

For the detection of miRNA expression, cDNA was synthesised using stem-loop reverse transcription primers as per the Taqman microRNA assay protocol (Applied Biosystems, Paisley, UK) according to the manufacturer’s instructions. Each reaction contained 2.5 µl of 2 ng/µl sample RNA, 0.25 mM of each deoxyribonucleotide triphosphate (dNTP), 3.33 U/µl multiscribe reverse transcriptase, 0.25 U/µl RNase inhibitor, 1 X Reverse Transcriptase buffer, 2.08 µl RNase-free water, and Taqman® miRNA Reverse Transcription Primers for the mature sequence of the miRNA of interest. Both human and mouse endogenous controls RNU48 and U6 were also performed for each sample to normalise changes in the miRNA expression. The mature sequence of miRNA of interest and endogenous

control sequences shown in table 2-6. cDNA synthesis reactions were incubated at 16 °C for 30 min, 42 °C for 30 min, and 85 °C for 5 min and then held at 4 °C. Samples were stored at -20 °C before quantitative PCR was performed.

**Table 2-6 MiRNA reverse transcription primers**

MiRNA/Control	Sequence	Species
Has-miR-143-3p	5'UGAGAUGAAGCACUGUAGCUC 3'	Human/mouse
Has-miR-143-5p	5' GGUGCAGUGCUGCAUCUCUGGU 3'	Human/mouse
Has-miR-145-5p	5' GUCCAGUUUCCCCAGGAAUCCCU 3'	Human/mouse
Has-miR-145-3p	5' GGAUUCCUGGAAAUACUGUUCU 3'	Human/mouse
RNU48	5'GATGACCCAGGTA ACTCTGAGTGTGT CGCTGATGCCATCACC GCAGCGCTCTGAC C 3'	Human
U6	5'GTGCTCGCTTCGGCAGCACATATACTAA AATTGGAACGATACAGAGAAGATTAGCAT GGCCCCTGCGCAAGGATGACACGCAA TTCGTGAAGCGTTCCATATTTT 3'	Mouse

### 2.13.2 mRNA Reverse Transcription

For gene expression analysis, cDNA was synthesised using the SuperScript™ II Reverse Transcriptase (RT) system. Each reaction contained 4 µl 5 X First strand buffer, 1µl 10 mM dNTP, 1 µl Random Primers (9 units), 1 µl 0.1 M DTT, 0.5 µl RNasin® Ribonuclease Inhibitor (2500 units) (Promega), 1 µl SuperScript™ II Reverse Transcriptase, 1.5 µl RNase-free H<sub>2</sub>O and 100-1000 ng RNA (diluted into 10 µl) to a total volume of 20 µl (same concentration of RNA used per experiment). Samples were incubated at 70 °C for 10 min, 4 °C for 10 min (mastermix added to each reaction), 25 °C 10 min, 42 °C 1 h, 72 °C 15 min and held at 4 °C. Samples were stored at -20 °C when not being used immediately.

## 2.14 Taqman Quantitative Real-Time PCR

Quantitative PCR is the second step in the real-time PCR assay. MiRNA qRT-PCR was performed using Taqman® miRNA Assay RT-PCR Probes and Taqman® Universal Mastermix II (containing AmpliTaq Gold® DNA polymerase, dNTP mixture and optimal salt conditions, no UNG; Invitrogen) in accordance with the manufacturer's instructions. Each reaction mastermix contained 250 nM Taqman probe, 1 X Taqman Universal PCR MasterMix II (Invitrogen) and nuclease-free H<sub>2</sub>O to a total volume of 9.33 µl per sample. cDNA was pipetted in technical triplicate into a 384 well plate 0.67 µl per well and the mastermix added to each well to give a total reaction volume of 10 µl. Human RNU48, or mouse U6 were used as an endogenous control in separate wells.

Quantitative qRT-PCR for mRNA expression samples was performed using Taqman® Gene Expression Assays and Taqman® Universal Mastermix II in accordance with the manufacturer's instructions. Each reaction mastermix contained 1 X Taqman® gene probe, 1 X Taqman® Mastermix and H<sub>2</sub>O to a total volume of 10 µl. cDNA samples were diluted with RNase-free H<sub>2</sub>O dependent on how much RNA was added to the RT reaction. For example, where 1000 ng RNA added per sample in RT reactions then cDNA was diluted to 200 µl with nuclease-free H<sub>2</sub>O. qRT-PCR reactions were performed using 2.5 µl diluted cDNA in technical triplicate into a 384 well plate and added with mastermix to give a total reaction volume of 12.5 µl.

MiRNA and mRNA expression was measured using the ABI Prism 7900HT sequence detection system (Applied Biosystems). Thermal cycling conditions began with 10 min incubation at 95 °C, then followed by 40 cycles of 15 sec at 95 °C and then 60 sec at 60 °C.

Results were shown relative to the control sample using the  $-2^{\Delta\Delta C_t}$  method and expressed as relative fold change. For miRNA expression, results were normalised to U6 and RNU48 for mouse and human samples, respectively. For mRNA and long non-coding RNA expression, results were normalised to 18S rRNA or UBC for experiments that involved hypoxia,

as this gene remains unchanged in hypoxic conditions. Experiments performed in normoxic conditions were normalised to GAPDH, as study showed that GAPDH expression was upregulated in hypoxic conditions (Yamaji et al., 2003).

## **2.15 Exosome Extraction, Purification and Quantification**

PASMCs were seeded in 6-well plates with cell number at  $2 \times 10^5$ /well with or without transfection. In the following day, cells were washed twice with PBS and replaced with 10% exosome free-FCS (exosome remove by 18 h ultracentrifugation) SMC medium and cells were incubated at 37 °C and 5% CO<sub>2</sub> for 36 - 48 h.

Cell culture medium was collected for each sample and centrifuged at 2,000 g for 30 min to remove cell debris at room temperature. Supernatants containing cell free cell media were transferred to a clean tube and held on ice until use. Supernatants were then combined with total exosome isolation reagent (Invitrogen) and mixed well by vortexing until a homogenous solution was formed. The samples were incubated at 4 °C overnight and then centrifuged at 4 °C at 10,000 g for 1 h. The supernatant was aspirated and discarded, and the exosome pellet was resuspended in PBS buffer, then stored at 4 °C for short term (1-7 day) and -20 °C for long term until use.

Exosomes were also extracted by ultracentrifugation for western blot analysis. Supernatants from PASMC cultures were collected and pre-cleared by centrifugation at 4,000 g for 10 min at 4 °C to remove cell debris. To pellet the exosomes, the supernatant was centrifuged at 23,000 g for 70 min at 4 °C. Supernatants were removed and discarded, and the pelleted exosomes were washed with ice-cold PBS and pelleted again by ultracentrifugation at 23,000 g for 70 min at 4 °C. Finally, the supernatant was removed and discarded and the pelleted exosomes were resuspended in 150 µl protein lysis buffer. After incubation on ice for 30 min, the lysed exosomes were centrifuged at 14,000 g for 10 min at 4 °C to harvest the supernatant (exosome protein) and store at -80 °C. Protein analysis by western blot for CD63 (H-193: sc-15363) and CD9 (H-110: sc-9148) were carried out to assess

the purity of the exosome isolation. RNA was extracted from exosomes by following the protocol for RNA extraction from cells described in section 2.12.1.

## **2.16 Nanoparticle Tracking Analysis (NTA)**

Exosomes isolated from cell culture media and the exosome size and numbers were measured using a NonoSight LM system. The instrument, which is based on a conventional optical microscope, uses a laser light source to illuminate nano-scale particles within a 0.3 ml sample introduced to the viewing unit with a 1ml disposable syringe. Enhance by a near perfect black background, particles appear individually as point scatters moving under Brownian motion. The NanoSight instrument tracks the Brownian motion of nanoparticles in liquid suspension (exosomes diluted in PBS) on a particle-by-particle basis. Subsequent application of the Stokes-Einstein equation allows the derivation of particle (exosomes) size and concentration. The size of exosome particles is from 30nm to 130 nm.

## **2.17 Microarray Analysis**

Microarray analysis was performed on PASMCM and PAECs transfected with scramble or pre-miR-143-3p. RNA quantity and quality were assessed by NanoDrop® Spectrophotometer (Thermo Scientific, Wilmington, DE, USA). RNA integrity was assessed with the Agilent 2100 bioanalyser using the RNA 6000 Nano Kit (Santa Clara, CA). The Illumina TotalPrep RNA amplification kit (Ambion) was used to generate biotinylated, amplified RNA, from 500 ng input RNA, for hybridization with the Illumina arrays (Applied Biosystems Carlsbad, California). The Illumina humanHumanHT-12 v4.0 Expression BeadChips were hybridised following the manufacturer's protocol, scanned with the Illumina BeadArray Reader and read into Illumina GenomeStudio® software (version 1.1.1).

For microarray data analysis and validation, quantile normalised and background subtracted intensity values were exported from GenomeStudio® software for data processing and analysis in R (<http://www.R-project.org>) in which limma statistical analysis was carried out (Ritchie et al., 2015), including pairwise comparisons between the 3 groups. The microarray data and experimental design was submitted online to the ArrayExpress database

([www.ebi.ac.uk/arrayexpress](http://www.ebi.ac.uk/arrayexpress)) following MIAME guidelines. The accessions E-MTAB-3566 and E-MTAB-3567 were allocated to the PAEC and PASMIC arrays respectively. To gain further biological insights into the gene expression profiling experiments, pathway analysis was performed using Ingenuity Pathway Analysis software (Ingenuity Systems, [www.ingenuity.com](http://www.ingenuity.com)). To account for potentially subtle changes in levels of gene expression caused by the action of miRNAs and to ensure these changes were included in the pathway analysis we used a fold change threshold of  $\pm 1.25$ .

## 2.18 Lentivirus Production and Titering

Lentiviral vectors were produced by triple transient transfection of HEK293T cells with a packaging plasmid (pCMV $\Delta$ 8.74), a plasmid encoding the envelope of vesicular stomatitis virus (VSVg) (pMDG) (Plasmid Factory, Bielefeld, Germany) and lentiviral vector (pFUGW) plasmid employing polyethylenimine. The lentiviral plasmid (pFUGW) carrying the *MYOSLID* transcript and vector control were generated as previously described (Zhao et al., 2016) and kindly gifted by Dr. Xiaochun Long (Albany Medical College, NY).

Briefly, HEK293T cells grown to 80% confluency in 3 T150 flasks and transfected using polyethylenimine (3  $\mu$ l (1 mg/ml) diluted in 5 ml OptiMEM) precomplexed with 50  $\mu$ g of the lentiviral vector along with 17.5  $\mu$ g pMDG envelope plasmid and 32.5  $\mu$ g packaging plasmid (pCMV $\Delta$ 8.74) diluted in 5 ml OptiMEM. The combination mixture was incubated for 20 min at room temperature to allow the DNA/PEI complexes formation. HEK293T cells were washed with 5 ml OptiMEM and 10 ml DNA/PEI complexes were added to each flask, with cells incubated at 37 °C and 5% CO<sub>2</sub> for 4 h. Transfection media were replaced after the 4h transfection period with 20 ml fresh complete MEM. Cell media were harvested at 48 h and 72 h, filtered through a 0.22  $\mu$ m Millipore™ Stericup™ Vacuum Filter Unit (Millipore) and lentiviruses were pelleted by centrifugation at 23,000 rpm for 1 h at 4 °C. The viral pellet was resuspended in 50  $\mu$ l OptiMEM per flask and left for 20 min on ice before aliquoting and storage at -80 °C.

The viral titer was determined using Lenti-X qRT-PCR titration kit (Clontech) according to the manufacturer's instructions. Briefly, viral RNA was isolated from the resuspended lentivirus. Viruses were first lysed by add 600  $\mu$ l Buffer RAV1 containing Carrier RNA to 150  $\mu$ l lentivirus and mixed well and incubated for 5 min at 70 °C. 600  $\mu$ l 100% ethanol was added to lysed lentiviruses and mixed by vortexing (10-15 s). Lysed samples were then loaded onto the NucleoSpin® Virus Columns and centrifuged for 1 min at 8,000 g at room temperature. Three washes were then performed: once 500  $\mu$ l Buffer RAW, once 600  $\mu$ l Buffer RAV3, and once 200  $\mu$ l Buffer RAV3. The last spin was at 11,000 g to remove ethanolic Buffer RVA3 completely. The NucleoSpin® Virus Columns were placed into new, sterile 1.5 ml microcentrifuge tubes and added 50  $\mu$ l nuclease-free H<sub>2</sub>O (preheated to 70 °C) and incubated for 2 min and centrifuged for 1 min at 11,000 g at room temperature.

QRT-PCR for the viral RNA samples was performed using Lenti-X primers and Quant-X Buffer in accordance with the manufacturer's instructions. Briefly, Master Reaction Mix were set up to contain 12.5  $\mu$ l Quant-X Buffer (2 X), 0.5  $\mu$ l Lenti-X Forward/Reverse Primer (10  $\mu$ M), ROX Reference Dye LSR or LMP (50 X), 0.5  $\mu$ l Quant-X Enzyme, 0.5  $\mu$ l RT-enzyme Mix, and 8  $\mu$ l H<sub>2</sub>O to a total volume of 23  $\mu$ l per well. Viral RNA and the diluted Lenti-X RNA control Template were pipetted in duplex into a 384 well plate with 2  $\mu$ l per well and the Master Reaction Mix added to each well to give a total reaction volume of 25  $\mu$ l. The plate was centrifuge at 2000 rpm for 2 min to remove any bubbles and installed the plate in the Applied Biosystems 7900T sequence detection system. Cycling condition were: RT Reaction step: 42 °C 5 min and 95 °C 10 sec; qRT-PCR step: 95 °C 5 sec and 60 °C 30 sec with 40 cycles; Dissociation Curve step: 95 °C 15 sec, 60 °C 30 sec and all (60 °C - 95 °C).

A standard curve was generated using the average Ct values from each of the Lenti-X RNA Control Template duplicate sample dilutions plotted against copy number (log scale) for the calculation of the quantity of viral RNA. Once an average Ct value for each sample was determined and then a corresponding value got from the standard curve, the copy number of sample viral RNA per ml was calculated using the equation below:

$$\text{Copies/ml} = \frac{(\text{copy number from CtS})(1000 \mu\text{l/ml})(50 \mu\text{l RNA elution})}{(150 \mu\text{l sample})(2 \mu\text{l added to eachwell})}$$

## 2.19 Co-culture Model

The co-culture model was showed in Figure 2.3. 6-well transwell inserts with 0.4  $\mu\text{m}$  pores were purchased from Greiner and used following the manufacturer's instructions. Briefly, PSMCs ( $1.5 \times 10^5$ ) were seeded in the well inserts and/or transfected with pre-miR143 (100 nM) using siPORT NeoFX Transfection Agent and cultured in full SMC medium for 24 h detailed in section 2.8.1. PAECs ( $2 \times 10^5$ ) were seeded into the 6-well plate with full EBM media. On the following day before starting the co-culture experiments, both PSMCs and PAECs were washed with PBS then the well insert seeded with transfected PSMC putted into the 6-well plate seeded with PAECs. All co-culture experiments were done in full EBM-2 media.

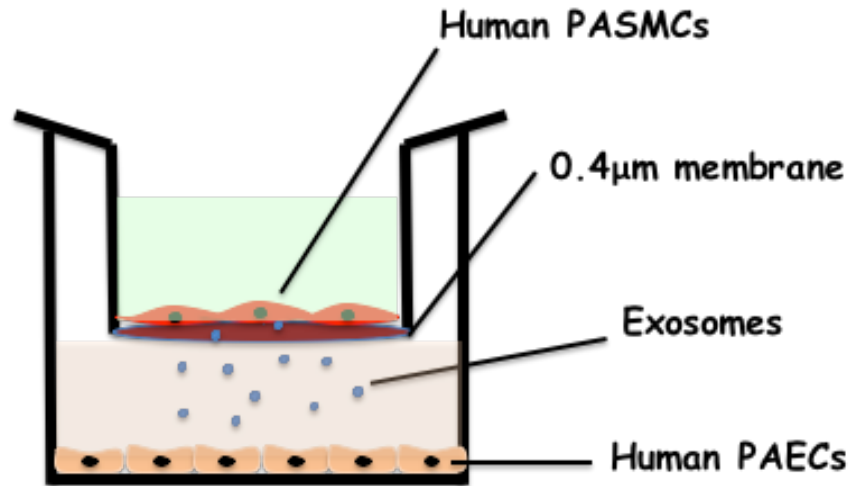


**Figure 2.5 Co-culture model of cell-to-cell communication**

A co-culture model was used for cell-to-cell communication between PASMCs and PAECs. PASMCs were seeded in the top well, and PAECs were seeded in the bottom well, and a 0.4 μm porous membrane between the 2 wells inhibiting cell-cell contact.

## **2.20 Labelling Pre-miR-143-3p Precursor with Cy3 *In Vitro***

Pre-miR miRNA precursor (has-miR-143-3p) was labelled with Label Cy3 using IT siRNA Tracker Cy3 Kit, according to the manufacturer's instructions (Mirus, Madison, WI, USA). Briefly, Label IT® siRNA Tracker Reagent was added 50 μl Label IT® Reconstitution Solution to completely reconstitute the pellet, mix well by gentle pipetting. The labelling reaction samples were prepared as follows: molecular biology-grade H<sub>2</sub>O 60 μl, 10 X Labeling Buffer A 10 μl, pre-miR-143-3p precursor 20 μl of a 40 μM stock, and the reconstituted Label IT® siRNA Tracker Reagent 10 μl. The reaction samples were incubated at 37 °C for 1 h and protected from light. After incubation, 0.1 volumes of 5 M sodium chloride and 2.5 volumes of ice cold 100% ethanol were added to reaction samples which were placed in -20 °C freezer for at least 30 min. This step was to remove the unreacted Label IT® siRNA Tracker Reagent from the labelled pre-miR precursor by ethanol precipitation. The reaction samples were further centrifuged at 14,000 g for 15 min at 4 °C to pellet the labelled pre-miR precursor, with supernatants carefully removed using a pipette. The labelled pellet was washed with 500 μl room temperature 70% ethanol and centrifuged at

14,000 g at 4 °C for 15 min and removed all traces of ethanol with a micropipette. The pellet was resuspended in 20 µl Dilution Buffer to bring the concentration to approximately 40 µM. Labelled pre-miRNAs were aliquoted and stored at -20 °C, protected from light.

## **2.21 Statistical Analysis**

All Taqman qRT-PCR results are expressed as mean and standard error of the mean (SEM). Statistical analysis was performed using Graphpad Prism 5 Software (California, USA) by unpaired student's t-test when comparing two experimental groups. When more than two groups were compared, a one-way ANOVA was performed followed by a Tukey's post hoc test. All statistics for individual experiments are showed in figure legends. Significance was determined as a *P* value of  $P < 0.05$ .

### **3 Evaluation of miR-143/145 in pulmonary arterial hypertension patient samples and in experimental animal models of PAH**

### 3.1 Introduction

The first study to identify the expression of miR-143 and miR-145 showed that their expression levels were reduced in precancerous and neoplastic colorectal tissue, indicating that these miRNAs may affect the early processes of tumorigenesis in the colon (Michael et al., 2003). MiR-143 and miR-145 have been deemed as “tumor suppressors” after extensive studies in human cancer (Akao et al., 2006, Zhang et al., 2012, Takagi et al., 2009, Kent et al., 2014). Later studies showed that miRNA expression broadly contributes to the tissue specificity of mRNA expression in many human tissues (Sood et al., 2006), underlining the importance of evaluating the pattern of miR-143/145 expression in different cell types in order to increase our understanding of the role of these miRNAs in the pathophysiological processes that drive human diseases.

The miR-143 encoding gene is highly conserved and lies with 1.4 kilobases (kb) of another conserved miRNA, miR-145, on mouse chromosome 18 and human chromosome 5. RT-PCR using primers from the stem-loop sequences of the miR-143/145 showed that they are derived from a common bicistronic precursor, indicating that they are co-transcribed from the same gene. Although miR-143 and miR-145 exist in a cluster, their mature forms exhibit no sequence homology (Cordes et al., 2009, Elia et al., 2009, Xin et al., 2009). The restricted expression of miR-143/145 was initially in early cardiomyocytes (E8.5 onward) but disappeared from cardiomyocytes at later stages (E16.5) and then express exclusively in SMCs. Interestingly, microarray experiments performed on various mouse tissues at different developmental stages revealed that the expression of miR-143 and miR-145 strongly correlated with the number of SMCs present in the organ analysed. For example, expression of these miRNAs was particularly high in aorta and bladder (Boettger et al., 2009). This observation was further confirmed by another study by evaluating the expression of miR-143/145 in various mouse tissues by northern blotting, which found that miR-143 and miR-145 is present in lung, skeletal muscle, heart, skin, and was most abundant in aorta and fat (Elia et al., 2009). Thus, miR-143/145 cluster is known as smooth muscle cell (SMCs)-enriched miRNAs.

There are several studies that have reported a role for miR-143/145 in vascular diseases in which SMCs play fundamental role in disease pathogenesis such as acute vascular injury (carotid artery balloon injury, wire injury, ligation injury), atherosclerosis, and cardiac disease (transverse aortic constriction (TAC) mouse model). In the carotid balloon injury model in male Sprague-Dawley rats, miR-143/145 expression was significantly downregulated at day 7, 14 and 28 days after balloon injury (Ji et al., 2007). Adenovirus-mediated restoration of miR-145 (Ad-miR-145) in balloon-injured arteries inhibited neointimal growth (Cheng et al., 2009), in line with similar studies performed by Elia et al using Ad-miR-145 and Ad-miR-143 (Elia et al, 2009). Using the carotid artery ligation model, which results in narrowing of the vascular lumen as a result of phenotypic modulation and proliferation of VSMCs, a significant downregulation of miR-143 and miR-145 expression was observed when injured vessels were compared to sham contralateral vessels (Cordes et al, 2009). Consistent with this results, miR-143/145 knockout (KO) aged mice (18 month) develop neointimal lesions in the femoral arteries (Boettger et al., 2009). However, another study use different miR-143/145 mutant mice following carotid artery ligation showed that miR-143 KO, miR-145 KO and miR-143/145 double KO mice dramatically reduced the neointimal formation (Xin et al., 2009). These data suggest that miR-143/145 cluster is key regulator in the response of vascular SMCs to vessel injury.

In atherosclerosis disease, apolipoprotein E (ApoE) knockout mice is a classic model to study atherosclerosis, which can induce vascular stress and damage by a hypercholesterolaemic diet (Breslow, 1996). The qRT-PCR results showed miR-143/145 expression level was significantly reduced in the aorta of ApoE KO mice, and the expression was further reduced with high fat diet (HFD) feeding (Elia et al., 2009). The downregulation of miR-145 in atherosclerosis was further confirm with ApoE KO mice maintained with Western diet for 12 weeks compared with WT control and before diet initiation. In human carotid artery segments with plaque containing also have reduced level of miR-145 compared with normal controls. Vascular smooth muscle cell (VSMC)-specific miR-145 lentivirus treated ApoE<sup>-/-</sup> mice markedly reduced atherosclerosis *in vivo* (Lovren et al., 2012).

In addition, the transcripts of miR-145 were downregulated to nearly undetectable levels in atherosclerotic lesions with significant neointimal formation (Cordes et al., 2009). In addition, the Dimmeler group demonstrated that shear stress could induce *KLF2* and miR-143/145 expression and *KLF2* also induced miR-143/145 increase in endothelial cells (ECs). These miRNAs packaged in EC secreted extracellular vesicles, which can transfer miR-143/145 to target VSMCs. In the atherosclerosis mouse model, the injection of extracellular vesicles from *KLF2* transduced mouse ECs that contained enriched miR-143/145 resulted in marked reduction of atherosclerosis in ApoE<sup>-/-</sup> mice (Hergenreider et al., 2012). All these studies suggested that miR-143/145 cluster have an anti-atherogenic role in atherosclerosis. In contrast with these observations, the genetic ablation of miR-143/145 attenuated the progression of atherosclerosis in *Ldlr*<sup>-/-</sup> mice due to the changes in VSMC functions and lipid metabolism (Sala et al., 2014). These discrepancies may be due to the disparities between the transient overexpression and genetic ablation of miR-143/145 *in vivo*.

In addition to the interventional animal studies described above, several studies have shown dysregulation of the miR-143/145 cluster in samples from patients suffering from cardiovascular disease and related conditions. In patients, miR-143/145 significantly decreased in aortic aneurysm compared with normal aortic biopsies (Elia et al., 2009). MiR-145 was also reported significantly reduced in the blood of patients with coronary artery disease (CAD) compared with healthy individuals (Fichtlscherer et al., 2010). In Type 2 diabetes derived saphenous vein SMCs, both miR-143 and miR-145 were significantly elevated compared with non-diabetic patients (Riches et al., 2014). *In vitro*, Elia et al also showed that miR-143/145 KO derived VSMCs showed increased migration towards PDGF (Elia et al., 2009). A follow-up study demonstrated that loss of miR-143/145 *in vitro* and *in vivo* results in the formation of podosomes, which are actin-rich membrane protrusions involved in the migration of several cell types, including SMCs (Quintavalle et al., 2010).

In PAH, previous studies have demonstrated the dysregulation of the miR-143/145 cluster in PAH. Taqman low density arrays (TLDA) performed in pulmonary artery smooth mus-

cle cells (PASMCs) derived from distal pulmonary arteries (PAs) of patients with idiopathic PAH and controls was the first to demonstrate that miR-145 was up-regulated in PASMCs from IPAH patients (Courboulin et al., 2011). This observation was further confirmed by Bockmeyer and colleagues and our group, who found that miR-143/145 expression levels were significantly higher in concentric lesions (CLs) than plexiform lesions in PAH patients (Bockmeyer et al., 2012) and that miR-145-5p was up-regulated in distal PASMCs and in lung tissues from IPAH and HPAH patients. In the mouse chronic hypoxia induced PH model, miR-145-5p expression was significantly increased in the total lungs and the right ventricle. To further study the role of miR-145 in the pathogenesis of PAH, Caruso et al. found that genetic ablation of miR-145 in female mice prevented the development of chronic hypoxia induced PH, showing a significant reduction of right ventricular systolic pressure, right ventricular hypertrophy and pulmonary vascular remodelling compared with hypoxic control WT mice (Caruso et al., 2012).

Gain of function and loss of function studies of specific miRNAs in animal disease models show that miRNAs are viable targets for therapeutics (van Rooij and Olson, 2012, Montgomery et al., 2011). In general, therapeutic approaches targeting ncRNAs involve inhibiting or overexpressing the ncRNAs. Currently, two major approaches are applied to modulate miRNA activity. First, restoring the function of specific miRNAs using either synthetic double-stranded miRNAs (e.g miRNA mimics, which imitate the mature miRNAs) or viral vector-based overexpression (Lentivirus or adenovirus vectors). Second, inhibiting the function of a miRNA using chemically modified single-stranded anti-miRNA oligonucleotides, which can bind irreversibly to the endogenous miRNAs and inactivate their function (van Rooij and Kauppinen, 2014, Samanta et al., 2016). Manipulation of miR-143/145 *in vivo* has been reported in several studies, showing efficacy in modulation of disease pathogenesis (Cheng et al., 2009, Elia et al., 2009, Cordes et al., 2009, Caruso et al., 2012, McLendon et al., 2015). In the context of PAH, therapeutic miRNA delivery to the lung in animal PAH models has been achieved via several routes: (a) subcutaneous injection (Caruso et al., 2012, Deng et al., 2015), (b) intravenous delivery (Bonci, 2010), (c) intranasal delivery (Kim et al., 2013), (d) Intratracheal delivery (Courboulin et al., 2011) and (e) in-

traperitoneal injection (Caruso et al., 2010).

An antimR-145-5p approach was used to investigate whether pharmacological inhibition of miR-145-5p produced similar results to genetic knockout in chronic hypoxia induced PH, showing that antimiR-14-5p treatment could significantly reduce the right ventricular systolic pressure and vascular remodelling, without inducing changes in right ventricular hypertrophy (Caruso et al., 2012). Another study used antimiR-145-5p formulated with Star: Star-mPEG lipid nanoparticles and delivered by intravenous in rat with SU5416/hypoxia induced PAH model. They showed Star:Star-mPEG delivery of anti-miR-145-5p elicited therapeutic effect in the PAH rat model through reduced pulmonary arteriopathy and cardiac dysfunction (McLendon et al., 2015). These studies demonstrate the important role that miR-145-5p plays in PAH, showing that manipulation of miR-145-5p is a potential therapeutic strategy in the treatment of PAH.

In general terms, *in vitro* studies have demonstrated the essential role for miR-143/145 in regulating SMC functions. Meanwhile, *in vivo* studies illustrate that specific knock down of miR-145 expression ameliorated the chronic hypoxia induced PH in mice. Further investigation the role of miR-143 in the development of pulmonary arterial hypertension would increase our depth of understanding the miR-143/145 cluster in PAH.

### 3.2 Aims

The miR-143/145 cluster has a pivotal role in VSMC differentiation and disease. Previous studies have demonstrated miR-145-5p expression upregulated in PASMCs from patients with PAH and miR-145-5p knocking down protected against the development of PH. However, it is not yet known about the role of miR-143 in PAH. The aims investigated in this chapter were:

- To evaluate the miR-143 expression profile in cells and tissues from pulmonary hypertension animal models and human patients with PAH.
- To assess whether miR-143 knockout can prevent the development of chronic hypoxia induced PH in a mouse model.
- To determine the effect of silencing miR-143-3p both in a prevention and rescue therapy study on the development of PH in the chronic hypoxia mouse model.
- To evaluate the therapeutic effect of intranasal delivery of antimiR-145-5p in the chronic hypoxia induced PH mouse model.

### 3.3 Results

#### 3.3.1 MiR-143 is Highly Expressed in PSMCs Compared to PAECs

To investigate miR-143 expression in female pulmonary artery smooth muscle cells (PSMCs) and pulmonary artery endothelial cells (PAECs), Taqman qRT-PCR assays for miR-143-3p (lead strand) and miR-143-5p (passenger strand) were performed in PSMCs and PAECs isolated from healthy female donors. We found that both miR-143 lead strand and passenger strand (miR-143-3p/5p) were expressed in PSMCs. However, only miR-143 lead strand (miR-143-3p) was expressed in PAECs (Figure 3.1).

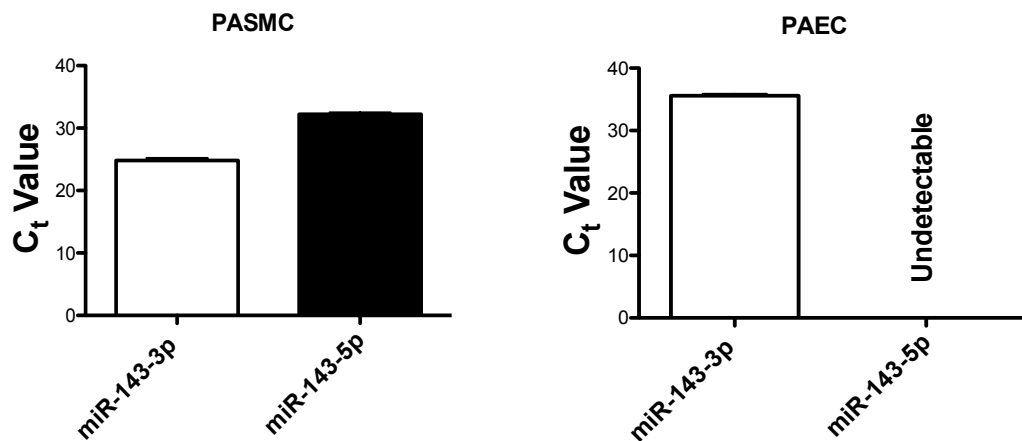


**Figure 3.1 Analysis of miR-143 expression levels in pulmonary vascular cells**

Pulmonary artery smooth muscle cells (PSMCs) and pulmonary artery endothelial cells (PAECs) from female healthy donors were cultured, RNA extracted and expression of miR-143-3p/5p was assessed using TaqMan qRT-PCR. n = 3 per group in triplicate.

### 3.3.2 MiR-143-3p is Upregulated in PAH Patients

Having shown that miR-143 is expressed mostly in the SMC compartment, we wished to examine the relative expression levels of miR-143 in PASMCs from PAH patients (both idiopathic and familial PAH (IPAH/FPAH)) and healthy controls. Here, we showed that miR-143-3p expression was significantly increased in PASMC from PAH patients compared with healthy donors (Figure 3.2 A) ( $P < 0.05$ ). However, there was no significant change in miR-143-5p (Figure 3.2 B). These results indicate miR-143-3p dysregulation may be involved in the pathogenesis of PAH. In order to further evaluate miR-143-3p expression in PAH patients, we use *in situ* hybridization to analyse miR-143-3p expression in the lung tissues from patients with PAH and healthy controls. The results showed that miR-143-3p appears to have a higher expression level in the smooth muscle cell layer (co-localised by staining with  $\alpha$ -SMC) in the constrictive lesions and complex lesions in patients (Figure 3.2 C). The constrictive lesions include medial hypertrophy, and intimal and adventitial thickening. And plexiform lesions, dilation lesions, and arteritis are classified as complex lesions.

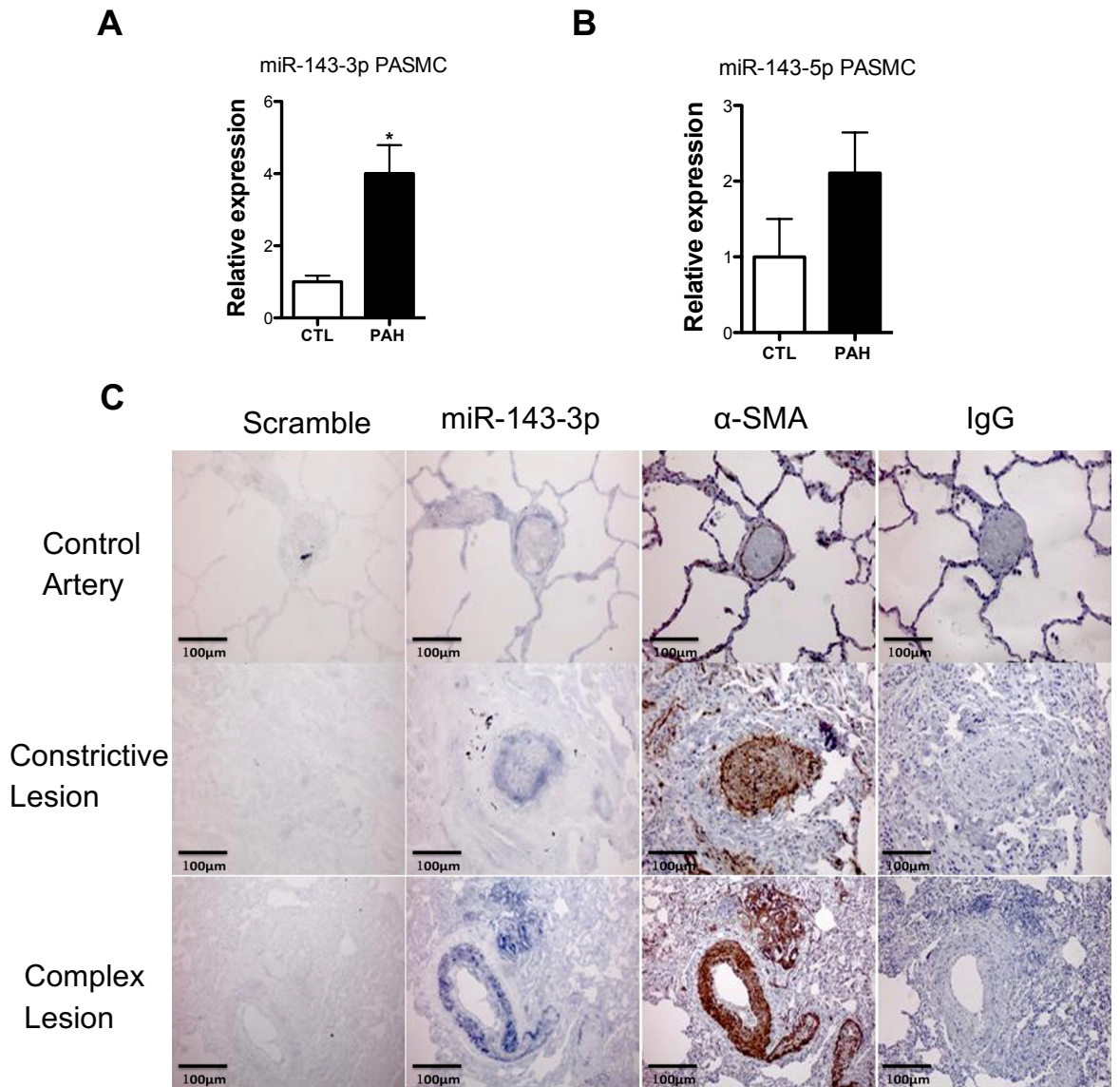


**Figure 3.2 Analysis of miR-143 expression in PAH patients and healthy controls**

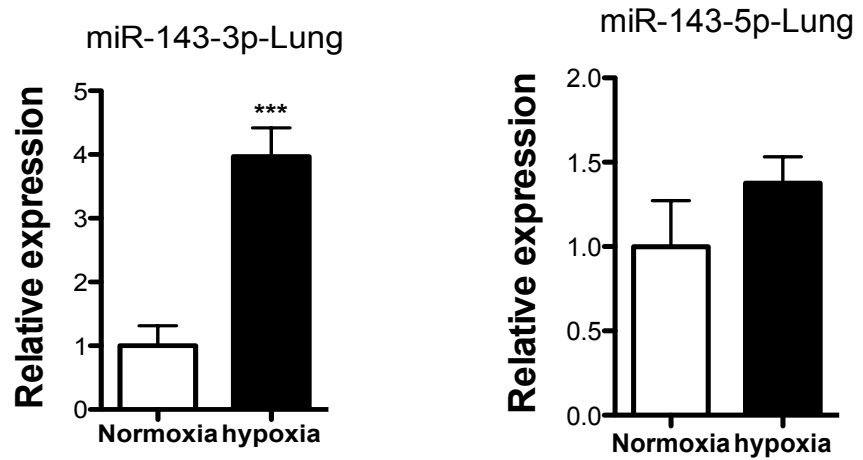
Taqman qRT-PCR analyses were performed on distal PASCs isolated from PAH patients and healthy controls to analyse the expression of miR-143. (A) MiR-143-3p was significantly upregulated in the patient cells compared with controls. (B) MiR-143-5p did not show any significant change. Data are expressed as mean  $\pm$  SEM and analysed by Student t-test; \* $P < 0.05$ .  $n = 3$  independent patients and performed in triplicate. (C) *In situ* hybridization of miR-143-3p in the lung tissues from PAH patients and healthy controls. In the patient group, miR-143-3p staining is much higher in the constrictive lesions and complex lesions. Localization of alpha smooth muscle action ( $\alpha$ -SMA) staining in lung was shown the smooth muscle cell layer in the pulmonary arteries.  $n = 3$  patient samples. Magnification X 10. Scale bar = 100  $\mu$ m. IgG = isotype control. This work was done by Dr. Ruifang Lu.

### 3.3.3 MiR-143-3p is Upregulated in Animal Models of Pulmonary Hypertension

In order to further investigate the dysregulation of miR-143 in PAH, we assessed the expression of miR-143 in different *in vivo* PAH models, including the chronic hypoxia induced PH mouse model, rat SU5416/hypoxia PH model, hypoxia neonatal calf model of PH, and Brisket Disease. There are no perfect animal models that completely recapitulate human PAH disease. However, different models provided valuable insight into various signalling pathways involved in the pathogenesis of PAH. First, we analysed miR-143 expression in the total lung and right ventricle (RV) from mice exposed to chronic hypoxia (the chronic hypoxia induced mouse pulmonary hypertension (PH) model). We found that miR-143-3p was significantly upregulated in both lung and right ventricle tissue from the chronic hypoxia group (Figure 3.3 A and B) ( $P < 0.01$ , and  $P < 0.001$ ), however, there was no difference in miR-143-5p levels between chronic hypoxia treated mice and normoxic controls (Figure 3.3 A and B). *In situ* staining in the mouse right ventricle showed highly expression of miR-143-3p in the chronic hypoxia group (Figure 3.4). To confirm this observation, we further analysed miR-143 expression in cardiomyocytes and fibroblasts from mouse heart, Taqman qRT-PCR results showed that miR-143-3p/5p were expressed in both cell types (Figure 3.5). Second, we analysed the miR-143-3p expression in the rat SU5416 model of PH. There were three groups in this analysis including normoxia/vehicle group, normoxia/SU5416, and hypoxia/SU5416. SU5416 is inhibitor of the vascular endothelial growth factor receptor-2 (VEGFR2), which is mainly expressed in endothelial cells and plays a vital role in the cell maintenance and functions (Lee et al., 2007). The hypoxia/SU5416 model of PH is characterised by endothelial dysfunction (Ciuclan et al., 2011). TaqMan qRT-PCR found that miR-143-3p significantly increased in hypoxia + SU5416 group compared with normoxic groups at different time-points (2 weeks, 3 weeks, 8 weeks, and 14 weeks) (Figure 3.6) ( $P < 0.01$  and  $P < 0.001$ ). Third, we analysed the expression of miR-143-3p in the new-born calves that develop severe pulmonary hypertension after exposure to hypoxia, which associated with many of the same functional and structural abnormalities observed in human infants with pulmonary hypertension (Stenmark et al.,

1987). *In situ* hybridization results revealed increased miR-143-3p level in the vascular wall of the small pulmonary arterioles. In addition, we further assessed the miR-143-3p level in the lung tissue of calves suffering from Brisket disease, which is a naturally occurring animal model of hypoxia induced pulmonary hypertension (Rhodes, 2005). *In situ* hybridization showed highly express of miR-143-3p in the vascular wall of distal pulmonary arterioles. Smooth muscle cell identity was confirmed by immunostaining for smooth muscle myosin (Figure 3.7). Taken together, miR-143-3p expression was significantly up-regulated in different animal models of pulmonary hypertension, which indicates that miR-143-3p may be involved in the pathogenesis of PAH.

A



B

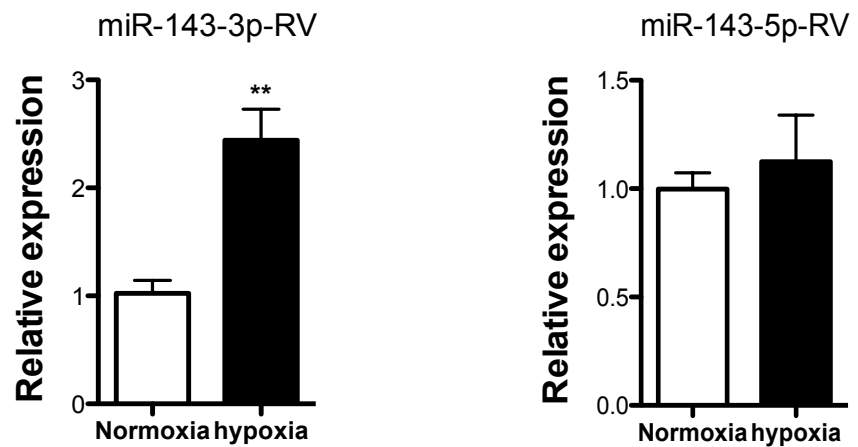


**Figure 3.3 Analysis of miR-143 in chronic hypoxia induced PH mouse model**

Mature miR-143 expression was detected by Taqman qRT-PCR in whole lung and right ventricle from female mice after 2 weeks exposure to normoxic and hypoxic conditions. (A) Taqman qRT-PCR showed that miR-143-3p was significantly upregulated in the lung in the chronic hypoxia group compared with normoxia group. There was no difference for miR-143-5p ( $n = 6$ ). (B) Taqman qRT-PCR showed that miR-143-3p significantly upregulated in the RV in the chronic hypoxia group compared with normoxia group. There was no difference for miR-143-5p ( $n = 3$ ). Data are expression as mean  $\pm$  SEM and analysed by Student t-test.  $**P < 0.01$ ,  $***P < 0.001$ .

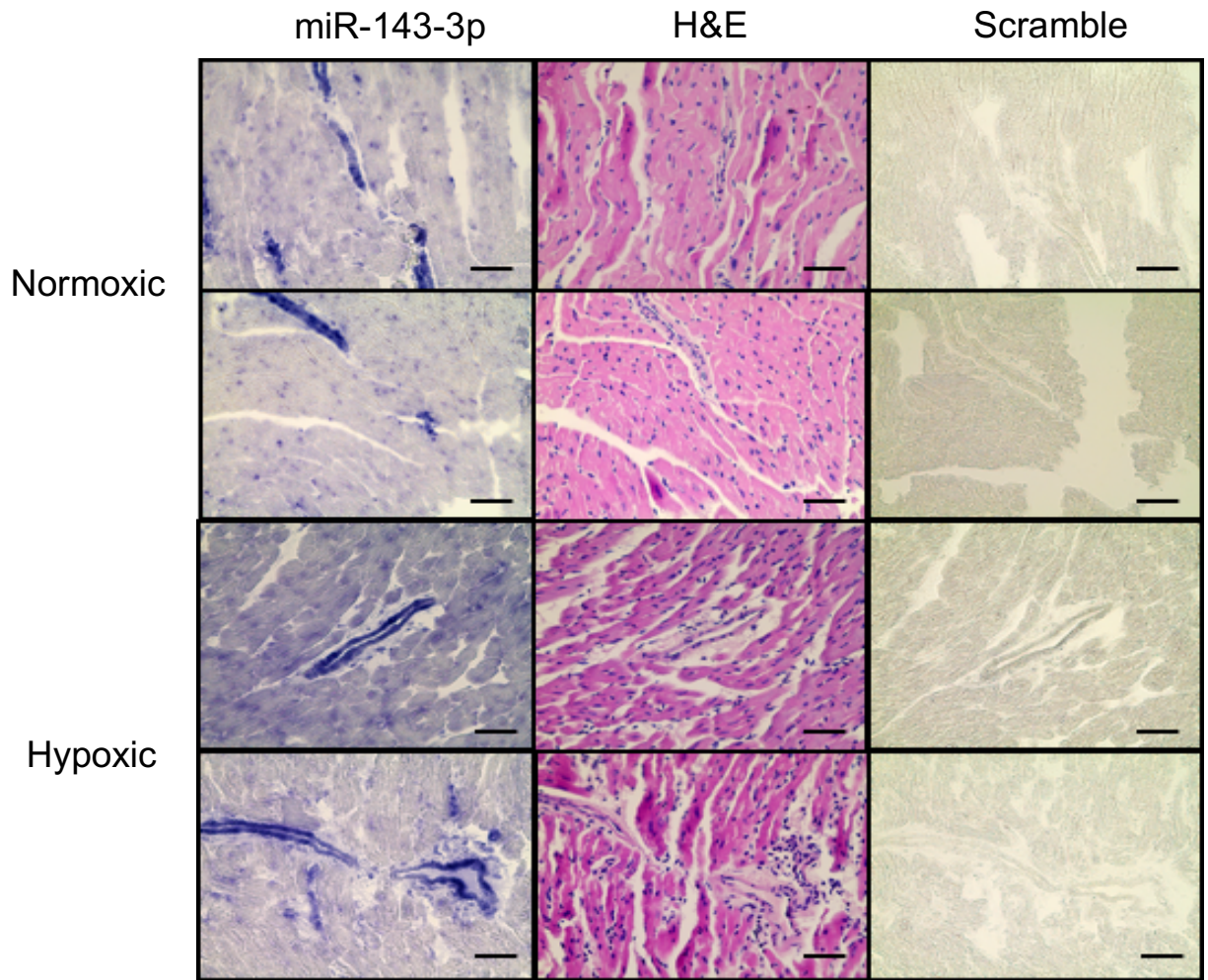


**Figure 3.4 *In situ* hybridization analysis of miR-143-3p in right ventricle**

Paraffin sections of RV with 5  $\mu\text{m}$  were rehydrated and incubated with miR-143-3p probe and scramble probe. *In situ* hybridization analysed the miR-143-3p expression in right ventricle of the hypoxic and normoxic mice. Right ventricular morphological changes were observed by Hematoxylin and eosin (H&E) staining. Images X 40 magnification. Scale bar = 50  $\mu\text{m}$ . n = 3 animals per group. This work was done by Dr. Hannah Stevens.

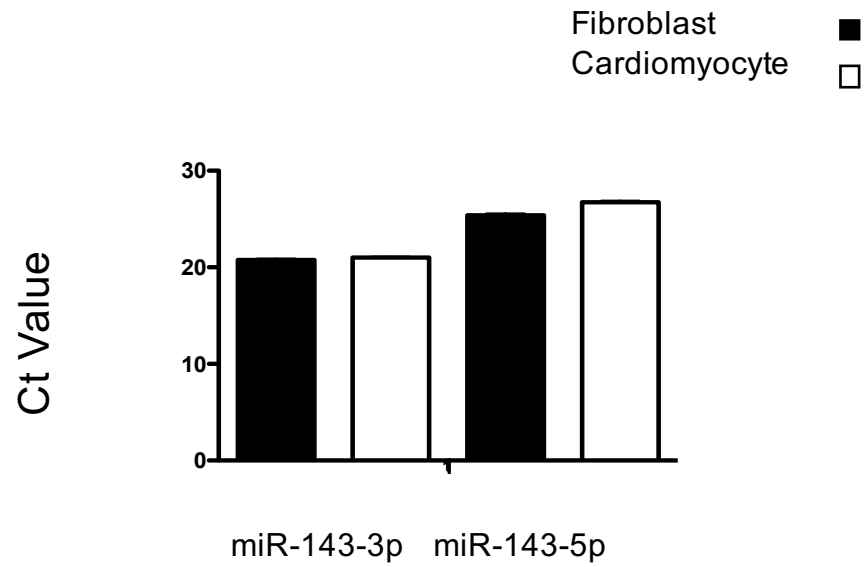


**Figure 3.5 Analysis of miR-143 expression in mouse cardiomyocytes and fibroblasts**

Taqman qRT-PCR was performed on isolated adult mouse cardiomyocytes and fibroblasts to analyse the expression of miR-143-3p and-5p. Results showed that miR-143-3p/5p were expressed in cardiomyocytes and fibroblasts. n = 3 individual mice and performed in triplicate. This work was done by Dr. Hannah Stevens.

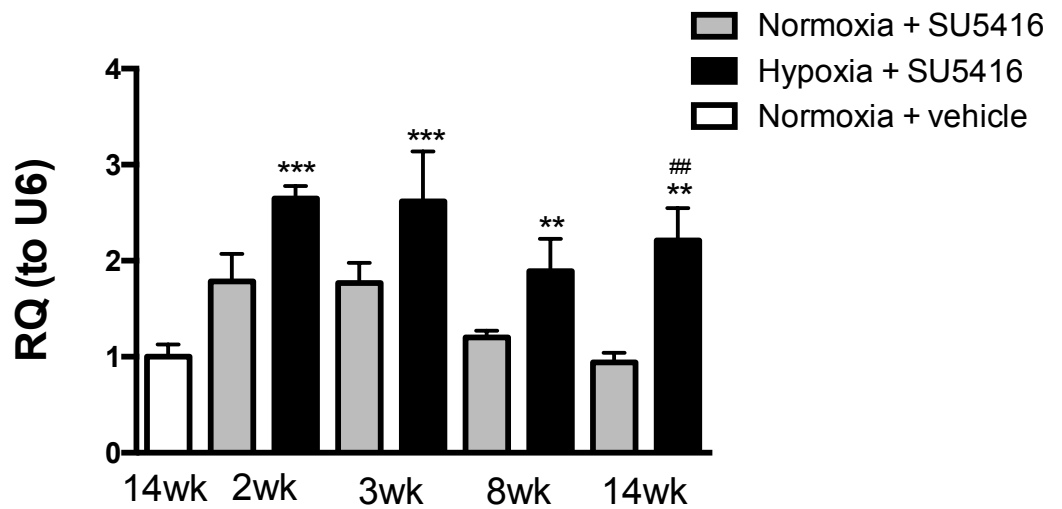


**Figure 3.6 Analysis of miR-143-3p expression in SU5416/hypoxia rat PH model**

MiR-143-3p detected by qRT-PCR in lung from male rats exposed to normoxic or hypoxic conditions for 2 weeks coupled with subcutaneous administration of 20 mg/kg SU5416 on day 0, followed by varying lengths of time in normoxic conditions. Total study time indicated on x-axis. Arbitrary value of 1 assigned to 14 wk normoxia + vehicle. Data represented as fold change  $\pm$  SEM and analysed by a one-way ANOVA followed by Tukey's post hoc test,  $n = 5$  animals per group. \* $P < 0.05$ , \*\* $P < 0.01$ , \*\*\* $P < 0.001$  vs 14 week normoxia + vehicle, # $P < 0.01$  vs time matched normoxia + SU5416.  $n = 5$  animals per group. RQ = Relative Quantification. This work was done by Dr. Jenny Grant.

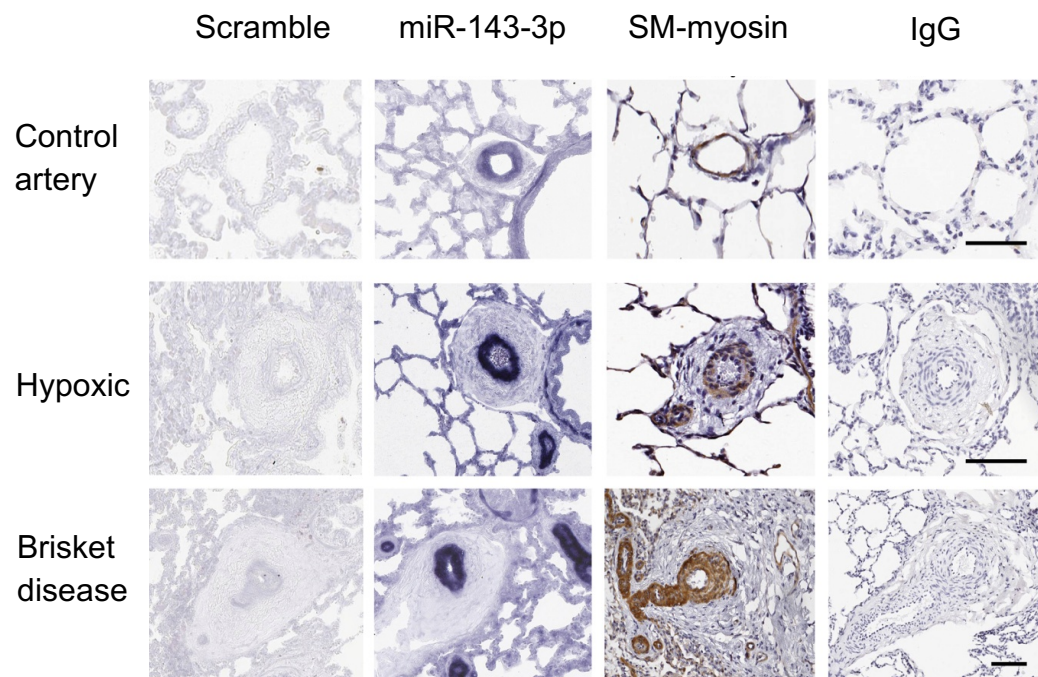


**Figure 3.7 *In situ* hybridization analysis of miR-143-3p expression in hypoxia neonatal calf PH model and brisket disease**

*In situ* hybridization and immunohistochemistry (IHC) were performed on fixed lung tissues of one-day-old Holstein calves were exposed to hypoxia for 2 weeks, and age-matched controls were kept at ambient altitude, and cattle naturally susceptible to pulmonary hypertension at high altitude (Brisket Disease, BD). *In situ* hybridization of miR-143-3p in lung tissue of hypoxic neonatal calf showed miR-143-3p level increased in the distal pulmonary arterioles compared with normoxic controls. In the brisket disease, miR-143-3p showed high expression level in the distal pulmonary arterioles. IHC for SM-myosin located the smooth muscle cell layer. n = 5 for hypoxia neonatal calves and control calves. n = 3 for brisket disease. This work was done by Prof. Kurt Stenmark lab.

### 3.3.4 Genetic Deletion of miR-143 in Mice Prevents Chronic Hypoxia Induced PH

Our previous data showed that miR-143-3p expression increased in animal models of PH and in PAH patients, suggesting that a reduction of miR-143-3p *in vivo* may attenuate the development of chronic hypoxia induced PH. We therefore used miR-143 knockout mice to study the effect of miR-143 genetic ablation in the chronic hypoxia induced PH model. The miR-143 mutant mice were generated by deletion of miR-143 stem loop (both miR-143-3p and -5p) (Xin et al., 2009). The targeting strategy was designed to replace the pre-miR-143 sequences with the neomycin resistance cassette flanked by loxP sites, which deleted both miR-143 stem loop and did not affect miR-145 level. MiR-143 KO mice and age-matched wild type control mice were exposure to hypoxic and normoxic conditions for 14 days, after which hemodynamic measurements, right ventricular hypertrophy and pulmonary vascular remodelling measurements were taken to assess the development of PH.

Systemic arterial pressure (SAP) was significantly increased after hypoxic exposure compared to basal conditions (normoxic). However, we did not observe any difference in SAP between the miR-143 KO and WT mice in both normoxic and chronic hypoxia (Figure 3.8 A). There was also no difference in heart rate between the two groups (Figure 3.8 B) and no difference in basal right ventricular systolic pressure (RVSP) between miR-143 KO and WT mice (normoxic condition) (Figure 3.9). In the hypoxia condition, both WT and miR-143 KO showed significantly increase in RVSP with hypoxia exposure ( $P < 0.05$  and  $P < 0.001$ ). In addition, compared with two groups in the chronic hypoxia condition, the RVSP of miR-143 KO mice significantly decreased compared with WT mice ( $P < 0.001$ ) (Figure 3.9). After 14 days chronic hypoxia exposure, right ventricular hypertrophy (RVH) significantly increased in the WT mice. However, there was no significant increase in RVH in miR-143 KO mice after hypoxic exposure and miR-143 KO mice showed significantly reduced RVH compared with WT mice in the chronic hypoxia (Figure 3.10 A) ( $P < 0.001$ ). In line with these results, miR-143 KO animals exhibited decreased pulmonary vascular

remodelling compared with WT mice in chronic hypoxia (Figure 3.10 B) ( $P < 0.05$ ).

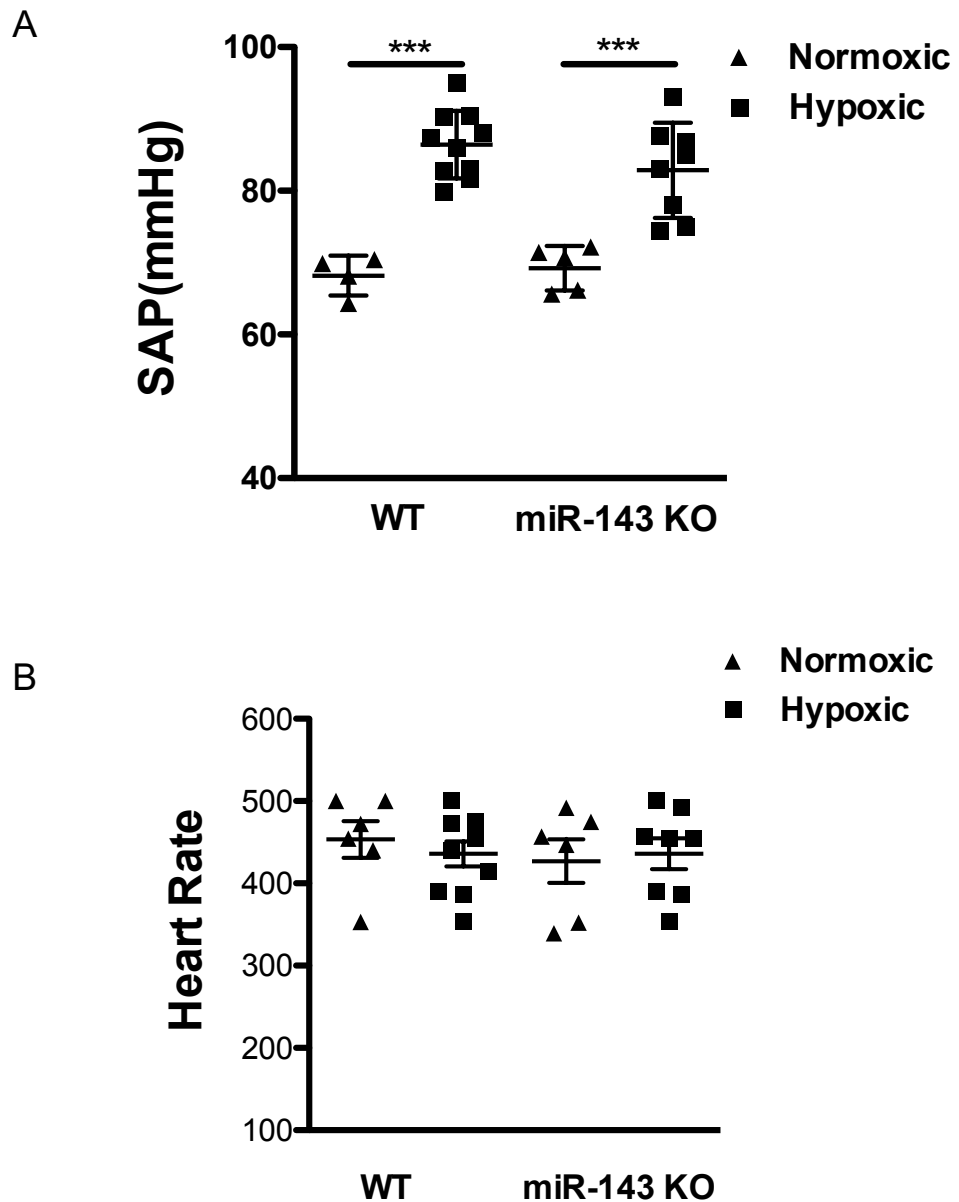
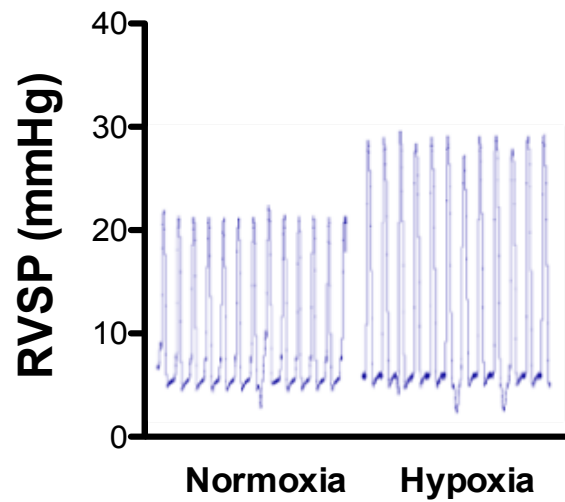


**Figure 3.8 Effect of miR-143 knockout on systemic arterial pressure and heart rate**

Mir-143 KO and WT control mice exposed to chronic hypoxia for 14 days together with normoxia controls. Quantification of (A) systemic arterial pressure (SAP) in female miR-143 KO and WT mice showed that SAP significantly increased in chronic hypoxia exposure compared with normoxia. However, no differences were observed between miR-143 KO and WT in both conditions. (B) Heart rate in female miR-143 KO and WT controls exposure to normoxic or hypoxic conditions for showed no changes. Data are expression as mean  $\pm$  SEM and analysed by Student t-test. \*\*\* $P < 0.001$ ,  $n = 6-10$  animals per group.

A



B

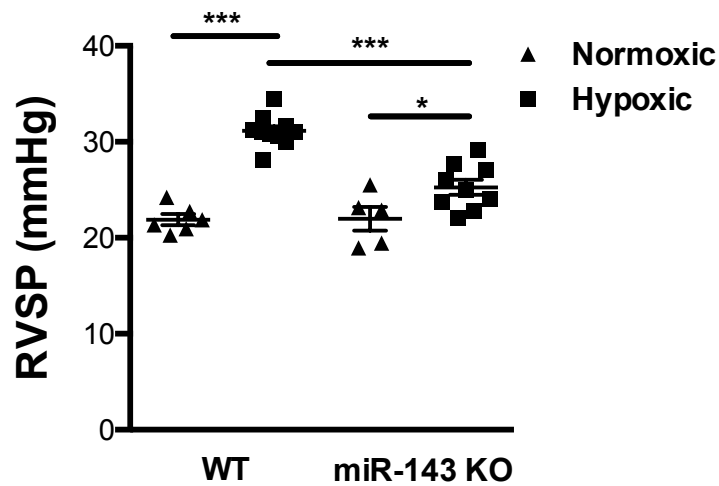
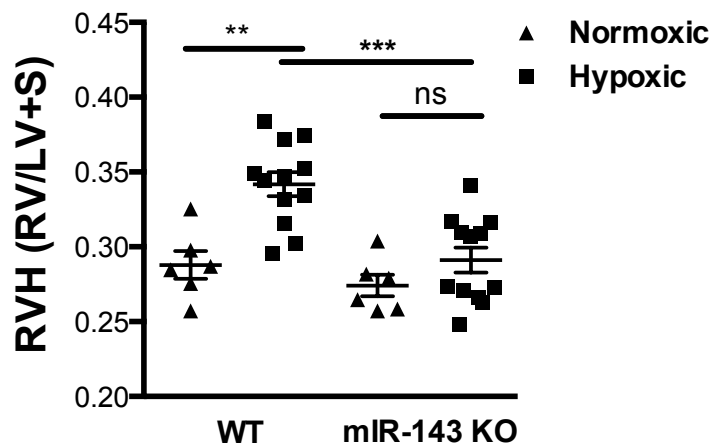


**Figure 3.9 Effect of miR-143 knockout on right ventricular systolic pressure**

Mir-143 KO and WT control mice were exposed to chronic hypoxia for 14 days together with normoxia conditions. (A) Representative recording of right ventricular pressure and (B) quantification of RVSP in female miR-143 KO and WT controls exposure to normoxic or hypoxic conditions. Both miR-143 KO and WT mice showed significantly increased RVSP in chronic hypoxia exposure compared with normoxia. And the elevation of RVSP in WT mice revealed significantly higher than miR-143 KO mice in the chronic hypoxia. Data are expression as mean  $\pm$  SEM and analysed by Student t-test  $*P < 0.5$ ,  $***P < 0.001$ . n = 6-9 animals per group.

A



B

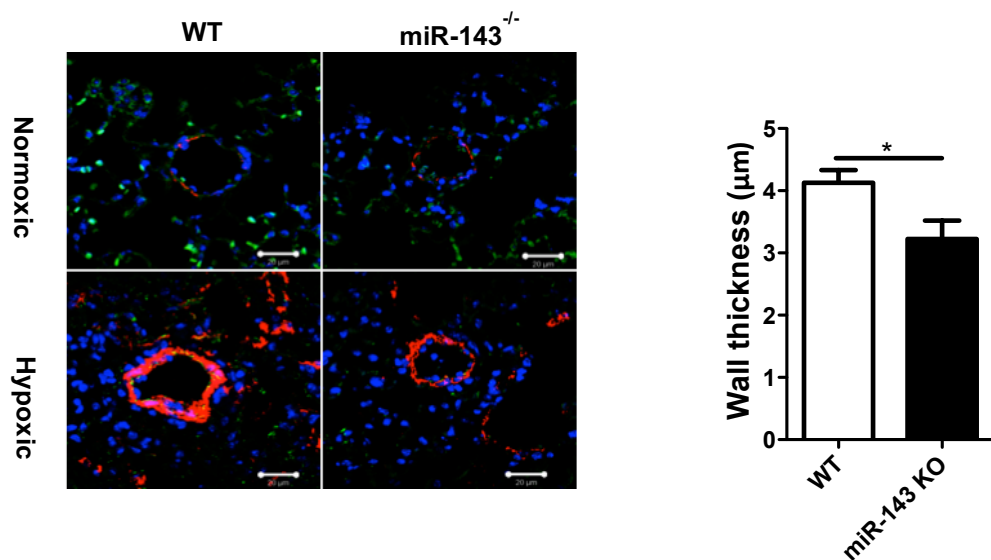


**Figure 3.10 Effect of miR-143 knockout on right ventricular hypertrophy and pulmonary vascular remodelling**

Mir-143 KO and WT control mice exposed to chronic hypoxia for 14 days together with normoxic controls. (A), quantification of right ventricular hypertrophy (RVH,  $n = 6-12$  mice per group) in WT and miR-143 KO mice showed that miR-143 KO mice had less RVH compared with WT mice in chronic hypoxia. And chronic hypoxia exposure significantly induced RVH in WT mice rather than miR-143 KO mice. (B) Distal pulmonary artery vessel wall thickness and remodelling were analysed by  $\alpha$ -smooth muscle actin ( $\alpha$ -SMA) (Red), CD31 (Green) and DAPI (Blue) staining in miR-143 KO mice compared with their WT littermate controls in both normoxic and chronic hypoxia ( $n = 4$  mice per group). MiR-143 KO mice showed decreased pulmonary vascular remodelling compared with WT control in chronic hypoxia. Data are expression as mean  $\pm$  SEM and analysed by Student t-test. Scale bar = 20  $\mu$ m. \* $P < 0.05$ , \*\* $P < 0.01$ , \*\*\* $P < 0.001$ .

### 3.3.5 Pharmacological Inhibition of miR-143-3p in Mice Alleviates the Development of PH

Genetic ablation of miR-143 proved to be beneficial in the chronic hypoxia induced PH mouse model. In order to assess the therapeutic role of miR-143-3p in PAH, silencing of miR-143-3p was applied *in vivo* in the mouse chronic hypoxia model of PH using anti-miRNA oligonucleotides inhibiting the mature miR-143-3p in competition with cellular target mRNAs leading to function inhibition of the miR-143-3p and derepression of their direct target mRNAs. Locked nucleic acid anti-miR probes bind to and form heteroduplexes with target miRNA, thereby sequestering and preventing the miRNA from binding to the 3' UTR of its target mRNAs (Giaid et al., 1993). AntimiR-143-3p is a 16-mer oligonucleotide comprising at least 9 LNAs with an LNA at both 5' and 3' ends and with full phosphorothioate linkages (In collaboration with MiRagen Therapeutics, Boulder, Colorado, USA). Administration of antimiR-143-3p was subcutaneously injected at day 0 and day 7 during the period of 14 days in both normoxia and chronic hypoxia at a 25 mg/kg concentration (Figure 3.11). To verify the knockdown of miR-143-3p by antimiR-143-3p treatment, lung, pulmonary artery (PA) and right ventricle (RV) were harvested and miR-143-3p expression was analysed by Taqman qRT-PCR. MiR-143-3p levels were significantly reduced in the antimiR-143-3p treated group compared with both control anti-miRNA (Scramble) and PBS treatment groups (Figure 3.12) ( $P < 0.01$  and  $P < 0.001$ ).

The effect of knockdown miR-143-3p on the development of chronic hypoxia induced PH in female mice was quantified by analysis of key indicators of PH including systemic arterial pressure (SAP), right ventricular systolic pressure (RVSP), right ventricular hypertrophy (RVH) and pulmonary vascular remodelling. There was no significant change in SAP between normoxia and chronic hypoxia groups. However, we observed that the basal (normoxic) SAP in the control (Scramble) group was significantly higher than basal SAP in animals treated with vehicle control (Figure 3.13 A) ( $P < 0.05$ ). This may result from off-target effects of the scramble control antimiRNA. Mice exposed to chronic hypoxia for 14 days displayed a significant increase in RVSP and RVH compared with normoxic

groups (Figure 3.13 B and C) ( $P < 0.001$ ). Notably, the RVSP in antimiR-143-3p treated group significantly reduced compared with control groups in chronic hypoxia condition, but no significant difference observed in normoxic condition (Figure 3.13 B) ( $P < 0.01$ ). In addition, pulmonary vascular remodelling did not have any changes between groups (Figure 3.14). Taken together, antimiR-143-3p treatment reduced the right ventricular systolic pressure in the chronic hypoxia induced PH mice model.

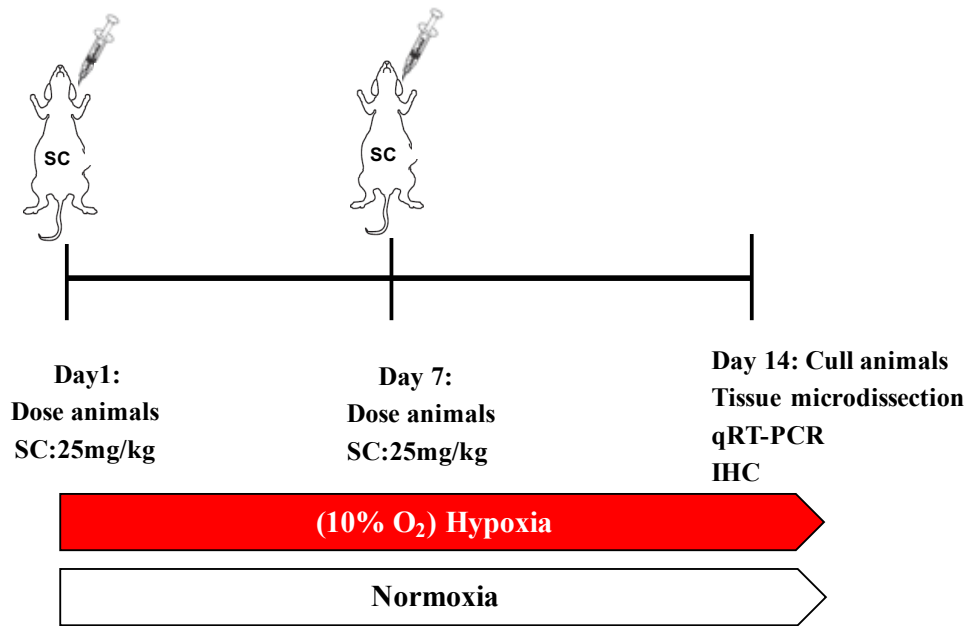


**Figure 3.11 Prevention study of antimiR-143-3p *in vivo* study design**

Female mice were administrated with antimiR-143-3p, control antimiRNA (Scramble) or PBS subcutaneously at 25 mg/kg every 7 days following 14 days normoxic or chronic hypoxia. On day 14, hemodynamic measurements were taken and tissues harvested.

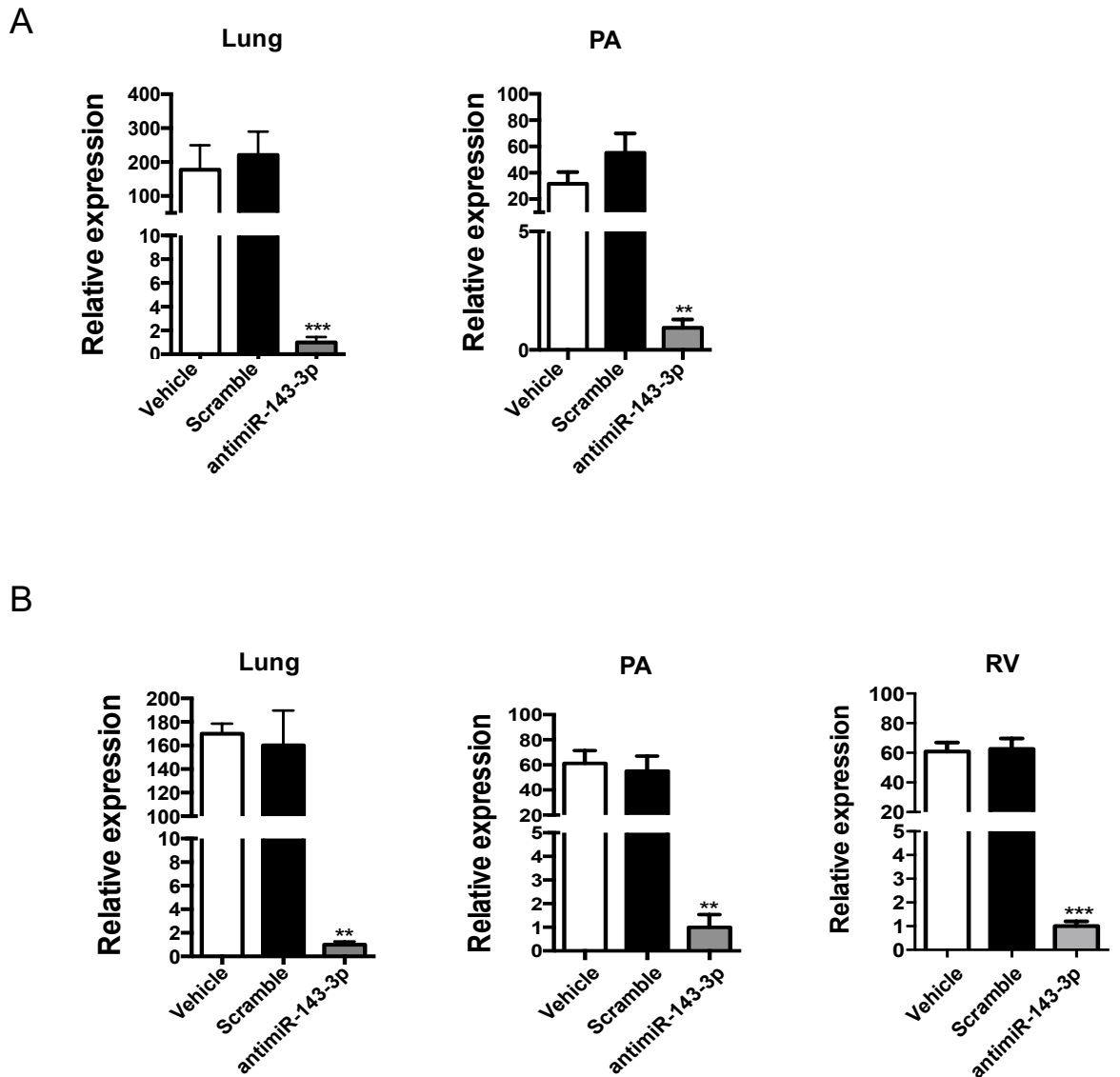
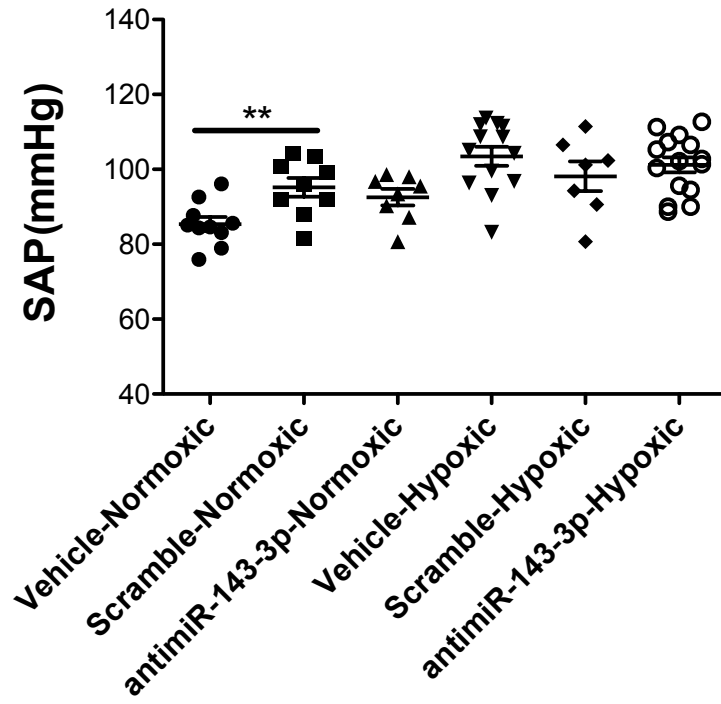
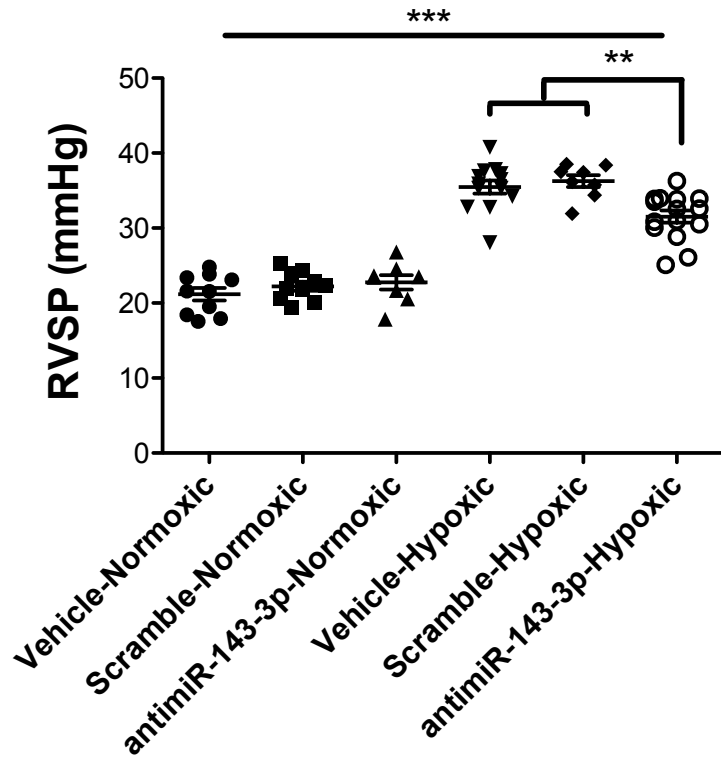


**Figure 3.12 Analysis of MiR-143-3p expression in lung, PA and RV of anti-miR-143-3p prevention study**  
 Expression of miR-143-3p in female mice lung tissue, pulmonary artery (PA) and right ventricle (RV) from anti-miR-143-3p prevention study were detected by qRT-PCR. (A) In the normoxia condition, miR-143-3p expression in lung (n = 10) and PA (n = 7) significantly reduced in the anti-miR-143-3p treated group compared with control groups. (B) In The hypoxia condition, miR-143-3p expression in lung (n = 5), PA (n = 6) and RV (n = 4) significantly reduced in the anti-miR-143-3p treated group compared with control groups. All data analysed by a one-way ANOVA followed by Tukey's post hoc tests. \*\* $P < 0.01$ , \*\*\* $P < 0.001$

A



B



C

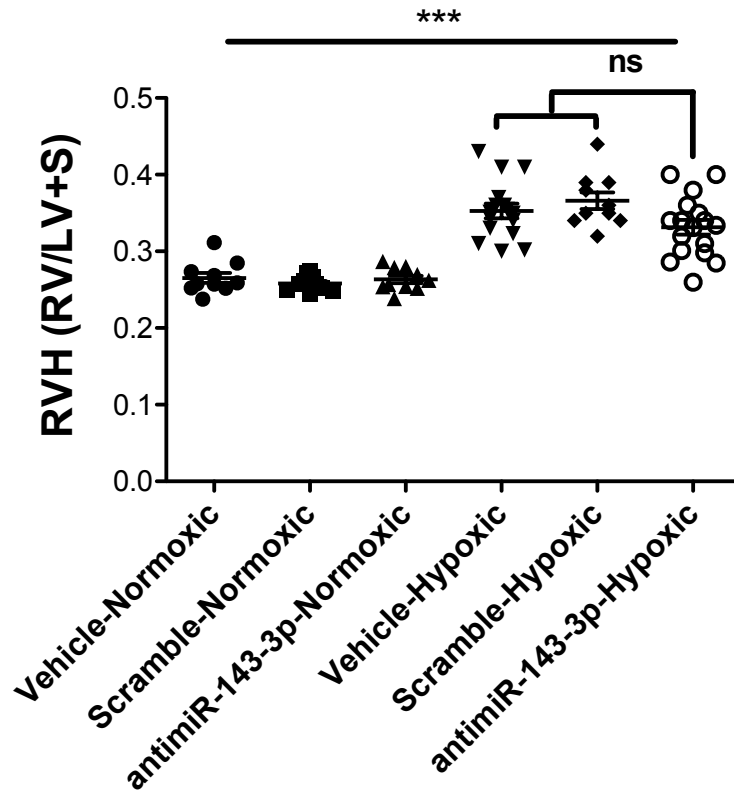


**Figure 3.13 Quantification of PH indices anti-miR-143-3p prevention study**

Quantification of (A) SAP, (B) RVSP and (C) RVH were performed in female mice from anti-miR-143-3p study at day 14. In normoxic condition, both RVSP and RVH showed no difference among three groups. However, SAP in the control anti-miRNA (Scramble) significantly increased compared with vehicle control. In the chronic hypoxia, there were no significant changes in SAP and RVH. However, RVSP in anti-miR-143-3p treated group significantly reduced compared with control groups. All data analysed by a one-way ANOVA followed by Tukey's post hoc tests.  $n = 7-16$  mice per group.  $**P < 0.01$ ,  $***P < 0.001$ .

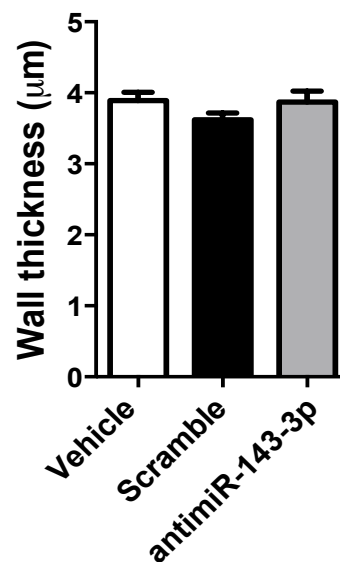
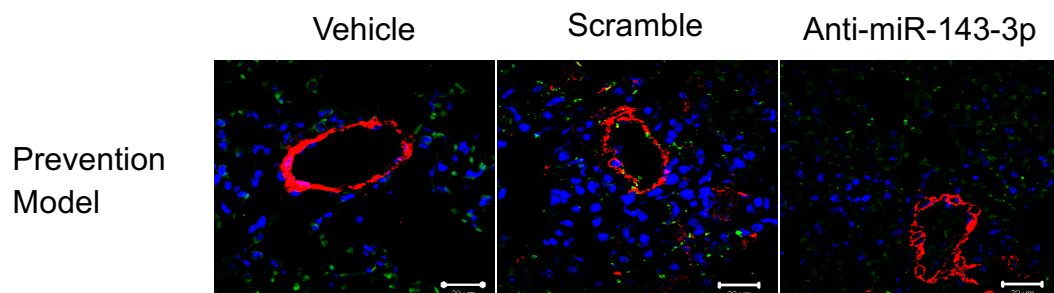


**Figure 3.14 Effect of anti-miR-143-3p treatment on the pulmonary vascular remodelling**

Distal pulmonary artery vessel wall thickness and remodelling were analysed by  $\alpha$ -smooth muscle actin ( $\alpha$ -SMC) and CD31 staining in prevention PH model by anti-miR-143-3p injection compared with control groups. There was no difference among groups. All data analysed by a one-way ANOVA followed by Tukey's post hoc tests. n =5 mice per group. Scale bar = 20  $\mu\text{m}$ .  $\alpha$ -SMC (red), CD31 (green), and DAPI (blue).

### 3.3.6 AntimiR-143-3p Treatment Shows Therapeutic Effect in Chronic Hypoxia Induced PH Mice

As the prevention study using anti-miR-143-3p treatment protected mice from the development of chronic hypoxia induced PH, we aimed to assess the therapeutic role of anti-miR-143-3p in established PH by performing a reversal study in female mice in established chronic hypoxia induced PH. In this reversal study, administration of anti-miR-143-3p or a scramble control anti-miRNA was performed at day 14 and day 21 during the period of 21 days exposure to chronic hypoxia (Figure 3.15). As in the prevention study, miR-143-3p knocking down in the total lung, pulmonary artery (PA) and right ventricle (RV) were analysed using Taqman qRT-PCR. Expressions of miR-143 were significantly down-regulated in the anti-miR-143-3p treated group compared to control anti-miRNA (Scramble) and vehicle treated group (Figure 3.16) ( $P < 0.05$ , and  $P < 0.001$ ).

The effect of knocking down miR-143-3p levels in mice with established PH was quantified by measuring the key indices of PH as for the prevention study. SAP did not differ between the three groups. However, we observed the SAP of two mice in the control anti-miRNA (Scramble) group was much higher than other mice. This may also result from off-target effects of the scramble anti-miRNA, as per the prevention study (Figure 3.17 A). Again, similar to the prevention study, the RVSP in the anti-miR-143-3p treated group was significantly decreased compared with the control groups (Figure 3.17 B) ( $P < 0.01$ ). Importantly, we observed a significant reduction of RVH in the anti-miR-143-3p treated group compared with control groups (Figure 3.17 C) ( $P < 0.01$  and  $P < 0.001$ ), while the prevention study did not have significant differences. In addition, there was a significant reduction in the pulmonary vascular remodelling in the anti-miR-143-3p treated mice compared to control groups (Figure 3.18) ( $P < 0.05$  and  $P < 0.01$ ). Taken together, anti-miR-143-3p treatment reversed the established PH in female mice, showing a therapeutic effect in the treatment of chronic hypoxia induced PH.

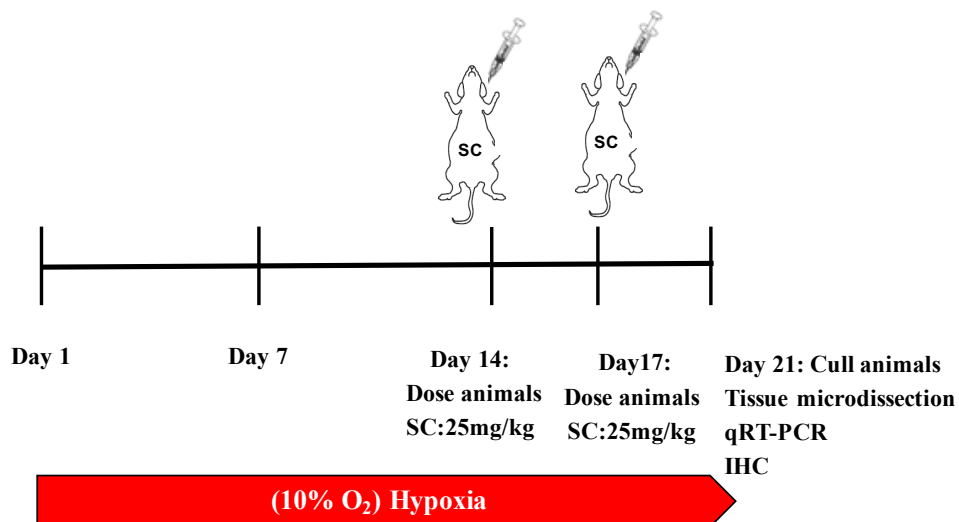


**Figure 3.15 Reverse study of antimiR-143-3p *in vivo* study design**

Female mice were administrated with antimiR-143-3p, control antimiRNA (Scramble) or PBS subcutaneously at 25 mg/kg on day 14 and 17 following 21 days chronic hypoxia. On day 21, hemodynamic measurements were taken and tissues harvested.

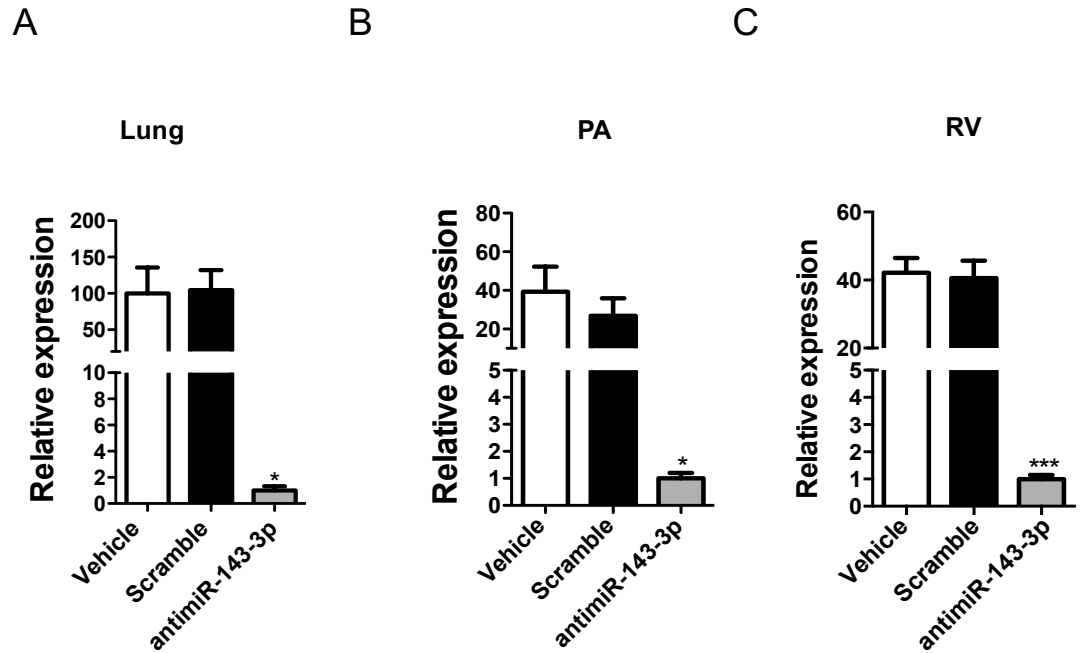


**Figure 3.16 Analysis of miR-143-3p expression in lung, PA and RV from anti-miR-143-3p prevention study**

Expression of miR-143-3p in female mice lung tissue, pulmonary artery (PA) and right ventricle (RV) from anti-miR-143-3p reversal study were detected by qRT-PCR. MiR-143-3p expression in lung (A), PA (B) and RV (C) significantly reduced in the anti-miR-143-3p treated group compared with control groups. All data were analysed by a one-way ANOVA followed by Tukey's post hoc tests.  $n = 5$  mice per group.  $*P < 0.05$ ,  $***P < 0.001$

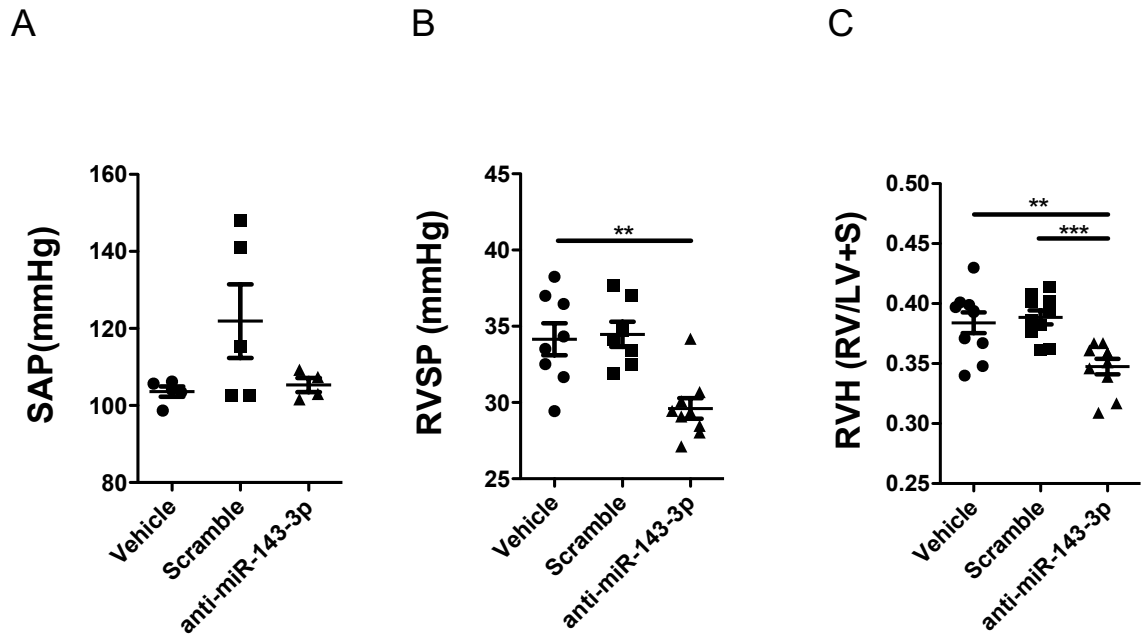


**Figure 3.17 Quantification of PH indices anti-miR-143-3p reversal study**

Quantification of SAP, RVSP and RVH in female mice from anti-miR-143-3p reversal study was performed at day 21. In the therapeutic study, there are no changes in SAP. However, RVSP and RVH in anti-miR-143-3p treated group significantly reduced compared with control groups. All data analysed by a one-way ANOVA followed by Tukey's post hoc tests. n = 6-10 mice per group. \*\* $P < 0.01$ , \*\*\* $P < 0.001$

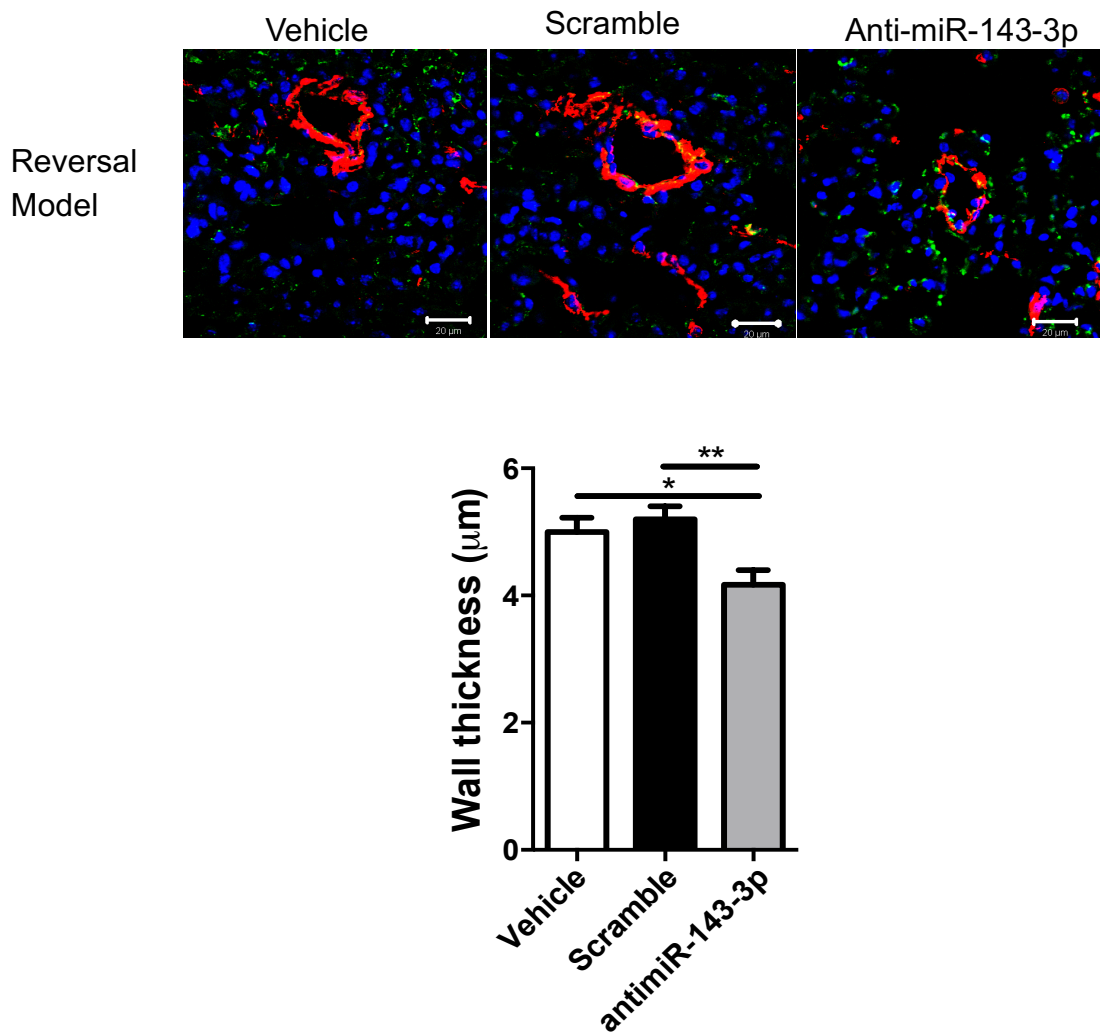


**Figure 3.18 Effect of anti-miR-143-3p reversal study on the pulmonary vascular remodelling.**

Distal pulmonary artery vessel wall thickness and remodelling were analysed by  $\alpha$ -smooth muscle actin ( $\alpha$ -SMC) and CD31 staining in reversal PH model by anti-miR-143-3p injection compared with control groups. The vascular remodelling in anti-miR-143-3p treated group was significantly reduced compared with control groups. All data analysed by a one-way ANOVA followed by Tukey's post hoc tests.  $n = 5$  mice per group. Scale bar =  $20 \mu\text{m}$ .  $*P < 0.05$ ,  $**P < 0.01$

### 3.3.7 Intranasal Delivery of anti-miR-145-5p Significantly Reduced the miR-145-5p Level in Pulmonary System

Previously our group found that increased expression of miR-145-5p in lung smooth muscle in wild-type mice exposed to chronic hypoxia and miR-145 knockout mice has a protective role on the development of chronic hypoxia induced pulmonary hypertension. Pharmacological inhibition of miR-145-5p *in vivo* also protected the development of chronic hypoxia induced PH mice model (Caruso et al., 2012). As pulmonary hypertension is a disease affecting the small pulmonary vessels, the localised topical therapy in the lungs of pulmonary hypertension can be developed as potential drug delivery route. This route makes it possible to deposit drugs more site-specifically at high concentrations with the diseased lung thereby reducing the drug amount given to patients, as well as increasing local drug activity while reducing systemic side effects and first-pass metabolism. This is a key area for miRNA therapeutics. Intranasal drug delivery has been recognised to be a useful and reliable alternative to oral and parenteral routes. Here, we addressed if blocking miR-145-5p following local delivery *in vivo* is able to attenuate chronic hypoxia induced PH. To answer this question, we use nucleic acid modified anti-miR-145-5p knockdown probes. The *in vivo* experiments were performed as described in (Figure 3.19). In this study, administration of anti-miR-145 intranasal was performed at day 1, 7, 14 and day 21 during the period of 28 days in the normoxic condition. To confirm knockdown of miR-145-5p in the lung, pulmonary artery (PA) and right ventricle (RV), expression of miR-145-5p was evaluated by Taqman qRT-PCR. As shown in, repeated intranasal delivery of anti-miR-145-5p significantly down-regulated the expression levels of miR-145-5p in lung tissue, pulmonary artery and right ventricle when assessed by Taqman qRT-PCR at day 28 in normoxic animals (Figure 3.20) ( $P < 0.001$ ). Furthermore, fibromodulin (*fmod*) and angiotensin-converting enzyme (*ace*), which are predicted targets of miR-145, were significantly upregulated in the anti-miR-145 treated group compared with control groups (Figure 3.21) ( $P < 0.05$ ). Meanwhile, other target gene such as SMAD family member 4 (*smad4*), Kruppel-like factor 5 (*klf5*), integrin, beta 1 (*itgb1*) and wen inhibitory factor-1 (*wif1*) were also upregulated, but not at significant levels (Figure 3.21).

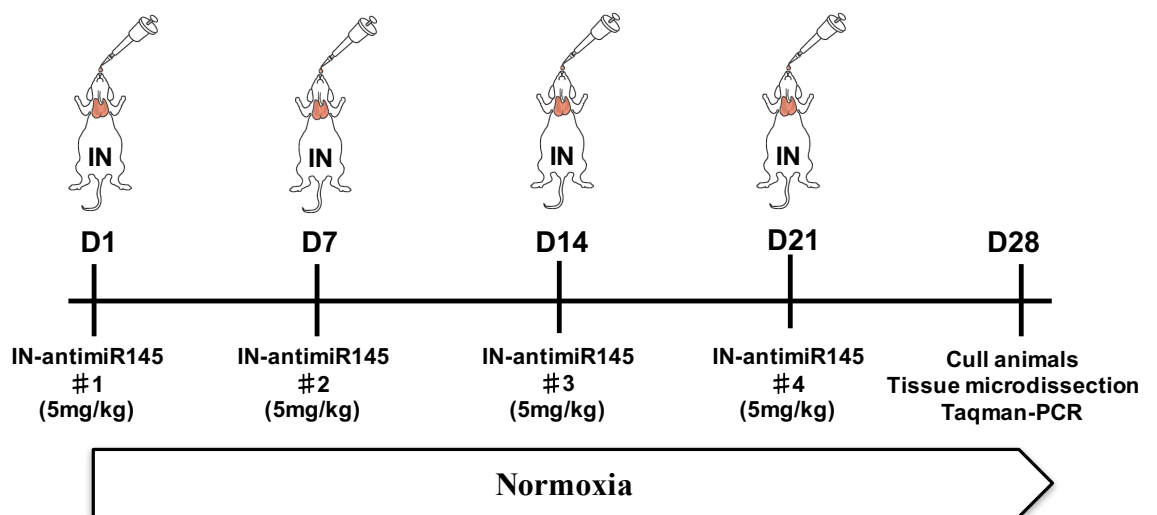


**Figure 3.19 Schematic of experimental normoxic mice model with anti-miR-145-5p administration**

Female mice were administrated with anti-miR-145 and control anti-miRNA (Scramble) intranasal at 5mg/kg on day 1, 7, 14, and 21 following 28 days normoxic. On day 28, were taken and tissues harvested.

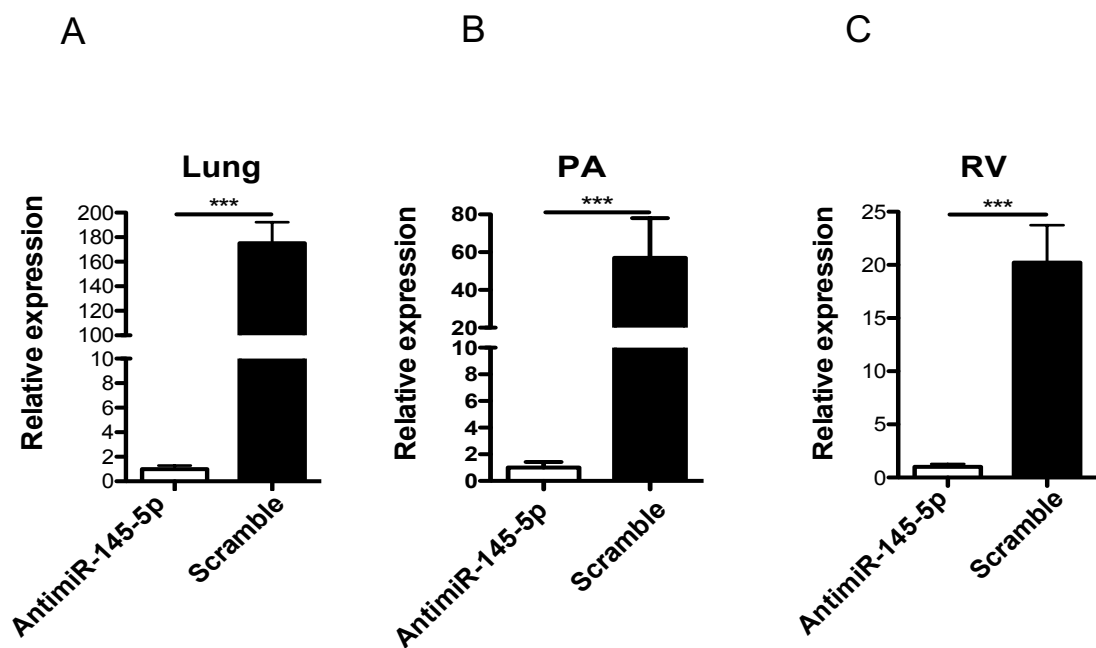


**Figure 3.20 Analysis of miR-145-5p lung, PA and RV from antimiR-145 treated mice**

Expression of miR-145-5p in female mice lung tissue, pulmonary artery (PA) and right ventricle (RV) from antimiR-145-5p intranasal delivery were detected by qRT-PCR. MiR-145-5p expression in lung (A), PA (B) and RV (C) significantly reduced in the antimiR-145-5p treated group compared with scramble control. Data are expression as mean  $\pm$  SEM and analysed by Student t-test. n = 6 mice per group. \*\*\* $P < 0.001$

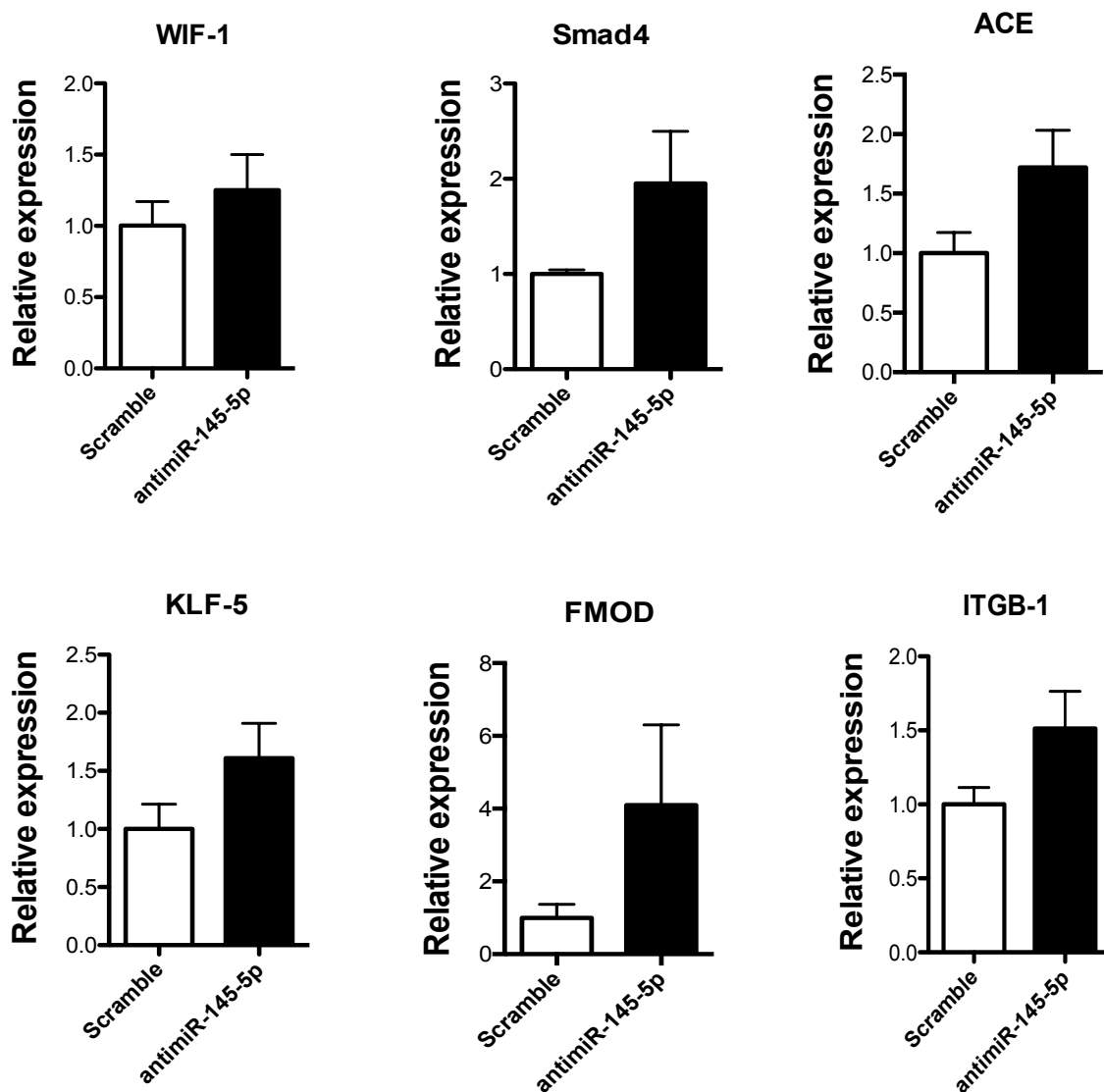


**Figure 3.21 Analysis of target genes expression of the anti-miR-145-5p treated mice**

The expression level of *fomd*, *ace*, *smad4*, *klf5*, *itgb1* and *wif1* was assessed by Taqman qRT-PCR in the total lung of scramble and anti-miR-145-5p treated mice. The predicted target gene fibromodulin (*fmod*) and angiotensin-converting enzyme (*ace*) were significantly upregulated. The other target genes did not show any significant differences. Data are expression as mean  $\pm$  SEM and analysed by Student t-test. n = 6 mice per group.

### **3.3.8 Intranasal Delivery of anti-miR-145-5p does not Attenuate Chronic Hypoxia Induced Pulmonary Arterial Hypertension**

Multiple doses of anti-miR-145-5p via intranasal delivery inhibited miR-145-5p expression and upregulated one target gene in total lung in the normoxic condition. In order to determine the effect of anti-miR-145-5p treatment in the chronic hypoxia induced PH mouse model, C57BL/6J wild-type female mice were intranasal delivered with anti-miR-145-5p at day 1, 7, 14 and day 21 during the period of 28 days in the normoxia and chronic hypoxia (Figure 3.22).

The miR-145-5p knocking down in the total lung was assessed by Taqman qRT-PCR. Expressions of miR-145-5p were significantly down-regulated in the anti-miR-145-5p treated group compared to control anti-miRNA (Scramble) and vehicle treated group ( $P < 0.001$ ) (Figure 3.23 A). Also, we selected some miR-145 target genes that were affected by intranasal delivery anti-miR-145-5p under normoxic condition. In chronic hypoxia induced lung tissue, only the *ace* gene was significantly upregulated in anti-miR-145-5p treated group compared with scramble and PBS control. There were no changes for other genes. (Figure 3.23 B) ( $P < 0.01$ ).

The effect of knocking down miR-145-5p by intranasal delivery was quantified by measuring the key indicators of disease, RVSP and RVH. We found that anti-miR-145-5p treatment did not attenuate chronic hypoxia induced PAH compared with scramble and PBS groups. As shown in (Figure 3.24), hemodynamic data of heart rate, right ventricular systolic pressure (RVSP) and systolic arterial pressures (SAP) in three groups did not have significant difference. There was no change in RVH (RV/LV + S) as well (Figure 3.24).

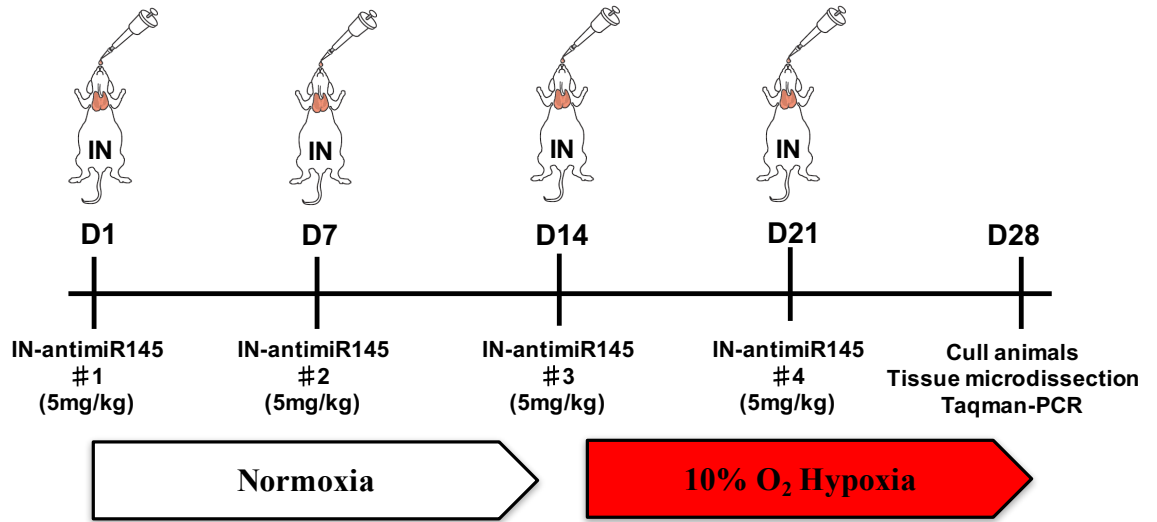


**Figure 3.22 Schematic of experimental mice PH model with antimiR-145-5p administration**

Female mice were administrated with antimiR-145-5p, control antimiRNA (Scramble) and PBS intranasal at 5mg/kg on day 1, 7, 14, and 21 following 28 days normoxic and chronic hypoxia. On day 28, hemodynamic measurements were taken and tissues harvested.

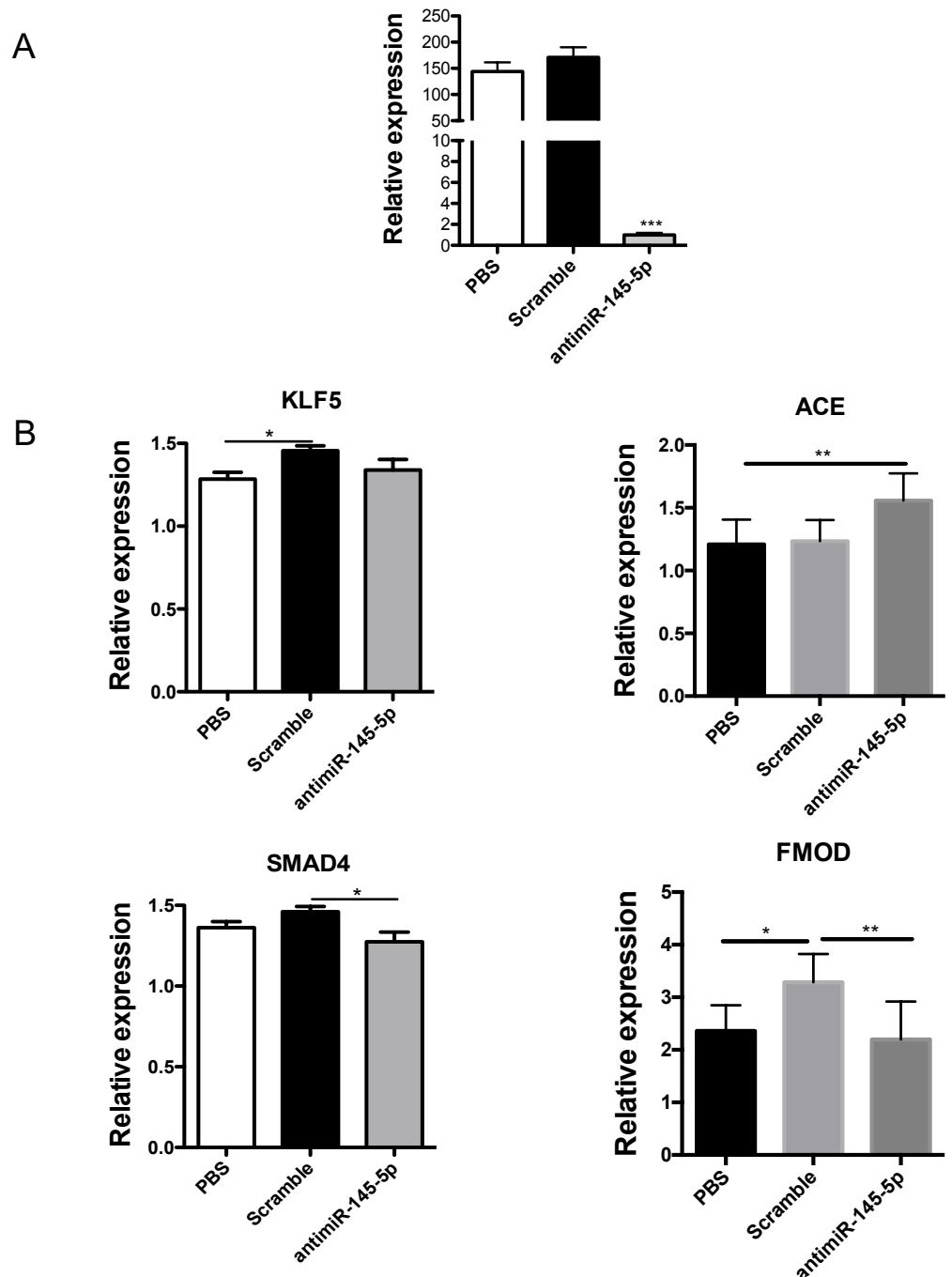


**Figure 3.23 Analysis of target genes expression of miR-145 in lung from the anti-miR-145 intranasal study**

RNA from lungs was isolated and miR-145 and its targets were determined by Taqman qRT-PCR. (A) MiR-145 expression was normalised to U6 and was significantly down-regulated upon treatment with anti-miR-145 in lung tissue of chronic hypoxia induced pulmonary arterial hypertension. (B) The expression level of *fmod*, *ace*, *smad4* and *klf5* was analysed. Data are expression as mean  $\pm$  SEM and analysed by Student t-test and by a one-way ANOVA followed by Tukey's post hoc tests. n = 8 mice per group. \* $P < 0.05$ , \*\* $P < 0.01$ .

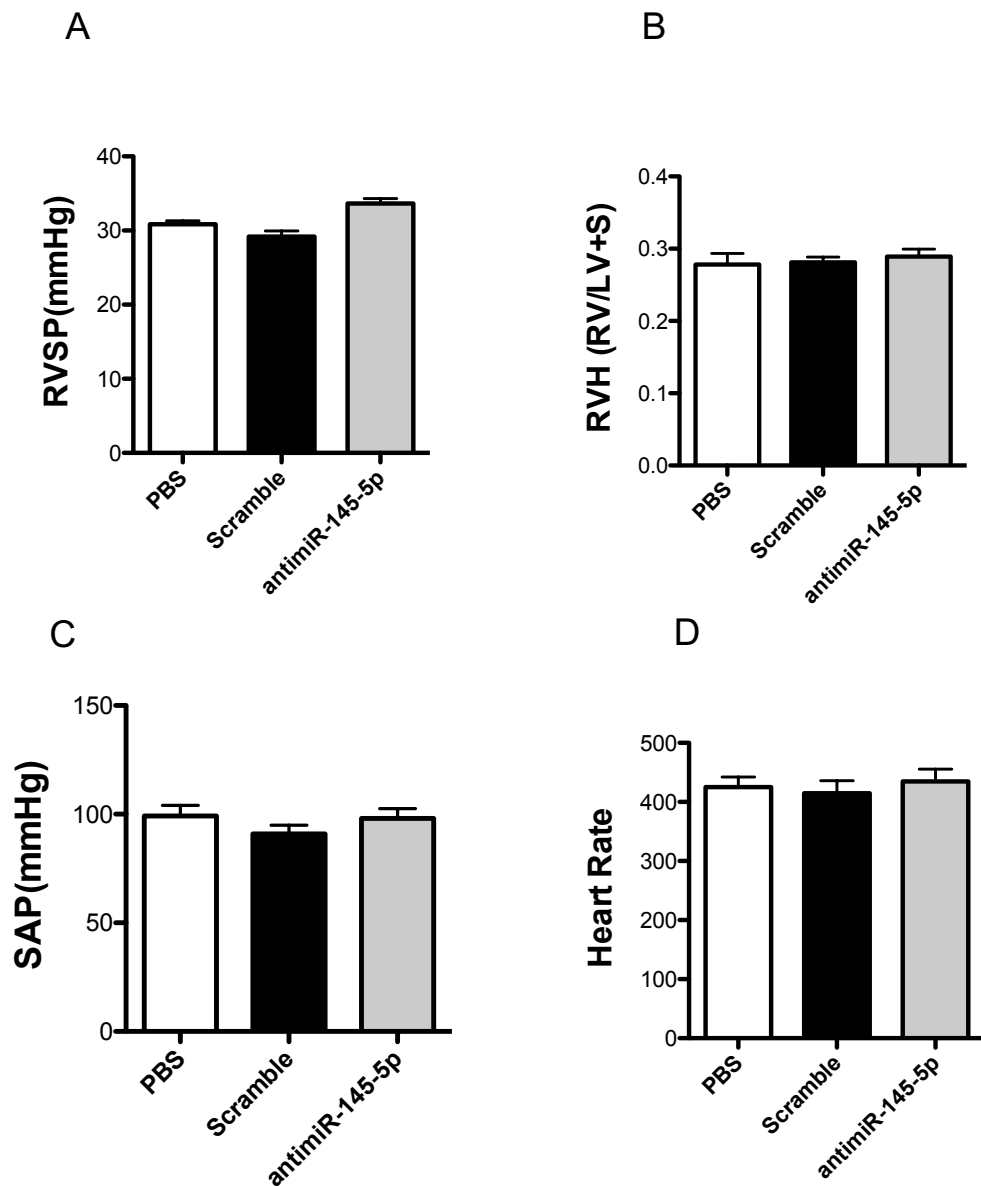


**Figure 3.24 Effect of miR-145-5p inhibition on the development of PAH**

Mice were administered anti-miR-145-5p, scramble or PBS by intranasal. Two weeks after chronic hypoxia exposure hemodynamic measurements were performed. (A) RVSP, (B) RVH, (C) SAP were assessed, (D) Heart rate, were measured. There were no significance changes among different groups. All data analysed by a one-way ANOVA followed by Tukey's post hoc tests. n = 6-10 mice per group.

### 3.4 Discussion

In the chapter, we have assessed the expression of miR-143 in several animal models of pulmonary hypertension, as well as in cells and tissues from patients with PAH, revealing that miR-143-3p expression levels significantly elevated in PASMCs from patients with PAH. In the miR-143 knockout (KO) study, genetic ablation of miR-143 in female mice showed significantly reduction of right ventricular systolic pressure (RVSP), right ventricular hypertrophy (RVH) and distal pulmonary vascular remodelling, which is beneficial in the hypoxic mouse model of PH. In the prevention study with antimiR-143-3p treatment, pharmacological repression of miR-143-3p in animals exposed to chronic hypoxia significantly reduced RVSP but had no effect on RVH and pulmonary vascular remodelling compared with control group, whereas similar results to the miR-143<sup>-/-</sup> study were observed in the antimiR-143-3p rescue study, with significantly decreased RVSP, RVH and pulmonary vascular remodelling. In addition, in the intranasal delivery study, knocking down miR-145-5p using antimiR-145-5p had no effect on RVSP, RVH and pulmonary vascular remodelling. Although, antimiR-145-5p treatment by intranasal delivery significantly reduced the miR-145-5p level in the lung, little effect on target genes and no effect on indices of PH were observed.

MiR-143 and miR-145 are transcribed as a cluster and are cardiac-specific and smooth-muscle-specific miRNAs (Cordes et al., 2009). Consistent with these findings, Taqman qRT-PCR and *in situ* hybridization analyses of miR-143-3p expression in mouse cardiomyocytes and right ventricle, and also in human PASMCs and pulmonary arteries, showed high expression of miR-143-3p. Moreover, we found miR-143-3p expression significantly increased in the total lung and right ventricles of mice in which experimental PH was induced by exposure to chronic hypoxia. Distal PASMCs isolated from patients with PAH showed significantly increased expression of miR-143-3p compared with healthy controls. In addition, *in situ* analyses of constrictive and complex lesions in diseased distal pulmonary arteries showed miR-143-3p is localised to the SMC layer of the lesions and appears to be highly expressed. This dysregulation of miR-143-3p in mouse PH model and

human patients were similar with our previous study in miR-145 (Caruso et al., 2012). A previous study revealed that miR-143-3p expression was much higher in concentric lesions (CLs) compared with plexiform lesions (PLs). However, this study also showed that miR-143 expression in plexiform lesions (PLs) was significantly lower than controls, which is not consistent with our finding (Bockmeyer et al., 2012). The possible reasons for the difference expression of miR-143-3p in PLs and CLs are the cell-specific expression of miR-143 and the structural differences between these lesions. MiR-143 is highly expressed in vascular SMC, whereas much lower expresses in endothelial cells (Zhang, 2009). In addition, plexiform lesions are composed of similar components of vascular SMCs and endothelial cells, and SMCs were predominant in the concentric lesions (Jonigk et al., 2011). This may partially explain the higher expression of miR-143-3p in CLs than PLs. There are no available perfect pre-clinical models that mimic human PAH disease. That is, no animal model can reproduce all the clinical pathological features of any groups of human PH. However, each animal model has its features, which are described in the chapter 1. The use of animal models of pulmonary hypertension has contributed to the understanding of PH pathophysiology and the development of experimental treatments. The animal models include single-pathological-insult models (SPI) (such as chronic hypoxia or MCT induced PH models) and multiple-pathological insult models (such as SU5416 and hypoxia induced PH models) (Maarman et al., 2013). Human PAH disease is triggered by genetic, environmental and other factors (Machado et al., 2009). Use different models with different pathological-insults will allow us to investigate the pathogenesis of PAH at various disease stages and also evaluate the therapeutic role of agents (Stenmark et al., 2009). Thus, in this study, we further analysed the miR-143-3p expression in rat SU5416/hypoxia model, hypoxia neonatal calves and high-altitude pulmonary hypertension in cattle (brisket disease). Consistent with the mouse chronic hypoxia model and human patients, miR-143-3p expression was significantly upregulated in the total lung of rat SU5416/hypoxia model and highly expressed in the distal pulmonary arteries of hypoxia neonatal calves and brisket disease. The brisket disease samples in particular share some common features of the human PAH disease, including right heart failure and the development of complex vascular lung lesions. Since expression of miR-143-3p appears high in both mouse chronic hypoxia

induced samples, rat SU5416/hypoxia samples, post-mortem human lung and brisket disease lung samples, which suggests that miR-143-3p expression is elevated and sustained during the pathogenesis of PAH, particularly evident in distal small pulmonary vessels.

Although we found miR-143-3p expression increased in PAH, there are studies in different vascular disease models demonstrated miR-143-3p decreased in the carotid artery balloon injury rat model and carotid artery ligation model. In addition, used adenovirus (Ad-miR-143) to overexpress miR-143-3p in WT mice stimulated with balloon injury in rat carotids found that miR-143-3p overexpression significantly reduced the balloon injury induced neointimal formation. These observations are consistent with miR-143-3p shown to be down-regulated during neointimal formation in the carotid artery of the rat (Cordes et al., 2009, Elia et al., 2009, Ji et al., 2007). The expression profile of miRNAs is disease status-dependent, dependent on the type and nature of the stimuli and the surrounding environment. Particular pathological processes and stimulations are associated with the expression of specific group of miRNAs in different diseases.

Genetic ablation of the miR-143 stem loop markedly prevented the development of PH assessed by RVSP, RVH and pulmonary vascular remodelling. This phenotype we also found in the miR-145<sup>-/-</sup> mice (Caruso et al., 2012). Both miR-143-3p and miR-143-5p were deleted in the miR-143 knockout mice. The *in vitro* studies demonstrated that only miR-143-3p (guide strand) is functional affected the cell behaviours. Specific pharmacological inhibition of miR-143-3p rather than miR-143-5p with *in vivo* exerts protective therapeutic role in the disease development and treatment. Thus, this data suggest that the guide strand of miR-143 acts as mature functional miRNA in the pathogenesis of PAH.

There is still no definite cure treatment for pulmonary arterial hypertension (PAH). As we noticed that miR-143<sup>-/-</sup> could inhibit the development of chronic hypoxia induced PH, we used a pharmacological inhibition strategy to knock down miR-143 *in vivo* to test whether knocking down miR-143 can alleviate PH pathogenesis in the chronic hypoxia model of PH. Both prevention and reverse models revealed a protective role of antimiR-143-3p

treatment in the development of chronic hypoxia induced PH mice model. Concerning the indexes of evaluation of PAH disease features, the reverse therapeutic study showed greater efficacy than the prevention study, which only showed a significant decrease in right ventricular systolic pressure. And miR-143-3p knocking down significantly reduced the pulmonary vascular remodelling and RVH in the reverse therapeutic model. Here we observed a discrepancy results between prevention model and reversal model with anti-miR-143-3p treatment, both use the same delivery route and same concentration of anti-miR-143-3p. Chronic Hypoxia exposure activated several signalling pathways in pulmonary hypertension (Stenmark et al., 2006b). The reason to explain the difference in results between prevention and reversal study may be due to the activation of different signalling pathways, which some pathways will change with miR-143-3p silence by anti-miR-143-3p administration at different stages. In addition, the reversal therapeutic strategy is much more clinically relevant than prevention route.

In our previous study, we found that the expression of miR-145-5p was enhanced in the lungs of mice with chronic hypoxia induced PH mouse model and PAH patients. Genetic deletion and pharmacological inhibition of miR-145-5p in mice protected against the development of PH. This study used subcutaneous injection route, a strategy for systemic delivery, for anti-miR-145-5p and clearly shown an important role for miR-145-5p in PH (Junion et al., 2012). Here, we want to evaluate the efficacy of established mediator of PH (miR-145) by using local delivery strategy in the development of chronic hypoxia induced PH. As the lungs are capable of absorbing pharmaceuticals either for local and systemic delivery, one of the widely use local delivery routes is intranasal route for therapeutic purposes (Patil and Sarasija, 2012). The administration of substances to mice by the intranasal route is an effect, non-invasive technique that can be employed for the delivery of drugs or gene therapy to the lung (Ciuclan et al., 2013). Previous studies using intranasal administration of mature let-7 mimic showed efficiently delivery to the lung, with repression of the let-7 target IL-13 (Savai et al., 2012) while intranasal delivery of let-7 anti-miRNA reduced tumour growth in mouse models of lung cancer (Dorfmuller and Humbert, 2012). Until now, there has been only one study to use the intranasal route to study PH. In this

study, lentivirus encoding miR-424 and miR-503 was administered via intranasal delivery to the lung, which exhibited a protective role in the development of PH. Analysis of intranasal delivery efficiency showed that endothelial cells were infected with lentivirus delivery (Kim et al., 2013). So, we first use intranasal delivery strategy to deliver anti-miR-145-5p in mouse chronic hypoxia induced PH model. In order to confirm the intranasal anti-miR-145-5p delivery efficiency, we used the mouse normoxic model to assess the efficiency. First, RNA extracted from lung tissue, pulmonary artery, and right ventricle and we used Taqman qRT-PCR to analyse the miR-145-5p expression level. The levels were approximately 170 fold, 50 fold and 20-fold downregulated in lung tissue, pulmonary artery and right ventricle separately. Second, the targets of miR-145-5p are upregulated in lung, especially *fmod* and *ace* that have statistically significant derepression.

However, we employed an established mouse chronic hypoxia induced pulmonary hypertension. Antagonization of miR-145-5p by intranasal delivery of anti-miR-145-5p did not protect against the development of PH assessed by hemodynamic data. The target genes expression levels of anti-miR-145-5p treated mice were not altered except just the *ace* gene. The possible reason of these results maybe including: 1) the miR-145-5p was being significantly knockdown by anti-miR-145-5p treatment in the total lung, however only one target gene was modulated. Although we did not analyse many potential target genes of miR-145, this suggesting that the local deliver of anti-miR-145-5p is potentially not optimal. More work need to assess other tissues such as heart, liver and kidney for the targeting effect of anti-miR-145-5p, as well as specific cell types in the lung and the effects on direct mRNA targets. 2) As miR-145-5p is predominantly expressed vascular SMCs layer, we observed that miR-145-5p expression was significantly downregulated in the large pulmonary arteries that contain different cell compartments. However, whether the anti-miR-145-5p can reach to SMCs layer of the distal pulmonary vessels to knock down miR-145 was not investigated, as PAH is characterised by progressive remodelling of the distal pulmonary arteries. 3) Several circulating miRNAs such as miR-23a/b, miR-451, miR-130a, miR-191 et al have been demonstrated as potential maker for PAH. Although lung tissue is the most downregulated tissue in mice, there still may have circulating miR-145 in blood that may-

be influences disease development, although this is less likely. Also miR-143/145 can be secreted from endothelial cells and crosstalk with SMCs in the vasculature, this study also highlights the cell-to-cell communication between cell types by miR-143/145 (see Chapter 4). In addition to this local communications, the secreted miRNAs in the bloodstream also can mediate distant cell-to-cell communication, although this remains an area with little scientific research to date. One possible explain is the secreted miR-145 (e.g. exosomal miR-145) from other parts can circulate to pulmonary vessels to affect the vascular functions. 4) Different antimiRNA (or drug) delivery routes may have different therapeutic effect on established disease model. The aim of local delivery is to target specific tissues in order to minimise the “off-target” effect or targeting unintended tissues. However, the systemic delivery will target nearly all the tissues and have more side effects, limiting translational appeal.

In summary, miR-143-3p expression is induced in multiple models of PAH and in human patients. Silencing of miR-143-3p using genetic ablation or antimiRNA treatment provides a beneficial effect in female mice exposed to chronic hypoxia induced PH model. This data suggest miR-143-3p is potential therapeutic target in the treatment of PAH. Further studies are required to explore the smooth muscle cell and endothelial cell functions and the mechanisms including target genes and pathways underlie the beneficial effects.

## **4 The role of miR-143 regulation of smooth muscle and endothelial cell crosstalk in pulmonary arterial hypertension**

## 4.1 Introduction

Pulmonary arterial hypertension (PAH) is a deadly disease characterised by vasoconstriction and abnormal remodelling of pulmonary vessels. The endothelial cells (ECs), smooth muscle cells (SMCs), and fibroblasts of the pulmonary vessel walls, as well as inflammatory cells and platelets have been demonstrated have a role during the pathogenesis of PAH (Yildiz, 2009). The interplay among these cell population is regulated by several mediators contributing to the pathophysiologic features of PAH (Nogueira-Ferreira et al., 2014). In the pulmonary vasculature, both SMCs and ECs are the key cell types involved and play a key role in pulmonary vascular remodelling associated with PAH, as both smooth muscle cell-dependent medial thickening and endothelial cell-dependent angio-obliteration occur during the development of PAH. (Yuan and Rubin, 2005). The plexiform lesion, a histological hallmark of the pulmonary vessels of patients with PAH, has been demonstrated to result from disordered endothelial cell proliferation, migration along with concurrent neoangiogenesis, and recruitment of other cell types (e.g. macrophages, endothelial progenitor cells) (Sakao et al., 2009). Pulmonary artery smooth muscle cell (PASMC) hypertrophy, proliferation, migration and anti-apoptosis also contribute to plexiform lesion formation (Tajsic and Morrell, 2011).

More recently, miRNAs have been demonstrated as key regulators of a wide range of cellular processes such as proliferation, migration and apoptosis and play a pivotal role in vascular remodelling of PAH diseases. MiRNAs are expressed in a cell-and tissue-specific manner involved in various biological processes including vascular remodelling in pulmonary vasculature. A number of miRNAs have been shown to regulate PASMCs and PAECs behaviours during the pathogenesis of PAH disease such as miR-145, miR-21, miR-204, miR-17/92, miR-34a, miR-424/503, miR-210 et al (Bienertova-Vasku et al., 2015).

MiR-143 together with miR-145 has been identified as regulators of VSMC contractile phenotype. *In vitro* studies have shown that the promoter region of the miR-143/145 cluster there is a region contained a conserved serum response factor SRF-binding site [CC

(A/T)6GG], known as a CArG box. Luciferase reporter assays have shown that the transcription of miR-143/145 can be activated by SRF and its co-factors myocardin-related transcription factors (MRTF) and myocardin through binding to this CArG box (Xin et al., 2009, Davis-Dusenbery et al., 2011, Rangrez et al., 2011, Cordes et al., 2009). TGF- $\beta$  and BMP4 are known to induced SMC contractile phenotype. One of the mechanisms involved in this phenotype is TGF- $\beta$  and BMP4 induce myocardin and MRTF separately that further activate the miR-143/145 (Davis-Dusenbery et al., 2011). MiR-143/145 expression levels are decreased in VSMCs treated with PDGF, which has been proven to induce migration through podosome formation. And the PDGF induce podosome formation in VSMCs through regulation of miR-143/145 via Scr and p53 pathway (Quintavalle et al., 2010, Wang et al., 2010b). VSMCs isolated from miR-143/145 KO mice showed the KO cells were more migratory than WT cells. In addition, Rat VSMC line A7r5 cells showed decreased proliferation with Ad-miR-143/145 transduction (Elia et al., 2009). Overexpression of miR-143 in VSMCs significantly enhanced H<sub>2</sub>O<sub>2</sub> induced VSMC senescence, and recued proliferation and migration with interaction between MEF2A (Zhao et al., 2015b). These studies revealed that miR-143 play a vital role in regulation of SMC behaviours. MiR-143 particularly enriched in SMCs and expressed low levels in other cell types such as endothelial cells. The dysregulation of miR-143 in endothelial cells also found in various disease conditions (Climent et al., 2015, Hergenreider et al., 2012, Zhao et al., 2015a). However, the miR-143 mediated effects in the pulmonary vasculature are unknown.

The precise and dynamic interactions between smooth muscle cells (SMCs) and endothelial cells are important for maintaining vascular homeostasis through careful regulation of cell proliferation, apoptosis, differentiation, migration and survival. Aberrant interactions between these cell types have been shown to lead to pathological changes in the vascular compartment, including pulmonary vascular remodelling and pulmonary arterial hypertension (Heydarkhan-Hagvall et al., 2003, Eddahibi et al., 2006). Generally, in the vessel wall, there are three broad areas of cellular communications: paracrine signalling (e.g. through secretion and exchange of soluble bioactive factors); physical connections (e.g. gap junctions and potassium channels); and exocytosis (Wheelhouse et al., 2003, Lilly, 2014, Dia-

mant et al., 2004, Freyssinet, 2003, Billaud et al., 2014). In the pulmonary vasculature, it is well recognised that endothelial cells can regulate the functions of SMCs by releasing various factors such as nitric oxide (NO), prostaglandin, prostacyclin, endothelin-1, and (Torporsian et al., 2005, Dora, 2001). However, the interactions between ECs and SMCs is not a simple one-way interaction from the endothelium to the smooth muscle cells but are more complicated interactions between each cell types (Gao et al., 2016). In addition to such paracrine regulation, there are more complicated communication patterns. Myoendothelial junction (MEJ) is described as the structural location at which an EC or VSMC extension protrudes through the internal elastic lamina, resulting in plasma membrane juxtaposition with the opposite cell type (Heberlein et al., 2009). There are gap junctions at the tip of the MEJ composed of two hemi-channels termed connexions, some of which are associated with MEJ including connexion 37, 40, and 43. And the smaller arteries are containing more numerous MEJ than the larger diameter arteries (Gao et al., 2016). In the pulmonary vasculature, PAECs co-cultured with PASMCs by direct contact each other activate the TGF- $\beta$  signalling in PASMCs, which exert a more contractile-like phenotype and maintaining the TGF- $\beta$ -dependent PASMC differentiation. These communications are mediated through myoendothelial gap junctions (connexion 43) from PAECs to PASMCs, which suggest that dysregulation of this direct interaction is involved in the pathogenesis of pulmonary vascular remodelling (Gairhe et al., 2011). Another connected cell to cell communication is tunnelling nanotubes (TNTs), which represent a subset of F-actin-rich structures containing membranous nanotubes between cells and facilitate the intercellular transport of various cellular components (Gurke et al., 2008). Recently, the miR-143/145 cluster has been demonstrated to act as communication molecules between SMCs and ECs via TNTs (Climent et al., 2015).

Extracellular vesicles include apoptotic bodies, microparticles/microvesicles, and exosomes. Several studies showed cell-to-cell communication can be mediated by exosomes, which contain miRNAs (McCoy-Simandle et al., 2016, Ciardiello et al., 2016). Exosomes are 40 to 100nm in size and represent a specific subtype of secreted membrane vesicles formed through the fusion of multivesicular endosomes with the plasma membrane (Inter-

national et al., 2000). Exosomes are released by many types of cell, and have been identified in most body fluids, including as plasma, urine, saliva, cerebrospinal, amniotic and synovial fluids. Exosomes are now known to carry a wide array of molecules including: proteins, DNAs, mRNAs, miRNAs and lncRNAs, depending on a variety of factors including the cell type from which the exosome originates, the state of health of the host, and extracellular stimuli (Newman et al., 2004). Exosomes can be taken up by neighbouring or distant cells and can be functional in the recipient cells by fusion with the plasma membrane, via receptor-mediated uptake or by internalization via endocytosis or macropinocytosis (Valadi et al., 2007). Since the discovery of miRNA in exosomes, a number of studies have focused on the identification and function of exosomal miRNAs in cancer (Kosaka, 2016) and cardiovascular diseases (Waldenstrom and Ronquist, 2014, Yellon and Davidson, 2014, Sahoo and Losordo, 2014, Loyer et al., 2014, Kishore and Khan, 2016). Interestingly, cancer cell derived exosomes contain key components of microRNA biogenesis including RISC, AGO2, Dicer, and TRBP, which displayed cell-independent capacity to process precursor miRNAs into mature miRNAs (Melo et al., 2014).

DNA damage in cells is caused by intrinsic and extrinsic genotoxic stresses, including ultraviolet (UV) radiation, ionizing radiation (IR), chemo- and radiotherapeutic agents, reactive oxygen species, as well as the strong inflammation environment which is known to be toxic for the cells (Suzuki et al., 2009). Inflammatory cytokines (e.g. TNF- $\alpha$  and IL-6) and growth factors (e.g. PDGF) also induce DNA damages (Fehsel et al., 1991, Yun et al., 2012, Squatrito and Holland, 2011, Soon et al., 2010). One of the features of PAH is inflammation, which is characterised by sustained elevation of circulating pro-inflammatory molecules such as tumour necrosis factor  $\alpha$  (TNF- $\alpha$ ) and interleukin 6 (IL-6) in patients with PAH (Caruso et al., 2012). In the human distal pulmonary arteries (PAs), DNA damage is significantly increased in PAH patients compared with normal tissue controls. Consistent with the findings in PAs, PASMCs isolated from patients with PAH also showed increased DNA damage in comparison with healthy control cells (Shiloh, 2001). Several studies have demonstrated that DNA damage can regulate miRNAs expression at the transcriptional level and regulate miRNAs by modulating the miRNA processing and maturation steps

(Bottai et al., 2014, Bienertova-Vasku et al., 2015). Several miRNAs including miR-143/145 have been found to be upregulated by DNA damage induced by irradiation (Hu and Gatti, 2011). However, the role of miR-143 response to DNA damage in PAH still unknown.

In the chapter 3, we showed a consistent up-regulation of miR-143-3p expression in different animal PH models and PAH patients. In addition, miR-143-3p knockdown significantly alleviated the development of chronic hypoxia induced PH mice model. Thus, this chapter was designed to study the mechanisms underlie the protective role of miR-143 ablation in the development of PAH, and assess the effects of modulating miR-143-3p expression in PSMCs and PAECs with respect to cell functions and target gene expression. In addition, we also aimed to use an *in vitro* cell-to-cell communication co-culture model to investigate the crosstalk between PSMCs and PAECs via miR-143-3p in the pulmonary vasculature.

## 4.2 Aims

- To analyse the effect of miR-143 on PASMC and PAEC proliferation, migration, apoptosis and angiogenesis and identify the potential pathways of miR-143-3p *in vitro*
- To purify the exosomes secreted by PASMCs and identify the enrichment of miR-143 in PASMC-derived exosomes
- To assess whether PAECs can ingest miR-143-3p enriched exosomes secreted by PASMCs, and the effect this may have on PAEC behaviour.

## 4.3 Results

### 4.3.1 MiR-143 Expression is Significantly Upregulated During Scratch Closure in PASMCs

In the previous chapter, we demonstrated that miR-143 was enriched in SMC, and that knockdown could inhibit the development of PAH. PASMC proliferation, migration and apoptosis contribute to the development of vascular remodelling, which is central to the pathobiology of PAH (Tajsic and Morrell, 2011). We therefore sought to understand whether manipulation of miR-143 in PASMC could affect these cellular processes *in vitro* (These PASMCs were derived from proximal pulmonary arteries). In order to understand whether manipulation of miR-143 could affect cell migration, we first created multiple scratch wounds in cultured PASMCs to analyse expression levels of the miR-143/145 cluster at different time points after scratch. We showed rapid transcriptional activation of the pri-miR-143/145 precursors at 3 h post-scratch, which was maintained over time for pri-miR-143 but was later repressed for pri-miR-145 (Figure 4.1) ( $P < 0.05$ ,  $P < 0.01$ , and  $P < 0.001$ ). We further analysed the expression of mature lead and passenger strands of miR-143 and -145 during PASMC migration. Although the mature form of miR-143-3p lead strand was significantly upregulated in a time-dependent manner after scratch wounding, the expression of the miR-145-5p lead strand did not significantly change (Figure 4.2 A) ( $P < 0.05$ ,  $P < 0.01$ , and  $P < 0.001$ ). In addition, the expression of miR-143-5p and miR-145-3p passenger strands did not change significantly during the PASMC migration (Figure 4.2 B). Taken together, these results show that miR-143-3p expression is selectively induced in migrating PASMCs.

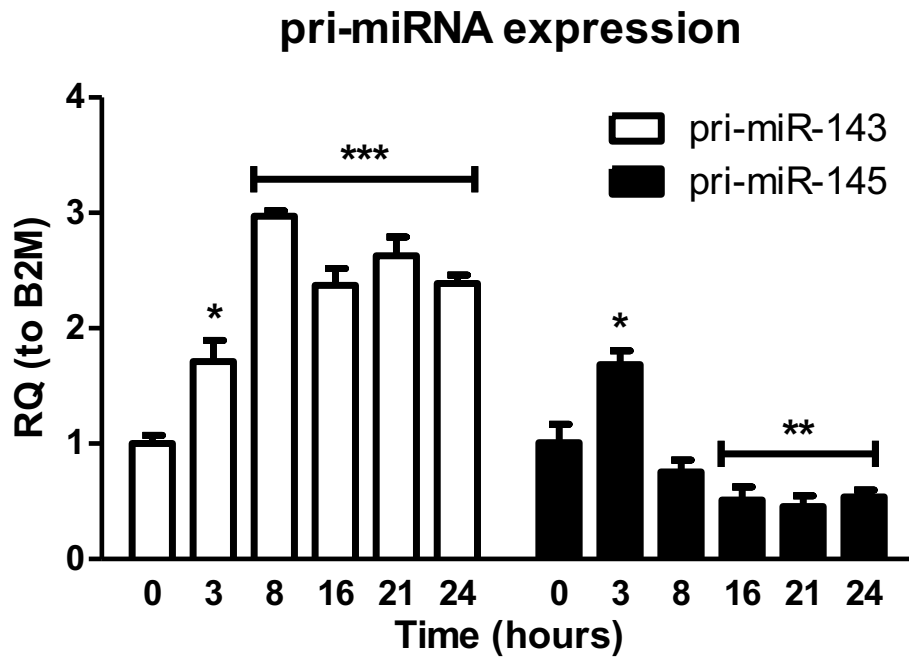
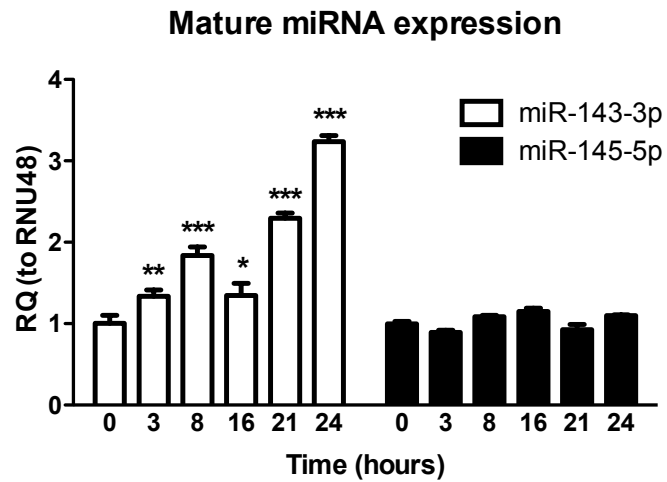


**Figure 4.1 Analysis of the expression of pri-miR-143 and pri-miR-145 during PASC migration *in vitro***

Multiple scratches were performed on PASCs to induce cell migration. TaqMan qRT-PCR analyses were performed to evaluate the expression of pri-miR-143 and pri-miR-145 during PASC scratch closure at different time points. Pri-miR-143 was significantly increased at all time points after scratch compared with control. Pri-miR-145 was significantly upregulated 3 h after injury and then significantly downregulated from 16 to 24 h. Data represented as fold change  $\pm$  SEM and analysed by a one-way ANOVA followed by Tukey's post hoc tests.  $n = 3$  per group in triplicate. \* $P < 0.05$ , \*\* $P < 0.01$ , \*\*\* $P < 0.001$ . This work was done by Dr. Francisco J. Blanco.

A



B

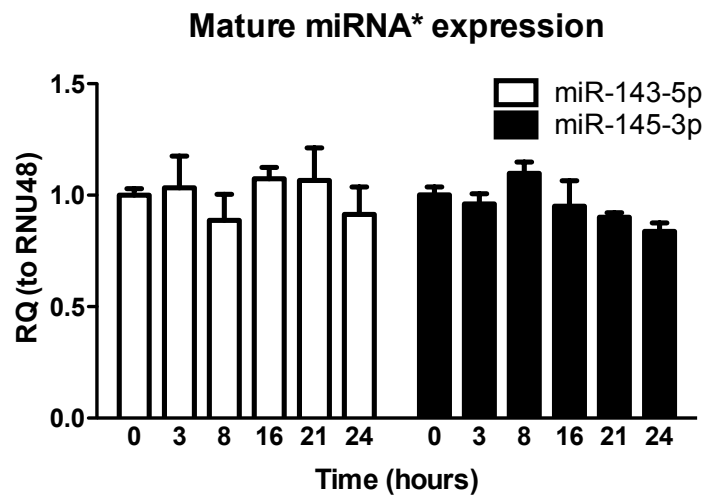


**Figure 4.2 Analysis of the expression of miR-143/145 lead and passenger strands during PASMCM migration *in vitro*.**

Multiple scratches were performed on PASMCMs to induce cell migration. Taqman qRT-PCR analyses were performed to evaluate the expression of the mature forms of miR-143 and miR-145 during PASMCM scratch closure at different time points. (A) The expression of the miR-143 lead strand (miR-143-3p) was significantly increased after scratch while the expression of the miR-145 lead strand (miR-145-5p) remained unchanged. (B) The expression of both passenger strands of miR-143 (miR-143-5p) and miR-145 (miR-145-3p) did not change during scratch closure of PASMCM. Data represented as fold change  $\pm$  SEM and analysed by a one-way ANOVA followed by Tukey's post hoc test.  $n = 3$  per group in triplicate. \* $P < 0.05$ , \*\* $P < 0.01$ , \*\*\* $P < 0.001$ . This work was done by Dr. Francisco J. Blanco.

### **4.3.2 MiR-143-3p Expression is Dysregulated During Scratch Closure in Distal PSMCs from HPAH/IPAH Patients and Controls**

We observed that both primary and mature forms of miR-143-3p expressions were significantly upregulated in wound healing assays performed in healthy human PSMCs. In order to assess miR-143-3p expression during wound healing in the context of disease, we analysed miR-143-3p expression in distal PSMCs isolated from patients with HPAH and healthy controls with multiple scratch. In PSMCs from healthy controls, pri-miR-143 expression was significantly induced 3 h after scratch. This increase in expression was sustained to the 8 h time point (Figure 4.3A) ( $P < 0.01$  and  $P < 0.001$ ). Pri-miR-145 expression was significantly increased at 1 and 3 h then decreased at 8 h post-scratch (Figure 4.3 A) ( $P < 0.001$ ). Only the mature form of miR-143-3p expression was significantly increased at different time point (Figure 4.3 B) ( $P < 0.05$  and  $P < 0.001$ ). There was no difference in the expression of miR-145-5p mature form (Figure 4.3 B). This data is consistent with the data we obtained from PSMCs isolated from the larger pulmonary arteries (section 4.3.1). In PSMCs from HPAH patients, pri-miR-143 expression was significantly upregulated during scratch closure (Figure 4.4 A) ( $P < 0.01$  and  $P < 0.001$ ), while the expression of pri-miR-145 was significantly decreased at 1 and 3 h (Fig. 4.4 A) ( $P < 0.05$  and  $P < 0.01$ ). We also observed that the expression of both mature form of miR-143-3p/miR-145-5p significantly induced (Figure 4.4 B) ( $P < 0.05$  and  $P < 0.001$ ). In PSMCs from patients with IPAH, a similar pattern of miR-143/145 expression was observed, with pri-miR-143 expression significantly upregulated and pri-miR-145 expression significantly downregulated during scratch closure (Figure 4.5 A) ( $P < 0.05$ ,  $P < 0.01$ , and  $P < 0.001$ ). Mature form of miR-143-3p not miR-145-5p significantly increased during the wound healing (Figure 4.5 B) ( $P < 0.001$ ). Taken together, we observed the same patterns of miR-143/145 expression in distal PSMCs from HPAH/IPAH patients and healthy controls during scratch closure, compared to culture PSMCs from the larger pulmonary arteries.

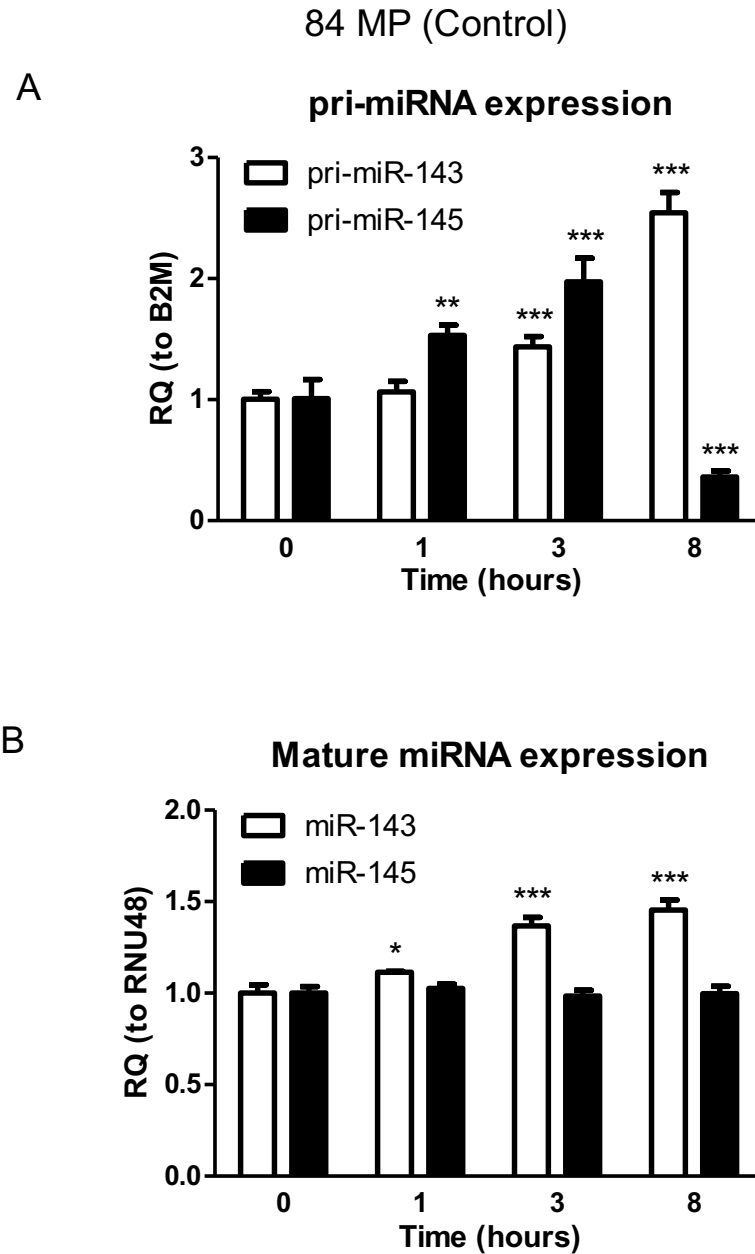
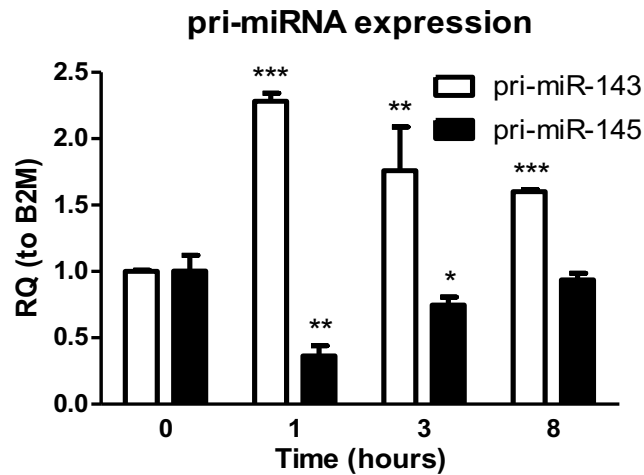


**Figure 4.3 Comparative analysis of migration in distal PASMC from healthy donors**

Cells were grown in monolayer and the expression levels of miR-143 and miR-145 precursors and mature forms were detected by Taqman qRT-PCR at the indicated time after multiple scratches in control distal PASMC (84MP). (A) The pri-miR-143 expression significantly increased time dependently and pri-miR-145 expression increased at first and then decreased. (B) The mature form of miR-143-3p expression significantly increased but no change in miR-145-5p mature form. Data represented as fold change  $\pm$  SEM and analysed by a one-way ANOVA followed by Tukey's post hoc test. Experiments were performed in one control patient cells.  $n = 3$  per group in triplicate.  $*P < 0.05$ ,  $**P < 0.01$ ,  $***P < 0.001$ . This work was done by Dr. Francisco J. Blanco.

## 73MP (HPAH)

A



B

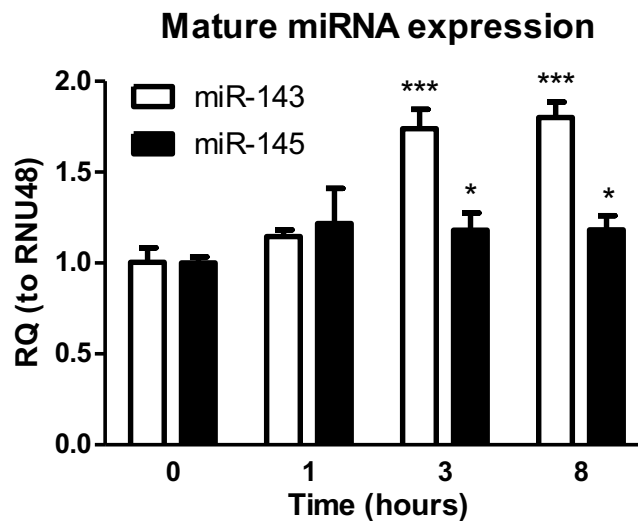


**Figure 4.4 Comparative analysis of migration in distal PASMC from HPAH patients**

Cells were grown in monolayer and the expression levels of miR-143 and miR-145 precursors and mature forms were detected by Taqman qRT-PCR at the indicated time after multiple scratches in heritable PAH patients distal PASMCs (73MP (HPAH)). (A) The pri-miR-143 significantly increased at all the time points and pri-miR-145 significantly decreased. (B) The mature forms of both miR-143-3p and miR-145-5p were significantly increased. Data represented as fold change  $\pm$  SEM and analysed by a one-way ANOVA followed by Tukey's post hoc test. Experiments were performed in one HPAH patient cells.  $n = 3$  per group in triplicate.  $*P < 0.05$ ,  $**P < 0.01$ ,  $***P < 0.001$ . This work was done by Dr. Francisco J. Blanco.

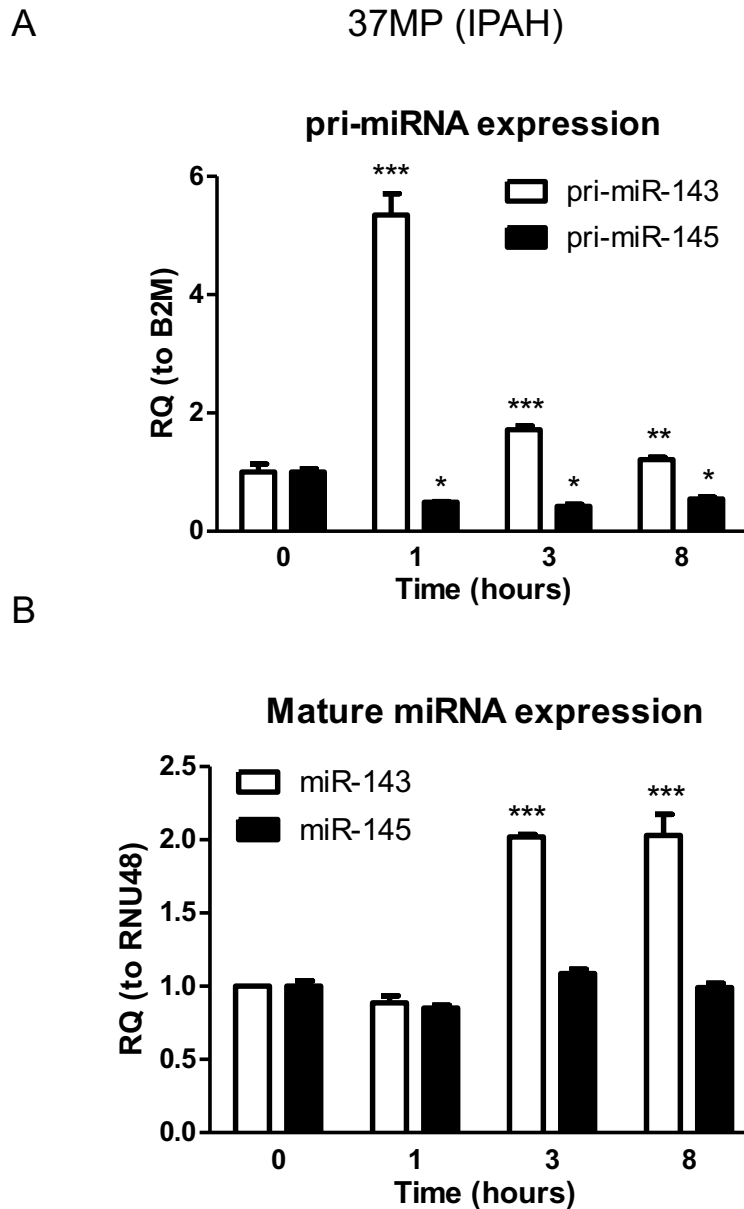


**Figure 4.5 Comparative analysis of migration in distal PASMC from IPAH patients**

Cells were grown in monolayer and the expression levels of miR-143 and miR-145 precursors and mature forms were detected by Taqman qRT-PCR at the indicated time after multiple scratches in idiopathic PAH patients distal PASMCs (37MP (IPAH)). (A) The pri-miR-143 was significantly increased at all the time points and pri-miR-145 was significantly decreased. (B) The mature form miR-143-3p was significantly increased but no difference for miR-145-5p mature form. Data represented as fold change  $\pm$  SEM and analysed by a one-way ANOVA followed by Tukey's post hoc test. Experiments were performed in one IPAH patient cells. n = 3 per group in triplicate. \* $P < 0.05$ , \*\* $P < 0.01$ , \*\*\* $P < 0.001$ . This work was done by Dr. Francisco J. Blanco.

### **4.3.3 Overexpression and Knockdown of miR-143-3p in PASMCs Affects Cell Migration**

As we observed that miR-143-3p expression was increased during scratch wound healing both in the PASMCs from larger healthy human pulmonary arteries and distal pulmonary arteries from PAH patients and healthy donors, we next aimed to manipulate miR-143-3p levels *in vitro* to identify whether miR-143-3p plays an important role in PASMC migration phenotype. First, we overexpressed miR-143-3p in PASMC by transfecting cells with a synthetic pre-miR-143-3p. Overexpression of miR-143-3p was confirmed by Taqman qRT-PCR (Figure 4.6 B) ( $P < 0.001$ ). Transfection with pre-miR-143-3p significantly induced PASMC migration in a scratch wound healing assay (Figure 4.6 A) ( $P < 0.05$ ). Meanwhile, knockdown of miR-143-3p using the anti-miR-143-3p significantly inhibited PASMC migration (Figure 4.7 A) ( $P < 0.01$ ). Knockdown of miR-143-3p was confirmed by Taqman qRT-PCR (Figure 4.7 B) ( $P < 0.01$ ). Taken together, these results demonstrate that miR-143-3p can induce the migration of PASMCs *in vitro*.

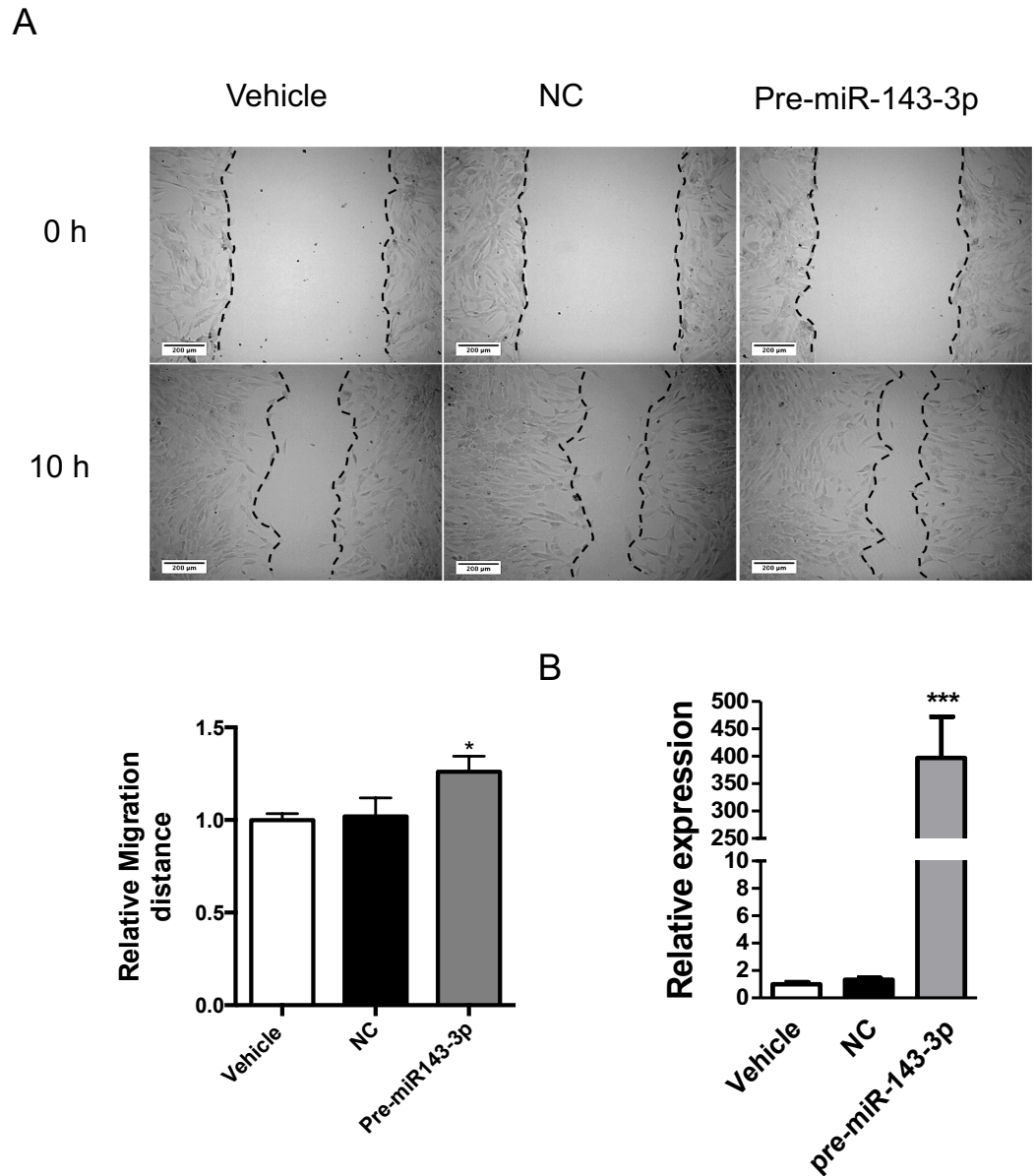


**Figure 4.6 Assessment of miR-143-3p overexpression on cell migration in wound healing assay**

Single scratch was applied on monolayer PSMCs, and capture of images at time point 0 h and 10 h. Migration distance between these two time-points was analysed by Image J. (A) Representative micrographs and quantification of a wound-healing assay after miR-143-3p overexpression by pre-miR-143-3p transfection, in comparison with vehicle and negative control (NC). MiR-143-3p overexpression significantly induced cell migration. (B) MiR-143-3p significantly increased with pre-miR-143-3p transfection confirm by Taqman qRT-PCR. Data represented as fold change  $\pm$  SEM and analysed by a one-way ANOVA followed by Tukey's post hoc test.  $n = 3$  per group in triplicate. \* $P < 0.05$ , \*\*\* $P < 0.001$ . Scale bar = 200  $\mu\text{m}$ .

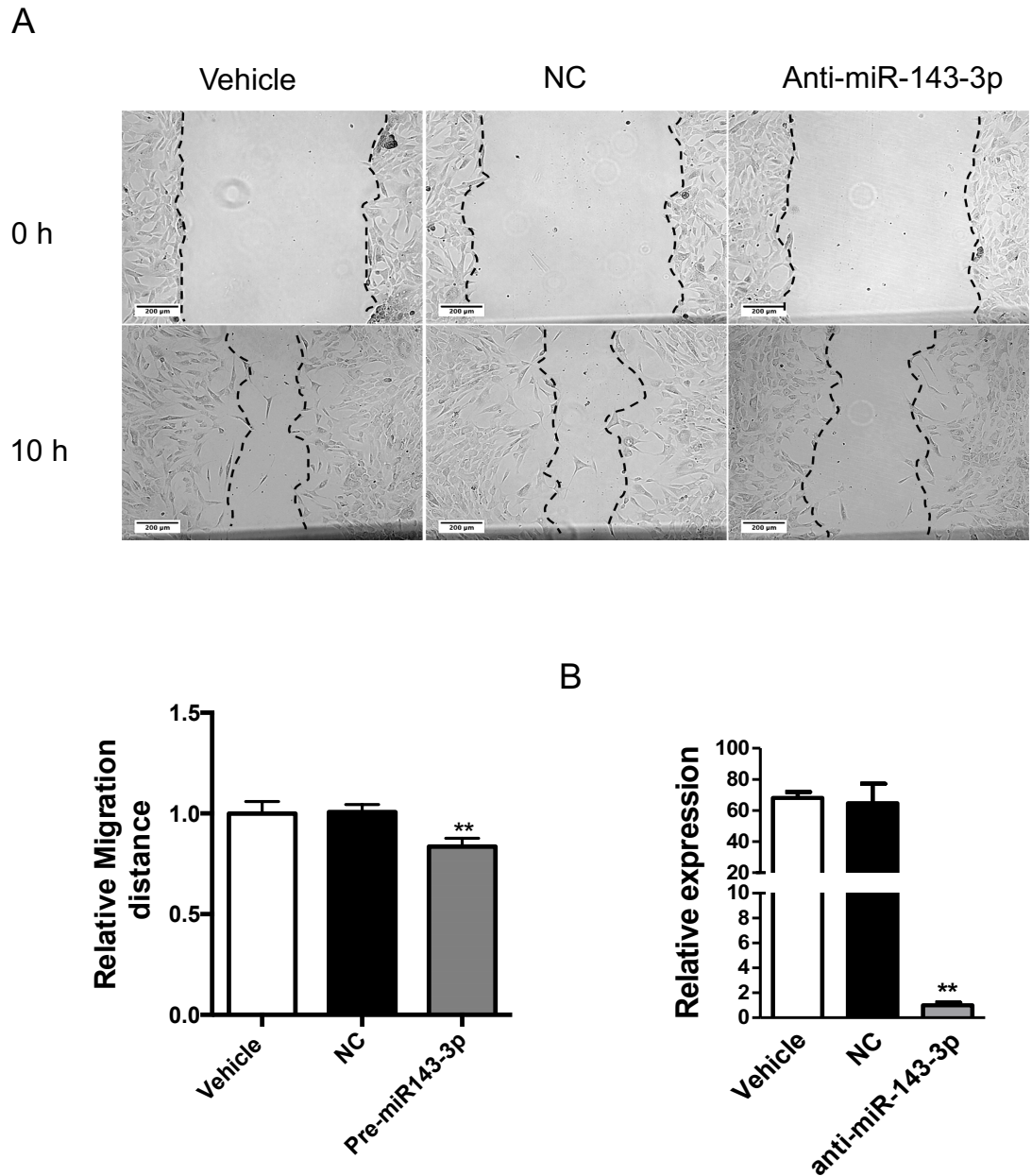


**Figure 4.7 Assessment of miR-143-3p knockdown on cell migration in wound healing assay**

Single scratch was applied on monolayer PSMCs, and capture of images at time point 0 h and 10 h. Migration distance between these two time-points was analysed by Image J. (A) Representative micrographs and quantification of a wound-healing assay after miR-143-3p knockdown by anti-miR-143-3p transfection, in comparison with vehicle and negative control (NC). MiR-143-3p knockdown significantly inhibited cell migration. (B) MiR-143-3p was significantly knockdown with anti-miR-143-3p transfection confirm by Taqman qRT-PCR. Data represented as fold change  $\pm$  SEM and analysed by a one-way ANOVA followed by Tukey's post hoc test.  $n = 3$  per group in triplicate.  $**P < 0.01$ . Scale bar = 200  $\mu\text{m}$ .

#### **4.3.4 Manipulation of miR-143-3p Affects PASMCMigration but not Proliferation**

Having identified a role for miR-143-3p in the regulation of PASMCMigration, we next aimed to assess the effect of miR-143-3p manipulation on PASMCMigration and apoptosis. To be consistent with our migration assays, we utilised pre-miR-143-3p transfection and anti-miR-143-3p treatment to increase or decrease the expression of miR-143-3p, respectively. BrdU incorporation assay and western blotting for PCNA analysed cell proliferation of PASMCMigration, while apoptosis was evaluated by measuring Caspase3/7 activity. First, we observed that PDGF treatment significantly induced PASMCMigration proliferation compared with controls (Figure 4.8 A) ( $P < 0.001$ ). However, pre-miR-143-3p treatment of PDGF-stimulated PASMCMigration had no effect on proliferation (Figure 4.8 A). Consistent with the Absorbance<sub>450</sub> results, a PCNA western blot showed no difference in PCNA expression between pre-miR-143-3p treated cells compared with controls (Figure 4.8 B). In addition, anti-miR-143-3p treatment significantly induced apoptosis in H<sub>2</sub>O<sub>2</sub>-treated PASMCMigration compared to controls (Figure 4.9) ( $P < 0.001$ ), and treatment with pre-miR-143-3p significantly inhibited the apoptosis compared with scramble control (Figure 4.9) ( $P < 0.001$ ).

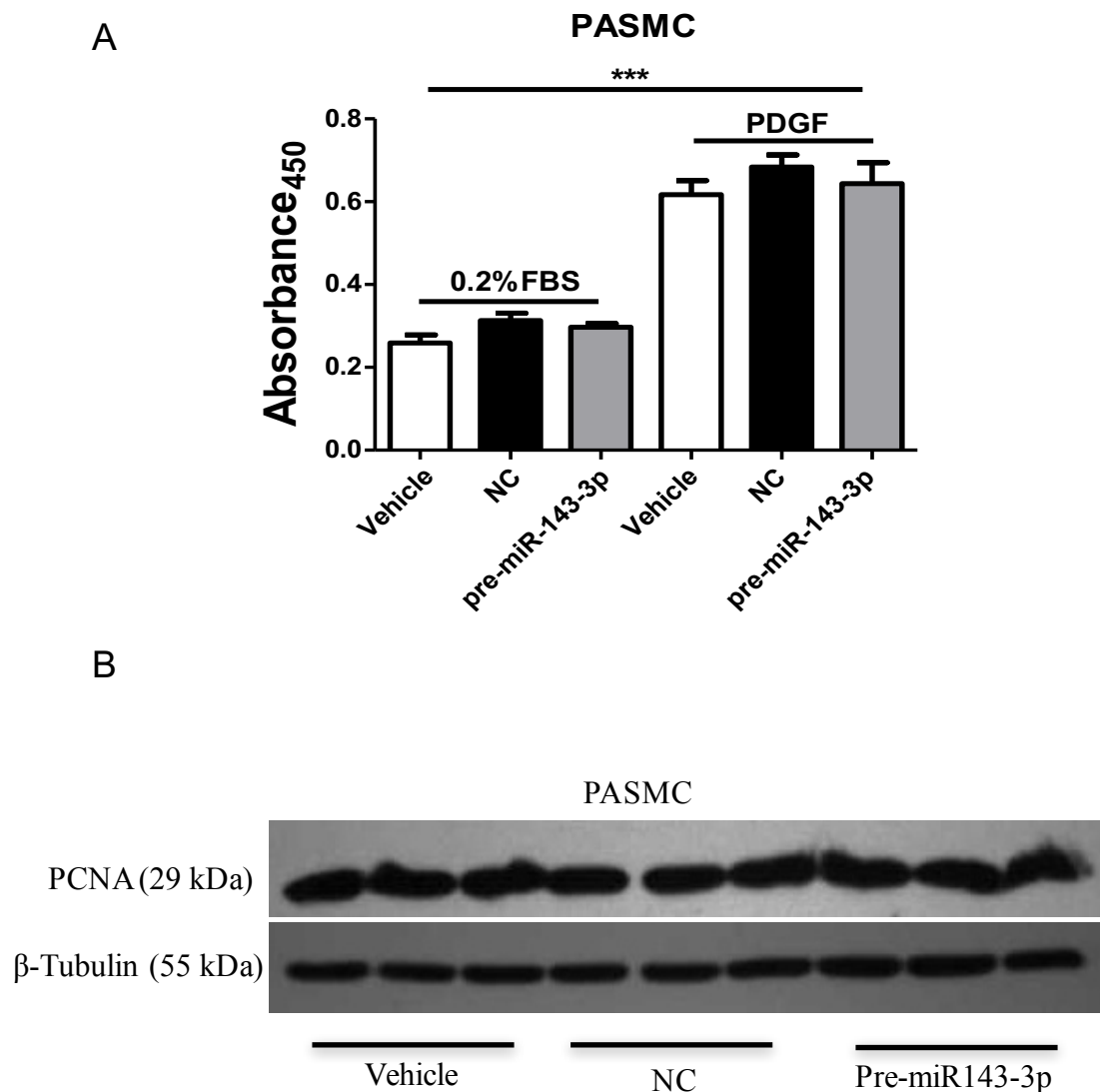


**Figure 4.8 Evaluation of the proliferation of PASMCs after transfection with pre-miR-143-3p**

PASMCs were transfected with pre-miR-143-3p and negative controls. BrdU incorporation assay and western blot assay were performed. (A) There was no difference in BrdU incorporation assay analysis in PASMC with miR-143-3p overexpression (n = 5). (B) Western blot assessed the PCNA protein level in PASMC with miR-143-3p over expression did not show any difference.  $\beta$ -Tubulin was used as internal control (n = 3). Data represented as fold change  $\pm$  SEM and analysed by a one-way ANOVA followed by Tukey's post hoc test. \*\*\*  $P < 0.001$ .

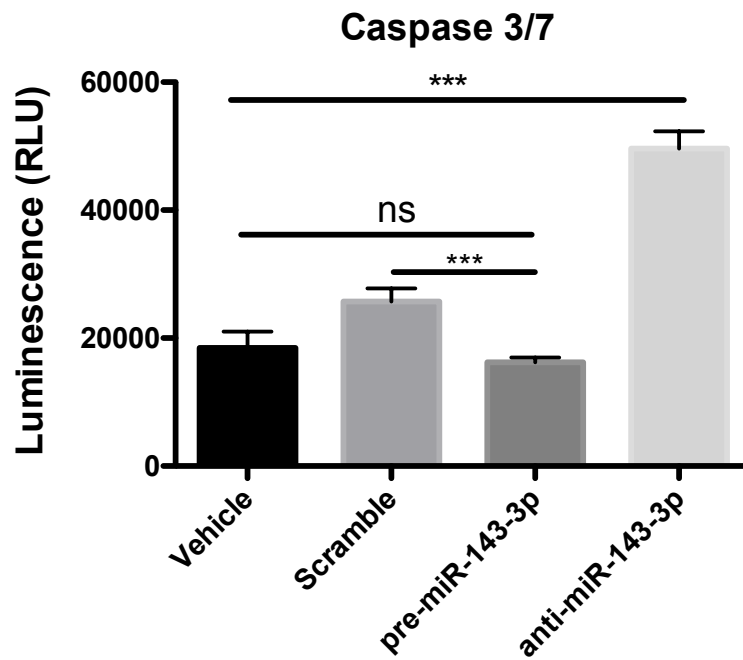


**Figure 4.9 Analysis of apoptosis in PSMCs with miR-143-3p overexpression and knockdown**

Caspase 3/7 assay for PSMC apoptosis induced by H<sub>2</sub>O<sub>2</sub> treatment with miR-143-3p overexpression and knockdown by transfected with pre-miR-143-3p and anti-miR-143-3p. AntimiR-143-3p treatment significantly induced cell apoptosis, and pre-miR-143-3p treatment inhibited but not significantly to the cell apoptosis. Data represented as fold change  $\pm$  SEM and analysed by a one-way ANOVA followed by Tukey's post hoc test. n = 8 wells per group. \*\*\* $P < 0.001$ .

### 4.3.5 DNA Damage in PASMCs Induces miR-143-3p Expression

DNA damage is known to be caused by highly inflammatory cellular environments, which are toxic for cells (Wheelhouse et al., 2003, Fehsel et al., 1991, Gorenne et al., 2013). The development of PAH involves a chronic inflammatory response, characterised by sustained elevation of circulating pro-inflammatory molecules such as tumour necrosis factor  $\alpha$  (TNF- $\alpha$ ) and interleukin-6 (IL-6) (Soon et al., 2010), and recent studies indicate that the Poly (ADP-ribose) polymerase-1 (PARP-1) DNA damage pathway is activated in human distal pulmonary arteries and cultured PASMCs from PAH patients (Meloche et al., 2014b). Given the potential importance of the DNA damage pathway in PAH pathogenesis, we assessed the influence of DNA damage on miR-143-3p expression in PASMC. PASMC were treated with TNF- $\alpha$  (100 ng/mL), IL-6 (100  $\mu$ M) or PDGF (30 ng/mL) for 48 h to induce DNA damage.  $\gamma$ H2AX nuclear staining confirmed DNA damage in PASMC (Figure 4.10 B) and Taqman qRT-PCR analyses revealed a significant upregulation of miR-143-3p following different inductions of DNA damage (Figure 4.10 A) ( $P < 0.05$ ,  $P < 0.01$ ).

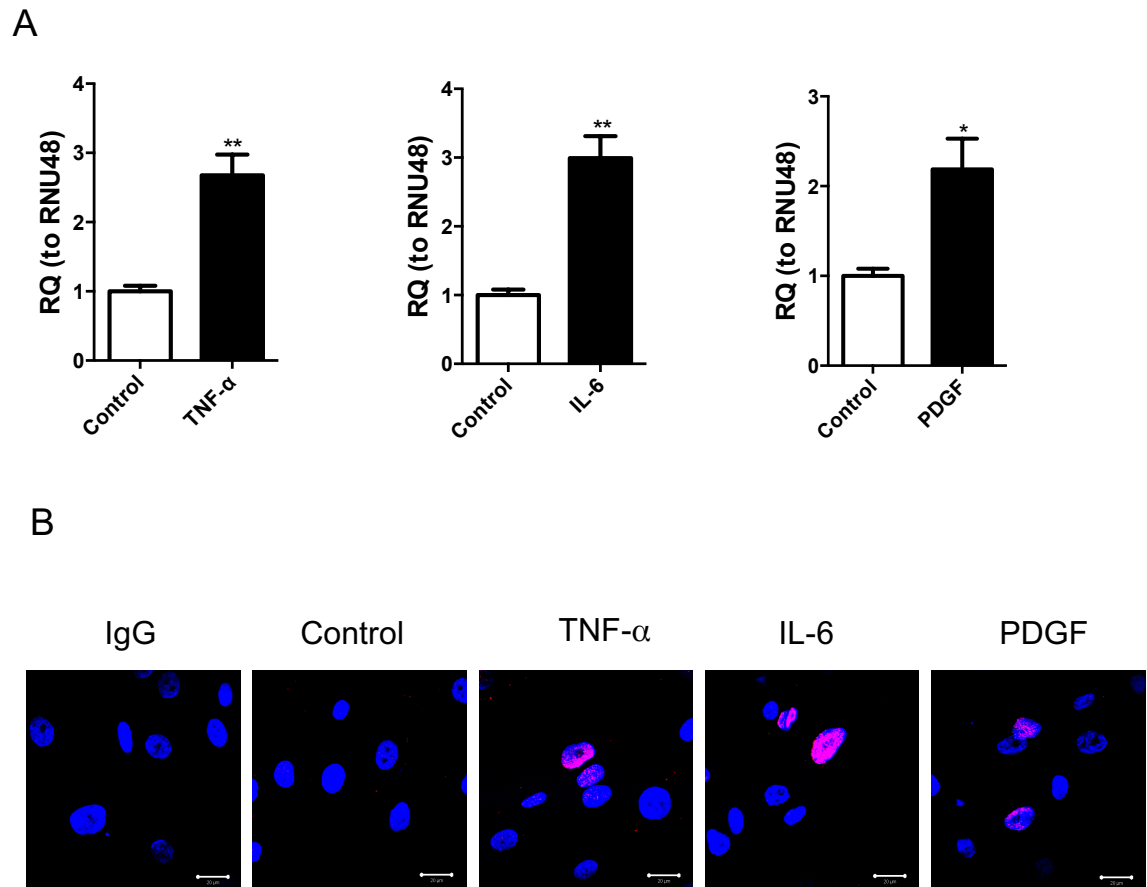


**Figure 4.10 Analysis of miR-143-3p expression following induction of DNA damage in PASC**

Taqman qRT-PCR analysed miR-143-3p in PASCs treated with TNF- $\alpha$  (100 ng/mL), IL-6 (100  $\mu$ M) or PDGF (30 ng/mL) for 48 h. (A) MiR-143-3p expression significantly induced with DNA damage stimulation. (B) Immunofluorescence for  $\gamma$ H2AX nuclear staining for DNA damage in PASCs. Data are expression as mean  $\pm$  SEM and analysed by Student t-test. n = 3 per group in triplicate. \* $P < 0.05$ , \*\* $P < 0.01$ . Scale bar = 20  $\mu$ m.

### **4.3.6 Extracellular Vesicles from PASMC-derived Culture Medium can Transfer miR-143-3p to PAECs**

As shown above, we observed that manipulation of miR-143-3p expression could affect PASMC migration and apoptosis. Previous studies have shown that miR-143/145 mediates cell-to-cell communication between smooth muscle cells and endothelial cells (Hergenreider et al., 2012). In order to explore whether miR-143-3p was involved in cell-to-cell communication between PASMCs and PAECs, we performed a co-culture assay of PAEC with PASMC in Boyden chambers, in which cells were physically separated by 0.4  $\mu\text{m}$  membrane to prevent direct cell-cell contact and transfer of larger vesicles (Figure 4.11 A). MiR-143-3p is more highly expressed in smooth muscle cells in contrast to endothelial cells, which show very low levels of expression of miR-143-3p. In the co-culture experiments, the basal level of miR-143-3p in PAECs was significantly upregulated by co-culture with PASMCs showing the transfer of endogenous miR-143-3p from PASMCs to PAECs (Figure 4.11 B) ( $P < 0.05$ ). In order to visualise whether miRNAs released from PASMCs in extracellular vesicles are transported to PAECs, we transfected PASMC with a Cy3-labeled precursor miRNA prior to co-culturing with PAECs for 24 h. Fluorescence imaging of PAECs showed that Cy3-labeled miRNAs derived from PASMCs could be detected in PAECs in the co-culture system (Figure 4.11 C). In addition, pre-miR-143-3p transfected PASMCs co-cultured with PAECs significantly induced miR-143-3p level in PAECs at 24 h (Figure 4.12 A) ( $P < 0.001$ ) and 48 h (Figure 4.12 B) ( $P < 0.001$ ) after co-culture.

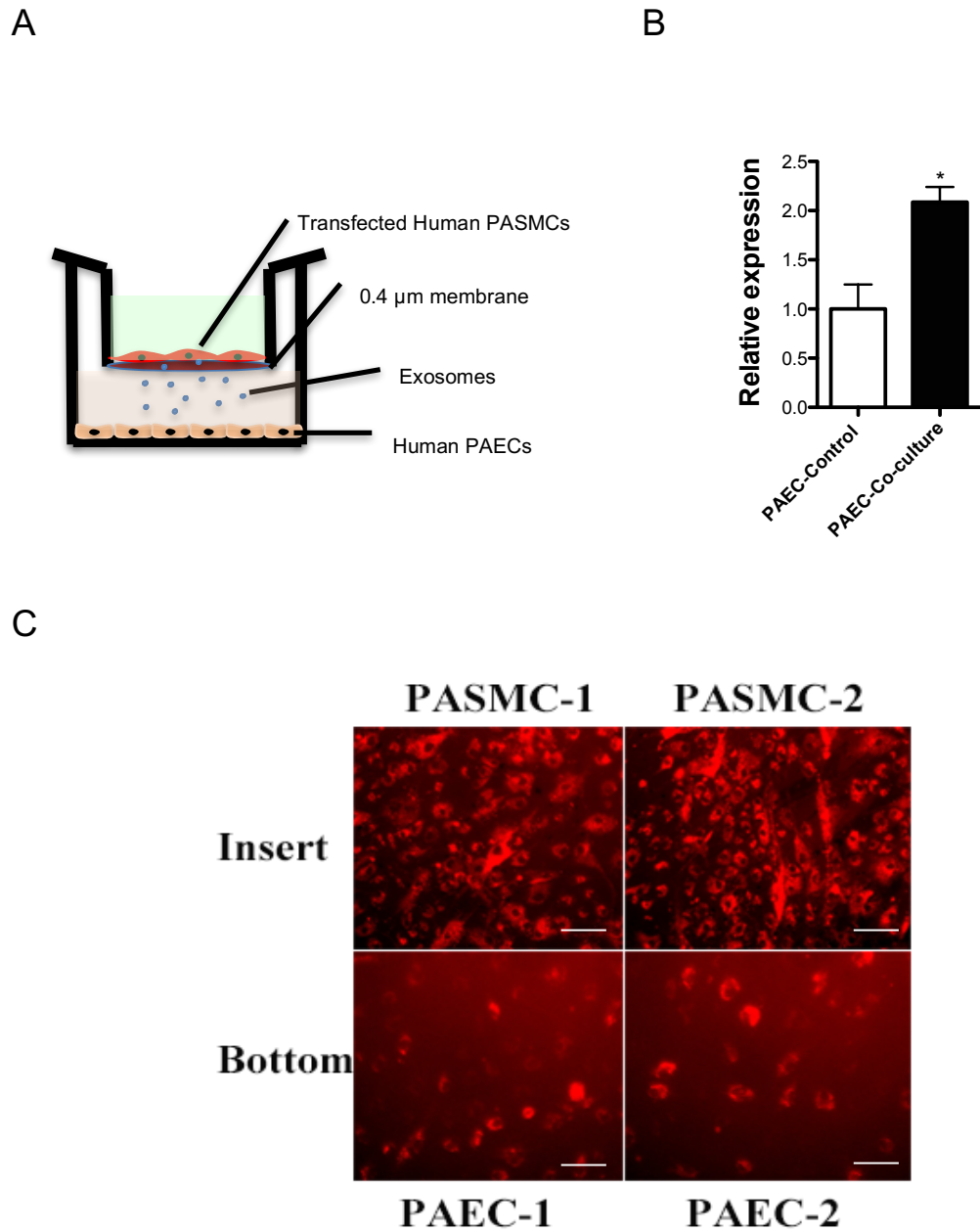


**Figure 4.11 Analysis of cell-to-cell communication between PASMCs and PAECs**

(A) Diagram of the transwell used for the *in vitro* co-culture system. (B) Co-culture system applied with PASMCs (insert) and PAECs (bottom) for 48 h to assess the transfer of endogenous miR-143-3p from PASMCs to PAECs. Taqman qRT-PCR showed that the expression of miR-143-3p was significantly increased in PAECs compared with control after co-culture with PASMCs ( $n = 6$  wells per group). (C) PASMCs in the upper chamber were transfected with Cy3-pre-miRNA. Cy3-labeled miRNA were released and transferred to PAEC in the lower chamber after 24 h. Data are expression as mean  $\pm$  SEM and analysed by Student t-test.  $n = 3$  per group in triplicate.  $*P < 0.05$ . Scale bar = 50  $\mu\text{m}$ .

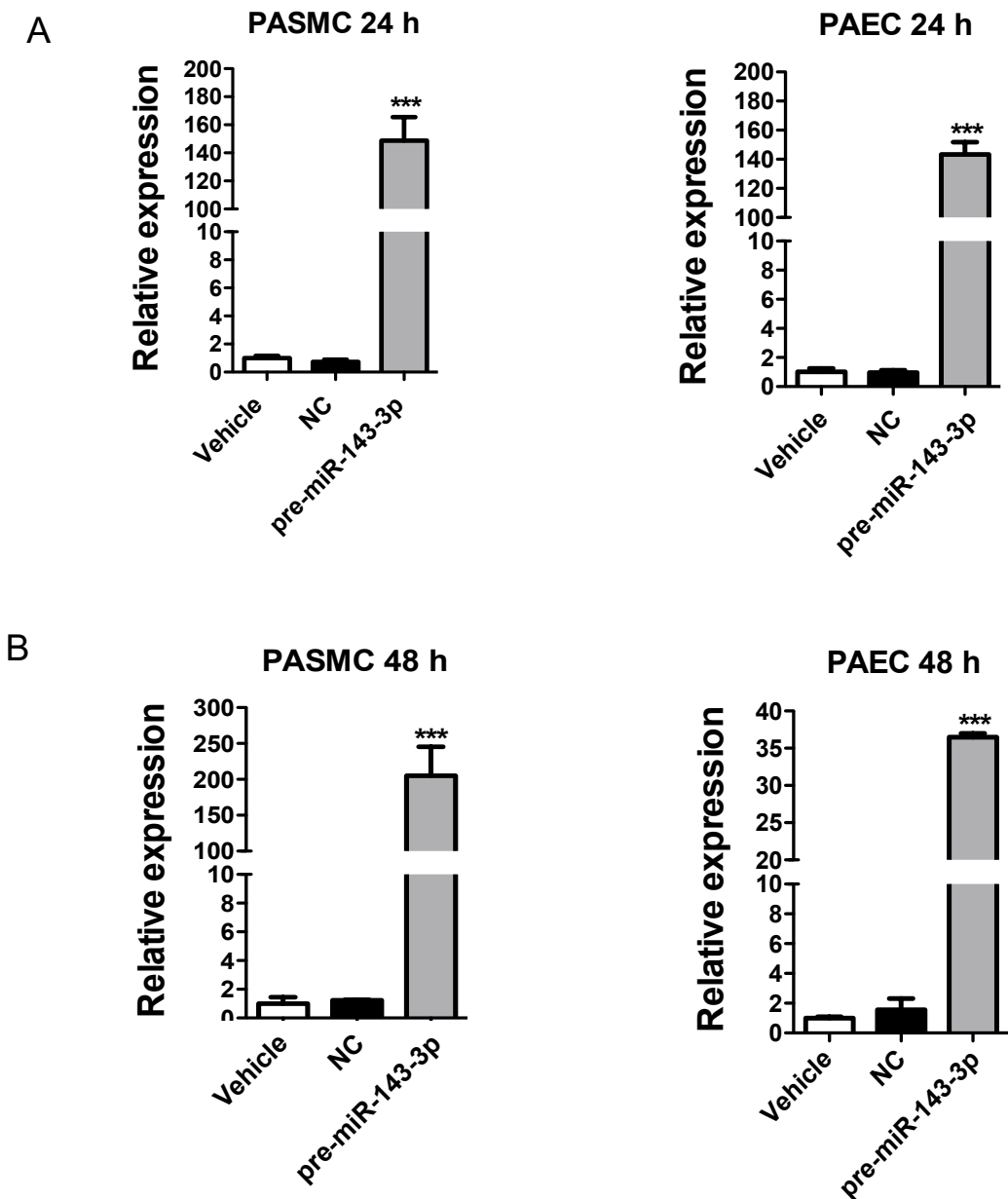


**Figure 4.12** Analysis the cell-to-cell communications between PASMCs and PAECs via miR-143-3p  
 PASMCs were transfected with pre-miR-143-3p or negative control (NC), then co-cultured with PAECs for 24 (A) or 48 h (B) and expression of miR-143-3p was measured in PASMCs and PAECs by Taqman qRT-PCR. MiR-143-3p expression levels in both PASMCs and PAEC were significantly upregulated at 24 h and 48 h after co-culture. Data represented as fold change  $\pm$  SEM and analysed by a one-way ANOVA followed by Tukey's post hoc test.  $n = 3$  per group in triplicate. \*\*\* $P < 0.001$ .

### 4.3.7 MiR-143-3p Secreted by PASMCM Induces PAEC Cell Migration

We had observed that miR-143-3p secreted from PASMCMs could be taken up by PAEC during *in vitro* co-culture. Here, we further investigated whether miR-143-3p secreted from PASMCM can affect PAEC migration. PASMCMs were transfected with pre-miR-143-3p prior to co-culture. Wound healing assay showed that miR-143-3p overexpression significantly induce PAEC migration in the co-culture model (Figure 4.13 A) ( $P < 0.05$ ). The overexpression of miR-143-3p confirm by Taqman qRT-PCR (Figure 4.13 B) ( $P < 0.001$ ). In addition, conditioned medium taken from the transfected PASMCMs with pre-miR-143-3p also significantly increased miR-143-3p expression (Figure 4.14 B) ( $P < 0.01$ ) and induced cell migration in PAECs (Figure 4.14 A) ( $P < 0.05$ ). Taken together, miR-143-3p secreted from PASMCMs affected endothelial cell migration, which demonstrated the cell-to-cell communication between PASMCMs and PAECs through miR-143-3p.

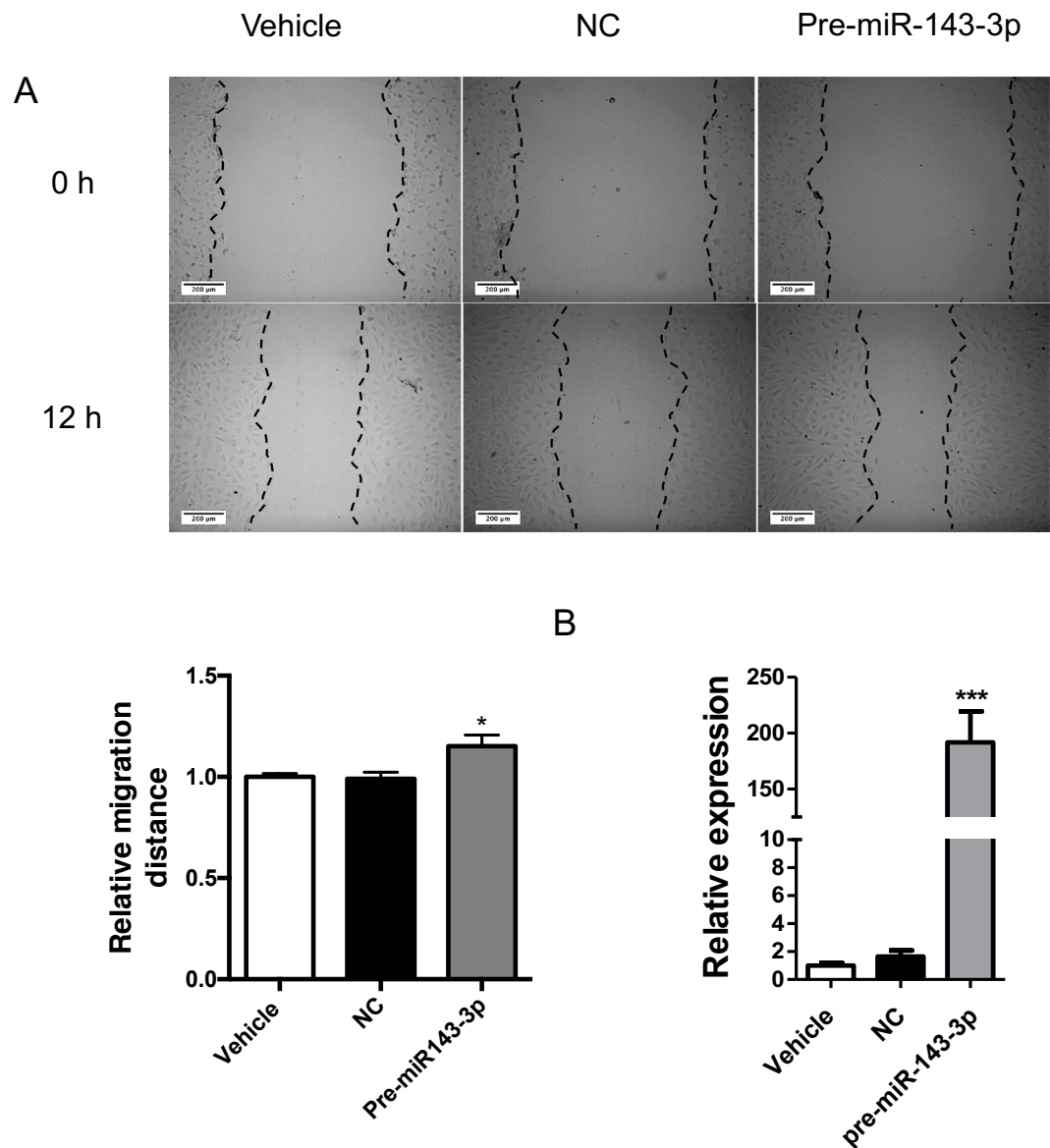


**Figure 4.13 Analysis cell migration of PAECs in co-culture with PSMCs with pre-miR-143-3p transfection**

PASMCs were transfected with pre-miR-143-3p, co-culture was set up with PAECs after 24 h transfection. A single scratch was applied to the PAEC monolayer, with images of scratch captured at the 0h and 12h time points. Image J was used to analyse the migration distance between these two time-points. (A) Representative micrographs and relative migration distance of PAEC migration during scratch closure in co-culture with pre-miR-143-3p-transfected PASMC showed miR-143-3p significantly induced cell migration. (B) Taqman qRT-PCR confirmed the overexpression of miR-143-3p in PAEC compared with controls. Data represented as fold change  $\pm$  SEM and analysed by a one-way ANOVA followed by Tukey's post hoc test.  $n = 3$  per group in triplicate. \* $P < 0.05$ , \*\*\* $P < 0.001$ . Scale bar = 200  $\mu$ m.

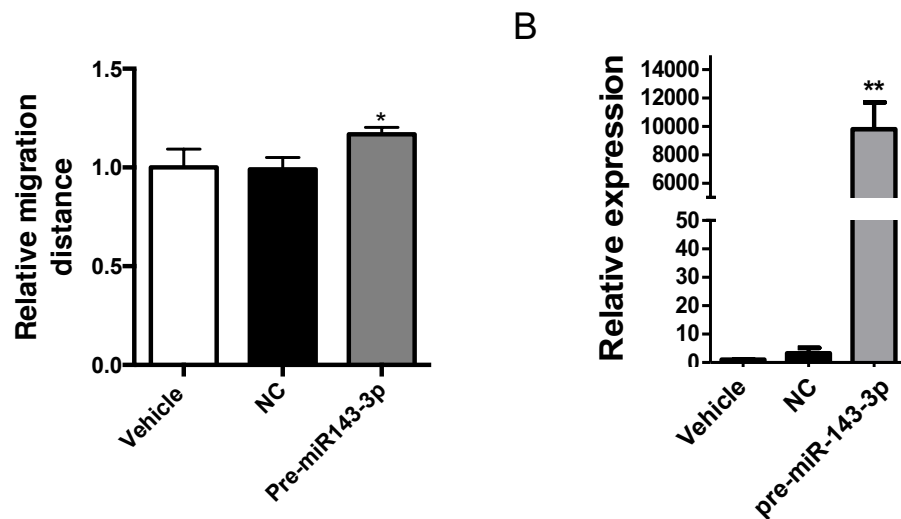
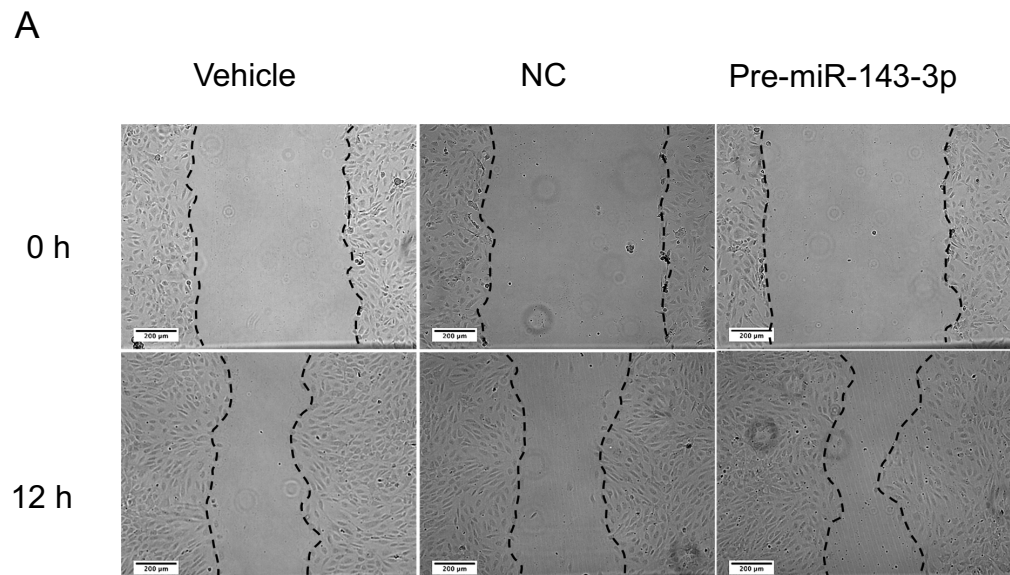


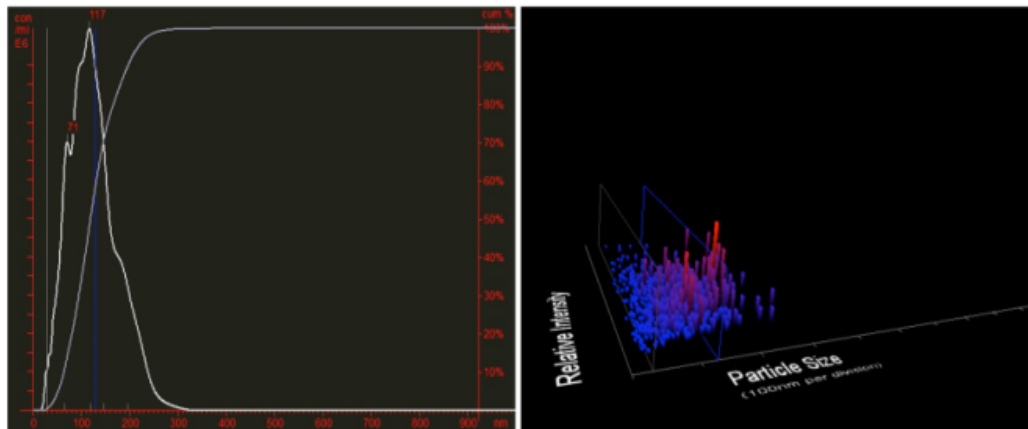
**Figure 4.14 Analysis cell migration of PAECs treated with conditioned medium from PSMCs with pre-miR-143-3p transfection**

Conditioned medium was harvest from PSMCs transfected with pre-miR-143-3p after 48 h and then cultured with PAECs for 24 h. A single scratch was applied to the PAEC monolayer, with images of scratch captured at the 0h and 12h time points. Image J was used to analyse the migration distance between these two time-points. (A) Representative micrographs and relative migration distance of PAECs during scratch closure in the presence of conditioned medium from pre-miR-143-3p transfected PSMCs showed miR-143-3p significantly induced cell migration. (B) Taqman qRT-PCR confirmed the overexpression of miR-143-3p in PAEC compared with controls. Data represented as fold change  $\pm$  SEM and analysed by a one-way ANOVA followed by Tukey's post hoc test.  $n = 3$  per group in triplicate. \* $P < 0.05$ , \*\* $P < 0.01$ . Scale bar = 200  $\mu\text{m}$ .

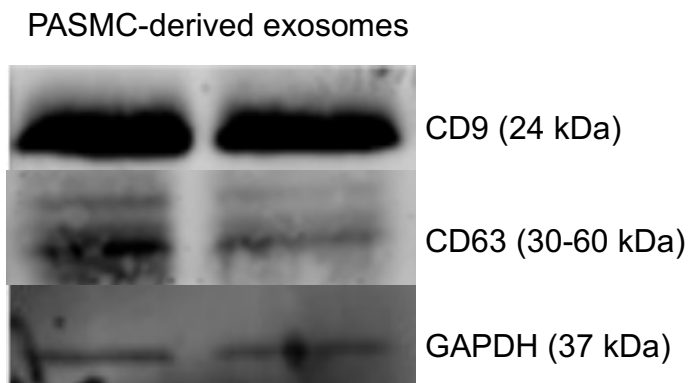
### 4.3.8 Isolation and Characterisation of Exosomes Derived from PSMCs

Previous studies have reported that exosomes can carry functional miRNAs between cells (Valadi et al., 2007, Shimbo et al., 2014). To investigate the function of the extracellular vesicles containing miR-143-3p in the co-culture system and in conditioned medium, we first isolated exosomes from conditioned PSMC medium and assessed the exosomes by NanoSight and western blot. Exosomes were of the expected diameter and size (between 30-130 nm) and showed expression of the exosome specific markers CD9 and CD63 (Figure 4.15 A and B). In order to analyse whether both strands of miR-143 were present within PSMC-derived exosomes, Taqman qRT-PCR analysis was performed, showing that miR-143-3p/5p was present at high levels in the RNA isolated from PSMC-derived exosomes. MiR-143-3p showed higher expression levels than miR-143-5p. As a positive control, the Ct value of miR-143-3p expression in PSMCs is shown, which showed higher levels of miR-143-3p expression compared to PSMC exosomes (Figure 4.15 C). In addition, we isolated exosomes from the medium of PSMCs transfected with different concentrations of pre-miR-143-3p and quantified the levels of miR-143-3p in the exosomes and transfected cells. The incorporation of miR-143-3p into exosomes was confirmed by Taqman qRT-PCR assessing both the cell-associated and extracellular levels of miR-143-3p 24 h post-transfection. As expected, we found a dose-dependent increase in miR-143-3p in PSMCs (Figure 4.16 A) ( $P < 0.001$ ) and accumulation of miR-143-3p in exosomes derived from PSMCs (Figure 4.16 B) ( $P < 0.001$ ). Taken together, this data clearly demonstrates that miR-143-3p is present in exosomes derived from PSMCs. In addition, the quantity of miR-143-3p incorporated into PSMC exosomes is positively correlated with the expression level of miR-143-3p in PSMCs.

A



B



C

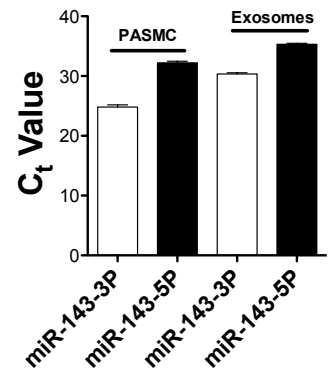
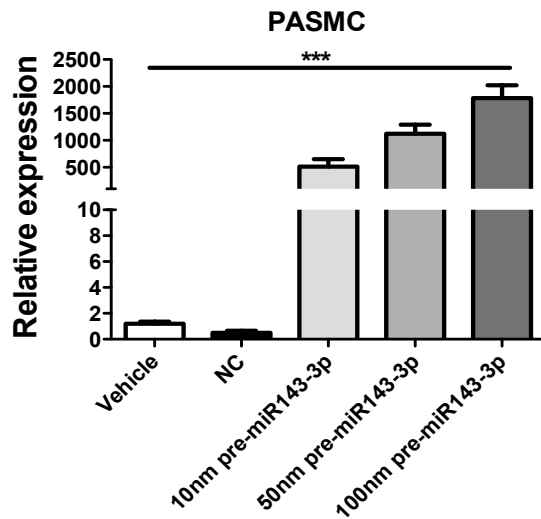


**Figure 4.15 Identification of PASM-derived exosomes and analysis of miR-143 expression in exosomes**

Exosomes were isolated from PASM culture medium by ultracentrifugation. (A) The exosome pellet was re-suspended in PBS and visualised on the NanoSight instrument. The analysis shows the size of isolated exosomes is between 30-130nm. (B) Western Blot for the exosomes markers CD9 and CD63 in PASM derived exosome protein, n = 2 per group in duplicate. (C) Taqman qRT-PCR shows Ct value analysis of miR-143-3p/5p in PASM and exosomes derived from PASM. n = 3 in per group in triplicate.

A



B

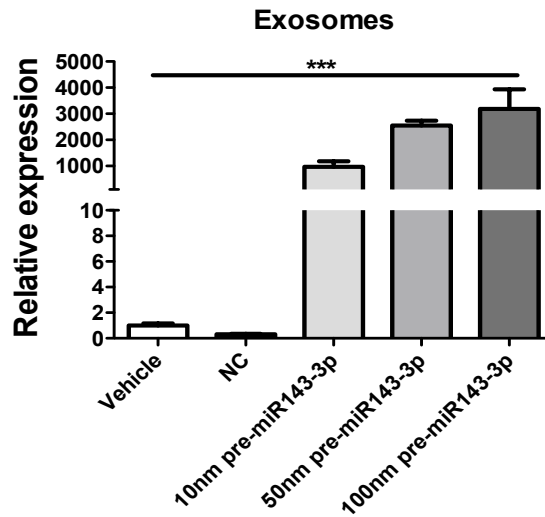


**Figure 4.16 Analysis of miR-143-3p exosomes derived from PASMCS with pre-miR-143-3p transfection at different concentration**

PASMCS were transfected with different concentration with pre-miR-143-3p, and exosomes were purified from the culture medium 48 h after transfection. (A and B) Taqman qRT-PCR analysis of miR-143-3p expression in PASMCS and PASMCS-derived exosomes after the cells were transfected with negative control or pre-miR143-3p (10nM, 50nM and 100nM). MiR-143-3p expression increased with dose dependent manner in exosomes. RNU48 and cel-miR-39 were used as internal loading controls for cells and exosomes respectively. Data represented as fold change  $\pm$  SEM and analysed by a one-way ANOVA followed by Tukey's post hoc test. n =3 per group in triplicate. \*\*\* $P < 0.001$

### **4.3.9 MiR-143-3p Enriched Exosomes Treatment and Direct Transfection of pre-miR-143-3p Induced Cell migration and Angiogenesis in PAECs**

We have demonstrated that miR-143-3p secreted by PASMCs induces cell migration in PAECs, and that miR-143-3p is enriched in PASMC-derived exosomes. In order to investigate the functions of miR-143-3p in PASMC exosomes, we performed a wound-healing assay to examine whether exosome-derived miR-143-3p has similar functional effects on PAECs to that observed in the co-culture and conditioned medium experiments. PASMC-derived exosomes induced PAEC migration in a similar manner to that observed in co-culture and conditioned medium experiments (Figure 4.17 A) ( $P < 0.05$ , and  $P < 0.01$ ), with a corresponding increase in the intracellular levels of miR-143-3p (Figure 4.17 B) ( $P < 0.01$ ). We further performed wound-healing assay in PAECs with pre-miR-143-3p direct transfection. Consistent with our experiments using miR-143-3p enriched exosomes, direct transfection of PAECs with pre-miR-143-3p significantly induced cell migration (Figure 4.18 A) ( $P < 0.05$ ) and increased the miR-143-3p expression level (Figure 4.8 B) ( $P < 0.001$ ) (Figure 4.18 B). In addition, disordered angiogenesis contributed to the plexiform lesions formation (Pietra et al., 2004). Here, we observed that miR-143-3p overexpression via the uptake of miR-143-3p enriched exosomes derived from PASMCs and pre-miR-143-3p transfection significantly induced angiogenesis in matrigel assays in PAEC (Figure 4.19) ( $P < 0.01$ ,  $P < 0.001$ ).

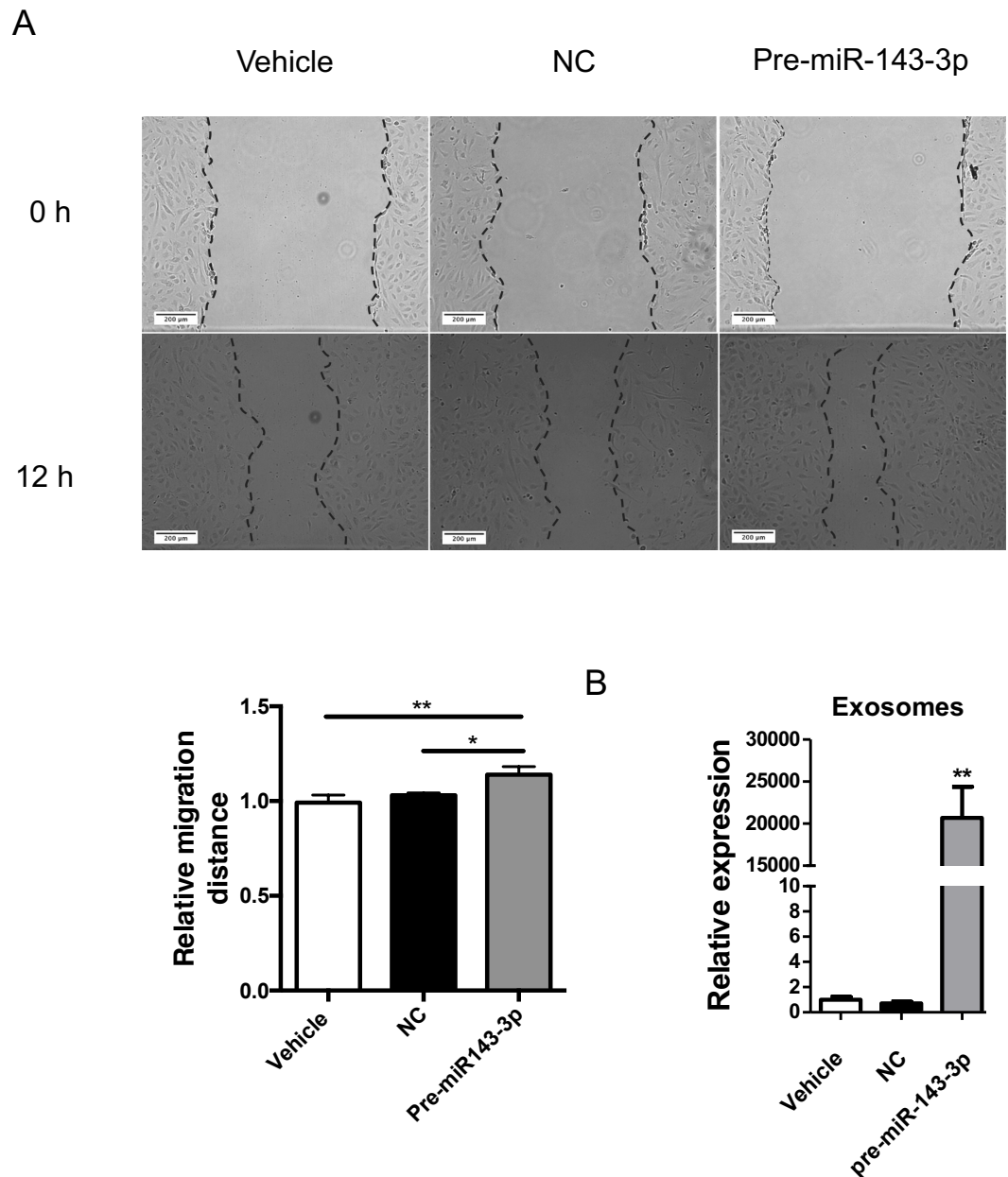


**Figure 4.17 Analysis cell migration of PAECs treated miR-143-3p enriched exosomes derived from PASMCS with pre-miR-143-3p transfection**

A single scratch was applied to the PAEC monolayer, with images of scratch captured at the 0 h and 12 h time points. Image J was used to analyse the migration distance between these two time-points. (A) Representative micrographs and relative migration distance of PAECs during scratch closure, after treatment with isolated exosomes derived from PASMCS transfected with pre-miR-143-3p, vehicle or negative control (NC). The results showed that miR-143-3p significantly induced cell migration. (B) Taqman qRT-PCR confirmed the overexpression of miR-143-3p in PAEC compared with controls. Data represented as fold change  $\pm$  SEM and analysed by a one-way ANOVA followed by Tukey's post hoc test.  $n = 3$  per group in triplicate. Scale bar = 200  $\mu\text{m}$ . \* $P < 0.05$ , \*\* $P < 0.01$ .

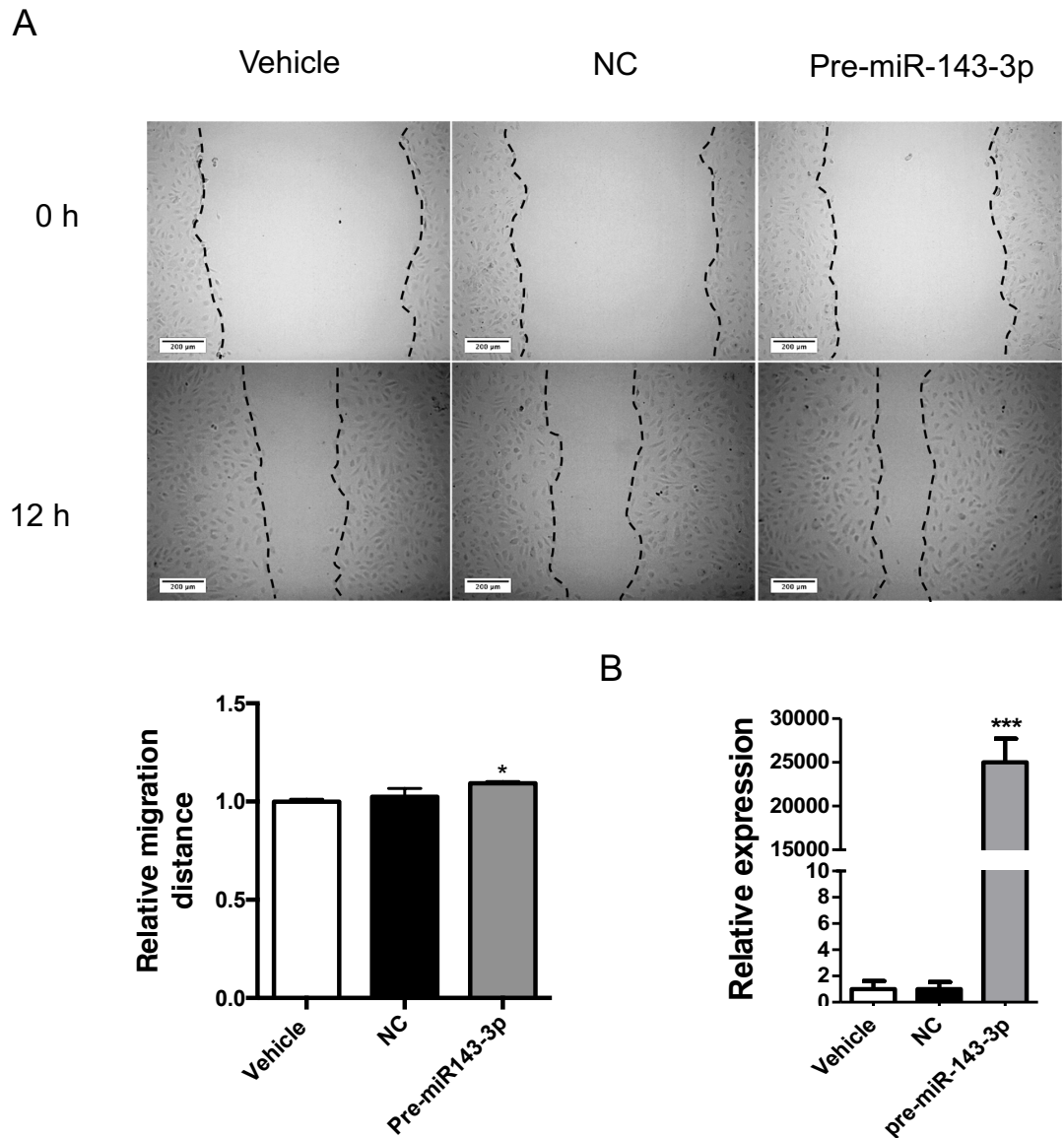


**Figure 4.18 Analysis cell migration of PAECs with pre-miR-143-3p transfection**

A single scratch was applied to the PAEC monolayer, with images of scratch captured at the 0h and 12h time points. Image J was used to analyse the migration distance between these two time-points. (A) Representative micrographs and relative migration distance of PAECs during scratch closure after direct transfection with pre-miR-143-3p. The results showed that miR-143-3p significantly induced cell migration. (B) Taqman qRT-PCR confirmed the overexpression of miR-143-3p in PAEC compared with controls. Data represented as fold change  $\pm$  SEM and analysed by a one-way ANOVA followed by Tukey's post hoc test.  $n = 3$  per group in triplicate. Scale bar = 200  $\mu$ m. \* $P < 0.05$ , \*\*\* $P < 0.001$ .

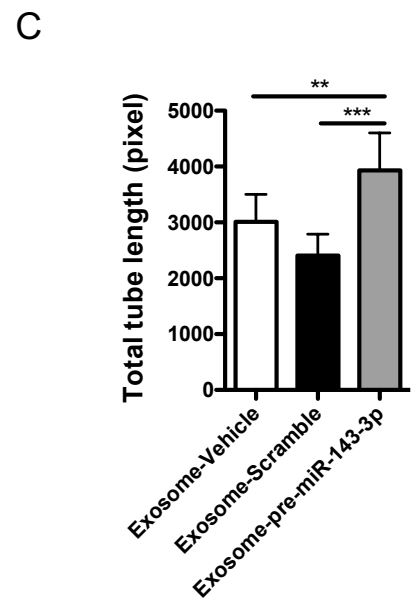
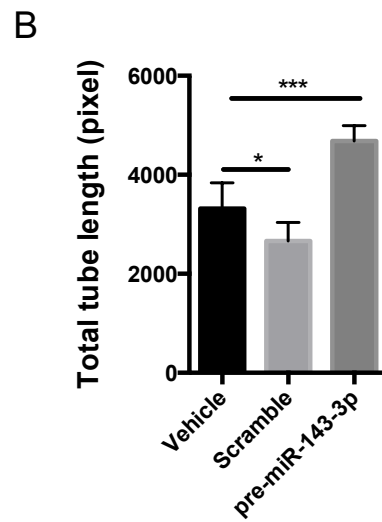
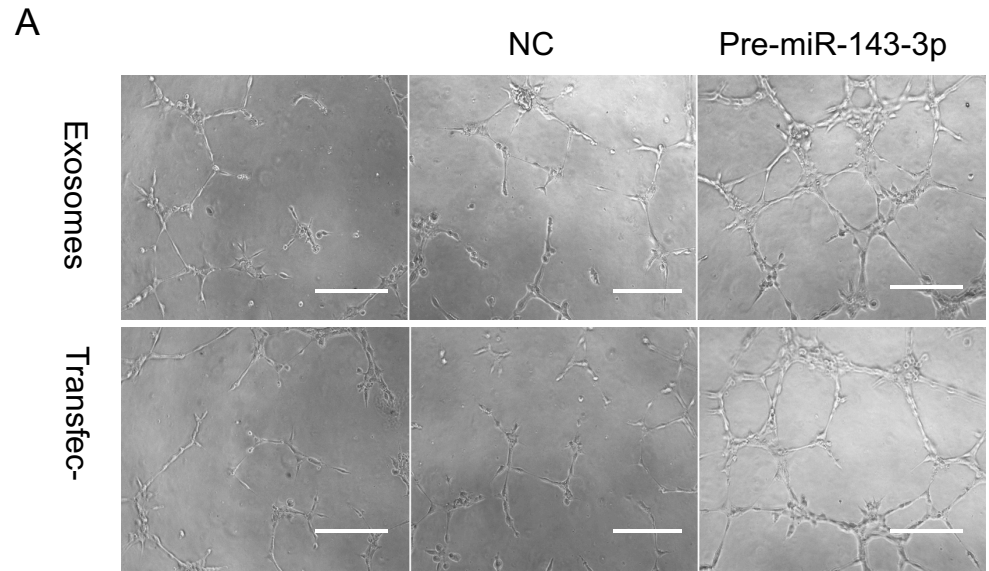


**Figure 4.19** Angiogenesis analysis of PAECs with miR-143-3p overexpression via treated with miR-143-3p enriched exosomes and transfected with pre-miR-143-3p

(A) Matrigel angiogenesis assay analysis in PAECs transfected with pre-miR-143-3p or loaded with miR-143-3p enriched exosomes derived from PSMCs with pre-miR-143-3p transfection. (B) Quantification of total tube lengths in PAECs treated with exosomes from pre-miR-143-3p transfection and (C) Quantification of total tube lengths in PAECs transfected with premiR-143-3p. Data represented as fold change  $\pm$  SEM and analysed by a one-way ANOVA followed by Tukey's post hoc test.  $n = 6$  wells per group. Scale bar = 250  $\mu\text{m}$ . \* $P < 0.05$ , \*\* $P < 0.01$ , \*\*\*  $P < 0.001$ .

#### **4.3.10 Overexpression of miR-143-3p in PAECs Has No Effect on Cell Proliferation and Apoptosis**

In addition to analysing the role of miR-143-3p during PAEC migration and tube formation, we also assessed the effect of miR-143-3p on PAEC proliferation and apoptosis. Overexpression of miR-143-3p was achieved via pre-miR-143-3p transfection, while cell proliferation was analysed by BrdU incorporation assay and evaluation of PCNA protein levels by western. We observed that VEGF significantly induced PAEC proliferation compared to unstimulated control cells (Figure 4.20 A) ( $P < 0.001$ ). However, there was no difference between pre-miR-143-3p treated groups compared with control groups. Consistent with our BrdU results, PCNA western blots showed that there was no difference in pre-miR-143-3p treated cells compared with controls (Figure 4.20 B). Cell apoptosis was analysed using a Caspase3/7 activity assay. Neither pre-miR-143-3p transfection nor exposure to miR-143-3p enriched exosomes affected PAEC apoptosis when assayed in this way (Figure 4.21 A and B). However, we observed the Scramble transfected group significantly induced the apoptosis (Figure 4.21 B) ( $P < 0.001$ ) compared control and pre-miR-143-3p. This may due to the target effect of scramble control.

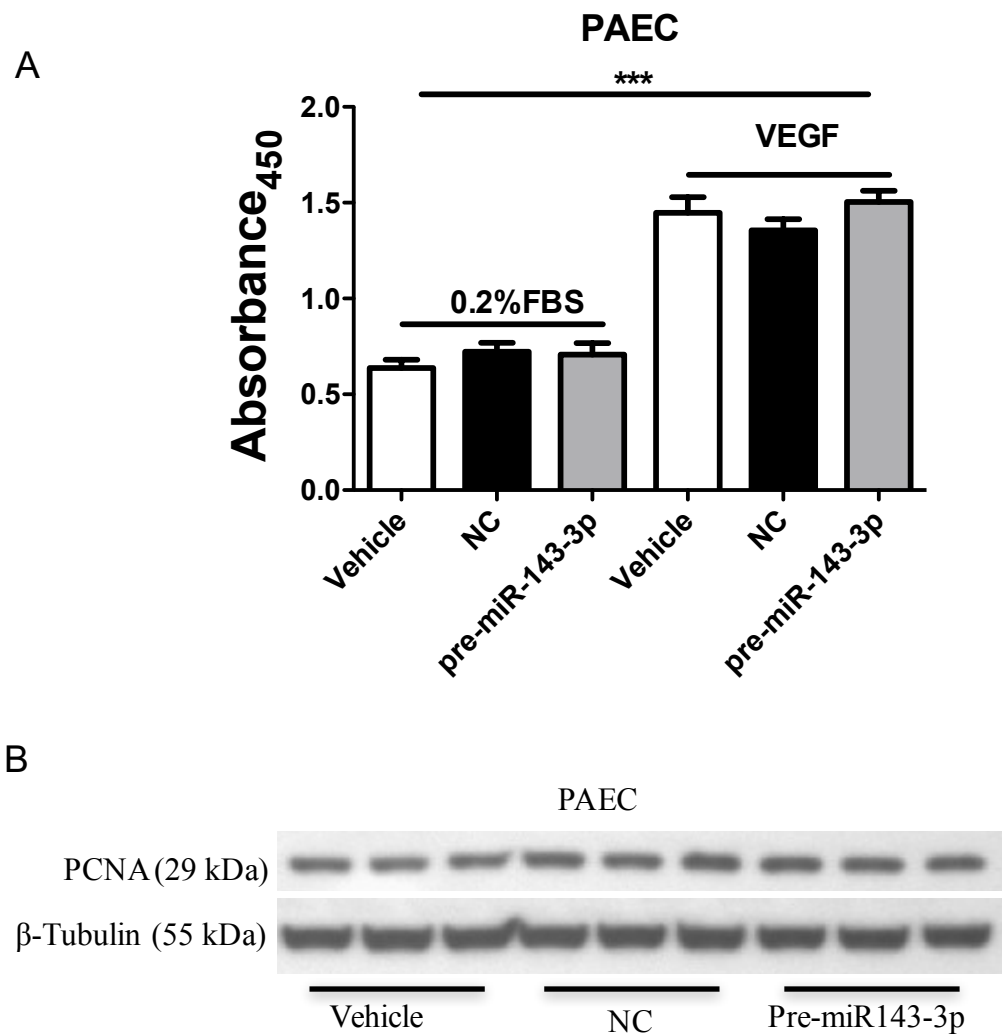


**Figure 4.20 Proliferation analysis of PAECs with miR-143-3p transfection**

PAECs were transfected with pre-miR-143-3p. BrdU incorporation assays and PCNA western blot assays were performed to evaluate PAEC proliferation (A) There was no difference in BrdU incorporation by PAEC following miR-143-3p overexpression (n = 5). (B) Western blots analysis did not reveal any effect on PCNA protein expression in PAEC following miR-143-3p overexpression.  $\beta$ -Tubulin was used as internal loading control (n = 3). Data represented as fold change  $\pm$  SEM and analysed by a one-way ANOVA followed by Tukey's post hoc test. \*\*\*  $P < 0.001$ .

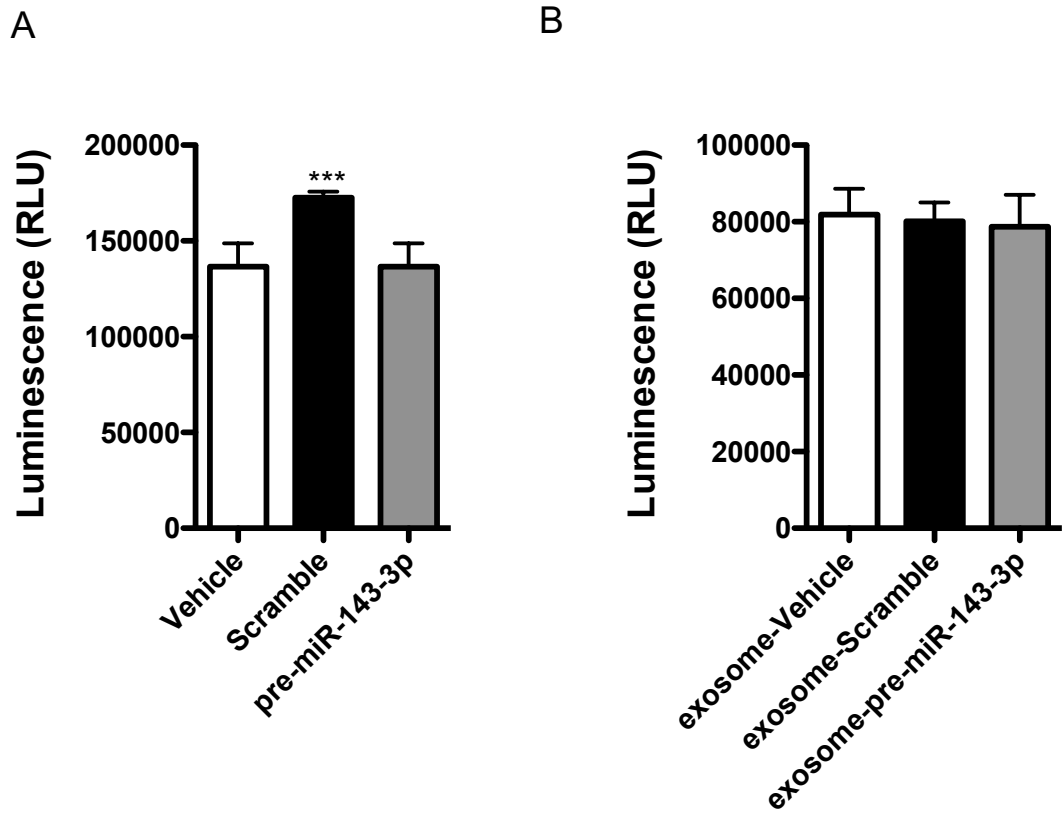


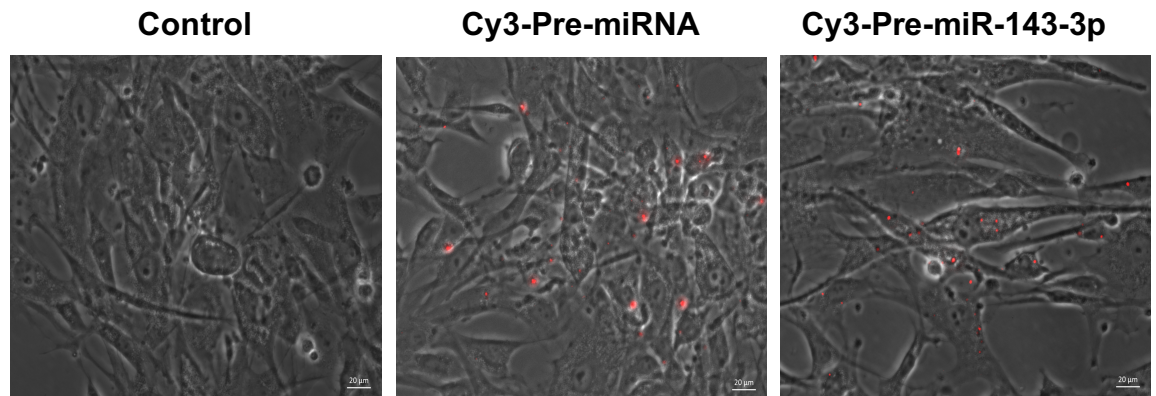
**Figure 4.21 Apoptosis analysis of PAECs with miR-143-3p overexpression via pre-miR-143-3p transfection and treated with miR-143-3p enriched exosomes**

PAEC apoptosis was assessed by performing Caspase 3/7 activity assays on cells following TNF- $\alpha$  and Cycloheximide (CHX) treatment in the presence or absence of miR-143-3p overexpression (pre-miR-143-3p transfection) or miR-143-3p enriched PASCs exosomes. Neither condition affected PAEC apoptosis compared with controls. Data represented as fold change  $\pm$  SEM and analysed by a one-way ANOVA followed by Tukey's post hoc test. n = 8 well per group. \*\*\* $P < 0.001$ .

### **4.3.11 Cy3-labelled pre-miR-143-3p is Transferred from PSMC to PAEC in Exosomes**

We have demonstrated that exosomes mediate the cell-to-cell communication between PSMCs and PAECs, with transfer of miR-143-3p between the two cell types. In order to track the secretion and uptake of miR-143-3p during cell-to-cell communication, we labelled pre-miR-143-3p with Cy3 and then transfected PSMCs with Cy3-labelled pre-miR-143-3p. Cy3-labelling pre-miRNA, which can be transfer from PSMCs to PAECs in the co-culture model, used as positive control. Confocal microscopy analysis showed red fluorescence in transfected PSMC, which demonstrated the transfection success (Figure 4.22 A). To show direct transfer of Cy3-labelled pre-miR-143-3p between PSMCs and PAECs, exosomes purified from the culture medium 48 h after PSMC transfection were incubated with PAECs for a period of 24 h. Confocal microscopy analysis of fluorescence showed high levels of Cy3 fluorescence in PAEC transfected with labelled pre-miR-143-3p and positive control pre-miR, compared to control (Figure 4.22 B).

A



B

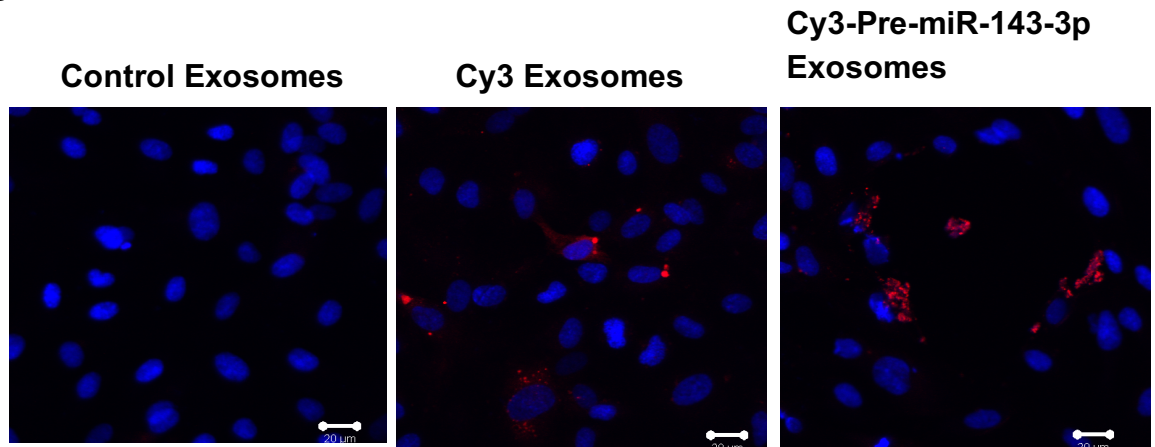


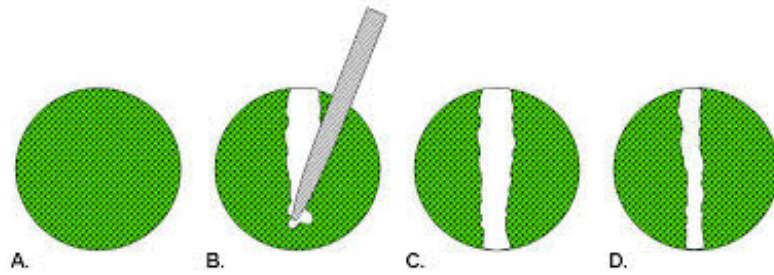
**Figure 4.22 Tracking analysis of cell-to-cell communication between PSMCs and PAECs via Cy3-labeled pre-miR-143-3p**

(A) PSMC transfected with Cy3-labeled pre-miRNA and Cy3-labeled pre-miR-143-3p. Confocal images were taken after 48 h showed red fluorescence (Cy3). (B) Exosomes were purified from the supernatants of PSMC transfected with Cy3-labelled pre-miRNA or Cy3-labeled pre-miR-143-3p. Confocal microscopy analysis was performed following 24 h of PAEC exposure to exosomes, showed red fluorescence compared with control exosomes. n = 3 per group in triplicate.

#### **4.3.12 AntimiR-143-3p Treatment Reversed the Pro-migratory Effect of miR-143-3p Enriched Exosomes Derived from PSMCs**

In order to further confirm that PSMC-derived miR-143-3p enriched exosomes are involved in the cell-to-cell communication between PSMCs and PAECs and regulate the migration behaviour, we performed reverse experiments to investigate whether inhibiting the exosome-induced overexpression of miR-143-3p in PAEC could inhibit migration. The experimental design is showed in (Figure 4.23). We first verified the miR-143-3p expression levels in PAECs exposed to various treatments. In the exosome-free groups, anti-miR-143-3p transfection significantly reduced the expression of miR-143-3p level (undetectable by Taqman qRT-PCR) compared with vehicle and scramble groups. As shown previously, the PSMC-derived exosome treated groups had a much higher level of miR-143-3p than the exosome-free groups. In particular, miR-143-3p expression in PAECs exposed to exosomes from PSMCs transfected with pre-miR-143-3p was dramatically increased compared with all other groups. AntimiR-143-3p transfection significantly reduced miR-143-3p expression in these cells, although levels were still higher than vehicle and scramble exosomes treated cells (Figure 4.24 A) ( $P < 0.01$ ). Importantly, the wound healing assay showed that treatment of PAECs with exosomes derived from pre-miR-143-3p transfected PSMCs significantly induced cell migration compared with all other groups, while transfection of anti-miR-143-3p reversed this increase in cell migration (Figure 4.24 B) ( $P < 0.05$ ). Taken together, these data show that the induction of PAEC migration in the presence of PSMC derived exosomes are mediated by transfer of exosomal miR-143-3p between these two cell types.

A



B

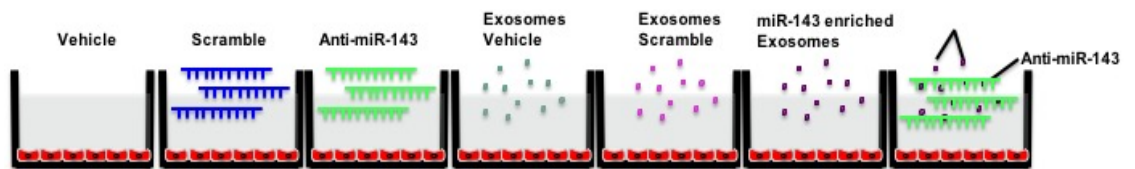
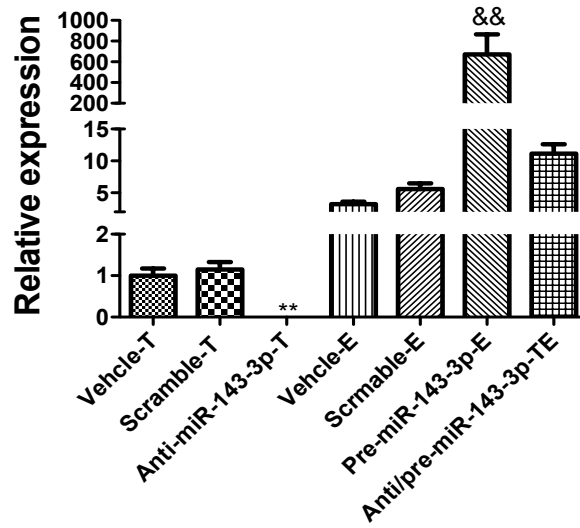


**Figure 4.23 Schematic diagrams to shown the experiments work model**

(A) Cartoon showing the wound-healing assay in PAECs with a single scratch. (B) Design of reversal experiments evaluating the effect of miR-143-3p enriched PASMCMC exosomes on PAEC migration. There are seven groups, which are vehicle, scramble transfection, antimiR-143-3p transfection, vehicle (exosomes derived from untransfected PASMCMCs), scramble (exosomes derived from PASMCMCs transfected with a scramble control), miR-143-3p-enriched exosomes (derived from PASMCMCs transfected with pre-miR-143-3p), and antimiR-143-3p transfection together with treatment of miR-143-3p-enriched exosomes derived from PASMCMCs transfected with pre-miR-143-3p.

A



B

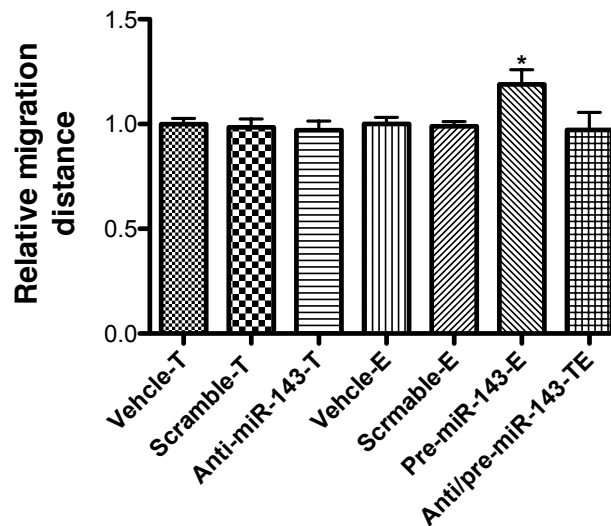


**Figure 4.24 Migration analysis of PAECs with modulation of miR-143-3p expression with transfection and/or miR-143-3p enriched exosome treatment**

(A) Analysis of miR-143-3p expression in PAEC with different treatments. PAECs were transfected with anti-miR-143-3p, or pre-miR-143-3p, or combination of pre-miR-143-3p transfection and treatment with miR-143-3p enriched exosomes derived from PSMCs transfected with pre-miR-143-3p. (B) Analysis of relative migration distance in PAEC showed that anti-miR-143-3p transfection could inhibit the increase in migration caused by exposure to miR-143-3p enriched exosomes from PSMCs. Data represented as fold change  $\pm$  SEM and analysed by a one-way ANOVA followed by Tukey's post hoc test.  $n = 3$  per group in triplicate.  $**P < 0.01$  compared with Vehicle-T and Scramble-T,  $\&\& P < 0.01$  compared with any other groups.  $*P < 0.05$  compared with all other groups.

### 4.3.13 Pathway Analysis of PSMCs and PAECs

In order to identify potential pathways that may be involved in the miR-143-3p-mediated regulation of PSMC and PAEC migration, we carried out expression microarray on PSMCs and PAECs. PSMCs were transfected with pre-miR-143-3p and PAECs were treated with miR-143-3p enriched exosomes derived from PSMCs transfected with pre-miR-143-3p. Taqman qRT-PCR confirmed up-regulation of miR-143-3p in PSMC and PAEC following transfection and exosome treatment respectively (Figure 4.25) ( $P < 0.01$ ). In PSMCs transfected with pre-miR-143-3p, 68 regulated targets known to be involved in cell migration were identified (Table 4-1). Further, “migration of cancer cells” was identified as a significantly enriched pathway ( $P = 0.0001$ ) identified by ingenuity pathway analysis (Table 4-2 and Figure 4.26). These findings are consistent with the hypothesis that miR-143-3p can increase migration in PSMCs. In PAECs exposed to miR-143-3p-loaded PSMC exosomes, we observed the regulation of multiple targets involved in cell death and survival (Table 4-3 and 4-4). Further these targets might suggest that miR-143-3p reduces cell death in PAEC (Figure 4.27).

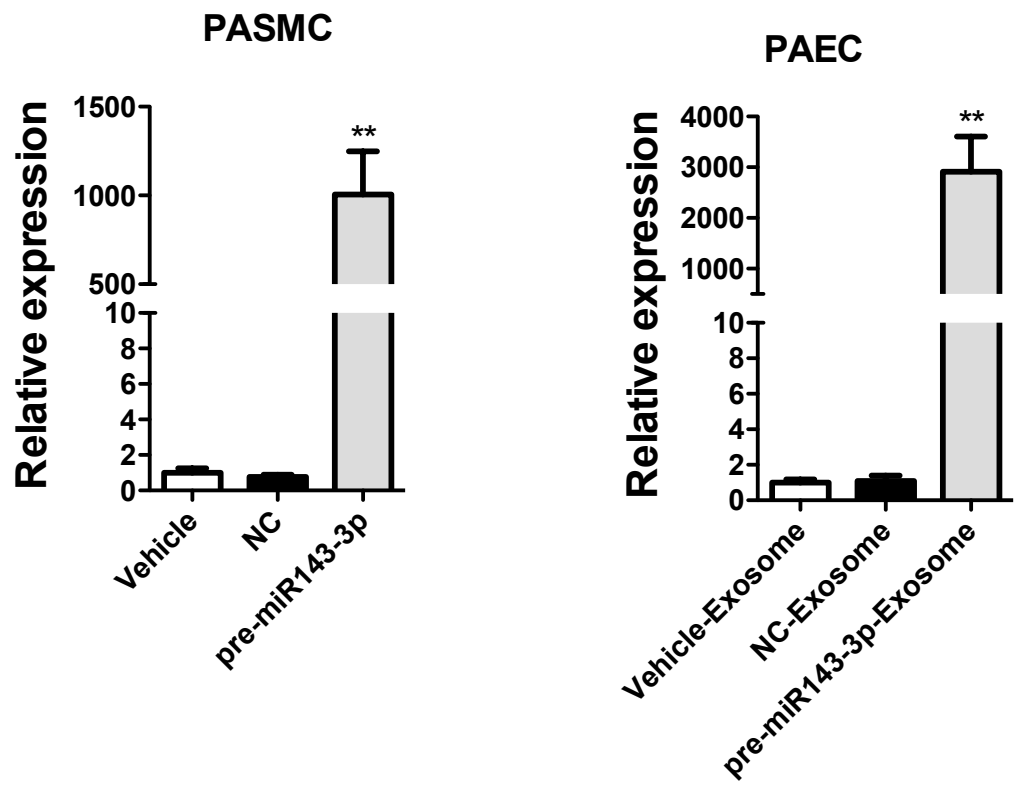


**Figure 4.25 Validation of miR-143-3p expression in PASMCS and PAECs array samples**

PASMCS were transfected with pre-miR-143-3p or a negative control for 48 h. PAECs were treated with miR-143-3p-enriched exosomes derived from PASC transfected with pre-miR-143-3p. Taqman qRT-PCR analysis of these samples showed a significant increase in miR-143-3p compared to controls. Data represented as fold change  $\pm$  SEM and analysed by a one-way ANOVA followed by Tukey's post hoc test. n = 4 wells in per group. \*\* $P < 0.01$

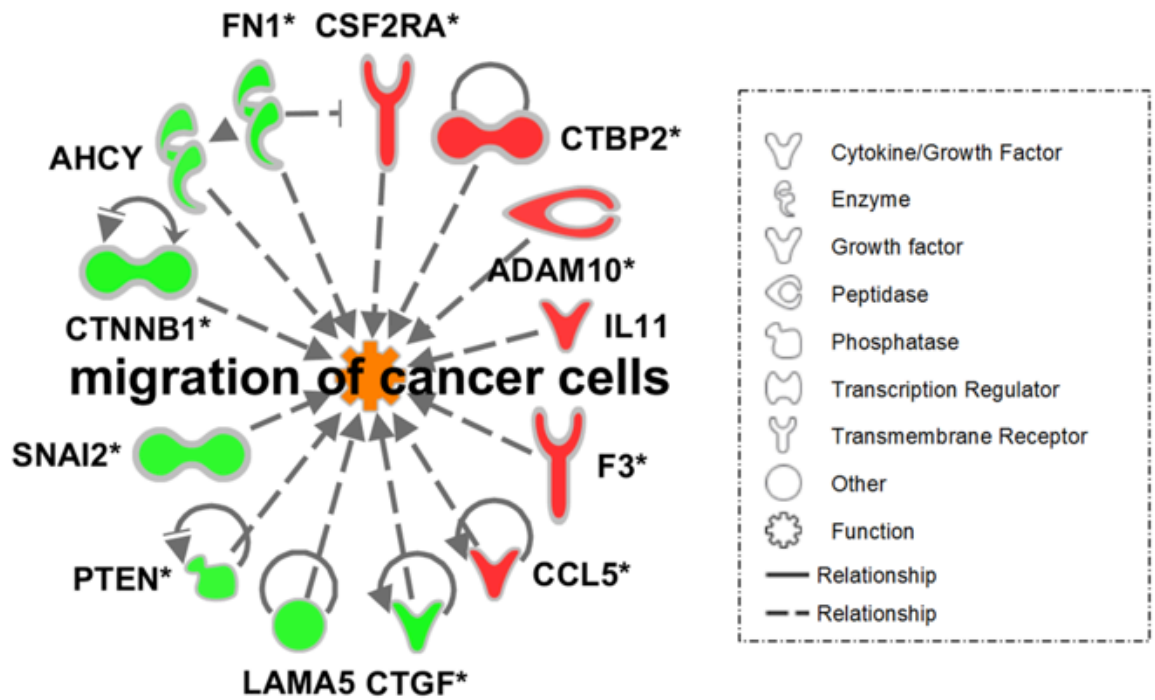


**Figure 4.26 Pathway analysis in PASMC by microarray**

Selected significant functional annotation relating to increased 'migration of cancer cells' ( $P < 1.43 \times 10^{-4}$ ) using Ingenuity Pathway Analysis. Orange represents an increase in migration of cancer cells, green fill represents decrease and red an increase in gene expression levels in miR-143-3p transfected cells compared to controls.

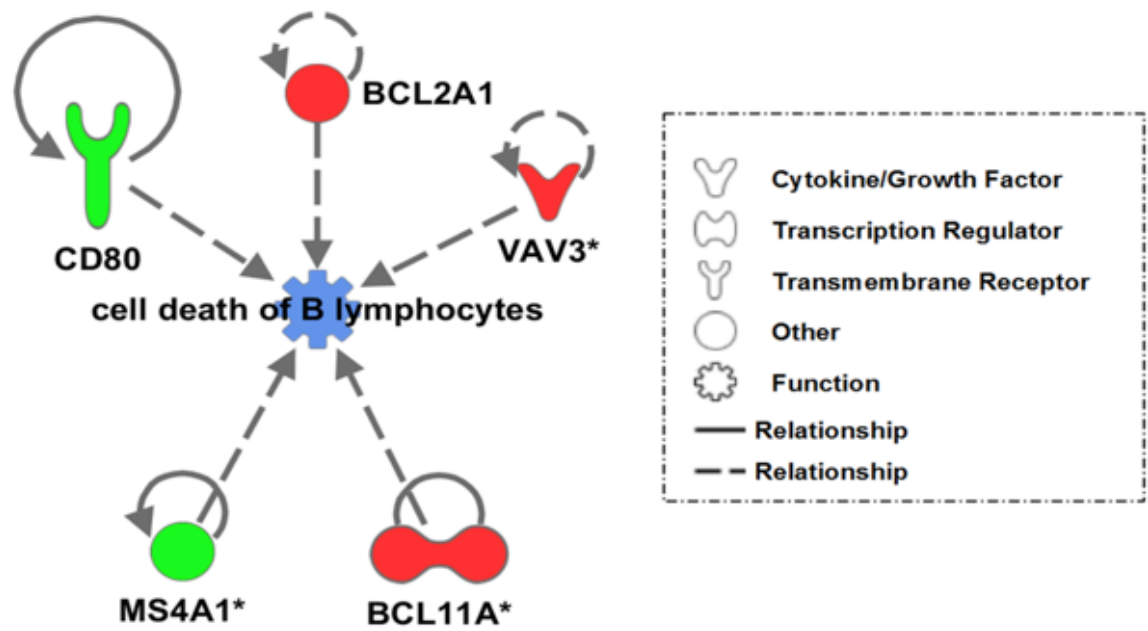


**Figure 4.27 Pathway analysis in PAEC by microarray**

Selected significant functional annotation relating to decrease in 'cell death and survival' ( $P < 1.56 \times 10^{-3}$ ) using Ingenuity Pathway Analysis. Blue represents a decrease in 'cell death of B lymphocytes', green fill represents decrease and red an increase in gene expression levels in miR-143-3p-enriched exosome treated cells compared to controls.

**Table 4-1 Disease and function annotation relating to migration in the smooth muscle cell gene expression dataset.**

Categories	Diseases or Functions Annotation	p-Value	Gene Count	Molecules
Cellular Movement	migration of brain cells	5.53E-05	9	APP,BTG2,CDK5,FN1,FUT10,GNA13,LAMA1,PTEN,RERE
	migration of breast cancer cell lines	2.96E-03	12	ANKS1A,CCL5,CTGF,CTNNB1,CTSL,DDR2,FLNA,FN1,GIT1,MLLT4,SNAI2,TGM2
	migration of cancer cells	1.43E-04	13	AD-AM10,AHCY,CCL5,CSF2RA,CTBP2,CTGF,CTNNB1,F3,FN1,IL11,LAMA5,PTEN,SNAI2
	migration of cells	3.64E-04	68	AD-AM10,ADORA1,AHCY,ANGPTL4,ANKS1A,APP,ARHGDI3,ASAP2,BBS1,BTG2,CCL5,CCR5,CD58,CD63,CDK5,CSF2RA,CTBP1,CTBP2,CTGF,CTNNA1,CTNNB1,CTSL,DDR2,DIAPH1,DOCK3,F3,FCAR,FLNA,FN1,FUT10,FUT8,GIT1,GNA13,GNG12,HDAC3,HDC,HLA-G,HRH1,IL11,JAK1,LAMA1,LAMA5,LDLR,LPA,MATN2,MLLT4,MYOCD,PKD1,PKM,PLEC,PRRX1,PTEN,PTPRU,RERE,RHOG,SCARB1,SEMA3E,SLC3A2,SLC9A1,SNAI2,SPRY4,TGM2,TP53INP1,TPT1,TRPV1,WHSC1,YWHAE,YY1AP1
	migration of central nervous system cells	2.37E-05	10	APP,BTG2,CDK5,CTGF,FN1,FUT10,GNA13,LAMA1,PTEN,RERE
	migration of chondrosarcoma cells	1.03E-02	2	CCL5,IL11
	migration of embryonic cells	3.08E-03	7	CCL5,CDK5,FN1,IL11,LAMA1,LAMA5,SLC3A2
	migration of endothelial cells	9.72E-03	14	AD-AM10,ANGPTL4,CCL5,CD63,CTGF,F3,FLNA,FN1,HRH1,PKM,PTEN,SCARB1,SEMA3E,SPRY4

migration of extravillous trophoblast cells	3.00E-03	2	CCL5,IL11
migration of fibroblast cells	3.48E-03	8	CTNNB1, FN1, GNG12, PKD1, PTEN, RHOG, TGM2, TP53INP1
migration of glioma cells	9.43E-03	3	CSF2RA, CTGF, F3
migration of hepatic stellate cells	6.56E-03	3	CCL5, CCR5, CTGF
migration of kidney cell lines	1.57E-03	7	ANKS1A, APP, CCL5, CCR5, FN1, PKD1, RHOG
migration of leukemia cells	5.33E-04	7	APP, CCL5, CCR5, FLNA, FN1, GNA13, TGM2
migration of melanoma cells	8.41E-03	3	ADAM10, FN1, SNAI2
migration of monocytes	6.45E-03	6	APP, CCL5, CTGF, FN1, JAK1, LDLR
migration of mononuclear leukocytes	6.50E-03	16	AD-AM10, APP, CCL5, CCR5, CD58, CTGF, DIAPH1, FN1, GNA13, HDC, HLA-G, JAK1, LDLR, PLEC, PTEN, TGM2
migration of neural precursor cells	2.12E-03	3	APP, BTG2, FUT10
migration of neuroglia	9.97E-03	5	APP, CTGF, FN1, MATN2, PTEN
migration of neurons	2.06E-03	13	AD-AM10, BBS1, CDK5, CTNNB1, DIAPH1, FLNA, FN1, GNA13, LAMA1, MATN2, PTEN, RERE, YWHAE
migration of	2.92E-03	4	CDK5, FN1, PRRX1, TP53INP1

pancreatic cancer cell lines				
migration of pericytes	7.70E-04	4	CCL5,CCR5,CTGF,FN1	
migration of phagocytes	1.16E-02	12	APP,CCL5,CCR5,CD58,CTGF,DDR2,FLNA,FN1,JAK1,LDLR,PTEN,TRPV1	
migration of prostate cells	4.45E-03	2	FN1,WHSC1	
migration of Purkinje cells	4.24E-05	4	CDK5,GNA13,PTEN,RERE	

**Table 4-2 Gene expression data from the ‘migration of cancer cell’ functional annotation relating to migration in the smooth muscle cell gene expression dataset.**

Symbol	Illumina	p-value	Log Ratio	Entrez Gene ID for Human
ADAM10	ILMN_2148360	0.00749	0.32705	102
AHCY	ILMN_1657862	0.00741	-0.33416	191
CCL5	ILMN_2098126	0.00023	0.45211	6352
CSF2RA	ILMN_1661196	0.00239	0.44034	1438
CTBP2	ILMN_3250209	0.00809	0.39629	1488
CTGF	ILMN_2115125	0.00012	-0.61260	1490
CTNNB1	ILMN_1746396	0.00256	-0.36541	1499
F3	ILMN_2129572	0.00201	0.37686	2152
FN1	ILMN_1778237	0.00041	-0.45445	2335
IL11	ILMN_1788107	0.00526	0.33755	3589
LAMA5	ILMN_1773567	0.04814	-0.34166	3911
PTEN	ILMN_1880406	0.00718	-0.32989	5728
SNAI2	ILMN_1655740	0.03198	-0.34327	6591

**Table 4-3 Gene expression data from the ‘cell death and survival’ functional annotation relating to survival in the endothelial cell gene expression dataset.**

Categories	Diseases or Functions Annotation	p-Value	Gene Count	Molecules
Cell Death and Survival	apoptosis of follicular B lymphocytes	1.25E-03	2	BCL2A1,CD80
	cell death of B lymphocytes	1.56E-03	5	BCL11A,BCL2A1,CD80,MS4A1,VAV3
	apoptosis of pro-B lymphocytes	4.58E-03	2	BCL11A,VAV3
	apoptosis of B-2 lymphocytes	6.00E-03	1	BCL2A1
	apoptosis of B lymphocytes	7.40E-03	4	BCL11A,BCL2A1,CD80,VAV3
	apoptosis of germinal center B lymphocytes	1.79E-02	1	CD80
	loss of long-lived plasma cell	1.79E-02	1	CD80
	cell death of lymphoblastoid cell lines	2.12E-02	3	RAP1GDS1,TGIF2LX,VAV3
	apoptosis of leukocyte cell lines	2.71E-02	4	BCL2A1,IKZF3,MS4A1,PMAIP1
	apoptosis of prostate cancer cell lines	2.85E-02	4	HOXC6,IGFBP1,ILK,PMAIP1
apoptosis of	4.02E-02	3	BCL2A1,MS4A1,PMAIP1	

B-lymphocyte derived cell lines				
cell viability of germ cell tumor cell lines	4.13E-02	1		PMAIP1
apoptosis of fibro-sarcoma cell lines	4.31E-02	2		BCL2A1,PMAIP1
anoikis of breast cell lines	4.70E-02	1		ILK

**Table 4-4 Gene expression data from the ‘cell death and survival’ functional annotation relating to survival in the endothelial cell gene expression dataset.**

Symbol	Illumina	p-value	Log Ratio	Entrez Gene ID for Human
BCL11A	ILMN_1752899	0.00215	0.36538	53335
BCL2A1	ILMN_1769229	0.00205	0.35285	597
CD80	ILMN_1716736	0.00333	-0.32993	941
MS4A1	ILMN_1776939	0.00339	-0.39392	931
VAV3	ILMN_2290068	0.00137	0.35903	10451

## 4.4 Discussion

In this chapter, *in vitro* techniques have been used to assess the role of miR-143-3p in vascular cell function and in cell-to-cell communication between PASMCs and PAECs. The potential gene targets of miR-143-3p and dysregulated signalling pathways in vascular cells were also investigated. In summary, using cultured PASMCs, over-expression or knockdown of miR-143-3p promoted or reduced migration, and inhibited or induced apoptosis respectively. However, modulation of miR-143-3p had no effect on cellular proliferation. Using an *in vitro* co-culture model, we showed that PASMCs secrete miR-143-3p-enriched exosomes that can be taken up by PAECs, further inducing endothelial cell migration and tube formation but with no effect on proliferation and apoptosis. Concerted efforts were made to identify the potential target genes of miR-143-3p in PASMCs and PAECs, however we were unable to validate any of the putative targets previously identified in the literature. Furthermore, we performed gene expression microarray experiments on PASMCs transfected with pre-miR-143-3p and PAECs treated with miR-143-3p-enriched exosomes derived from PASMCs and identified 68 regulated targets that are involved in cell migration in PASMCs and multiple targets involved in cell death and survival in PAECs. We further performed the same experiments in distal PASMCs from PAH patients (IPAH and HPAH) and healthy donor controls. The similar responses were also observed but even enhanced in distal PASMCs from PAH patients. This may partially contribute to the up-regulation of miR-143-3p observed in PAH patient cells.

Increased muscularisation of the small pulmonary vessels, driven partly by increased proliferation and migration of pulmonary arterial smooth muscle cells (PASMCs), is a key component of the vascular remodelling process that drives the development of PAH. Dysregulation of PASMC normal cells function is associated with the development of PAH pathophysiology, as many *in vivo* and *in vitro* studies have previously shown (Humbert et al., 2004b, Archer et al., 2010, Cordes et al., 2009, Leggett et al., 2012). Many different

growth factors and transcription factors such as PDGF, VEGF, Oct-4, and Notch-3 play a key role in influencing PASMOC dysfunction. In addition, several recent studies have reported that miRNAs associated with vascular remodelling can regulate PASMOC proliferation and migration, albeit not always in parallel (Grant et al., 2013). For example, previous *in vitro* study on miR-145 demonstrated that delivery of miR-145 mimic inhibits PASMOC proliferation, but has no effect on cell migration (Caruso et al., 2012). In addition, other studies have shown that miR-143 and miR-145 are not redundant and hence do not always act in parallel *in vitro* and *in vivo* (Xin et al., 2009, Cordes et al., 2009). Here, we used a wound healing assay to evaluate the role of miR-143 in PASMOC or PAEC migration. This assay is based on the principle that after creating multiple wounds to intact cell monolayers, a high proportion of cells will migrate to fill the scratch (or wound). In this study we first applied multiple scratches to PASMOC monolayer, then harvested the cells at different time-points to analyse the expression of the miR-143/145 cluster during cell migration. We found that both pri-miR-143 and the lead strand of miR-143 (miR-143-3p) were significantly increased during cell migration, with a sustained up-regulation from 3 h to 24 h after scratch. The expression of the miR-143 passenger strand (miR-143-5p) remained unchanged. This sustained upregulation of miR-143 suggested that miR-143-3p may specifically be involved in the biological processes underlying PASMOC migration. Conversely, although pri-miR-145 expression was upregulated at 3 h post-scratch, it was then significantly reduced at the ensuing time points (16-24 h). We did not observe any changes in expression of mature miR-145-5p. These data are consistent with the previous study from our group that showed miR-145-5p did not affect PASMOC migration (Caruso et al., 2012).

During miRNA biogenesis, it has been generally thought that the “passenger” strand of the miRNA duplex is rapidly degraded and only the lead strand (guide strand) remains bound to Ago as mature miRNA to become the functional strand (Wahid et al., 2010). Recently, several studies have demonstrated that passenger strands are loaded into RISC and can also target mRNAs, thereby playing a biological role in pathologies such as cancer and cardiovascular disease (Yang et al., 2013, Shan et al., 2013, Bang et al., 2014). In chapter 3, *in vivo* animal models and PAH patients showed that only miR-143-3p expression was sig-

nificantly elevated in the disease conditions and pharmacological inhibition of miR-143-3p prevented the development of chronic hypoxia induced PH. Here, we also showed that miR-143-3p expression was increased in migrated PSMCs and manipulation of miR-143-3p affected the cell behaviour of PSMCs and PAECs. In addition, previous study also demonstrated that only miR-145-5p knockdown exert a protective role in the development of chronic hypoxia induced PH (Caruso et al., 2012). All of which indicate that the lead strands of miR-143/145 are functional in the setting of PAH. However, genetic ablation of both miR-143 and miR-145 *in vivo* showed the same protective effect in the development of hypoxic-induced PH (Caruso et al., 2012). As the genetic ablation inhibited both strands of miR-143 and miR-145, whether the inhibition of miR-143-5p or miR-145-3p will exert protective role in the development of PAH need to be further investigated. The *in vitro* data showed that miR-145-5p inhibited the PSMCs proliferation but no effect on cell migration (Caruso et al., 2012), and we showed that miR-143-3p induced the cell migration and prevented cell apoptosis in PSMCs. In addition, we also observed the different expression profiles of pri-miR-143/145 and mature form of miR-143/145 in the migrated PSMCs. This suggests that there may be differential post-transcriptional regulation of each individual miRNA within the cluster. This alternative processing has been already reported for other miRNA clusters, for example the up-regulation of all members of the polycistronic miR-17-92 cluster during endothelial differentiation of mouse embryonic stem cells apart from miR-92a, which is repressed (Treguer et al., 2012). Another explanation is that the miR-143-5p is believed to be degraded and inactivated but need further experimental validation. As accumulating evidence has suggested that passenger miRNA strands can be loaded into Ago2 protein and contributed to the regulating mRNA translation (Mah et al., 2010). In summary, we demonstrate that miR-143-3p significantly increases during cell migration in PSMCs. However, miR-145 expression is not significantly changed during the cell migration, which indicates that miR-143-3p is involved in the cell migration process in PSMCs.

In order to further confirm that miR-143-3p is an important regulator of PSMC migration, we use gain-of-function and loss-of-function approaches to evaluate the effect of modulat-

ing miR-143-3p expression on wound healing. Our results indicate that miR-143-3p overexpression induces PASMC migration, whereas miR-143-3p knockdown inhibits this effect. This reduction in cell migration with miR-143-3p knockdown *in vitro* is consistent with *in vivo* data showing that miR-143 knockout (KO) mice (and mice treated with anti-miR-143-3p) exhibit protection from chronic hypoxia induced PH (chapter 3). By contrast, we did not observe any effect of miR-143-3p on the proliferation of PASMCs both *in vivo* and *in vitro*, as measured by PCNA expression and BrdU analysis. miR-143-3p has been previously reported as a tumor suppressor by inhibiting proliferation and migration in several cancer cells (Ma et al., 2013, Xu et al., 2011, Zhang et al., 2012) which suggests that miR-143-3p function strongly depends on the specific cellular context.

In addition to increases in vascular cell proliferation and migration, PAH also characterised by the development of an anti-apoptotic phenotype (Couboulin et al., 2012). In PAH, PASMC apoptosis is suppressed (Couboulin et al., 2012). There are several miRNAs have been demonstrated regulate PASMCs apoptosis; for example, inhibition of miR-204 in PASMC resulted in an increased resistance to apoptosis (Vaidya and Gupta, 2015), overexpression of miR-138 suppressed PASMC apoptosis (Li et al., 2013) and overexpression of miR-328 induced PASMC apoptosis (Guo et al., 2012). In this study, we found that overexpression or knockdown of miR-143-3p in PASMCs resulted in resistance to apoptosis or augmentation of apoptosis respectively. This is the first time that an anti-apoptotic role for miR-143-3p has been demonstrated, as previous studies in cancer cell lines indicate that miR-143-3p promotes apoptosis (Liu et al., 2012, Zhang et al., 2013b). Although PAH shares some similarities of mechanism with cancer (Couboulin et al., 2016), these results indicate that the functions of miRNAs in different diseases and settings may not be consistent. This might be expected considering the target mRNA transcriptome in these different settings will be substantially different.

Mechanistically, we used an unbiased approach to assess the effect of miR-143-3p overexpression on the transcriptional profile of PASMCs by microarray. Informatic analysis of the data highlighted a migratory phenotype. There are a number of genes related to migra-

tion significantly changed, which including *adam10*, *ahcy*, *ccl5*, *csf2ra*, *ctbp2*, *ctgf*, *ctnnb1*, *f3*, *fn1*, *ill1*, *lama5*, *pten*, and *snai2*. In addition, an expression microarray also carried out on PAECs treated with miR-143-3p enriched exosome derived from PSMCs transfection with scramble and pre-miR-143-3p. We observed the regulation of multiple targets, which involved in cell death and survival. The significantly changed genes include *bcl11a*, *bcl2a1*, *cd80*, *ms4a1*, and *vav3*. However, we did not do any validation of these significantly change genes in this study. Further work need to address on the validation of these genes, which might be a target of miR-143-3p and involved in the protective role of miR-143-3p knockdown in the development of PAH.

DNA damage is a normal and frequent phenomenon in the human body, as we are constantly exposed to genotoxic agents at the molecular level (De Bont and van Larebeke, 2004, Kawanishi et al., 2006). To respond to the threat of DNA damage, cells have evolved mechanisms to detect DNA lesions, signal their presence and promote their repair, which is termed the DNA damage response (DDR) (Harper and Elledge, 2007, Rouse and Jackson, 2002, Harrison and Haber, 2006). Previous studies have shown that DNA damage and DNA damage repair pathways are etiologically implicated in PAH patients (Caruso et al., 2012). In the clinical scenario, DNA damage has been suspected to be responsible for the occurrence of PH after etoposide treatment, an anticancer drug promoting DNA damage (Yeh et al., 2004). PAH is characterised by sustained sterile inflammation and elevated circulating cytokines such as TNF- $\alpha$  and IL-6, which are known to promote DNA damage (Wheelhouse et al., 2003, Fehsel et al., 1991). Moreover, the cytokine driven inflammatory process is a major contributor to the development of PAH (Soon et al., 2010, Groth et al., 2014). In addition, the right ventricle of rats (SU5416/hypoxia rat PH model) exhibits extensive DNA damage (Gomez-Arroyo et al., 2013). We therefore aimed to assess the role of miR-143-3p in DNA damage. Firstly, we demonstrated that PSMCs exposed to known inducers of PAH (TNF- $\alpha$ , IL-6 and PDGF) showed increased DNA damage, measured by immunocytochemistry for  $\gamma$ -H2AX. MiR-143-3p expression was significantly increased in PSMCs following induction of DNA damage, indicating that miR-143-3p may be involved in the DNA damage process during PAH pathogenesis. Another study showed that

miR-143/145-dependent *MDM2* turnover contributes to the control of p53 dynamics in response to DNA damage in cancer cells (Zhang et al., 2013a) further indicating that miR-143-3p is responsible for DNA damage.

Several studies revealed the emerging role of exosomes in the development of PH. Lee et al. carried out intravenous delivery of mesenchymal stromal cell (MSC)-derived exosomes inhibited vascular remodelling and exert a pleiotropic protective effect on the lung and chronic hypoxia induced PH in mice. The mechanism of this protective effect is through suppression of hyperproliferative pathways including STAT3-mediated signalling induced by chronic hypoxia (Lee et al., 2012a). Extracellular vesicles isolated from the circulation or lungs of mice with monocrotaline-induced pulmonary hypertension (MCT-PH) induced right ventricular hypertrophy (RVH) and pulmonary vascular remodelling when injected in to healthy mice (Aliotta et al., 2013). In order to determine which extracellular vesicles contributed to the disease induction, the same group found that the exosomes isolated from mice with MCT-PH are responsible for inducing pulmonary hypertensive changes in healthy mice, and that exosomes isolated from MSC can prevent or reverses MCT-PH. The mechanism underlying this phenotype was shown to be loading of miRNAs known to be involved in the pathogenesis of PAH into MCT-PH-derived exosomes, whereas MSC-derived exosomes contained increased levels of miRNAs that blunt angiogenesis, inhibit proliferation of neoplastic cells, and induced senescence of vascular SMCs and endothelial progenitor cells (EPCs) (Aliotta et al., 2016).

The studies described above demonstrate that exosomes can participate in the development of PAH. However, there is no report about exosomal miRNA in the PAH disease. Therefore, it is reasonable to investigate the role exosomal miRNAs in this disease setting. Previous studies demonstrated that exosomes derived from endothelial cells transfer both miR-143-3p and miR-145-5p to smooth muscle cells, affecting the SMC functions and regulate target genes (Hergenreider et al., 2012). In addition, miR-143-3p-enriched exosomes are known to be secreted from mesenchymal stem cells, and were able to suppress the migration of osteosarcoma cells following exposure (Shimbo et al., 2014). These stud-

ies revealed that exosomal miR-143-3p can functionally mediated cell to cell communications between vascular SMC/EC cells and other cell types. In order to investigate whether exosomal miR-143-3p can mediate the cell to cell communications between PSMCs and PAECs, in this study, we first demonstrated that PSMCs could communicate with PAECs by miRNA via the co-culture experiment between PSMCs with Cy-3 labelled pre-miRNA transfected and PAECs, which found Cy3-labelling miRNA in the PAECs. MiR-143-3p is highly expressed in smooth muscle cells and very low expressed in endothelial cell. We applied the co-culture experiment between PSMCs and PAECs without any stimulation. Taqman qRT-PCR analysis showed that the miR-143-3p is significantly increased in PAECs compared with cell without co-culture application. This suggest that endogenous miR-143-3p in PSMCs can be transferred and uptake by PAECs. Function assessment of PAECs co-cultured with PSMC transfected pre-miR-143-3p or treated with conditioned medium taken from PSMCs transfected with pre-miR-143-3p found that miR-143-3p secreted from PSMCs significantly induced PAEC migration. It was recently reported that exosomes are effective carriers of miRNAs, and the identification of exosomal miRNAs has been performed by a number of researchers (Loyer et al., 2014). We purified exosomes from PSMCs and found that isolated exosomes from PSMC culture medium are enriched in miR-143-3p, and to a lesser extent, the miR-143-5p passenger strand. Functional study revealed that exosomal miR-143-3p derived from PSMCs induced PAECs migration and angiogenesis. We further performed a reverse experiment, which PAECs first treated with miR-143-3p enriched exosomes derived from PSMCs and then transfected with anti-miR-143-3p to decrease the miR-143-3p level in PAECs. Migration assay analysis showed that anti-miR-143-3p transfection in PAECs prevented the pro-migratory effect of PAECs mediated by miR-143-3p enriched exosome derived from PSMCs. These data suggested that exosomal miR-143-3p secreted by PSMCs specifically regulate the migration behaviour of PAECs. Thus, we provide the first evidence that miR-143-3p acts as a paracrine signalling mediator and is involved in the induction of PAEC migration and angiogenesis but not proliferation and apoptosis. This cell-cell communication by exosomal miR-143-3p in the pulmonary vascular system is relevant to the functional changes in cell behaviour that help drive the pathogenesis of PAH, which indicate that exosomes contain-

ing miR-143-3p and secreted by PAH-PASMCs might enhance the development of lesions associated with pulmonary hypertension and could be of clinical importance. Furthermore, we observed a reduction in microvessel density in the miR-143<sup>-/-</sup> hypoxic lungs compared to WT, suggesting that miR-143-3p transport in exosomes might contribute to the enhancing microvessel density and lung perfusion. Further experiments will be needed to address this effect *in vivo*.

Moreover, miR-143-3p may act via multiple mechanisms in PASMCs and indeed PAECs following exosome-mediated transport and uptake, including cell migration and apoptosis (PASMC), cell death/survival and angiogenesis (PAEC). A recent study highlighted another important cell to cell communication route tunnelling nanotubes (TNTs), which mediated the cell to cell communications between SMCs and ECs via miR-143/145 cluster. The mechanisms underlying these functional miR-143/145 mediated angiogenesis and proliferation in PAECs are through targeting hexokinase II (*hk II*) and integrin beta 8 (*itgb8*) (Climent et al., 2015). Another study showed the endothelial cells can secrete and transfer functional exosomal miR-143/145 to SMCs to mediate an atheroprotective SMC phenotype via leading to an enhanced repression of miR-143/145 target genes and de-differentiation-associated gene expression (Hergenreider et al., 2012). Clearly, cell-to-cell communication of miR-143-3p is of fundamental importance in related pathological settings including PAH diseases. The mechanisms involve this exosomal miR-143-3p mediated PASMCs and PAECs communications still unknown. This will require detailed further analysis but suggest a complex environment where miR-143-3p up-regulation in hypoxia or inhibition (therapeutically) can modulate phenotypes in both PASMC and PAEC compartments. As we observed both cardiac and lung phenotypes with miR-143 loss, the generation of conditional knockouts will help define cell-specific contributions to the underpinning role of miR-143 in this setting.

In conclusion, we have demonstrated that miR-143-3p induced migration and inhibited apoptosis in PASMCs. This is also the first time that miRNAs have been shown to be involved in cell-to-cell communication between PASMCs and PAECs in PAH. Mechanisti-

cally, miR-143-3p -enriched exosomes derived from PASMCs induced PAEC migration and angiogenesis, which indicates that exosomal miR-143-3p may act as a crucial paracrine signalling mediator during the remodelling of the pulmonary vasculature. The proposed mechanism of miR-143/145 cluster in PAH (Figure 4.28).

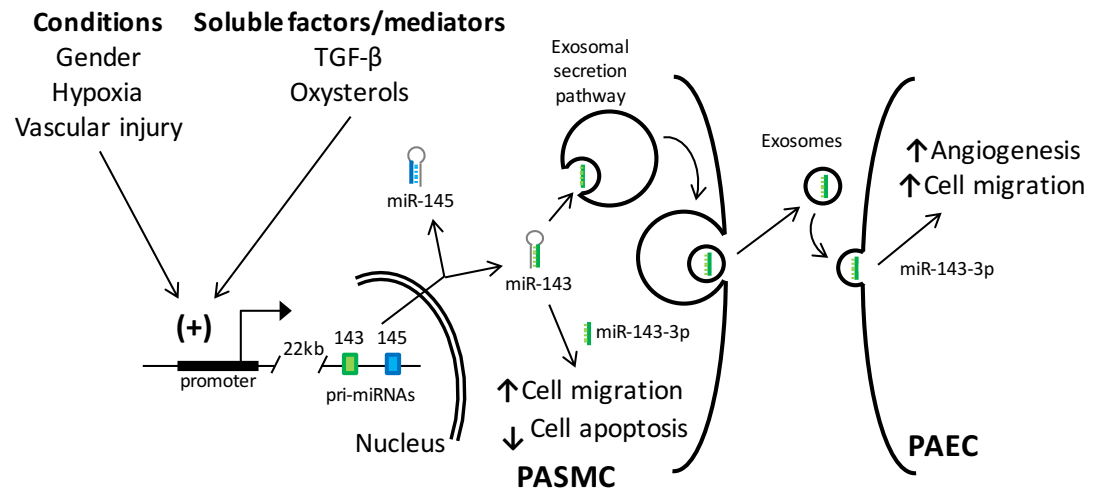


**Figure 4.28 Proposed mechanism of miR-143/145 cluster in PAH**

Several signalling pathways related to the pathogenesis of PAH regulate miR-143/145 expression by activating the promoter region of the miR-143/145 cluster in PASMCs. MiR-143-3p can affect cellular migration and apoptosis and acts as a paracrine signalling mediator during vascular remodelling. During the development of PAH, PASMCs secrete exosomes enriched with miR-143-3p, which are transported to PAEC, inducing migration and angiogenesis. Adapted from (Deng et al., 2015).

## **5 The role of long non-coding RNA in PAH**

## 5.1 Introduction

Mutations in the *bmpr2* gene have been found in more 70% of HPAH. In addition, up to 25% of patients with apparently sporadic IPAH have been demonstrated to harbour similar mutations. *BMPR2* is a member of the transforming growth factor-beta (TGF- $\beta$ ) receptor superfamily (Atkinson et al., 2002, Aldred et al., 2006, Cogan et al., 2006, Thomson et al., 2000). Consistent with the mutations of *bmpr2*, PAH patients without mutation of *bmpr2* and the experimental models of PAH showed decreased expression levels of *BMPR2* (Atkinson et al., 2002). *BMPR2* is highly expressed in the endothelium of the pulmonary arteries and expressed at lower levels in PASMCs and fibroblasts (Morrell, 2006). Further, *BMPR2* signalling showed a critical role in preventing vascular remodelling through promoting survival of pulmonary arterial endothelial cells (Atkinson et al., 2002). *BMPR2* signalling can inhibit proliferation, induce apoptosis (Hansmann et al., 2008, Zhang et al., 2003, Morrell et al., 2001), promote motility (Spiekerkoetter et al., 2009), repress growth (Perez et al., 2011), and differentiation in PASMCs (Yu et al., 2008). In addition, *BMPR2* signalling exerts anti-inflammatory effects, with loss of *BMPR2* activity that results in unopposed IL-6 production (Hagen et al., 2007). These observations suggest that the aberrant expression of *BMPR2* is critical mediator to the pathogenesis of PAH.

The penetrance of the *bmpr2* mutation is low with an estimated lifetime risk of 20% and this develops into PAH disease (Loyd et al., 1995, Rich et al., 1987, Sztrymf et al., 2007, West et al., 2008a). Thus, indicating that the mutation of the *bmpr2* receptor alone is insufficient to cause the disease onset and also suggesting that there could be other secondary genetic and /or environmental factors that may be required for the clinical manifestation of PAH (Liu and Morrell, 2013). In the context of multifactorial events, several factors can trigger inappropriate cellular responses in the background of genetic susceptibility. Triggers for disease may include inflammation, hypoxia, shear stress and vascular injury (Humbert et al., 2004b).

Previous studies demonstrated that BMP/TGF- $\beta$  signalling pathways play an important

role in the pathobiology of PAH. Bone morphogenetic proteins (BMPs) activate the canonical Smad 1/5/9 pathway via BMPR2. TGF- $\beta$  activates the Smad2/3 pathway via the ALK5 in a complex with the TGF- $\beta$  type II receptor (TGF- $\beta$ R-II) (Upton and Morrell, 2013). In the monocrotaline (MCT-PAH) rat model, the BMP signalling was reduced and the transforming growth factor- $\beta$ 1 signalling was enhanced (Steinle et al., 2002, Morty et al., 2007). BMP4 inhibited proliferation of PASMCs isolated from proximal pulmonary arteries via a SMAD-dependent pathway. However, BMP4 stimulated proliferation of PASMCs from peripheral arteries, conferred protection from apoptosis, which was dependent on p38 and ERK signalling pathways (Yang et al., 2005). *In vivo* data demonstrated that Smad3 signalling was significantly increased in the lungs of MCT-PAH and on the contrary it was decreased in chronic hypoxia induced pulmonary hypertension (Steinle et al., 2002). In addition, several studies have shown that the TGF- $\beta$  signalling pathway inhibitor (such as IN-1233, SB525334, and SD208) attenuated the disease progression in MCT-PAH (Steinle et al., 2002, Zaiman et al., 2008, Thomas et al., 2009). *In vitro*, TGF- $\beta$  inhibits the serum-induced proliferation of proximal PASMCs from healthy individuals, whereas PASMCs from idiopathic PAH patients showed enhanced proliferation to TGF- $\beta$  stimulation (Morrell et al., 2001). The loss of repressive effects of TGF- $\beta$  on PASMCs proliferation was directly associated with reduced *bmpr2* (Davies et al., 2012). In addition, TGF- $\beta$  inhibited BMP4-mediated target genes transcription in both control and HPAH PASMCs with *bmpr2* mutations (Upton et al., 2013).

Growth factors, including platelet-derived growth factor (PDGF), vascular endothelial growth factor (VEGF), serotonin, and fibroblast growth factor 2 (FGF2) are important inhibitors of apoptosis in vascular cells and are also involved in the remodelling of vasculature during PAH (Perros et al., 2008, Hassoun et al., 2009). PDGF and PDGF receptor mRNA (PDGFR) expression levels were increased in the small pulmonary arteries from patients with PAH. In addition, the protein levels of both PDGF/PDGFR were shown to be expressed in PASMCs and endothelial cell in pulmonary arteries of PAH patients. *In vitro*, PDGF induces the proliferation and migration of PASMCs, which can be specifically inhibited by imatinib (Perros et al., 2008). Several studies have demonstrated the therapeutic

role of PDGF inhibition by imatinib in PAH disease (Schermyly et al., 2005, Souza et al., 2006, Patterson et al., 2006, Ghofrani et al., 2005). VEGF is an endothelial cell-specific mitogen and survival factor in the lung and affects functional properties including NO and prostacyclin synthesis (Voelkel et al., 2006). The platelet VEGF levels were elevated in patients with PAH (Eddahibi et al., 2000) as well as systemic sclerosis patients with sPAP  $\geq 35$  mmHg (Papaioannou et al., 2009). As blockade of VEGF function will induce endothelial cell dysfunction and death promote apoptosis-resistant endothelial cell proliferation. Overexpression of VEGF exerted a protective role against the hypoxic pulmonary hypertension (Partovian et al., 2000) and ameliorated the pulmonary hypertension indexes in the rat model of idiopathic pulmonary fibrosis (IPF) (Farkas et al., 2009). On the contrary, blockade of VEGF results in severe pulmonary hypertension by inducing endothelial cell dysfunction (Sakao et al., 2009). VEGF receptor (VEGFR) inhibitor SU5416 impaired pulmonary vascular growth and postnatal alveolarisation and caused severe pulmonary hypertension in new-born rats (Phan, 2002). The protein levels of FGF2 in pulmonary artery endothelial cells (PAECs) were markedly increased in patients with IPAH compared with healthy controls and *in situ* hybridization further confirmed the FGF2 predominantly expressed in the remodelled vascular endothelium of lungs from patients with IPAH. In addition, FGF2-siRNA and FGFR1 inhibitor SU5402 treatment reversed the rat MCT-PAH model (Izikki et al., 2009). The conditioned medium of PAECs from IPAH significantly increased PSMCs proliferation compared with control PAEC conditioned medium.

Several studies demonstrated that inflammatory cytokines and chemokines are key factors contributing to the pathogenesis of pulmonary hypertension (Stenmark et al., 2011, Stenmark et al., 2006a, Durmowicz et al., 1994). Both pulmonary vascular cells and inflammatory cells are important local sources of cytokines and chemokines that can affect pulmonary vascular remodelling in PAH (Touyz and Schiffrin, 2004, Prockop, 1997). Inflammatory cytokines including TNF- $\alpha$ , interferon- $\gamma$ , IL-1, 2, 4, 6, 8, and 10 were significantly elevated in the serum levels of patients with idiopathic and heritable PAH compared with control subjects. In addition, the elevated levels of IL-6 correlated with decreased survival in PAH patients (Stenmark et al., 2002, Gao et al., 2003, Touyz and Briones, 2011). Fur-

thermore, several chemokine ligands including CXCL2 (Stenmark et al., 2002), CXCL5 (Li et al., 2008), CXCL10 (Shi-Wen et al., 2004), CXCL13 (Gallucci et al., 2006), CXCL12, and CXCL16 (Meier et al., 1989) expression levels have also showed significantly increased in plasma of PAH patients compared with healthy controls.

Apart from inflammatory cytokines and chemokines, ncRNAs also have shown important roles in PAH. The role of miRNAs in PAH has been widely demonstrated in recent years (Boucherat et al., 2015, Bienertova-Vasku et al., 2015, Zhou et al., 2015, Meloche et al., 2014a). Dysregulation of lncRNAs is associated with several human diseases, including cancers (Bartoniccek et al., 2016, Lavorogna et al., 2016, Schmitt and Chang, 2016), cardiovascular diseases (Archer et al., 2015, Lorenzen and Thum, 2016), and respiratory diseases (Liu et al., 2015, Booton and Lindsay, 2014). In addition, accumulating early evidence suggests that lncRNAs may play an important role in vascular cell pathophysiology. Early studies identified ANRIL, a lncRNA to be expressed in VSMC, and shown to regulate CDKN2A/B expression in aortic VSMC and attenuate proliferation in atherosclerosis (Congrains et al., 2012b, Motterle et al., 2012, Congrains et al., 2012a) as well as modulate inflammatory responses in coronary artery disease (Zhou et al., 2016). Lnc-Ang362, harbouring the miR-221 and miR-222 genes, first identified to be regulated by angiotensin II in VSMC, and was in turn able to modulate VSMC proliferation, vascular remodelling and neointimal hyperplasia in concert with miR-221 and miR-222 (Moledina et al., 2011, Chistiakov et al., 2015, Liu et al., 2009). These studies showed that lncRNA were involved in the control of cell proliferation, and could be regulated alongside proximal miRNAs in VSMCs. RNA-seq analysis of human coronary artery SMC revealed a novel lncRNA, LncRNA SENCR is expressed in both VSMCs and ECs. In VSMC, knockdown of SENCR decreased the expression of myocardin and numerous smooth muscle contractile genes and increased a number of pro-migratory genes (namely MDK and PTN). Inhibition of these two genes reversed the increased VSMC migration mediated by SENCR silencing, which suggested that the expression of these genes was partially regulated by SENCR in these cells. However, the functions of SENCR in ECs were not reported in this study (Bell et al., 2014). Our group further revealed that SENCR induced the proliferation, migration and

angiogenesis of HUVECs. In patient samples, SENCN expression was altered in vascular tissues and cells derived from patients with critical limb ischemia and premature coronary artery disease compared with healthy controls (Boulberdaa et al., 2016). These two studies revealed that SENCN could modulate the behaviour of both smooth muscle and ECs, and exhibited altered expression patterns in vascular tissues and cells from human vascular disease patients. However, the exact molecular targets and mechanisms of SENCN in pathological vascular remodelling remain to be determined.

Similar to SENCN, LincRNA-p21 is expressed in both VSMC and vascular ECs. In human VSMC, lincRNA-p21 repressed cell proliferation and induce apoptosis *in vitro*. LincRNA-p21 also inhibited neointima formation in carotid arteries and repressed proliferation and induced apoptosis in carotid artery injury model *in vivo*. The authors further confirmed that lincRNA-p21 was decreased in patients with coronary heart disease (Wu et al., 2014). In mouse vascular ECs, lincRNA-p21 induced cell apoptosis and cell cycle progression. In addition, lincRNA-p21 inhibited cell proliferation through binding miR-130b (He et al., 2015). Unlike many lncRNAs, LincRNA-p21 is a conserved lncRNA, which provided the possibility of using an *in vivo* animal model to study the role of this lncRNA (Tang et al., 2015). These data identified lincRNA-p21 is a key regulator of cell proliferation and apoptosis in vascular cells, which are primary contributors to vascular remodelling. Consistent with the human *in vitro* data, knockdown of lincRNA-p21 resulted in dramatic neointimal hyperplasia in a mouse model of carotid artery injury, which indicated that lincRNA-p21 could serve as therapeutic target to treat vascular remodelling diseases (Wu et al., 2014).

Using RNA-seq, we recently defined a novel smooth muscle specific lncRNA *SMILR*, which could be induced by IL-1 $\alpha$  and PDGF in human saphenous vein smooth muscle cells (HSVSMCs). Knockdown of *SMILR* markedly reduced HSVSMC proliferation, likely through regulation of the HAS2 gene, located proximal to the genetic locus for *SMILR*. In human samples, *SMILR* expression increased in unstable atherosclerotic plaques and plas-

ma from patients with high plasma C-reactive protein (Ballantyne et al., 2016b). These data suggested that inhibiting *SMILR* expression could be a potential target for treating vascular diseases characterised by VSMC proliferation.

In the context to ECs, studies have shown that the lncRNA MALAT1 could regulate retinal vessel remodelling by affecting retinal EC proliferation, migration and tube formation, as genetic ablation of MALAT1 inhibited the proliferation of ECs and reduced neonatal retina vascularization *in vivo* (Liu et al., 2014, Michalik et al., 2014). In human aortic ECs, knockdown of the lncRNA H19 reduced cell proliferation and activated p21/CDKN1A, increasing apoptosis, decreasing angiogenesis, and diminishing the number of cells in G0/G1 and S phases in cell cycle (Voellenkle et al., 2016). These two lncRNAs are highly expressed in ECs and were shown to be multifunctional both *in vivo* and *in vitro*. In this context, although numerous lncRNAs have been investigated in vascular cells, the role for lncRNAs in pulmonary vascular cells and PAH disease still unknown.

In this study, we collaborated with Joseph Miano (University of Rochester) and Xiaochun Long (Albany Medical Center) to study novel vascular smooth muscle cell (VSMC)-specific lncRNAs in PAH. They used RNA-seq in Myocardin (MYOCD) over-expressing human coronary artery SMCs (HCSMCs) to identify new lncRNAs. Here, we investigate two new lncRNAs they found based on the RNA-seq data, MYOcardin-induced Smooth Muscle Long noncoding RNA, Inducer of Differentiation (*MYOSLID*) and MYOcardin-lncRNA16 (*Myolnc16*).

## 5.2 Aims

- To functionally characterise two novel lncRNAs *MYOSLID* and *Myolnc16* in the pulmonary vasculature
- To understand the cellular functions of *MYOSLID* and *Myolnc16*
- To find the potential signalling pathways of *MYOSLID* and *Myolnc16*

## 5.3 Results

### 5.3.1 LncRNA *MYOSLID*

#### 5.3.1.1 Identification and Genomic Location of *MYOSLID*

This work was done by Joseph Miano (University of Rochester) and Xiaochun Long. Human coronary artery SMCs (HCASMs) transduced with adenovirus carrying Myocardin (MYOCD), a potent SRF cofactor for the vascular SMC differentiation program. RNA-seq performed in these conditions to identify lncRNAs associated with vascular SMC differentiation. A total of 265 lncRNAs were found to be expressed in HCASMs, among which, 54 were annotated lncRNAs in the UCSC Genome Browser and the remaining were novel lncRNAs. In addition, 137 lncRNAs were significantly regulated by MYOCD with 79 up-regulated and 46 downregulated. QRT-PCR validated 13 selected lncRNAs and finally chooses *MYOSLID* and *Myolnc16* for further study.

*MYOSLID* is located in a lncRNA-rich genomic region of chromosome 2 where the closest protein coding genes are 70 kb (KLF7) and 200 kb (CREB1) away from its 5' end and 3' end, respectively (Figure 5.1).

### Genomic location of *MYOSLID*

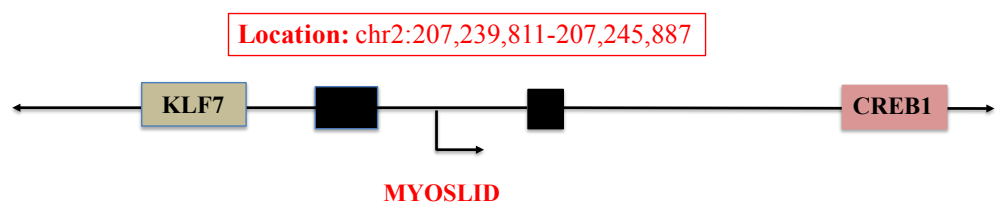
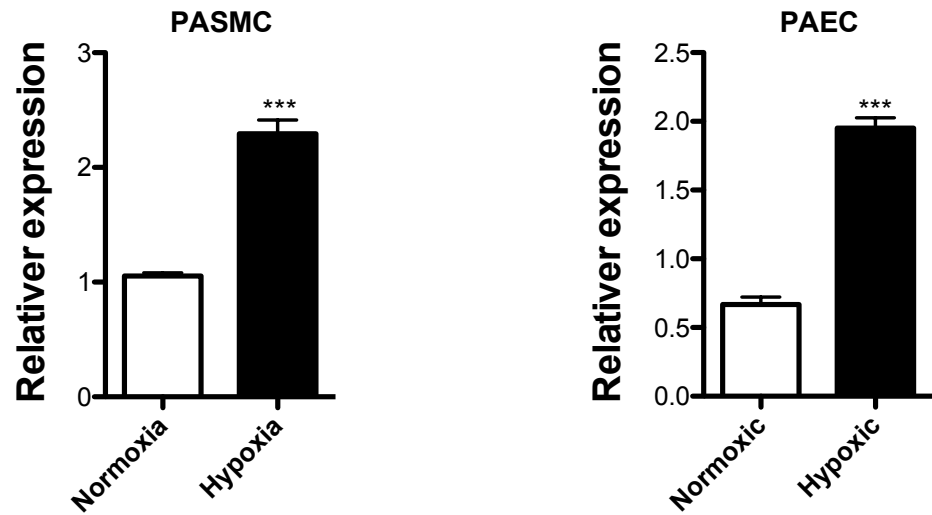


Figure 5.1 Genomic location of *MYOSLID*

### 5.3.1.2 *MYOSLID* is Upregulated by Multiple Triggers of PH in PASMCMC and PAH Patients

To validate *MYOSLID* expression in the pulmonary system, we aimed to determine whether *MYOSLID* was regulated by any known triggers of PH and hence analysed its expression in hypoxic conditions. Previous studies demonstrated that chronic hypoxia alone can induce pulmonary hypertension by promoting significant structural remodelling of pulmonary arteries in humans (Arias-Stella and Saldana, 1963). We found that *MYOSLID* is significantly unregulated upon exposure to hypoxia (1% O<sub>2</sub>) in PASMCMCs ( $P < 0.05$ ) and PAECs ( $P < 0.01$ ) (Figure 5.2). As bone morphogenetic protein (BMP) and transforming growth factor- $\beta$  (TGF- $\beta$ ) signalling pathways are dysregulated in pulmonary arterial hypertension (Morty et al., 2007, Ogo et al., 2013), we assessed *MYOSLID* expression in response to BMP4 and TGF- $\beta$ . PASMCMCs were treated with TGF- $\beta$  (10 ng/ml) and BMP4 (10 ng/ml) and their corresponding inhibitors for 24 h and found that *MYOSLID* expression is significantly induced both BMP4 ( $P < 0.01$ ) and TGF- $\beta$  ( $P < 0.05$ ) (Figure 5.3 A and B). Conversely, treatment of TGF- $\beta$  stimulated PASMCMC with the TGF- $\beta$  type I receptor inhibitor, SB525334 (1 nM) reversed the effect of TGF- $\beta$  stimulation (Figure 5.3 A) ( $P < 0.01$ ), while treatment of BMP4-stimulated cells with an inhibitor of BMP signalling (K02288) abolished the BMP4-mediated increase in *MYOSLID* expression ( $P < 0.01$ ) (Fig 5.2 B). Interestingly, we found that the TGF- $\beta$  type I receptor inhibitor (SB525334) treatment also significantly inhibited the *MYOSLID* expression. This finding suggests that *MYOSLID* maybe the direct target of TGF- $\beta$  signalling pathway. Apart from BMP and TGF- $\beta$  treatment, we further investigated the effect of PDGF, VEGF, and FGF2 treatment in pulmonary vascular cells. In our results, we found that *MYOSLID* was significantly upregulated in PASMCMCs with PDGF treatment ( $P < 0.01$ ) and in PAECs with FGF2 and VEGF stimulation (Figure 5.4) ( $P < 0.01$ ). In addition, we found that *MYOSLID* expression was increased in distal PASMCMCs from PAH patients (IPAH and FPAH) compared to healthy controls (Figure 5.5 A). There were no significant changes of the *MYOSLID* expression level in *bmpr2*-mutant endothelial progenitor cells (EPCs) from patient with PAH compared with controls (Figure 5.5 B) ( $P = 0.28$ ). Taken together, these data demonstrated that

*MYOSLID* might be involved in several pathways related to the pathogenesis of PAH.



**Figure 5.2 Analysis of *MYOSLID* in the cells with hypoxia exposure**

PASMCs and PAECs seeded in 6-well plates were exposed to hypoxia with 1%O<sub>2</sub> for 24 h. TaqMan qRT-PCR assessed the *MYOSLID* expression in these cell types. The results showed that *MYOSLID* expression significantly upregulated in the hypoxia condition in both PASMCs and PAECs. Data are expression as mean  $\pm$  SEM and analysed by Student t-test. All experiments were repeated at least 3 independent times. n = 3 per group in triplicate. \*\*\*  $P < 0.001$ .

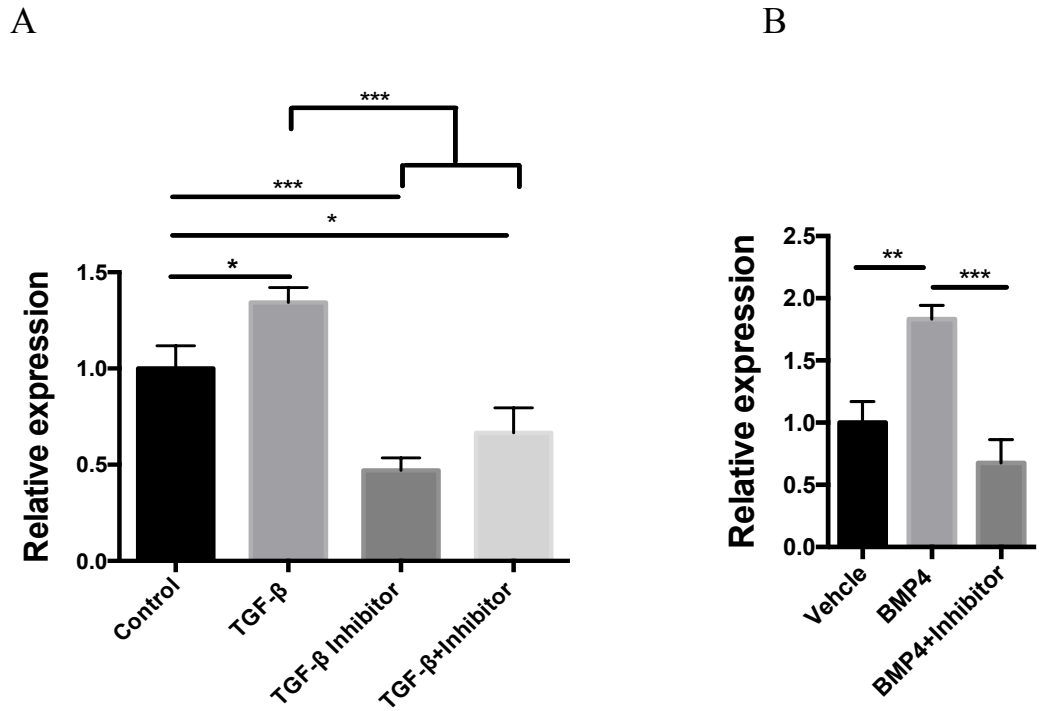


**Figure 5.3 Analysis of *MYOSLID* expression in PASMCs with TGF- $\beta$  and BMP4 stimulation**

PASMCs were seeded in 6-well plates and stimulated with TGF- $\beta$  and BMP4. The inhibitors of TGF- $\beta$  and BMP4 signalling were added to the cells 1 h before the stimulation. TaqMan qRT-PCR assessed the *MYOSLID* expression in these treated cells and controls. (A) TGF- $\beta$  and (B) BMP4 stimulation significantly induced *MYOSLID* expression and the expression was reversed by TGF- $\beta$  type I receptor inhibitor (SB525334 (1 nM)) and type I bone morphogenic protein (BMP) receptors (K02288 (10 nM)). Data represented as fold change  $\pm$  SEM and analysed by a one-way ANOVA followed by Tukey's post hoc test. All experiments were repeated at least 3 independent times. n = 3 per group in triplicate. \* $P < 0.05$ , \*\* $P < 0.01$ , \*\*\* $P < 0.001$ .

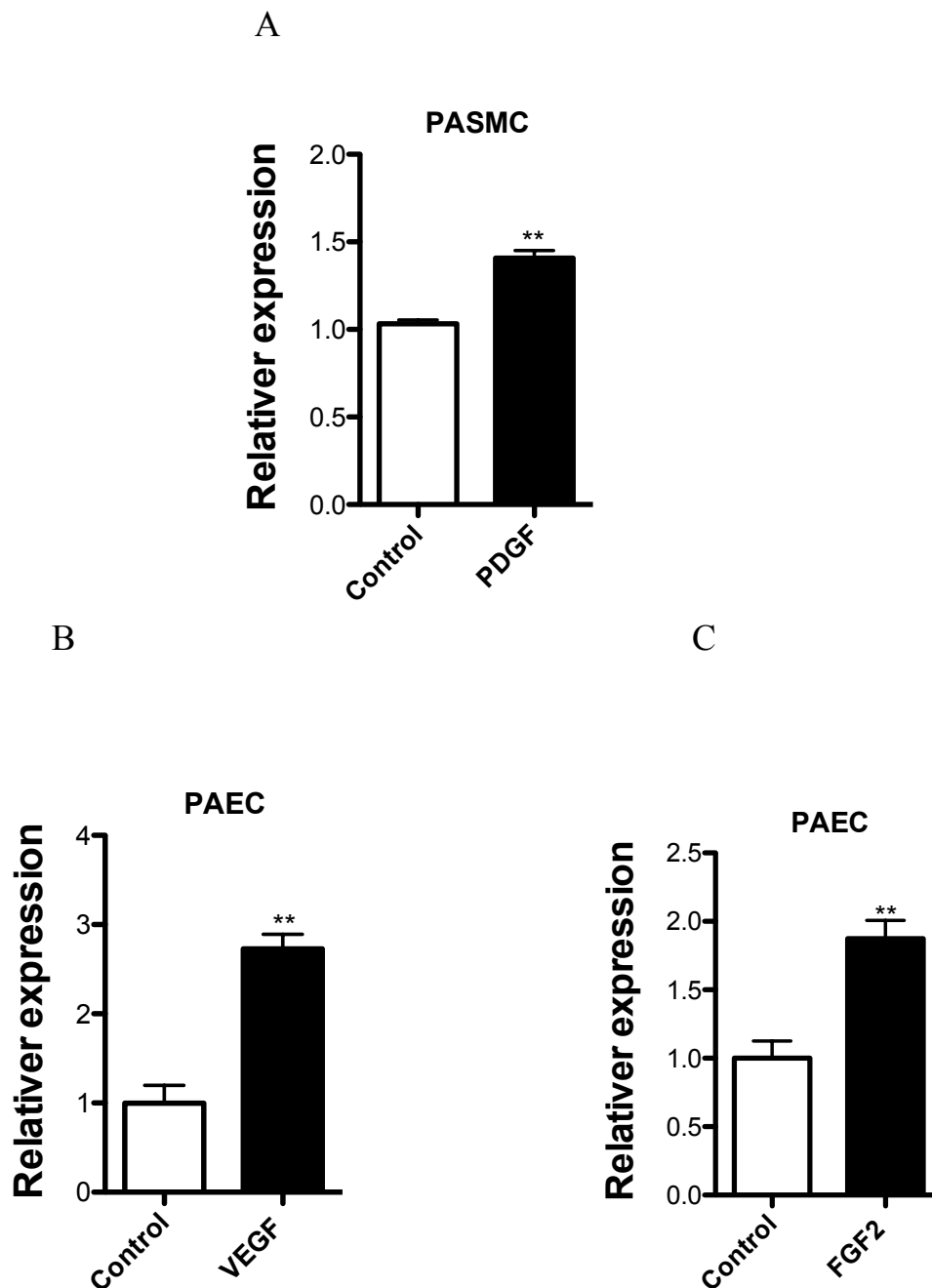
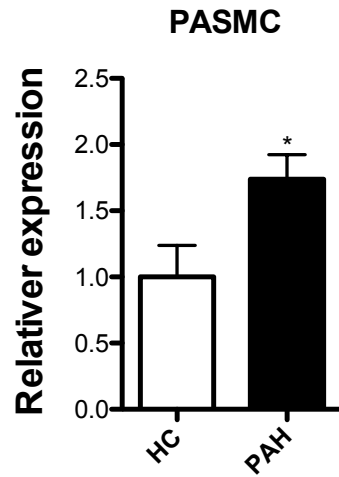


**Figure 5.4 Analysis of *MYOSLID* in PSMCs and PAECs with various stimulations**

PASMCs and PAECs were seeded into 6-well plates and then stimulated with PDGF (20 ng/ml), VEGF (50 ng/ml) and FGF2 (25 ng/ml) for 24 h. Taqman qRT-PCR assessed the *MYOSLID* expression in these stimulated cell types. (A) PDGF stimulation significantly induced the expression of *MYOSLID* in PSMCs. (B) and (C) *MYOSLID* expression significantly increased in PAECs with VEGF and FGF2 stimulations. Data are represented as mean  $\pm$  SEM and analysed by Student t-test. All experiments were repeated at least 3 independent times. n = 3 per group in triplicate. \*\*  $P < 0.01$ .

A



B

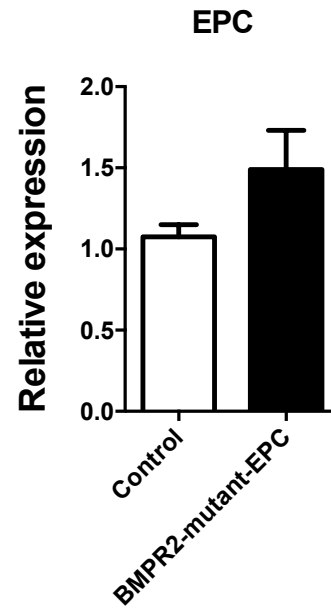


**Figure 5.5 Analysis of *MYOSLID* in PAH patients**

Distal PASMCS and EPC cells were obtained from patients with PAH and healthy controls. (A) Taqman qRT-PCR analysed the *MYOSLID* expression in the distal PASMCS from patients with PAH (IPAH and FPAH), which showed significantly upregulated compared with healthy controls (n = 4 healthy control and n = 6 PAH patients). (B) Taqman qRT-PCR analysed the *MYOSLID* expression in EPC cells from *bmpr2* mutant patients and controls, which showed no significant changes (P = 0.28) (n = 2 control patients and n = 3 *bmpr2* mutant patients). Data is represented as mean  $\pm$  SEM and analysed by Student t-test. \*P < 0.05.

### 5.3.1.3 Downregulation *MYOSLID* Induces Apoptosis and Inhibits Cellular Migration in PSMCs

Previous data showed that *MYOSLID* expressions were altered with various stimulations (Hypoxia, PDGF, BMP4 and TGF- $\beta$ ) and in distal PSMC obtained from PAH patients. We further sought to assess the impact of knockdown of *MYOSLID* on PSMCs functions including migration, proliferation and apoptosis to assess functional consequences. We first sought to evaluate the expression profile of *MYOSLID* during cell migration processes (by making a multiple scratches) in PSMCs. The *MYOSLID* expression was induced at 8 h and was significantly upregulated at 24 h (Figure 5.6). Since we observed that *MYOSLID* expression was increased in the PSMC migrating cells, we performed wound-healing assay by knocking down *MYOSLID* (using siRNAs) and found that *MYOSLID* significantly reduced the cell migration in PSMCs ( $P < 0.01$ ) (Figure 5.7 A). *MYOSLID* knockdown was confirmed by Taqman qRT-PCR, and the expression was significantly reduced compared with control groups (Figure 5.7 B) ( $P < 0.001$ ). In addition, Caspase3/7 assay showed that knockdown of *MYOSLID* significantly induced PSMC apoptosis with hydrogen peroxide ( $H_2O_2$ ) treatment (Figure 5.8 A) ( $P < 0.01$ ). However, assessment of PSMC proliferation using the EdU incorporation assay showed no significant change with *MYOSLID* knockdown (Figure 5.8 B). Taken together, knocking down *MYOSLID* affected the cell migration and apoptosis but not proliferation in PSMCs.

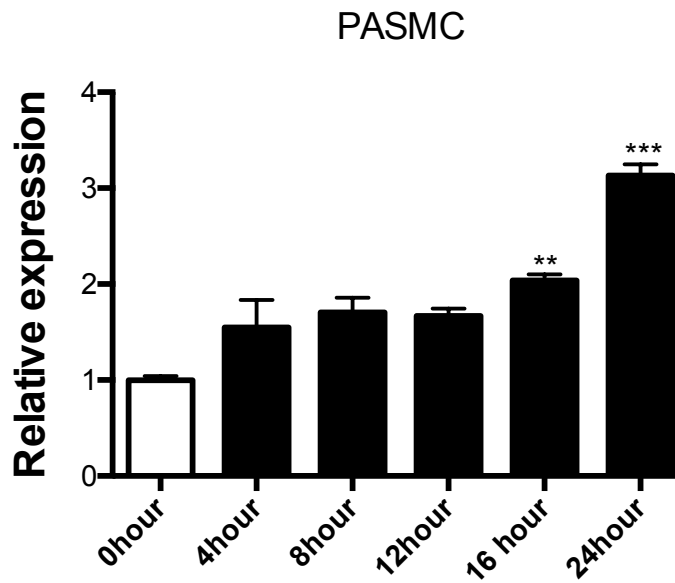


**Figure 5.6 Analysis of *MYOSLID* in PASMCs during the cell migrations**

Multiple scratches were applied in PASMC monolayer and cells harvested at different time points after scratches. Taqman qRT-PCR analysed the *MYOSLID* expressions at different time points showed that *MYOSLID* was significantly induced during migration at 8 h and sustained the upregulation till 24 h. Data represented as fold change  $\pm$  SEM and analysed by a one-way ANOVA followed by Tukey's post hoc test. n = 3 per group in triplicate.  $**P < 0.01$ , and  $***P < 0.01$ .

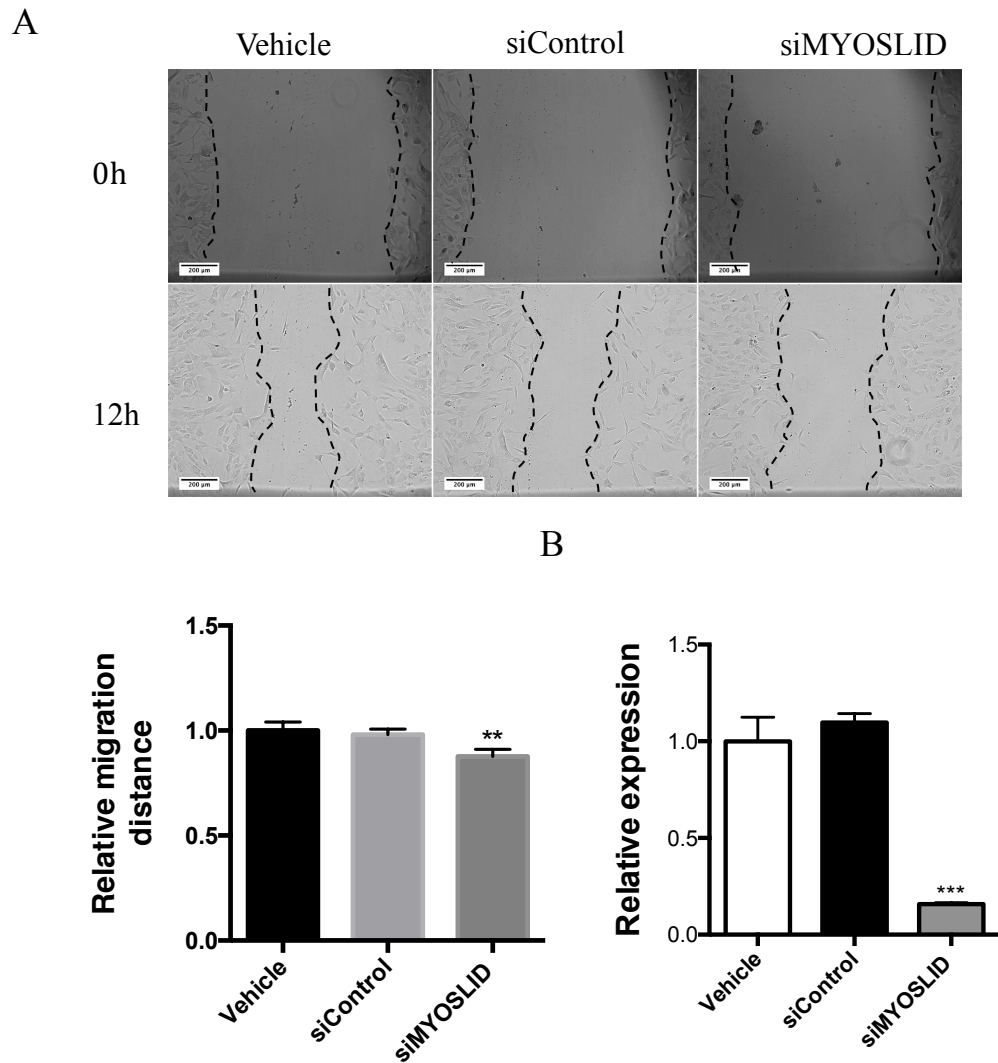
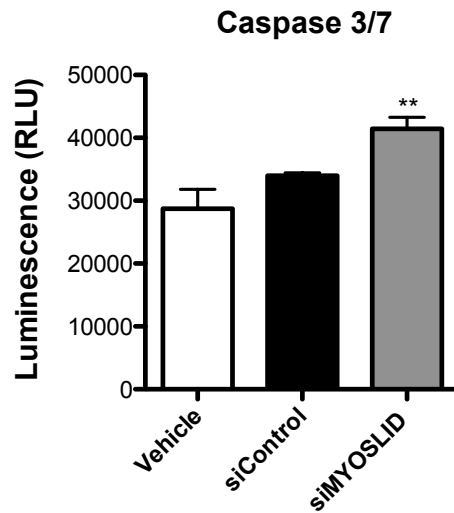


**Figure 5.7 Analysis of the migration of PSMCs with *MYOSLID* knock down**

PASMCs were transfected with si*MYOSLID* and a single scratch was applied on monolayer PASMCs, and the pictures were captured and analysed the migrated distances at time point 0 h and 12 h. (A) Representative micrographs and quantification of a wound healing assay after *MYOSLID* knockdown in comparison with vehicle and siRNA control. *MYOSLID* knockdown significantly inhibited cell migration. (B) Taqman qRT-PCR confirmed the knocking down of *MYOSLID* in PASMCs by si*MYOSLID* transfection. Data represented as fold change  $\pm$  SEM and analysed by a one-way ANOVA followed by Tukey's post hoc test. All experiments were repeated at least 3 independent times.  $n = 3$  per group in triplicate. \*\* $P < 0.01$ , and \*\*\* $P < 0.001$ .

A



B

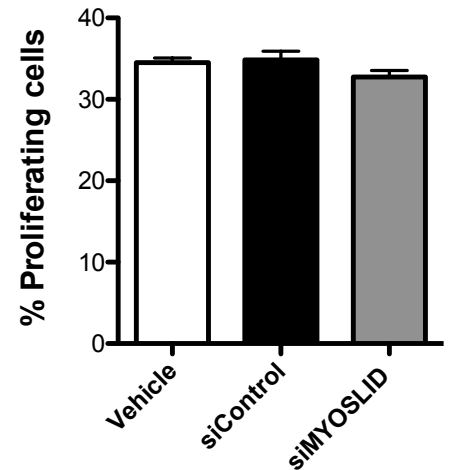


**Figure 5.8 Analysis of proliferation and apoptosis of PSMCs with *MYOSLID* knock down**

PASMCs were transfected with si*MYOSLID*. (A) Caspase 3/7 activity assay was assessed in PSMCs induced by H<sub>2</sub>O<sub>2</sub>. Knocking down *MYOSLID* significantly induced cell apoptosis compared with controls. (B) Edu incorporation assay was performed in transfected cells and controls. There was no change in cell proliferation with *MYOSLID* knocking down. Data represented as fold change  $\pm$  SEM and analysed by one-way ANOVA followed by Tukey's post hoc test. Experiments were done by once. n = 8 wells per group. \*\**P* < 0.01.

#### **5.3.1.4 *MYOSLID* Knockdown Decreased the Proliferation of PAEC**

We have demonstrated that *MYOSLID* knockdown affected the cell function of PSMCs. Here we further assessed the functions of PAECs with *MYOSLID* knockdown. Wound healing assay showed that knocking down *MYOSLID* had no effect on cell migration (Figure 5.9). The cell proliferation of PAECs was induced by VEGF stimulation and analysed by BrdU incorporation and PCNA protein level. These results showed that *MYOSLID* knockdown significantly decreased the cell proliferation in PAECs ( $P < 0.05$ , and  $P < 0.001$ ) (Figure 5.10). Taken together, this data revealed that *MYOSLID* affected the proliferation and had no affect on the migration of PAECs.

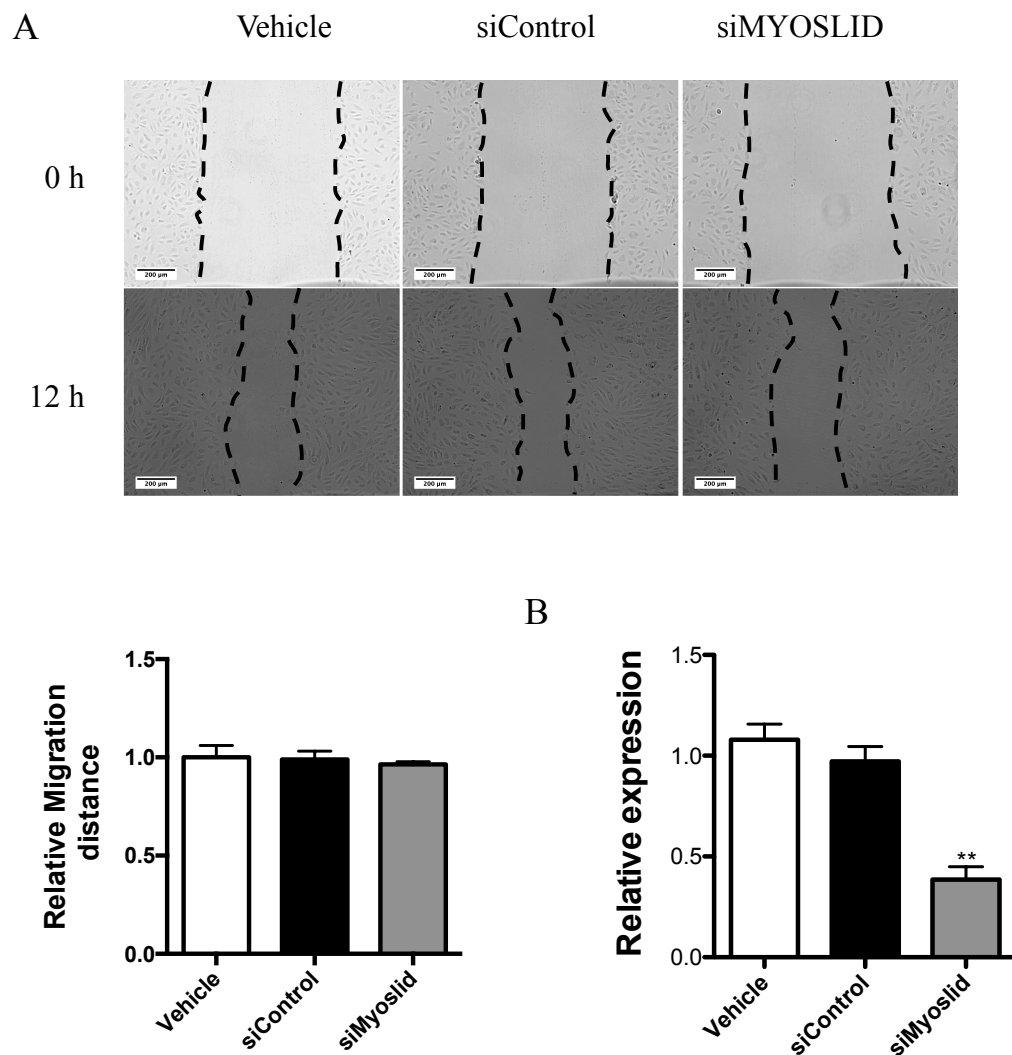
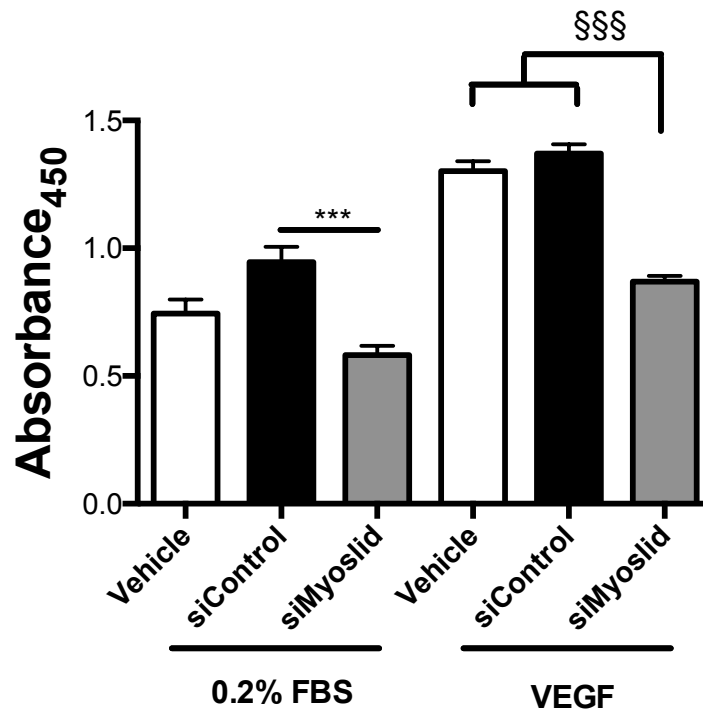


**Figure 5.9 Analysis of cell migration of PAECs upon *MYOSLID* knockdown**

PAECs were transfected with si*MYOSLID*. Then single scratch was made on monolayer PAECs, and the pictures were captured and the migratory distances were analysed at time point 0 h and 12 h. (A) Representative micrographs and quantification of a wound healing assay after *MYOSLID* knockdown in comparison with vehicle and siRNA control. *MYOSLID* knockdown had no effect on cell migration. (B) *MYOSLID* expression was analysed by Taqman qRT-PCR, which showed that *MYOSLID* significantly decreased in si*MYOSLID* transfected group compared with control groups. Data represented as fold change  $\pm$  SEM and analysed by a one-way ANOVA followed by Tukey's post hoc test. All experiments were repeated at least 3 independent times. n = 3 per group in triplicate. \*\* $P < 0.01$

A



B

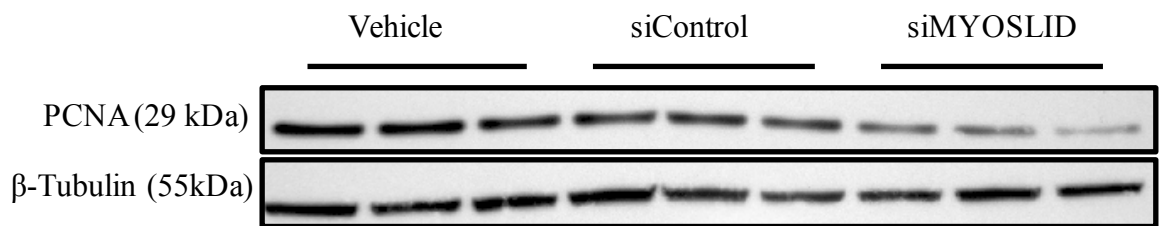


**Figure 5.10 Analysis of proliferation in PAECs with *MYOSLID* knocking down**

PAECs were transfected with *siMYOSLID*. (A) transfected and control cells were stimulated with VEGF and 0.2% FBS for 48 h. Proliferation assay by BrdU incorporation showed that *MYOSLID* knocking down significantly reduced cell proliferation in both 0.2% FBS and VEGF stimulation conditions (n = 5). (B) Western blot of PCNA showed that knocking down of *MYOSLID* decreased the PCNA expression in PAECs.  $\beta$ -Tubulin was used as internal control (n = 3). Data represented as fold change  $\pm$  SEM and analysed by a one-way ANOVA followed by Tukey's post hoc test. \*\*\* $P < 0.001$  and §§§ $P < 0.001$ .

### 5.3.1.5 *MYOSLID* Knockdown Modulates the Expression of BMP Pathway Components in PASMIC

In our previous results, we had showed that *MYOSLID* expression is significantly induced by BMP4 stimulation (Figure 5.3 B). As BMP signalling plays a prominent role in PAH pathogenesis, we went on to assess the effect of *MYOSLID* modulation on the expression of BMP signalling pathway components and target genes. SiRNA-mediated knockdown of *MYOSLID* significantly induced the expression of BMP signalling pathway receptor *BMPR1 $\alpha$*  and *BMPR2*, as well as the BMP4 target genes *ID1* and *ID3* (Figure 5.11) ( $P < 0.05$ ). The *MYOSLID* expression was significantly decreased with SiRNA transfection ( $P < 0.001$ ) (Figure 5.11). In addition, we performed *MYOSLID* overexpression in PASMICs by lentivirus transduction and analysed the receptors and target genes expression. We found that overexpression of *MYOSLID* did not affect the *bmpr1 $\alpha$* , *bmpr2*, *id1*, and *id3* expression, although the *MYOSLID* expression was significantly elevated with lentivirus-*MYOSLID* transduction (Figure 5.12) ( $P < 0.001$ ). It has been demonstrated that mutations in the *bmpr2* gene have been found in approximately 70% of familial PAH (FPAH) (Machado et al., 2006), and up to 25% of sporadic IPAH patients also have been found to harbour similar mutations (Thomson et al., 2000). We further analysed the protein level of *BMPR2* with *MYOSLID* knockdown and overexpression in PASMICs and PAECs. In the PASMICs, we found knocking down *MYOSLID* increased the *BMPR2* protein level (Figure 5.13 A), and overexpression of *MYOSLID* reduced the *BMPR2* protein level (Figure 5.13 B). However, we did not find any change in PAECs with *MYOSLID* knocking down (Figure 5.12 C). Furthermore, in the non-canonical BMP pathway, we found that ERK1/2 protein levels were decreased in both control and BMP4 stimulated cell (30 min and 1 h) with *MYOSLID* knockdown (Figure 5.14 A). In the canonical BMP pathway, the p-SMAD1/5/9 protein level was decreased at 30 min with BMP4 stimulation in PASMICs but slightly increased at 1 h in the *MYOSLID* knockdown condition (Figure 5.14 B).

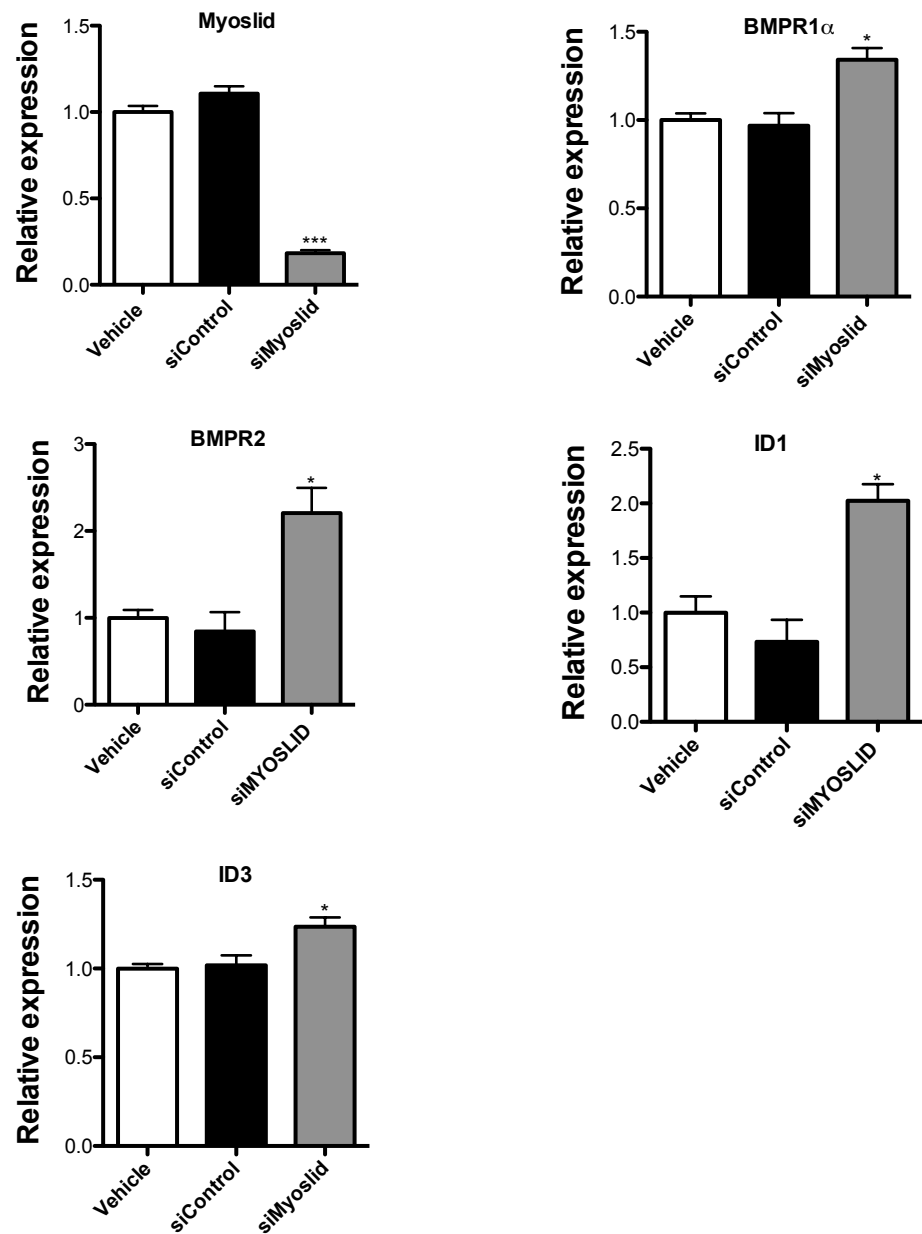


**Figure 5.11 Analysis of BMP pathway components with *MYOSLID* knockdown**

PASMCs were transfected with si*MYOSLID* and control siRNAs for 48 h. Taqman qRT-PCR analysed the gene expressions of receptors and target of BMP signalling. *MYOSLID* expression was significantly reduced with si*MYOSLID* transfection. *bmpr1 $\alpha$* , *bmpr2*, *id1*, and *id3* expression were significantly increased with *MYOSLID* knockdown. Data represented as fold change  $\pm$  SEM and analysed by a one-way ANOVA followed by Tukey's post hoc test. All experiments were repeated with at least  $n = 3$  independent replicates.  $n = 3$  per group in triplicate. \* $P < 0.05$ , and \*\*\* $P < 0.001$ .

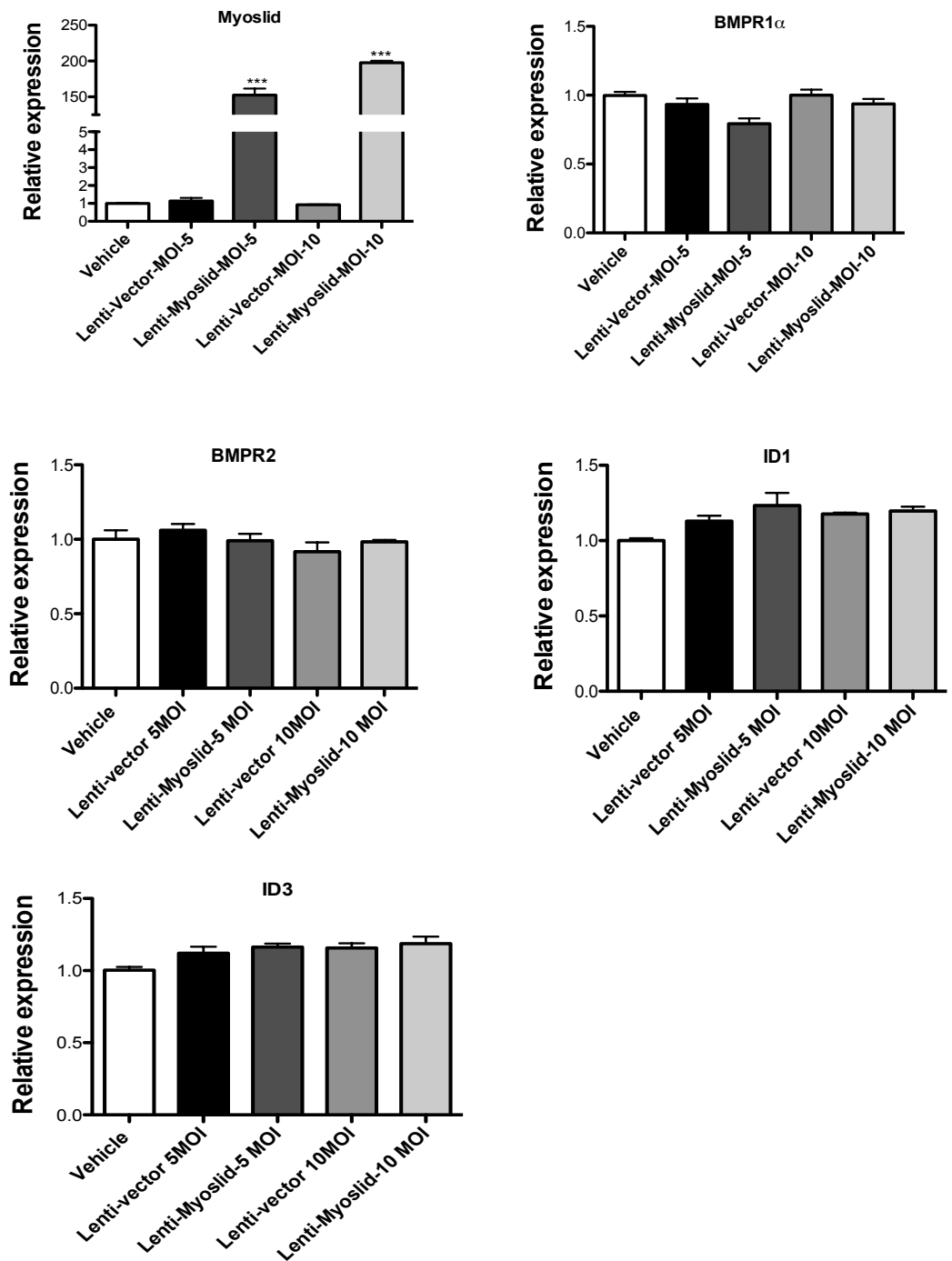


**Figure 5.12 Analysis of BMP pathway components with *MYOSLID* overexpression**

PASMCs were infected with lentivirus of *MYOSLID* and control lentivirus for 48 h. Taqman qRT-PCR analysed the gene expressions of receptors and target of BMP signalling. *MYOSLID* expression was significantly increased with lentivirus infection at different multiplicity of infection (MOI). *bmpr1a*, *bmpr2*, *id1*, and *id3* expression have no change with *MYOSLID* overexpression. Data represented as fold change  $\pm$  SEM and analysed by a one-way ANOVA followed by Tukey's post hoc test. All experiments were repeated at least  $n = 3$  independent times.  $n = 3$  per group in triplicate. \*\*\* $P < 0.001$ .

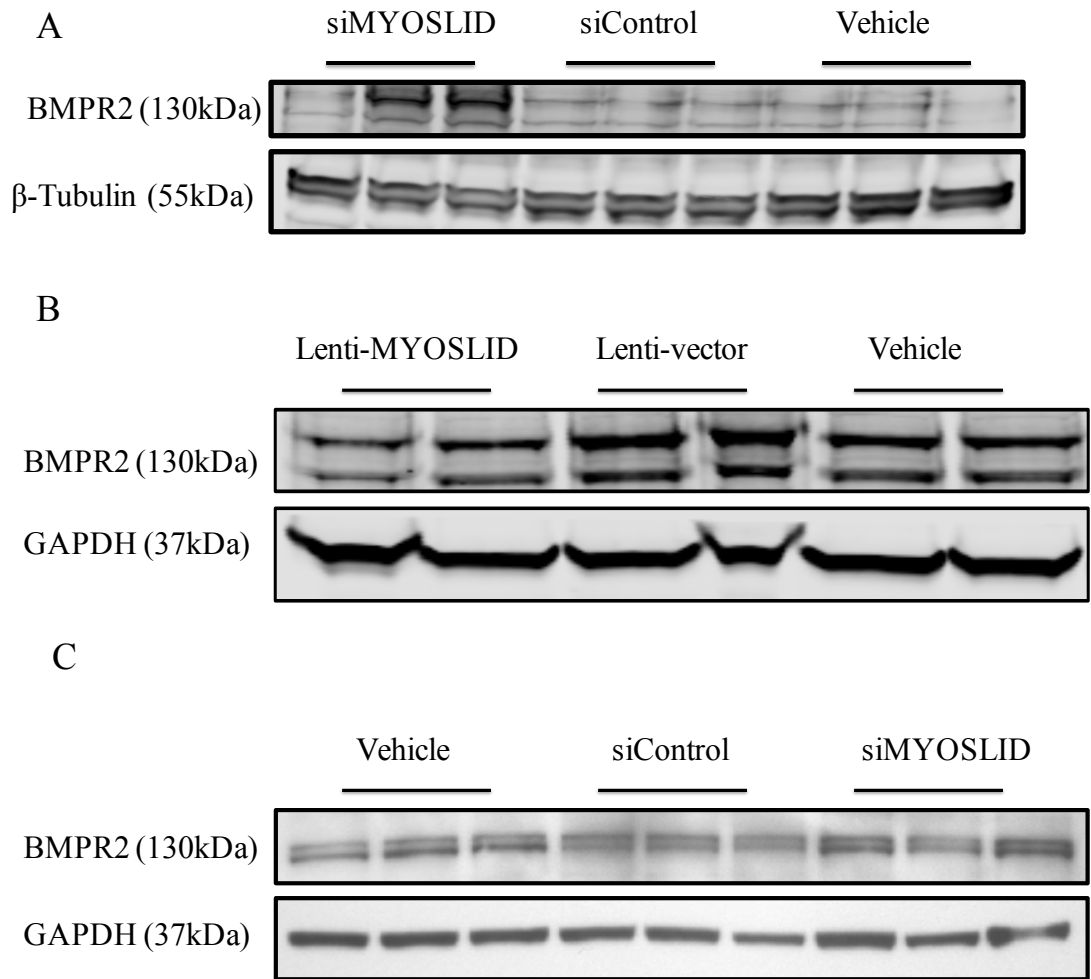


**Figure 5.13 Analysis of *BMPR2* protein level with *MYOSLID* knockdown and overexpression**

PASCs were transfected with si*MYOSLID* and infected with lentivirus of *MYOSLID* and controls for 48 h. Western blot was performed and *BMPR2* protein levels were analysed. (A) *BMPR2* protein level was increased in PASCs with *MYOSLID* knockdown compared with controls. (B) *BMPR2* protein level was decreased in PASCs with *MYOSLID* overexpression compared with controls. (C) Change in *BMPR2* protein level in PAEC with *MYOSLID* knockdown. All experiments were repeated at least n = 3 independent times. n = 2/3 wells per group.

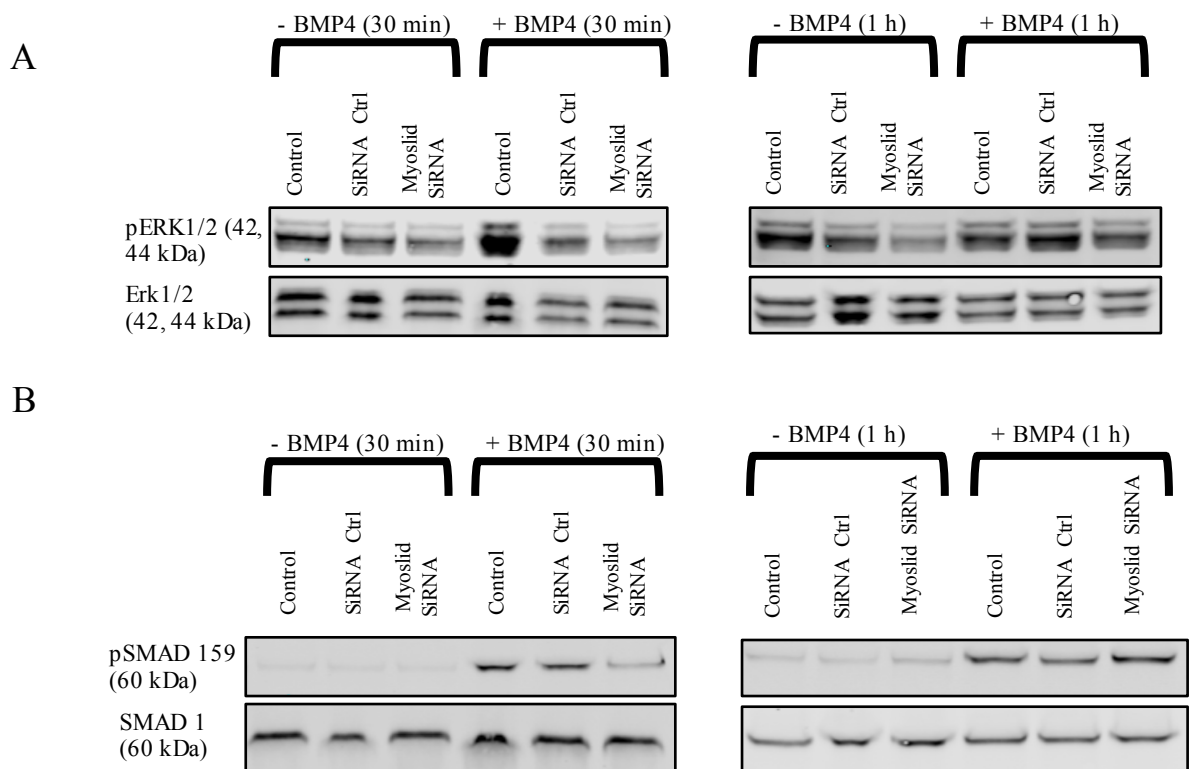


**Figure 5.14 Effect of *MYOSLID* knockdown on the canonical and non-canonical BMP pathway**

PASMCs were transfected with si*MYOSLID* and then stimulated with BMP4 (10 ng/ml) for 30 min and 1 h time points and western blots were performed (A) p-ERK1/2 protein levels were analysed for non-canonical BMP pathway, which showed significant decrease in p-ERK1/2 levels upon *MYOSLID* knockdown. (B) p-SMAD1/5/9 protein levels were accessed to check the activation of the canonical BMP pathway, which was blocked upon *MYOSLID* knockdown at 30 min and was slightly enhanced at 1 h with BMP4 stimulation. All experiments were performed in twice. n = 1 well per condition.

## 5.3.2 LncRNA *Myolnc16*

### 5.3.2.1 Genomic Location of *Myolnc16*

*Myolnc16* is identified through RNA-seq same as *MYOSLID* discussed above. *Myolnc16* is located in the chromosome 4 where several chemokine protein-coding genes are locating from its 3' end. These chemokine genes include CXCL1, CXCL2, CXCL3, CXCL4, CXCL5, CXCL6, CXCL7, and CXCL8 (Figure 5.15).

### Genomic loaction of *Myolnc16*

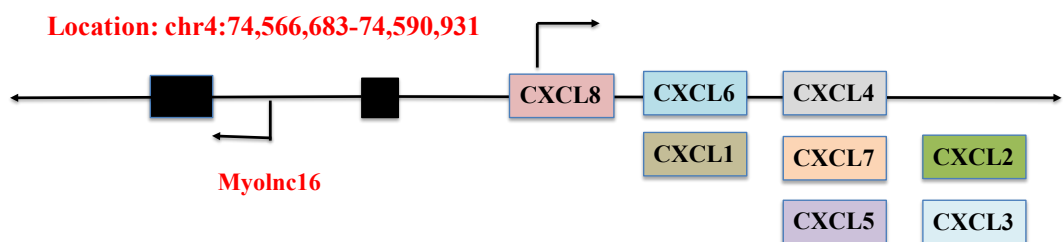
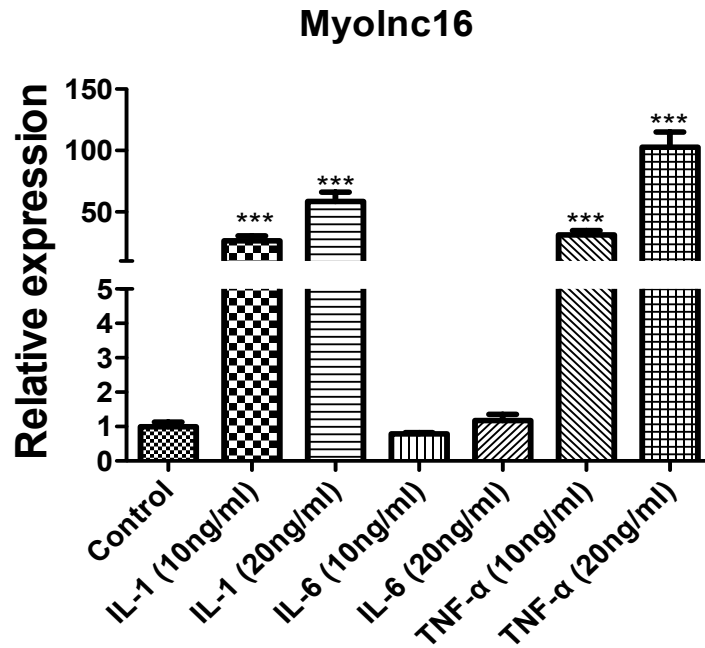


Figure 5.15 Genomic location of *Myolnc16*

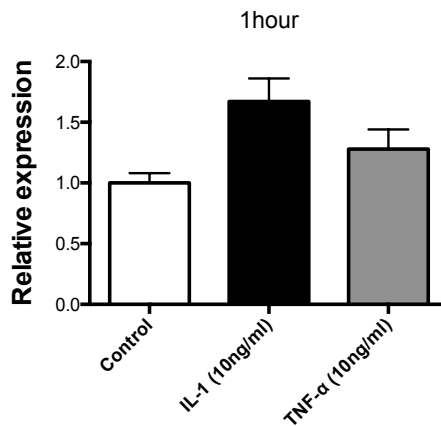
### 5.3.2.2 Inflammatory Cytokines Induced *Myolnc16* Expression in PSMC

Based on the information from the genomic location of *Myolnc16*. We found several cytokines located downstream of this lncRNA. Previous studies demonstrated that inflammatory cytokines are triggers of PH, including IL-1, IL-6 and TNF- $\alpha$  (Humbert et al., 1995, Soon et al., 2010). In order to assess the *Myolnc16* expression in response to inflammatory cytokines, we treated PSMCs with IL-1, IL-6 and TNF- $\alpha$  at two different concentrations (10 ng/ml and 20 ng/ml). The results showed that IL-1 and TNF- $\alpha$  significantly induced *Myolnc16* dose-dependently in PSMCs (Figure 5.16 A) ( $P < 0.001$ ). However, there was no change with IL-6 stimulation (Figure 5.16 A). In addition, we analysed the expression of *Myolnc16* during early time points and found that *Myolnc16* to be induced at 1 h and was significantly upregulated at 6 h with IL-1 and TNF- $\alpha$  stimulation in PSMCs (Figure 5.16 B) ( $P < 0.05$ , and  $P < 0.01$ ).

A



B



C

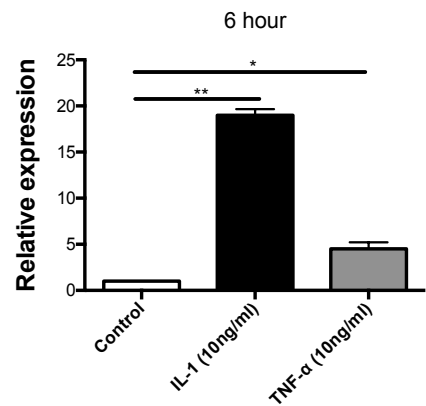


**Figure 5.16 Analysis of *MyoInc16* expression with inflammatory cytokines stimulation**

PASMCs were stimulated with IL-1, IL-6 and TNF- $\alpha$ . (A) Taqman qTR-PCR analysed the *MyoInc16* expression with IL-1 (10 ng/ml, and 20 ng/ml), IL-6 (10 ng/ml, and 20 ng/ml) and TNF- $\alpha$  (10 ng/ml, and 20 ng/ml) for 24 h. IL-1 and TNF- $\alpha$  stimulation significantly increased the *MyoInc16* expression in PASMCs. (B) and (C) Taqman qTR-PCR analysed the *MyoInc16* expression with IL-1 (10 ng/ml) and TNF- $\alpha$  (10 ng/ml) at 1 h and 6 h. *MyoInc16* was significantly upregulated at 6 h with IL-1 and TNF- $\alpha$  stimulation. Data are expression as mean  $\pm$  SEM and analysed by Student t-test. All experiments were repeated twice. n = 3 per group in triplicate. \*  $P < 0.05$ , \*\*  $P < 0.01$ , and \*\*\*  $P < 0.001$ .

### **5.3.2.3 *Myolnc16* Knockdown Induced IL-1 and TNF- $\alpha$ Expression and Inhibited IL-6 Expression**

As we observed that *Myolnc16* was upregulated to IL-1 and TNF- $\alpha$  stimulation. We further aimed to functionally characterise the role of *Myolnc16* and its effect on inflammatory cytokines in PASMCs. Hence, we performed *Myolnc16* knockdowns in PASMCs with siRNAs and then stimulated with or without TNF- $\alpha$  (10 ng/ml) for 24 h. Taqman qRT-PCR showed *Myolnc16* expression was significantly decreased with siRNA transfection in with or without TNF- $\alpha$  stimulation ( $P < 0.001$ ) (Figure 5.17 A). Consistent with previous data, TNF- $\alpha$  significantly induced *Myolnc16* expression (Figure 5.17 A). In addition, TNF- $\alpha$  significantly induced IL-6 expression in PASMCs and *Myolnc16* knockdown significantly decreased the elevation of IL-6 mRNA expression level (Figure 5.17 B) ( $P < 0.05$ ). But in the unstimulated condition, there was no change of IL-6 expression with *Myolnc16* knockdown (Figure 5.17 B). Furthermore, knockdown of *Myolnc16* significantly induced IL-1 and TNF- $\alpha$  expression in both unstimulated and with TNF- $\alpha$  stimulation condition (Figure 5. 18) ( $P < 0.01$ , and  $P < 0.001$ ).

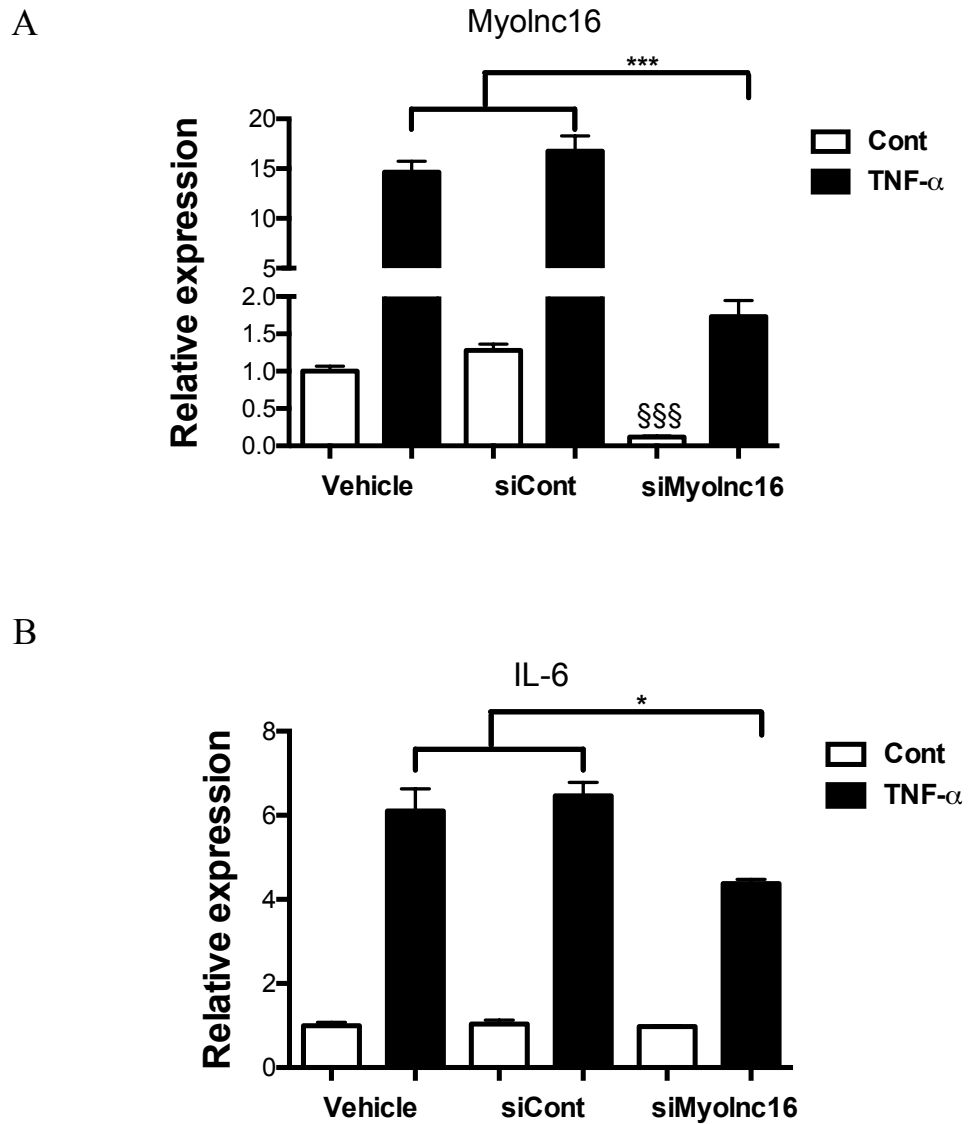


**Figure 5.17 Analysis of IL-6 expression with *Myolnc16* knockdown with or without TNF- $\alpha$  stimulation**

PASMCs were transfected with si*Myolnc16* and then stimulated with or without TNF- $\alpha$  for 24 h. (A) Taqman qRT-PCR was performed to analyse the knockdown of *Myolnc16* in PASMCs with or without TNF- $\alpha$  stimulation. *Myolnc16* expression was significantly reduced with si*Myolnc16* transfection. (B) Taqman qRT-PCR analysed the expression of IL-6 in PASMCs with *Myolnc16* knockdown with or without TNF- $\alpha$  stimulation. IL-6 expression was significantly decreased in the TNF- $\alpha$  stimulated condition. Data are represented as fold change  $\pm$  SEM and analysed by a one-way ANOVA followed by Tukey's post hoc test. All experiments were done by once. n = 3 per group in triplicate. \* $P < 0.05$ , \*\*\* $P < 0.001$ , and §§§ $P < 0.001$ .

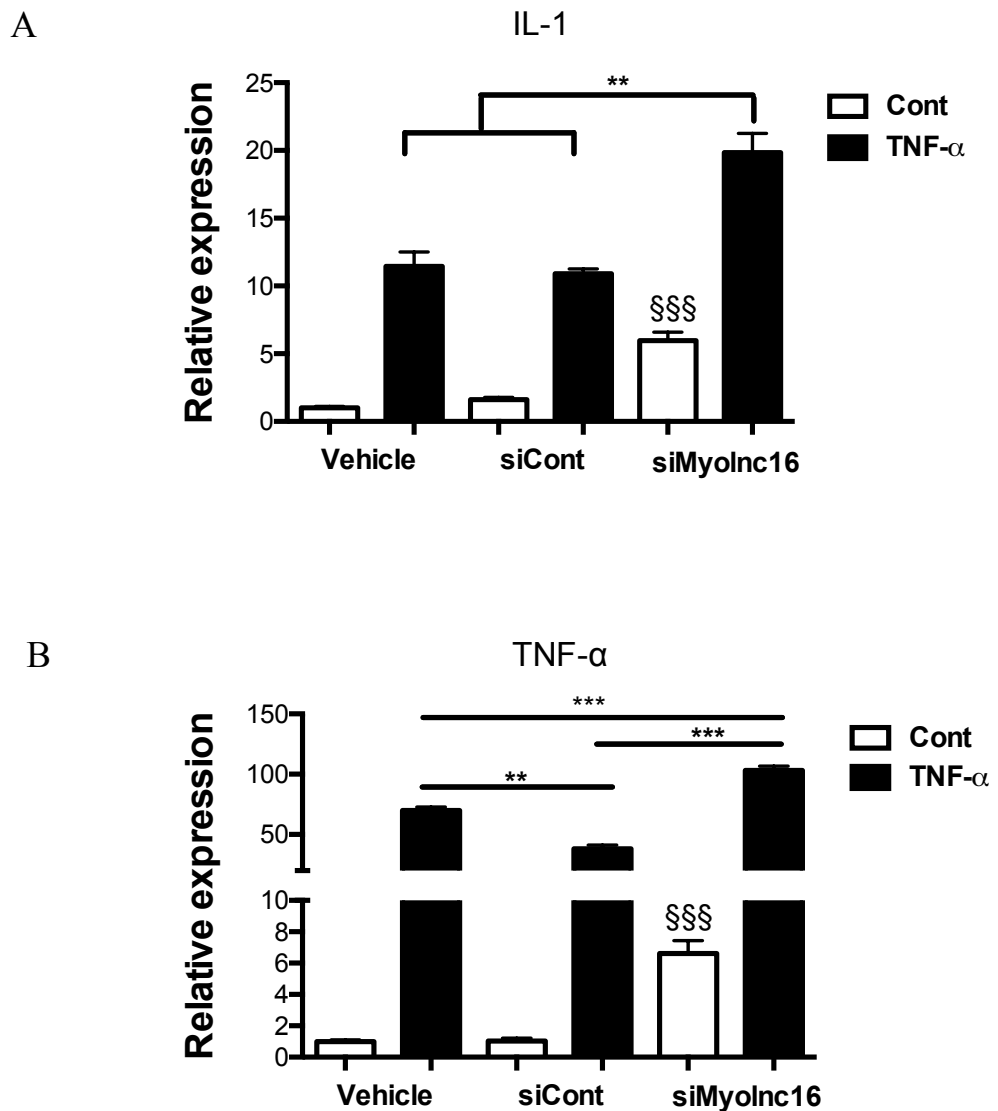
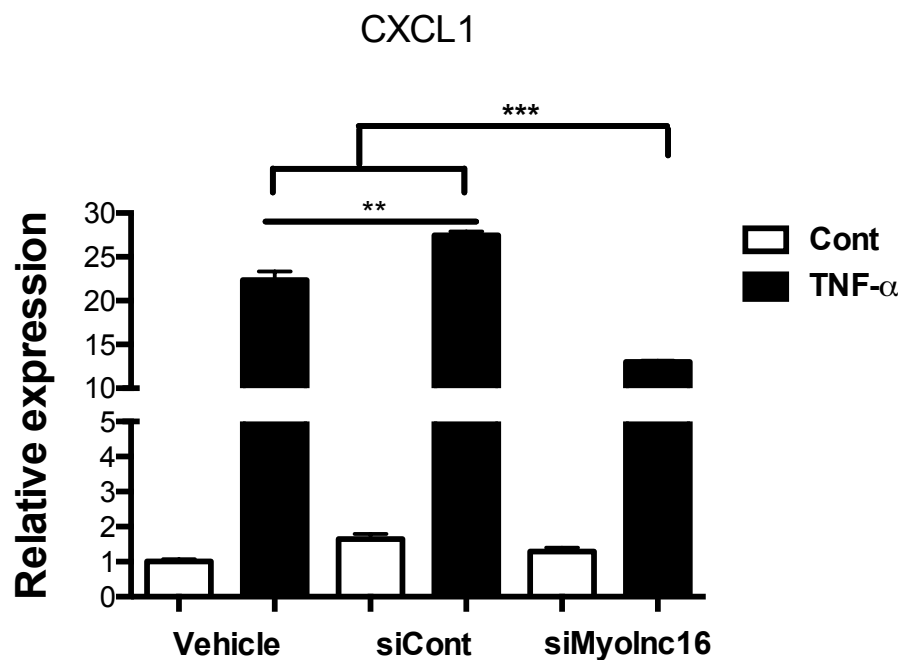


**Figure 5.18 Analysis of IL-1 and TNF- $\alpha$  expression in PSMCs with *Myolnc16* knockdown**

PASMCs were transfected with *siMyolnc16* and then stimulated with or without TNF- $\alpha$  for 24 h. Taqman qRT-PCR analysed the expression of (A) IL-1 and (B) TNF- $\alpha$  in PSMCs with *Myolnc16* knockdown with or without TNF- $\alpha$  stimulation. IL-1 and TNF- $\alpha$  expressions were significantly increased with *Myolnc16* knockdown in both with and without TNF- $\alpha$  stimulation condition compared with controls. Data are represented as fold change  $\pm$  SEM and analysed by a one-way ANOVA followed by Tukey's post hoc test. All experiments were done by once. n = 3 per group in triplicate. \*\* $P$  < 0.01, \*\*\* $P$  < 0.001, and §§§ $P$  < 0.001.

### 5.3.2.4 *Myolnc16* Knockdown Decreased the Chemokine 1,6 8 Expression

Based on the genomic location of *Myolnc16*, there are several chemokine genes located near to the *Myolnc16*. In order to investigate the effect of *Myolnc16* knockdown on the expression of chemokine genes, we stimulated PSMCs with or without TNF- $\alpha$  for 24 h. In the unstimulated condition, *Myolnc16* knockdown had no effect on CXCL1, CXCL6, and CXCL8 expression. However, we found *Myolnc16* knockdown significantly reduced CXCL1, CXCL6, and CXCL8 expression with TNF- $\alpha$  stimulation (Figure 5.19) ( $P < 0.05$ ,  $P < 0.01$ , and  $P < 0.001$ ).



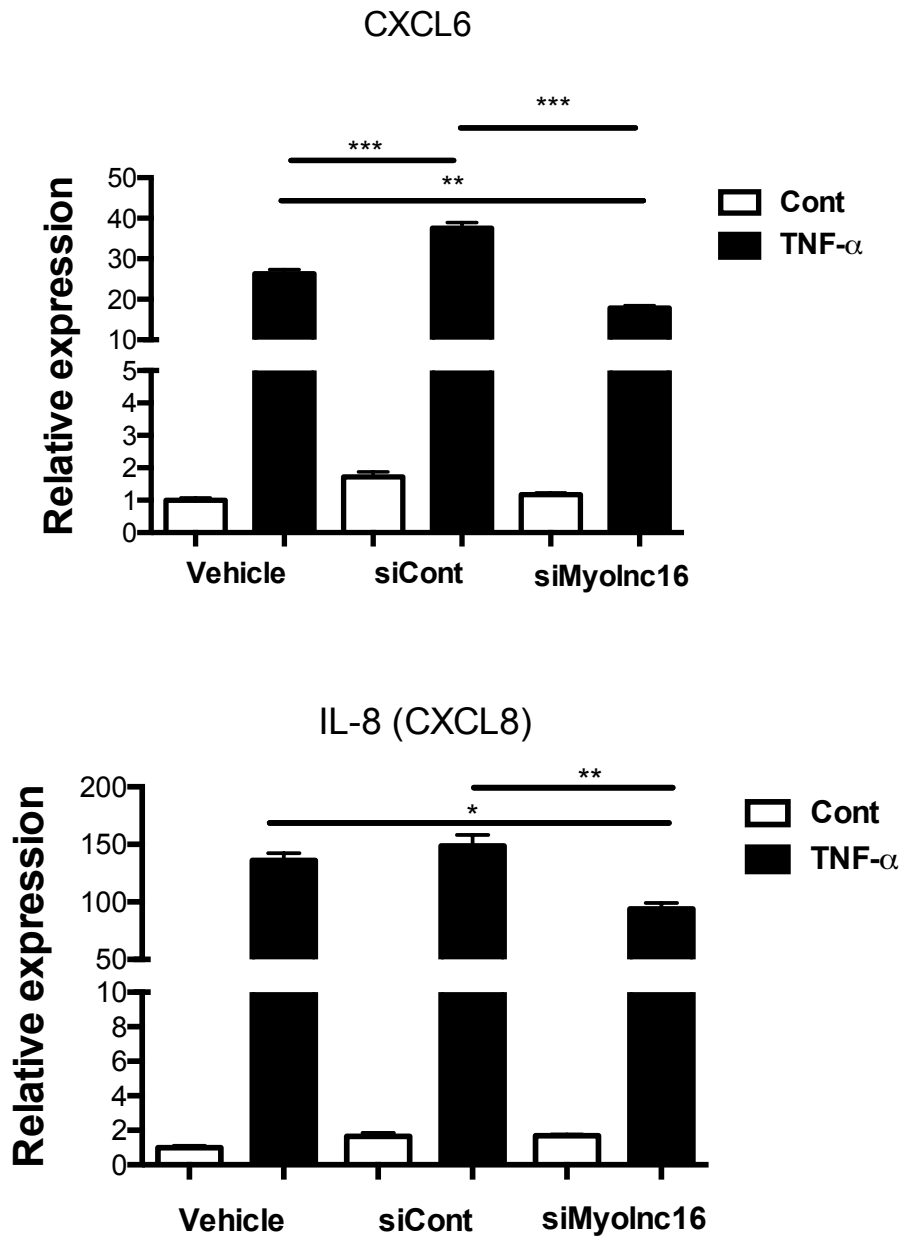


**Figure 5.19 Analysis of chemokine gene expression in PSMCs with *Myolnc16* knockdown**

PASMCs were transfected with *siMyolnc16* and then stimulated with or without TNF- $\alpha$  for 24 h. Taqman qRT-PCR analysed the expression of CXCL1, CXCL6, and CXCL8 in PSMCs with *Myolnc16* knockdown with or without TNF- $\alpha$  stimulation. CXCL1, CXCL6, and CXCL8 expressions were significantly decreased with *siMyolnc16* with TNF- $\alpha$  stimulation condition compared with controls. Data are represented as fold change  $\pm$  SEM and analysed by a one-way ANOVA followed by Tukey's post hoc test. All experiments were done by once. n = 3 per group in triplicate. \* $P < 0.05$ , \*\* $P < 0.01$ , and \*\*\* $P < 0.001$ .

### 5.3.2.5 *Myolnc16* Knockdown Decreased the MAPK/ERK Pathway

Previous study demonstrated that inhibition of mitogen-activated protein kinase attenuates monocrotaline-induced pulmonary hypertension in rats (Lu et al., 2004). Activation of mitogen-activated protein kinase pathways including p38, ERK1/2, and JNK can be induced by TNF- $\alpha$  (Bian et al., 2001). Here we investigated the effect of *Myolnc16* knockdown on ERK1/2 and p38 activation. Our results showed that the pERK1/2, and pp38 protein levels were decreased upon *Myolnc16* inhibition in both control and TNF- $\alpha$  stimulated condition (Figure 5.20). However, this experiments need to repeat to confirm the knockdown of *Myolnc16* affecting the protein levels of p-ERK1/2, and p-p38.

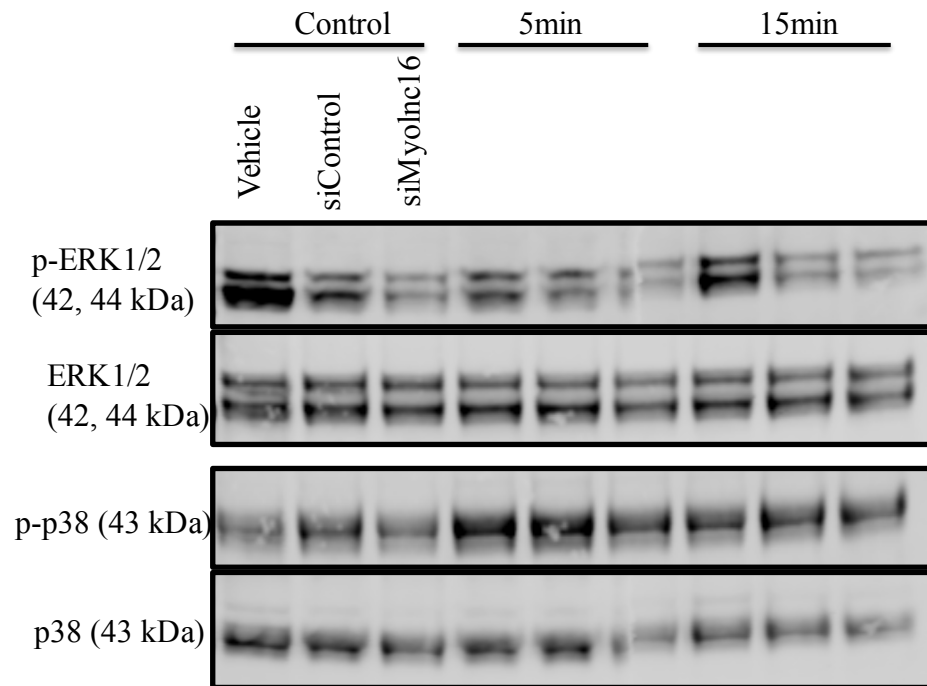
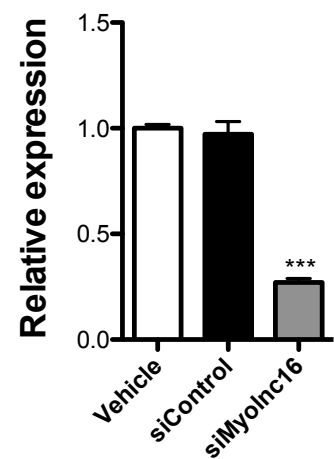
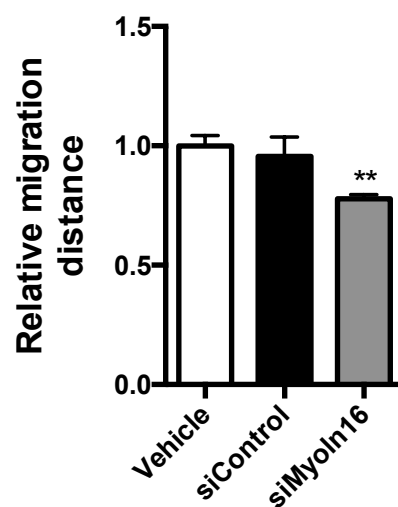
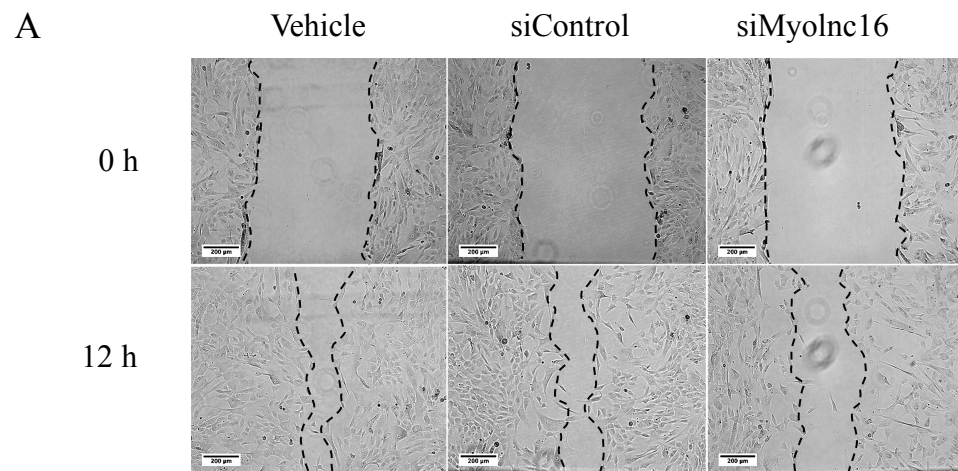


**Figure 5.20 Effect of *MyoInc16* knockdown on ERK1/2 and p38 activation in PSMCs**

PASMCs were transfected with si*MyoInc16* and then stimulated with TNF- $\alpha$  for 5 min and 15 min. Western blot analysed the protein level of ERK1/2 and p38. *MyoInc16* knockdown decreased the protein levels of ERK1/2 and p38 in control and TNF- $\alpha$  stimulation condition compared with vehicle and siRNA control groups. All experiments were performed once. n = 1 well per condition.

### 5.3.2.6 *Myolnc16* Knockdown Decreased the Migration and Proliferation in PSMCs

In order to investigate the effect of *Myolnc16* knockdown on the cellular function of PSMCs, we analysed the migration and proliferation of PSMCs with *Myolnc16* knockdown. Wound healing assay demonstrated that *Myolnc16* knockdown significantly inhibited the cell migration (Figure 5.21 A) ( $P < 0.01$ ). Taqman qRT-PCR confirmed the knockdown of *Myolnc16* (Figure 5.21 B) ( $P < 0.001$ ). In addition, employing EdU incorporation assay clearly showed that *Myolnc16* knockdown significantly decreased the cell proliferation (Figure 5.21 C).



C

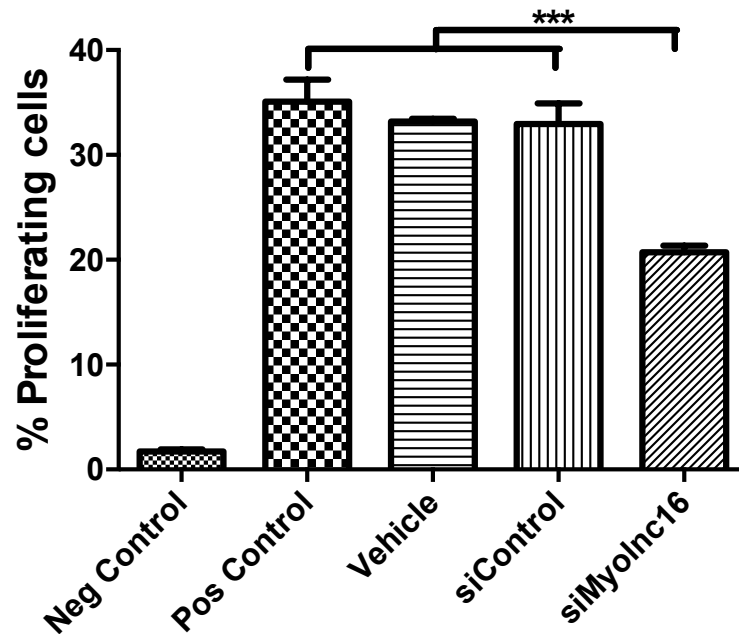


**Figure 5.21 Effect of *Myolnc16* knockdown on PSMC cell functions**

PASMCs were transfected with si*Myolnc16*. A single scratch was applied on monolayer PAECs, and the microscopic pictures were captured and the migrated distances at time point 0 and 12 h were analysed. (A) Representative micrographs and quantification of a wound healing assay after *Myolnc16* knockdown in comparison with vehicle and siRNA control. *Myolnc16* knockdown significantly inhibited cell migration. (B) Taqman qRT-PCR analysed the expression of *Myolnc16*, which showed that *Myolnc16* significantly decreased in si*Myolnc16*-transfected group compared to control groups. (C) EdU incorporation assay assessed the proliferation of PSMCs with *Myolnc16* knockdown, which revealed that *Myolnc16* knockdown significantly inhibited the cell proliferation. Data are represented as fold change  $\pm$  SEM and analysed by a one-way ANOVA followed by Tukey's post hoc test.  $n = 3$  per group in triplicate.  $**P < 0.01$ , and  $***P < 0.001$ .

## 5.4 Discussion

Mammalian genomes encode numerous long non-coding RNAs (LncRNAs), which are defined as non-protein-coding transcripts over 200nt in length. LncRNAs have been shown to perform important functions within the cell, including chromatin modification, RNA processing and structural scaffolding, which affects cell behaviours on cell and tissue processes such as proliferation, migration, apoptosis, invasion, etc. Despite the biological importance of lncRNAs, it is not yet clear whether lncRNAs are involved in the regulation of PAH. In this study, we report that several growth factors that trigger PAH/PH induce *MYOSLID* expression. These are hypoxia, PDGF, VEGF, FGF2, BMP4, and TGF- $\beta$  treatment in pulmonary vascular cells (PASMCs and PAECs) *in vitro*. In addition, *MYOSLID* expression is significantly increased in distal PASMCs from patients with PAH disease (IPAH, FPAH and *bmpr2* mutant PAH patients) and compared to healthy controls. Towards functional studies, *MYOSLID* knockdown in PASMCs induced cell apoptosis and inhibited cell migration but had no effect on cell proliferation. In PAECs, *MYOSLID* knockdown prevented the cell proliferation without any effect on cell migration. Furthermore, *MYOSLID* knockdown modulated the expression of BMP pathway components and affected the BMP-Smad and BMP-non-Smad signalling pathways in PASMCs. *Myolnc16*, which is an inflammatory lncRNA, was induced by inflammatory cytokines (IL-1 and TNF- $\alpha$ ) treatment in PASMCs. Knockdown *Myolnc16* in PASMCs affected the expression levels of inflammatory cytokines (IL-1, IL-6 and TNF- $\alpha$ ) and decreased the expression of chemokines (*cxcl1*, *cxcl6* and *cxcl8*). In addition, *Myolnc16* knockdown decreased the MAP kinase signalling pathway and inhibited cell migration and proliferation in PASMCs.

Hypoxia is an important factor in the pathogenesis of pulmonary hypertension and pulmonary vascular remodelling (Aaronson et al., 2006). Chronic hypoxia is a well-known stimulus for abnormal proliferation and migration of vascular smooth muscle cells and remodelling in patients with PAH (Zhou et al., 2009, Eul et al., 2006, Sarkar et al., 2010). However, few studies have been done on hypoxia of PAECs. In the bovine PAECs, hypoxia exposure showed a decrease in PAEC proliferation after 5 days of exposure to 0% oxygen

and a decrease in DNA synthesis after exposure to 0% for 24 and 48 h. Another study using human pulmonary microvascular endothelial cells revealed that 1% oxygen exposure significantly induced cell proliferation during 5 days incubation. In our study, *MYOSLID* significantly increased in both PASMCs and PAECs with 1% oxygen exposure for 24 h. This data indicated that *MYOSLID* might be hypoxia-sensitive lncRNA in vascular cells and could be involved in the hypoxia induced cellular changes in the pulmonary vasculature and thus might affect the vascular remodelling and development of PAH. Although there are no reports on hypoxia induced lncRNAs (hypoxic-lncRNAs) in the pulmonary vascular cells, there are several novel hypoxia-sensitive lncRNAs found in endothelial cells and play a significant role in the hypoxic response of endothelial cells. The first lncRNA to be described in endothelial cell was an overlapping antisense transcript (sONE, known as eNOS antisense) to eNOS/NOS3 that was implicated in the post-transcriptional regulation of eNOS. In hypoxic ECs, sONE expression negatively correlated with eNOS expression and RNA interference-mediated degradation of the sONE transcript blunted the fall in eNOS RNA and protein during prolonged hypoxia (Fish et al., 2007). RNA-seq analysis of HUVECs revealed high expression levels and conserved lincRNA MALAT1 induced by hypoxia. Knockdown of MALAT1 in ECs results in a pro-migratory phenotype *in vitro* and reduced capillary density and blood flow in a hindlimb ischemia model *in vivo* (Michalik et al., 2014). Another study used both microarray and RNA-seq approaches to analyse the hypoxia-sensitive lncRNAs in HUVEC exposure to hypoxia. Two novel hypoxia-sensitive lncRNAs (LINC00323-003 and MIR503HG) were identified and further characterised by applying loss-and gain of function assessments revealing an important role for both these lncRNAs in endothelial biology (Fiedler et al., 2015). Recently, paired-end sequencing of polyadenylated RNA derived from HUVECs exposed to 1% O<sub>2</sub> or normoxia was performed and identified 122 lncRNAs that differentially expressed. They further validated several lncRNAs including H19, MIR210HG, MEG0, MALAT1 and MIR22HG and found them to be induced in a mouse model of hindlimb ischemia and they further investigated the effect H19 knockdown on endothelial cell growth and angiogenesis (Voellenkle et al., 2016). In contrast to ECs, there are no reports suggesting hypoxia regulated lncRNAs in the VSMCs. However, there are a number studies on hypoxia

regulated lncRNAs identified in cancer diseases (Chang et al., 2016). Taken together, our findings show that *MYOSLID* is hypoxia responsive lncRNA in pulmonary vascular cells. These findings suggest that lncRNAs are important regulators of hypoxia signalling pathway in various disease conditions. Our work on *MYOSLID* is ongoing and we are currently investigating the cellular functions of this lncRNA during hypoxia conditions to explore its functional relevance and mechanisms that underlie the hypoxic processes.

It is well accepted that in PASMCs during vascular remodelling, there is excessive proliferation, migration and resistance to apoptosis. Besides, PASMCs, PAECs in the intima are also involved in the vascular remodelling and in the development of PAH. There is an increase in PAECs proliferation in plexiform lesion, a complex pathological vascular structure seen in the late stage of PAH (Jeffery and Wanstall, 2001). In addition, several studies have demonstrated the PAECs dysfunctions involved in the pathogenesis of PAH (Humbert et al., 2004b, Archer et al., 2010, Cordes et al., 2009). Our data shows that knockdown of *MYOSLID* can inhibit PASMC migration and induce PASMC apoptosis but have no effect on PASMC proliferation. In addition, *MYOSLID* knockdown inhibited PAEC proliferation but had no effect on cell migration. Regarding to another lncRNA *Myolnc16*, we found knockdown of *Myolnc16* significantly reduced cell migration and proliferation in PASMCs. Taken together, these data demonstrated that manipulation of *MYOSLID* and *Myolnc16* affected the cell behaviours of pulmonary vascular cells including proliferation, migration, and apoptosis, which are key contributors to the vascular remodelling in the development. This suggests that *MYOSLID* and *Myolnc16* may play a vital role in the vascular remodelling processes in PAH.

The BMP signalling involves binding to its BMP Type 1 and Type 2 serine/threonine kinase receptors and the subsequent activation of Smad-dependent (Smad1/5/9) and Smad-independent (ERK1/2 and p38 MAPK) pathways, resulting in the regulation of plethora of genes to cell functions (Derynck and Zhang, 2003, Yang et al., 2005, Yang et al., 2007). The Smad pathway is the canonical pathway that mediates the anti-proliferative or pro-apoptotic effects of various BMP ligands. In the PAH setting, BMP4 was demon-

strated as an important factor mediating the process of pulmonary arterial remodelling including the regulation of cell proliferation, migration, intracellular calcium homeostasis (Eickelberg and Morty, 2007, Frank et al., 2005, Long et al., 2006). Germline mutations in the bone morphogenetic protein type II receptor (*bmpr2*) gene, a transforming growth factor- $\beta$  (TGF- $\beta$ ) receptor superfamily member, cause in majority of cases heritable pulmonary arterial hypertension (HPAH) (Beppu et al., 2004, International et al., 2000, Machado et al., 2006). *bmpr2* mutations in PASMCs reduce downstream Smad1/5 phosphorylation. And loss of *bmpr2* function or knockdown of *id1*, a key target gene in response to BMP signalling, both lead to loss of the growth suppressive effects of BMPs (Yang et al., 2008, Miyazono et al., 2005, Yang et al., 2005). Hence *bmpr2* mutation leads to a proproliferative, apoptosis-resistant cell phenotype in PASMCs that may contribute to the process of vascular remodelling observed in the lung of patients with PAH (Morrell et al., 2001). In our study, we found that both BMP4 and TGF- $\beta$  stimulation can significantly induce *MYOSLID* expression in PASMCs, and these effects could be rescued with respective specific inhibitors. This data indicates that *MYOSLID* is involved in the TGF- $\beta$  and BMP4 signalling. We further found *MYOSLID* knockdown significantly increased both the mRNA and protein levels of *BMPR2* in PASMCs. In addition, *BMPR1 $\alpha$*  and target genes of BMP signalling *id1* and *id3* were significantly increased with *MYOSLID* knockdown in PASMCs. However, when we overexpress *MYOSLID* using lentivirus transduction in PASMCs, we found the overexpression of *MYOSLID* did not affect the mRNA expression levels of *bmpr2*, *bmpr1 $\alpha$*  and BMP pathway target genes *id1* and *id3*. However, the *BMPR2* protein level was decreased. This data indicate that *MYOSLID* knockdown restored the *BMPR2* levels and increased the BMP signalling in PASMCs, which is beneficial to the treatment of PAH disease. Here, we did not found any difference of gene expression in the *MYOSLID* overexpression conditions. The possible reasons may include: the endogenous level of *MYOSLID* is already high, and the additional overexpression cannot affect the *MYOSLID* mediated pathways; we performed this experiment on the non-stimulation condition, and the effect of knockdown *MYOSLID* may not affect the BMP signalling without BMP4 stimulation; we found the *BMPR2* protein level was decreased with *MYOSLID* overexpression but not mRNA level, and may due to the post-transcriptional regulation of *MYOSLID*.

Furthermore, we found that *MYOSLID* knockdown at 30 min decreased Smad1/5/9 phosphorylation upon BMP4 stimulation but increased phosphorylation of Smad1/5/9 at 1 h stimulation with BMP4 in PSMCs. To understand the BMP signalling dynamics upon knockdown and overexpression (via lentiviral transductions) of *MYOSLID*, our ongoing studies are focusing towards optimizing the time-course experiments and possibly this will shed light on the *MYOSLID* mediated regulation of BMP signalling.

Apart from activation of canonical Smad-dependent signalling pathway, there is accumulating evidence that MAPKs, mainly ERK1/2 and p38 MAPK, are also activated by BMP4 in several cell types (including human PSMCs) through Smad-independent pathways (Nohe et al., 2004, Zhou et al., 2007, Moon et al., 2009, Jeffery et al., 2005, Yang et al., 2005, Morty et al., 2007, Yu et al., 2008). The BMP signalling can stimulate MAPK pathways has been demonstrated and is functionally linked to the proliferative responses and to the regulation of numerous gene expressions involved in cell growth and differentiation. In PSMCs, the p38 MAPK and ERK1/2 is pro-proliferative and anti-apoptotic whereas Smad signalling is anti-proliferative. (Jeffery et al., 2005, Dewachter et al., 2009, Lee et al., 2012b, Yang et al., 2005, Frank et al., 2005). Previous studies demonstrated that phosphorylation of p38 MAPK and ERK1/2 is increased in PSMCs from PAH patients and experimental models of pulmonary hypertension (Welsh et al., 2001, Zeng et al., 2010, Long et al., 2006, West et al., 2008b). Inhibition of MAPK signalling decreases the excessive proliferation of PAH-PSMCs and prevents the development of the disease in model systems, suggesting that Smad-independent pathways play a key role in disease pathogenesis (Weerackody et al., 2009, Dewachter et al., 2009). Our study showed that *MYOSLID* knockdown decreased the phosphorylation of ERK1/2 in PSMCs upon BMP4 treatment at both 30 min and 60 min time-point, which suggest that knockdown of *MYOSLID* affects the Smad-independent pathway in PSMCs. The decreased phosphorylation of ERK1/2 with *MYOSLID* knockdown can be explained by induced apoptosis with *MYOSLID* knockdown in PSMCs, as p38 MAPK and ERK1/2 exert anti-apoptotic effect in PSMCs. Apart from BMP mediated Smad-independent pathways, our current ongoing studies are also focusing towards understanding the role of *MYOSLID* during

TGF- $\beta$ -Smad-independent pathways as we found that *MYOSLID* expression was significantly induced with TGF- $\beta$  treatment in PSMCs.

We found that *MYOSLID* expression was significantly elevated in the PSMCs from patients with PAH (IPAH and FPAH) compared with controls. In addition, several studies have showed that endothelial progenitor cells were beneficial to treatment of pulmonary hypertension (Fadini et al., 2010, Takahashi et al., 2004, Zhao et al., 2005, Zeng et al., 2007, Wang et al., 2007, Ward et al., 2007, Yip et al., 2008, Sun et al., 2009). And we found that *MYOSLID* expression increased in the circulating endothelial progenitor cells (ECPs) from PAH patients with *bmpr2* mutant compared to controls. The upregulation of *MYOSLID* in these two cell types from patients with PAH suggested that *MYOSLID* dysregulation might contribute to the pathogenesis of PAH.

Cytokines and chemokines emerged as important contributing factors that can lead to pulmonary vascular remodelling and participate into the pathogenesis of PAH (Huertas et al., 2014, Ricard et al., 2014, Groth et al., 2014). In this study, we found the novel lncRNA *Myolnc16* was significantly induced by IL-1 and TNF- $\alpha$  stimulation in PSMCs, which suggests that *Myolnc16* is an inflammatory lncRNA. Knockdown of *Myolnc16* significantly decreased the TNF- $\alpha$  induced IL-6 mRNA expression in PSMCs. Previous studies demonstrated that IL-6 is one of the most important cytokines involved in the pathogenesis of PAH and chronic hypoxia induced pulmonary hypertension. Experimental evidences from animal model studies showed that IL-6 mRNA levels in total lung were increased in MCT-rats, and treatment with immunosuppressive steroids decreased the levels of IL-6 and further reduced pulmonary pressures and RVH (Bhargava et al., 1999). Similar study in mice injecting supraphysiological high doses of IL-6 resulted in pulmonary hypertension and showed a severe disease phenotype under chronic hypoxia conditions (Golembeski et al., 2005). Furthermore, other studies also used lung-specific IL-6 overexpression transgenic mice to investigate the role of IL-6 in pulmonary hypertension. These mice exhibited elevated right ventricular systolic pressures and right ventricular hypertrophy with corresponding pulmonary vasculopathic changes. In addition, IL-6 overexpression enhanced

muscularisation of both the proximal arterial tree and the distal arteriolar vessels that were characterised with the formation of occlusive neointimal angioproliferative lesions composed of endothelial cells and T-lymphocytes, and all of these diseases features were exacerbated in the chronic hypoxia conditions (Steiner et al., 2009). Furthermore, IL-6 genetic ablation mice showed decreased in RVSP, RVH, and the number and media thickness of muscular pulmonary vessels compared to wild-type mice in the chronic hypoxia condition. On the contrary, chronic hypoxia IL-6<sup>-/-</sup> mice showed less inflammatory cell recruitment in the lungs compared with wild-type mice. *In vitro* studies showed that IL-6 was prominently synthesised by PASMCs compared to microvascular endothelial cells and IL-6 also stimulated PASMC migration (Savale et al., 2009). All these studies demonstrated that low levels of IL-6 *in vivo* and *in vitro* are beneficial to the development of PAH.

However, we found *Myolnc16* knockdown in PASMCs significantly induced IL-1 and TNF- $\alpha$  expression with both with or without TNF- $\alpha$  stimulation. And these two inflammatory cytokines levels have been founded elevated in the patients with PAH (Soon et al., 2010). In the rat pulmonary hypertension model, high levels of IL-1 were founded in the MCT rat model and treatment with recombinant human interleukin-1 receptor antagonist reduced pulmonary hypertension and right ventricular hypertrophy, while no protective effect was observed in the chronic hypoxia rat model (Voelkel et al., 1994). Rats fed with recombinant human TNF- $\alpha$  resulted in increased vascular reactivity to hypoxia and ANG II, which could cause the development of pulmonary hypertension (Stevens et al., 1992). Similarly, TNF- $\alpha$  overexpressed in alveolar type II cells resulted in chronic pulmonary inflammation, severe alveolar air space enlargement, septal destruction, bronchiolitis, and pulmonary hypertension (Fujita et al., 2001). Injection of TNF- $\alpha$  antagonist Etanercept prevented and reversed MCT-induced pulmonary hypertension in rat *in vivo*. In PASMCs treated with TNF- $\alpha$ , pyruvate dehydrogenase (PDH) activity was significantly decreased, which plays an important role towards providing resistance to apoptosis (Sutendra et al., 2011). In the endotoxemic-shock-induced pig pulmonary hypertension models, etanercept treatment reduced both pulmonary arterial pressure and pulmonary vascular resistance compared with pigs without etanercept therapy (Mutschler et al., 2006). In another study,

rats treated with TNF- $\alpha$  antagonist, recombinant TNF- $\alpha$  receptor II: IgG Fc fusion protein (rhTNFRFc), attenuated the process of MCT-induced PH through the anti-inflammatory responses (Wang et al., 2013). On the contrary, other studies showed that TNF- $\alpha$  antagonists (infliximab, and etanercept) have no improvement of pulmonary hypertension (Chung et al., 2003, Henriques-Coelho et al., 2008a). In addition, we also found that the lncRNA *Myolnc16* knockdown reduced the phosphorylation of both ERK1/2 and p38 MAPK in PSMCs with TNF- $\alpha$  stimulation. As studies have demonstrated that inhibition of p38 MAPK pathway prevented the development of PH (Weerackody et al., 2009, Church et al., 2015), knockdown *Myolnc16* may exert a protective role in the development of PH. Taken together, IL-1, IL-6, TNF- $\alpha$  and p38 MAPK pathway play an important role in the development of pulmonary hypertension, and studies showed that inhibition these cytokines production and p38 MAPK pathway is beneficial to PAH disease. In this study we showed *Myolnc16* knockdown increased the *il-1* and *tnf- $\alpha$*  mRNA levels in PSMCs while decreasing the IL-6 levels in PSMCs. In addition, *Myolnc16* knockdown inhibited the p38 MAPK pathway. Currently, in our ongoing studies, we further analyse the protein level of these cytokines secreted in PSMCs. Also, the follow up study will focus on the mechanistic regulation of *Myolnc16* in the inflammatory cytokine signalling and p38 MAPK pathway and its effects on the IL-1, IL6 and TNF- $\alpha$ .

In addition to the inflammatory cytokines, we found that *Myolnc16* knockdown significantly reduced the mRNA levels of chemokines including *cxcl1*, *cxcl6* and *cxcl8*. Previous studies showed that CXCL8 (IL-8) was elevated in the serum of PAH patients and CXCL8 have pro-angiogenic and anti-apoptotic activities and acts as a growth factor to endothelial cells (Li et al., 2005). These effects are in consistent with higher CXCL8 serum levels were detected in PAH patients in association with connective tissue diseases compared with patients without PAH (Ricciari et al., 2011). There is no report about CXCL1 and CXCL6 in pulmonary hypertension disease. However, CXCL6 antibody blockade attenuated acute inflammation and reduced lung toxicity associated with bleomycin treatment in mice (Besnard et al., 2013) and enhanced CXCL1 production induced pulmonary angiogenesis (Mohsenin et al., 2007). There are several chemokines levels have been demon-

strated elevated in PAH patients including *CXCL2*, *CXCL5*, *CXCL10*, *CXCL12*, *CXCL13*, and *CXCL16* (see introduction). Taken together, we found that *Myolnc16* knockdown can inhibit chemokine production in PASMCs, which suggest that inhibition of chemokines production by *Myolnc16* can be serve as a potential therapeutic target.

In summary, our study identified two novel lncRNAs *MYOLSID* and *Myolnc16* that are regulated by discrete signalling pathways in PASMCs and down-regulation of these lncRNAs can modulate vascular cell behaviours, which suggest that inhibition of these lncRNAs can serve as a novel therapeutic strategy for PAH treatment.

## 6 General Discussion

PAH is a rare, severe and progressive disease characterised by vasoconstriction and remodelling that mainly affects the small pulmonary arteries with an estimated prevalence of ~ 15-50 cases per million population (Thenappan et al., 2012). The consequences of this is increased pulmonary arterial pressure, right heart failure and eventual death if left untreated. The etiology of PAH is still not entirely clear, but a genetic component is contributed. From the pathophysiology of this disease, the PAH disease is based on genetic predisposition (e.g. *bmpr2*), vessel injury, vascular tone imbalance, increased proliferation and resistance to apoptosis of PSMCs and PAECs, increased proliferation of fibroblasts in the adventitial layer of the vascular wall, inflammation, and *in situ* thrombosis (Biener-tova-Vasku et al., 2015). Despite the modern therapeutic advances, the survival rates of PAH patients remain unacceptably low. Therefore, new treatments and therapeutic strategies (such as ncRNAs) that target disease progression and focus at alleviating vascular remodelling are desperately needed to improve the outcome of patients with PAH.

The first study to demonstrate that miRNA expression profiles are dysregulated during the development of PAH was carried out by our lab, using chronic hypoxia or monocrotaline (MCT) induced PH models (Caruso et al., 2010). This study indicated that miRNA dysregulation might participate in the pathogenesis of PAH and highlighted the potential importance of miRNAs in disease progression, and also their possible role as therapeutic targets. While numerous studies have since elucidated the roles of specific miRNA in PAH, miRNA therapies remain to be applied in the clinical setting. However, the lncRNA field has only recently been developed and the lncRNA studies are considerably less advanced in the PAH field in comparison to studies on miRNAs. Recently, another similar study analysed the expression profile of long noncoding RNA in the chronic hypoxia induced rat model. Hundreds of lncRNAs were identified to be significantly differentially expressed, indicating that lncRNAs might also be involved in the pathogenesis of PAH and may potentially provide novel therapeutic targets (Wang et al., 2016). However, to date no indi-

vidual lncRNA has been investigated in this disease setting. Thus, it is important to further explore the role of miRNAs and lncRNAs in PAH.

This thesis has focused on identifying the role of noncoding RNAs (miRNAs and lncRNAs) during the development of PAH. We were particularly focused on four individual noncoding RNAs: miR-143, miR-145, *MYOSLID*, and *Myolnc16*, aiming to establish the roles of these ncRNAs during PAH pathogenesis and explore the potential mechanisms involved using both *in vivo* and *in vitro* models.

MiR-143 expression is often downregulated in cancer cells and has been associated with reduced migration, proliferation and metastasis (Lee et al., 2013, Xu et al., 2011). MiR-143 expression is also reduced following vascular injury. Overexpression of miR-143 decreased neointimal formation in a rat model of balloon injury (Elia et al., 2009). These studies demonstrated that miR-143 exerted a protective role in the cancer disease and certain vascular disease. In the PAH setting, previous study performed in our lab showed that miR-143 expression was significantly upregulated in lung and right ventricle samples from mice with chronic hypoxia induced PH, potentially due to a release from BMPR2-mediated transcriptional suppression (Caruso et al., 2012). However, this study did not further investigate the expression profile in different PH models and patients with PAH. The lack of evidence of manipulation of miR-143 *in vivo* also founded in this study. Thus, the studies described in chapter 3 aimed at investigating the expression profiles of miR-143 using four different small and large animal models of PH and PAH patient samples. We showed that MiR-143-3p expression is consistently upregulated across all animal models of PH that were assessed (chronic hypoxia induced PH mice model, hypoxia/SU5416 rat model, hypoxia neonatal calves model, brisket disease) as well as in PASMCs and lung samples from PAH patients. In addition, miR-143 genetic knockout and miR-143-3p knockdown via anti-miR-143-3p treatment (both prevention and reversal studies) in the chronic hypoxia induced mice PH model demonstrated a protective effect on the development of PH. Therefore, inhibition of miR-143-3p might be a novel therapeutic target in PAH.

One of the limitations of this study is only using the chronic hypoxia induced PH mice model to investigate the therapeutic role of miR-143-3p knockdown. This model is characterised by hypoxic pulmonary vasoconstriction and subsequently leads to increased pulmonary arterial pressure. As a number of various animal models of PH can simulate the different disease stages or features of human PAH, and also can reflect various pathophysiological pathways involved in PAH development. The chronic hypoxia induced PH model cannot fully recapitulate certain stages/clinical features of PAH. (Stenmark et al., 2009). Thus, more animal PH models such as monocrotaline (MCT) and hypoxia/SU5416 mice/rat PH models should be used to further investigate the important role of miR-143-3p knockdown in PH development. These animals can help to understand the pulmonary vascular remodelling and plexiform lesions progress characteristic of human PAH. Another limitation of this study is lacking of *in vivo* signalling pathways mediated by miR-143-3p in the development of chronic hypoxia induced PH. Previous studies have demonstrated the dysregulation of BMP and TGF- $\beta$  signalling in both the chronic hypoxia and monocrotaline models of PAH. Reduced *BMPR2* expression in lung and reduced signalling via the downstream Smad1/5 pathway are observed. However, TGF- $\beta$  signalling is increased, with increased Smad3 phosphorylation and increased expression of TGF- $\beta$  target genes (Long et al., 2009). These observations are greater in the monocrotaline model compared with chronic hypoxia model. Interestingly, miR-143 and miR-145 are co-transcribed from a common bicistronic precursor and the expression of miR-143/145 is transcriptionally activated by signalling molecules including TGF- $\beta$  and BMP4. The activation of miR-143/145 by TGF- $\beta$  and BMP4 leads to down-regulation of their target genes KLF4 and KLF5 resulting in increased expression of smooth muscle specific genes (Davis-Dusenbery et al., 2011, Long and Miano, 2011, Cordes et al., 2009, Xin et al., 2009). Thus, it is valuable to investigate whether the protective role of miR-143-3p knock-out/knockdown is via affecting the TGF- $\beta$ /BMP4 signalling *in vivo* in both chronic hypoxia and monocrotaline PH models.

At the clinical level, the incidence of nearly all classifications of PH and PAH show an en-

hanced female susceptibility with about 4:1 in ratio between females and males (Rich et al., 1987, Humbert et al., 2006, Badesch et al., 2010, Ling et al., 2012). This sex-ratio imbalance suggests that gender is involved in the development of PAH. However, female PAH patients appear to have longer survival time than males and females develop lesser degree of disease than males (Humbert et al., 2010a, Humbert et al., 2010b). The sex hormone oestrogen is thought to exert a protective role in PAH, based on studies showing that bilateral ovariectomy of female rats results in an exacerbation of PH and cardiac remodeling in response to monocrotaline, an effect that could be reversed with estradiol administration (Ahn et al., 2003). Interestingly, several miRNAs exhibit gender-specific differences in regulation, such as miR-96, which plays a role in the development of PH in a sex-dependent manner by regulating 5-hydroxytryptamine 1B receptor (5-HT<sub>1B</sub>R) expression and hence serotonin-induced proliferation (Wallace et al., 2015) and miR-223, which expression levels are significantly decreased in female patients rather than male patients (Zeng et al., 2016). Understanding the different roles of miRNAs between the genders and the effect of sex hormones on miRNA expression in the pulmonary system is essential if these miRNAs are to be developed as therapeutic targets for PAH treatment. Our lab has recently showed that miR-143 expression levels were significantly elevated with estradiol treatment in PSMCs (Deng et al., 2015). However, we still do not know whether miR-143 acts in a gender-specific manner, which should be validated in future studies.

Pre-miRNAs and anti-miRNAs were used successfully to induce and knockdown miR-143-3p expression in pulmonary vascular cells (PSMCs and PAECs). In chapter 4, *in vitro* modulation of miR-143-3p showed that miR-143-3p overexpression promoted migration and inhibited apoptosis while miR-143-3p knockdown prevented migration and induced apoptosis in PSMCs. No effect of miR-143-3p modulation on PSMC proliferation was observed. We focus on PSMC behaviours due to their documented highly proliferative, migratory, and apoptotic response to PH stimuli (Rabinovitch, 2012, Gerthoffer, 2007, Tajsic and Morrell, 2011). There is also a significant increase in the muscularisation of distal small pulmonary arteries leading to the vascular remodelling of these vessels, which highlights the importance of PSMCs in the pulmonary vascular remodelling pro-

cess. In addition to this, we evaluated the functional effect of miR-143-3p modulation in PAECs, which also play a vital role in the cellular response to PH; notably, ECs are the principal cell type involved in the formation of plexiform lesions in PAH patients (Wideman et al., 2011). In chapter 4, we showed that miR-143-3p overexpression significantly induced cell migration and angiogenesis of PAECs but had no effect on proliferation and apoptosis. Thus, manipulation of miR-143-3p affects PASMCM and PAEC function *in vitro*, which contributes to the vascular aberrant remodelling observed in PAH pathogenesis.

PASMCs and PAECs are two key cell components of the pulmonary vasculature that play a major role in the pathobiology of PH. Under physiological conditions, interactions between PASMCs and PAECs are required to maintain pulmonary vascular homeostasis; aberrant interactions between these two cell types may lead to disease onset or contribute to PAH disease progression (Gao et al., 2016). Several previous studies have investigated the role of miRNAs in PAH disease (Zhou et al., 2015), and one important study has shown the role of miRNA mediated crosstalk between PASMCs and PAECs (Kim et al., 2013). MiR-424 and miR-503 are expressed at higher levels in PAECs compared with PASMCs, and the expression levels of these two miRNAs are significantly downregulated in PAH PAECs but no significant changes in PAH PASMCs compared to control cells. Conditioned media from control PAECs resulted in a significant increase in PASMC proliferation, and conditioned media from PAH PAECs induced a greater degree of PASMC proliferation. In addition, conditioned media from either control or PAH PAECs transfected with miR-424 and miR-503 significantly reduced the proliferation of PASMCs. Mechanistically, the miR-424/503 effect was abrogated by concurrently transfecting PAECs with an FGF2 overexpression construct, demonstrating FGF2 reversed the PAEC derived paracrine effect of miR-424/503. Conditioned media from normal PAECs with APLN knockdown significantly induced PASMC proliferation, which was reversed by overexpression of miR-424/503 in PAECs. PAECs with FGF2 knockdown also led to decreased proliferation PASMCs exposure to PAEC conditioned media. Moreover, the proliferative response of PASMCs to conditioned media from PAEC with APLN knockdown was rescued by concurrent FGF2 knockdown. This study showed APLN-miR-424/503-FGF2 signalling path-

way in PAECs could regulate PASMCM proliferation in a paracrine manner (Kim et al., 2013), which is the first study showing miRNA mediated cell-to-cell communication between PAECs and PASMCMs. These findings are also consistent with the emerging role of PAEC-PASMC crosstalk in the pathogenesis of PAH (Izikki et al., 2009, Eddahibi et al., 2006, Dewachter et al., 2006).

In chapter 4, we evaluated exosomal cell-to-cell communication between PASMCMs and PAECs, focusing on the role of miR-143-3p in this process. MiR-143-3p is expressed at much higher levels in PASMCMs compared to PAECs. Co-culture experiments showed that miR-143-3p expression was significantly increased in PAECs co-cultured with PASMCMs with or without pre-miR-143-3p transfection. PAEC migration was increased following co-culture with PASMCM transfected with pre-miR-143-3p, as well as in the presence of conditioned media from transfected PASMCMs. In further validating the crosstalk between PASMCMs and PAECs, we found that PASMCM-derived exosomes were enriched in miR-143-3p and exosomal miR-143-3p derived from PASMCM transfected with pre-miR-143-3p significantly induced PAEC migration and tube formation in angiogenesis assays. To complement this data, we have recently published studies identifying several PAH-related signalling pathway elements that regulate miR-143/145 expression by binding the promoter region of the miR-143/145 cluster. Firstly, estradiol (E2) treatment activated the estrogen receptor and significantly triggered the expression of miR-143/145 cluster, which is consistent with the fact that gender *per se* is a risk factor in the pathogenesis of PAH (Mair et al., 2014). In the same way, PASMCMs treated with 9-*cis*-retinoic acid (9cRA) and/or 22R-hydroxycholesterol (22R) upregulated miR-143/145 expression. In addition, hypoxia exposure and TGF- $\beta$  but not BMP4 induced the expression of miR-143/145 cluster (Deng et al., 2015). Taken together, these results are the first demonstration of the promoter sequence controlling transcription of the miR-143/145 cluster, unravelling the most significant signalling pathways involved. Many of these signalling pathways have previously been implicated in the development of PAH, in which the expression of miR-143 is increased. Moreover, this is also the first report about exosomal miRNA-mediated crosstalk in pulmonary vasculature homeostasis, in which exosomal miR-143-3p from PASMCM

can regulate PAEC behaviour in a paracrine manner.

However, in chapter 4, we did not investigate signalling pathways and target genes involved in miR-143-3p modulation effect on pulmonary vascular function and the exosomal miR-143-3p mediated crosstalk between PASMCs and PAECs. As described in the previous paragraph, there are several signalling pathways known to regulate miR-143-3p expression in PASMCs and these pathways are involved in PAH disease. The further study will be required to investigate whether miR-143 modulation will affect these signalling pathways in PASMCs. In addition, activation all these signalling pathways induce the expression of miR-143-3p expression in PASMCs. Theoretically, the miR-143-3p expression levels in the PASMCs are positively correlated with the miR-143-3p expression levels in PASMC-derived exosomes. As we have demonstrated that miR-143-3p levels in PASMC are positively correlated with expression levels in exosomes with different concentration of pre-miR-143-3p transfection. But, whether exosomes derived from PASMCs with these signalling pathways activation will functionally affect the PAEC behaviours need to be further investigated. Conversely, if the activation of these signalling pathways induce PASMC dysfunction and also regulate the PAEC behaviours via cell-to-cell communication by exosomes, we are still not knowing whether this effect is specifically mediated by exosomal miR-143-3p derived from PASMCs. Therefore, a reversal study (by decreasing the expression level of miR-143-3p to baseline) should be carried out to address this question, as activation of pathogenic signalling pathways in PASMCs definitely will affect the expression of a number of miRNAs or other biological substances. To identify potential target genes of miR-143-3p, we performed two gene expression microarrays in PASMCs and PAECs overexpressing miR-143-3p and identified a number of dysregulated genes, including 68 genes involved in cell migration (in PASMC arrays; Chapter 4) and multiple targets involved in cell death and survival (in PAEC arrays; Chapter 4). However, due to time constraints we did not validate any of these potential targets. Individual miRNA can target several hundreds of mRNAs on the basis of sequence complementarity, and a substantial fraction of these predicted interactions may depend on cell type and context (Jacobsen et al., 2013). It is possible that the predicted but not validated targets of

miR-143-3p may also contribute to the cellular and *in vivo* consequences of manipulation of miR-143-3p. Thus, further studies should be performed to validate predicted targets of miR-143-3p in the context of PAH.

In summary, in chapters 3 and 4, we have demonstrated that miR-143-3p expression is elevated in several animal PH models and in PASMCs and lung tissue from human patients of PAH. Studies performed in the chronic hypoxia induced mouse model of PH showed that genetic ablation of miR-143 and pharmacological inhibition of miR-143-3p exerted a protective role in the development of PH. In addition, this is the first study to show that exosomal miRNAs are involved in the cell-to-cell communications between PASMCs and PAECs in the pulmonary vasculature, suggesting that miR-143-3p may act as a crucial paracrine signalling mediator during pulmonary vascular remodelling. Thus, this study illustrates a novel role for miR-143-3p as a potential therapeutic target in the treatment of PAH.

In addition to miRNA, there is another group of noncoding RNAs that have emerged as important players in the regulation of cell function and behaviour in vascular homeostasis and dysfunction. As described in the introduction to chapter 5, ncRNAs work through multiple mechanisms. Of particular relevance to this project, lncRNA can act as endogenous sponges to regulate miRNA functions and miRNA have been shown to bind and regulate lncRNA stability (Ballantyne et al., 2016a). There is very little known about the expression and function of lncRNA in vascular diseases such as pulmonary hypertension. In order to identify whether lncRNAs can regulate the miR-143/145 cluster in the setting of PAH, our group recently cloned a novel promoter region that is rich in lncRNAs (miR-143-3p/145HG lncRNA). Preliminary evidence (unpublished data, Anderson and Baker) suggests that manipulation of miR-143HG modulates miR-143 expression in PASMCs, suggesting that miR-143HG lncRNA may play a role in the pathogenesis of PH. Further studies will focus on several aspects of miR-143HG biology, including the expression profile of miR-143HG in animal models of PH and in PAH patients; the regulation of the miR-143HG axis in response to pathogenic stimuli; the impact and function of the

miR-143HG axis on the expression and function of the miR-143/145 cluster, and the effect of miR-143HG modulation on the development of PH. This study may further strengthen the important role of lncRNA-miRNA-143 axis in PAH development.

In chapter 5, we show preliminary evidence of the function and mechanisms of two novel lncRNAs (*MYOSLID* and *Myolnc16*) in pulmonary vascular cells. *MYOSLID* expression is elevated in PASMCs following exposure to numerous PAH stimuli such as hypoxia, BMP4, TGF- $\beta$ , and PDGF. Knockdown of *MYOSLID* induced the mRNA expression of BMP signalling pathway components include *bmpr1a*, *bmpr2*, *id1*, and *id3*. However, lentivirus overexpression of *MYOSLID* did not have the opposite effect. The possible reason is that the *MYOSLID* knockdown by siRNA is in a sequence-specific manner, which can directly affect the expression level of *MYOSLID* in the genomic location. *MYOSLID* overexpression was achieved using a lentiviral approach. As lentiviral vectors favour integration in active transcription units, the local chromosomal environment into which integration has occurred can affect transgene expression. The functional consequence can be varied depend on where the lncRNA is overexpressed. Similar findings in our lab showed that RNA-interference-mediated knockdown of smooth muscle-induced lncRNA enhances replication (*SMILR*) significantly decreased the proximal gene hyaluronan synthase 2 (*HAS2*) expression. However, lentiviral-mediated overexpression of *SMILR* did not affect *HAS2* expression (Ballantyne et al., 2016c). Thus, further work need to localise the cellular localisation of *MYOSLID* in basic condition and with lentivirus overexpression. Because the cellular localization of lncRNA will affect the silencing efficiency of lncRNA (Lennox and Behlke, 2016).

In addition to modulating mRNA expression of BMP signalling pathway components, *MYOSLID* was able to regulate BMPR2 protein expression. Functional study revealed that *MYOSLID* knockdown inhibited the cell migration and induced cell apoptosis of PASMCs. Mechanistically, *MYOSLID* knockdown reduced the protein levels of pERK1/2 and affected the protein levels of Smad1/5/9. Previous study showed in normal PASMCs, BMP4 activated Smad15/9 as well as p38 MAPK and ERK1/2. Smad signalling was an-

ti-proliferative, whereas p38 MAPK and ERK1/2 signalling were pro-proliferative and anti-apoptotic (Yang et al., 2005). In PASMCs from PAH patients with BMPR2 mutations, Smad signalling was defective and the cells were unresponsive to the anti-proliferative effect of BMP4. The BMPR2 mutations also can lead to unopposed the activation of pro-proliferative p38 MAPK and ERK1/2 signalling (Yang et al., 2008). In consistent with these finding, PASMCs from heritable PAH patients show no BMP4-induced Smad1/5/9 phosphorylation but BMP4-induced activation of p38 MAPK pathway. PASMCs from PAH patients with an *in vitro* proliferative and anti-apoptotic pattern that can be inhibited by BMP4 in idiopathic PAH but no in heritable PAH (Dewachter et al., 2009). Our data may indicate that *MYOSLID* knockdown increased the BMP4-Smad signalling pathway and reduced the p38 MAPK and ERK1/2 signalling leading to inhibition of cell migration and induced cell apoptosis. However, to confirm this regulation of *MYOSLID*, more experiments need to be addressed including analysing the protein levels of p38 MAPK, and the Smad1/5/9 at various time point. Whether lentiviral overexpression of *MYOSLID* also affected these two signalling pathways need to be analysed. Furthermore, the expression levels of *MYOSLID* is elevated in PASMCs from PAH patients. In order to analyse the effect of *MYOSLID* in regulating the signalling pathways in PAH disease, PASMCs with and/or without BMPR2 mutations cells need to be used for analysis. The *MYOSLID* knockdown may compensate the defective BMP4-Smad signalling pathway to exert a protective phenotype. We found not all the patient cells express high levels of *MYOSLID*, exploring the underlying mechanisms of this difference will be done.

Apart from PASMCs, *MYOSLID* is also expressed in PAECs. *MYOSLID* knockdown significantly decreased PAEC proliferation. In chapter 4, we showed cell-to-cell communication between PASMCs and PAECs by exosomal miRNA may contribute to the vascular remodelling process during PAH pathogenesis. Similar to miRNAs, recent studies have reported that lncRNA are present in exosomes and account for 20.19% of exosomal RNA extracted from the plasma of castration-resistant prostate cancer patients (Huang et al., 2015). Other exosomal lncRNAs include HOTAIR (Botti et al., 2015), H19 (Conigliaro et al., 2015), ROR (Takahashi et al., 2014a), Linc-VLDLR (Takahashi et al., 2014b), TUC339

(Kogure et al., 2013), lncRNA-p21 (Isin et al., 2015). For example, sunitinib resistance is a major challenge for advanced renal cell carcinoma, and developing effective strategies against sunitinib resistance are highly desired in the clinical treatment. In this study, lncARSR was shown to be secreted by resistant cells via exosomes, and could be taken up by sunitinib-sensitive cells to transform sunitinib-sensitive cells into resistant cells (Qu et al., 2016). This study revealed that exosomal lncRNAs could functionally mediate cell-to-cell communication in disease context. Thus, it would be interesting to investigate whether PSMCs and/or PAEC-derived exosomes contain *MYOSLID*, and whether exosomal *MYOSLID* can mediate the functional crosstalk between PSMCs and PAECs.

*Myolnc16* is another novel lncRNA investigated in this chapter. In PSMCs, the expression of *Myolnc16* is significantly induced by inflammatory cytokines (TNF- $\alpha$  and IL-1) at very early time points. *Myolnc16* knockdown significantly reduced the expression levels of *il-6*, *cxcl1*, *cxcl6*, and *cxcl8*, which were activated by TNF- $\alpha$  treatment in PSMCs. Mechanistically, knockdown of *Myolnc16* reduced p38 MAPK and ERK1/2 signalling pathway activation in PSMCs, which are known to drive proliferation and inhibit apoptosis of PSMCs (Yang et al., 2005). Consistent with this observation, *in vitro* functional experiments showed that *Myolnc16* knockdown inhibited the proliferation and migration of PSMCs, potentially via inhibition of p38 MAPK and ERK1/2 signalling. Further experiments are required to analyse the cell apoptosis of PSMCs with *Myolnc16* knockdown. Given that inflammatory pathways appear to be the key targets of *Myolnc16*, it would be important to evaluate the role of *Myolnc16* in NF- $\kappa$ B pathway. Nuclear factor  $\kappa$ -B (NF- $\kappa$ B) is activated in the pulmonary vessels of PAH patients (Price et al., 2013) and NF- $\kappa$ B inhibition exerts an anti-remodelling effect in PSMCs (Hosokawa et al., 2013, Ogbozor et al., 2015). *In vivo* inhibition of NF- $\kappa$ B prevents monocrotaline-induced PH in mice (Li et al., 2014). As *Myolnc16* is induced by inflammatory cytokines and NF- $\kappa$ B pathway plays a vital role in inflammatory signalling pathways, it is important for further studies focusing on the role of modulation of *Myolnc16* in the NF- $\kappa$ B pathway in PAH setting. In addition, overexpression of *Myolnc16* should be considered in all these experiments to assess whether *Myolnc16* could reverse the cell functions and signalling pathways.

The translation of ncRNAs from bench to bedside has received considerable attention in the context of PAH. In general, therapeutic approaches involve the inhibition or overexpression of ncRNAs. Several approaches to manipulate ncRNAs are currently in use pre-clinically, including miRNA antagonists, miRNA mimics, antisense oligonucleotide (ASO), small interfering RNA (siRNA), and GapmeRs. The first anti-miRNA (Miravirsen) to enter clinical trials is a locked nucleic acid-modified DNA phosphorothioate antisense oligonucleotide targeting miR-122, which sequesters mature miR-122 to treat patients with hepatitis C. Miravirsen is currently in phase 2 clinical trials (Sanchez-Nino and Ortiz, 2013, Janssen et al., 2013). MRX34, a double-stranded miR-34 RNA mimic encapsulated in a liposomal nanoparticle formulation, is the first miRNA mimic to enter phase I clinical trials (Adams et al., 2015). Several antimicroRNA/mimic therapeutics targeting miRNAs are currently under development, including Let-7, miR-21, miR-208, miR-195, miR-221, miR-29, miR-155, miR-10b, and miR-103/107. Four of these miRNA-based therapeutic drugs have entered into phase 1 clinical trials (Trajkovski et al., 2011, Li and Rana, 2014, Xiao et al., 2012, Butovsky et al., 2015, van Rooij and Kauppinen, 2014). Therefore, pharmacological targeting disease related miRNAs is showing promising therapeutic potential and miRNA-based therapeutics can be expected to apply in the human disease treatment.

Despite intensive studies of miRNAs in vascular disease, there are currently no miRNA-based therapeutics entering clinical trials for PAH treatment. The obstacles impeding development of miRNA-based therapeutics are low delivery efficacy to the vasculature and the likely need for repeated delivery, which means that high concentrations with substantial risks of off-target effects are required for vascular delivery. The administration route for miRNA therapies is also an important consideration in the PAH setting. PAH mainly targets the small pulmonary arteries, so ideally, local administration (such as intranasal and intratracheal delivery) direct to the pulmonary circulation should be used to minimise off-target effects and maximise therapeutic effects. Some existing PAH treatments (e.g. aerosolised iloprost and trepostinil) are delivered directly to the lungs via the inhalational

route, enhancing the pulmonary specificity and reducing systemic adverse effects. However this route requires frequent administration and has a tendency to cause airway symptoms (Hill et al., 2015). Formulation of inhalable miRNA drugs and stability of these drugs during the inhalation process are key challenges to solve.

Off-target effects of therapies are a particular concern with miRNAs, as individual miRNAs can target hundreds of mRNAs and direct modulation of miRNAs may lead to off target effects *in vivo* due to the pleiotropic effect of these small RNA molecules. The key function of miRNAs is to regulate their targets to participating the pathophysiological process and the expression levels of miRNAs in different cells and tissues are various. Moreover, directly targeting miRNA target genes in the pre-clinical and clinical setting may prove to be beneficial, while also reducing concerns regarding the diversity of genes targeted by individual miRNAs. Thus, the identification of genuine target genes is key not only to understanding the mechanisms of miRNA action, but also for the development of new PAH treatments. However, despite the challenges of therapeutic modulation of miRNA, pharmacological manipulation of disease-associated miRNAs shows promising therapeutic potential in pre-clinical models of PAH. With more and intensive studies of miRNAs *in vitro* and *in vivo* pre-clinical models and in tissues from human patients, we hope that the application of miRNA-based therapeutics in the clinic can become a reality.

As stated previously, to date there is no specific lncRNA has been intensively investigated in PAH disease. As the important role of lncRNAs in human disease, it is no doubt that the understanding of lncRNAs in the development of PAH will contribute to the disease treatment in the future. In general, there are several obstacles facing the development of lncRNA-based therapeutics. First, the functions of, and mechanisms used by lncRNAs are much more complex and diversified than miRNAs (Ballantyne et al., 2016a). Despite recent advances in our understanding of lncRNA biology, lncRNAs are still largely an “unknown” with regards to their cellular functions and molecular mechanisms. Second, the majority of lncRNAs that localise to the nucleus are thought to act as epigenetic regulators (Djebali et al., 2012). This feature makes it hard to target lncRNAs using siRNA, which is

a potential therapeutic strategy. Recently, *in vivo* animal work using GapmeR-mediated silencing of lncRNA *Chast* (cardiac hypertrophy-associated transcript) prevented and attenuated transverse aortic constriction (TAC)-induced pathological cardiac remodelling with no obvious side-effects (Viereck et al., 2016). This study revealed that inhibition of specific lncRNA by GapmeRs *in vivo* provided a potential therapeutic strategy for the pre-clinical and clinical development of drugs. Third, most lncRNAs lack conservation between species, which restricts the utility of pre-clinical disease models. One possible strategy to overcome these issues is to identify the direct targets of disease-associated lncRNAs and use pre-clinical disease models to assess the therapeutic role of these targets in disease pathogenesis and/or use innovative human-based model systems *ex vivo* and *in vitro*.

In summary, the evidence presented in this thesis extends our understanding of ncRNA biology in the setting of PAH. MiR-143-3p is consistently dysregulated across several small and large animal models of PH, as well as in lung samples from patients with PAH. Genetic ablation and pharmacological inhibition of miR-143-3p protected animals against the development of chronic hypoxia induced PH. Modulation of miR-143-3p had significant effects on pulmonary vascular cell migration, apoptosis and angiogenesis, while miR143-3p in exosomes was shown to mediate crosstalk between PSMCs and PAECs. However, the exact mechanisms involved in the protective role of miR-143 in PAH require further investigation. In addition, we have shown that local delivery of anti-miR-145-5p had no protective effect on PH development compared to systemic delivery, indicating that local anti-miRNA delivery approaches require further refinement before they can be utilised in the pre-clinical setting. Further, our preliminary data have showed modulation of lncRNA *MYOSLID* and *Myolnc16* regulated several signalling pathways related to the pathogenesis of PAH and regulated cell functions in pulmonary vascular cells. Future work will continue focus on the functions and mechanisms of these lncRNAs in the PAH setting.

This thesis has demonstrated the involvement of specific ncRNAs in the development of PAH. In the future perspective, the therapeutic target of these ncRNAs may provide potential treatment strategy in patients with PAH.

## 7 Bibliography

1973. Primary pulmonary hypertension: a fatality during pulmonary angiography. Clinical conference from Boston University School of Medicine. *Chest*, 64, 628-35.
- AARONSON, P. I., ROBERTSON, T. P., KNOCK, G. A., BECKER, S., LEWIS, T. H., SNETKOV, V. & WARD, J. P. 2006. Hypoxic pulmonary vasoconstriction: mechanisms and controversies. *J Physiol*, 570, 53-8.
- ABE, K., TOBA, M., ALZOUBI, A., ITO, M., FAGAN, K. A., COOL, C. D., VOELKEL, N. F., MCMURTRY, I. F. & OKA, M. 2010. Formation of plexiform lesions in experimental severe pulmonary arterial hypertension. *Circulation*, 121, 2747-54.
- ABRAMOVITZ, M., ADAM, M., BOIE, Y., CARRIERE, M., DENIS, D., GODBOUT, C., LAMONTAGNE, S., ROCHETTE, C., SAWYER, N., TREMBLAY, N. M., BELLEY, M., GALLANT, M., DUFRESNE, C., GAREAU, Y., RUEL, R., JUTEAU, H., LABELLE, M., OUIMET, N. & METTERS, K. M. 2000. The utilization of recombinant prostanoid receptors to determine the affinities and selectivities of prostaglandins and related analogs. *Biochim Biophys Acta*, 1483, 285-93.
- ADAMS, B. D., PARSONS, C. & SLACK, F. J. 2015. The tumor-suppressive and potential therapeutic functions of miR-34a in epithelial carcinomas. *Expert Opin Ther Targets*, 1-17.
- AGGARWAL, S., GROSS, C. M., SHARMA, S., FINEMAN, J. R. & BLACK, S. M. 2013. Reactive oxygen species in pulmonary vascular remodeling. *Compr Physiol*, 3, 1011-34.
- AHN, B. H., PARK, H. K., CHO, H. G., LEE, H. A., LEE, Y. M., YANG, E. K. & LEE, W. J. 2003. Estrogen and enalapril attenuate the development of right ventricular hypertrophy induced by monocrotaline in ovariectomized rats. *J Korean Med Sci*, 18, 641-8.
- AKAO, Y., NAKAGAWA, Y. & NAOE, T. 2006. MicroRNAs 143 and 145 are possible common onco-microRNAs in human cancers. *Oncol Rep*, 16, 845-50.
- AL-NEDAWI, K., MEEHAN, B., KERBEL, R. S., ALLISON, A. C. & RAK, J. 2009. Endothelial expression of autocrine VEGF upon the uptake of tumor-derived microvesicles containing oncogenic EGFR. *Proc Natl Acad Sci U S A*, 106, 3794-9.
- ALDRED, M. A., VIJAYAKRISHNAN, J., JAMES, V., SOUBRIER, F., GOMEZ-SANCHEZ, M. A., MARTENSSON, G., GALIE, N., MANES, A., CORRIS, P., SIMONNEAU, G., HUMBERT, M., MORRELL, N. W. & TREMBATH, R. C. 2006. BMPR2 gene rearrangements account for a significant proportion of mutations in familial and idiopathic pulmonary arterial hypertension. *Hum Mutat*, 27, 212-3.
- ALIOTTA, J. M., PEREIRA, M., AMARAL, A., SOROKINA, A., IGBINOBA, Z., HASSLINGER, A., EL-BIZRI, R., ROUNDS, S. I., QUESENBERRY, P. J. & KLINGER, J. R. 2013. Induction of pulmonary hypertensive changes by extracellular vesicles from monocrotaline-treated mice. *Cardiovasc Res*, 100, 354-62.
- ALIOTTA, J. M., PEREIRA, M., WEN, S., DOONER, M. S., DEL TATTO, M., PAPA, E.,

- GOLDBERG, L. R., BAIRD, G. L., VENTETUOLO, C. E., QUESENBERRY, P. J. & KLINGER, J. R. 2016. Exosomes induce and reverse monocrotaline-induced pulmonary hypertension in mice. *Cardiovasc Res*, 110, 319-30.
- AMBARTSUMIAN, N., KLINGELHOFER, J., GRIGORIAN, M., KARLSTROM, O., SIDENIUS, N., GEORGIEV, G. & LUKANIDIN, E. 1998. Tissue-specific posttranscriptional downregulation of expression of the S100A4(mts1) gene in transgenic animals. *Invasion Metastasis*, 18, 96-104.
- AMESHIMA, S., GOLPON, H., COOL, C. D., CHAN, D., VANDIVIER, R. W., GARDAL, S. J., WICK, M., NEMENOFF, R. A., GERACI, M. W. & VOELKEL, N. F. 2003. Peroxisome proliferator-activated receptor gamma (PPARgamma) expression is decreased in pulmonary hypertension and affects endothelial cell growth. *Circ Res*, 92, 1162-9.
- ARCHER, K., BROSKOVA, Z., BAYOUMI, A. S., TEOH, J. P., DAVILA, A., TANG, Y., SU, H. & KIM, I. M. 2015. Long Non-Coding RNAs as Master Regulators in Cardiovascular Diseases. *Int J Mol Sci*, 16, 23651-67.
- ARCHER, S. L., WEIR, E. K. & WILKINS, M. R. 2010. Basic science of pulmonary arterial hypertension for clinicians: new concepts and experimental therapies. *Circulation*, 121, 2045-66.
- ARIAS-STELLA, J. & SALDANA, M. 1963. The Terminal Portion of the Pulmonary Arterial Tree in People Native to High Altitudes. *Circulation*, 28, 915-25.
- ARONOFF, D. M., PERES, C. M., SEREZANI, C. H., BALLINGER, M. N., CARSTENS, J. K., COLEMAN, N., MOORE, B. B., PEEBLES, R. S., FACCIOLI, L. H. & PETERS-GOLDEN, M. 2007. Synthetic prostacyclin analogs differentially regulate macrophage function via distinct analog-receptor binding specificities. *J Immunol*, 178, 1628-34.
- ARRIGO, M. & HUBER, L. C. 2013. Eponyms in cardiopulmonary reflexes. *Am J Cardiol*, 112, 449-53.
- ASLAM, M., BAVEJA, R., LIANG, O. D., FERNANDEZ-GONZALEZ, A., LEE, C., MITSIALIS, S. A. & KOUREMBANAS, S. 2009. Bone marrow stromal cells attenuate lung injury in a murine model of neonatal chronic lung disease. *Am J Respir Crit Care Med*, 180, 1122-30.
- ATKINSON, C., STEWART, S., UPTON, P. D., MACHADO, R., THOMSON, J. R., TREMBATH, R. C. & MORRELL, N. W. 2002. Primary pulmonary hypertension is associated with reduced pulmonary vascular expression of type II bone morphogenetic protein receptor. *Circulation*, 105, 1672-8.
- AUSTIN, E. D., LAHM, T., WEST, J., TOFOVIC, S. P., JOHANSEN, A. K., MACLEAN, M. R., ALZOUBI, A. & OKA, M. 2013. Gender, sex hormones and pulmonary hypertension. *Pulm Circ*, 3, 294-314.
- AUSTIN, E. D. & LOYD, J. E. 2013. Heritable forms of pulmonary arterial hypertension. *Semin Respir Crit Care Med*, 34, 568-80.
- AUSTIN, E. D. & LOYD, J. E. 2014. The genetics of pulmonary arterial hypertension. *Circ Res*, 115, 189-202.
- AUSTIN, E. D., PHILLIPS, J. A., COGAN, J. D., HAMID, R., YU, C., STANTON, K. C., PHILLIPS, C. A., WHEELER, L. A., ROBBINS, I. M., NEWMAN, J. H. & LOYD, J. E. 2009.

- Truncating and missense BMP2 mutations differentially affect the severity of heritable pulmonary arterial hypertension. *Respir Res*, 10, 87.
- BADESCH, D. B., ABMAN, S. H., SIMONNEAU, G., RUBIN, L. J. & MCLAUGHLIN, V. V. 2007. Medical therapy for pulmonary arterial hypertension: updated ACCP evidence-based clinical practice guidelines. *Chest*, 131, 1917-28.
- BADESCH, D. B., RASKOB, G. E., ELLIOTT, C. G., KRICHMAN, A. M., FARBER, H. W., FROST, A. E., BARST, R. J., BENZA, R. L., LIOU, T. G., TURNER, M., GILES, S., FELDKIRCHER, K., MILLER, D. P. & MCGOON, M. D. 2010. Pulmonary arterial hypertension: baseline characteristics from the REVEAL Registry. *Chest*, 137, 376-87.
- BADESCH, D. B., TAPSON, V. F., MCGOON, M. D., BRUNDAGE, B. H., RUBIN, L. J., WIGLEY, F. M., RICH, S., BARST, R. J., BARRETT, P. S., KRAL, K. M., JOBSIS, M. M., LOYD, J. E., MURALI, S., FROST, A., GIRGIS, R., BOURGE, R. C., RALPH, D. D., ELLIOTT, C. G., HILL, N. S., LANGLEBEN, D., SCHILZ, R. J., MCLAUGHLIN, V. V., ROBBINS, I. M., GROVES, B. M., SHAPIRO, S. & MEDSGER, T. A., JR. 2000. Continuous intravenous epoprostenol for pulmonary hypertension due to the scleroderma spectrum of disease. A randomized, controlled trial. *Ann Intern Med*, 132, 425-34.
- BALLANTYNE, M. D., MCDONALD, R. A. & BAKER, A. H. 2016a. lncRNA/MicroRNA interactions in the vasculature. *Clin Pharmacol Ther*, 99, 494-501.
- BALLANTYNE, M. D., PINEL, K., DAKIN, R., VESEY, A. T., DIVER, L., MACKENZIE, R., GARCIA, R., WELSH, P., SATTAR, N., HAMILTON, G., JOSHI, N., DWECK, M. R., MIANO, J. M., MCBRIDE, M. W., NEWBY, D. E., MCDONALD, R. A. & BAKER, A. H. 2016b. Smooth Muscle Enriched Long Non-Coding RNA (SMILR) Regulates Cell Proliferation. *Circulation*.
- BALLANTYNE, M. D., PINEL, K., DAKIN, R., VESEY, A. T., DIVER, L., MACKENZIE, R., GARCIA, R., WELSH, P., SATTAR, N., HAMILTON, G., JOSHI, N., DWECK, M. R., MIANO, J. M., MCBRIDE, M. W., NEWBY, D. E., MCDONALD, R. A. & BAKER, A. H. 2016c. Smooth Muscle Enriched Long Noncoding RNA (SMILR) Regulates Cell Proliferation. *Circulation*, 133, 2050-65.
- BANG, C., BATKAI, S., DANGWAL, S., GUPTA, S. K., FOINQUINOS, A., HOLZMANN, A., JUST, A., REMKE, J., ZIMMER, K., ZEUG, A., PONIMASKIN, E., SCHMIEDL, A., YIN, X., MAYR, M., HALDER, R., FISCHER, A., ENGELHARDT, S., WEI, Y., SCHOBER, A., FIEDLER, J. & THUM, T. 2014. Cardiac fibroblast-derived microRNA passenger strand-enriched exosomes mediate cardiomyocyte hypertrophy. *J Clin Invest*, 124, 2136-46.
- BARST, R. J., RUBIN, L. J., LONG, W. A., MCGOON, M. D., RICH, S., BADESCH, D. B., GROVES, B. M., TAPSON, V. F., BOURGE, R. C., BRUNDAGE, B. H., KOERNER, S. K., LANGLEBEN, D., KELLER, C. A., MURALI, S., URETSKY, B. F., CLAYTON, L. M., JOBSIS, M. M., BLACKBURN, S. D., SHORTINO, D., CROW, J. W. & PRIMARY PULMONARY HYPERTENSION STUDY, G. 1996. A comparison of continuous intravenous epoprostenol (prostacyclin) with conventional therapy for primary pulmonary hypertension. *N Engl J Med*, 334, 296-301.
- BARTEL, D. P. 2004. MicroRNAs: genomics, biogenesis, mechanism, and function. *Cell*,

116, 281-97.

- BARTONICEK, N., MAAG, J. L. & DINGER, M. E. 2016. Long noncoding RNAs in cancer: mechanisms of action and technological advancements. *Mol Cancer*, 15, 43.
- BASKERVILLE, S. & BARTEL, D. P. 2005. Microarray profiling of microRNAs reveals frequent coexpression with neighboring miRNAs and host genes. *RNA*, 11, 241-7.
- BATISTA, P. J. & CHANG, H. Y. 2013. Long noncoding RNAs: cellular address codes in development and disease. *Cell*, 152, 1298-307.
- BEACH, A., ZHANG, H. G., RATAJCZAK, M. Z. & KAKAR, S. S. 2014. Exosomes: an overview of biogenesis, composition and role in ovarian cancer. *J Ovarian Res*, 7, 14.
- BELL, R. D., LONG, X., LIN, M., BERGMANN, J. H., NANDA, V., COWAN, S. L., ZHOU, Q., HAN, Y., SPECTOR, D. L., ZHENG, D. & MIANO, J. M. 2014. Identification and initial functional characterization of a human vascular cell-enriched long noncoding RNA. *Arterioscler Thromb Vasc Biol*, 34, 1249-59.
- BENNETT, J. A., RIEGEL, B., BITTNER, V. & NICHOLS, J. 2002. Validity and reliability of the NYHA classes for measuring research outcomes in patients with cardiac disease. *Heart Lung*, 31, 262-70.
- BENZA, R. L., MILLER, D. P., GOMBERG-MAITLAND, M., FRANTZ, R. P., FOREMAN, A. J., COFFEY, C. S., FROST, A., BARST, R. J., BADESCH, D. B., ELLIOTT, C. G., LIOU, T. G. & MCGOON, M. D. 2010. Predicting survival in pulmonary arterial hypertension: insights from the Registry to Evaluate Early and Long-Term Pulmonary Arterial Hypertension Disease Management (REVEAL). *Circulation*, 122, 164-72.
- BEPPU, H., ICHINOSE, F., KAWAI, N., JONES, R. C., YU, P. B., ZAPOL, W. M., MIYAZONO, K., LI, E. & BLOCH, K. D. 2004. BMPR-II heterozygous mice have mild pulmonary hypertension and an impaired pulmonary vascular remodeling response to prolonged hypoxia. *Am J Physiol Lung Cell Mol Physiol*, 287, L1241-7.
- BEPPU, H., KAWABATA, M., HAMAMOTO, T., CHYTIL, A., MINOWA, O., NODA, T. & MIYAZONO, K. 2000. BMP type II receptor is required for gastrulation and early development of mouse embryos. *Dev Biol*, 221, 249-58.
- BESNARD, A. G., STRUYF, S., GUABIRABA, R., FAUCONNIER, L., ROUXEL, N., PROOST, P., UYTENHOVE, C., VAN SNICK, J., COUILLIN, I. & RYFFEL, B. 2013. CXCL6 antibody neutralization prevents lung inflammation and fibrosis in mice in the bleomycin model. *J Leukoc Biol*, 94, 1317-23.
- BHARGAVA, A., KUMAR, A., YUAN, N., GEWITZ, M. H. & MATHEW, R. 1999. Monocrotaline induces interleukin-6 mRNA expression in rat lungs. *Heart Dis*, 1, 126-32.
- BIAN, Z. M., ELNER, S. G., YOSHIDA, A., KUNKEL, S. L., SU, J. & ELNER, V. M. 2001. Activation of p38, ERK1/2 and NIK pathways is required for IL-1beta and TNF-alpha-induced chemokine expression in human retinal pigment epithelial cells. *Exp Eye Res*, 73, 111-21.
- BIENERTOVA-VASKU, J., NOVAK, J. & VASKU, A. 2015. MicroRNAs in pulmonary arterial hypertension: pathogenesis, diagnosis and treatment. *J Am Soc Hypertens*, 9, 221-34.

- BILLAUD, M., LOHMAN, A. W., JOHNSTONE, S. R., BIWER, L. A., MUTCHLER, S. & ISAKSON, B. E. 2014. Regulation of cellular communication by signaling microdomains in the blood vessel wall. *Pharmacol Rev*, 66, 513-69.
- BOCKMEYER, C. L., MAEGEL, L., JANCIAUSKIENE, S., RISCHE, J., LEHMANN, U., MAUS, U. A., NICKEL, N., HAVERICH, A., HOEPER, M. M., GOLPON, H. A., KREIPE, H., LAENGER, F. & JONIGK, D. 2012. Plexiform vasculopathy of severe pulmonary arterial hypertension and microRNA expression. *J Heart Lung Transplant*, 31, 764-72.
- BOETTGER, T., BEETZ, N., KOSTIN, S., SCHNEIDER, J., KRUGER, M., HEIN, L. & BRAUN, T. 2009. Acquisition of the contractile phenotype by murine arterial smooth muscle cells depends on the Mir143/145 gene cluster. *J Clin Invest*, 119, 2634-47.
- BONCI, D. 2010. MicroRNA-21 as therapeutic target in cancer and cardiovascular disease. *Recent Pat Cardiovasc Drug Discov*, 5, 156-61.
- BONNET, S., ROCHEFORT, G., SUTENDRA, G., ARCHER, S. L., HAROMY, A., WEBSTER, L., HASHIMOTO, K., BONNET, S. N. & MICHELAKIS, E. D. 2007. The nuclear factor of activated T cells in pulmonary arterial hypertension can be therapeutically targeted. *Proc Natl Acad Sci U S A*, 104, 11418-23.
- BOOTON, R. & LINDSAY, M. A. 2014. Emerging role of MicroRNAs and long noncoding RNAs in respiratory disease. *Chest*, 146, 193-204.
- BOTTAI, G., PASCULLI, B., CALIN, G. A. & SANTARPIA, L. 2014. Targeting the microRNA-regulating DNA damage/repair pathways in cancer. *Expert Opin Biol Ther*, 14, 1667-83.
- BOTTI, G., MARRA, L., MALZONE, M. G., ANNICIELLO, A., BOTTI, C., FRANCO, R. & CANTILE, M. 2015. LncRNA HOTAIR as prognostic circulating marker and potential therapeutic target in patients with tumor diseases. *Curr Drug Targets*.
- BOUCHERAT, O., POTUS, F. & BONNET, S. 2015. microRNA and Pulmonary Hypertension. *Adv Exp Med Biol*, 888, 237-52.
- BOULBERDAA, M., SCOTT, E., BALLANTYNE, M., GARCIA, R., DESCAMPS, B., ANGELINI, G. D., BRITTAN, M., HUNTER, A., MCBRIDE, M., MCCLURE, J., MIANO, J. M., EMANUELI, C., MILLS, N. L., MOUNTFORD, J. C. & BAKER, A. H. 2016. A Role for the Long Noncoding RNA SENCER in Commitment and Function of Endothelial Cells. *Mol Ther*.
- BRAUER, P. R. 2006. MMPs--role in cardiovascular development and disease. *Front Biosci*, 11, 447-78.
- BRESLOW, J. L. 1996. Mouse models of atherosclerosis. *Science*, 272, 685-8.
- BROCK, M., SAMILLAN, V. J., TRENKMANN, M., SCHWARZWALD, C., ULRICH, S., GAY, R. E., GASSMANN, M., OSTERGAARD, L., GAY, S., SPEICH, R. & HUBER, L. C. 2014. AntagomiR directed against miR-20a restores functional BMP2 signalling and prevents vascular remodelling in hypoxia-induced pulmonary hypertension. *Eur Heart J*, 35, 3203-11.
- BROCK, M., TRENKMANN, M., GAY, R. E., MICHEL, B. A., GAY, S., FISCHLER, M., ULRICH, S., SPEICH, R. & HUBER, L. C. 2009. Interleukin-6 modulates the expression of the bone morphogenic protein receptor type II through a novel

- STAT3-microRNA cluster 17/92 pathway. *Circ Res*, 104, 1184-91.
- BUERMANS, H. P., REDOUT, E. M., SCHIEL, A. E., MUSTERS, R. J., ZUIDWIJK, M., EIJK, P. P., VAN HARDEVELD, C., KASANMOENTALIB, S., VISSER, F. C., YLSTRA, B. & SIMONIDES, W. S. 2005. Microarray analysis reveals pivotal divergent mRNA expression profiles early in the development of either compensated ventricular hypertrophy or heart failure. *Physiol Genomics*, 21, 314-23.
- BULL, T. M., COLDREN, C. D., GERACI, M. W. & VOELKEL, N. F. 2007. Gene expression profiling in pulmonary hypertension. *Proc Am Thorac Soc*, 4, 117-20.
- BURKE, D. L., FRID, M. G., KUNRATH, C. L., KAROOR, V., ANWAR, A., WAGNER, B. D., STRASSHEIM, D. & STENMARK, K. R. 2009. Sustained hypoxia promotes the development of a pulmonary artery-specific chronic inflammatory microenvironment. *Am J Physiol Lung Cell Mol Physiol*, 297, L238-50.
- BUTOVSKY, O., JEDRYCHOWSKI, M. P., CIALIC, R., KRASEMANN, S., MURUGAIYAN, G., FANEK, Z., GRECO, D. J., WU, P. M., DOYKAN, C. E., KINER, O., LAWSON, R. J., FROSCH, M. P., POCHET, N., FATIMY, R. E., KRICHEVSKY, A. M., GYGI, S. P., LASSMANN, H., BERRY, J., CUDKOWICZ, M. E. & WEINER, H. L. 2015. Targeting miR-155 restores abnormal microglia and attenuates disease in SOD1 mice. *Ann Neurol*, 77, 75-99.
- CABILI, M. N., TRAPNELL, C., GOFF, L., KOZIOL, M., TAZON-VEGA, B., REGEV, A. & RINN, J. L. 2011. Integrative annotation of human large intergenic noncoding RNAs reveals global properties and specific subclasses. *Genes Dev*, 25, 1915-27.
- CABY, M. P., LANKAR, D., VINCENDEAU-SCHERRER, C., RAPOSO, G. & BONNEROT, C. 2005. Exosomal-like vesicles are present in human blood plasma. *Int Immunol*, 17, 879-87.
- CAI, X., HAGEDORN, C. H. & CULLEN, B. R. 2004. Human microRNAs are processed from capped, polyadenylated transcripts that can also function as mRNAs. *RNA*, 10, 1957-66.
- CAI, Y., HAN, M., LUO, L., SONG, W. & ZHOU, X. 1996. Increased expression of PDGF and c-myc genes in lungs and pulmonary arteries of pulmonary hypertensive rats induced by hypoxia. *Chin Med Sci J*, 11, 152-6.
- CALIN, G. A., SEVIGNANI, C., DUMITRU, C. D., HYSLOP, T., NOCH, E., YENDAMURI, S., SHIMIZU, M., RATTAN, S., BULLRICH, F., NEGRINI, M. & CROCE, C. M. 2004. Human microRNA genes are frequently located at fragile sites and genomic regions involved in cancers. *Proc Natl Acad Sci U S A*, 101, 2999-3004.
- CAMPION, M. E., HARDZIYENKA, M., DE BRUIN, K., VAN ECK-SMIT, B. L., DE BAKKER, J. M., VERBERNE, H. J. & TAN, H. L. 2010. Early inflammatory response during the development of right ventricular heart failure in a rat model. *Eur J Heart Fail*, 12, 653-8.
- CAMPION, M. E., HARDZIYENKA, M., MICHEL, M. C. & TAN, H. L. 2006. How valid are animal models to evaluate treatments for pulmonary hypertension? *Naunyn Schmiedebergs Arch Pharmacol*, 373, 391-400.
- CARUSO, P., DEMPSIE, Y., STEVENS, H. C., MCDONALD, R. A., LONG, L., LU, R., WHITE, K., MAIR, K. M., MCCLURE, J. D., SOUTHWOOD, M., UPTON, P., XIN, M., VAN ROOIJ, E., OLSON, E. N., MORRELL, N. W., MACLEAN, M. R. & BAKER, A. H. 2012. A role

- for miR-145 in pulmonary arterial hypertension: evidence from mouse models and patient samples. *Circ Res*, 111, 290-300.
- CARUSO, P., MACLEAN, M. R., KHANIN, R., MCCLURE, J., SOON, E., SOUTHGATE, M., MACDONALD, R. A., GREIG, J. A., ROBERTSON, K. E., MASSON, R., DENBY, L., DEMPSIE, Y., LONG, L., MORRELL, N. W. & BAKER, A. H. 2010. Dynamic changes in lung microRNA profiles during the development of pulmonary hypertension due to chronic hypoxia and monocrotaline. *Arterioscler Thromb Vasc Biol*, 30, 716-23.
- CECH, T. R. & STEITZ, J. A. 2014. The noncoding RNA revolution-trashing old rules to forge new ones. *Cell*, 157, 77-94.
- CHANG, Y. N., ZHANG, K., HU, Z. M., QI, H. X., SHI, Z. M., HAN, X. H., HAN, Y. W. & HONG, W. 2016. Hypoxia-regulated lncRNAs in cancer. *Gene*, 575, 1-8.
- CHANNICK, R. N., SIMONNEAU, G., SITBON, O., ROBBINS, I. M., FROST, A., TAPSON, V. F., BADESCH, D. B., ROUX, S., RAINISIO, M., BODIN, F. & RUBIN, L. J. 2001. Effects of the dual endothelin-receptor antagonist bosentan in patients with pulmonary hypertension: a randomised placebo-controlled study. *Lancet*, 358, 1119-23.
- CHEMLA, D., CASTELAIN, V., HERVE, P., LECARPENTIER, Y. & BRIMIOULLE, S. 2002. Haemodynamic evaluation of pulmonary hypertension. *Eur Respir J*, 20, 1314-31.
- CHEN, C. N., WATSON, G. & ZHAO, L. 2013. Cyclic guanosine monophosphate signalling pathway in pulmonary arterial hypertension. *Vascul Pharmacol*, 58, 211-8.
- CHEN, J. Y., AN, R., LIU, Z. J., WANG, J. J., CHEN, S. Z., HONG, M. M., LIU, J. H., XIAO, M. Y. & CHEN, Y. F. 2014a. Therapeutic effects of mesenchymal stem cell-derived microvesicles on pulmonary arterial hypertension in rats. *Acta Pharmacol Sin*, 35, 1121-8.
- CHEN, T., ZHOU, G., ZHOU, Q., TANG, H., IBE, J. C., CHENG, H., GOU, D., CHEN, J., YUAN, J. X. & RAJ, J. U. 2015. Loss of microRNA-17 approximately 92 in smooth muscle cells attenuates experimental pulmonary hypertension via induction of PDZ and LIM domain 5. *Am J Respir Crit Care Med*, 191, 678-92.
- CHEN, W. X., LIU, X. M., LV, M. M., CHEN, L., ZHAO, J. H., ZHONG, S. L., JI, M. H., HU, Q., LUO, Z., WU, J. Z. & TANG, J. H. 2014b. Exosomes from drug-resistant breast cancer cells transmit chemoresistance by a horizontal transfer of microRNAs. *PLoS One*, 9, e95240.
- CHENG, H., KIMURA, K., PETER, A. K., CUI, L., OUYANG, K., SHEN, T., LIU, Y., GU, Y., DALTON, N. D., EVANS, S. M., KNOWLTON, K. U., PETERSON, K. L. & CHEN, J. 2010. Loss of enigma homolog protein results in dilated cardiomyopathy. *Circ Res*, 107, 348-56.
- CHENG, Y., LIU, X., YANG, J., LIN, Y., XU, D. Z., LU, Q., DEITCH, E. A., HUO, Y., DELPHIN, E. S. & ZHANG, C. 2009. MicroRNA-145, a novel smooth muscle cell phenotypic marker and modulator, controls vascular neointimal lesion formation. *Circ Res*, 105, 158-66.
- CHESNEY, C. F. & ALLEN, J. R. 1973a. Endocardial fibrosis associated with monocrotaline-induced pulmonary hypertension in nonhuman primates (*Macaca arctoides*). *Am J Vet Res*, 34, 1577-81.

- CHESNEY, C. F. & ALLEN, J. R. 1973b. Monocrotaline induced pulmonary vascular lesions in non-human primates. *Cardiovasc Res*, 7, 508-18.
- CHESTER, A. H. & YACOUB, M. H. 2014. The role of endothelin-1 in pulmonary arterial hypertension. *Glob Cardiol Sci Pract*, 2014, 62-78.
- CHISTIYAKOV, D. A., SOBENIN, I. A., OREKHOV, A. N. & BOBRY SHEV, Y. V. 2015. Human miR-221/222 in Physiological and Atherosclerotic Vascular Remodeling. *Biomed Res Int*, 2015, 354517.
- CHRISTMAN, B. W., MCPHERSON, C. D., NEWMAN, J. H., KING, G. A., BERNARD, G. R., GROVES, B. M. & LOYD, J. E. 1992. An imbalance between the excretion of thromboxane and prostacyclin metabolites in pulmonary hypertension. *N Engl J Med*, 327, 70-5.
- CHUNG, E. S., PACKER, M., LO, K. H., FASANMADE, A. A., WILLERSON, J. T. & ANTI, T. N. F. T. A. C. H. F. I. 2003. Randomized, double-blind, placebo-controlled, pilot trial of infliximab, a chimeric monoclonal antibody to tumor necrosis factor-alpha, in patients with moderate-to-severe heart failure: results of the anti-TNF Therapy Against Congestive Heart Failure (ATTACH) trial. *Circulation*, 107, 3133-40.
- CHURCH, A. C., MARTIN, D. H., WADSWORTH, R., BRYSON, G., FISHER, A. J., WELSH, D. J. & PEACOCK, A. J. 2015. The reversal of pulmonary vascular remodeling through inhibition of p38 MAPK-alpha: a potential novel anti-inflammatory strategy in pulmonary hypertension. *Am J Physiol Lung Cell Mol Physiol*, 309, L333-47.
- CIARDIELLO, C., CAVALLINI, L., SPINELLI, C., YANG, J., REIS-SOBREIRO, M., DE CANDIA, P., MINCIACCHI, V. R. & DI VIZIO, D. 2016. Focus on Extracellular Vesicles: New Frontiers of Cell-to-Cell Communication in Cancer. *Int J Mol Sci*, 17.
- CIUCLAN, L., BONNEAU, O., HUSSEY, M., DUGGAN, N., HOLMES, A. M., GOOD, R., STRINGER, R., JONES, P., MORRELL, N. W., JARAI, G., WALKER, C., WESTWICK, J. & THOMAS, M. 2011. A novel murine model of severe pulmonary arterial hypertension. *Am J Respir Crit Care Med*, 184, 1171-82.
- CIUCLAN, L., HUSSEY, M. J., BURTON, V., GOOD, R., DUGGAN, N., BEACH, S., JONES, P., FOX, R., CLAY, I., BONNEAU, O., KONSTANTINOVA, I., PEARCE, A., ROWLANDS, D. J., JARAI, G., WESTWICK, J., MACLEAN, M. R. & THOMAS, M. 2013. Imatinib attenuates hypoxia-induced pulmonary arterial hypertension pathology via reduction in 5-hydroxytryptamine through inhibition of tryptophan hydroxylase 1 expression. *Am J Respir Crit Care Med*, 187, 78-89.
- CLIMENT, M., QUINTAVALLE, M., MIRAGOLI, M., CHEN, J., CONDORELLI, G. & ELIA, L. 2015. TGFbeta Triggers miR-143/145 Transfer From Smooth Muscle Cells to Endothelial Cells, Thereby Modulating Vessel Stabilization. *Circ Res*, 116, 1753-64.
- COGAN, J. D., PAUCIUOLO, M. W., BATCHMAN, A. P., PRINCE, M. A., ROBBINS, I. M., HEDGES, L. K., STANTON, K. C., WHEELER, L. A., PHILLIPS, J. A., 3RD, LOYD, J. E. & NICHOLS, W. C. 2006. High frequency of BMPR2 exonic deletions/duplications in familial pulmonary arterial hypertension. *Am J Respir Crit Care Med*, 174, 590-8.

- COLOMBO, M., RAPOSO, G. & THERY, C. 2014. Biogenesis, secretion, and intercellular interactions of exosomes and other extracellular vesicles. *Annu Rev Cell Dev Biol*, 30, 255-89.
- COMROE, J. H., JR. 1966. The main functions of the pulmonary circulation. *Circulation*, 33, 146-58.
- CONGRAINS, A., KAMIDE, K., KATSUYA, T., YASUDA, O., OGURO, R., YAMAMOTO, K., OHISHI, M. & RAKUGI, H. 2012a. CVD-associated non-coding RNA, ANRIL, modulates expression of atherogenic pathways in VSMC. *Biochem Biophys Res Commun*, 419, 612-6.
- CONGRAINS, A., KAMIDE, K., OGURO, R., YASUDA, O., MIYATA, K., YAMAMOTO, E., KAWAI, T., KUSUNOKI, H., YAMAMOTO, H., TAKEYA, Y., YAMAMOTO, K., ONISHI, M., SUGIMOTO, K., KATSUYA, T., AWATA, N., IKEBE, K., GONDO, Y., OIKE, Y., OHISHI, M. & RAKUGI, H. 2012b. Genetic variants at the 9p21 locus contribute to atherosclerosis through modulation of ANRIL and CDKN2A/B. *Atherosclerosis*, 220, 449-55.
- CONIGLIARO, A., COSTA, V., LO DICO, A., SAEVA, L., BUCCHERI, S., DIELI, F., MANNO, M., RACCOSTA, S., MANCONE, C., TRIPODI, M., DE LEO, G. & ALESSANDRO, R. 2015. CD90+ liver cancer cells modulate endothelial cell phenotype through the release of exosomes containing H19 lncRNA. *Mol Cancer*, 14, 155.
- CONSORTIUM, E. P. 2004. The ENCODE (ENCyclopedia Of DNA Elements) Project. *Science*, 306, 636-40.
- COOL, C. D., GROSHONG, S. D., OAKEY, J. & VOELKEL, N. F. 2005. Pulmonary hypertension: cellular and molecular mechanisms. *Chest*, 128, 565S-571S.
- COOL, C. D., STEWART, J. S., WERAHERA, P., MILLER, G. J., WILLIAMS, R. L., VOELKEL, N. F. & TUDER, R. M. 1999. Three-dimensional reconstruction of pulmonary arteries in plexiform pulmonary hypertension using cell-specific markers. Evidence for a dynamic and heterogeneous process of pulmonary endothelial cell growth. *Am J Pathol*, 155, 411-9.
- CORBIN, J. D., BEASLEY, A., BLOUNT, M. A. & FRANCIS, S. H. 2005. High lung PDE5: a strong basis for treating pulmonary hypertension with PDE5 inhibitors. *Biochem Biophys Res Commun*, 334, 930-8.
- CORDES, K. R., SHEEHY, N. T., WHITE, M. P., BERRY, E. C., MORTON, S. U., MUTH, A. N., LEE, T. H., MIANO, J. M., IVEY, K. N. & SRIVASTAVA, D. 2009. miR-145 and miR-143 regulate smooth muscle cell fate and plasticity. *Nature*, 460, 705-10.
- COURBOULIN, A., BARRIER, M., PERREAULT, T., BONNET, P., TREMBLAY, V. L., PAULIN, R., TREMBLAY, E., LAMBERT, C., JACOB, M. H., BONNET, S. N., PROVENCHER, S. & BONNET, S. 2012. Plumbagin reverses proliferation and resistance to apoptosis in experimental PAH. *Eur Respir J*, 40, 618-29.
- COURBOULIN, A., PAULIN, R., GIGUERE, N. J., SAKSOUK, N., PERREAULT, T., MELOCHE, J., PAQUET, E. R., BIARDEL, S., PROVENCHER, S., COTE, J., SIMARD, M. J. & BONNET, S. 2011. Role for miR-204 in human pulmonary arterial hypertension. *J Exp Med*, 208, 535-48.
- COURBOULIN, A., RANCHOUX, B., COHEN-KAMINSKY, S., PERROS, F. & BONNET, S. 2016. MicroRNA networks in pulmonary arterial hypertension: share

- mechanisms with cancer? *Curr Opin Oncol*, 28, 72-82.
- CROSSWHITE, P. & SUN, Z. 2014. Molecular mechanisms of pulmonary arterial remodeling. *Mol Med*, 20, 191-201.
- D'ALONZO, G. E., BARST, R. J., AYRES, S. M., BERGOFSKY, E. H., BRUNDAGE, B. H., DETRE, K. M., FISHMAN, A. P., GOLDRING, R. M., GROVES, B. M., KERNIS, J. T. & ET AL. 1991. Survival in patients with primary pulmonary hypertension. Results from a national prospective registry. *Ann Intern Med*, 115, 343-9.
- DAHAL, B. K., KOSANOVIC, D., KAULEN, C., CORNITESCU, T., SAVAI, R., HOFFMANN, J., REISS, I., GHOFrani, H. A., WEISSMANN, N., KUEBLER, W. M., SEEGER, W., GRIMMINGER, F. & SCHERMULY, R. T. 2011. Involvement of mast cells in monocrotaline-induced pulmonary hypertension in rats. *Respir Res*, 12, 60.
- DAS, M., BOUCHEY, D. M., MOORE, M. J., HOPKINS, D. C., NEMENOFF, R. A. & STENMARK, K. R. 2001. Hypoxia-induced proliferative response of vascular adventitial fibroblasts is dependent on g protein-mediated activation of mitogen-activated protein kinases. *J Biol Chem*, 276, 15631-40.
- DAS, M., DEMPSEY, E. C., BOUCHEY, D., REYLAND, M. E. & STENMARK, K. R. 2000. Chronic hypoxia induces exaggerated growth responses in pulmonary artery adventitial fibroblasts: potential contribution of specific protein kinase c isozymes. *Am J Respir Cell Mol Biol*, 22, 15-25.
- DAS, M., DEMPSEY, E. C., REEVES, J. T. & STENMARK, K. R. 2002. Selective expansion of fibroblast subpopulations from pulmonary artery adventitia in response to hypoxia. *Am J Physiol Lung Cell Mol Physiol*, 282, L976-86.
- DAS, M., FESSEL, J., TANG, H. & WEST, J. 2012. A process-based review of mouse models of pulmonary hypertension. *Pulm Circ*, 2, 415-33.
- DAVIE, N., HALEEN, S. J., UPTON, P. D., POLAK, J. M., YACOUB, M. H., MORRELL, N. W. & WHARTON, J. 2002. ET(A) and ET(B) receptors modulate the proliferation of human pulmonary artery smooth muscle cells. *Am J Respir Crit Care Med*, 165, 398-405.
- DAVIES, R. J., HOLMES, A. M., DEIGHTON, J., LONG, L., YANG, X., BARKER, L., WALKER, C., BUDD, D. C., UPTON, P. D. & MORRELL, N. W. 2012. BMP type II receptor deficiency confers resistance to growth inhibition by TGF-beta in pulmonary artery smooth muscle cells: role of proinflammatory cytokines. *Am J Physiol Lung Cell Mol Physiol*, 302, L604-15.
- DAVIS, E., CAIMENT, F., TORDOIR, X., CAVAILLE, J., FERGUSON-SMITH, A., COCKETT, N., GEORGES, M. & CHARLIER, C. 2005. RNAi-mediated allelic trans-interaction at the imprinted Rtl1/Peg11 locus. *Curr Biol*, 15, 743-9.
- DAVIS-DUSENBERY, B. N., CHAN, M. C., RENO, K. E., WEISMAN, A. S., LAYNE, M. D., LAGNA, G. & HATA, A. 2011. down-regulation of Kruppel-like factor-4 (KLF4) by microRNA-143/145 is critical for modulation of vascular smooth muscle cell phenotype by transforming growth factor-beta and bone morphogenetic protein 4. *J Biol Chem*, 286, 28097-110.
- DE BONT, R. & VAN LAREBEKE, N. 2004. Endogenous DNA damage in humans: a review of quantitative data. *Mutagenesis*, 19, 169-85.
- DELCROIX, M. & HOWARD, L. 2015. Pulmonary arterial hypertension: the burden of

- disease and impact on quality of life. *Eur Respir Rev*, 24, 621-9.
- DEMPSEY, E. C., WICK, M. J., KAROOR, V., BARR, E. J., TALLMAN, D. W., WEHLING, C. A., WALCHAK, S. J., LAUDI, S., LE, M., OKA, M., MAJKA, S., COOL, C. D., FAGAN, K. A., KLEMM, D. J., HERSH, L. B., GERARD, N. P., GERARD, C. & MILLER, Y. E. 2009. Nprilysin null mice develop exaggerated pulmonary vascular remodeling in response to chronic hypoxia. *Am J Pathol*, 174, 782-96.
- DENG, H., HERSHENSON, M. B., LEI, J., ANYANWU, A. C., PINSKY, D. J. & BENTLEY, J. K. 2010. Pulmonary artery smooth muscle hypertrophy: roles of glycogen synthase kinase-3beta and p70 ribosomal S6 kinase. *Am J Physiol Lung Cell Mol Physiol*, 298, L793-803.
- DENG, L., BLANCO, F. J., STEVENS, H., LU, R., CAUDRILLIER, A., MCBRIDE, M., MCCLURE, J. D., GRANT, J., THOMAS, M., FRID, M., STENMARK, K., WHITE, K., SETO, A. G., MORRELL, N. W., BRADSHAW, A. C., MACLEAN, M. R. & BAKER, A. H. 2015. MicroRNA-143 Activation Regulates Smooth Muscle and Endothelial Cell Crosstalk in Pulmonary Arterial Hypertension. *Circ Res*, 117, 870-83.
- DERRIEN, T., JOHNSON, R., BUSSOTTI, G., TANZER, A., DJEBALI, S., TILGNER, H., GUERNEC, G., MARTIN, D., MERKEL, A., KNOWLES, D. G., LAGARDE, J., VEERAVALLI, L., RUAN, X., RUAN, Y., LASSMANN, T., CARNINCI, P., BROWN, J. B., LIPOVICH, L., GONZALEZ, J. M., THOMAS, M., DAVIS, C. A., SHIEKHATTAR, R., GINGERAS, T. R., HUBBARD, T. J., NOTREDAME, C., HARROW, J. & GUIGO, R. 2012. The GENCODE v7 catalog of human long noncoding RNAs: analysis of their gene structure, evolution, and expression. *Genome Res*, 22, 1775-89.
- DERYNCK, R. & ZHANG, Y. E. 2003. Smad-dependent and Smad-independent pathways in TGF-beta family signalling. *Nature*, 425, 577-84.
- DESMOULIERE, A., CHAPONNIER, C. & GABBIANI, G. 2005. Tissue repair, contraction, and the myofibroblast. *Wound Repair Regen*, 13, 7-12.
- DEWACHTER, L., ADNOT, S., FADEL, E., HUMBERT, M., MAITRE, B., BARLIER-MUR, A. M., SIMONNEAU, G., HAMON, M., NAEIJE, R. & EDDAHIBI, S. 2006. Angiopoietin/Tie2 pathway influences smooth muscle hyperplasia in idiopathic pulmonary hypertension. *Am J Respir Crit Care Med*, 174, 1025-33.
- DEWACHTER, L., ADNOT, S., GUIGNABERT, C., TU, L., MARCOS, E., FADEL, E., HUMBERT, M., DARTEVELLE, P., SIMONNEAU, G., NAEIJE, R. & EDDAHIBI, S. 2009. Bone morphogenetic protein signalling in heritable versus idiopathic pulmonary hypertension. *Eur Respir J*, 34, 1100-10.
- DEYO, J. A. & KERKVLIT, N. I. 1990. Immunotoxicity of the pyrrolizidine alkaloid monocrotaline following subchronic administration to C57Bl/6 mice. *Fundam Appl Toxicol*, 14, 842-9.
- DEYO, J. A. & KERKVLIT, N. I. 1991. Tier-2 studies on monocrotaline immunotoxicity in C57BL/6 mice. *Toxicology*, 70, 313-25.
- DI SALVO, T. G., GUO, Y., SU, Y. R., CLARK, T., BRITTAI, E., ABSI, T., MALTAIS, S. & HEMNES, A. 2015. Right ventricular long noncoding RNA expression in human heart failure. *Pulm Circ*, 5, 135-61.
- DIAMANT, M., TUSHUIZEN, M. E., STURK, A. & NIEUWLAND, R. 2004. Cellular microparticles: new players in the field of vascular disease? *Eur J Clin Invest*, 34,

392-401.

- DING, K., YIN, Y., CAO, K., CHRISTENSEN, G. E., LIN, C. L., HOFFMAN, E. A. & REINHARDT, J. M. 2009. Evaluation of lobar biomechanics during respiration using image registration. *Med Image Comput Comput Assist Interv*, 12, 739-46.
- DJEBALI, S., DAVIS, C. A., MERKEL, A., DOBIN, A., LASSMANN, T., MORTAZAVI, A., TANZER, A., LAGARDE, J., LIN, W., SCHLESINGER, F., XUE, C., MARINOV, G. K., KHATUN, J., WILLIAMS, B. A., ZALESKI, C., ROZOWSKY, J., RODER, M., KOKOCINSKI, F., ABDELHAMID, R. F., ALIOTO, T., ANTOSHECHKIN, I., BAER, M. T., BAR, N. S., BATUT, P., BELL, K., BELL, I., CHAKRABORTTY, S., CHEN, X., CHRAST, J., CURADO, J., DERRIEN, T., DRENKOW, J., DUMAIS, E., DUMAIS, J., DUTTAGUPTA, R., FALCONNET, E., FASTUCA, M., FEJES-TOTH, K., FERREIRA, P., FOISSAC, S., FULLWOOD, M. J., GAO, H., GONZALEZ, D., GORDON, A., GUNAWARDENA, H., HOWALD, C., JHA, S., JOHNSON, R., KAPRANOV, P., KING, B., KINGSWOOD, C., LUO, O. J., PARK, E., PERSAUD, K., PREALL, J. B., RIBECA, P., RISK, B., ROBYR, D., SAMMETH, M., SCHAFFER, L., SEE, L. H., SHAHAB, A., SKANCKE, J., SUZUKI, A. M., TAKAHASHI, H., TILGNER, H., TROUT, D., WALTERS, N., WANG, H., WROBEL, J., YU, Y., RUAN, X., HAYASHIZAKI, Y., HARROW, J., GERSTEIN, M., HUBBARD, T., REYMOND, A., ANTONARAKIS, S. E., HANNON, G., GIDDINGS, M. C., RUAN, Y., WOLD, B., CARNINCI, P., GUIGO, R. & GINGERAS, T. R. 2012. Landscape of transcription in human cells. *Nature*, 489, 101-8.
- DORA, K. A. 2001. Cell-cell communication in the vessel wall. *Vasc Med*, 6, 43-50.
- DORFMULLER, P. & HUMBERT, M. 2012. Progress in pulmonary arterial hypertension pathology: relighting a torch inside the tunnel. *Am J Respir Crit Care Med*, 186, 210-2.
- DORFMULLER, P., MONTANI, D. & HUMBERT, M. 2010. Beyond arterial remodelling: pulmonary venous and cardiac involvement in patients with systemic sclerosis-associated pulmonary arterial hypertension. *Eur Respir J*, 35, 6-8.
- DORFMULLER, P., PERROS, F., BALABANIAN, K. & HUMBERT, M. 2003. Inflammation in pulmonary arterial hypertension. *Eur Respir J*, 22, 358-63.
- DRAGOVIC, R. A., GARDINER, C., BROOKS, A. S., TANNETTA, D. S., FERGUSON, D. J., HOLE, P., CARR, B., REDMAN, C. W., HARRIS, A. L., DOBSON, P. J., HARRISON, P. & SARGENT, I. L. 2011. Sizing and phenotyping of cellular vesicles using Nanoparticle Tracking Analysis. *Nanomedicine*, 7, 780-8.
- DRESDALE, D. T., SCHULTZ, M. & MICHOM, R. J. 1951. Primary pulmonary hypertension. I. Clinical and hemodynamic study. *Am J Med*, 11, 686-705.
- DREXLER, E. S., BISCHOFF, J. E., SLIFKA, A. J., MCCOWAN, C. N., QUINN, T. P., SHANDAS, R., IVY, D. D. & STENMARK, K. R. 2008. Stiffening of the Extrapulmonary Arteries From Rats in Chronic Hypoxic Pulmonary Hypertension. *J Res Natl Inst Stand Technol*, 113, 239-49.
- DU, T. & ZAMORE, P. D. 2005. microPrimer: the biogenesis and function of microRNA. *Development*, 132, 4645-52.
- DUMITRASCU, R., KOEBRICH, S., DONY, E., WEISSMANN, N., SAVAI, R., PULLAMSETTI, S. S., GHOFrani, H. A., SAMIDURAI, A., TRAUPE, H., SEEGER, W., GRIMMINGER, F. & SCHERMULY, R. T. 2008. Characterization of a murine model of

- monocrotaline pyrrole-induced acute lung injury. *BMC Pulm Med*, 8, 25.
- DURMOWICZ, A. G., PARKS, W. C., HYDE, D. M., MECHAM, R. P. & STENMARK, K. R. 1994. Persistence, re-expression, and induction of pulmonary arterial fibronectin, tropoelastin, and type I procollagen mRNA expression in neonatal hypoxic pulmonary hypertension. *Am J Pathol*, 145, 1411-20.
- EBRALIDZE, A., TULCHINSKY, E., GRIGORIAN, M., AFANASYEVA, A., SENIN, V., REVAZOVA, E. & LUKANIDIN, E. 1989. Isolation and characterization of a gene specifically expressed in different metastatic cells and whose deduced gene product has a high degree of homology to a Ca<sup>2+</sup>-binding protein family. *Genes Dev*, 3, 1086-93.
- EDDAHIBI, S., GUIGNABERT, C., BARLIER-MUR, A. M., DEWACHTER, L., FADEL, E., DARTEVELLE, P., HUMBERT, M., SIMONNEAU, G., HANOUN, N., SAURINI, F., HAMON, M. & ADNOT, S. 2006. Cross talk between endothelial and smooth muscle cells in pulmonary hypertension: critical role for serotonin-induced smooth muscle hyperplasia. *Circulation*, 113, 1857-64.
- EDDAHIBI, S., HUMBERT, M., SEDIAME, S., CHOUAID, C., PARTOVIAN, C., MAITRE, B., TEIGER, E., RIDEAU, D., SIMONNEAU, G., SITBON, O. & ADNOT, S. 2000. Imbalance between platelet vascular endothelial growth factor and platelet-derived growth factor in pulmonary hypertension. Effect of prostacyclin therapy. *Am J Respir Crit Care Med*, 162, 1493-9.
- EDWARDS, A. L., GUNNINGHAM, S. P., CLARE, G. C., HAYMAN, M. W., SMITH, M., FRAMPTON, C. M., ROBINSON, B. A., TROUGHTON, R. W. & BECKERT, L. E. 2013. Professional killer cell deficiencies and decreased survival in pulmonary arterial hypertension. *Respirology*, 18, 1271-7.
- EGUCHI, S., HIRATA, Y. & MARUMO, F. 1993. Endothelin subtype B receptors are coupled to adenylate cyclase via inhibitory G protein in cultured bovine endothelial cells. *J Cardiovasc Pharmacol*, 22 Suppl 8, S161-3.
- EICKELBERG, O. & MORTY, R. E. 2007. Transforming growth factor beta/bone morphogenic protein signaling in pulmonary arterial hypertension: remodeling revisited. *Trends Cardiovasc Med*, 17, 263-9.
- ELIA, L., QUINTAVALLE, M., ZHANG, J., CONTU, R., COSSU, L., LATRONICO, M. V., PETERSON, K. L., INDOLFI, C., CATALUCCI, D., CHEN, J., COURTNEIDGE, S. A. & CONDORELLI, G. 2009. The knockout of miR-143 and -145 alters smooth muscle cell maintenance and vascular homeostasis in mice: correlates with human disease. *Cell Death Differ*, 16, 1590-8.
- ESTELLER, M. 2011. Non-coding RNAs in human disease. *Nat Rev Genet*, 12, 861-74.
- EUL, B., ROSE, F., KRICK, S., SAVAI, R., GOYAL, P., KLEPETKO, W., GRIMMINGER, F., WEISSMANN, N., SEEGER, W. & HANZE, J. 2006. Impact of HIF-1alpha and HIF-2alpha on proliferation and migration of human pulmonary artery fibroblasts in hypoxia. *FASEB J*, 20, 163-5.
- EULALIO, A., MANO, M., DAL FERRO, M., ZENTILIN, L., SINAGRA, G., ZACCHIGNA, S. & GIACCA, M. 2012. Functional screening identifies miRNAs inducing cardiac regeneration. *Nature*, 492, 376-81.
- EVANS, J. D., GIRERD, B., MONTANI, D., WANG, X. J., GALIE, N., AUSTIN, E. D., ELLIOTT,

- G., ASANO, K., GRUNIG, E., YAN, Y., JING, Z. C., MANES, A., PALAZZINI, M., WHEELER, L. A., NAKAYAMA, I., SATOH, T., EICHSTAEDT, C., HINDERHOFER, K., WOLF, M., ROSENZWEIG, E. B., CHUNG, W. K., SOUBRIER, F., SIMONNEAU, G., SITBON, O., GRAF, S., KAPTOGE, S., DI ANGELANTONIO, E., HUMBERT, M. & MORRELL, N. W. 2016. BMP2 mutations and survival in pulmonary arterial hypertension: an individual participant data meta-analysis. *Lancet Respir Med*, 4, 129-37.
- FADINI, G. P., AVOGARO, A., FERRACCIOLI, G. & AGOSTINI, C. 2010. Endothelial progenitors in pulmonary hypertension: new pathophysiology and therapeutic implications. *Eur Respir J*, 35, 418-25.
- FARBER, H. W., MILLER, D. P., MELTZER, L. A. & MCGOON, M. D. 2013. Treatment of patients with pulmonary arterial hypertension at the time of death or deterioration to functional class IV: insights from the REVEAL Registry. *J Heart Lung Transplant*, 32, 1114-22.
- FARBER, H. W., MILLER, D. P., POMS, A. D., BADESCH, D. B., FROST, A. E., MUROS-LE ROUZIC, E., ROMERO, A. J., BENTON, W. W., ELLIOTT, C. G., MCGOON, M. D. & BENZA, R. L. 2015. Five-Year outcomes of patients enrolled in the REVEAL Registry. *Chest*, 148, 1043-54.
- FARHA, S., SHARP, J., ASOSINGH, K., PARK, M., COMHAIR, S. A., TANG, W. H., THOMAS, J., FARVER, C., HSIEH, F., LOYD, J. E. & ERZURUM, S. C. 2012. Mast cell number, phenotype, and function in human pulmonary arterial hypertension. *Pulm Circ*, 2, 220-8.
- FARKAS, L., FARKAS, D., ASK, K., MOLLER, A., GAULDIE, J., MARGETTS, P., INMAN, M. & KOLB, M. 2009. VEGF ameliorates pulmonary hypertension through inhibition of endothelial apoptosis in experimental lung fibrosis in rats. *J Clin Invest*, 119, 1298-311.
- FEHSEL, K., KOLB-BACHOFEN, V. & KOLB, H. 1991. Analysis of TNF alpha-induced DNA strand breaks at the single cell level. *Am J Pathol*, 139, 251-4.
- FESSEL, J. P., LOYD, J. E. & AUSTIN, E. D. 2011. The genetics of pulmonary arterial hypertension in the post-BMP2 era. *Pulm Circ*, 1, 305-19.
- FICHTLSCHERER, S., DE ROSA, S., FOX, H., SCHWIETZ, T., FISCHER, A., LIEBETRAU, C., WEBER, M., HAMM, C. W., ROXE, T., MULLER-ARDOGAN, M., BONAUER, A., ZEIHNER, A. M. & DIMMELER, S. 2010. Circulating microRNAs in patients with coronary artery disease. *Circ Res*, 107, 677-84.
- FIEDLER, J., BRECKWOLDT, K., REMMELE, C. W., HARTMANN, D., DITTRICH, M., PFANNE, A., JUST, A., XIAO, K., KUNZ, M., MULLER, T., HANSEN, A., GEFFERS, R., DANDEKAR, T., ESCHENHAGEN, T. & THUM, T. 2015. Development of Long Noncoding RNA-Based Strategies to Modulate Tissue Vascularization. *J Am Coll Cardiol*, 66, 2005-15.
- FILIPOWICZ, W., BHATTACHARYYA, S. N. & SONENBERG, N. 2008. Mechanisms of post-transcriptional regulation by microRNAs: are the answers in sight? *Nat Rev Genet*, 9, 102-14.
- FISH, J. E., MATOUK, C. C., YEBOAH, E., BEVAN, S. C., KHAN, M., PATIL, K., OHH, M. & MARSDEN, P. A. 2007. Hypoxia-inducible expression of a natural cis-antisense

- transcript inhibits endothelial nitric-oxide synthase. *J Biol Chem*, 282, 15652-66.
- FLYNN, R. A. & CHANG, H. Y. 2014. Long noncoding RNAs in cell-fate programming and reprogramming. *Cell Stem Cell*, 14, 752-61.
- FONG, T. A., SHAWVER, L. K., SUN, L., TANG, C., APP, H., POWELL, T. J., KIM, Y. H., SCHRECK, R., WANG, X., RISAU, W., ULLRICH, A., HIRTH, K. P. & MCMAHON, G. 1999. SU5416 is a potent and selective inhibitor of the vascular endothelial growth factor receptor (Flk-1/KDR) that inhibits tyrosine kinase catalysis, tumor vascularization, and growth of multiple tumor types. *Cancer Res*, 59, 99-106.
- FRANK, D. B., ABTAHI, A., YAMAGUCHI, D. J., MANNING, S., SHYR, Y., POZZI, A., BALDWIN, H. S., JOHNSON, J. E. & DE CAESTECKER, M. P. 2005. Bone morphogenetic protein 4 promotes pulmonary vascular remodeling in hypoxic pulmonary hypertension. *Circ Res*, 97, 496-504.
- FRANK, D. B., LOWERY, J., ANDERSON, L., BRINK, M., REESE, J. & DE CAESTECKER, M. 2008. Increased susceptibility to hypoxic pulmonary hypertension in Bmpr2 mutant mice is associated with endothelial dysfunction in the pulmonary vasculature. *Am J Physiol Lung Cell Mol Physiol*, 294, L98-109.
- FREYSSINET, J. M. 2003. Cellular microparticles: what are they bad or good for? *J Thromb Haemost*, 1, 1655-62.
- FRUMKIN, L. R. 2012. The pharmacological treatment of pulmonary arterial hypertension. *Pharmacol Rev*, 64, 583-620.
- FUJITA, M., SHANNON, J. M., IRVIN, C. G., FAGAN, K. A., COOL, C., AUGUSTIN, A. & MASON, R. J. 2001. Overexpression of tumor necrosis factor-alpha produces an increase in lung volumes and pulmonary hypertension. *Am J Physiol Lung Cell Mol Physiol*, 280, L39-49.
- GABBAY, E., FRASER, J. & MCNEIL, K. 2007. Review of bosentan in the management of pulmonary arterial hypertension. *Vasc Health Risk Manag*, 3, 887-900.
- GAIRHE, S., BAUER, N. N., GEBB, S. A. & MCMURTRY, I. F. 2011. Myoendothelial gap junctional signaling induces differentiation of pulmonary arterial smooth muscle cells. *Am J Physiol Lung Cell Mol Physiol*, 301, L527-35.
- GALIE, N., BRUNDAGE, B. H., GHOFRANI, H. A., OUDIZ, R. J., SIMONNEAU, G., SAFDAR, Z., SHAPIRO, S., WHITE, R. J., CHAN, M., BEARDSWORTH, A., FRUMKIN, L., BARST, R. J., PULMONARY ARTERIAL, H. & RESPONSE TO TADALAFIL STUDY, G. 2009a. Tadalafil therapy for pulmonary arterial hypertension. *Circulation*, 119, 2894-903.
- GALIE, N., CORRIS, P. A., FROST, A., GIRGIS, R. E., GRANTON, J., JING, Z. C., KLEPETKO, W., MCGOON, M. D., MCLAUGHLIN, V. V., PRESTON, I. R., RUBIN, L. J., SANDOVAL, J., SEEGER, W. & KEOGH, A. 2013. Updated treatment algorithm of pulmonary arterial hypertension. *J Am Coll Cardiol*, 62, D60-72.
- GALIE, N., GHOFRANI, H. A., TORBICKI, A., BARST, R. J., RUBIN, L. J., BADESCH, D., FLEMING, T., PARPIA, T., BURGESS, G., BRANZI, A., GRIMMINGER, F., KURZYNA, M., SIMONNEAU, G. & SILDENAFIL USE IN PULMONARY ARTERIAL HYPERTENSION STUDY, G. 2005. Sildenafil citrate therapy for pulmonary

arterial hypertension. *N Engl J Med*, 353, 2148-57.

- GALIE, N., HOEPER, M. M., HUMBERT, M., TORBICKI, A., VACHIERY, J. L., BARBERA, J. A., BEGHETTI, M., CORRIS, P., GAINE, S., GIBBS, J. S., GOMEZ-SANCHEZ, M. A., JONDEAU, G., KLEPETKO, W., OPITZ, C., PEACOCK, A., RUBIN, L., ZELLWEGER, M., SIMONNEAU, G. & GUIDELINES, E. S. C. C. F. P. 2009b. Guidelines for the diagnosis and treatment of pulmonary hypertension: the Task Force for the Diagnosis and Treatment of Pulmonary Hypertension of the European Society of Cardiology (ESC) and the European Respiratory Society (ERS), endorsed by the International Society of Heart and Lung Transplantation (ISHLT). *Eur Heart J*, 30, 2493-537.
- GALIE, N., HUMBERT, M., VACHIERY, J. L., GIBBS, S., LANG, I., TORBICKI, A., SIMONNEAU, G., PEACOCK, A., VONK NOORDEGRAAF, A., BEGHETTI, M., GHOFRANI, A., GOMEZ SANCHEZ, M. A., HANSMANN, G., KLEPETKO, W., LANCELLOTTI, P., MATUCCI, M., MCDONAGH, T., PIERARD, L. A., TRINDADE, P. T., ZOMPATORI, M. & HOEPER, M. 2015. 2015 ESC/ERS Guidelines for the diagnosis and treatment of pulmonary hypertension: The Joint Task Force for the Diagnosis and Treatment of Pulmonary Hypertension of the European Society of Cardiology (ESC) and the European Respiratory Society (ERS): Endorsed by: Association for European Paediatric and Congenital Cardiology (AEPC), International Society for Heart and Lung Transplantation (ISHLT). *Eur Respir J*, 46, 903-75.
- GALIE, N., HUMBERT, M., VACHIERY, J. L., GIBBS, S., LANG, I., TORBICKI, A., SIMONNEAU, G., PEACOCK, A., VONK NOORDEGRAAF, A., BEGHETTI, M., GHOFRANI, A., GOMEZ SANCHEZ, M. A., HANSMANN, G., KLEPETKO, W., LANCELLOTTI, P., MATUCCI, M., MCDONAGH, T., PIERARD, L. A., TRINDADE, P. T., ZOMPATORI, M., HOEPER, M., ABOYANS, V., VAZ CARNEIRO, A., ACHENBACH, S., AGEWALL, S., ALLANORE, Y., ASTEGGIANO, R., PAOLO BADANO, L., ALBERT BARBERA, J., BOUVAIST, H., BUENO, H., BYRNE, R. A., CARERJ, S., CASTRO, G., EROL, C., FALK, V., FUNCK-BRENTANO, C., GORENFLO, M., GRANTON, J., IUNG, B., KIELY, D. G., KIRCHHOF, P., KJELLSTROM, B., LANDMESSER, U., LEKAKIS, J., LIONIS, C., LIP, G. Y., ORFANOS, S. E., PARK, M. H., PIEPOLI, M. F., PONIKOWSKI, P., REVEL, M. P., RIGAU, D., ROSENKRANZ, S., VOLLER, H. & LUIS ZAMORANO, J. 2016. 2015 ESC/ERS Guidelines for the diagnosis and treatment of pulmonary hypertension: The Joint Task Force for the Diagnosis and Treatment of Pulmonary Hypertension of the European Society of Cardiology (ESC) and the European Respiratory Society (ERS): Endorsed by: Association for European Paediatric and Congenital Cardiology (AEPC), International Society for Heart and Lung Transplantation (ISHLT). *Eur Heart J*, 37, 67-119.
- GALIE, N. & SIMONNEAU, G. 2013. The Fifth World Symposium on Pulmonary Hypertension. *J Am Coll Cardiol*, 62, D1-3.
- GALLUCCI, R. M., LEE, E. G. & TOMASEK, J. J. 2006. IL-6 modulates alpha-smooth muscle actin expression in dermal fibroblasts from IL-6-deficient mice. *J Invest Dermatol*, 126, 561-8.
- GAO, P. J., LI, Y., SUN, A. J., LIU, J. J., JI, K. D., ZHANG, Y. Z., SUN, W. L., MARCHE, P. & ZHU,

- D. L. 2003. Differentiation of vascular myofibroblasts induced by transforming growth factor-beta1 requires the involvement of protein kinase Calpha. *J Mol Cell Cardiol*, 35, 1105-12.
- GAO, Y., CHEN, T. & RAJ, J. U. 2016. Endothelial and Smooth Muscle Cell Interactions in the Pathobiology of Pulmonary Hypertension. *Am J Respir Cell Mol Biol*, 54, 451-60.
- GERACI, M. W., BULL, T. M. & TUDER, R. M. 2010. Genomics of pulmonary arterial hypertension: implications for therapy. *Heart Fail Clin*, 6, 101-14.
- GERACI, M. W., GAO, B., SHEPHERD, D. C., MOORE, M. D., WESTCOTT, J. Y., FAGAN, K. A., ALGER, L. A., TUDER, R. M. & VOELKEL, N. F. 1999. Pulmonary prostacyclin synthase overexpression in transgenic mice protects against development of hypoxic pulmonary hypertension. *J Clin Invest*, 103, 1509-15.
- GERASIMOVSKAYA, E., KRATZER, A., SIDIKOVA, A., SALYS, J., ZAMORA, M. & TARASEVICIENE-STEWART, L. 2012. Interplay of macrophages and T cells in the lung vasculature. *Am J Physiol Lung Cell Mol Physiol*, 302, L1014-22.
- GERASIMOVSKAYA, E. V., TUCKER, D. A. & STENMARK, K. R. 2005. Activation of phosphatidylinositol 3-kinase, Akt, and mammalian target of rapamycin is necessary for hypoxia-induced pulmonary artery adventitial fibroblast proliferation. *J Appl Physiol (1985)*, 98, 722-31.
- GERTHOFFER, W. T. 2007. Mechanisms of vascular smooth muscle cell migration. *Circ Res*, 100, 607-21.
- GHOFRANI, H. A. & HUMBERT, M. 2014. The role of combination therapy in managing pulmonary arterial hypertension. *Eur Respir Rev*, 23, 469-75.
- GHOFRANI, H. A., OSTERLOH, I. H. & GRIMMINGER, F. 2006. Sildenafil: from angina to erectile dysfunction to pulmonary hypertension and beyond. *Nat Rev Drug Discov*, 5, 689-702.
- GHOFRANI, H. A., SEEGER, W. & GRIMMINGER, F. 2005. Imatinib for the treatment of pulmonary arterial hypertension. *N Engl J Med*, 353, 1412-3.
- GHOFRANI, H. A., WIEDEMANN, R., ROSE, F., OLSCHIEWSKI, H., SCHERMULY, R. T., WEISSMANN, N., SEEGER, W. & GRIMMINGER, F. 2002. Combination therapy with oral sildenafil and inhaled iloprost for severe pulmonary hypertension. *Ann Intern Med*, 136, 515-22.
- GIAID, A., YANAGISAWA, M., LANGLEBEN, D., MICHEL, R. P., LEVY, R., SHENNIB, H., KIMURA, S., MASAKI, T., DUGUID, W. P. & STEWART, D. J. 1993. Expression of endothelin-1 in the lungs of patients with pulmonary hypertension. *N Engl J Med*, 328, 1732-9.
- GOLEMBESKI, S. M., WEST, J., TADA, Y. & FAGAN, K. A. 2005. Interleukin-6 causes mild pulmonary hypertension and augments hypoxia-induced pulmonary hypertension in mice. *Chest*, 128, 572S-573S.
- GOMEZ-ARROYO, J., MIZUNO, S., SZCZEPANEK, K., VAN TASSELL, B., NATARAJAN, R., DOS REMEDIOS, C. G., DRAKE, J. I., FARKAS, L., KRASKAUSKAS, D., WIJESINGHE, D. S., CHALFANT, C. E., BIGBEE, J., ABBATE, A., LESNEFSKY, E. J., BOGAARD, H. J. & VOELKEL, N. F. 2013. Metabolic gene remodeling and mitochondrial dysfunction in failing right ventricular hypertrophy secondary to pulmonary

- arterial hypertension. *Circ Heart Fail*, 6, 136-44.
- GOMEZ-ARROYO, J. G., FARKAS, L., ALHUSSAINI, A. A., FARKAS, D., KRASKAUSKAS, D., VOELKEL, N. F. & BOGAARD, H. J. 2012. The monocrotaline model of pulmonary hypertension in perspective. *Am J Physiol Lung Cell Mol Physiol*, 302, L363-9.
- GORENNE, I., KUMAR, S., GRAY, K., FIGG, N., YU, H., MERCER, J. & BENNETT, M. 2013. Vascular smooth muscle cell sirtuin 1 protects against DNA damage and inhibits atherosclerosis. *Circulation*, 127, 386-96.
- GRANT, J. S., WHITE, K., MACLEAN, M. R. & BAKER, A. H. 2013. MicroRNAs in pulmonary arterial remodeling. *Cell Mol Life Sci*, 70, 4479-94.
- GREEN, D. E., MURPHY, T. C., KANG, B. Y., SEARLES, C. D. & HART, C. M. 2015. PPARgamma Ligands Attenuate Hypoxia-Induced Proliferation in Human Pulmonary Artery Smooth Muscle Cells through Modulation of MicroRNA-21. *PLoS One*, 10, e0133391.
- GREENWAY, S., VAN SUYLEN, R. J., DU MARCHIE SARVAAS, G., KWAN, E., AMBARTSUMIAN, N., LUKANIDIN, E. & RABINOVITCH, M. 2004. S100A4/Mts1 produces murine pulmonary artery changes resembling plexogenic arteriopathy and is increased in human plexogenic arteriopathy. *Am J Pathol*, 164, 253-62.
- GREGORY, R. I., YAN, K. P., AMUTHAN, G., CHENDRIMADA, T., DORATOTAJ, B., COOCH, N. & SHIEKHATTAR, R. 2004. The Microprocessor complex mediates the genesis of microRNAs. *Nature*, 432, 235-40.
- GRIMSON, A., FARH, K. K., JOHNSTON, W. K., GARRETT-ENGELE, P., LIM, L. P. & BARTEL, D. P. 2007. MicroRNA targeting specificity in mammals: determinants beyond seed pairing. *Mol Cell*, 27, 91-105.
- GROTE, P., WITTLER, L., HENDRIX, D., KOCH, F., WAHRISCH, S., BEISAW, A., MACURA, K., BLASS, G., KELLIS, M., WERBER, M. & HERRMANN, B. G. 2013. The tissue-specific lncRNA Fendrr is an essential regulator of heart and body wall development in the mouse. *Dev Cell*, 24, 206-14.
- GROTH, A., VRUGT, B., BROCK, M., SPEICH, R., ULRICH, S. & HUBER, L. C. 2014. Inflammatory cytokines in pulmonary hypertension. *Respir Res*, 15, 47.
- GU, S., LI, G., ZHANG, X., YAN, J., GAO, J., AN, X., LIU, Y. & SU, P. 2015. Aberrant expression of long noncoding RNAs in chronic thromboembolic pulmonary hypertension. *Mol Med Rep*, 11, 2631-43.
- GUBRIJ, I. B., MARTIN, S. R., PANGLE, A. K., KURTEN, R. & JOHNSON, L. G. 2014. Attenuation of monocrotaline-induced pulmonary hypertension by luminal adeno-associated virus serotype 9 gene transfer of prostacyclin synthase. *Hum Gene Ther*, 25, 498-505.
- GUENTHER, M. G., LEVINE, S. S., BOYER, L. A., JAENISCH, R. & YOUNG, R. A. 2007. A chromatin landmark and transcription initiation at most promoters in human cells. *Cell*, 130, 77-88.
- GUO, L., QIU, Z., WEI, L., YU, X., GAO, X., JIANG, S., TIAN, H., JIANG, C. & ZHU, D. 2012. The microRNA-328 regulates hypoxic pulmonary hypertension by targeting at insulin growth factor 1 receptor and L-type calcium channel-alpha1C.

*Hypertension*, 59, 1006-13.

- GURKE, S., BARROSO, J. F. & GERDES, H. H. 2008. The art of cellular communication: tunneling nanotubes bridge the divide. *Histochem Cell Biol*, 129, 539-50.
- GUSACHENKO, O. N., ZENKOVA, M. A. & VLASSOV, V. V. 2013. Nucleic acids in exosomes: disease markers and intercellular communication molecules. *Biochemistry (Mosc)*, 78, 1-7.
- HAGEN, M., FAGAN, K., STEUDEL, W., CARR, M., LANE, K., RODMAN, D. M. & WEST, J. 2007. Interaction of interleukin-6 and the BMP pathway in pulmonary smooth muscle. *Am J Physiol Lung Cell Mol Physiol*, 292, L1473-9.
- HAN, J., LEE, Y., YEOM, K. H., KIM, Y. K., JIN, H. & KIM, V. N. 2004. The Drosha-DGCR8 complex in primary microRNA processing. *Genes Dev*, 18, 3016-27.
- HANSMANN, G., DE JESUS PEREZ, V. A., ALASTALO, T. P., ALVIRA, C. M., GUIGNABERT, C., BEKKER, J. M., SCHELLONG, S., URASHIMA, T., WANG, L., MORRELL, N. W. & RABINOVITCH, M. 2008. An antiproliferative BMP-2/PPARgamma/apoE axis in human and murine SMCs and its role in pulmonary hypertension. *J Clin Invest*, 118, 1846-57.
- HAO, H., GABBIANI, G. & BOCHATON-PIALLAT, M. L. 2003. Arterial smooth muscle cell heterogeneity: implications for atherosclerosis and restenosis development. *Arterioscler Thromb Vasc Biol*, 23, 1510-20.
- HARPER, J. W. & ELLEDGE, S. J. 2007. The DNA damage response: ten years after. *Mol Cell*, 28, 739-45.
- HARRISON, J. C. & HABER, J. E. 2006. Surviving the breakup: the DNA damage checkpoint. *Annu Rev Genet*, 40, 209-35.
- HASSOUN, P. M., MOUTHON, L., BARBERA, J. A., EDDAHIBI, S., FLORES, S. C., GRIMMINGER, F., JONES, P. L., MAITLAND, M. L., MICHELAKIS, E. D., MORRELL, N. W., NEWMAN, J. H., RABINOVITCH, M., SCHERMULY, R., STENMARK, K. R., VOELKEL, N. F., YUAN, J. X. & HUMBERT, M. 2009. Inflammation, growth factors, and pulmonary vascular remodeling. *J Am Coll Cardiol*, 54, S10-9.
- HASSOUN, P. M., THOMPSON, B. T., STEIGMAN, D. & HALES, C. A. 1989. Effect of heparin and warfarin on chronic hypoxic pulmonary hypertension and vascular remodeling in the guinea pig. *Am Rev Respir Dis*, 139, 763-8.
- HATA, A. N. & BREYER, R. M. 2004. Pharmacology and signaling of prostaglandin receptors: multiple roles in inflammation and immune modulation. *Pharmacol Ther*, 103, 147-66.
- HAYASHI, S., MITSUMORI, K., IMAIDA, K., IMAZAWA, T., YASUHARA, K., UNEYAMA, C. & HAYASHI, Y. 1995. Establishment of an animal model for pulmonary fibrosis in mice using monocrotaline. *Toxicol Pathol*, 23, 63-71.
- HE, C., DING, J. W., LI, S., WU, H., JIANG, Y. R., YANG, W., TENG, L., YANG, J. & YANG, J. 2015. The Role of Long Intergenic Noncoding RNA p21 in Vascular Endothelial Cells. *DNA Cell Biol*, 34, 677-83.
- HE, L., THOMSON, J. M., HEMANN, M. T., HERNANDO-MONGE, E., MU, D., GOODSON, S., POWERS, S., CORDON-CARDO, C., LOWE, S. W., HANNON, G. J. & HAMMOND, S. M. 2005. A microRNA polycistron as a potential human oncogene. *Nature*, 435, 828-33.

- HEATH, D., SHABA, J., WILLIAMS, A., SMITH, P. & KOMBE, A. 1975. A pulmonary hypertension-producing plant from Tanzania. *Thorax*, 30, 399-404.
- HEBERLEIN, K. R., STRAUB, A. C. & ISAKSON, B. E. 2009. The myoendothelial junction: breaking through the matrix? *Microcirculation*, 16, 307-22.
- HENRIQUES-COELHO, T., BRANDAO-NOGUEIRA, A., MOREIRA-GONCALVES, D., CORREIA-PINTO, J. & LEITE-MOREIRA, A. F. 2008a. Effects of TNF-alpha blockade in monocrotaline-induced pulmonary hypertension. *Rev Port Cardiol*, 27, 341-8.
- HENRIQUES-COELHO, T., OLIVEIRA, S. M., MOURA, R. S., RONCON-ALBUQUERQUE, R., JR., NEVES, A. L., SANTOS, M., NOGUEIRA-SILVA, C., LA FUENTE CARVALHO, F., BRANDAO-NOGUEIRA, A., CORREIA-PINTO, J. & LEITE-MOREIRA, A. F. 2008b. Thymulin inhibits monocrotaline-induced pulmonary hypertension modulating interleukin-6 expression and suppressing p38 pathway. *Endocrinology*, 149, 4367-73.
- HERGENREIDER, E., HEYDT, S., TREGUER, K., BOETTGER, T., HORREVOETS, A. J., ZEIHNER, A. M., SCHEFFER, M. P., FRANGAKIS, A. S., YIN, X., MAYR, M., BRAUN, T., URBICH, C., BOON, R. A. & DIMMELER, S. 2012. Atheroprotective communication between endothelial cells and smooth muscle cells through miRNAs. *Nat Cell Biol*, 14, 249-56.
- HERGET, J., SUGGETT, A. J., LEACH, E. & BARER, G. R. 1978. Resolution of pulmonary hypertension and other features induced by chronic hypoxia in rats during complete and intermittent normoxia. *Thorax*, 33, 468-73.
- HERRMANN, J., BEST, P. J., RITMAN, E. L., HOLMES, D. R., LERMAN, L. O. & LERMAN, A. 2002. Chronic endothelin receptor antagonism prevents coronary vasa vasorum neovascularization in experimental hypercholesterolemia. *J Am Coll Cardiol*, 39, 1555-61.
- HEYDARKHAN-HAGVALL, S., HELENIUS, G., JOHANSSON, B. R., LI, J. Y., MATTSSON, E. & RISBERG, B. 2003. Co-culture of endothelial cells and smooth muscle cells affects gene expression of angiogenic factors. *J Cell Biochem*, 89, 1250-9.
- HILL, N. S., PRESTON, I. R. & ROBERTS, K. E. 2015. Inhaled Therapies for Pulmonary Hypertension. *Respir Care*, 60, 794-802; discussion 802-5.
- HIROSE, S., HOSODA, Y., FURUYA, S., OTSUKI, T. & IKEDA, E. 2000. Expression of vascular endothelial growth factor and its receptors correlates closely with formation of the plexiform lesion in human pulmonary hypertension. *Pathol Int*, 50, 472-9.
- HISLOP, A. & REID, L. 1976. New findings in pulmonary arteries of rats with hypoxia-induced pulmonary hypertension. *Br J Exp Pathol*, 57, 542-54.
- HOEPER, M. M., BOGAARD, H. J., CONDLIFFE, R., FRANTZ, R., KHANNA, D., KURZYNA, M., LANGLEBEN, D., MANES, A., SATOH, T., TORRES, F., WILKINS, M. R. & BADESCH, D. B. 2013. Definitions and diagnosis of pulmonary hypertension. *J Am Coll Cardiol*, 62, D42-50.
- HOEPER, M. M. & WELTE, T. 2006. Sildenafil citrate therapy for pulmonary arterial hypertension. *N Engl J Med*, 354, 1091-3; author reply 1091-3.
- HONG, K. H., LEE, Y. J., LEE, E., PARK, S. O., HAN, C., BEPPU, H., LI, E., RAIZADA, M. K.,

- BLOCH, K. D. & OH, S. P. 2008. Genetic ablation of the BMPR2 gene in pulmonary endothelium is sufficient to predispose to pulmonary arterial hypertension. *Circulation*, 118, 722-30.
- HOSHIKAWA, Y., NANA-SINKAM, P., MOORE, M. D., SOTTO-SANTIAGO, S., PHANG, T., KEITH, R. L., MORRIS, K. G., KONDO, T., TUDER, R. M., VOELKEL, N. F. & GERACI, M. W. 2003. Hypoxia induces different genes in the lungs of rats compared with mice. *Physiol Genomics*, 12, 209-19.
- HOSHIKAWA, Y., VOELKEL, N. F., GESELL, T. L., MOORE, M. D., MORRIS, K. G., ALGER, L. A., NARUMIYA, S. & GERACI, M. W. 2001. Prostacyclin receptor-dependent modulation of pulmonary vascular remodeling. *Am J Respir Crit Care Med*, 164, 314-8.
- HOSOKAWA, S., HARAGUCHI, G., SASAKI, A., ARAI, H., MUTO, S., ITAI, A., DOI, S., MIZUTANI, S. & ISOBE, M. 2013. Pathophysiological roles of nuclear factor kappaB (NF-kB) in pulmonary arterial hypertension: effects of synthetic selective NF-kB inhibitor IMD-0354. *Cardiovasc Res*, 99, 35-43.
- HU, H. & GATTI, R. A. 2011. MicroRNAs: new players in the DNA damage response. *J Mol Cell Biol*, 3, 151-8.
- HU, J., XU, Q., MCTIERNAN, C., LAI, Y. C., OSEI-HWEDIEH, D. & GLADWIN, M. 2015. Novel Targets of Drug Treatment for Pulmonary Hypertension. *Am J Cardiovasc Drugs*, 15, 225-34.
- HUANG, J., ZHAO, L., XING, L. & CHEN, D. 2010. MicroRNA-204 regulates Runx2 protein expression and mesenchymal progenitor cell differentiation. *Stem Cells*, 28, 357-64.
- HUANG, W., YEN, R. T., MCLAURINE, M. & BLEDSOE, G. 1996. Morphometry of the human pulmonary vasculature. *J Appl Physiol (1985)*, 81, 2123-33.
- HUANG, X., YUAN, T., LIANG, M., DU, M., XIA, S., DITTMAR, R., WANG, D., SEE, W., COSTELLO, B. A., QUEVEDO, F., TAN, W., NANDY, D., BEVAN, G. H., LONGENBACH, S., SUN, Z., LU, Y., WANG, T., THIBODEAU, S. N., BOARDMAN, L., KOHLI, M. & WANG, L. 2015. Exosomal miR-1290 and miR-375 as prognostic markers in castration-resistant prostate cancer. *Eur Urol*, 67, 33-41.
- HUARTE, M. 2015. The emerging role of lncRNAs in cancer. *Nat Med*, 21, 1253-61.
- HUARTE, M., GUTTMAN, M., FELDSER, D., GARBER, M., KOZIOL, M. J., KENZELMANN-BROZ, D., KHALIL, A. M., ZUK, O., AMIT, I., RABANI, M., ATTARDI, L. D., REGEV, A., LANDER, E. S., JACKS, T. & RINN, J. L. 2010. A large intergenic noncoding RNA induced by p53 mediates global gene repression in the p53 response. *Cell*, 142, 409-19.
- HUERTAS, A., PERROS, F., TU, L., COHEN-KAMINSKY, S., MONTANI, D., DORFMULLER, P., GUIGNABERT, C. & HUMBERT, M. 2014. Immune dysregulation and endothelial dysfunction in pulmonary arterial hypertension: a complex interplay. *Circulation*, 129, 1332-40.
- HUMBERT, M., BARST, R. J., ROBBINS, I. M., CHANNICK, R. N., GALIE, N., BOONSTRA, A., RUBIN, L. J., HORN, E. M., MANES, A. & SIMONNEAU, G. 2004a. Combination of bosentan with epoprostenol in pulmonary arterial hypertension: BREATHE-2. *Eur Respir J*, 24, 353-9.

- HUMBERT, M. & GHOFrani, H. A. 2016. The molecular targets of approved treatments for pulmonary arterial hypertension. *Thorax*, 71, 73-83.
- HUMBERT, M., MONTI, G., BRENOT, F., SITBON, O., PORTIER, A., GRANGEOT-KEROS, L., DUROUX, P., GALANAUD, P., SIMONNEAU, G. & EMILIE, D. 1995. Increased interleukin-1 and interleukin-6 serum concentrations in severe primary pulmonary hypertension. *Am J Respir Crit Care Med*, 151, 1628-31.
- HUMBERT, M., MORRELL, N. W., ARCHER, S. L., STENMARK, K. R., MACLEAN, M. R., LANG, I. M., CHRISTMAN, B. W., WEIR, E. K., EICKELBERG, O., VOELKEL, N. F. & RABINOVITCH, M. 2004b. Cellular and molecular pathobiology of pulmonary arterial hypertension. *J Am Coll Cardiol*, 43, 13S-24S.
- HUMBERT, M., SEGAL, E. S., KIELY, D. G., CARLSEN, J., SCHWIERIN, B. & HOEPER, M. M. 2007. Results of European post-marketing surveillance of bosentan in pulmonary hypertension. *Eur Respir J*, 30, 338-44.
- HUMBERT, M., SITBON, O., CHAOUAT, A., BERTOCCHI, M., HABIB, G., GRESSIN, V., YAICI, A., WEITZENBLUM, E., CORDIER, J. F., CHABOT, F., DROMER, C., PISON, C., REYNAUD-GAUBERT, M., HALOUN, A., LAURENT, M., HACHULLA, E., COTTIN, V., DEGANI, B., JAIS, X., MONTANI, D., SOUZA, R. & SIMONNEAU, G. 2010a. Survival in patients with idiopathic, familial, and anorexigen-associated pulmonary arterial hypertension in the modern management era. *Circulation*, 122, 156-63.
- HUMBERT, M., SITBON, O., CHAOUAT, A., BERTOCCHI, M., HABIB, G., GRESSIN, V., YAICI, A., WEITZENBLUM, E., CORDIER, J. F., CHABOT, F., DROMER, C., PISON, C., REYNAUD-GAUBERT, M., HALOUN, A., LAURENT, M., HACHULLA, E. & SIMONNEAU, G. 2006. Pulmonary arterial hypertension in France: results from a national registry. *Am J Respir Crit Care Med*, 173, 1023-30.
- HUMBERT, M., SITBON, O. & SIMONNEAU, G. 2004c. Treatment of pulmonary arterial hypertension. *N Engl J Med*, 351, 1425-36.
- HUMBERT, M., SITBON, O., YAICI, A., MONTANI, D., O'CALLAGHAN, D. S., JAIS, X., PARENT, F., SAVALE, L., NATALI, D., GUNTHER, S., CHAOUAT, A., CHABOT, F., CORDIER, J. F., HABIB, G., GRESSIN, V., JING, Z. C., SOUZA, R., SIMONNEAU, G. & FRENCH PULMONARY ARTERIAL HYPERTENSION, N. 2010b. Survival in incident and prevalent cohorts of patients with pulmonary arterial hypertension. *Eur Respir J*, 36, 549-55.
- HUNG, T., WANG, Y., LIN, M. F., KOEGEL, A. K., KOTAKE, Y., GRANT, G. D., HORLINGS, H. M., SHAH, N., UMBRIGHT, C., WANG, P., WANG, Y., KONG, B., LANGEROD, A., BORRESEN-DALE, A. L., KIM, S. K., VAN DE VIJVER, M., SUKUMAR, S., WHITFIELD, M. L., KELLIS, M., XIONG, Y., WONG, D. J. & CHANG, H. Y. 2011. Extensive and coordinated transcription of noncoding RNAs within cell-cycle promoters. *Nat Genet*, 43, 621-9.
- INTERNATIONAL, P. P. H. C., LANE, K. B., MACHADO, R. D., PAUCIULO, M. W., THOMSON, J. R., PHILLIPS, J. A., 3RD, LOYD, J. E., NICHOLS, W. C. & TREMBATH, R. C. 2000. Heterozygous germline mutations in BMPR2, encoding a TGF-beta receptor, cause familial primary pulmonary hypertension. *Nat Genet*, 26, 81-4.
- ISIN, M., UYSALER, E., OZGUR, E., KOSEOGLU, H., SANLI, O., YUCEL, O. B., GEZER, U. &

- DALAY, N. 2015. Exosomal lncRNA-p21 levels may help to distinguish prostate cancer from benign disease. *Front Genet*, 6, 168.
- IZIKKI, M., GUIGNABERT, C., FADEL, E., HUMBERT, M., TU, L., ZADIGUE, P., DARTEVELLE, P., SIMONNEAU, G., ADNOT, S., MAITRE, B., RAFFESTIN, B. & EDDAHIBI, S. 2009. Endothelial-derived FGF2 contributes to the progression of pulmonary hypertension in humans and rodents. *J Clin Invest*, 119, 512-23.
- JACOBSEN, A., SILBER, J., HARINATH, G., HUSE, J. T., SCHULTZ, N. & SANDER, C. 2013. Analysis of microRNA-target interactions across diverse cancer types. *Nat Struct Mol Biol*, 20, 1325-32.
- JAMES, W. R. & THOMAS, A. J. 1968. The effect of hypoxia on the heart and pulmonary arterioles of mice. *Cardiovasc Res*, 2, 278-83.
- JANSSEN, H. L., REESINK, H. W., LAWITZ, E. J., ZEUZEM, S., RODRIGUEZ-TORRES, M., PATEL, K., VAN DER MEER, A. J., PATICK, A. K., CHEN, A., ZHOU, Y., PERSSON, R., KING, B. D., KAUPPINEN, S., LEVIN, A. A. & HODGES, M. R. 2013. Treatment of HCV infection by targeting microRNA. *N Engl J Med*, 368, 1685-94.
- JASMIN, J. F., LUCAS, M., CERNACEK, P. & DUPUIS, J. 2001. Effectiveness of a nonselective ET(A/B) and a selective ET(A) antagonist in rats with monocrotaline-induced pulmonary hypertension. *Circulation*, 103, 314-8.
- JAZBUTYTE, V. & THUM, T. 2010. MicroRNA-21: from cancer to cardiovascular disease. *Curr Drug Targets*, 11, 926-35.
- JEFFERY, T. K. & MORRELL, N. W. 2002. Molecular and cellular basis of pulmonary vascular remodeling in pulmonary hypertension. *Prog Cardiovasc Dis*, 45, 173-202.
- JEFFERY, T. K., UPTON, P. D., TREMBATH, R. C. & MORRELL, N. W. 2005. BMP4 inhibits proliferation and promotes myocyte differentiation of lung fibroblasts via Smad1 and JNK pathways. *Am J Physiol Lung Cell Mol Physiol*, 288, L370-8.
- JEFFERY, T. K. & WANSTALL, J. C. 2001. Pulmonary vascular remodeling: a target for therapeutic intervention in pulmonary hypertension. *Pharmacol Ther*, 92, 1-20.
- JI, R., CHENG, Y., YUE, J., YANG, J., LIU, X., CHEN, H., DEAN, D. B. & ZHANG, C. 2007. MicroRNA expression signature and antisense-mediated depletion reveal an essential role of MicroRNA in vascular neointimal lesion formation. *Circ Res*, 100, 1579-88.
- JIN, Y., JIN, Y., CHEN, B., TIPPLE, T. E. & NELIN, L. D. 2014. Arginase II is a target of miR-17-5p and regulates miR-17-5p expression in human pulmonary artery smooth muscle cells. *Am J Physiol Lung Cell Mol Physiol*, 307, L197-204.
- JONIGK, D., GOLPON, H., BOCKMEYER, C. L., MAEGEL, L., HOEPER, M. M., GOTTLIEB, J., NICKEL, N., HUSSEIN, K., MAUS, U., LEHMANN, U., JANCIAUSKIENE, S., WELTE, T., HAVERICH, A., RISCHE, J., KREIPE, H. & LAENGER, F. 2011. Plexiform lesions in pulmonary arterial hypertension composition, architecture, and microenvironment. *Am J Pathol*, 179, 167-79.
- JUNION, G., SPIVAKOV, M., GIRARDOT, C., BRAUN, M., GUSTAFSON, E. H., BIRNEY, E. & FURLONG, E. E. 2012. A transcription factor collective defines cardiac cell fate and reflects lineage history. *Cell*, 148, 473-86.

- KAKIMOTO, Y., ITO, S., ABIRU, H., KOTANI, H., OZEKI, M., TAMAKI, K. & TSURUYAMA, T. 2013. Sorbin and SH3 domain-containing protein 2 is released from infarcted heart in the very early phase: proteomic analysis of cardiac tissues from patients. *J Am Heart Assoc*, 2, e000565.
- KALLURI, R. 2016. The biology and function of exosomes in cancer. *J Clin Invest*, 126, 1208-15.
- KANG, H., DAVIS-DUSENBERY, B. N., NGUYEN, P. H., LAL, A., LIEBERMAN, J., VAN AELST, L., LAGNA, G. & HATA, A. 2012. Bone morphogenetic protein 4 promotes vascular smooth muscle contractility by activating microRNA-21 (miR-21), which down-regulates expression of family of dedicator of cytokinesis (DOCK) proteins. *J Biol Chem*, 287, 3976-86.
- KAWANISHI, S., HIRAKU, Y., PINLAOR, S. & MA, N. 2006. Oxidative and nitrative DNA damage in animals and patients with inflammatory diseases in relation to inflammation-related carcinogenesis. *Biol Chem*, 387, 365-72.
- KAY, J. M. 1994. Dietary pulmonary hypertension. *Thorax*, 49 Suppl, S33-8.
- KAY, J. M., HARRIS, P. & HEATH, D. 1967. Pulmonary hypertension produced in rats by ingestion of *Crotalaria spectabilis* seeds. *Thorax*, 22, 176-9.
- KELLER, S., SANDERSON, M. P., STOECK, A. & ALTEVOGT, P. 2006. Exosomes: from biogenesis and secretion to biological function. *Immunol Lett*, 107, 102-8.
- KENT, O. A., MCCALL, M. N., CORNISH, T. C. & HALUSHKA, M. K. 2014. Lessons from miR-143/145: the importance of cell-type localization of miRNAs. *Nucleic Acids Res*, 42, 7528-38.
- KILNER, P. J. 2004. Pulmonary resistance in cardiovascular context. *Int J Cardiol*, 97 Suppl 1, 3-6.
- KIM, J., KANG, Y., KOJIMA, Y., LIGHTHOUSE, J. K., HU, X., ALDRED, M. A., MCLEAN, D. L., PARK, H., COMHAIR, S. A., GREIF, D. M., ERZURUM, S. C. & CHUN, H. J. 2013. An endothelial apelin-FGF link mediated by miR-424 and miR-503 is disrupted in pulmonary arterial hypertension. *Nat Med*, 19, 74-82.
- KISHORE, R. & KHAN, M. 2016. More Than Tiny Sacks: Stem Cell Exosomes as Cell-Free Modality for Cardiac Repair. *Circ Res*, 118, 330-43.
- KOGURE, T., YAN, I. K., LIN, W. L. & PATEL, T. 2013. Extracellular Vesicle-Mediated Transfer of a Novel Long Noncoding RNA TUC339: A Mechanism of Intercellular Signaling in Human Hepatocellular Cancer. *Genes Cancer*, 4, 261-72.
- KOLETTIS, T., VLAHOS, A. P., LOUKA, M., HATZISTERGOS, K. E., BALTOGIANNIS, G. G., AGELAKI, M. M., MITSIS, A. & MALAMOU-MITSIS, V. 2007. Characterisation of a rat model of pulmonary arterial hypertension. *Hellenic J Cardiol*, 48, 206-10.
- KOS, A., OLDE LOOHUIS, N. F., WIECZOREK, M. L., GLENNON, J. C., MARTENS, G. J., KOLK, S. M. & ASCHRAFI, A. 2012. A potential regulatory role for intronic microRNA-338-3p for its host gene encoding apoptosis-associated tyrosine kinase. *PLoS One*, 7, e31022.
- KOSAKA, N. 2016. Decoding the Secret of Cancer by Means of Extracellular Vesicles. *J Clin Med*, 5.
- KRICK, S., HANZE, J., EUL, B., SAVAI, R., SEAY, U., GRIMMINGER, F., LOHMEYER, J.,

- KLEPETKO, W., SEEGER, W. & ROSE, F. 2005. Hypoxia-driven proliferation of human pulmonary artery fibroblasts: cross-talk between HIF-1 $\alpha$  and an autocrine angiotensin system. *FASEB J*, 19, 857-9.
- KUWANO, K., HASHINO, A., NODA, K., KOSUGI, K. & KUWABARA, K. 2008. A long-acting and highly selective prostacyclin receptor agonist prodrug, 2-{4-[(5,6-diphenylpyrazin-2-yl)(isopropyl)amino]butoxy}-N-(methylsulfonyl)acetamide (NS-304), ameliorates rat pulmonary hypertension with unique relaxant responses of its active form, {4-[(5,6-diphenylpyrazin-2-yl)(isopropyl)amino]butoxy}acetic acid (MRE-269), on rat pulmonary artery. *J Pharmacol Exp Ther*, 326, 691-9.
- LAGOS-QUINTANA, M., RAUHUT, R., LENDECKEL, W. & TUSCHL, T. 2001. Identification of novel genes coding for small expressed RNAs. *Science*, 294, 853-8.
- LAI, Y. C., POTOKA, K. C., CHAMPION, H. C., MORA, A. L. & GLADWIN, M. T. 2014. Pulmonary arterial hypertension: the clinical syndrome. *Circ Res*, 115, 115-30.
- LAKKARAJU, A. & RODRIGUEZ-BOULAN, E. 2008. Itinerant exosomes: emerging roles in cell and tissue polarity. *Trends Cell Biol*, 18, 199-209.
- LAMMERS, S. R., KAO, P. H., QI, H. J., HUNTER, K., LANNING, C., ALBIETZ, J., HOFMEISTER, S., MECHAM, R., STENMARK, K. R. & SHANDAS, R. 2008. Changes in the structure-function relationship of elastin and its impact on the proximal pulmonary arterial mechanics of hypertensive calves. *Am J Physiol Heart Circ Physiol*, 295, H1451-9.
- LASSER, C., ALIKHANI, V. S., EKSTROM, K., ELDH, M., PAREDES, P. T., BOSSIOS, A., SJOSTRAND, M., GABRIELSSON, S., LOTVALL, J. & VALADI, H. 2011. Human saliva, plasma and breast milk exosomes contain RNA: uptake by macrophages. *J Transl Med*, 9, 9.
- LAU, N. C., LIM, L. P., WEINSTEIN, E. G. & BARTEL, D. P. 2001. An abundant class of tiny RNAs with probable regulatory roles in *Caenorhabditis elegans*. *Science*, 294, 858-62.
- LAVORGNA, G., VAGO, R., SARMINI, M., MONTORSI, F., SALONIA, A. & BELLONE, M. 2016. Long non-coding RNAs as novel therapeutic targets in cancer. *Pharmacol Res*, 110, 131-138.
- LE CONTEL, C., BEIGNEUX, A. P., HUANG, J. & PARANT, M. A. 1995. Regulation of lipopolysaccharide-induced tumor necrosis factor production by cyclosporin A in mice primed with muramyl dipeptide. *FEMS Immunol Med Microbiol*, 11, 297-305.
- LEE, C., MITSIALIS, S. A., ASLAM, M., VITALI, S. H., VERGADI, E., KONSTANTINOPOULOS, G., SDRIMAS, K., FERNANDEZ-GONZALEZ, A. & KOUREMBANAS, S. 2012a. Exosomes mediate the cytoprotective action of mesenchymal stromal cells on hypoxia-induced pulmonary hypertension. *Circulation*, 126, 2601-11.
- LEE, H. K., BIER, A., CAZACU, S., FINNISS, S., XIANG, C., TWITO, H., POISSON, L. M., MIKKELSEN, T., SLAVIN, S., JACOBY, E., YALON, M., TOREN, A., REMPEL, S. A. & BRODIE, C. 2013. MicroRNA-145 is downregulated in glial tumors and regulates glioma cell migration by targeting connective tissue growth factor. *PLoS One*, 8, e54652.

- LEE, J. S., HA, L., PARK, J. H. & LIM, J. Y. 2012b. Mechanical stretch suppresses BMP4 induction of stem cell adipogenesis via upregulating ERK but not through downregulating Smad or p38. *Biochem Biophys Res Commun*, 418, 278-83.
- LEE, R. C., FEINBAUM, R. L. & AMBROS, V. 1993. The *C. elegans* heterochronic gene *lin-4* encodes small RNAs with antisense complementarity to *lin-14*. *Cell*, 75, 843-54.
- LEE, S., CHEN, T. T., BARBER, C. L., JORDAN, M. C., MURDOCK, J., DESAI, S., FERRARA, N., NAGY, A., ROOS, K. P. & IRUELA-ARISPE, M. L. 2007. Autocrine VEGF signaling is required for vascular homeostasis. *Cell*, 130, 691-703.
- LEE, Y., EL ANDALOUSSI, S. & WOOD, M. J. 2012c. Exosomes and microvesicles: extracellular vesicles for genetic information transfer and gene therapy. *Hum Mol Genet*, 21, R125-34.
- LEE, Y., JEON, K., LEE, J. T., KIM, S. & KIM, V. N. 2002. MicroRNA maturation: stepwise processing and subcellular localization. *EMBO J*, 21, 4663-70.
- LEE, Y., KIM, M., HAN, J., YEOM, K. H., LEE, S., BAEK, S. H. & KIM, V. N. 2004. MicroRNA genes are transcribed by RNA polymerase II. *EMBO J*, 23, 4051-60.
- LEE, Y., YANG, X., HUANG, Y., FAN, H., ZHANG, Q., WU, Y., LI, J., HASINA, R., CHENG, C., LINGEN, M. W., GERSTEIN, M. B., WEICHSELBAUM, R. R., XING, H. R. & LUSSIER, Y. A. 2010. Network modeling identifies molecular functions targeted by miR-204 to suppress head and neck tumor metastasis. *PLoS Comput Biol*, 6, e1000730.
- LEGGETT, K., MAYLOR, J., UNDEM, C., LAI, N., LU, W., SCHWEITZER, K., KING, L. S., MYERS, A. C., SYLVESTER, J. T., SIDHAYE, V. & SHIMODA, L. A. 2012. Hypoxia-induced migration in pulmonary arterial smooth muscle cells requires calcium-dependent upregulation of aquaporin 1. *Am J Physiol Lung Cell Mol Physiol*, 303, L343-53.
- LENNOX, K. A. & BEHLKE, M. A. 2016. Cellular localization of long non-coding RNAs affects silencing by RNAi more than by antisense oligonucleotides. *Nucleic Acids Res*, 44, 863-77.
- LEWIS, B. P., SHIH, I. H., JONES-RHOADES, M. W., BARTEL, D. P. & BURGE, C. B. 2003. Prediction of mammalian microRNA targets. *Cell*, 115, 787-98.
- LI, A., VARNEY, M. L., VALASEK, J., GODFREY, M., DAVE, B. J. & SINGH, R. K. 2005. Autocrine role of interleukin-8 in induction of endothelial cell proliferation, survival, migration and MMP-2 production and angiogenesis. *Angiogenesis*, 8, 63-71.
- LI, C. H. & CHEN, Y. 2013. Targeting long non-coding RNAs in cancers: progress and prospects. *Int J Biochem Cell Biol*, 45, 1895-910.
- LI, L., WEI, C., KIM, I. K., JANSSEN-HEININGER, Y. & GUPTA, S. 2014. Inhibition of nuclear factor-kappaB in the lungs prevents monocrotaline-induced pulmonary hypertension in mice. *Hypertension*, 63, 1260-9.
- LI, M., RIDDLE, S. R., FRID, M. G., EL KASMI, K. C., MCKINSEY, T. A., SOKOL, R. J., STRASSHEIM, D., MEYRICK, B., YEAGER, M. E., FLOCKTON, A. R., MCKEON, B. A., LEMON, D. D., HORN, T. R., ANWAR, A., BARAJAS, C. & STENMARK, K. R. 2011. Emergence of fibroblasts with a proinflammatory epigenetically altered

- phenotype in severe hypoxic pulmonary hypertension. *J Immunol*, 187, 2711-22.
- LI, S., RAN, Y., ZHANG, D., CHEN, J., LI, S. & ZHU, D. 2013. MicroRNA-138 plays a role in hypoxic pulmonary vascular remodelling by targeting Mst1. *Biochem J*, 452, 281-91.
- LI, S., TABAR, S. S., MALEC, V., EUL, B. G., KLEPETKO, W., WEISSMANN, N., GRIMMINGER, F., SEEGER, W., ROSE, F. & HANZE, J. 2008. NOX4 regulates ROS levels under normoxic and hypoxic conditions, triggers proliferation, and inhibits apoptosis in pulmonary artery adventitial fibroblasts. *Antioxid Redox Signal*, 10, 1687-98.
- LI, Z. & RANA, T. M. 2014. Therapeutic targeting of microRNAs: current status and future challenges. *Nat Rev Drug Discov*, 13, 622-38.
- LILLY, B. 2014. We have contact: endothelial cell-smooth muscle cell interactions. *Physiology (Bethesda)*, 29, 234-41.
- LIN, J., LI, J., HUANG, B., LIU, J., CHEN, X., CHEN, X. M., XU, Y. M., HUANG, L. F. & WANG, X. Z. 2015. Exosomes: novel biomarkers for clinical diagnosis. *ScientificWorldJournal*, 2015, 657086.
- LING, Y., JOHNSON, M. K., KIELY, D. G., CONDLIFFE, R., ELLIOT, C. A., GIBBS, J. S., HOWARD, L. S., PEPKE-ZABA, J., SHEARES, K. K., CORRIS, P. A., FISHER, A. J., LORDAN, J. L., GAINE, S., COGLAN, J. G., WORT, S. J., GATZOULIS, M. A. & PEACOCK, A. J. 2012. Changing demographics, epidemiology, and survival of incident pulmonary arterial hypertension: results from the pulmonary hypertension registry of the United Kingdom and Ireland. *Am J Respir Crit Care Med*, 186, 790-6.
- LIU, D. & MORRELL, N. W. 2013. Genetics and the molecular pathogenesis of pulmonary arterial hypertension. *Curr Hypertens Rep*, 15, 632-7.
- LIU, D., WANG, J., KINZEL, B., MUELLER, M., MAO, X., VALDEZ, R., LIU, Y. & LI, E. 2007. Dosage-dependent requirement of BMP type II receptor for maintenance of vascular integrity. *Blood*, 110, 1502-10.
- LIU, J., CARMELL, M. A., RIVAS, F. V., MARSDEN, C. G., THOMSON, J. M., SONG, J. J., HAMMOND, S. M., JOSHUA-TOR, L. & HANNON, G. J. 2004. Argonaute2 is the catalytic engine of mammalian RNAi. *Science*, 305, 1437-41.
- LIU, J. Y., YAO, J., LI, X. M., SONG, Y. C., WANG, X. Q., LI, Y. J., YAN, B. & JIANG, Q. 2014. Pathogenic role of lncRNA-MALAT1 in endothelial cell dysfunction in diabetes mellitus. *Cell Death Dis*, 5, e1506.
- LIU, L., YU, X., GUO, X., TIAN, Z., SU, M., LONG, Y., HUANG, C., ZHOU, F., LIU, M., WU, X. & WANG, X. 2012. miR-143 is downregulated in cervical cancer and promotes apoptosis and inhibits tumor formation by targeting Bcl-2. *Mol Med Rep*, 5, 753-60.
- LIU, X., CHENG, Y., ZHANG, S., LIN, Y., YANG, J. & ZHANG, C. 2009. A necessary role of miR-221 and miR-222 in vascular smooth muscle cell proliferation and neointimal hyperplasia. *Circ Res*, 104, 476-87.
- LIU, Y., ZHANG, R. & YING, K. 2015. Long noncoding RNAs: novel links in respiratory diseases (review). *Mol Med Rep*, 11, 4025-31.

- LOEWER, S., CABILI, M. N., GUTTMAN, M., LOH, Y. H., THOMAS, K., PARK, I. H., GARBER, M., CURRAN, M., ONDER, T., AGARWAL, S., MANOS, P. D., DATTA, S., LANDER, E. S., SCHLAEGER, T. M., DALEY, G. Q. & RINN, J. L. 2010. Large intergenic non-coding RNA-RoR modulates reprogramming of human induced pluripotent stem cells. *Nat Genet*, 42, 1113-7.
- LONG, L., CROSBY, A., YANG, X., SOUTHWOOD, M., UPTON, P. D., KIM, D. K. & MORRELL, N. W. 2009. Altered bone morphogenetic protein and transforming growth factor-beta signaling in rat models of pulmonary hypertension: potential for activin receptor-like kinase-5 inhibition in prevention and progression of disease. *Circulation*, 119, 566-76.
- LONG, L., MACLEAN, M. R., JEFFERY, T. K., MORECROFT, I., YANG, X., RUDARAKANCHANA, N., SOUTHWOOD, M., JAMES, V., TREMBATH, R. C. & MORRELL, N. W. 2006. Serotonin increases susceptibility to pulmonary hypertension in BMPR2-deficient mice. *Circ Res*, 98, 818-27.
- LONG, X. & MIANO, J. M. 2011. Transforming growth factor-beta1 (TGF-beta1) utilizes distinct pathways for the transcriptional activation of microRNA 143/145 in human coronary artery smooth muscle cells. *J Biol Chem*, 286, 30119-29.
- LORENZEN, J. M. & THUM, T. 2016. Long noncoding RNAs in kidney and cardiovascular diseases. *Nat Rev Nephrol*, 12, 360-73.
- LOVREN, F., PAN, Y., QUAN, A., SINGH, K. K., SHUKLA, P. C., GUPTA, N., STEER, B. M., INGRAM, A. J., GUPTA, M., AL-OMRAN, M., TEOH, H., MARSDEN, P. A. & VERMA, S. 2012. MicroRNA-145 targeted therapy reduces atherosclerosis. *Circulation*, 126, S81-90.
- LOYD, J. E., BUTLER, M. G., FOROUD, T. M., CONNEALLY, P. M., PHILLIPS, J. A., 3RD & NEWMAN, J. H. 1995. Genetic anticipation and abnormal gender ratio at birth in familial primary pulmonary hypertension. *Am J Respir Crit Care Med*, 152, 93-7.
- LOYER, X., VION, A. C., TEDGUI, A. & BOULANGER, C. M. 2014. Microvesicles as cell-cell messengers in cardiovascular diseases. *Circ Res*, 114, 345-53.
- LU, J., SHIMPO, H., SHIMAMOTO, A., CHONG, A. J., HAMPTON, C. R., SPRING, D. J., YADA, M., TAKAO, M., ONODA, K., YADA, I., POHLMAN, T. H. & VERRIER, E. D. 2004. Specific inhibition of p38 mitogen-activated protein kinase with FR167653 attenuates vascular proliferation in monocrotaline-induced pulmonary hypertension in rats. *J Thorac Cardiovasc Surg*, 128, 850-9.
- LUO, L., LI, S. & CAI, Y. 1996. Effect of hypoxia on DNA synthesis and c-myc gene expression of pulmonary artery smooth muscle cells. *Chin Med Sci J*, 11, 224-7.
- LUTTER, D., MARR, C., KRUMSIEK, J., LANG, E. W. & THEIS, F. J. 2010. Intronic microRNAs support their host genes by mediating synergistic and antagonistic regulatory effects. *BMC Genomics*, 11, 224.
- LYTLE, J. R., YARIO, T. A. & STEITZ, J. A. 2007. Target mRNAs are repressed as efficiently by microRNA-binding sites in the 5' UTR as in the 3' UTR. *Proc Natl Acad Sci U S A*, 104, 9667-72.
- MA, Q., JIANG, Q., PU, Q., ZHANG, X., YANG, W., WANG, Y., YE, S., WU, S., ZHONG, G., REN, J., ZHANG, Y., LIU, L. & ZHU, W. 2013. MicroRNA-143 inhibits migration and

- invasion of human non-small-cell lung cancer and its relative mechanism. *Int J Biol Sci*, 9, 680-92.
- MAARMAN, G., LECOUR, S., BUTROUS, G., THIENEMANN, F. & SLIWA, K. 2013. A comprehensive review: the evolution of animal models in pulmonary hypertension research; are we there yet? *Pulm Circ*, 3, 739-56.
- MACHADO, R. D., ALDRED, M. A., JAMES, V., HARRISON, R. E., PATEL, B., SCHWALBE, E. C., GRUENIG, E., JANSSEN, B., KOEHLER, R., SEEGER, W., EICKELBERG, O., OLSCHESKI, H., ELLIOTT, C. G., GLISSMEYER, E., CARLQUIST, J., KIM, M., TORBICKI, A., FIJALKOWSKA, A., SZEWCZYK, G., PARMA, J., ABRAMOWICZ, M. J., GALIE, N., MORISAKI, H., KYOTANI, S., NAKANISHI, N., MORISAKI, T., HUMBERT, M., SIMONNEAU, G., SITBON, O., SOUBRIER, F., COULET, F., MORRELL, N. W. & TREMBATH, R. C. 2006. Mutations of the TGF-beta type II receptor BMPR2 in pulmonary arterial hypertension. *Hum Mutat*, 27, 121-32.
- MACHADO, R. D., EICKELBERG, O., ELLIOTT, C. G., GERACI, M. W., HANAOKA, M., LOYD, J. E., NEWMAN, J. H., PHILLIPS, J. A., 3RD, SOUBRIER, F., TREMBATH, R. C. & CHUNG, W. K. 2009. Genetics and genomics of pulmonary arterial hypertension. *J Am Coll Cardiol*, 54, S32-42.
- MAH, S. M., BUSKE, C., HUMPHRIES, R. K. & KUCHENBAUER, F. 2010. miRNA\*: a passenger stranded in RNA-induced silencing complex? *Crit Rev Eukaryot Gene Expr*, 20, 141-8.
- MAIR, K. M., JOHANSEN, A. K., WRIGHT, A. F., WALLACE, E. & MACLEAN, M. R. 2014. Pulmonary arterial hypertension: basis of sex differences in incidence and treatment response. *Br J Pharmacol*, 171, 567-79.
- MANDEGAR, M., FUNG, Y. C., HUANG, W., REMILLARD, C. V., RUBIN, L. J. & YUAN, J. X. 2004. Cellular and molecular mechanisms of pulmonary vascular remodeling: role in the development of pulmonary hypertension. *Microvasc Res*, 68, 75-103.
- MASRI, F. A., XU, W., COMHAIR, S. A., ASOSINGH, K., KOO, M., VASANJI, A., DRAZBA, J., ANAND-APTE, B. & ERZURUM, S. C. 2007. Hyperproliferative apoptosis-resistant endothelial cells in idiopathic pulmonary arterial hypertension. *Am J Physiol Lung Cell Mol Physiol*, 293, L548-54.
- MATHIVANAN, S., FAHNER, C. J., REID, G. E. & SIMPSON, R. J. 2012. ExoCarta 2012: database of exosomal proteins, RNA and lipids. *Nucleic Acids Res*, 40, D1241-4.
- MATHIVANAN, S., JI, H. & SIMPSON, R. J. 2010. Exosomes: extracellular organelles important in intercellular communication. *J Proteomics*, 73, 1907-20.
- MATHIVANAN, S. & SIMPSON, R. J. 2009. ExoCarta: A compendium of exosomal proteins and RNA. *Proteomics*, 9, 4997-5000.
- MCCOY-SIMANDLE, K., HANNA, S. J. & COX, D. 2016. Exosomes and nanotubes: Control of immune cell communication. *Int J Biochem Cell Biol*, 71, 44-54.
- MCGOON, M. D. 2014. Upfront triple therapy for pulmonary arterial hypertension: is three a crowd or critical mass? *Eur Respir J*, 43, 1556-9.
- MCLAUGHLIN, V. V. & MCGOON, M. D. 2006. Pulmonary arterial hypertension. *Circulation*, 114, 1417-31.
- MCLAUGHLIN, V. V., SHILLINGTON, A. & RICH, S. 2002. Survival in primary pulmonary hypertension: the impact of epoprostenol therapy. *Circulation*, 106, 1477-82.

- MCLENDON, J. M., JOSHI, S. R., SPARKS, J., MATAR, M., FEWELL, J. G., ABE, K., OKA, M., MCMURTRY, I. F. & GERTHOFFER, W. T. 2015. Lipid nanoparticle delivery of a microRNA-145 inhibitor improves experimental pulmonary hypertension. *J Control Release*, 210, 67-75.
- MEIER, B., RADEKE, H. H., SELLE, S., YOUNES, M., SIES, H., RESCH, K. & HABERMEHL, G. G. 1989. Human fibroblasts release reactive oxygen species in response to interleukin-1 or tumour necrosis factor-alpha. *Biochem J*, 263, 539-45.
- MEISTER, G., LANDTHALER, M., PATKANIOWSKA, A., DORSETT, Y., TENG, G. & TUSCHL, T. 2004. Human Argonaute2 mediates RNA cleavage targeted by miRNAs and siRNAs. *Mol Cell*, 15, 185-97.
- MELO, S. A., SUGIMOTO, H., O'CONNELL, J. T., KATO, N., VILLANUEVA, A., VIDAL, A., QIU, L., VITKIN, E., PERELMAN, L. T., MELO, C. A., LUCCI, A., IVAN, C., CALIN, G. A. & KALLURI, R. 2014. Cancer exosomes perform cell-independent microRNA biogenesis and promote tumorigenesis. *Cancer Cell*, 26, 707-21.
- MELOCHE, J., PFLIEGER, A., VAILLANCOURT, M., GRAYDON, C., PROVENCHER, S. & BONNET, S. 2014a. miRNAs in PAH: biomarker, therapeutic target or both? *Drug Discov Today*, 19, 1264-9.
- MELOCHE, J., PFLIEGER, A., VAILLANCOURT, M., PAULIN, R., POTUS, F., ZERVOPOULOS, S., GRAYDON, C., COURBOULIN, A., BREUILS-BONNET, S., TREMBLAY, E., COUTURE, C., MICHELAKIS, E. D., PROVENCHER, S. & BONNET, S. 2014b. Role for DNA damage signaling in pulmonary arterial hypertension. *Circulation*, 129, 786-97.
- MERKLINGER, S. L., WAGNER, R. A., SPIEKERKOETTER, E., HINEK, A., KNUTSEN, R. H., KABIR, M. G., DESAI, K., HACKER, S., WANG, L., CANN, G. M., AMBARTSUMIAN, N. S., LUKANIDIN, E., BERNSTEIN, D., HUSAIN, M., MECHAM, R. P., STARCHER, B., YANAGISAWA, H. & RABINOVITCH, M. 2005. Increased fibulin-5 and elastin in S100A4/Mts1 mice with pulmonary hypertension. *Circ Res*, 97, 596-604.
- MEYRICK, B., GAMBLE, W. & REID, L. 1980. Development of Crotalaria pulmonary hypertension: hemodynamic and structural study. *Am J Physiol*, 239, H692-702.
- MEYRICK, B. & REID, L. 1980. Endothelial and subintimal changes in rat hilar pulmonary artery during recovery from hypoxia. A quantitative ultrastructural study. *Lab Invest*, 42, 603-15.
- MEYRICK, B. O. & PERKETT, E. A. 1989. The sequence of cellular and hemodynamic changes of chronic pulmonary hypertension induced by hypoxia and other stimuli. *Am Rev Respir Dis*, 140, 1486-9.
- MICHAEL, M. Z., SM, O. C., VAN HOLST PELLEKAAN, N. G., YOUNG, G. P. & JAMES, R. J. 2003. Reduced accumulation of specific microRNAs in colorectal neoplasia. *Mol Cancer Res*, 1, 882-91.
- MICHALIK, K. M., YOU, X., MANAVSKI, Y., DODDABALLAPUR, A., ZORNIG, M., BRAUN, T., JOHN, D., PONOMAREVA, Y., CHEN, W., UCHIDA, S., BOON, R. A. & DIMMELER, S. 2014. Long noncoding RNA MALAT1 regulates endothelial cell function and vessel growth. *Circ Res*, 114, 1389-97.
- MICHELAKIS, E., TYMCHAK, W., LIEN, D., WEBSTER, L., HASHIMOTO, K. & ARCHER, S. 2002. Oral sildenafil is an effective and specific pulmonary vasodilator in

- patients with pulmonary arterial hypertension: comparison with inhaled nitric oxide. *Circulation*, 105, 2398-403.
- MIRANDA, C. L., HENDERSON, M. C., SCHMITZ, J. A. & BUHLER, D. R. 1983. Protective role of dietary butylated hydroxyanisole against chemical-induced acute liver damage in mice. *Toxicol Appl Pharmacol*, 69, 73-80.
- MITCHELL, J. A., AHMETAJ-SHALA, B., KIRKBY, N. S., WRIGHT, W. R., MACKENZIE, L. S., REED, D. M. & MOHAMED, N. 2014. Role of prostacyclin in pulmonary hypertension. *Glob Cardiol Sci Pract*, 2014, 382-93.
- MITCHELL, J. A., ALI, F., BAILEY, L., MORENO, L. & HARRINGTON, L. S. 2008. Role of nitric oxide and prostacyclin as vasoactive hormones released by the endothelium. *Exp Physiol*, 93, 141-7.
- MIYAUCHI, T., YORIKANE, R., SAKAI, S., SAKURAI, T., OKADA, M., NISHIKIBE, M., YANO, M., YAMAGUCHI, I., SUGISHITA, Y. & GOTO, K. 1993. Contribution of endogenous endothelin-1 to the progression of cardiopulmonary alterations in rats with monocrotaline-induced pulmonary hypertension. *Circ Res*, 73, 887-97.
- MIYAZONO, K., MAEDA, S. & IMAMURA, T. 2005. BMP receptor signaling: transcriptional targets, regulation of signals, and signaling cross-talk. *Cytokine Growth Factor Rev*, 16, 251-63.
- MOHSENIN, A., BURDICK, M. D., MOLINA, J. G., KEANE, M. P. & BLACKBURN, M. R. 2007. Enhanced CXCL1 production and angiogenesis in adenosine-mediated lung disease. *FASEB J*, 21, 1026-36.
- MOLEDINA, S., DE BRUYN, A., SCHIEVANO, S., OWENS, C. M., YOUNG, C., HAWORTH, S. G., TAYLOR, A. M., SCHULZE-NEICK, I. & MUTHURANGU, V. 2011. Fractal branching quantifies vascular changes and predicts survival in pulmonary hypertension: a proof of principle study. *Heart*, 97, 1245-9.
- MOLTENI, A., WARD, W. F., TS'AO, C. H. & SOLLIDAY, N. H. 1989. Monocrotaline pneumotoxicity in mice. *Virchows Arch B Cell Pathol Incl Mol Pathol*, 57, 149-55.
- MONTGOMERY, R. L., HULLINGER, T. G., SEMUS, H. M., DICKINSON, B. A., SETO, A. G., LYNCH, J. M., STACK, C., LATIMER, P. A., OLSON, E. N. & VAN ROOIJ, E. 2011. Therapeutic inhibition of miR-208a improves cardiac function and survival during heart failure. *Circulation*, 124, 1537-47.
- MOON, B. S., YOON, J. Y., KIM, M. Y., LEE, S. H., CHOI, T. & CHOI, K. Y. 2009. Bone morphogenetic protein 4 stimulates neuronal differentiation of neuronal stem cells through the ERK pathway. *Exp Mol Med*, 41, 116-25.
- MORRELL, N. W. 2006. Pulmonary hypertension due to BMPR2 mutation: a new paradigm for tissue remodeling? *Proc Am Thorac Soc*, 3, 680-6.
- MORRELL, N. W. 2010. Role of bone morphogenetic protein receptors in the development of pulmonary arterial hypertension. *Adv Exp Med Biol*, 661, 251-64.
- MORRELL, N. W., ADNOT, S., ARCHER, S. L., DUPUIS, J., JONES, P. L., MACLEAN, M. R., MCMURTRY, I. F., STENMARK, K. R., THISTLETHWAITE, P. A., WEISSMANN, N., YUAN, J. X. & WEIR, E. K. 2009. Cellular and molecular basis of pulmonary

- arterial hypertension. *J Am Coll Cardiol*, 54, S20-31.
- MORRELL, N. W., YANG, X., UPTON, P. D., JOURDAN, K. B., MORGAN, N., SHEARES, K. K. & TREMBATH, R. C. 2001. Altered growth responses of pulmonary artery smooth muscle cells from patients with primary pulmonary hypertension to transforming growth factor-beta(1) and bone morphogenetic proteins. *Circulation*, 104, 790-5.
- MORSE, J. H., JONES, A. C., BARST, R. J., HODGE, S. E., WILHELMSSEN, K. C. & NYGAARD, T. G. 1997. Mapping of familial primary pulmonary hypertension locus (PPH1) to chromosome 2q31-q32. *Circulation*, 95, 2603-6.
- MORTY, R. E., NEJMAN, B., KWAPISZEWSKA, G., HECKER, M., ZAKRZEWICZ, A., KOURI, F. M., PETERS, D. M., DUMITRASCU, R., SEEGER, W., KNAUS, P., SCHERMULY, R. T. & EICKELBERG, O. 2007. Dysregulated bone morphogenetic protein signaling in monocrotaline-induced pulmonary arterial hypertension. *Arterioscler Thromb Vasc Biol*, 27, 1072-8.
- MOTTERLE, A., PU, X., WOOD, H., XIAO, Q., GOR, S., NG, F. L., CHAN, K., CROSS, F., SHOHREH, B., POSTON, R. N., TUCKER, A. T., CAULFIELD, M. J. & YE, S. 2012. Functional analyses of coronary artery disease associated variation on chromosome 9p21 in vascular smooth muscle cells. *Hum Mol Genet*, 21, 4021-9.
- MUBARAK, K. K. 2010. A review of prostaglandin analogs in the management of patients with pulmonary arterial hypertension. *Respir Med*, 104, 9-21.
- MUTSCHLER, D., WIKSTROM, G., LIND, L., LARSSON, A., LAGRANGE, A. & ERIKSSON, M. 2006. Etanercept reduces late endotoxin-induced pulmonary hypertension in the pig. *J Interferon Cytokine Res*, 26, 661-7.
- MYERS, S. A., AHEARN, G. S., ANGELICA SELIM, M. & TAPSON, V. F. 2004. Cutaneous findings in patients with pulmonary arterial hypertension receiving long-term epoprostenol therapy. *J Am Acad Dermatol*, 51, 98-102.
- NAGAYA, N., YOKOYAMA, C., KYOTANI, S., SHIMONISHI, M., MORISHITA, R., UEMATSU, M., NISHIKIMI, T., NAKANISHI, N., OGIHARA, T., YAMAGISHI, M., MIYATAKE, K., KANEDA, Y. & TANABE, T. 2000. Gene transfer of human prostacyclin synthase ameliorates monocrotaline-induced pulmonary hypertension in rats. *Circulation*, 102, 2005-10.
- NAKAOKA, T., GONDA, K., OGITA, T., OTAWARA-HAMAMOTO, Y., OKABE, F., KIRA, Y., HARI, K., MIYAZONO, K., TAKUWA, Y. & FUJITA, T. 1997. Inhibition of rat vascular smooth muscle proliferation in vitro and in vivo by bone morphogenetic protein-2. *J Clin Invest*, 100, 2824-32.
- NARUMIYA, S. 2007. Physiology and pathophysiology of prostanoid receptors. *Proc Jpn Acad Ser B Phys Biol Sci*, 83, 296-319.
- NEWMAN, J. H., TREMBATH, R. C., MORSE, J. A., GRUNIG, E., LOYD, J. E., ADNOT, S., COCCOLO, F., VENTURA, C., PHILLIPS, J. A., 3RD, KNOWLES, J. A., JANSSEN, B., EICKELBERG, O., EDDAHIBI, S., HERVE, P., NICHOLS, W. C. & ELLIOTT, G. 2004. Genetic basis of pulmonary arterial hypertension: current understanding and future directions. *J Am Coll Cardiol*, 43, 33S-39S.
- NEWMAN, J. H., WHEELER, L., LANE, K. B., LOYD, E., GADDIPATI, R., PHILLIPS, J. A.,

- 3RD & LOYD, J. E. 2001. Mutation in the gene for bone morphogenetic protein receptor II as a cause of primary pulmonary hypertension in a large kindred. *N Engl J Med*, 345, 319-24.
- NICOLLS, M. R., MIZUNO, S., TARASEVICIENE-STEWART, L., FARKAS, L., DRAKE, J. I., AL HUSSEINI, A., GOMEZ-ARROYO, J. G., VOELKEL, N. F. & BOGAARD, H. J. 2012. New models of pulmonary hypertension based on VEGF receptor blockade-induced endothelial cell apoptosis. *Pulm Circ*, 2, 434-42.
- NOGUEIRA-FERREIRA, R., FERREIRA, R. & HENRIQUES-COELHO, T. 2014. Cellular interplay in pulmonary arterial hypertension: implications for new therapies. *Biochim Biophys Acta*, 1843, 885-93.
- NOHE, A., KEATING, E., KNAUS, P. & PETERSEN, N. O. 2004. Signal transduction of bone morphogenetic protein receptors. *Cell Signal*, 16, 291-9.
- NOREL, X. 2007. Prostanoid receptors in the human vascular wall. *ScientificWorldJournal*, 7, 1359-74.
- NOTTROTT, S., SIMARD, M. J. & RICHTER, J. D. 2006. Human let-7a miRNA blocks protein production on actively translating polyribosomes. *Nat Struct Mol Biol*, 13, 1108-14.
- NOZIK-GRAYCK, E., SULIMAN, H. B., MAJKA, S., ALBIETZ, J., VAN RHEEN, Z., ROUSH, K. & STENMARK, K. R. 2008. Lung EC-SOD overexpression attenuates hypoxic induction of Egr-1 and chronic hypoxic pulmonary vascular remodeling. *Am J Physiol Lung Cell Mol Physiol*, 295, L422-30.
- O'DONNELL, K. A., WENTZEL, E. A., ZELLER, K. I., DANG, C. V. & MENDELL, J. T. 2005. c-Myc-regulated microRNAs modulate E2F1 expression. *Nature*, 435, 839-43.
- OGBOZOR, U. D., OPENE, M., RENTERIA, L. S., MCBRIDE, S. & IBE, B. O. 2015. Mechanism by which nuclear factor-kappa beta (NF-kB) regulates ovine fetal pulmonary vascular smooth muscle cell proliferation. *Mol Genet Metab Rep*, 4, 11-8.
- OGO, T., CHOWDHURY, H. M., YANG, J., LONG, L., LI, X., TORRES CLEUREN, Y. N., MORRELL, N. W., SCHERMULY, R. T., TREMBATH, R. C. & NASIM, M. T. 2013. Inhibition of overactive transforming growth factor-beta signaling by prostacyclin analogs in pulmonary arterial hypertension. *Am J Respir Cell Mol Biol*, 48, 733-41.
- OHTA-OGO, K., HAO, H., ISHIBASHI-UEDA, H., HIROTA, S., NAKAMURA, K., OHE, T. & ITO, H. 2012. CD44 expression in plexiform lesions of idiopathic pulmonary arterial hypertension. *Pathol Int*, 62, 219-25.
- OIDA, H., NAMBA, T., SUGIMOTO, Y., USHIKUBI, F., OHISHI, H., ICHIKAWA, A. & NARUMIYA, S. 1995. In situ hybridization studies of prostacyclin receptor mRNA expression in various mouse organs. *Br J Pharmacol*, 116, 2828-37.
- ORTON, E. C., REEVES, J. T. & STENMARK, K. R. 1988. Pulmonary vasodilation with structurally altered pulmonary vessels and pulmonary hypertension. *J Appl Physiol (1985)*, 65, 2459-67.
- PAN, B. T., TENG, K., WU, C., ADAM, M. & JOHNSTONE, R. M. 1985. Electron microscopic evidence for externalization of the transferrin receptor in vesicular form in sheep reticulocytes. *J Cell Biol*, 101, 942-8.

- PAPAIOANNOU, A. I., ZAKYNTHINOS, E., KOSTIKAS, K., KIROPOULOS, T., KOUTSOKERA, A., ZIOGAS, A., KOUTROUMPAS, A., SAKKAS, L., GOURGOULIANIS, K. I. & DANIL, Z. D. 2009. Serum VEGF levels are related to the presence of pulmonary arterial hypertension in systemic sclerosis. *BMC Pulm Med*, 9, 18.
- PARANT, M. A., POUILLART, P., LE CONTEL, C., PARANT, F. J., CHEDID, L. A. & BAHR, G. M. 1995. Selective modulation of lipopolysaccharide-induced death and cytokine production by various muramyl peptides. *Infect Immun*, 63, 110-5.
- PARIKH, V. N., JIN, R. C., RABELLO, S., GULBAHCE, N., WHITE, K., HALE, A., COTTRILL, K. A., SHAIK, R. S., WAXMAN, A. B., ZHANG, Y. Y., MARON, B. A., HARTNER, J. C., FUJIWARA, Y., ORKIN, S. H., HALEY, K. J., BARABASI, A. L., LOSCALZO, J. & CHAN, S. Y. 2012. MicroRNA-21 integrates pathogenic signaling to control pulmonary hypertension: results of a network bioinformatics approach. *Circulation*, 125, 1520-32.
- PARTOVIAN, C., ADNOT, S., RAFFESTIN, B., LOUZIER, V., LEVAME, M., MAVIER, I. M., LEMARCHAND, P. & EDDAHIBI, S. 2000. Adenovirus-mediated lung vascular endothelial growth factor overexpression protects against hypoxic pulmonary hypertension in rats. *Am J Respir Cell Mol Biol*, 23, 762-71.
- PATEL, K. M., CRISOSTOMO, P., LAHM, T., MARKEL, T., HERRING, C., WANG, M., MELDRUM, K. K., LILLEMOR, K. D. & MELDRUM, D. R. 2007. Mesenchymal stem cells attenuate hypoxic pulmonary vasoconstriction by a paracrine mechanism. *J Surg Res*, 143, 281-5.
- PATIL, J. S. & SARASIJA, S. 2012. Pulmonary drug delivery strategies: A concise, systematic review. *Lung India*, 29, 44-9.
- PATTERSON, K. C., WEISSMANN, A., AHMADI, T. & FARBER, H. W. 2006. Imatinib mesylate in the treatment of refractory idiopathic pulmonary arterial hypertension. *Ann Intern Med*, 145, 152-3.
- PEACOCK, A. J., MURPHY, N. F., MCMURRAY, J. J., CABALLERO, L. & STEWART, S. 2007. An epidemiological study of pulmonary arterial hypertension. *Eur Respir J*, 30, 104-9.
- PEDRON, T., GIRARD, R., LASFARGUES, A. & CHABY, R. 1993. Differential effects of a monoclonal antibody recognizing 3-deoxy-D-manno-2-octulosonic acid on endotoxin-induced activation of pre-B cells and macrophages. *Cell Immunol*, 148, 18-31.
- PEREZ, V. A., ALI, Z., ALASTALO, T. P., IKENO, F., SAWADA, H., LAI, Y. J., KLEISLI, T., SPIEKERKOEETTER, E., QU, X., RUBINOS, L. H., ASHLEY, E., AMIEVA, M., DEDHAR, S. & RABINOVITCH, M. 2011. BMP promotes motility and represses growth of smooth muscle cells by activation of tandem Wnt pathways. *J Cell Biol*, 192, 171-88.
- PERROS, F., MONTANI, D., DORFMULLER, P., DURAND-GASSELIN, I., TCHERAKIAN, C., LE PAVEC, J., MAZMANIAN, M., FADEL, E., MUSSOT, S., MERCIER, O., HERVE, P., EMILIE, D., EDDAHIBI, S., SIMONNEAU, G., SOUZA, R. & HUMBERT, M. 2008. Platelet-derived growth factor expression and function in idiopathic pulmonary arterial hypertension. *Am J Respir Crit Care Med*, 178, 81-8.
- PETERSEN, C. P., BORDELEAU, M. E., PELLETIER, J. & SHARP, P. A. 2006. Short RNAs

- repress translation after initiation in mammalian cells. *Mol Cell*, 21, 533-42.
- PFEIFER, P., WERNER, N. & JANSEN, F. 2015. Role and Function of MicroRNAs in Extracellular Vesicles in Cardiovascular Biology. *Biomed Res Int*, 2015, 161393.
- PHAN, S. H. 2002. The myofibroblast in pulmonary fibrosis. *Chest*, 122, 286S-289S.
- PIETRA, G. G., CAPRON, F., STEWART, S., LEONE, O., HUMBERT, M., ROBBINS, I. M., REID, L. M. & TUDER, R. M. 2004. Pathologic assessment of vasculopathies in pulmonary hypertension. *J Am Coll Cardiol*, 43, 25S-32S.
- PITTMAN, R. N. 2011. *Regulation of Tissue Oxygenation*. San Rafael (CA).
- PRICE, L. C., CARAMORI, G., PERROS, F., MENG, C., GAMBARYAN, N., DORFMULLER, P., MONTANI, D., CASOLARI, P., ZHU, J., DIMOPOULOS, K., SHAO, D., GIRERD, B., MUMBY, S., PROUDFOOT, A., GRIFFITHS, M., PAPI, A., HUMBERT, M., ADCOCK, I. M. & WORT, S. J. 2013. Nuclear factor kappa-B is activated in the pulmonary vessels of patients with end-stage idiopathic pulmonary arterial hypertension. *PLoS One*, 8, e75415.
- PRICE, L. C., WORT, S. J., PERROS, F., DORFMULLER, P., HUERTAS, A., MONTANI, D., COHEN-KAMINSKY, S. & HUMBERT, M. 2012. Inflammation in pulmonary arterial hypertension. *Chest*, 141, 210-21.
- PROCKOP, D. J. 1997. Marrow stromal cells as stem cells for nonhematopoietic tissues. *Science*, 276, 71-4.
- PUGLIESE, S. C., POTH, J. M., FINI, M. A., OLSCHESKI, A., EL KASMI, K. C. & STENMARK, K. R. 2015. The role of inflammation in hypoxic pulmonary hypertension: from cellular mechanisms to clinical phenotypes. *Am J Physiol Lung Cell Mol Physiol*, 308, L229-52.
- PULLAMSETTI, S. S., DOEBELE, C., FISCHER, A., SAVAI, R., KOJONAZAROV, B., DAHAL, B. K., GHOFRANI, H. A., WEISSMANN, N., GRIMMINGER, F., BONAUER, A., SEEGER, W., ZEIHNER, A. M., DIMMELER, S. & SCHERMULY, R. T. 2012. Inhibition of microRNA-17 improves lung and heart function in experimental pulmonary hypertension. *Am J Respir Crit Care Med*, 185, 409-19.
- PULLAMSETTI, S. S., SAVAI, R., JANSSEN, W., DAHAL, B. K., SEEGER, W., GRIMMINGER, F., GHOFRANI, H. A., WEISSMANN, N. & SCHERMULY, R. T. 2011. Inflammation, immunological reaction and role of infection in pulmonary hypertension. *Clin Microbiol Infect*, 17, 7-14.
- QU, L., DING, J., CHEN, C., WU, Z. J., LIU, B., GAO, Y., CHEN, W., LIU, F., SUN, W., LI, X. F., WANG, X., WANG, Y., XU, Z. Y., GAO, L., YANG, Q., XU, B., LI, Y. M., FANG, Z. Y., XU, Z. P., BAO, Y., WU, D. S., MIAO, X., SUN, H. Y., SUN, Y. H., WANG, H. Y. & WANG, L. H. 2016. Exosome-Transmitted lncARSR Promotes Sunitinib Resistance in Renal Cancer by Acting as a Competing Endogenous RNA. *Cancer Cell*, 29, 653-68.
- QUINTAVALLE, M., ELIA, L., CONDORELLI, G. & COURTNEIDGE, S. A. 2010. MicroRNA control of podosome formation in vascular smooth muscle cells in vivo and in vitro. *J Cell Biol*, 189, 13-22.
- RABINOVITCH, M. 2012. Molecular pathogenesis of pulmonary arterial hypertension. *J Clin Invest*, 122, 4306-13.
- RABINOVITCH, M., GUIGNABERT, C., HUMBERT, M. & NICOLLS, M. R. 2014. Inflammation and immunity in the pathogenesis of pulmonary arterial

- hypertension. *Circ Res*, 115, 165-75.
- RAJA, S. G. 2010. Endothelin receptor antagonists for pulmonary arterial hypertension: an overview. *Cardiovasc Ther*, 28, e65-71.
- RAJA, S. G. & DREYFUS, G. D. 2008. Current status of bosentan for treatment of pulmonary hypertension. *Ann Card Anaesth*, 11, 6-14.
- RAJENDRAN, L., BALI, J., BARR, M. M., COURT, F. A., KRAMER-ALBERS, E. M., PICOU, F., RAPOSO, G., VAN DER VOS, K. E., VAN NIEL, G., WANG, J. & BREAKFIELD, X. O. 2014. Emerging roles of extracellular vesicles in the nervous system. *J Neurosci*, 34, 15482-9.
- RANGREZ, A. Y., MASSY, Z. A., METZINGER-LE MEUTH, V. & METZINGER, L. 2011. miR-143 and miR-145: molecular keys to switch the phenotype of vascular smooth muscle cells. *Circ Cardiovasc Genet*, 4, 197-205.
- RAPOSO, G. & STLOORVOGEL, W. 2013. Extracellular vesicles: exosomes, microvesicles, and friends. *J Cell Biol*, 200, 373-83.
- RATAJCZAK, J., MIEKUS, K., KUCIA, M., ZHANG, J., RECA, R., DVORAK, P. & RATAJCZAK, M. Z. 2006. Embryonic stem cell-derived microvesicles reprogram hematopoietic progenitors: evidence for horizontal transfer of mRNA and protein delivery. *Leukemia*, 20, 847-56.
- REHWINKEL, J., BEHM-ANSMANT, I., GATFIELD, D. & IZAURRALDE, E. 2005. A crucial role for GW182 and the DCP1:DCP2 decapping complex in miRNA-mediated gene silencing. *RNA*, 11, 1640-7.
- REINHART, B. J., SLACK, F. J., BASSON, M., PASQUINELLI, A. E., BETTINGER, J. C., ROUGVIE, A. E., HORVITZ, H. R. & RUVKUN, G. 2000. The 21-nucleotide let-7 RNA regulates developmental timing in *Caenorhabditis elegans*. *Nature*, 403, 901-6.
- RENSSEN, S. S., DOEVENDANS, P. A. & VAN EYS, G. J. 2007. Regulation and characteristics of vascular smooth muscle cell phenotypic diversity. *Neth Heart J*, 15, 100-8.
- RHOADES, M. W., REINHART, B. J., LIM, L. P., BURGE, C. B., BARTEL, B. & BARTEL, D. P. 2002. Prediction of plant microRNA targets. *Cell*, 110, 513-20.
- RHODES, J. 2005. Comparative physiology of hypoxic pulmonary hypertension: historical clues from brisket disease. *J Appl Physiol (1985)*, 98, 1092-100.
- RICARD, N., TU, L., LE HIRESS, M., HUERTAS, A., PHAN, C., THUILLET, R., SATTTLER, C., FADEL, E., SEFERIAN, A., MONTANI, D., DORFMULLER, P., HUMBERT, M. & GUIGNABERT, C. 2014. Increased pericyte coverage mediated by endothelial-derived fibroblast growth factor-2 and interleukin-6 is a source of smooth muscle-like cells in pulmonary hypertension. *Circulation*, 129, 1586-97.
- RICCIERI, V., STEFANANTONI, K., VASILE, M., MACRI, V., SCIARRA, I., IANNACE, N., ALESSANDRI, C. & VALESINI, G. 2011. Abnormal plasma levels of different angiogenic molecules are associated with different clinical manifestations in patients with systemic sclerosis. *Clin Exp Rheumatol*, 29, S46-52.
- RICH, J. D. & RICH, S. 2014. Clinical diagnosis of pulmonary hypertension. *Circulation*, 130, 1820-30.

- RICH, S., DANTZKER, D. R., AYRES, S. M., BERGOFSKY, E. H., BRUNDAGE, B. H., DETRE, K. M., FISHMAN, A. P., GOLDRING, R. M., GROVES, B. M., KOERNER, S. K. & ET AL. 1987. Primary pulmonary hypertension. A national prospective study. *Ann Intern Med*, 107, 216-23.
- RICHES, K., ALSHANWANI, A. R., WARBURTON, P., O'REGAN, D. J., BALL, S. G., WOOD, I. C., TURNER, N. A. & PORTER, K. E. 2014. Elevated expression levels of miR-143/5 in saphenous vein smooth muscle cells from patients with Type 2 diabetes drive persistent changes in phenotype and function. *J Mol Cell Cardiol*, 74, 240-50.
- RINN, J. L. & CHANG, H. Y. 2012. Genome regulation by long noncoding RNAs. *Annu Rev Biochem*, 81, 145-66.
- RITCHIE, M. E., PHIPSON, B., WU, D., HU, Y., LAW, C. W., SHI, W. & SMYTH, G. K. 2015. limma powers differential expression analyses for RNA-sequencing and microarray studies. *Nucleic Acids Res*, 43, e47.
- RODRIGUEZ, A., GRIFFITHS-JONES, S., ASHURST, J. L. & BRADLEY, A. 2004. Identification of mammalian microRNA host genes and transcription units. *Genome Res*, 14, 1902-10.
- ROUSE, J. & JACKSON, S. P. 2002. Interfaces between the detection, signaling, and repair of DNA damage. *Science*, 297, 547-51.
- RUBENS, C., EWERT, R., HALANK, M., WENSEL, R., ORZECZOWSKI, H. D., SCHULTHEISS, H. P. & HOEFFKEN, G. 2001. Big endothelin-1 and endothelin-1 plasma levels are correlated with the severity of primary pulmonary hypertension. *Chest*, 120, 1562-9.
- RUBIN, L. J. 1995. Pathology and pathophysiology of primary pulmonary hypertension. *Am J Cardiol*, 75, 51A-54A.
- RUBIN, L. J. 2012. Endothelin receptor antagonists for the treatment of pulmonary artery hypertension. *Life Sci*, 91, 517-21.
- RUBIN, L. J. & AMERICAN COLLEGE OF CHEST, P. 2004. Diagnosis and management of pulmonary arterial hypertension: ACCP evidence-based clinical practice guidelines. *Chest*, 126, 7S-10S.
- RUBIN, L. J., BADESCH, D. B., BARST, R. J., GALIE, N., BLACK, C. M., KEOGH, A., PULIDO, T., FROST, A., ROUX, S., LECONTE, I., LANDZBERG, M. & SIMONNEAU, G. 2002. Bosentan therapy for pulmonary arterial hypertension. *N Engl J Med*, 346, 896-903.
- RUBIN, L. J., BADESCH, D. B., FLEMING, T. R., GALIE, N., SIMONNEAU, G., GHOFrani, H. A., OAKES, M., LAYTON, G., SERDAREVIC-PEHAR, M., MCLAUGHLIN, V. V., BARST, R. J. & GROUP, S.-S. 2011. Long-term treatment with sildenafil citrate in pulmonary arterial hypertension: the SUPER-2 study. *Chest*, 140, 1274-83.
- RUBIN, L. J., MENDOZA, J., HOOD, M., MCGOON, M., BARST, R., WILLIAMS, W. B., DIEHL, J. H., CROW, J. & LONG, W. 1990. Treatment of primary pulmonary hypertension with continuous intravenous prostacyclin (epoprostenol). Results of a randomized trial. *Ann Intern Med*, 112, 485-91.
- RUFFENACH, G., CHABOT, S., TANGUAY, V. F., COURBOULIN, A., BOUCHERAT, O., POTUS, F., MELOCHE, J., PFLIEGER, A., BREUILS-BONNET, S., NADEAU, V., PARADIS, R.,

- TREMBLAY, E., GIRERD, B., HAUTEFORT, A., MONTANI, D., FADEL, E., DORFMULLER, P., HUMBERT, M., PERROS, F., PAULIN, R., PROVENCHER, S. & BONNET, S. 2016. Role for RUNX2 in Proliferative and Calcified Vascular Lesions in Pulmonary Arterial Hypertension. *Am J Respir Crit Care Med*.
- RYAN, J., BLOCH, K. & ARCHER, S. L. 2011. Rodent models of pulmonary hypertension: harmonisation with the world health organisation's categorisation of human PH. *Int J Clin Pract Suppl*, 15-34.
- SAHOO, S. & LOSORDO, D. W. 2014. Exosomes and cardiac repair after myocardial infarction. *Circ Res*, 114, 333-44.
- SAHU, A., SINGHAL, U. & CHINNAIYAN, A. M. 2015. Long noncoding RNAs in cancer: from function to translation. *Trends Cancer*, 1, 93-109.
- SAKAO, S., TARASEVICIENE-STEWART, L., LEE, J. D., WOOD, K., COOL, C. D. & VOELKEL, N. F. 2005. Initial apoptosis is followed by increased proliferation of apoptosis-resistant endothelial cells. *FASEB J*, 19, 1178-80.
- SAKAO, S., TATSUMI, K. & VOELKEL, N. F. 2009. Endothelial cells and pulmonary arterial hypertension: apoptosis, proliferation, interaction and transdifferentiation. *Respir Res*, 10, 95.
- SALA, F., ARANDA, J. F., ROTLLAN, N., RAMIREZ, C. M., ARYAL, B., ELIA, L., CONDORELLI, G., CATAPANO, A. L., FERNANDEZ-HERNANDO, C. & NORATA, G. D. 2014. MiR-143/145 deficiency attenuates the progression of atherosclerosis in Ldlr<sup>-/-</sup> mice. *Thromb Haemost*, 112, 796-802.
- SAMANTA, S., BALASUBRAMANIAN, S., RAJASINGH, S., PATEL, U., DHANASEKARAN, A., DAWN, B. & RAJASINGH, J. 2016. MicroRNA: A new therapeutic strategy for cardiovascular diseases. *Trends Cardiovasc Med*.
- SANCHEZ-NINO, M. D. & ORTIZ, A. 2013. HCV infection and miravirsin. *N Engl J Med*, 369, 877-8.
- SARKAR, J., GOU, D., TURAKA, P., VIKTOROVA, E., RAMCHANDRAN, R. & RAJ, J. U. 2010. MicroRNA-21 plays a role in hypoxia-mediated pulmonary artery smooth muscle cell proliferation and migration. *Am J Physiol Lung Cell Mol Physiol*, 299, L861-71.
- SAVAI, R., AL-TAMARI, H. M., SEDDING, D., KOJONAZAROV, B., MUECKE, C., TESKE, R., CAPECCHI, M. R., WEISSMANN, N., GRIMMINGER, F., SEEGER, W., SCHERMULY, R. T. & PULLAMSETTI, S. S. 2014. Pro-proliferative and inflammatory signaling converge on FoxO1 transcription factor in pulmonary hypertension. *Nat Med*, 20, 1289-300.
- SAVAI, R., PULLAMSETTI, S. S., KOLBE, J., BIENIEK, E., VOSWINCKEL, R., FINK, L., SCHEED, A., RITTER, C., DAHAL, B. K., VATER, A., KLUSMANN, S., GHOFRANI, H. A., WEISSMANN, N., KLEPETKO, W., BANAT, G. A., SEEGER, W., GRIMMINGER, F. & SCHERMULY, R. T. 2012. Immune and inflammatory cell involvement in the pathology of idiopathic pulmonary arterial hypertension. *Am J Respir Crit Care Med*, 186, 897-908.
- SAVALE, L., TU, L., RIDEAU, D., IZZIKI, M., MAITRE, B., ADNOT, S. & EDDAHIBI, S. 2009. Impact of interleukin-6 on hypoxia-induced pulmonary hypertension and lung inflammation in mice. *Respir Res*, 10, 6.

- SCHAFER, B. W. & HEIZMANN, C. W. 1996. The S100 family of EF-hand calcium-binding proteins: functions and pathology. *Trends Biochem Sci*, 21, 134-40.
- SCHELLER, J., CHALARIS, A., SCHMIDT-ARRAS, D. & ROSE-JOHN, S. 2011. The pro- and anti-inflammatory properties of the cytokine interleukin-6. *Biochim Biophys Acta*, 1813, 878-88.
- SCHERMULY, R. T., DONY, E., GHOFRANI, H. A., PULLAMSETTI, S., SAVAI, R., ROTH, M., SYDYKOV, A., LAI, Y. J., WEISSMANN, N., SEEGER, W. & GRIMMINGER, F. 2005. Reversal of experimental pulmonary hypertension by PDGF inhibition. *J Clin Invest*, 115, 2811-21.
- SCHERMULY, R. T., KREISSELMEIER, K. P., GHOFRANI, H. A., YILMAZ, H., BUTROUS, G., ERMERT, L., ERMERT, M., WEISSMANN, N., ROSE, F., GUENTHER, A., WALMRATH, D., SEEGER, W. & GRIMMINGER, F. 2004. Chronic sildenafil treatment inhibits monocrotaline-induced pulmonary hypertension in rats. *Am J Respir Crit Care Med*, 169, 39-45.
- SCHMITT, A. M. & CHANG, H. Y. 2016. Long Noncoding RNAs in Cancer Pathways. *Cancer Cell*, 29, 452-63.
- SCHONROCK, N., HARVEY, R. P. & MATTICK, J. S. 2012. Long noncoding RNAs in cardiac development and pathophysiology. *Circ Res*, 111, 1349-62.
- SCHOREY, J. S. & HARDING, C. V. 2016. Extracellular vesicles and infectious diseases: new complexity to an old story. *J Clin Invest*, 126, 1181-9.
- SEO, B., OEMAR, B. S., SIEBENMANN, R., VON SEGESSER, L. & LUSCHER, T. F. 1994. Both ETA and ETB receptors mediate contraction to endothelin-1 in human blood vessels. *Circulation*, 89, 1203-8.
- SHAH, M., PATEL, K. & SEHGAL, P. B. 2005. Monocrotaline pyrrole-induced endothelial cell megalocytosis involves a Golgi blockade mechanism. *Am J Physiol Cell Physiol*, 288, C850-62.
- SHAN, S. W., FANG, L., SHATSEVA, T., RUTNAM, Z. J., YANG, X., DU, W., LU, W. Y., XUAN, J. W., DENG, Z. & YANG, B. B. 2013. Mature miR-17-5p and passenger miR-17-3p induce hepatocellular carcinoma by targeting PTEN, GalNT7 and vimentin in different signal pathways. *J Cell Sci*, 126, 1517-30.
- SHAO, D., PARK, J. E. & WORT, S. J. 2011. The role of endothelin-1 in the pathogenesis of pulmonary arterial hypertension. *Pharmacol Res*, 63, 504-11.
- SHI, Y., PATEL, S., NICULESCU, R., CHUNG, W., DESROCHERS, P. & ZALEWSKI, A. 1999. Role of matrix metalloproteinases and their tissue inhibitors in the regulation of coronary cell migration. *Arterioscler Thromb Vasc Biol*, 19, 1150-5.
- SHI-WEN, X., CHEN, Y., DENTON, C. P., EASTWOOD, M., RENZONI, E. A., BOU-GHARIOS, G., PEARSON, J. D., DASHWOOD, M., DU BOIS, R. M., BLACK, C. M., LEASK, A. & ABRAHAM, D. J. 2004. Endothelin-1 promotes myofibroblast induction through the ETA receptor via a rac/phosphoinositide 3-kinase/Akt-dependent pathway and is essential for the enhanced contractile phenotype of fibrotic fibroblasts. *Mol Biol Cell*, 15, 2707-19.
- SHILOH, Y. 2001. ATM and ATR: networking cellular responses to DNA damage. *Curr Opin Genet Dev*, 11, 71-7.

- SHIMBO, K., MIYAKI, S., ISHITOBI, H., KATO, Y., KUBO, T., SHIMOSE, S. & OCHI, M. 2014. Exosome-formed synthetic microRNA-143 is transferred to osteosarcoma cells and inhibits their migration. *Biochem Biophys Res Commun*, 445, 381-7.
- SHIMODA, L. A. & LAURIE, S. S. 2013. Vascular remodeling in pulmonary hypertension. *J Mol Med (Berl)*, 91, 297-309.
- SHORT, M., NEMENOFF, R. A., ZAWADA, W. M., STENMARK, K. R. & DAS, M. 2004. Hypoxia induces differentiation of pulmonary artery adventitial fibroblasts into myofibroblasts. *Am J Physiol Cell Physiol*, 286, C416-25.
- SIME, F., BANCHERO, N., PENALOZA, D., GAMBOA, R., CRUZ, J. & MARTICORENA, E. 1963. Pulmonary hypertension in children born and living at high altitudes. *Am J Cardiol*, 11, 143-9.
- SIMONNEAU, G., GALIE, N., RUBIN, L. J., LANGLEBEN, D., SEEGER, W., DOMENIGHETTI, G., GIBBS, S., LEBREC, D., SPEICH, R., BEGHETTI, M., RICH, S. & FISHMAN, A. 2004. Clinical classification of pulmonary hypertension. *J Am Coll Cardiol*, 43, 5S-12S.
- SIMONNEAU, G., GATZOULIS, M. A., ADATIA, I., CELERMAJER, D., DENTON, C., GHOFRANI, A., GOMEZ SANCHEZ, M. A., KRISHNA KUMAR, R., LANDZBERG, M., MACHADO, R. F., OLSCHESKI, H., ROBBINS, I. M. & SOUZA, R. 2013. Updated clinical classification of pulmonary hypertension. *J Am Coll Cardiol*, 62, D34-41.
- SIMONNEAU, G., ROBBINS, I. M., BEGHETTI, M., CHANNICK, R. N., DELCROIX, M., DENTON, C. P., ELLIOTT, C. G., GAINES, S. P., GLADWIN, M. T., JING, Z. C., KROWKA, M. J., LANGLEBEN, D., NAKANISHI, N. & SOUZA, R. 2009. Updated clinical classification of pulmonary hypertension. *J Am Coll Cardiol*, 54, S43-54.
- SIMPSON, R. J., JENSEN, S. S. & LIM, J. W. 2008. Proteomic profiling of exosomes: current perspectives. *Proteomics*, 8, 4083-99.
- SIMPSON, R. J., LIM, J. W., MORITZ, R. L. & MATHIVANAN, S. 2009. Exosomes: proteomic insights and diagnostic potential. *Expert Rev Proteomics*, 6, 267-83.
- SITBON, O., JAIS, X., SAVALE, L., COTTIN, V., BERGOT, E., MACARI, E. A., BOUVAIST, H., DAUPHIN, C., PICARD, F., BULIFON, S., MONTANI, D., HUMBERT, M. & SIMONNEAU, G. 2014. Upfront triple combination therapy in pulmonary arterial hypertension: a pilot study. *Eur Respir J*, 43, 1691-7.
- SITBON, O. & MORRELL, N. 2012. Pathways in pulmonary arterial hypertension: the future is here. *Eur Respir Rev*, 21, 321-7.
- SOBIN, S. S., TREMER, H. M., HARDY, J. D. & CHIOLDI, H. P. 1983. Changes in arteriole in acute and chronic hypoxic pulmonary hypertension and recovery in rat. *J Appl Physiol Respir Environ Exerc Physiol*, 55, 1445-55.
- SOMMER, N., DIETRICH, A., SCHERMULY, R. T., GHOFRANI, H. A., GUDERMANN, T., SCHULZ, R., SEEGER, W., GRIMMINGER, F. & WEISSMANN, N. 2008. Regulation of hypoxic pulmonary vasoconstriction: basic mechanisms. *Eur Respir J*, 32, 1639-51.
- SONG, J. J., SMITH, S. K., HANNON, G. J. & JOSHUA-TOR, L. 2004. Crystal structure of Argonaute and its implications for RISC slicer activity. *Science*, 305, 1434-7.
- SONG, Y., JONES, J. E., BEPPU, H., KEANEY, J. F., JR., LOSCALZO, J. & ZHANG, Y. Y. 2005. Increased susceptibility to pulmonary hypertension in heterozygous

- BMPR2-mutant mice. *Circulation*, 112, 553-62.
- SOOD, P., KREK, A., ZAVOLAN, M., MACINO, G. & RAJEWSKY, N. 2006. Cell-type-specific signatures of microRNAs on target mRNA expression. *Proc Natl Acad Sci U S A*, 103, 2746-51.
- SOON, E., HOLMES, A. M., TREACY, C. M., DOUGHTY, N. J., SOUTHGATE, L., MACHADO, R. D., TREMBATH, R. C., JENNINGS, S., BARKER, L., NICKLIN, P., WALKER, C., BUDD, D. C., PEPKE-ZABA, J. & MORRELL, N. W. 2010. Elevated levels of inflammatory cytokines predict survival in idiopathic and familial pulmonary arterial hypertension. *Circulation*, 122, 920-7.
- SOUZA, R., SITBON, O., PARENT, F., SIMONNEAU, G. & HUMBERT, M. 2006. Long term imatinib treatment in pulmonary arterial hypertension. *Thorax*, 61, 736.
- SPIEKERKOETTER, E., GUIGNABERT, C., DE JESUS PEREZ, V., ALASTALO, T. P., POWERS, J. M., WANG, L., LAWRIE, A., AMBARTSUMIAN, N., SCHMIDT, A. M., BERRYMAN, M., ASHLEY, R. H. & RABINOVITCH, M. 2009. S100A4 and bone morphogenetic protein-2 codependently induce vascular smooth muscle cell migration via phospho-extracellular signal-regulated kinase and chloride intracellular channel 4. *Circ Res*, 105, 639-47, 13 p following 647.
- SQUATRITO, M. & HOLLAND, E. C. 2011. DNA damage response and growth factor signaling pathways in gliomagenesis and therapeutic resistance. *Cancer Res*, 71, 5945-9.
- SREEKUMAR, P. G., KANNAN, R., KITAMURA, M., SPEE, C., BARRON, E., RYAN, S. J. & HINTON, D. R. 2010. alphaB crystallin is apically secreted within exosomes by polarized human retinal pigment epithelium and provides neuroprotection to adjacent cells. *PLoS One*, 5, e12578.
- STACHER, E., GRAHAM, B. B., HUNT, J. M., GANDJEVA, A., GROSHONG, S. D., MCLAUGHLIN, V. V., JESSUP, M., GRIZZLE, W. E., ALDRED, M. A., COOL, C. D. & TUDER, R. M. 2012. Modern age pathology of pulmonary arterial hypertension. *Am J Respir Crit Care Med*, 186, 261-72.
- STEINER, M. K., SYRKINA, O. L., KOLLIPUTI, N., MARK, E. J., HALES, C. A. & WAXMAN, A. B. 2009. Interleukin-6 overexpression induces pulmonary hypertension. *Circ Res*, 104, 236-44, 28p following 244.
- STEINLE, J. J., PIERCE, J. D., CLANCY, R. L. & P, G. S. 2002. Increased ocular blood vessel numbers and sizes following chronic sympathectomy in rat. *Exp Eye Res*, 74, 761-8.
- STENMARK, K. R., DAVIE, N., FRID, M., GERASIMOVSKAYA, E. & DAS, M. 2006a. Role of the adventitia in pulmonary vascular remodeling. *Physiology (Bethesda)*, 21, 134-45.
- STENMARK, K. R., FAGAN, K. A. & FRID, M. G. 2006b. Hypoxia-induced pulmonary vascular remodeling: cellular and molecular mechanisms. *Circ Res*, 99, 675-91.
- STENMARK, K. R., FASULES, J., HYDE, D. M., VOELKEL, N. F., HENSON, J., TUCKER, A., WILSON, H. & REEVES, J. T. 1987. Severe pulmonary hypertension and arterial adventitial changes in newborn calves at 4,300 m. *J Appl Physiol (1985)*, 62, 821-30.
- STENMARK, K. R., GERASIMOVSKAYA, E., NEMENOFF, R. A. & DAS, M. 2002. Hypoxic

- activation of adventitial fibroblasts: role in vascular remodeling. *Chest*, 122, 326S-334S.
- STENMARK, K. R., MEYRICK, B., GALIE, N., MOOI, W. J. & MCMURTRY, I. F. 2009. Animal models of pulmonary arterial hypertension: the hope for etiological discovery and pharmacological cure. *Am J Physiol Lung Cell Mol Physiol*, 297, L1013-32.
- STENMARK, K. R., NOZIK-GRAYCK, E., GERASIMOVSKAYA, E., ANWAR, A., LI, M., RIDDLE, S. & FRID, M. 2011. The adventitia: Essential role in pulmonary vascular remodeling. *Compr Physiol*, 1, 141-61.
- STEVENS, T., JANSSEN, P. L. & TUCKER, A. 1992. Acute and long-term TNF-alpha administration increases pulmonary vascular reactivity in isolated rat lungs. *J Appl Physiol (1985)*, 73, 708-12.
- STITHAM, J., MIDGETT, C., MARTIN, K. A. & HWA, J. 2011. Prostacyclin: an inflammatory paradox. *Front Pharmacol*, 2, 24.
- STOW, J. L., LOW, P. C., OFFENHAUSER, C. & SANGERMANI, D. 2009. Cytokine secretion in macrophages and other cells: pathways and mediators. *Immunobiology*, 214, 601-12.
- STRINGHAM, R. & SHAH, N. R. 2010. Pulmonary arterial hypertension: an update on diagnosis and treatment. *Am Fam Physician*, 82, 370-7.
- SUN, C. K., LEE, F. Y., SHEU, J. J., YUEN, C. M., CHUA, S., CHUNG, S. Y., CHAI, H. T., CHEN, Y. T., KAO, Y. H., CHANG, L. T. & YIP, H. K. 2009. Early combined treatment with cilostazol and bone marrow-derived endothelial progenitor cells markedly attenuates pulmonary arterial hypertension in rats. *J Pharmacol Exp Ther*, 330, 718-26.
- SUN, M. & KRAUS, W. L. 2015. From discovery to function: the expanding roles of long noncoding RNAs in physiology and disease. *Endocr Rev*, 36, 25-64.
- SUTENDRA, G., DROMPARIS, P., BONNET, S., HAROMY, A., MCMURTRY, M. S., BLEACKLEY, R. C. & MICHELAKIS, E. D. 2011. Pyruvate dehydrogenase inhibition by the inflammatory cytokine TNFalpha contributes to the pathogenesis of pulmonary arterial hypertension. *J Mol Med (Berl)*, 89, 771-83.
- SUZUKI, H. I., YAMAGATA, K., SUGIMOTO, K., IWAMOTO, T., KATO, S. & MIYAZONO, K. 2009. Modulation of microRNA processing by p53. *Nature*, 460, 529-33.
- SZTRYMF, B., YAICI, A., GIRERD, B. & HUMBERT, M. 2007. Genes and pulmonary arterial hypertension. *Respiration*, 74, 123-32.
- TAJSIC, T. & MORRELL, N. W. 2011. Smooth muscle cell hypertrophy, proliferation, migration and apoptosis in pulmonary hypertension. *Compr Physiol*, 1, 295-317.
- TAKAGI, T., IIO, A., NAKAGAWA, Y., NAOE, T., TANIGAWA, N. & AKAO, Y. 2009. Decreased expression of microRNA-143 and -145 in human gastric cancers. *Oncology*, 77, 12-21.
- TAKAHASHI, K., YAN, I. K., KOGURE, T., HAGA, H. & PATEL, T. 2014a. Extracellular vesicle-mediated transfer of long non-coding RNA ROR modulates chemosensitivity in human hepatocellular cancer. *FEBS Open Bio*, 4, 458-67.
- TAKAHASHI, K., YAN, I. K., WOOD, J., HAGA, H. & PATEL, T. 2014b. Involvement of extracellular vesicle long noncoding RNA (linc-VLDLR) in tumor cell responses

- to chemotherapy. *Mol Cancer Res*, 12, 1377-87.
- TAKAHASHI, M., NAKAMURA, T., TOBA, T., KAJIWARA, N., KATO, H. & SHIMIZU, Y. 2004. Transplantation of endothelial progenitor cells into the lung to alleviate pulmonary hypertension in dogs. *Tissue Eng*, 10, 771-9.
- TAKEMIYA, K., KAI, H., YASUKAWA, H., TAHARA, N., KATO, S. & IMAIZUMI, T. 2010. Mesenchymal stem cell-based prostacyclin synthase gene therapy for pulmonary hypertension rats. *Basic Res Cardiol*, 105, 409-17.
- TAMOSIUNIENE, R., TIAN, W., DHILLON, G., WANG, L., SUNG, Y. K., GERA, L., PATTERSON, A. J., AGRAWAL, R., RABINOVITCH, M., AMBLER, K., LONG, C. S., VOELKEL, N. F. & NICOLLS, M. R. 2011. Regulatory T cells limit vascular endothelial injury and prevent pulmonary hypertension. *Circ Res*, 109, 867-79.
- TANG, S. S., ZHENG, B. Y. & XIONG, X. D. 2015. LincRNA-p21: Implications in Human Diseases. *Int J Mol Sci*, 16, 18732-40.
- TANZER, A. & STADLER, P. F. 2004. Molecular evolution of a microRNA cluster. *J Mol Biol*, 339, 327-35.
- TAPSON, V. F., JING, Z. C., XU, K. F., PAN, L., FELDMAN, J., KIELY, D. G., KOTLYAR, E., MCSWAIN, C. S., LALIBERTE, K., ARNESON, C., RUBIN, L. J. & TEAM, F.-C. S. 2013. Oral treprostinil for the treatment of pulmonary arterial hypertension in patients receiving background endothelin receptor antagonist and phosphodiesterase type 5 inhibitor therapy (the FREEDOM-C2 study): a randomized controlled trial. *Chest*, 144, 952-8.
- TAPSON, V. F., TORRES, F., KERMEEN, F., KEOGH, A. M., ALLEN, R. P., FRANTZ, R. P., BADESCH, D. B., FROST, A. E., SHAPIRO, S. M., LALIBERTE, K., SIGMAN, J., ARNESON, C. & GALIE, N. 2012. Oral treprostinil for the treatment of pulmonary arterial hypertension in patients on background endothelin receptor antagonist and/or phosphodiesterase type 5 inhibitor therapy (the FREEDOM-C study): a randomized controlled trial. *Chest*, 142, 1383-90.
- TARASEVICIENE-STEWART, L., KASAHARA, Y., ALGER, L., HIRTH, P., MC MAHON, G., WALTENBERGER, J., VOELKEL, N. F. & TUDER, R. M. 2001. Inhibition of the VEGF receptor 2 combined with chronic hypoxia causes cell death-dependent pulmonary endothelial cell proliferation and severe pulmonary hypertension. *FASEB J*, 15, 427-38.
- TASK FORCE FOR, D., TREATMENT OF PULMONARY HYPERTENSION OF EUROPEAN SOCIETY OF, C., EUROPEAN RESPIRATORY, S., INTERNATIONAL SOCIETY OF, H., LUNG, T., GALIE, N., HOEPER, M. M., HUMBERT, M., TORBICKI, A., VACHIERY, J. L., BARBERA, J. A., BEGHETTI, M., CORRIS, P., GAINE, S., GIBBS, J. S., GOMEZ-SANCHEZ, M. A., JONDEAU, G., KLEPETKO, W., OPITZ, C., PEACOCK, A., RUBIN, L., ZELLWEGER, M. & SIMONNEAU, G. 2009. Guidelines for the diagnosis and treatment of pulmonary hypertension. *Eur Respir J*, 34, 1219-63.
- TAY, Y., ZHANG, J., THOMSON, A. M., LIM, B. & RIGOUTSOS, I. 2008. MicroRNAs to Nanog, Oct4 and Sox2 coding regions modulate embryonic stem cell differentiation. *Nature*, 455, 1124-8.
- TEICHERT-KULISZEWSKA, K., KUTRYK, M. J., KULISZEWSKI, M. A., KAROUBI, G., COURTMAN, D. W., ZUCCO, L., GRANTON, J. & STEWART, D. J. 2006. Bone

- morphogenetic protein receptor-2 signaling promotes pulmonary arterial endothelial cell survival: implications for loss-of-function mutations in the pathogenesis of pulmonary hypertension. *Circ Res*, 98, 209-17.
- THENAPPAN, T., RYAN, J. J. & ARCHER, S. L. 2012. Evolving epidemiology of pulmonary arterial hypertension. *Am J Respir Crit Care Med*, 186, 707-9.
- THERY, C., BOUSSAC, M., VERON, P., RICCIARDI-CASTAGNOLI, P., RAPOSO, G., GARIN, J. & AMIGORENA, S. 2001. Proteomic analysis of dendritic cell-derived exosomes: a secreted subcellular compartment distinct from apoptotic vesicles. *J Immunol*, 166, 7309-18.
- THERY, C., REGNAULT, A., GARIN, J., WOLFERS, J., ZITVOGEL, L., RICCIARDI-CASTAGNOLI, P., RAPOSO, G. & AMIGORENA, S. 1999. Molecular characterization of dendritic cell-derived exosomes. Selective accumulation of the heat shock protein hsc73. *J Cell Biol*, 147, 599-610.
- THERY, C., ZITVOGEL, L. & AMIGORENA, S. 2002. Exosomes: composition, biogenesis and function. *Nat Rev Immunol*, 2, 569-79.
- THIENEMANN, F., HENZ, B. M. & BABINA, M. 2004. Regulation of mast cell characteristics by cytokines: divergent effects of interleukin-4 on immature mast cell lines versus mature human skin mast cells. *Arch Dermatol Res*, 296, 134-8.
- THOMAS, M., DOCX, C., HOLMES, A. M., BEACH, S., DUGGAN, N., ENGLAND, K., LEBLANC, C., LEBRET, C., SCHINDLER, F., RAZA, F., WALKER, C., CROSBY, A., DAVIES, R. J., MORRELL, N. W. & BUDD, D. C. 2009. Activin-like kinase 5 (ALK5) mediates abnormal proliferation of vascular smooth muscle cells from patients with familial pulmonary arterial hypertension and is involved in the progression of experimental pulmonary arterial hypertension induced by monocrotaline. *Am J Pathol*, 174, 380-9.
- THOMPSON, P. & MCRAE, C. 1970. Familial pulmonary hypertension. Evidence of autosomal dominant inheritance. *Br Heart J*, 32, 758-60.
- THOMSON, J. R., MACHADO, R. D., PAUCIULO, M. W., MORGAN, N. V., HUMBERT, M., ELLIOTT, G. C., WARD, K., YACOB, M., MIKHAIL, G., ROGERS, P., NEWMAN, J., WHEELER, L., HIGENBOTTAM, T., GIBBS, J. S., EGAN, J., CROZIER, A., PEACOCK, A., ALLCOCK, R., CORRIS, P., LOYD, J. E., TREMBATH, R. C. & NICHOLS, W. C. 2000. Sporadic primary pulmonary hypertension is associated with germline mutations of the gene encoding BMPR-II, a receptor member of the TGF-beta family. *J Med Genet*, 37, 741-5.
- THUM, T. & CONDORELLI, G. 2015. Long noncoding RNAs and microRNAs in cardiovascular pathophysiology. *Circ Res*, 116, 751-62.
- TIAN, L. & CHESLER, N. C. 2012. In vivo and in vitro measurements of pulmonary arterial stiffness: A brief review. *Pulm Circ*, 2, 505-17.
- TOPORSIAN, M., GROS, R., KABIR, M. G., VERA, S., GOVINDARAJU, K., EIDELMAN, D. H., HUSAIN, M. & LETARTE, M. 2005. A role for endoglin in coupling eNOS activity and regulating vascular tone revealed in hereditary hemorrhagic telangiectasia. *Circ Res*, 96, 684-92.
- TOUYZ, R. M. & BRIONES, A. M. 2011. Reactive oxygen species and vascular biology:

- implications in human hypertension. *Hypertens Res*, 34, 5-14.
- TOUYZ, R. M. & SCHIFFRIN, E. L. 2004. Reactive oxygen species in vascular biology: implications in hypertension. *Histochem Cell Biol*, 122, 339-52.
- TOWNSLEY, M. I. 2012. Structure and composition of pulmonary arteries, capillaries, and veins. *Compr Physiol*, 2, 675-709.
- TRAJKOVSKI, M., HAUSSER, J., SOUTSCHEK, J., BHAT, B., AKIN, A., ZAVOLAN, M., HEIM, M. H. & STOFFEL, M. 2011. MicroRNAs 103 and 107 regulate insulin sensitivity. *Nature*, 474, 649-53.
- TREGUER, K., HEINRICH, E. M., OHTANI, K., BONAUER, A. & DIMMELER, S. 2012. Role of the microRNA-17-92 cluster in the endothelial differentiation of stem cells. *J Vasc Res*, 49, 447-60.
- TSAI, M. C., MANOR, O., WAN, Y., MOSAMMAPARAST, N., WANG, J. K., LAN, F., SHI, Y., SEGAL, E. & CHANG, H. Y. 2010. Long noncoding RNA as modular scaffold of histone modification complexes. *Science*, 329, 689-93.
- TU, L., DEWACHTER, L., GORE, B., FADEL, E., DARTEVELLE, P., SIMONNEAU, G., HUMBERT, M., EDDAHIBI, S. & GUIGNABERT, C. 2011. Autocrine fibroblast growth factor-2 signaling contributes to altered endothelial phenotype in pulmonary hypertension. *Am J Respir Cell Mol Biol*, 45, 311-22.
- TUDER, R. M., COOL, C. D., GERACI, M. W., WANG, J., ABMAN, S. H., WRIGHT, L., BADESCH, D. & VOELKEL, N. F. 1999. Prostacyclin synthase expression is decreased in lungs from patients with severe pulmonary hypertension. *Am J Respir Crit Care Med*, 159, 1925-32.
- TUDER, R. M., GROVES, B., BADESCH, D. B. & VOELKEL, N. F. 1994. Exuberant endothelial cell growth and elements of inflammation are present in plexiform lesions of pulmonary hypertension. *Am J Pathol*, 144, 275-85.
- UCHIDA, S. & DIMMELER, S. 2015. Long noncoding RNAs in cardiovascular diseases. *Circ Res*, 116, 737-50.
- ULRICH, S., TARASEVICIENE-STEWART, L., HUBER, L. C., SPEICH, R. & VOELKEL, N. 2008. Peripheral blood B lymphocytes derived from patients with idiopathic pulmonary arterial hypertension express a different RNA pattern compared with healthy controls: a cross sectional study. *Respir Res*, 9, 20.
- UPTON, P. D., DAVIES, R. J., TAJASIC, T. & MORRELL, N. W. 2013. Transforming growth factor-beta(1) represses bone morphogenetic protein-mediated Smad signaling in pulmonary artery smooth muscle cells via Smad3. *Am J Respir Cell Mol Biol*, 49, 1135-45.
- UPTON, P. D. & MORRELL, N. W. 2013. The transforming growth factor-beta-bone morphogenetic protein type signalling pathway in pulmonary vascular homeostasis and disease. *Exp Physiol*, 98, 1262-6.
- VAIDYA, B. & GUPTA, V. 2015. Novel therapeutic approaches for pulmonary arterial hypertension: Unique molecular targets to site-specific drug delivery. *J Control Release*, 211, 118-33.
- VAKRILOVA, L. 2014. [Pulmonary hypertension of the newborn - mechanisms of failed circulatory adaptation after birth, clinical presentation and diagnosis]. *Akush Ginekol (Sofia)*, 53, 34-40.

- VALADI, H., EKSTROM, K., BOSSIOS, A., SJOSTRAND, M., LEE, J. J. & LOTVALL, J. O. 2007. Exosome-mediated transfer of mRNAs and microRNAs is a novel mechanism of genetic exchange between cells. *Nat Cell Biol*, 9, 654-9.
- VAN NIEL, G., PORTO-CARREIRO, I., SIMOES, S. & RAPOSO, G. 2006. Exosomes: a common pathway for a specialized function. *J Biochem*, 140, 13-21.
- VAN ROOIJ, E. 2011. The art of microRNA research. *Circ Res*, 108, 219-34.
- VAN ROOIJ, E. & KAUPPINEN, S. 2014. Development of microRNA therapeutics is coming of age. *EMBO Mol Med*, 6, 851-64.
- VAN ROOIJ, E. & OLSON, E. N. 2007. MicroRNAs: powerful new regulators of heart disease and provocative therapeutic targets. *J Clin Invest*, 117, 2369-76.
- VAN ROOIJ, E. & OLSON, E. N. 2012. MicroRNA therapeutics for cardiovascular disease: opportunities and obstacles. *Nat Rev Drug Discov*, 11, 860-72.
- VIERECK, J., KUMARSWAMY, R., FOINQUINOS, A., XIAO, K., AVRAMOPOULOS, P., KUNZ, M., DITTRICH, M., MAETZIG, T., ZIMMER, K., REMKE, J., JUST, A., FENDRICH, J., SCHERF, K., BOLESANI, E., SCHAMBACH, A., WEIDEMANN, F., ZWEIGERDT, R., DE WINDT, L. J., ENGELHARDT, S., DANDEKAR, T., BATKAI, S. & THUM, T. 2016. Long noncoding RNA Chast promotes cardiac remodeling. *Sci Transl Med*, 8, 326ra22.
- VITALI, S. H., HANSMANN, G., ROSE, C., FERNANDEZ-GONZALEZ, A., SCHEID, A., MITSIALIS, S. A. & KOUREMBANAS, S. 2014. The Sugen 5416/hypoxia mouse model of pulmonary hypertension revisited: long-term follow-up. *Pulm Circ*, 4, 619-29.
- VOELKEL, N. F. & TUDER, R. M. 1997. Cellular and molecular biology of vascular smooth muscle cells in pulmonary hypertension. *Pulm Pharmacol Ther*, 10, 231-41.
- VOELKEL, N. F. & TUDER, R. M. 2000. Hypoxia-induced pulmonary vascular remodeling: a model for what human disease? *J Clin Invest*, 106, 733-8.
- VOELKEL, N. F., TUDER, R. M., BRIDGES, J. & AREND, W. P. 1994. Interleukin-1 receptor antagonist treatment reduces pulmonary hypertension generated in rats by monocrotaline. *Am J Respir Cell Mol Biol*, 11, 664-75.
- VOELKEL, N. F., VANDIVIER, R. W. & TUDER, R. M. 2006. Vascular endothelial growth factor in the lung. *Am J Physiol Lung Cell Mol Physiol*, 290, L209-21.
- VOELLENKLE, C., GARCIA-MANTEIGA, J. M., PEDROTTI, S., PERFETTI, A., DE TOMA, I., DA SILVA, D., MAIMONE, B., GRECO, S., FASANARO, P., CREO, P., ZACCAGNINI, G., GAETANO, C. & MARTELLI, F. 2016. Implication of Long noncoding RNAs in the endothelial cell response to hypoxia revealed by RNA-sequencing. *Sci Rep*, 6, 24141.
- WAHID, F., SHEHZAD, A., KHAN, T. & KIM, Y. Y. 2010. MicroRNAs: synthesis, mechanism, function, and recent clinical trials. *Biochim Biophys Acta*, 1803, 1231-43.
- WALDENSTROM, A. & RONQUIST, G. 2014. Role of exosomes in myocardial remodeling. *Circ Res*, 114, 315-24.
- WALKER, B. R., BEREND, N. & VOELKEL, N. F. 1984. Comparison of muscular pulmonary arteries in low and high altitude hamsters and rats. *Respir Physiol*,

56, 45-50.

- WALLACE, E., MORRELL, N. W., YANG, X. D., LONG, L., STEVENS, H., NILSEN, M., LOUGHLIN, L., MAIR, K. M., BAKER, A. H. & MACLEAN, M. R. 2015. A Sex-Specific MicroRNA-96/5-Hydroxytryptamine 1B Axis Influences Development of Pulmonary Hypertension. *Am J Respir Crit Care Med*, 191, 1432-42.
- WANG, F. E., ZHANG, C., MAMINISHKIS, A., DONG, L., ZHI, C., LI, R., ZHAO, J., MAJERCIK, V., GAUR, A. B., CHEN, S. & MILLER, S. S. 2010a. MicroRNA-204/211 alters epithelial physiology. *FASEB J*, 24, 1552-71.
- WANG, J., HENDRIX, A., HERNOT, S., LEMAIRE, M., DE BRUYNE, E., VAN VALCKENBORGH, E., LAHOUTTE, T., DE WEVER, O., VANDERKERKEN, K. & MENU, E. 2014. Bone marrow stromal cell-derived exosomes as communicators in drug resistance in multiple myeloma cells. *Blood*, 124, 555-66.
- WANG, K. C. & CHANG, H. Y. 2011. Molecular mechanisms of long noncoding RNAs. *Mol Cell*, 43, 904-14.
- WANG, Q., ZUO, X. R., WANG, Y. Y., XIE, W. P., WANG, H. & ZHANG, M. 2013. Monocrotaline-induced pulmonary arterial hypertension is attenuated by TNF-alpha antagonists via the suppression of TNF-alpha expression and NF-kappaB pathway in rats. *Vascul Pharmacol*, 58, 71-7.
- WANG, X., HU, G. & ZHOU, J. 2010b. Repression of versican expression by microRNA-143. *J Biol Chem*, 285, 23241-50.
- WANG, X., YAN, C., XU, X., DONG, L., SU, H., HU, Y., ZHANG, R. & YING, K. 2016. Long noncoding RNA expression profiles of hypoxic pulmonary hypertension rat model. *Gene*, 579, 23-8.
- WANG, X. X., ZHANG, F. R., SHANG, Y. P., ZHU, J. H., XIE, X. D., TAO, Q. M., ZHU, J. H. & CHEN, J. Z. 2007. Transplantation of autologous endothelial progenitor cells may be beneficial in patients with idiopathic pulmonary arterial hypertension: a pilot randomized controlled trial. *J Am Coll Cardiol*, 49, 1566-71.
- WARD, M., MCEWAN, C., MILLS, J. D. & JANITZ, M. 2015. Conservation and tissue-specific transcription patterns of long noncoding RNAs. *J Hum Transcr*, 1, 2-9.
- WARD, M. R., STEWART, D. J. & KUTRYK, M. J. 2007. Endothelial progenitor cell therapy for the treatment of coronary disease, acute MI, and pulmonary arterial hypertension: current perspectives. *Catheter Cardiovasc Interv*, 70, 983-98.
- WEERACKODY, R. P., WELSH, D. J., WADSWORTH, R. M. & PEACOCK, A. J. 2009. Inhibition of p38 MAPK reverses hypoxia-induced pulmonary artery endothelial dysfunction. *Am J Physiol Heart Circ Physiol*, 296, H1312-20.
- WELSH, D. J., PEACOCK, A. J., MACLEAN, M. & HARNETT, M. 2001. Chronic hypoxia induces constitutive p38 mitogen-activated protein kinase activity that correlates with enhanced cellular proliferation in fibroblasts from rat pulmonary but not systemic arteries. *Am J Respir Crit Care Med*, 164, 282-9.
- WEST, J., COGAN, J., GERACI, M., ROBINSON, L., NEWMAN, J., PHILLIPS, J. A., LANE, K., MEYRICK, B. & LOYD, J. 2008a. Gene expression in BMPR2 mutation carriers

- with and without evidence of pulmonary arterial hypertension suggests pathways relevant to disease penetrance. *BMC Med Genomics*, 1, 45.
- WEST, J., FAGAN, K., STEUDEL, W., FOUTY, B., LANE, K., HARRAL, J., HOEDT-MILLER, M., TADA, Y., OZIMEK, J., TUDER, R. & RODMAN, D. M. 2004. Pulmonary hypertension in transgenic mice expressing a dominant-negative BMPRII gene in smooth muscle. *Circ Res*, 94, 1109-14.
- WEST, J., HARRAL, J., LANE, K., DENG, Y., ICKES, B., CRONA, D., ALBU, S., STEWART, D. & FAGAN, K. 2008b. Mice expressing BMPRII<sup>R899X</sup> transgene in smooth muscle develop pulmonary vascular lesions. *Am J Physiol Lung Cell Mol Physiol*, 295, L744-55.
- WHEELHOUSE, N. M., CHAN, Y. S., GILLIES, S. E., CALDWELL, H., ROSS, J. A., HARRISON, D. J. & PROST, S. 2003. TNF-alpha induced DNA damage in primary murine hepatocytes. *Int J Mol Med*, 12, 889-94.
- WHITE, K., DEMPSIE, Y., CARUSO, P., WALLACE, E., MCDONALD, R. A., STEVENS, H., HATLEY, M. E., VAN ROOIJ, E., MORRELL, N. W., MACLEAN, M. R. & BAKER, A. H. 2014. Endothelial apoptosis in pulmonary hypertension is controlled by a microRNA/programmed cell death 4/caspase-3 axis. *Hypertension*, 64, 185-94.
- WHITTLE, B. J., SILVERSTEIN, A. M., MOTTOLA, D. M. & CLAPP, L. H. 2012. Binding and activity of the prostacyclin receptor (IP) agonists, treprostinil and iloprost, at human prostanoid receptors: treprostinil is a potent DP1 and EP2 agonist. *Biochem Pharmacol*, 84, 68-75.
- WIDEMAN, R. F., HAMAL, K. R., BAYONA, M. T., LORENZONI, A. G., CROSS, D., KHAJALI, F., RHOADS, D. D., ERF, G. F. & ANTHONY, N. B. 2011. Plexiform lesions in the lungs of domestic fowl selected for susceptibility to pulmonary arterial hypertension: incidence and histology. *Anat Rec (Hoboken)*, 294, 739-55.
- WILKINS, M. R. 2012. Pulmonary hypertension: the science behind the disease spectrum. *Eur Respir Rev*, 21, 19-26.
- WILSON, R. J. & GILES, H. 2005. Piglet saphenous vein contains multiple relaxatory prostanoid receptors: evidence for EP4, EP2, DP and IP receptor subtypes. *Br J Pharmacol*, 144, 405-15.
- WINTER, J., JUNG, S., KELLER, S., GREGORY, R. I. & DIEDERICHS, S. 2009. Many roads to maturity: microRNA biogenesis pathways and their regulation. *Nat Cell Biol*, 11, 228-34.
- WOJCIAK-STOTHARD, B., ZHAO, L., OLIVER, E., DUBOIS, O., WU, Y., KARDASSIS, D., VASILAKI, E., HUANG, M., MITCHELL, J. A., HARRINGTON, L. S., PRENDERGAST, G. C. & WILKINS, M. R. 2012. Role of RhoB in the regulation of pulmonary endothelial and smooth muscle cell responses to hypoxia. *Circ Res*, 110, 1423-34.
- WONG, W. K., KNOWLES, J. A. & MORSE, J. H. 2005. Bone morphogenetic protein receptor type II C-terminus interacts with c-Src: implication for a role in pulmonary arterial hypertension. *Am J Respir Cell Mol Biol*, 33, 438-46.
- WOODS, K., THOMSON, J. M. & HAMMOND, S. M. 2007. Direct regulation of an oncogenic micro-RNA cluster by E2F transcription factors. *J Biol Chem*, 282, 2130-4.

- WOODWARD, D. F., JONES, R. L. & NARUMIYA, S. 2011. International Union of Basic and Clinical Pharmacology. LXXXIII: classification of prostanoid receptors, updating 15 years of progress. *Pharmacol Rev*, 63, 471-538.
- WU, L., FAN, J. & BELASCO, J. G. 2006. MicroRNAs direct rapid deadenylation of mRNA. *Proc Natl Acad Sci U S A*, 103, 4034-9.
- XIAO, J., MENG, X. M., HUANG, X. R., CHUNG, A. C., FENG, Y. L., HUI, D. S., YU, C. M., SUNG, J. J. & LAN, H. Y. 2012. miR-29 inhibits bleomycin-induced pulmonary fibrosis in mice. *Mol Ther*, 20, 1251-60.
- XIN, M., SMALL, E. M., SUTHERLAND, L. B., QI, X., MCANALLY, J., PLATO, C. F., RICHARDSON, J. A., BASSEL-DUBY, R. & OLSON, E. N. 2009. MicroRNAs miR-143 and miR-145 modulate cytoskeletal dynamics and responsiveness of smooth muscle cells to injury. *Genes Dev*, 23, 2166-78.
- XU, B., NIU, X., ZHANG, X., TAO, J., WU, D., WANG, Z., LI, P., ZHANG, W., WU, H., FENG, N., WANG, Z., HUA, L. & WANG, X. 2011. miR-143 decreases prostate cancer cells proliferation and migration and enhances their sensitivity to docetaxel through suppression of KRAS. *Mol Cell Biochem*, 350, 207-13.
- YAMAJI, R., FUJITA, K., TAKAHASHI, S., YONEDA, H., NAGAO, K., MASUDA, W., NAITO, M., TSURUO, T., MIYATAKE, K., INUI, H. & NAKANO, Y. 2003. Hypoxia up-regulates glyceraldehyde-3-phosphate dehydrogenase in mouse brain capillary endothelial cells: involvement of Na<sup>+</sup>/Ca<sup>2+</sup> exchanger. *Biochim Biophys Acta*, 1593, 269-76.
- YANG, H., FU, H., XU, W. & ZHANG, X. 2016. Exosomal non-coding RNAs: a promising cancer biomarker. *Clin Chem Lab Med*.
- YANG, J., DAVIES, R. J., SOUTHWOOD, M., LONG, L., YANG, X., SOBOLEWSKI, A., UPTON, P. D., TREMBATH, R. C. & MORRELL, N. W. 2008. Mutations in bone morphogenetic protein type II receptor cause dysregulation of Id gene expression in pulmonary artery smooth muscle cells: implications for familial pulmonary arterial hypertension. *Circ Res*, 102, 1212-21.
- YANG, S., BANERJEE, S., FREITAS, A., CUI, H., XIE, N., ABRAHAM, E. & LIU, G. 2012. miR-21 regulates chronic hypoxia-induced pulmonary vascular remodeling. *Am J Physiol Lung Cell Mol Physiol*, 302, L521-9.
- YANG, X., DU, W. W., LI, H., LIU, F., KHORSHIDI, A., RUTNAM, Z. J. & YANG, B. B. 2013. Both mature miR-17-5p and passenger strand miR-17-3p target TIMP3 and induce prostate tumor growth and invasion. *Nucleic Acids Res*, 41, 9688-704.
- YANG, X., LEE, P. J., LONG, L., TREMBATH, R. C. & MORRELL, N. W. 2007. BMP4 induces HO-1 via a Smad-independent, p38MAPK-dependent pathway in pulmonary artery myocytes. *Am J Respir Cell Mol Biol*, 37, 598-605.
- YANG, X., LONG, L., SOUTHWOOD, M., RUDARAKANCHANA, N., UPTON, P. D., JEFFERY, T. K., ATKINSON, C., CHEN, H., TREMBATH, R. C. & MORRELL, N. W. 2005. Dysfunctional Smad signaling contributes to abnormal smooth muscle cell proliferation in familial pulmonary arterial hypertension. *Circ Res*, 96, 1053-63.
- YASUDA, T., TADA, Y., TANABE, N., TATSUMI, K. & WEST, J. 2011. Rho-kinase inhibition alleviates pulmonary hypertension in transgenic mice expressing a

- dominant-negative type II bone morphogenetic protein receptor gene. *Am J Physiol Lung Cell Mol Physiol*, 301, L667-74.
- YASUHARA, K., MITSUMORI, K., SHIMO, T., ONODERA, H., TAKAHASHI, M. & HAYASHI, Y. 1997. Mice with focal pulmonary fibrosis caused by monocrotaline are insensitive to urethane induction of lung tumorigenesis. *Toxicol Pathol*, 25, 574-81.
- YEH, E. T., TONG, A. T., LENIHAN, D. J., YUSUF, S. W., SWAFFORD, J., CHAMPION, C., DURAND, J. B., GIBBS, H., ZAFARMAND, A. A. & EWER, M. S. 2004. Cardiovascular complications of cancer therapy: diagnosis, pathogenesis, and management. *Circulation*, 109, 3122-31.
- YELLON, D. M. & DAVIDSON, S. M. 2014. Exosomes: nanoparticles involved in cardioprotection? *Circ Res*, 114, 325-32.
- YI, R., QIN, Y., MACARA, I. G. & CULLEN, B. R. 2003. Exportin-5 mediates the nuclear export of pre-microRNAs and short hairpin RNAs. *Genes Dev*, 17, 3011-6.
- YILDIZ, P. 2009. Molecular mechanisms of pulmonary hypertension. *Clin Chim Acta*, 403, 9-16.
- YIP, H. K., CHANG, L. T., SUN, C. K., SHEU, J. J., CHIANG, C. H., YOUSSEF, A. A., LEE, F. Y., WU, C. J. & FU, M. 2008. Autologous transplantation of bone marrow-derived endothelial progenitor cells attenuates monocrotaline-induced pulmonary arterial hypertension in rats. *Crit Care Med*, 36, 873-80.
- YU, B., ZHANG, X. & LI, X. 2014. Exosomes derived from mesenchymal stem cells. *Int J Mol Sci*, 15, 4142-57.
- YU, P. B., DENG, D. Y., BEPPU, H., HONG, C. C., LAI, C., HOYNG, S. A., KAWAI, N. & BLOCH, K. D. 2008. Bone morphogenetic protein (BMP) type II receptor is required for BMP-mediated growth arrest and differentiation in pulmonary artery smooth muscle cells. *J Biol Chem*, 283, 3877-88.
- YUAN, J. X. & RUBIN, L. J. 2005. Pathogenesis of pulmonary arterial hypertension: the need for multiple hits. *Circulation*, 111, 534-8.
- YUN, U. J., PARK, S. E., JO, Y. S., KIM, J. & SHIN, D. Y. 2012. DNA damage induces the IL-6/STAT3 signaling pathway, which has anti-senescence and growth-promoting functions in human tumors. *Cancer Lett*, 323, 155-60.
- ZAIMAN, A. L., PODOWSKI, M., MEDICHERLA, S., GORDY, K., XU, F., ZHEN, L., SHIMODA, L. A., NEPTUNE, E., HIGGINS, L., MURPHY, A., CHAKRAVARTY, S., PROTTER, A., SEHGAL, P. B., CHAMPION, H. C. & TUDER, R. M. 2008. Role of the TGF-beta/Alk5 signaling pathway in monocrotaline-induced pulmonary hypertension. *Am J Respir Crit Care Med*, 177, 896-905.
- ZANGIABADI, A., DE PASQUALE, C. G. & SAJKOV, D. 2014. Pulmonary hypertension and right heart dysfunction in chronic lung disease. *Biomed Res Int*, 2014, 739674.
- ZENG, C., WANG, X., HU, X., CHEN, J. & WANG, L. 2007. Autologous endothelial progenitor cells transplantation for the therapy of primary pulmonary hypertension. *Med Hypotheses*, 68, 1292-5.
- ZENG, Y., YI, R. & CULLEN, B. R. 2003. MicroRNAs and small interfering RNAs can inhibit mRNA expression by similar mechanisms. *Proc Natl Acad Sci U S A*, 100, 9779-84.

- ZENG, Y., ZHANG, X., KANG, K., CHEN, J., WU, Z., HUANG, J., LU, W., CHEN, Y., ZHANG, J., WANG, Z., ZHAI, Y., QU, J., RAMCHANDRAN, R., RAJ, J. U., WANG, J. & GOU, D. 2016. MicroRNA-223 Attenuates Hypoxia-induced Vascular Remodeling by Targeting RhoB/MLC2 in Pulmonary Arterial Smooth Muscle Cells. *Sci Rep*, 6, 24900.
- ZENG, Z., LI, Y., JIANG, Z., WANG, C., LI, B. & JIANG, W. 2010. The extracellular signal-regulated kinase is involved in the effects of sildenafil on pulmonary vascular remodeling. *Cardiovasc Ther*, 28, 23-9.
- ZHANG, C. 2009. MicroRNA-145 in vascular smooth muscle cell biology: a new therapeutic target for vascular disease. *Cell Cycle*, 8, 3469-73.
- ZHANG, J., SUN, Q., ZHANG, Z., GE, S., HAN, Z. G. & CHEN, W. T. 2013a. Loss of microRNA-143/145 disturbs cellular growth and apoptosis of human epithelial cancers by impairing the MDM2-p53 feedback loop. *Oncogene*, 32, 61-9.
- ZHANG, N., SU, Y. & XU, L. 2013b. Targeting PKCepsilon by miR-143 regulates cell apoptosis in lung cancer. *FEBS Lett*, 587, 3661-7.
- ZHANG, S., FANTOZZI, I., TIGNO, D. D., YI, E. S., PLATOSHYN, O., THISTLETHWAITE, P. A., KRIETT, J. M., YUNG, G., RUBIN, L. J. & YUAN, J. X. 2003. Bone morphogenetic proteins induce apoptosis in human pulmonary vascular smooth muscle cells. *Am J Physiol Lung Cell Mol Physiol*, 285, L740-54.
- ZHANG, X., YUAN, X., SHI, H., WU, L., QIAN, H. & XU, W. 2015. Exosomes in cancer: small particle, big player. *J Hematol Oncol*, 8, 83.
- ZHANG, Y., WANG, Z., CHEN, M., PENG, L., WANG, X., MA, Q., MA, F. & JIANG, B. 2012. MicroRNA-143 targets MACC1 to inhibit cell invasion and migration in colorectal cancer. *Mol Cancer*, 11, 23.
- ZHANG, Y., YANG, P., SUN, T., LI, D., XU, X., RUI, Y., LI, C., CHONG, M., IBRAHIM, T., MERCATALI, L., AMADORI, D., LU, X., XIE, D., LI, Q. J. & WANG, X. F. 2013c. miR-126 and miR-126\* repress recruitment of mesenchymal stem cells and inflammatory monocytes to inhibit breast cancer metastasis. *Nat Cell Biol*, 15, 284-94.
- ZHAO, J., ZHANG, W., LIN, M., WU, W., JIANG, P., TOU, E., XUE, M., RICHARDS, A., JOURD'HEUIL, D., ASIF, A., ZHENG, D., SINGER, H. A., MIANO, J. M. & LONG, X. 2016. MYOSLID Is a Novel Serum Response Factor-Dependent Long Noncoding RNA That Amplifies the Vascular Smooth Muscle Differentiation Program. *Arterioscler Thromb Vasc Biol*.
- ZHAO, L., MASON, N. A., MORRELL, N. W., KOJONAZAROV, B., SADYKOV, A., MARIPOV, A., MIRRAKHIMOV, M. M., ALDASHEV, A. & WILKINS, M. R. 2001. Sildenafil inhibits hypoxia-induced pulmonary hypertension. *Circulation*, 104, 424-8.
- ZHAO, W., ZHAO, S. P. & ZHAO, Y. H. 2015a. MicroRNA-143/-145 in Cardiovascular Diseases. *Biomed Res Int*, 2015, 531740.
- ZHAO, W., ZHENG, X. L., PENG, D. Q. & ZHAO, S. P. 2015b. Myocyte Enhancer Factor 2A Regulates Hydrogen Peroxide-Induced Senescence of Vascular Smooth Muscle Cells Via microRNA-143. *J Cell Physiol*, 230, 2202-11.
- ZHAO, W., ZHENG, X. L. & ZHAO, S. P. 2015c. Exosome and its roles in cardiovascular

- diseases. *Heart Fail Rev*, 20, 337-48.
- ZHAO, Y. D., COURTMAN, D. W., DENG, Y., KUGATHASAN, L., ZHANG, Q. & STEWART, D. J. 2005. Rescue of monocrotaline-induced pulmonary arterial hypertension using bone marrow-derived endothelial-like progenitor cells: efficacy of combined cell and eNOS gene therapy in established disease. *Circ Res*, 96, 442-50.
- ZHOU, G., CHEN, T. & RAJ, J. U. 2015. MicroRNAs in pulmonary arterial hypertension. *Am J Respir Cell Mol Biol*, 52, 139-51.
- ZHOU, L., CHEN, Z., VANDERSLICE, P., SO, S. P., RUAN, K. H., WILLERSON, J. T. & DIXON, R. A. 2013. Endothelial-like progenitor cells engineered to produce prostacyclin rescue monocrotaline-induced pulmonary arterial hypertension and provide right ventricle benefits. *Circulation*, 128, 982-94.
- ZHOU, Q., HEINKE, J., VARGAS, A., WINNIK, S., KRAUSS, T., BODE, C., PATTERSON, C. & MOSER, M. 2007. ERK signaling is a central regulator for BMP-4 dependent capillary sprouting. *Cardiovasc Res*, 76, 390-9.
- ZHOU, W., NEGASH, S., LIU, J. & RAJ, J. U. 2009. Modulation of pulmonary vascular smooth muscle cell phenotype in hypoxia: role of cGMP-dependent protein kinase and myocardin. *Am J Physiol Lung Cell Mol Physiol*, 296, L780-9.
- ZHOU, X., HAN, X., WITTFELDT, A., SUN, J., LIU, C., WANG, X., GAN, L. M., CAO, H. & LIANG, Z. 2016. Long non-coding RNA ANRIL regulates inflammatory responses as a novel component of NF-kappaB pathway. *RNA Biol*, 13, 98-108.